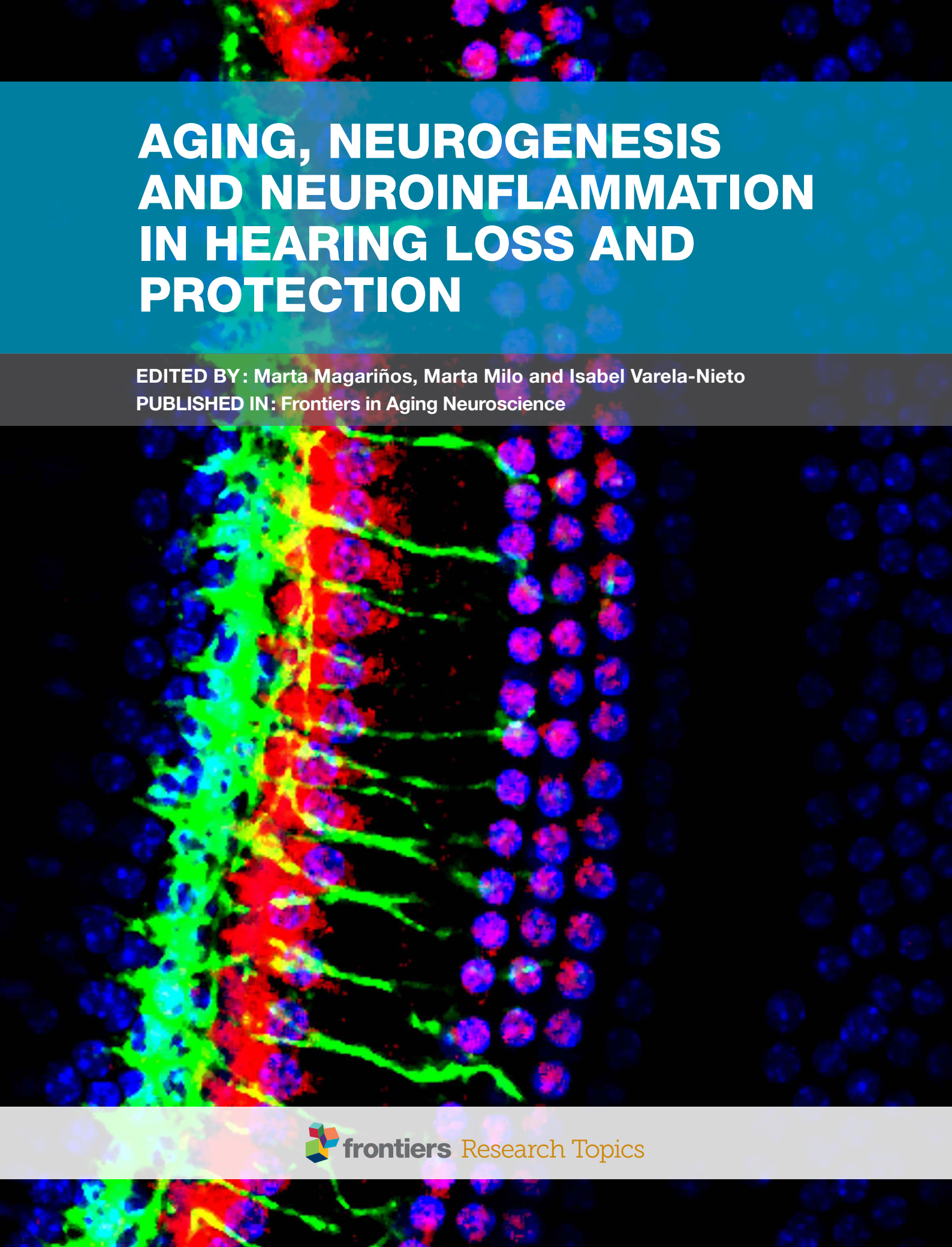

AGING, NEUROGENESIS AND NEUROINFLAMMATION IN HEARING LOSS AND PROTECTION

EDITED BY: Marta Magariños, Marta Milo and Isabel Varela-Nieto

PUBLISHED IN: Frontiers in Aging Neuroscience

frontiers Research Topics

frontiers

ISSN 1664-8714
ISBN 978-2-88919-644-9
DOI 10.3389/978-2-88919-644-9

About Frontiers

Frontiers is more than just an open-access publisher of scholarly articles: it is a pioneering approach to the world of academia, radically improving the way scholarly research is managed. The grand vision of Frontiers is a world where all people have an equal opportunity to seek, share and generate knowledge. Frontiers provides immediate and permanent online open access to all its publications, but this alone is not enough to realize our grand goals.

Frontiers Journal Series

The Frontiers Journal Series is a multi-tier and interdisciplinary set of open-access, online journals, promising a paradigm shift from the current review, selection and dissemination processes in academic publishing. All Frontiers journals are driven by researchers for researchers; therefore, they constitute a service to the scholarly community. At the same time, the Frontiers Journal Series operates on a revolutionary invention, the tiered publishing system, initially addressing specific communities of scholars, and gradually climbing up to broader public understanding, thus serving the interests of the lay society, too.

Dedication to Quality

Each Frontiers article is a landmark of the highest quality, thanks to genuinely collaborative interactions between authors and review editors, who include some of the world's best academicians. Research must be certified by peers before entering a stream of knowledge that may eventually reach the public - and shape society; therefore, Frontiers only applies the most rigorous and unbiased reviews.
Frontiers revolutionizes research publishing by freely delivering the most outstanding research, evaluated with no bias from both the academic and social point of view.
By applying the most advanced information technologies, Frontiers is catapulting scholarly publishing into a new generation.

What are Frontiers Research Topics?

Frontiers Research Topics are very popular trademarks of the Frontiers Journals Series: they are collections of at least ten articles, all centered on a particular subject. With their unique mix of varied contributions from Original Research to Review Articles, Frontiers Research Topics unify the most influential researchers, the latest key findings and historical advances in a hot research area! Find out more on how to host your own Frontiers Research Topic or contribute to one as an author by contacting the Frontiers Editorial Office: **researchtopics@frontiersin.org**

AGING, NEUROGENESIS AND NEUROINFLAMMATION IN HEARING LOSS AND PROTECTION

Topic Editors:
Marta Magariños, Instituto de Investigaciones Biomédicas "Alberto Sols", CSIC-UAM, Spain; CIBERER, Unit 761, Instituto de Salud Carlos III, Spain; Universidad Autónoma de Madrid, Spain
Marta Milo, University of Sheffield, UK
Isabel Varela-Nieto, Instituto de Investigaciones Biomédicas "Alberto Sols", CSIC-UAM, Spain; CIBERER, Unit 761, Instituto de Salud Carlos III, Spain; IdiPAZ, Instituto de Investigación Sanitaria, Spain

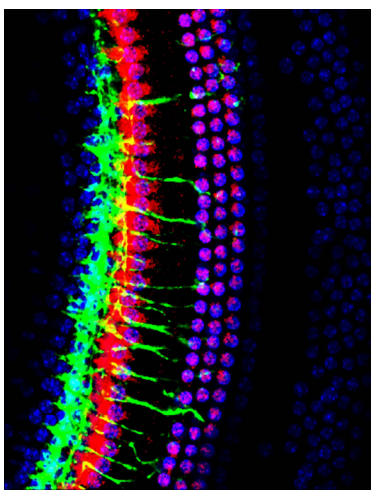

This image shows the middle turn of a 10 month old mouse cochlea stained with anti-Myo7a (red), anti-neurofilament (green) and Hoechst nuclear stain (blue). The image presents a confocal stack through the entire organ of Corti that has been collapsed along the Z-axis using Leica confocal microscopy software. Note the dense innervation of the single row of inner hair cells (left) and the extension of fibers to the three rows of outer hair cells (right). There is an occasional loss of outer hair cells that shows no obvious correlation with innervation (bottom).

Image taken from: Kersigo, J., and Fritzsch, B. (2015). Inner ear hair cells deteriorate in mice engineered to have no or diminished innervation. Front. Aging Neurosci. 7, 33. doi:10.3389/fnagi.2015.00033.

Worldwide, 278 million people are estimated to have moderate to profound hearing loss. Age-related hearing loss, also known as presbyacusis, affects approximately half of the population over 60 years old, making it the second most common cause of disability in older people. Hearing loss occurs when the sensory cells and neurons of the cochlea degenerate and die. The vestibular system, which holds the sense of balance, shares a common embryonic origin with the cochlea and together conform the inner ear. Balance problems are a trait of ageing to the point

that balance ability is considered a sensor of physical decline and vestibular degeneration is the most common cause of falls in the elderly. Still the molecular bases of ageing in the vestibular system have not been studied in detail. Genetic and environmental factors contribute to the progression of age-related hearing loss (ARHL). Being noise the main environmental noxious agent for human hearing in the industrialized societies.

There is no restorative treatment for deafness but functional replacement by means of prosthesis. Therefore, prevention and treatment of hearing loss is an unmet medical need. To develop innovative medical strategies against hearing loss, it is critical to understand the causes of ARHL and the essential pathways responsible for the manifestation of this complex disease.

In this research topic, experts will discuss the stages and molecular elements of the damage and repair processes involved in ARHL, from cellular processes to molecules involved in aging. Oxidative stress takes a central stage as an essential element in the progression of injury and cell loss, and a target for cell protection strategies. Finally, the mechanisms of action and the potential of novel therapies for hair cell repair and protection will be discussed along with drug delivery strategies.

Citation: Magariños, M., Milo, M., Varela-Nieto, I., eds. (2015). Aging, Neurogenesis and Neuroinflammation in Hearing Loss and Protection. Lausanne: Frontiers Media. doi: 10.3389/978-2-88919-644-9

Table of Contents

frontiers in Aging Neuroscience

EDITORIAL
published: 17 July 2015
doi: 10.3389/fnagi.2015.00138

Editorial: Aging, neurogenesis and neuroinflammation in hearing loss and protection

Marta Magariños[1,2,3], *Marta Milo*[4] *and Isabel Varela-Nieto*[1,2,5]*

[1] *Departamento de Fisiopatología Endocrina y del Sistema Nervioso, Instituto de Investigaciones Biomédicas "Alberto Sols," CISC-UAM, Madrid, Spain,* [2] *CIBERER, Unit 761, Instituto de Salud Carlos III, Madrid, Spain,* [3] *Departamento de Biología, Universidad Autónoma de Madrid, Madrid, Spain,* [4] *Department of Biomedical Science, University of Sheffield, Sheffield, UK,* [5] *Área de Cáncer y Genética Molecular Humana, IdiPAZ, Instituto de Investigación Sanitaria, Madrid, Spain*

Keywords: ARHL, hair cells, drug delivery, lipid homeostasis, noise, redox balance, spiral neurons, TGF-β

Hearing loss affects 360 million people worldwide and it is estimated that this number will exceed 900 million by 2025 (World Health Organization. Fact sheet N°300, March 2015). Hearing loss has different etiologies; it severely affects quality of life by reducing individual communication, a fact that has different implications depending on age.

Age-related hearing loss (ARHL), also called presbycusis, is an increasing health, social, and economic problem as the affected population represents a continuously increasing percentage of the world population. Associated with ARHL is an acceleration of cognitive decline, and its links with developing neurodegenerative diseases, including Alzheimer's and frailty, are currently under study. Excessive exposure to noise and/or ototoxic drugs are additional factors in the worldwide increase of ARHL. Both noise-induced hearing loss (NIHL) and ARHL share common molecular mechanisms that involve redox imbalance and inflammation.

Sensorineural hearing loss is associated with damage or death of cochlear cells, including neurons and sensory hair cells. Hearing insults decrease cell survival pathways and promote apoptotic programs. In the first article of this eBook, "Aging, neurogenesis and neuroinflammation in hearing loss and protection," the mechanisms behind sensorineural cell damage are reviewed (Wong and Ryan, 2015). Neuronal degeneration is typically considered secondary to hair cell loss, and another interesting article reviews the key role that innervation has on long-term hair cell maintenance (Kersigo and Fritzsch, 2015). Indeed, cochlear stressors affect not only sensorineural elements but also central components such as the auditory cortex (Fetoni et al., 2015). Similarly, aging affects the rat central auditory system in specific neuronal regions, where the expression of neurofilaments is more affected than are neuron numbers (Burianová et al., 2015). The efferent response is also altered in the senescent gerbil, indeed vestibular and cochlear efferent neurons are differentially modified (Radtke-Schuller et al., 2015). Auditory and vestibular organs have a common developmental origin (Magariños et al., 2012) and the parallel and gradual deterioration of both is strongly associated with aging. Older human adults showing hearing loss generally have increased audiometric thresholds. However, those suffering auditory deafferentation are difficult to diagnose by conventional methods. This topic explored and a novel method of diagnosis is proposed (Marmel et al., 2015).

People suffering from profound hearing loss can benefit from using hearing aids, the importance of which is being recognized by numerous awards including the 2013 Lasker-DeBakey Clinical Medical Research and the 2015 Fritz J. and Dolores H. Russ Prize Awards for the development of the modern cochlear implant. There is no other specific therapy available, but there is a boom of research efforts aimed at developing cell therapy, gene therapy, and small-molecule based pharmacological approaches. These exciting developments are based on the knowledge generated from basic neurobiology and developmental studies. Laboratory animals are essential

OPEN ACCESS

Edited and reviewed by:
Rodrigo Orlando Kuljiš, Zdrav Mozak Limitada, Chile

***Correspondence:**
Isabel Varela-Nieto, ivarela@iib.uam.es

Received: *22 June 2015*
Accepted: *06 July 2015*
Published: *17 July 2015*

Citation:
Magariños M, Milo M and Varela-Nieto I (2015) Editorial: Aging, neurogenesis and neuroinflammation in hearing loss and protection. Front. Aging Neurosci. 7:138. doi: 10.3389/fnagi.2015.00138

for generating accurate models of human hearing loss. One of the articles included in this eBook describes novel models for studying NIHL, based on the use of different sound stimuli, which provide solid ground on which to study potential therapeutic molecules (Sanz et al., 2015). Another important matter that must be addressed is the delivery of potential drugs to the cochlea. The isolation and difficult access of the inner ear and the delicate balance of its internal fluids makes this problem extremely challenging. Thus, we have included an article which explores the possibilities of "smart" nanoparticles for local drug delivery (Glueckert et al., 2015).

Finally, authors herein illustrate and discuss small molecule-based novel therapies directed to confer otoprotection or reduce injury. The role of oxidative stress in hearing loss has prompted study of the potential of a combination of antioxidants and vasodilators on hearing loss remediation (Alvarado et al., 2015). Inflammation and the immune response contribute both to hearing protection as well as to hearing damage. Thus, the description of the use of TGF-β inhibitors in the protection and repair of NIHL injury (Murillo-Cuesta et al., 2015) is of particular interest. Lipid metabolism is central to neuronal degenerative diseases although its role in inner ear pathologies is essentially unknown. The role of cholesterol (Malgrange et al., 2015) and sphingosine 1-P (Romero-Guevara et al., 2015) in the physiology of hearing as well as advance future strategies based on their derivatives to fight hearing loss are explored.

Funding

This work was supported by Spanish grant from the Ministerio de Economía y Competitividad SAF2014-53979-R and European FP7-PEOPLE-IAPP-TARGEAR. The cost of this publication has been paid in part by FEDER funds.

References

Alvarado, J. C., Fuentes-Santamaría, V., Melgar-Rojas, P., Valero, M. L., Gabaldón-Ull, M. C., Miller, J. M., et al. (2015). Synergistic effects of free radical scavengers and cochlear vasodilators: a new otoprotective strategy for age-related hearing loss. *Front. Aging Neurosci.* 7:86. doi: 10.3389/fnagi.2015.00086

Burianová, J., Ouda, L., and Syka, J. (2015). The influence of aging on the number of neurons and levels of non-phosporylated neurofilament proteins in the central auditory system of rats. *Front. Aging Neurosci.* 7:27. doi: 10.3389/fnagi.2015.00027

Fetoni, A. R., Troiani, D., Petrosini, L., and Paludetti, G. (2015). Cochlear injury and adaptive plasticity of the auditory cortex. *Front. Aging Neurosci.* 7:8. doi: 10.3389/fnagi.2015.00008

Glueckert, R., Pritz, C. O., Roy, S., Dudas, J., and Schrott-Fischer, A. (2015). Nanoparticle mediated drug delivery of rolipram to tyrosine kinase B positive cells in the inner ear with targeting peptides and agonistic antibodies. *Front. Aging Neurosci.* 7:71. doi: 10.3389/fnagi.2015.00071

Kersigo, J., and Fritzsch, B. (2015). Inner ear hair cells deteriorate in mice engineered to have no or diminished innervation. *Front. Aging Neurosci.* 7:33. doi: 10.3389/fnagi.2015.00033

Magariños, M., Contreras, J., Aburto, M. R., and Varela-Nieto, I. (2012). Early development of the vertebrate inner ear. *Anat. Rec. (Hoboken)* 295, 1775–1790. doi: 10.1002/ar.22575

Malgrange, B., Varela-Nieto, I., de Medina, P., and Paillasse, M. R. (2015). Targeting cholesterol homeostasis to fight hearing loss: a new perspective. *Front. Aging Neurosci.* 7:3. doi: 10.3389/fnagi.2015.00003

Marmel, F., Rodríguez-Mendoza, M. A., and Lopez-Poveda, E. A. (2015). Stochastic undersampling steepens auditory threshold/duration functions: implications for understanding auditory deafferentation and aging. *Front. Aging Neurosci.* 7:63. doi: 10.3389/fnagi.2015.00063

Murillo-Cuesta, S., Rodríguez-de la Rosa, L., Contreras, J., Celaya, A. M., Camarero, G., Rivera, T., et al. (2015). Transforming growth factor β1 inhibition protects from noise-induced hearing loss. *Front. Aging Neurosci.* 7:32. doi: 10.3389/fnagi.2015.00032

Radtke-Schuller, S., Seeler, S., and Grothe, B. (2015). Restricted loss of olivocochlear but not vestibular efferent neurons in the senescent gerbil (Meriones unguiculatus). *Front. Aging Neurosci.* 7:4. doi: 10.3389/fnagi.2015.00004

Romero-Guevara, R., Cencetti, F., Donati, C., and Bruni, P. (2015). Sphingosine 1-phosphate signaling pathway in inner ear biology. New therapeutic strategies for hearing loss? *Front. Aging Neurosci.* 7:60. doi: 10.3389/fnagi.2015.00060

Sanz, L., Murillo-Cuesta, S., Cobo, P., Cediel-Algovia, R., Contreras, J., Rivera, T., et al. (2015). Swept-sine noise-induced damage as a hearing loss model for preclinical assays. *Front. Aging Neurosci.* 7:7. doi: 10.3389/fnagi.2015.00007

Wong, A. C. Y., and Ryan, A. F. (2015). Mechanisms of sensorineural cell damage, death and survival in the cochlea. *Front. Aging Neurosci.* 7:58. doi: 10.3389/fnagi.2015.00058

Conflict of Interest Statement: The authors declare that the research was conducted in the absence of any commercial or financial relationships that could be construed as a potential conflict of interest.

frontiers in Aging Neuroscience

REVIEW
published: 21 April 2015
doi: 10.3389/fnagi.2015.00058

Mechanisms of sensorineural cell damage, death and survival in the cochlea

Ann C. Y. Wong[1,2] *and Allen F. Ryan*[1,3,4]*

[1] Department of Surgery/Division of Otolaryngology, University of California, San Diego School of Medicine, La Jolla, CA, USA, [2] Department of Physiology and Translational Neuroscience Facility, School of Medical Sciences, University of New South Wales, Sydney, NSW, Australia, [3] Veterans Administration Medical Center, La Jolla, CA, USA, [4] Department of Neurosciences, University of California, San Diego School of Medicine, La Jolla, CA, USA

The majority of acquired hearing loss, including presbycusis, is caused by irreversible damage to the sensorineural tissues of the cochlea. This article reviews the intracellular mechanisms that contribute to sensorineural damage in the cochlea, as well as the survival signaling pathways that can provide endogenous protection and tissue rescue. These data have primarily been generated in hearing loss not directly related to age. However, there is evidence that similar mechanisms operate in presbycusis. Moreover, accumulation of damage from other causes can contribute to age-related hearing loss (ARHL). Potential therapeutic interventions to balance opposing but interconnected cell damage and survival pathways, such as antioxidants, anti-apoptotics, and pro-inflammatory cytokine inhibitors, are also discussed.

Keywords: presbycusis, age-related hearing loss (ARHL), hair cells (HCs), spiral ganglion neurons (SGN), reactive oxygen species (ROS), c-Jun terminal kinase (JNK), inflammation, cell survival signaling

OPEN ACCESS

Edited by:
Marta Magarinos, Universidad Autonoma de Madrid, Spain

Reviewed by:
Gilda Kalinec, University of California, Los Angeles, USA
Joana Neves, Buck Institute for Research on Aging, USA

***Correspondence:**
Allen F. Ryan, Department of Surgery/Division of Otolaryngology, University of California, San Diego School of Medicine, 9500 Gilman Drive – MC#0666, La Jolla, CA 92093-0666, USA
Tel: +1.858.534.4594,
Fax: +1.858.534.5319
afryan@ucsd.edu

Received: *26 January 2015*
Accepted: *05 April 2015*
Published: *21 April 2015*

Citation:
Wong ACY and Ryan AF (2015) Mechanisms of sensorineural cell damage, death and survival in the cochlea. Front. Aging Neurosci. 7:58. doi: 10.3389/fnagi.2015.00058

Introduction

Acquired Sensorineural Hearing Loss (SNHL)

Sensorineural hearing loss (SNHL) is a common sensory deficit, the WHO estimating in 2012 that globally over 360 million people have disabling hearing loss (Duthey, 2013). SNHL is often defined as the loss of hearing sensitivity due to peripheral tissue damage and/or cell death in the hearing organ, the cochlea. However, it is increasingly recognized that the central auditory structures of the brain can also play an independent role in SNHL. The etiology of SNHL is multifactorial, with overexposure to sound, certain drugs, infection or immune-induced inflammation being common causes. Perhaps the most common form of hearing loss is presbycusis, age-related cochlear or central auditory tissue damage or degeneration, often aggravated by other factors including a history of noise exposure, diabetes or high blood pressure. These factors lead to damage and death of the sensory receptor cells in the cochlea and the neurons that relay auditory information from the inner ear to the central auditory circuitry, and then process information as it ascends the central auditory pathway. Damage restricted to the central auditory pathway also plays a role in age-associated hearing loss (e.g., Ouda et al., 2015).

The sensorineural tissues of the cochlea have very limited repair capacity. The mature cochlear receptor cells, the inner and outer hair cells (HCs), as well as the cochlear neurons do not regenerate, making any cellular loss permanent. An overarching aim in preclinical auditory research is to identify the myriad of cellular molecular mechanisms impacting the

damage and survival of cochlear sensorineural tissue, so as to translate into avenues for therapeutic interventions. Here, we review the mechanisms of cochlear HC and neuronal loss and survival, with focus on the role of intracellular pathways and immunity/inflammation in hearing loss. This includes presbycusis, since there is evidence that sensorineural cell damage occurs via similar mechanisms in most forms of SNHL. Moreover, at least some presbycusis is thought to represent the accumulation of hearing loss due to various etiologies over a lifetime.

Cochlear Structure and Function

A newborn human cochlea has ∼3500 inner HCs and a total of ∼12000 outer HCs, while the mouse, an important experimental animal in hearing research has ∼3300 HCs in one cochlea (Ehret and Frankenreiter, 1977). Cochlear HCs are interdigitated with supporting cells to form an epithelial layer on top of the basilar membrane, these receptor cells are bound by two different cellular fluids: apical stereocilia bath in high K^+ endolymph and its basal synaptic pole in perilymph with ionic concentration similar to extracellular fluid.

Sound energy produces fluidic pressure differences across the basilar membrane upon which the sensory cells sit, leading to membrane motion and deflection of bundles of stereocilia on their apical surfaces. This in turn activates mechanoelectrical transduction (MET) channels leading to K^+ influx and HC receptor potentials. Depolarization of outer HCs produces electromotility and amplification of basilar membrane motion, which forms the basis for cochlear sensitivity and frequency resolution. Depolarized inner HCs release glutamate from ribbon synapses at their basal poles. Innervating the inner HCs are dendrites of the afferent neurons of the cochlear nerve, known as spiral ganglion neurons (SGN). These bipolar neurons provide afferent auditory neurotransmission to the central auditory system. There are ∼35,000 afferent SGNs in one human cochlea and ∼7000 in a C57 mouse cochlea (Schettino and Lauer, 2013). Cochlear HCs and SGNs are the foundation of hearing function, and as noted above they do not regenerate after death. It is therefore important to curb the cellular mechanisms that contribute to HC and SGN death (**Figure 1**).

SNHL and HC Loss

The most common histological sign of SNHL in humans is damage to or the loss of cochlear sensory cells (Schuknecht et al., 1973). This phenomenon has been well studied in animals. For example, very intense noise can cause direct mechanical disruption of the HC stereocilia bundles (Liberman and Beil, 1979; Slepecky, 1986; Patuzzi et al., 1989), reducing or eliminating their function. Even more intense stimulation can disrupt the cellular organization of the sensory epithelium, producing profound damage directly or indirectly via potassium exposure of the HC basal poles. However, most damaging levels of noise are below the threshold of mechanical damage and produce the loss of HCs via biochemical pathways within the cells themselves. Such pathways are also involved in HC loss due to non-traumatic causes. These include ototoxic drugs, such as the aminoglycoside antibiotics (Schacht, 1986; Hiel et al., 1992; Richardson et al., 1997; Alharazneh et al., 2011), loop diuretics or some anticancer medications. Most critical for this review, they are important mediators of age-related hearing loss (ARHL).

Cochlear Neural Contributions to SNHL

Afferent SGNs depend at least partially for their survival upon the support of neurotrophic factors including neurotrophin-3 (NT-3), brain-derived neurotrophic factor (BDNF), and glial cell line-derived neurotrophic factor (GDNF), released from the HCs and supporting cells of the cochlear sensory epithelium (Schimmang et al., 2003; Sun and Salvi, 2009; Barclay et al., 2011). When HCs die, the afferent dendrites of SGNs retract, and secondary loss of SGN somata is observed (Liberman and Kiang, 1978; Spoendlin, 1984; Sugawara et al., 2005; Kujawa and Liberman, 2009; Moser et al., 2013). Recent evidence from ototoxic and age-related SNHL suggests that SGN damage or loss can be independent from HC loss. SGN afferent terminals and somata have been found to be primary injury sites after carboplatin treatment (Wang et al., 2003a). Similarly, with loud sound injury, SGN afferent terminals juxtaposed to the inner HCs swell immediately after exposure and prior to observable HC damage likely due to glutamate toxicity (Robertson, 1983; Puel et al., 1998). Kujawa and Liberman (2009) found that noise exposure at levels too low to produce permanent threshold shift can nevertheless cause the loss of a substantial number of the afferent synapses between inner HCs and SGNs. Moreover, they also found that such noise exposure potentiated age-related SNHL, also by disrupting cochlear ribbon synapses immediately post noise exposure, leading to selective SGN axonal fiber loss without destroying cochlear sensory cells (Kujawa and Liberman, 2009; Furman et al., 2013). In aged mice never exposed to loud noise, afferent SGN-inner HC innervation reduction was observed before SGN loss, supporting a role for SGNs in addition to HCs as a primary site of age-related SNHL (Sergeyenko et al., 2013). The mechanisms responsible for inner HC synapse loss have not been determined with certainty, but glutamate toxicity is a strong candidate.

On the central projection of SGN axons, electron microscopy analysis showed with repeated exposure to loud noise (100 dB SPL, 3 h per day over 3 days) marked elongation of the nodes of Ranvier and a moderate retraction of the paranodes was observed together with a reduced number of lamellar wraps and decreased myelin thickness (Tagoe et al., 2014). These morphological changes parallel physiological measurements of reduced auditory nerve conduction velocity and increased auditory thresholds.

Presbycusis

ARHL or persbycusis is most frequently associated with damage to HCs and SGNs. It has been suggested that a substantial contribution to presbycusis is accumulated, low-level damage due to noise and other insults (Gates and Mills, 2005). However, even in the absence of such stimuli, as when animals spend their lives in silence, ARHL is still observed (Sergeyenko et al.,

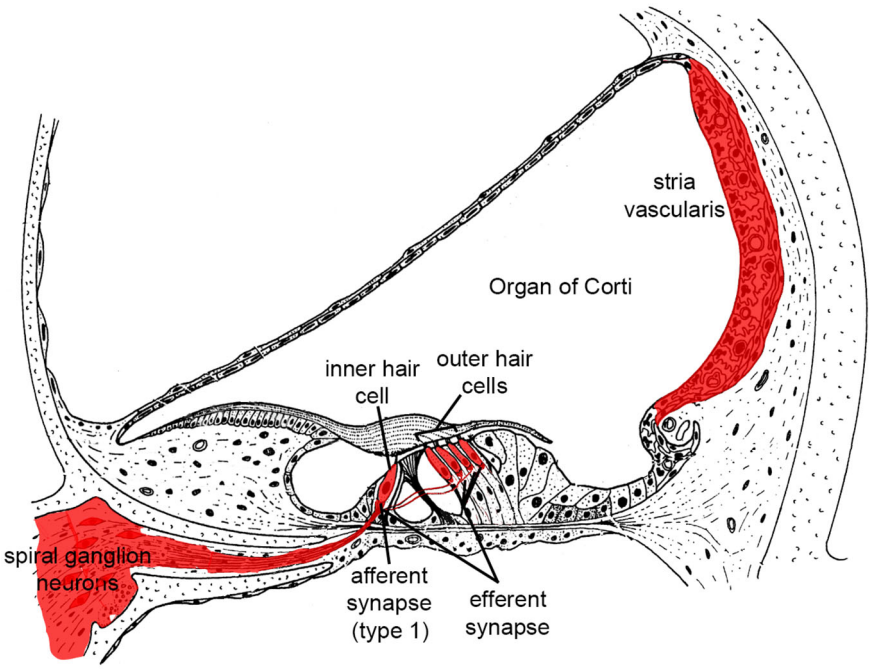

FIGURE 1 | Illustration highlighting cochlear tissues that are prone to irreversible damage and cell death in SNHL in red. Damage to any of these tissues reduces hearing.

2013; Yan et al., 2013). Damage to other tissues, in particular the stria vascularis, is also associated with aging (Schuknecht, 1964; Fetoni et al., 2011). Given the highly active and metabolic nature of many cochlear tissues, and their delicacy, it is perhaps not surprising that age results in damage independent of extrinsic causes. The inbred mouse model of C57BL/6J background has shown high-frequency hearing loss and cochlea basal turn cytostructural degeneration from 6-months of age, in part caused by the presence of the ARHL susceptibility allele (*Ahl*), which encodes for caderhin 23 expressed in the stereocilia of HCs (Zheng et al., 1999). Fransen et al. (2015) performed a genome-wide association study to identify the genes responsible for ARHL, and found no indication for the presence of any major genes. However, independent post-association pathway analysis suggested the involvement of the arachidonic acid secretion pathway, the JAK/STAT and TGFβ signaling pathways though the authors concluded the findings remain exploratory.

The central auditory system is also subject to changes related to age. Many of the alterations that have been documented in the aging central auditory system are related to the expression of potassium channels (Frisina, 2009) and neurotransmitters (Ling et al., 2005; Wang et al., 2009). For example, Zettel et al. (2007) found declines in Kv3.1 in the auditory midbrain structures of aging mice, which could contribute to reduced discharge and synchrony of auditory evoked neural activity. Similarly, Caspary et al. (2008) and Ouda and Syka (2012) noted reduced glycine and GABA expression in auditory midbrain structures with age, accompanied by altered expression of their receptors. This would alter the excitatory/inhibitory balance of auditory neurons and affect signal processing. Such changes are likely to alter the transmission of information in the ascending auditory pathway, and presumably contribute to altered perception of sounds that are independent of peripheral changes in thresholds. They can also influence the cochlea. Jacobson et al. (2003) observed dramatic declines in contralateral suppression known to be mediated by the olivocochlear efferents, in aged mice.

Intracellular Mechanisms of HC Loss

Free Radical Accumulation and Calcium Homeostasis

Generation of reactive oxygen species (ROS) and reactive nitrogen species (RNS) in the cochlea are triggered by exposure of loud sound and ototoxic drugs often followed by caspase-mediated cell death by apoptosis (Shi and Nuttall, 2003; Henderson et al., 2006; Hu et al., 2006). ROS have been detected in cochlear tissue immediately after noise exposure (Yamane et al., 1995) and seen to persist for 7–10 days after, spreading from the basal end of the organ of Corti to the apical turn; the RNS product peroxynitrite (ONOO−), generated by the combination of nitric oxide (NO) and superoxide has also been found (Yamashita et al., 2004a). This prolonged oxidative stress can induce the delay and continued cochlear injury. Apoptosis-inducing factor (AIF) and the apoptotic nuclease EndoG are also released by mitochondria into the cytosol of cochlear HCs following noise exposure (Yamashita et al., 2004b). Translocation of these pro-apoptotic

factors into the nucleus triggers apoptosis. Activation of the c-Jun *N*-terminal kinase/mitogen-activated protein kinase (JNK/MAPK) signaling pathway is also implicated in outer HC apoptosis in response to oxidative stress (Wang et al., 2007).

Free radicals (ROS and RNS) can cause damage by reacting with DNA, proteins, cytosolic molecules, cell surface receptors, and breaking down membrane lipids. ROS produced by the mitochondria induce lipid peroxidation in the cochlea through the formation of malondialdehyde and 4-hydroxynonenal byproducts (Yamashita et al., 2004a). This overloads the cochlear antioxidant enzyme system, including superoxide dismutase (SOD), catalase (CAT), glutathione peroxidase and glutathione reductase, and depletes glutathione, the endogenous antioxidant. In addition to apoptosis, ROS generation also leads to inflammation, and production of the pro-inflammatory cytokines interleukin-6 (IL-6; Wakabayashi et al., 2010) and tumor necrosis factor α (TNFα; Keithley et al., 2008). The presence of vasoactive lipid peroxidation products such as isoprostanes potentially also leads to the reduced cochlear blood flow associated with excessive noise (Thorne et al., 1987; Seidman et al., 1999; Ohinata et al., 2000; Jaumann et al., 2012). Noise-induced ischemia and subsequent re-perfusion further potentiate the generation of ROS. Expression of nicotinamide adenine dinucleotide phosphate (NADPH) oxidases, a key component in the cellular antioxidation system, is altered in the HCs and supporting cells of noise-exposed cochleae (Vlajkovic et al., 2013). Maulucci and colleagues have shown further that acoustic overstimulation reduced NADPH oxidation, decreasing plasma membrane fluidity of outer HCs as a consequence of excess peroxidation induced by an altered metabolic state (Maulucci et al., 2014). Interestingly, Fetoni and colleagues have recently identified endogenous coenzymes Q_9 and Q_{10} to be reduced in the cochlea after exposure to 60 min of 100 dB SPL sound for 10 consecutive days (Fetoni et al., 2013). Systematic administration of exogenous $CoQ_{10,}$ beginning 3 days prior to the noise insult, has been shown to improve hearing threshold, reducing HC bundle disorientation and SGN loss in the mid-cochlear turn, likely due to lowered noise-induced oxidative stress on the sensorineural tissues. Accumulation of highly-reactive oxygen species (hROS) in HCs is also found in cultured organ of Corti explants exposed to gentamicin (Choung et al., 2009).

Mitochondria are a potent source of ROS and loss of mitochondrial integrity can lead to increased ROS production and release of ROS into the cytoplasm (Batandier et al., 2004). Recent work by Esterberg and colleagues suggests that aminoglycoside antibiotics may induce cytoplasmic ROS in HCs by disrupting calcium homeostasis between the endoplasmic reticulum (ER) and mitochondria (Esterberg et al., 2013, 2014). Their data suggest that these drugs enhance calcium flow into mitochondria, leading to increases in mitochondrial membrane permeability, release of calcium as well as increased ROS production and release into the cytoplasm, with subsequent HC damage and death.

Excessive noise also leads to an increase in free Ca^{2+} in cochlear HCs immediately post-noise (Fridberger et al., 1998). This increase can be caused by Ca^{2+} entry through ion channels, such as L-type Ca^{2+} channels an $P2X_2$ ATP receptor subunit, and lead to further release of Ca^{2+} from intracellular stores such as the ER and mitochondria (Orrenius et al., 2003). Elevated Ca^{2+} levels in the cochlea may link to ROS production as well as triggering apoptotic and necrotic cell death pathways independent of ROS formation (Orrenius et al., 2003). In knock-out mice lacking expression of the canonical transient receptor potential channel subtype 3 (TRPC3), a non-selective cation-permeable receptor expressed in sensorineural cochlear tissue (Raybould et al., 2007; Phan et al., 2010; Tadros et al., 2010), cochlear HCs displayed approximately 40% reduction in Ca^{2+} re-entry following intracellular calcium depletion. The TRPC knockout mice have hyperacusis at frequencies tonotopically encoded by mid-apical basilar membrane, a region highly reliant on outer HC cochlear amplification (Wong et al., 2013b). The consequence of disrupted calcium homeostasis on noise susceptibility is also demonstrated in plasma membrane Ca^{2+}-ATPase isoform 2 (*Pmca2* or *Atp2b2*) mutant mice. The *C*-terminally truncated PMCA2a is the only isoform detected in the stereocilia of HCs (Furuta et al., 1998; Dumont et al., 2001). *Pmca2* null mice are deaf while their heterozygous littermates have significant hearing loss (Kozel et al., 1998). People carrying a homozygous mutation in cadherin 23 (*CDH23*) and a heterozygous, hypofunctional variant in *PMCA2* have exaggerated hearing loss compared to those having *CDH23* mutation alone (Schultz et al., 2005).

Another mode of action of calcium is to modulate the activity of MAPK and other intracellular signaling cascades, including apoptosis (e.g., Agell et al., 2002; Harr and Distelhorst, 2010). There is ample evidence that these cascades play a significant role in damage to both HCs and SGN.

MAPK Signaling Pathways

There is substantial evidence that sensorineural cell damage and death involve intracellular signaling pathways. MAPKs are important intracellular proteins that, when phosphorylated, regulate diverse cellular processes in response to a variety of extracellular and intracellular stimuli. MAPKs mediate plasma membrane bound receptor signals to activate transcription factors in the nucleus, facilitating gene expression, coordinately regulating cell proliferation, differentiation, motility, and survival (Johnson, 2011). They can also respond to intracellular events such as ROS or intracellular receptors (Torres, 2003). Among this family of signaling proteins, the classical MAPKs include the extracellular signal-regulated kinases 1, 2 and 5 (ERK1, 2 and 5), stress-activated protein kinase/JNK1-3, and p38 (α, β, γ, δ). MAPKs together regulate a large number of substrates, including members of a family of protein Ser/Thr kinases known as MAPK-activated protein kinases (MAPK-APK). Stress-activated protein kinases of the JNK and p38 families are key mediators of stress and inflammation responses evoked by a variety of physical, chemical and biological stress stimuli, while the ERK1/2 cascade is most often induced by growth factors and mediates tissue growth and survival. p38 MAPK activation is a major component deciding cell fate in

response to cisplatin, primarily to induce apoptosis (Brozovic and Osmak, 2007).

In animals exposed to intense noise, MAPK phosphorylation in the cochlea is altered, ERK1/2 in the sensory and support cells of the cochlear sensory epithelium are activated by phosphorylation; while JNK and p38 MAPKs showed late activation in the SGN, de novo syntheses of the MAPKs are also observed (Meltser et al., 2010; Jamesdaniel et al., 2011; Maeda et al., 2013; Patel et al., 2013). Radiation therapy for the treatment of head and neck cancers produces severe ototoxicity due to the increased production of ROS. In a cochlea derived cell line model, pharmacological inhibition of p38 prior to radiation exposure has prevented radiation ototoxicity (Shin et al., 2014). Inhibitors of JNK have demonstrated protection against noise-induced and aminoglycoside-induced HC loss (Pirvola et al., 2000; Wang et al., 2003b, 2007). Inhibition of upstream activators of the JNK pathway, including kRas, Rac/cdc42 and mixed lineage kinases also provides protection to HCs (Bodmer et al., 2002a,b; Battaglia et al., 2003).

Apoptosis

Following the activation of MAPK and ROS stress pathways, cochlear HCs can undergo apoptosis following intense noise exposure, aminoglycoside or cisplatin ototoxicity, or aging (Hu et al., 2000, 2002a,b; Nicotera et al., 2003; Wang et al., 2003b; Yang et al., 2004). Apoptosis can occur through the sequential actions of caspases, initiated by their associated extrinsic and intrinsic pathways (Yakovlev and Faden, 2001). The extrinsic pathway is initiated by extracellular stimuli through the activation of transmembrane death receptors, which cleave caspase-8 and activate the downstream execution pathway mediated by caspase-3. The intrinsic pathway is initiated by a change in mitochondrial membrane permeability, which not only activates caspase-9 and the downstream execution pathway via cytochrome C release, but also releases ROS. The execution pathway results in distinctive structural pathology including cell shrinkage, chromatin condensation, formation of cytoplasmic blebs and apoptotic bodies and finally phagocytosis of the apoptotic bodies by adjacent parenchymal cells, neoplastic cells or macrophages. Alternatively, there are caspase-independent processes that lead to apoptosis, mediated by other factors including receptor-interacting serine/threonine-protein kinase 1 (RIP-1) or AIF (Tait and Green, 2008).

The caspase-mediated cell death pathway has been widely implicated in programmed cell death of HCs (Nicotera et al., 2003; Yang et al., 2004; Bohne et al., 2007; Tadros et al., 2008), with the preponderance of evidence implicating the intrinsic pathway (e.g., Tabuchi et al., 2007; Esterberg et al., 2013, 2014), but evidence also for extrinsic pathway involvement (Bodmer et al., 2002b).

Infection, Immunity and Inflammation

Invasion of tissue by bacteria or viruses provokes an immediate response based on innate immunity that is independent of prior sensitization, and a delayed response based on acquired, cognate immunity. The processes of inflammation form an important party of both forms of immune defence, generating bioactive mediators that attack or impede infecting organisms, recruiting immune cells to the site and promoting the death of pathogens. However, inflammation is also known to damage or kill host cells via bystander injury. Pro-inflammatory cytokines such as IL-1β and TNFα produce toxicity through multiple pathways including complement activation, production of arachidonic acid metabolites and ROS formation (Neher et al., 2011). TNFα can also activate the extrinsic pathway of apoptosis via TNF "death" receptors common on the surface of cells. Leukocytes drawn to sites of inflammation by cytokines and chemokines may also cause tissue damage. For example, neutrophils are potent sources of ROS, and their release can cause harm to host cells (Wright et al., 2010).

Infection of the inner ear by viruses or bacteria causes varying degrees of inflammation, depending upon the nature of the organism and the host response. Bacterial labyrinthitis, especially when caused by invasive organisms such as *Streptococcus pneumoniae* or *Haemophilus influenzae* type B (Dodge et al., 1984; Wiedermann et al., 1986) is devastating to the delicate tissue of the inner ear, and immunization against these pathogens provides significant protection (Schuchat et al., 1997). On the other hand, there is evidence that the immune response to less damaging pathogens may produce a more severe reaction than the original infection. For example, cytomegalovirus (CMV) infection of the adult cochlea, unlike during the prenatal period, typically causes mild hearing loss and cochlear damage (Juanjuan et al., 2011; Wang et al., 2013). However, Woolf et al. (1985) found that infection of the adult guinea pig cochlea was far more damaging in animals that had previously been immunized systemically with the virus. This indicates that CMV can cause a relatively benign infection in the adult cochlea, while immune-mediated inflammation leads to damage and hearing loss.

Infections outside of the inner ear can also cause cochlear damage. Middle ear infections have been shown to damage especially the basal turn of the cochlea, even when the infection does not enter the labyrinth (Hunter et al., 1996). This is likely due to the relative permeability of the round window membrane, which can allow inflammatory mediators to enter the cochlea. Several studies have found that when such mediators are applied to the round window, they are detected in perilymph and can lead to sensorineural damage and hearing loss (Huang et al., 1990; Kubo et al., 1998).

In addition to the response to infection, tissue damage itself can initiate inflammation, through the release of damage-associated molecules including arachadonic acid metabolites, free extracellular matrix molecules, nucleotides and others (Van Crombruggen et al., 2013). This cochlear damage due to a variety of causes can initiate the inflammatory cascade in the absence of infection. Noise-induced hearing loss has been found to induce inflammation as evidenced by the observation of pro-inflammatory cytokines (Wakabayashi et al., 2010), leukotrienes (Park et al., 2014) and leukocytes (Hirose et al., 2005; Tornabene et al., 2006) within the inner ear. Similarly, ototoxicity can also induce inner ear inflammation (Sato et al., 2008, 2010; Dinh et al., 2013).

Autoimmunity has also been implicated as a mechanism of SNHL. This was originally based upon the observation that some forms of idiopathic hearing loss improve with steroid treatment, and may worsen upon the termination of therapy (Wilson et al., 1980). Identification of cochlear autoimmune antigenic targets has been difficult, although the most recent evidence implicates cochlin, one of the most prevalent proteins in the cochlea (Baruah, 2014). Interestingly, it has been suggested that this may be related to homology between cochlin and proteins present in certain molds that induce innate immune and allergic responses (Pathak et al., 2013).

Of particular interest for this review, an association between systemic inflammation and ARHL has recently been noted in human studies (Verschuur et al., 2012; Nash et al., 2014). A recent review by Franceschi and Campisi (2014) more broadly discusses the relationship between inflammation and aging ("inflammaging"). They cite extensive evidence to support the role of chronic inflammation in the aging process. In particular, low-grade production of pro-inflammatory cytokines including IL-6, IL-1β and TNFα appear to be significant mediators of age-related damage to a wide variety of tissues. Expression of these cytokines is associated with JAK/STAT signaling. As noted above, a genome-wide association study has implicated the JAK/STAT pathway in ARHL (Fransen et al., 2015), which provides further evidence to support a role for chronic inflammation.

HC Survival Signaling

Many cellular processes that lead to cell damage and death are tightly regulated to reduce unwanted cellular losses, as noted above for apoptosis. Inflammatory damage can be opposed by anti-inflammatory cytokines such as IL-10 and anti-inflammatory cellular phenotypes such as alternatively activated macrophages. Similarly, there are intracellular pro-survival pathways that oppose the death and damage signaling of stress pathways such as ROS, the JNK and p38 cascades.

ROS-Opposing Mechanisms

Antioxidants react with ROS, reducing them to eliminate or reduce toxicity. Cochlear HCs contain the antioxidant glutathione, which is the substrate by which glutathione transferases detoxify ROS. The levels of glutathione is lower in the basal cochlear turn HCs increasing towards the apex (Sha et al., 2001), which may be one reason why basal turn HCs are more vulnerable to most forms of SNHL. Glutathione peroxidases (GPxs) and SODs are enzymes that alter ROS to less damaging forms. Studies in mice deficient in SOD1 or GPx1 found increased susceptibility to noise, further indicating that natural defense mechanisms against ROS are important to the survival of HCs under stress. Polymorphisms in glutathione transferase genes, which catalyze the response of glutathione with ROS, have been linked to ototoxicity and noise sensitivity in humans (Peters et al., 2000; Lin et al., 2009; Shen et al., 2012).

Bared et al. (2010) compared polymorphisms in genes encoding glutathione S transferase and N-acetyltransferase, another antioxidant enzyme, in normal hearing subjects vs. presbycusis patients. They found significant associations with presbycusis and polymorphisms that reduce enzyme function. Moreover, Angeli et al. (2012) found that presbycusis patients with glutathione transferase gene polymorphisms were associated with preferential high-frequency hearing loss in patients with presbycusis. The evidence strongly suggests that HCs are equipped with multiple mechanisms with which to neutralize ROS. It seems likely that only when these mechanisms have been exhausted do ROS cause significant harm.

ROS accumulation is linked to activation of the JNK signaling pathway (Son et al., 2013). Interestingly, the calcium binding protein calmodulin, which is highly expressed in HCs, preferentially binds to and inhibits kRas in a calcium-dependent manner (Villalonga et al., 2001). This would be expected to reduce the activity of JNK signaling.

ERK MAPK Pathway

When Battaglia et al. (2003) evaluated the effects of Ras inhibition on ototoxin-induced HC loss, they noted that high levels of the inhibitor FTI-277 were protective, consistent with reducing downstream JNK signaling. However, lower levels of the inhibitor enhanced HC loss. This is related to the differential sensitivity of Ras isoforms to FTI-277. High concentrations inhibit kRas, which leads to JNK activation, while low levels of FTI-277 inhibit hRas, which leads to inhibition of another MAPK, ERK (Sebti and Der, 2003). ERK is associated with cell survival and proliferation in other tissues (Xia et al., 1995; Xue et al., 2000). This finding suggested that ototoxins can activate two distinct and competing cell signaling pathways within HCs. The balance of signaling between these pathways plays a significant role in determining the fate of the cell. ERK signaling is frequently activated by growth factors, which may also explain why several growth factors have been shown to protect HCs from various insults (Endo et al., 2005; Hayashi et al., 2013, 2014). Mutations in the insulin-like growth factor 1 (*igf1*) gene cause syndromic hearing loss in both humans and mice (Cediel et al., 2006), supporting a role of growth factors in protecting hearing. Interestingly, IGF-1 deletion mice display delayed responses to acoustic stimuli that increase along the central auditory pathways, suggesting a central component to growth factor protection.

PI3K/PKC/AKT Signaling Pathway

Another well-recognized survival signaling pathway is mediated by phosphatidylinositol 3 kinase (PI3K), protein kinase c (PKC) and protein kinase b (also known as AKT). Chung et al. (2006) found that gentamicin exposure increased AKT activation in the organ of Corti, while an inhibitor of AKT reduced HC loss. Brand et al. (2011) found that simvastatin protects HCs against gentamicin toxicity via AKT signaling. These data indicate that ototoxins activate another survival pathway that competes with cell damage signaling.

Anti-Apoptotic Signaling

As in all cells, the activation of caspases in HCs appears to be tightly regulated to avoid inappropriate cell death. Inhibitor of apoptosis proteins (IAPs) are a family of endogenous caspase inhibitors, with X-linked inhibitor of apoptosis protein (XIAP) responsible for inhibiting caspase-3 and caspase-9 (Obexer and Ausserlechner, 2014). Adeno-associated virus-mediated delivery of XIAP has shown protection against cisplatin ototoxicity (Cooper et al., 2006; Chan et al., 2007). Tabuchi and coworkers have found inhibitors of XIAP to increase caspase-3 activation in gentamicin-treated organ of Corti culture, with increased auditory HC loss (Tabuchi et al., 2007). Their findings suggest that XIAP is normally present in HCs and that it acts to reduce HC apoptosis during gentamicin ototoxicity.

Apoptosis is also regulated by other processes, including the expression of apoptosis-promoting and inhibiting factors of the Bcl2 family. Pro-apoptotic Bcl2 factors such as Bad and Bax promote cell death by increasing mitochondrial membrane permeability, while inhibitory members such as Bcl2 and BclX oppose cell death by stabilizing the mitochondrial membrane. The balance of these factors can alter the outcome of apoptotic signaling. Over-expressing anti-apoptotic Bcl2 factors has been shown to reduce HC death due to ototoxins (Cunningham et al., 2004). Of particular relevance to this review, aged gerbil HCs show reduced expression of Bcl2 and enhanced expression of Bax (Alam et al., 2001), which may contribute to age-induced loss of hearing.

Purinergic Pathways

Adenosine is an endogenous nucleoside present in all cells of the body that exerts its pharmacologic effects by activation of purine adenosine receptors, also present in the HCs, supporting Deiters' cells and SGNs (Vlajkovic et al., 2007, 2009). Adenosine is released from tissue in response to stress as a cytoprotectant, augments antioxidant defense, increases oxygen supply, improves blood flow, inhibits the release of neurotransmitters, stabilizes cells by stimulating K^+ channels and inhibiting Ca^{2+} channels, triggers anti-inflammatory responses, and promotes anti-apoptotic pathways (Linden, 2005; Jacobson and Gao, 2006; Fredholm, 2007). It is administered as analgesics, vasodilator and anti-arrhythmia agents (compound summary is available through the PubChem Substance and compound database through the chemical structure identifier CID60961 (NCBI)),[1] and has been shown to exert a protective effect to noise-induced oxidative cochlear damage (Hu et al., 1997; Hight et al., 2003; Fredholm, 2007). Local or systemic administration of selective A_1 adenosine receptor agonists such as 2-chloro-N^6-cyclopentyladenosine (CCPA) and adenosine amine congener (ADAC), has further shown promise in ameliorating noise- and cisplatin-induced cochlear injury (Vlajkovic et al., 2010, 2014). Most importantly, unlike most other therapeutic agents currently in trial which offer prophylactics, ADAC can be both otoprotective and therapeutic; systematic administration after the cessation of noise exposure improved hearing thresholds with increased survival of HCs and reduced expression of oxidative stress markers in the cochlea (Vlajkovic et al., 2010), with a therapeutic window of $\leq$24 h post exposure at doses $>$50 μg/kg and pharmacokinetic half-life of 5 min (Vlajkovic et al., 2014). Vlajkovic and colleagues also investigated if enhancing extracellular adenosine by selectively inhibiting adenosine kinase, the key enzyme in adenosine metabolism, may provide protection against ARHL in C57/B6 mice (Vlajkovic et al., 2011). The study found continuous inhibitor administration from early and late adulthood (3- and 6-month old) to reduce hearing loss at 9-months of age.

A theory much revisited recently is the role of intrinsic feedback pathways providing endogenous cochlear tissue protection against noise damage. Purinergic signaling through ATP activation of the ATP-gated ion channel $P2X_2$ receptor subunit expressed in the sensory HCs and epithelial cells lining the scala media of the cochlea is known to modulate cochlear function through regulating ion homeostasis (Housley et al., 1999, 2002, 2009; Thorne et al., 2002; Wang et al., 2003c). In a recent study, Housley and colleagues have shown that ATP is released into the cochlear partition upon sound exposure, activating $P2X_2$ receptors, which reduce the sensitivity of the HCs through K^+ shunting (Housley et al., 2013). This purinergic regulation of hearing sensitivity was revealed by the absence of noise-induced temporary threshold shift (TTS) in $P2X_2$ receptor knockout mice. $P2X_2$ receptor knockout mice also showed higher threshold shifts in response to moderate noise exposure and more substantial permanent loss of hearing sensitivity compared to their wild-type littermates, supporting the otoprotective role of $P2X_2$ receptor signaling pathway. Noise-induced ATP release and $P2X_2$ is rapidly regulated by the ectonucleoside triphosphate diphosphohydrolases (E-NTPDase) family which hydrolyze extracellular nucleotides. NTPDase3 is expressed in the SGNs and the synaptic regions of the inner and outer HCs, which is upregulated in noise-exposed rat cochleae (Vlajkovic et al., 2006). Disrupted $P2X_2$ signaling in humans and the total lack of $P2X_2$ signaling in $P2X_2$ knockout mice also showed exacerbated ARHL, evident in a flattened sensory epithelium in the basal organ of Corti (Yan et al., 2013).

Mechanisms of Cochlear Neuronal Damage

Cochlear neurons are frequently lost secondary to HC loss. This is generally thought to be due to loss of neurotrophin exposure provided by the HCs, and can occur rather slowly, especially in humans. Primary loss of SGNs in the absence of HC damage also occurs. One cause of this is thought to be neurotropic viruses, but proof for this is difficult to obtain. However, an established mechanism of noise-induced cochlear neuronal damage is the excess release of the excitatory neurotransmitter glutamate at the inner HC afferent synapse. Glutamate excitotoxicity resulting from excessive glutamate release following noise overstimulation leads to an influx of

[1]NCBI National Center for Biotechnology Information; PubChem Compound Database; CID=60961. In: PubChem Compound Database.

cations such as Ca^{2+} across the post-synaptic membrane. Such created osmotic imbalance, resulting in cellular swelling (vacuolization) of the SGNs and the afferent dendritic endings that synapses onto the inner HCs (Pujol and Puel, 1999; Wang et al., 2002). This process has been replicated by administration of exogenous glutamate receptor agonists including AMPA and kainite to the cochlea (Ruel et al., 2000; Le Prell et al., 2004). Secondary to this cellular degeneration is excessive Ca^{2+} influx, leading to calcium-dependent caspase-mediated apoptosis by intrinsic (mitochondria-mediated) pathway (Puel et al., 1998; Pujol and Puel, 1999; Ruel et al., 2007).

Noise exposure can lead to loss of many afferent synapses and degeneration of type 1 SGNs within weeks and months after noise exposure (Kujawa and Liberman, 2009), even when the exposure results in no permanent threshold shift or HC loss. This form of damage is thought to result in degraded ability to process and analyze auditory input, and is almost certainly caused by glutamate toxicity (Pujol et al., 1990). Cellular mechanisms leading to SGN loss after noise are less clear, but Selivanova et al. (2007) found that JNK levels are increased and AKT levels decreased in SGNs after moderate noise exposure in guinea pigs. Interestingly, Zuccotti et al. (2012) found that conditional deletion of BDNF in HCs and SGNs lead to reduced activity and reduced numbers of afferent synapses on inner HCs, but also to reduced noise-induced loss of the remaining synapses. These data indicate that neurotrophic support is critical to both the function and survival of afferent cochlear synapses.

Mechanisms of Central Auditory Damage

The mechanisms that contribute to central auditory deficits associated with noise damage and aging have received much less attention than those underlying cochlear damage. However, there is evidence for overlap of some mechanisms. For example, since glutamate is the major excitatory neurotransmitter of the central auditory pathway, glutamate toxicity following noise has been proposed to explain central auditory neuronal losses (Feng et al., 2012). Similarly, gradual accumulation of glutamate-related damage over time may contribute to age-related declines in central auditory neuronal populations (Tadros et al., 2007), perhaps exacerbated by declining inhibitory inputs (Caspary et al., 2008). Similarly, ROS accumulation due to noise-induced activity has been suggested to damage central neurons, while the accumulation of ROS damage with age may underlie damage to the central auditory pathway as it is thought to do in other parts of the central nervous system (Mattson and Magnus, 2006). It has also been suggested that deafferentation of central auditory neurons due to loss of HCs and SGNs reduces leads to transneuronal degeneration, due to loss of neurotrophic support (e.g., Feng et al., 2012).

Clues as to mechanisms of central auditory damage can also be inferred from research on the senescence-accelerated mouse model. ROS damage has also been implicated in age-related changes in the central nervous system of the senescence-accelerated mice (Wang et al., 2014). They noted brain increases in the oxidative stress-related marker malondialdehyde and decreases in the protective enzyme SOD. There is also evidence to implicate inflammation. Hasegawa-Ishii et al. (2015) observed enhanced expression of cytokines and chemokines that would be expected to increase inflammation and the recruitment of inflammatory cells in the brains of senescence-accelerated mice. Similar effects seem likely to operate in the central auditory system, and may also occur in the cochlea.

Discussion

Balance of Damage and Survival Signaling Determines Cochlear Damage

The studies reviewed above indicate that damage to cochlear tissues can involve a variety of mechanisms. Many of these are specific to the particular mode of damage and the cell types involved. However, there are common pathways that appear to operate across several different damage etiologies, including presbycusis. These include ROS accumulation, MAPK signaling, and apoptosis pathways. It is also clear that pathogenic stimuli activate not only damage mechanisms in cochlear cells, but also pro-survival processes that attempt to rescue cells. It is likely the balance of pro-death vs. pro-survival signaling that determines the fate of cells. This provides two potential mechanisms by which to protect cochlear tissues from damage: inhibition of damage-promoting processes and enhancement of survival-promoting mechanisms (**Figure 2**).

ARHL and the Cumulative/Synergistic Damage Hypothesis

There is considerable disagreement regarding the mechanisms of ARHL. There is evidence to suggest that presbycusis includes the accumulation of cochlear damage from various sources, and especially that of noise exposure. A study of hearing in Mabaan natives of Sudan in 1962 (Rosen et al., 1962; Bergman, 1966), a pre-industrial people, revealed superior hearing in older individuals to that observed in US population studies. However, it can be argued that this difference might be caused by genetic differences between the populations. Goycoolea et al. (1986) studied the hearing of natives of Easter Island, 45 years of age or older, who at the time lived in a largely pre-industrial society. Included in the study were natives who had emigrated to mainland Chile and spent varying amounts of time in modern society. They found that hearing in males that had lived or were living in Chile was significantly worse than that of males who had lived their entire lives on Easter Island, and that this difference was related to years lived in modern society.

Another issue for presbycusis involves synergy between different etiologies of cochlear damage. The involvement of common pathways in some forms of cochlear pathogenesis suggests that the combination of two or more forms may lead to even greater damage. There is evidence that this can occur even when the exposures are not concurrent.

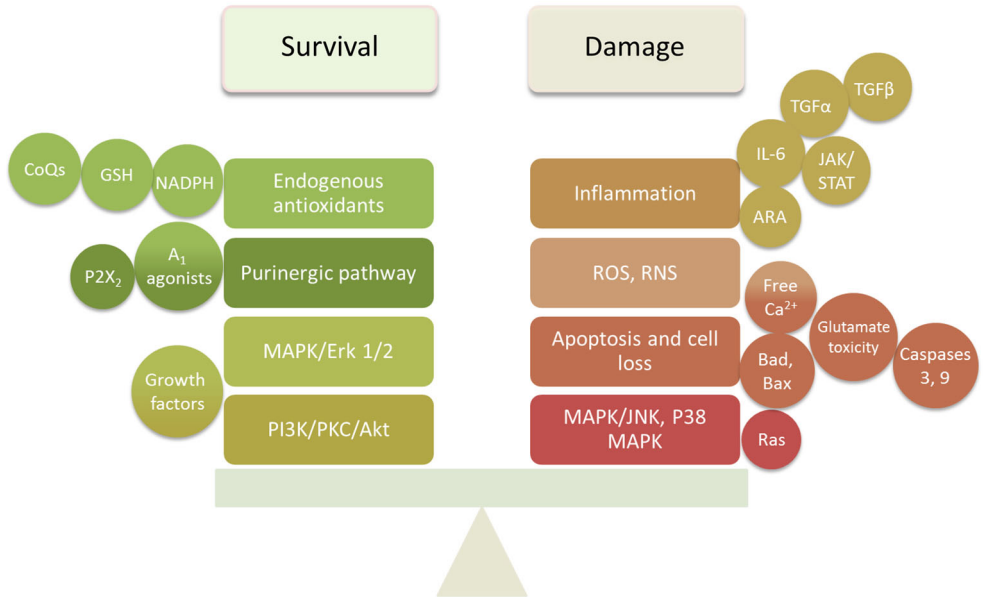

FIGURE 2 | Summary diagram of the survival and damaging factors in the cochlea that require balancing to prevent or delay SNHL.

Ryan and Bone (1982) found that prior exposure to noise that induced only TTS rendered animals more susceptible to later HC and hearing loss induced by aminoglycoside exposure. This finding also argues for the accumulation of damage from various etiologies as a contributing factor in presbycusis.

However, even in studies of pre-industrial societies, it was found that hearing decreased even in individuals for whom noise exposure was presumably restricted by lifestyle (Rosen et al., 1962; Bergman, 1966; Goycoolea et al., 1986). This suggests that a "pure" form of presbycusis exists. This could be driven by increased ROS accumulation in cochlear cells, due for example to age-related decreases in mitochondrial membrane integrity (Shigenaga et al., 1994). This would be expected to lead to MAPK cell damage signaling and enhanced probability of apoptosis (**Figure 3**).

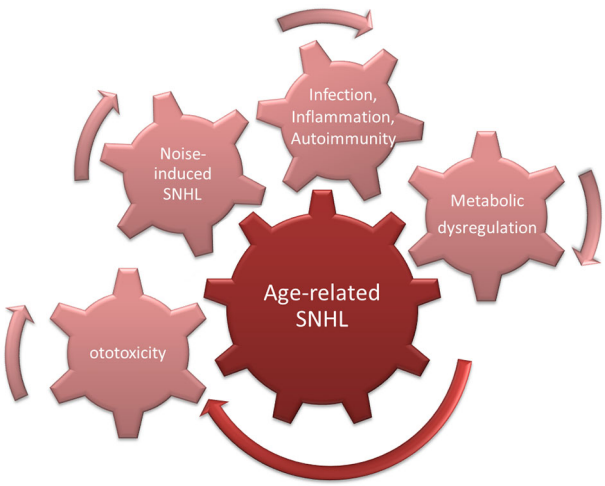

FIGURE 3 | Cumulative/synergistic damage hypothesis of age-related hearing loss (ARHL). Causes of SNHL that accumulate over a lifetime combine with endogenous susceptibility to exacerbate age-related SNHL.

Implications for Therapeutic Interventions

Because presbycusis is a predictable form of hearing loss and occurs over a long span of time, the therapeutic intervention for its prevention is feasible. As noted above, there are at least two potential strategies for therapeutic intervention to reduce cochlear damage. One is to inhibit processes or pathways that lead to the damage of cochlear cells. The other is to enhance processes that enhance cochlear cell survival. Both of these strategies have been attempted, with varying degrees of success.

Given the role of the MAPK-JNK signaling pathway in acoustic trauma and aminoglycoside induced HC apoptosis, studies have investigated the use of pharmacological blockers to protect sensorineural tissue from apoptosis (Pirvola et al., 2000; Hu et al., 2002a; Wang et al., 2003b). In particular, a peptide inhibitor of JNK kinase-mediated mitochondrial cell death pathway, D-JNKI-1 peptide, has shown promises in protecting the cochlea against noise-induced and aminoglycoside induced HC loss when delivered directly into the scala tympani or locally to the round window membrane (Wang et al., 2003b, 2007; Eshraghi et al., 2007). D-JNKI-1 has been developed under the name of AM-111 (Xigen/Auris Medical); a Phase 2b clinical trial has been completed in 2012 in three European countries and have shown promise for the treatment of acute

SNHL (ClinicalTrial.gov Identifier: NCT00802425). Other experimental otoprotective compounds and potential gene therapy options against SNHL have been recently reviewed in Wong et al. (2013a).

Perhaps the most promising therapeutic interventions thus far are the various antioxidants investigated as ARHL prophylaxis to enhance cochlear defense against oxidative stress. Seidman et al. (2000) found that oral supplementation of acetyl-L-carnitine or α-lipoic acid delayed ARHL in the aging rat model. In a study that investigates the involvement of mitochondrial proapoptotic Bcl-2 family member *Bak* in ARHL, Someya et al. (2009) looked at the effects of long-term dietary supplementation of 17 antioxidant compounds on ARHL development in C57BL/6J mice. They found compounds that act as mitochondrial antioxidants to delay high-frequency threshold elevation and maintain sensorineural tissue survival. Of which α-lipoic acid and N-acetyl-L-cysteine (NAC) are thiol compounds that are shown to reduce mitochondrial ROS production, and coenzyme Q10 is an essential mitochondrial electron transfer chain component that acts as a mitochondrial antioxidant. An antioxidant cocktail of L-cysteine-glutathione mixed disulfide (L-CySSG), ribose-cysteine, NW-nitro-L-arginine methyl ester (L-NAME), vitamin B12, folate, and ascorbic acid as a dietary supplement early in life has been shown to reduce age-related threshold shifts in C57BL/6 mice (Heman-Ackah et al., 2010). However, in CBA/J mice which do not have the *Cdh23*^{ahl} allele, an antioxidant-rich diet fails to provide advantage (Sha et al., 2012). In humans, a recent study correlated the dietary intake of β-carotene, vitamin C, vitamin E, and magnesium to a hearing threshold of ∼2500 US adults (Choi et al., 2014), has found higher intakes of the antioxidants and magnesium to associate with a lower hearing threshold, interpreted as less hearing loss. For the time being, an antioxidant rich diet with physical protection against overexposure of noise seems a sensible and feasible prevention to ARHL prone individuals.

Conclusions

With irreversible damages of the sensorineural tissue in the cochlea accumulating over a lifetime, ameliorating age-related SNHL seems daunting. However, we now understand far more of the cellular mechanisms leading to sensorineural damage, and the survival cellular signaling elements that can counterbalance and prevent it. Therapeutics that provide protection in the form of oral otoprotective formulations with antioxidant or other actions, or long-term local application of compounds that inhibit cell damage pathways or promote cell survival can readily be envisioned. Although a single mechanism responsible for ARHL is yet to be identified, and is rather unlikely with the multifactorial and cumulative nature of the damage, it is certain that ongoing research efforts to advance our understanding of SNHL, for example with transgenic animal models, high-throughput genome sequencing and proteomics, will further support evidence-based treatment. Advances in drug delivery to the inner ear will further support therapies for prebycusis.

Acknowledgments

AW: Garnett Passe and Rodney William Memorial Foundation for fellowship support. AFR: VA grants BX001205 and RX000977 and NIH/NIDCD grant DC000139.

References

Agell, N., Bachs, O., Rocamora, N., and Villalonga, P. (2002). Modulation of the Ras/Raf/MEK/ERK pathway by Ca(2+) and calmodulin. *Cell. Signal.* 14, 649–654. doi: 10.1016/s0898-6568(02)00007-4

Alam, S. A., Oshima, T., Suzuki, M., Kawase, T., Takasaka, T., and Ikeda, K. (2001). The expression of apoptosis-related proteins in the aged cochlea of Mongolian gerbils. *Laryngoscope* 111, 528–534. doi: 10.1097/00005537-200103000-00026

Alharazneh, A., Luk, L., Huth, M., Monfared, A., Steyger, P. S., Cheng, A. G., et al. (2011). Functional hair cell mechanotransducer channels are required for aminoglycoside ototoxicity. *PLoS One* 6:e22347. doi: 10.1371/journal.pone.0022347

Angeli, S. I., Bared, A., Ouyang, X., Du, L. L., Yan, D., and Zhong Liu, X. (2012). Audioprofiles and antioxidant enzyme genotypes in presbycusis. *Laryngoscope* 122, 2539–2542. doi: 10.1002/lary.23577

Barclay, M., Ryan, A. F., and Housley, G. D. (2011). Type I vs. type II spiral ganglion neurons exhibit differential survival and neuritogenesis during cochlear development. *Neural Dev.* 6:33. doi: 10.1186/1749-8104-6-33

Bared, A., Ouyang, X., Angeli, S., Du, L. L., Hoang, K., Yan, D., et al. (2010). Antioxidant enzymes, presbycusis and ethnic variability. *Otolaryngol. Head Neck Surg.* 143, 263–268. doi: 10.1016/j.otohns.2010.03.024

Baruah, P. (2014). Cochlin in autoimmune inner ear disease: is the search for an inner ear autoantigen over? *Auris Nasus Larynx* 41, 499–501. doi: 10.1016/j.anl.2014.08.014

Batandier, C., Leverve, X., and Fontaine, E. (2004). Opening of the mitochondrial permeability transition pore induces reactive oxygen species production at the level of the respiratory chain complex I. *J. Biol. Chem.* 279, 17197–17204. doi: 10.1074/jbc.m310329200

Battaglia, A., Pak, K., Brors, D., Bodmer, D., Frangos, J. A., and Ryan, A. F. (2003). Involvement of ras activation in toxic hair cell damage of the mammalian cochlea. *Neuroscience* 122, 1025–1035. doi: 10.1016/j.neuroscience.2003.08.041

Bergman, M. (1966). Hearing in the Mabaans. A critical review of related literature. *Arch. Otolaryngol.* 84, 411–415. doi: 10.1001/archotol.1966.00760030413007

Bodmer, D., Brors, D., Pak, K., Gloddek, B., and Ryan, A. (2002b). Rescue of auditory hair cells from aminoglycoside toxicity by Clostridium difficile toxin B, an inhibitor of the small GTPases Rho/Rac/Cdc42. *Hear. Res.* 172, 81–86. doi: 10.1016/s0378-5955(02)00514-2

Bodmer, D., Gloddek, B., Ryan, A. F., Huverstuhl, J., and Brors, D. (2002a). Inhibition of the c-Jun N-terminal kinase signaling pathway influences neurite outgrowth of spiral ganglion neurons *in vitro*. *Laryngoscope* 112, 2057–2061. doi: 10.1097/00005537-200211000-00028

Bohne, B. A., Harding, G. W., and Lee, S. C. (2007). Death pathways in noise-damaged outer hair cells. *Hear. Res.* 223, 61–70. doi: 10.1016/j.heares.2006.10.004

Brand, Y., Setz, C., Levano, S., Listyo, A., Chavez, E., Pak, K., et al. (2011). Simvastatin protects auditory hair cells from gentamicin-induced toxicity and activates Akt signaling *in vitro*. *BMC Neurosci.* 12:114. doi: 10.1186/1471-2202-12-114

Brozovic, A., and Osmak, M. (2007). Activation of mitogen-activated protein kinases by cisplatin and their role in cisplatin-resistance. *Cancer Lett.* 251, 1–16. doi: 10.1016/j.canlet.2006.10.007

Caspary, D. M., Ling, L., Turner, J. G., and Hughes, L. F. (2008). Inhibitory neurotransmission, plasticity and aging in the mammalian central auditory system. *J. Exp. Biol.* 211, 1781–1791. doi: 10.1242/jeb.013581

Cediel, R., Riquelme, R., Contreras, J., Díaz, A., and Varela-Nieto, I. (2006). Sensorineural hearing loss in insulin-like growth factor I-null mice: a new model of human deafness. *Eur. J. Neurosci.* 23, 587–590. doi: 10.1111/j.1460-9568.2005.04584.x

Chan, D. K., Lieberman, D. M., Musatov, S., Goldfein, J. A., Selesnick, S. H., and Kaplitt, M. G. (2007). Protection against cisplatin-induced ototoxicity by adeno-associated virus-mediated delivery of the X-linked inhibitor of apoptosis protein is not dependent on caspase inhibition. *Otol. Neurotol.* 28, 417–425. doi: 10.1097/01.mao.0000247826.28893.7a

Choi, Y. H., Miller, J. M., Tucker, K. L., Hu, H., and Park, S. K. (2014). Antioxidant vitamins and magnesium and the risk of hearing loss in the US general population. *Am. J. Clin. Nutr.* 99, 148–155. doi: 10.3945/ajcn.113.068437

Choung, Y. H., Taura, A., Pak, K., Choi, S. J., Masuda, M., and Ryan, A. F. (2009). Generation of highly-reactive oxygen species is closely related to hair cell damage in rat organ of Corti treated with gentamicin. *Neuroscience* 161, 214–226. doi: 10.1016/j.neuroscience.2009.02.085

Chung, W. H., Pak, K., Lin, B., Webster, N., and Ryan, A. F. (2006). A PI3K pathway mediates hair cell survival and opposes gentamicin toxicity in neonatal rat organ of Corti. *J. Assoc. Res. Otolaryngol.* 7, 373–382. doi: 10.1007/s10162-006-0050-y

Cooper, L. B., Chan, D. K., Roediger, F. C., Shaffer, B. R., Fraser, J. F., Musatov, S., et al. (2006). AAV-mediated delivery of the caspase inhibitor XIAP protects against cisplatin ototoxicity. *Otol. Neurotol.* 27, 484–490. doi: 10.1097/00129492-200606000-00009

Cunningham, L. L., Matsui, J. I., Warchol, M. E., and Rubel, E. W. (2004). Overexpression of Bcl-2 prevents neomycin-induced hair cell death and caspase-9 activation in the adult mouse utricle *in vitro*. *J. Neurobiol.* 60, 89–100. doi: 10.1002/neu.20006

Dinh, C., Bas, E., Dinh, J., Vu, L., Gupta, C., and Van De Water, T. R. (2013). Short interfering RNA against Bax attenuates TNFα-induced ototoxicity in rat organ of Corti explants. *Otolaryngol. Head Neck Surg.* 148, 834–840. doi: 10.1177/0194599813477631

Dodge, P. R., Davis, H., Feigin, R. D., Holmes, S. J., Kaplan, S. L., Jubelirer, D. P., et al. (1984). Prospective evaluation of hearing impairment as a sequela of acute bacterial meningitis. *N. Engl. J. Med.* 311, 869–874. doi: 10.1056/nejm198410043111401

Dumont, R. A., Lins, U., Filoteo, A. G., Penniston, J. T., Kachar, B., and Gillespie, P. G. (2001). Plasma membrane Ca2+-ATPase isoform 2a is the PMCA of hair bundles. *J. Neurosci.* 21, 5066–5078.

Duthey, B. (2013). *Background Paper 6.21 Hearing Loss*. Geneva: WHO Int.

Ehret, G., and Frankenreiter, M. (1977). Quantitative analysis of cochlear structures in the house mouse in relation to mechanisms of acoustical information processing. *J. Comp. Physiol.* 122, 65–85. doi: 10.1007/bf00611249

Endo, T., Nakagawa, T., Kita, T., Iguchi, F., Kim, T. S., Tamura, T., et al. (2005). Novel strategy for treatment of inner ears using a biodegradable gel. *Laryngoscope* 115, 2016–2020. doi: 10.1097/01.mlg.0000183020.32435.59

Eshraghi, A. A., Wang, J., Adil, E., He, J., Zine, A., Bublik, M., et al. (2007). Blocking c-Jun-N-terminal kinase signaling can prevent hearing loss induced by both electrode insertion trauma and neomycin ototoxicity. *Hear. Res.* 226, 168–177. doi: 10.1016/j.heares.2006.09.008

Esterberg, R., Hailey, D. W., Coffin, A. B., Raible, D. W., and Rubel, E. W. (2013). Disruption of intracellular calcium regulation is integral to aminoglycoside-induced hair cell death. *J. Neurosci.* 33, 7513–7525. doi: 10.1523/JNEUROSCI.4559-12.2013

Esterberg, R., Hailey, D. W., Rubel, E. W., and Raible, D. W. (2014). ER-mitochondrial calcium flow underlies vulnerability of mechanosensory hair cells to damage. *J. Neurosci.* 34, 9703–9719. doi: 10.1523/JNEUROSCI.0281-14.2014

Feng, J., Bendiske, J., and Morest, D. K. (2012). Degeneration in the ventral cochlear nucleus after severe noise damage in mice. *J. Neurosci. Res.* 90, 831–841. doi: 10.1002/jnr.22793

Fetoni, A. R., De Bartolo, P., Eramo, S. L., Rolesi, R., Paciello, F., Bergamini, C., et al. (2013). Noise-induced hearing loss (NIHL) as a target of oxidative stress-mediated damage: cochlear and cortical responses after an increase in antioxidant defense. *J. Neurosci.* 33, 4011–4023. doi: 10.1523/JNEUROSCI.2282-12.2013

Fetoni, A. R., Picciotti, P. M., Paludetti, G., and Troiani, D. (2011). Pathogenesis of presbycusis in animal models: a review. *Exp. Gerontol.* 46, 413–425. doi: 10.1016/j.exger.2010.12.003

Franceschi, C., and Campisi, J. (2014). Chronic inflammation (inflammaging) and its potential contribution to age-associated diseases. *J. Gerontol. A Biol. Sci. Med. Sci.* 69(Suppl. 1), S4–S9. doi: 10.1093/gerona/glu057

Fransen, E., Bonneux, S., Corneveaux, J. J., Schrauwen, I., Di Berardino, F., White, C. H., et al. (2015). Genome-wide association analysis demonstrates the highly polygenic character of age-related hearing impairment. *Eur. J. Hum. Genet.* 23, 110–115. doi: 10.1038/ejhg.2014.56

Fredholm, B. B. (2007). Adenosine, an endogenous distress signal, modulates tissue damage and repair. *Cell Death Differ.* 14, 1315–1323. doi: 10.1038/sj.cdd.4402132

Fridberger, A., Flock, A., Ulfendahl, M., and Flock, B. (1998). Acoustic overstimulation increases outer hair cell Ca2+ concentrations and causes dynamic contractions of the hearing organ. *Proc. Natl. Acad. Sci. U S A* 95, 7127–7132. doi: 10.1073/pnas.95.12.7127

Frisina, R. D. (2009). Age-related hearing loss. *Ann. N Y Acad. Sci.* 1170, 708–717. doi: 10.1111/j.1749-6632.2009.03931.x

Furman, A. C., Kujawa, S. G., and Liberman, M. C. (2013). Noise-induced cochlear neuropathy is selective for fibers with low spontaneous rates. *J. Neurophysiol.* 110, 577–586. doi: 10.1152/jn.00164.2013

Furuta, H., Luo, L., Hepler, K., and Ryan, A. F. (1998). Evidence for differential regulation of calcium by outer versus inner hair cells: plasma membrane Ca-ATPase gene expression. *Hear. Res.* 123, 10–26. doi: 10.1016/S0378-5955(98)00091-4

Gates, G. A., and Mills, J. H. (2005). Presbycusis. *Lancet* 366, 1111–1120. doi: 10.1016/S0140-6736(05)67423-5

Goycoolea, M. V., Goycoolea, H. G., Farfan, C. R., Rodriguez, L. G., Martinez, G. C., and Vidal, R. (1986). Effect of life in industrialized societies on hearing in natives of Easter Island. *Laryngoscope* 96, 1391–1396. doi: 10.1288/00005537-198612000-00015

Harr, M. W., and Distelhorst, C. W. (2010). Apoptosis and autophagy: decoding calcium signals that mediate life or death. *Cold Spring Harb. Perspect. Biol.* 2:a005579. doi: 10.1101/cshperspect.a005579

Hasegawa-Ishii, S., Inaba, M., Li, M., Shi, M., Umegaki, H., Ikehara, S., et al. (2015). Increased recruitment of bone marrow-derived cells into the brain associated with altered brain cytokine profile in senescence-accelerated mice. *Brain Struct. Funct.* doi: 10.1007/s00429-014-0987-2. [Epub ahead of print].

Hayashi, Y., Yamamoto, N., Nakagawa, T., and Ito, J. (2013). Insulin-like growth factor 1 inhibits hair cell apoptosis and promotes the cell cycle of supporting cells by activating different downstream cascades after pharmacological hair cell injury in neonatal mice. *Mol. Cell. Neurosci.* 56, 29–38. doi: 10.1016/j.mcn.2013.03.003

Hayashi, Y., Yamamoto, N., Nakagawa, T., and Ito, J. (2014). Insulin-like growth factor 1 induces the transcription of Gap43 and Ntn1 during hair cell protection in the neonatal murine cochlea. *Neurosci. Lett.* 560, 7–11. doi: 10.1016/j.neulet.2013.11.062

Heman-Ackah, S. E., Juhn, S. K., Huang, T. C., and Wiedmann, T. S. (2010). A combination antioxidant therapy prevents age-related hearing loss in C57BL/6 mice. *Otolaryngol. Head Neck Surg.* 143, 429–434. doi: 10.1016/j.otohns.2010.04.266

Henderson, D., Bielefeld, E. C., Harris, K. C., and Hu, B. H. (2006). The role of oxidative stress in noise-induced hearing loss. *Ear Hear.* 27, 1–19. doi: 10.1097/01.aud.0000191942.36672.f3

Hiel, H., Schamel, A., Erre, J. P., Hayashida, T., Dulon, D., and Aran, J. M. (1992). Cellular and subcellular localization of tritiated gentamicin in the guinea pig cochlea following combined treatment with ethacrynic acid. *Hear. Res.* 57, 157–165. doi: 10.1016/0378-5955(92)90148-g

Hight, N. G., McFadden, S. L., Henderson, D., Burkard, R. F., and Nicotera, T. (2003). Noise-induced hearing loss in chinchillas pre-treated with glutathione monoethylester and R-PIA. *Hear. Res.* 179, 21–32. doi: 10.1016/s0378-5955(03)00067-4

Hirose, K., Discolo, C. M., Keasler, J. R., and Ransohoff, R. (2005). Mononuclear phagocytes migrate into the murine cochlea after acoustic trauma. *J. Comp. Neurol.* 489, 180–194. doi: 10.1002/cne.20619

Housley, G. D., Bringmann, A., and Reichenbach, A. (2009). Purinergic signaling in special senses. *Trends Neurosci.* 32, 128–141. doi: 10.1016/j.tins.2009.01.001

Housley, G. D., Jagger, D. J., Greenwood, D., Raybould, N. P., Salih, S. G., Järlebark, L. E., et al. (2002). Purinergic regulation of sound transduction and auditory neurotransmission. *Audiol. Neurootol.* 7, 55–61. doi: 10.1159/000046865

Housley, G. D., Kanjhan, R., Raybould, N. P., Greenwood, D., Salih, S. G., Jarlebark, L., et al. (1999). Expression of the P2X(2) receptor subunit of the ATP-gated ion channel in the cochlea: implications for sound transduction and auditory neurotransmission. *J. Neurosci.* 19, 8377–8388.

Housley, G. D., Morton-Jones, R., Vlajkovic, S. M., Telang, R. S., Paramananthasivam, V., Tadros, S. F., et al. (2013). ATP-gated ion channels mediate adaptation to elevated sound levels. *Proc. Natl. Acad. Sci. U S A* 110, 7494–7499. doi: 10.1073/pnas.1222295110

Hu, B. H., Guo, W., Wang, P. Y., Henderson, D., and Jiang, S. C. (2000). Intense noise-induced apoptosis in hair cells of guinea pig cochleae. *Acta Otolaryngol.* 120, 19–24. doi: 10.1080/00016480750044443

Hu, B. H., Henderson, D., and Nicotera, T. M. (2002a). F-actin cleavage in apoptotic outer hair cells in chinchilla cochleas exposed to intense noise. *Hear. Res.* 172, 1–9. doi: 10.1016/s0378-5955(01)00361-6

Hu, B. H., Henderson, D., and Nicotera, T. M. (2002b). Involvement of apoptosis in progression of cochlear lesion following exposure to intense noise. *Hear. Res.* 166, 62–71. doi: 10.1016/s0378-5955(02)00286-1

Hu, B. H., Henderson, D., and Nicotera, T. M. (2006). Extremely rapid induction of outer hair cell apoptosis in the chinchilla cochlea following exposure to impulse noise. *Hear. Res.* 211, 16–25. doi: 10.1016/j.heares.2005.08.006

Hu, B. H., Zheng, X. Y., McFadden, S. L., Kopke, R. D., and Henderson, D. (1997). R-phenylisopropyladenosine attenuates noise-induced hearing loss in the chinchilla. *Hear. Res.* 113, 198–206. doi: 10.1016/s0378-5955(97)00143-3

Huang, M., Dulon, D., and Schacht, J. (1990). Outer hair cells as potential targets of inflammatory mediators. *Ann. Otol. Rhinol. Laryngol. Suppl.* 148, 35–38.

Hunter, L. L., Margolis, R. H., Rykken, J. R., Le, C. T., Daly, K. A., and Giebink, G. S. (1996). High frequency hearing loss associated with otitis media. *Ear Hear.* 17, 1–11. doi: 10.1097/00003446-199602000-00001

Jacobson, K. A., and Gao, Z. G. (2006). Adenosine receptors as therapeutic targets. *Nat. Rev. Drug Discov.* 5, 247–264. doi: 10.1038/nrd1983

Jacobson, M., Kim, S., Romney, J., Zhu, X., and Frisina, R. D. (2003). Contralateral suppression of distortion-product otoacoustic emissions declines with age: a comparison of findings in CBA mice with human listeners. *Laryngoscope* 113, 1707–1713. doi: 10.1097/00005537-200310000-00009

Jamesdaniel, S., Hu, B., Kermany, M. H., Jiang, H., Ding, D., Coling, D., et al. (2011). Noise induced changes in the expression of p38/MAPK signaling proteins in the sensory epithelium of the inner ear. *J. Proteomics* 75, 410–424. doi: 10.1016/j.jprot.2011.08.007

Jaumann, M., Dettling, J., Gubelt, M., Zimmermann, U., Gerling, A., Paquet-Durand, F., et al. (2012). cGMP-Prkg1 signaling and Pde5 inhibition shelter cochlear hair cells and hearing function. *Nat. Med.* 18, 252–259. doi: 10.1038/nm.2634

Johnson, G. L. (2011). Defining MAPK interactomes. *ACS Chem. Biol.* 6, 18–20. doi: 10.1021/cb100384z

Juanjuan, C., Yan, F., Li, C., Haizhi, L., Ling, W., Xinrong, W., et al. (2011). Murine model for congenital CMV infection and hearing impairment. *Virol. J.* 8:70. doi: 10.1186/1743-422X-8-70

Keithley, E. M., Wang, X., and Barkdull, G. C. (2008). Tumor necrosis factor alpha can induce recruitment of inflammatory cells to the cochlea. *Otol. Neurotol.* 29, 854–859. doi: 10.1097/MAO.0b013e31818256a9

Kozel, P. J., Friedman, R. A., Erway, L. C., Yamoah, E. N., Liu, L. H., Riddle, T., et al. (1998). Balance and hearing deficits in mice with a null mutation in the gene encoding plasma membrane Ca2+-ATPase isoform 2. *J. Biol. Chem.* 273, 18693–18696. doi: 10.1074/jbc.273.30.18693

Kubo, T., Anniko, M., Stenqvist, M., and Hsu, W. (1998). Interleukin-2 affects cochlear function gradually but reversibly. *ORL J. Otorhinolaryngol. Relat. Spec.* 60, 272–277. doi: 10.1159/000027609

Kujawa, S. G., and Liberman, M. C. (2009). Adding insult to injury: cochlear nerve degeneration after "temporary" noise-induced hearing loss. *J. Neurosci.* 29, 14077–14085. doi: 10.1523/JNEUROSCI.2845-09.2009

Le Prell, C. G., Yagi, M., Kawamoto, K., Beyer, L. A., Atkin, G., Raphael, Y., et al. (2004). Chronic excitotoxicity in the guinea pig cochlea induces temporary functional deficits without disrupting otoacoustic emissions. *J. Acoust. Soc. Am.* 116, 1044–1056. doi: 10.1121/1.1772395

Liberman, M. C., and Beil, D. G. (1979). Hair cell condition and auditory nerve response in normal and noise-damaged cochleas. *Acta Otolaryngol.* 88, 161–176. doi: 10.3109/00016487909137156

Liberman, M. C., and Kiang, N. Y. (1978). Acoustic trauma in cats. Cochlear pathology and auditory-nerve activity. *Acta Otolaryngol. Suppl.* 358, 1–63.

Lin, C. Y., Wu, J. L., Shih, T. S., Tsai, P. J., Sun, Y. M., and Guo, Y. L. (2009). Glutathione S-transferase M1, T1 and P1 polymorphisms as susceptibility factors for noise-induced temporary threshold shift. *Hear. Res.* 257, 8–15. doi: 10.1016/j.heares.2009.07.008

Linden, J. (2005). Adenosine in tissue protection and tissue regeneration. *Mol. Pharmacol.* 67, 1385–1387. doi: 10.1124/mol.105.011783

Ling, L. L., Hughes, L. F., and Caspary, D. M. (2005). Age-related loss of the GABA synthetic enzyme glutamic acid decarboxylase in rat primary auditory cortex. *Neuroscience* 132, 1103–1113. doi: 10.1016/j.neuroscience.2004.12.043

Maeda, Y., Fukushima, K., Omichi, R., Kariya, S., and Nishizaki, K. (2013). Time courses of changes in phospho- and total- MAP kinases in the cochlea after intense noise exposure. *PLoS One* 8:e58775. doi: 10.1371/journal.pone.0058775

Mattson, M. P., and Magnus, T. (2006). Ageing and neuronal vulnerability. *Nat. Rev. Neurosci.* 7, 278–294. doi: 10.1038/nrn1886

Maulucci, G., Troiani, D., Eramo, S. L., Paciello, F., Podda, M. V., Paludetti, G., et al. (2014). Time evolution of noise induced oxidation in outer hair cells: role of NAD(P)H and plasma membrane fluidity. *Biochim. Biophys. Acta* 1840, 2192–2202. doi: 10.1016/j.bbagen.2014.04.005

Meltser, I., Tahera, Y., and Canlon, B. (2010). Differential activation of mitogen-activated protein kinases and brain-derived neurotrophic factor after temporary or permanent damage to a sensory system. *Neuroscience* 165, 1439–1446. doi: 10.1016/j.neuroscience.2009.11.025

Moser, T., Predoehl, F., and Starr, A. (2013). Review of hair cell synapse defects in sensorineural hearing impairment. *Otol. Neurotol.* 34, 995–1004. doi: 10.1097/mao.0b013e3182814d4a

Nash, S. D., Cruickshanks, K. J., Zhan, W., Tsai, M. Y., Klein, R., Chappell, R., et al. (2014). Long-term assessment of systemic inflammation and the cumulative incidence of age-related hearing impairment in the epidemiology of hearing loss study. *J. Gerontol. A Biol. Sci. Med. Sci.* 69, 207–214. doi: 10.1093/gerona/glt075

Neher, M. D., Weckbach, S., Flierl, M. A., Huber-Lang, M. S., and Stahel, P. F. (2011). Molecular mechanisms of inflammation and tissue injury after major trauma–is complement the "bad guy"? *J. Biomed. Sci.* 18:90. doi: 10.1186/1423-0127-18-90

Nicotera, T. M., Hu, B. H., and Henderson, D. (2003). The caspase pathway in noise-induced apoptosis of the chinchilla cochlea. *J. Assoc. Res. Otolaryngol.* 4, 466–477. doi: 10.1007/s10162-002-3038-2

Obexer, P., and Ausserlechner, M. J. (2014). X-linked inhibitor of apoptosis protein–a critical death resistance regulator and therapeutic target for personalized cancer therapy. *Front. Oncol.* 4:197. doi: 10.3389/fonc.2014.00197

Ohinata, Y., Yamasoba, T., Schacht, J., and Miller, J. M. (2000). Glutathione limits noise-induced hearing loss. *Hear. Res.* 146, 28–34. doi: 10.1016/s0378-5955(00)00096-4

Orrenius, S., Zhivotovsky, B., and Nicotera, P. (2003). Regulation of cell death: the calcium-apoptosis link. *Nat. Rev. Mol. Cell Biol.* 4, 552–565. doi: 10.1038/nrm1150

Ouda, L., Profant, O., and Syka, J. (2015). Age-related changes in the central auditory system. *Cell Tissue Res.* doi: 10.1007/s00441-014-2107-2. [Epub ahead of print].

Ouda, L., and Syka, J. (2012). Immunocytochemical profiles of inferior colliculus neurons in the rat and their changes with aging. *Front. Neural Circuits* 6:68. doi: 10.3389/fncir.2012.00068

Park, J. S., Kang, S. J., Seo, M. K., Jou, I., Woo, H. G., and Park, S. M. (2014). Role of cysteinyl leukotriene signaling in a mouse model of noise-induced cochlear injury. *Proc. Natl. Acad. Sci. U S A* 111, 9911–9916. doi: 10.1073/pnas.1402261111

Patel, M., Cai, Q., Ding, D., Salvi, R., Hu, Z., and Hu, B. H. (2013). The miR-183/Taok1 target pair is implicated in cochlear responses to acoustic trauma. *PLoS One* 8:e58471. doi: 10.1371/journal.pone.0058471

Pathak, S., Hatam, L. J., Bonagura, V., and Vambutas, A. (2013). Innate immune recognition of molds and homology to the inner ear protein, cochlin, in patients with autoimmune inner ear disease. *J. Clin. Immunol.* 33, 1204–1215. doi: 10.1007/s10875-013-9926-x

Patuzzi, R. B., Yates, G. K., and Johnstone, B. M. (1989). Outer hair cell receptor current and sensorineural hearing loss. *Hear. Res.* 42, 47–72. doi: 10.1016/0378-5955(89)90117-2

Peters, U., Preisler-Adams, S., Hebeisen, A., Hahn, M., Seifert, E., Lanvers, C., et al. (2000). Glutathione S-transferase genetic polymorphisms and individual sensitivity to the ototoxic effect of cisplatin. *Anticancer Drugs* 11, 639–643. doi: 10.1097/00001813-200009000-00007

Phan, P. A., Tadros, S. F., Kim, Y., Birnbaumer, L., and Housley, G. D. (2010). Developmental regulation of TRPC3 ion channel expression in the mouse cochlea. *Histochem. Cell Biol.* 133, 437–448. doi: 10.1007/s00418-010-0686-x

Pirvola, U., Xing-Qun, L., Virkkala, J., Saarma, M., Murakata, C., Camoratto, A. M., et al. (2000). Rescue of hearing, auditory hair cells and neurons by CEP-1347/KT7515, an inhibitor of c-Jun N-terminal kinase activation. *J. Neurosci.* 20, 43–50.

Puel, J. L., Ruel, J., Gervais d'Aldin, C., and Pujol, R. (1998). Excitotoxicity and repair of cochlear synapses after noise-trauma induced hearing loss. *Neuroreport* 9, 2109–2114. doi: 10.1097/00001756-199806220-00037

Pujol, R., and Puel, J. L. (1999). Excitotoxicity, synaptic repair and functional recovery in the mammalian cochlea: a review of recent findings. *Ann. N Y Acad. Sci.* 884, 249–254. doi: 10.1111/j.1749-6632.1999.tb08646.x

Pujol, R., Rebillard, G., Puel, J. L., Lenoir, M., Eybalin, M., and Recasens, M. (1990). Glutamate neurotoxicity in the cochlea: a possible consequence of ischaemic or anoxic conditions occurring in ageing. *Acta Otolaryngol. Suppl.* 476, 32–36.

Raybould, N. P., Jagger, D. J., Kanjhan, R., Greenwood, D., Laslo, P., Hoya, N., et al. (2007). TRPC-like conductance mediates restoration of intracellular Ca2+ in cochlear outer hair cells in the guinea pig and rat. *J. Physiol.* 579, 101–113. doi: 10.1113/jphysiol.2006.122929

Richardson, G. P., Forge, A., Kros, C. J., Fleming, J., Brown, S. D., and Steel, K. P. (1997). Myosin VIIA is required for aminoglycoside accumulation in cochlear hair cells. *J. Neurosci.* 17, 9506–9519.

Robertson, D. (1983). Functional significance of dendritic swelling after loud sounds in the guinea pig cochlea. *Hear. Res.* 9, 263–278. doi: 10.1016/0378-5955(83)90031-x

Rosen, S., Bergman, M., Plester, D., El-Mofty, A., and Satti, M. H. (1962). Presbycusis study of a relatively noise-free population in the Sudan. *Ann. Otol. Rhinol. Laryngol.* 71, 727–743. doi: 10.1177/000348946207100313

Ruel, J., Bobbin, R. P., Vidal, D., Pujol, R., and Puel, J. L. (2000). The selective AMPA receptor antagonist GYKI 53784 blocks action potential generation and excitotoxicity in the guinea pig cochlea. *Neuropharmacology* 39, 1959–1973. doi: 10.1016/s0028-3908(00)00069-1

Ruel, J., Wang, J., Rebillard, G., Eybalin, M., Lloyd, R., Pujol, R., et al. (2007). Physiology, pharmacology and plasticity at the inner hair cell synaptic complex. *Hear. Res.* 227, 19–27. doi: 10.1016/j.heares.2006.08.017

Ryan, A. F., and Bone, R. C. (1982). Non-simultaneous interaction of exposure to noise and kanamycin intoxication in the chinchilla. *Am. J. Otolaryngol.* 3, 264–272. doi: 10.1016/s0196-0709(82)80065-3

Sato, E., Shick, H. E., Ransohoff, R. M., and Hirose, K. (2008). Repopulation of cochlear macrophages in murine hematopoietic progenitor cell chimeras: the role of CX3CR1. *J. Comp. Neurol.* 506, 930–942. doi: 10.1002/cne.21583

Sato, E., Shick, H. E., Ransohoff, R. M., and Hirose, K. (2010). Expression of fractalkine receptor CX3CR1 on cochlear macrophages influences survival of hair cells following ototoxic injury. *J. Assoc. Res. Otolaryngol.* 11, 223–234. doi: 10.1007/s10162-009-0198-3

Schacht, J. (1986). Molecular mechanisms of drug-induced hearing loss. *Hear. Res.* 22, 297–304. doi: 10.1016/0378-5955(86)90105-x

Schettino, A. E., and Lauer, A. M. (2013). The efficiency of design-based stereology in estimating spiral ganglion populations in mice. *Hear. Res.* 304, 153–158. doi: 10.1016/j.heares.2013.07.007

Schimmang, T., Tan, J., Müller, M., Zimmermann, U., Rohbock, K., Köpschall, I., et al. (2003). Lack of Bdnf and TrkB signalling in the postnatal cochlea leads to a spatial reshaping of innervation along the tonotopic axis and hearing loss. *Development* 130, 4741–4750. doi: 10.1242/dev.00676

Schuchat, A., Robinson, K., Wenger, J. D., Harrison, L. H., Farley, M., Reingold, A. L., et al. (1997). Bacterial meningitis in the United States in 1995. Active Surveillance Team. *N. Engl. J. Med.* 337, 970–976. doi: 10.1056/NEJM199710023371404

Schuknecht, H. F. (1964). Further observations on the pathology of presbycusis. *Arch. Otolaryngol.* 80, 369–382. doi: 10.1001/archotol.1964.00750040381003

Schuknecht, H. F., Kimura, R. S., and Naufal, P. M. (1973). The pathology of sudden deafness. *Acta Otolaryngol.* 76, 75–97. doi: 10.3109/00016487309121486

Schultz, J. M., Yang, Y., Caride, A. J., Filoteo, A. G., Penheiter, A. R., Lagziel, A., et al. (2005). Modification of human hearing loss by plasma-membrane calcium pump PMCA2. *N. Engl. J. Med.* 352, 1557–1564. doi: 10.1056/NEJMoa043899

Sebti, S. M., and Der, C. J. (2003). Opinion: searching for the elusive targets of farnesyltransferase inhibitors. *Nat. Rev. Cancer* 3, 945–951. doi: 10.1038/nrc1234

Seidman, M. D., Khan, M. J., Bai, U., Shirwany, N., and Quirk, W. S. (2000). Biologic activity of mitochondrial metabolites on aging and age-related hearing loss. *Am. J. Otol.* 21, 161–167. doi: 10.1016/s0196-0709(00)80003-4

Seidman, M. D., Quirk, W. S., and Shirwany, N. A. (1999). Mechanisms of alterations in the microcirculation of the cochlea. *Ann. N Y Acad. Sci.* 884, 226–232. doi: 10.1111/j.1749-6632.1999.tb08644.x

Selivanova, O., Brieger, J., Heinrich, U. R., and Mann, W. (2007). Akt and c-Jun N-terminal kinase are regulated in response to moderate noise exposure in the cochlea of guinea pigs. *ORL J. Otorhinolaryngol. Relat. Spec.* 69, 277–282. doi: 10.1159/000103871

Sergeyenko, Y., Lall, K., Liberman, M. C., and Kujawa, S. G. (2013). Age-related cochlear synaptopathy: an early-onset contributor to auditory functional decline. *J. Neurosci.* 33, 13686–13694. doi: 10.1523/JNEUROSCI.1783-13.2013

Sha, S. H., Kanicki, A., Halsey, K., Wearne, K. A., and Schacht, J. (2012). Antioxidant-enriched diet does not delay the progression of age-related hearing loss. *Neurobiol. Aging* 33, 1010.e15–1010.e16. doi: 10.1016/j.neurobiolaging.2011.10.023

Sha, S. H., Taylor, R., Forge, A., and Schacht, J. (2001). Differential vulnerability of basal and apical hair cells is based on intrinsic susceptibility to free radicals. *Hear. Res.* 155, 1–8. doi: 10.1016/s0378-5955(01)00224-6

Shen, H., Huo, X., Liu, K., Li, X., Gong, W., Zhang, H., et al. (2012). Genetic variation in GSTM1 is associated with susceptibility to noise-induced hearing loss in a Chinese population. *J. Occup. Environ. Med.* 54, 1157–1162. doi: 10.1097/jom.0b013e31825902ce

Shi, X., and Nuttall, A. L. (2003). Upregulated iNOS and oxidative damage to the cochlear stria vascularis due to noise stress. *Brain Res.* 967, 1–10. doi: 10.1016/s0006-8993(02)04090-8

Shigenaga, M. K., Hagen, T. M., and Ames, B. N. (1994). Oxidative damage and mitochondrial decay in aging. *Proc. Natl. Acad. Sci. U S A* 91, 10771–10778. doi: 10.1073/pnas.91.23.10771

Shin, Y. S., Hwang, H. S., Kang, S. U., Chang, J. W., Oh, Y. T., and Kim, C. H. (2014). Inhibition of p38 mitogen-activated protein kinase ameliorates radiation-induced ototoxicity in zebrafish and cochlea-derived cell lines. *Neurotoxicology* 40, 111–122. doi: 10.1016/j.neuro.2013.12.006

Slepecky, N. (1986). Overview of mechanical damage to the inner ear: noise as a tool to probe cochlear function. *Hear. Res.* 22, 307–321. doi: 10.1016/0378-5955(86)90107-3

Someya, S., Xu, J., Kondo, K., Ding, D., Salvi, R. J., Yamasoba, T., et al. (2009). Age-related hearing loss in C57BL/6J mice is mediated by Bak-dependent mitochondrial apoptosis. *Proc. Natl. Acad. Sci. U S A* 106, 19432–19437. doi: 10.1073/pnas.0908786106

Son, Y., Kim, S., Chung, H. T., and Pae, H. O. (2013). Reactive oxygen species in the activation of MAP kinases. *Methods Enzymol.* 528, 27–48. doi: 10.1016/B978-0-12-405881-1.00002-1

Spoendlin, H. (1984). Factors inducing retrograde degeneration of the cochlear nerve. *Ann. Otol. Rhinol. Laryngol. Suppl.* 112, 76–82.

Sugawara, M., Corfas, G., and Liberman, M. C. (2005). Influence of supporting cells on neuronal degeneration after hair cell loss. *J. Assoc. Res. Otolaryngol.* 6, 136–147. doi: 10.1007/s10162-004-5050-1

Sun, W., and Salvi, R. J. (2009). Brain derived neurotrophic factor and neurotrophic factor 3 modulate neurotransmitter receptor expressions on developing spiral ganglion neurons. *Neuroscience* 164, 1854–1866. doi: 10.1016/j.neuroscience.2009.09.037

Tabuchi, K., Pak, K., Chavez, E., and Ryan, A. F. (2007). Role of inhibitor of apoptosis protein in gentamicin-induced cochlear hair cell damage. *Neuroscience* 149, 213–222. doi: 10.1016/j.neuroscience.2007.06.061

Tadros, S. F., D'Souza, M., Zettel, M. L., Zhu, X., Waxmonsky, N. C., and Frisina, R. D. (2007). Glutamate-related gene expression changes with age in the mouse auditory midbrain. *Brain Res.* 1127, 1–9. doi: 10.1016/j.brainres.2006.09.081

Tadros, S. F., D'Souza, M., Zhu, X., and Frisina, R. D. (2008). Apoptosis-related genes change their expression with age and hearing loss in the mouse cochlea. *Apoptosis* 13, 1303–1321. doi: 10.1007/s10495-008-0266-x

Tadros, S. F., Kim, Y., Phan, P. A., Birnbaumer, L., and Housley, G. D. (2010). TRPC3 ion channel subunit immunolocalization in the cochlea. *Histochem. Cell Biol.* 133, 137–147. doi: 10.1007/s00418-009-0653-6

Tagoe, T., Barker, M., Jones, A., Allcock, N., and Hamann, M. (2014). Auditory nerve perinodal dysmyelination in noise-induced hearing loss. *J. Neurosci.* 34, 2684–2688. doi: 10.1523/JNEUROSCI.3977-13.2014

Tait, S. W., and Green, D. R. (2008). Caspase-independent cell death: leaving the set without the final cut. *Oncogene* 27, 6452–6461. doi: 10.1038/onc.2008.311

Thorne, P. R., Munoz, D. J., Nikolic, P., Mander, L., Jagger, D. J., Greenwood, D., et al. (2002). Potential role of purinergic signalling in cochlear pathology. *Audiol. Neurootol.* 7, 180–184. doi: 10.1159/000058307

Thorne, P. R., Nuttall, A. L., Scheibe, F., and Miller, J. M. (1987). Sound-induced artifact in cochlear blood flow measurements using the laser Doppler flowmeter. *Hear. Res.* 31, 229–234. doi: 10.1016/0378-5955(87)90192-4

Tornabene, S. V., Sato, K., Pham, L., Billings, P., and Keithley, E. M. (2006). Immune cell recruitment following acoustic trauma. *Hear. Res.* 222, 115–124. doi: 10.1016/j.heares.2006.09.004

Torres, M. (2003). Mitogen-activated protein kinase pathways in redox signaling. *Front. Biosci.* 8, d369–d391. doi: 10.2741/999

Van Crombruggen, K., Jacob, F., Zhang, N., and Bachert, C. (2013). Damage-associated molecular patterns and their receptors in upper airway pathologies. *Cell. Mol. Life Sci.* 70, 4307–4321. doi: 10.1007/s00018-013-1356-7

Verschuur, C. A., Dowell, A., Syddall, H. E., Ntani, G., Simmonds, S. J., Baylis, D., et al. (2012). Markers of inflammatory status are associated with hearing threshold in older people: findings from the Hertfordshire ageing study. *Age Ageing* 41, 92–97. doi: 10.1093/ageing/afr140

Villalonga, P., López-Alcalá, C., Bosch, M., Chiloeches, A., Rocamora, N., Gil, J., et al. (2001). Calmodulin binds to K-Ras, but not to H- or N-Ras and modulates its downstream signaling. *Mol. Cell. Biol.* 21, 7345–7354. doi: 10.1128/mcb.21.21.7345-7354.2001

Vlajkovic, S. M., Abi, S., Wang, C. J., Housley, G. D., and Thorne, P. R. (2007). Differential distribution of adenosine receptors in rat cochlea. *Cell Tissue Res.* 328, 461–471. doi: 10.1007/s00441-006-0374-2

Vlajkovic, S. M., Chang, H., Paek, S. Y., Chi, H. H., Sreebhavan, S., Telang, R. S., et al. (2014). Adenosine amine congener as a cochlear rescue agent. *Biomed Res. Int.* 2014:841489. doi: 10.1155/2014/841489

Vlajkovic, S. M., Guo, C. X., Telang, R., Wong, A. C., Paramananthasivam, V., Boison, D., et al. (2011). Adenosine kinase inhibition in the cochlea delays the onset of age-related hearing loss. *Exp. Gerontol.* 46, 905–914. doi: 10.1016/j.exger.2011.08.001

Vlajkovic, S. M., Housley, G. D., and Thorne, P. R. (2009). Adenosine and the auditory system. *Curr. Neuropharmacol.* 7, 246–256. doi: 10.2174/157015909789152155

Vlajkovic, S. M., Lee, K. H., Wong, A. C., Guo, C. X., Gupta, R., Housley, G. D., et al. (2010). Adenosine amine congener mitigates noise-induced cochlear injury. *Purinergic Signal.* 6, 273–281. doi: 10.1007/s11302-010-9188-5

Vlajkovic, S. M., Lin, S. C., Wong, A. C., Wackrow, B., and Thorne, P. R. (2013). Noise-induced changes in expression levels of NADPH oxidases in the cochlea. *Hear. Res.* 304, 145–152. doi: 10.1016/j.heares.2013.07.012

Vlajkovic, S. M., Vinayagamoorthy, A., Thorne, P. R., Robson, S. C., Wang, C. J., and Housley, G. D. (2006). Noise-induced up-regulation of NTPDase3 expression in the rat cochlea: implications for auditory transmission and cochlear protection. *Brain Res.* 1104, 55–63. doi: 10.1016/j.brainres.2006.05.094

Wakabayashi, K., Fujioka, M., Kanzaki, S., Okano, H. J., Shibata, S., Yamashita, D., et al. (2010). Blockade of interleukin-6 signaling suppressed cochlear inflammatory response and improved hearing impairment in noise-damaged mice cochlea. *Neurosci. Res.* 66, 345–352. doi: 10.1016/j.neures.2009.12.008

Wang, J., Ding, D., and Salvi, R. J. (2003a). Carboplatin-induced early cochlear lesion in chinchillas. *Hear. Res.* 181, 65–72. doi: 10.1016/s0378-5955(03)00176-x

Wang, Y., Hirose, K., and Liberman, M. C. (2002). Dynamics of noise-induced cellular injury and repair in the mouse cochlea. *J. Assoc. Res. Otolaryngol.* 3, 248–268. doi: 10.1007/s101620020028

Wang, J., Lei, H., Hou, J., and Liu, J. (2014). Involvement of oxidative stress in SAMP10 mice with age-related neurodegeneration. *Neurol. Sci.* doi: 10.1007/s10072-014-2029-5. [Epub ahead of print].

Wang, Y., Patel, R., Ren, C., Taggart, M. G., Firpo, M. A., Schleiss, M. R., et al. (2013). A comparison of different murine models for cytomegalovirus-induced sensorineural hearing loss. *Laryngoscope* 123, 2801–2806. doi: 10.1002/lary.24090

Wang, J. C., Raybould, N. P., Luo, L., Ryan, A. F., Cannell, M. B., Thorne, P. R., et al. (2003c). Noise induces up-regulation of P2X2 receptor subunit of ATP-gated ion channels in the rat cochlea. *Neuroreport* 14, 817–823. doi: 10.1097/00001756-200305060-00008

Wang, J., Ruel, J., Ladrech, S., Bonny, C., van de Water, T. R., and Puel, J. L. (2007). Inhibition of the c-Jun N-terminal kinase-mediated mitochondrial cell death pathway restores auditory function in sound-exposed animals. *Mol. Pharmacol.* 71, 654–666. doi: 10.1124/mol.106.028936

Wang, H., Turner, J. G., Ling, L., Parrish, J. L., Hughes, L. F., and Caspary, D. M. (2009). Age-related changes in glycine receptor subunit composition and binding in dorsal cochlear nucleus. *Neuroscience* 160, 227–239. doi: 10.1016/j.neuroscience.2009.01.079

Wang, J., Van De Water, T. R., Bonny, C., de Ribaupierre, F., Puel, J. L., and Zine, A. (2003b). A peptide inhibitor of c-Jun N-terminal kinase protects against both aminoglycoside and acoustic trauma-induced auditory hair cell death and hearing loss. *J. Neurosci.* 23, 8596–8607.

Wiedermann, B. L., Hawkins, E. P., Johnson, G. S., Lamberth, L. B., Mason, E. O., and Kaplan, S. L. (1986). Pathogenesis of labyrinthitis associated with Haemophilus influenzae type b meningitis in infant rats. *J. Infect. Dis.* 153, 27–32. doi: 10.1093/infdis/153.1.27

Wilson, W. R., Byl, F. M., and Laird, N. (1980). The efficacy of steroids in the treatment of idiopathic sudden hearing loss. A double-blind clinical study. *Arch. Otolaryngol.* 106, 772–776. doi: 10.1001/archotol.1980.00790360050013

Wong, A. C., Birnbaumer, L., and Housley, G. D. (2013b). Canonical transient receptor potential channel subtype 3-mediated hair cell Ca2+ entry regulates sound transduction and auditory neurotransmission. *Eur. J. Neurosci.* 37, 1478–1496. doi: 10.1111/ejn.12158

Wong, A. C. Y., Froud, K. E., and Hsieh, Y. S. Y. (2013a). Noise-induced hearing loss in the 21st century–a research and translational update. *World J. Otorhinolaryngol.* 3, 58–70. doi: 10.5319/wjo.v3.i3.58

Woolf, N. K., Harris, J. P., Ryan, A. F., Butler, D. M., and Richman, D. D. (1985). Hearing loss in experimental cytomegalovirus infection of the guinea pig inner ear: prevention by systemic immunity. *Ann. Otol. Rhinol. Laryngol.* 94, 350–356.

Wright, H. L., Moots, R. J., Bucknall, R. C., and Edwards, S. W. (2010). Neutrophil function in inflammation and inflammatory diseases. *Rheumatology (Oxford)* 49, 1618–1631. doi: 10.1093/rheumatology/keq045

Xia, Z., Dickens, M., Raingeaud, J., Davis, R. J., and Greenberg, M. E. (1995). Opposing effects of ERK and JNK-p38 MAP kinases on apoptosis. *Science* 270, 1326–1331. doi: 10.1126/science.270.5240.1326

Xue, L., Murray, J. H., and Tolkovsky, A. M. (2000). The Ras/phosphatidylinositol 3-kinase and Ras/ERK pathways function as independent survival modules each of which inhibits a distinct apoptotic signaling pathway in sympathetic neurons. *J. Biol. Chem.* 275, 8817–8824. doi: 10.1074/jbc.275.12.8817

Yakovlev, A. G., and Faden, A. I. (2001). Caspase-dependent apoptotic pathways in CNS injury. *Mol. Neurobiol.* 24, 131–144. doi: 10.1385/mn:24:1-3:131

Yamane, H., Nakai, Y., Takayama, M., Iguchi, H., Nakagawa, T., and Kojima, A. (1995). Appearance of free radicals in the guinea pig inner ear after noise-induced acoustic trauma. *Eur. Arch. Otorhinolaryngol.* 252, 504–508. doi: 10.1007/bf02114761

Yamashita, D., Jiang, H. Y., Schacht, J., and Miller, J. M. (2004a). Delayed production of free radicals following noise exposure. *Brain Res.* 1019, 201–209. doi: 10.1016/j.brainres.2004.05.104

Yamashita, D., Miller, J. M., Jiang, H. Y., Minami, S. B., and Schacht, J. (2004b). AIF and EndoG in noise-induced hearing loss. *Neuroreport* 15, 2719–2722.

Yan, D., Zhu, Y., Walsh, T., Xie, D., Yuan, H., Sirmaci, A., et al. (2013). Mutation of the ATP-gated P2X2 receptor leads to progressive hearing loss and increased susceptibility to noise. *Proc. Natl. Acad. Sci. U S A* 110, 2228–2233. doi: 10.1073/pnas.1222285110

Yang, W. P., Henderson, D., Hu, B. H., and Nicotera, T. M. (2004). Quantitative analysis of apoptotic and necrotic outer hair cells after exposure to different levels of continuous noise. *Hear. Res.* 196, 69–76. doi: 10.1016/j.heares.2004.04.015

Zettel, M. L., Zhu, X., O'Neill, W. E., and Frisina, R. D. (2007). Age-related decline in Kv3.1b expression in the mouse auditory brainstem correlates with functional deficits in the medial olivocochlear efferent system. *J. Assoc. Res. Otolaryngol.* 8, 280–293. doi: 10.1007/s10162-007-0075-x

Zheng, Q. Y., Johnson, K. R., and Erway, L. C. (1999). Assessment of hearing in 80 inbred strains of mice by ABR threshold analyses. *Hear. Res.* 130, 94–107. doi: 10.1016/s0378-5955(99)00003-9

Zuccotti, A., Kuhn, S., Johnson, S. L., Franz, C., Singer, W., Hecker, D., et al. (2012). Lack of brain-derived neurotrophic factor hampers inner hair cell synapse physiology, but protects against noise-induced hearing loss. *J. Neurosci.* 32, 8545–8553. doi: 10.1523/JNEUROSCI.1247-12.2012

Conflict of Interest Statement: The authors declare that the research was conducted in the absence of any commercial or financial relationships that could be construed as a potential conflict of interest.

frontiers in Aging Neuroscience

ORIGINAL RESEARCH
published: 18 March 2015
doi: 10.3389/fnagi.2015.00033

Inner ear hair cells deteriorate in mice engineered to have no or diminished innervation

*Jennifer Kersigo and Bernd Fritzsch **

Department of Biology, University of Iowa, Iowa City, IA, USA

The innervation of the inner ear critically depends on the two neurotrophins Ntf3 and Bdnf. In contrast to this molecularly well-established dependency, evidence regarding the need of innervation for long-term maintenance of inner ear hair cells is inconclusive, due to experimental variability. Mutant mice that lack both neurotrophins could shed light on the long-term consequences of innervation loss on hair cells without introducing experimental variability, but do not survive after birth. Mutant mice with conditional deletion of both neurotrophins lose almost all innervation by postnatal day 10 and show an initially normal development of hair cells by this stage. No innervation remains after 3 weeks and complete loss of all innervation results in near complete loss of outer and many inner hair cells of the organ of Corti within 4 months. Mutants that retain one allele of either neurotrophin have only partial loss of innervation of the organ of Corti and show a longer viability of cochlear hair cells with more profound loss of inner hair cells. By 10 months, hair cells disappear with a base to apex progression, proportional to the residual density of innervation and similar to carboplatin ototoxicity. Similar to reports of hair cell loss after aminoglycoside treatment, blobbing of stereocilia of apparently dying hair cells protrude into the cochlear duct. Denervation of vestibular sensory epithelia for several months also resulted in variable results, ranging from unusual hair cells resembling the aberrations found in the organ of Corti, to near normal hair cells in the canal cristae. Fusion and/or resorption of stereocilia and loss of hair cells follows a pattern reminiscent of Myo6 and Cdc42 null mice. Our data support a role of innervation for long-term maintenance but with a remarkable local variation that needs to be taken into account when attempting regeneration of the organ of Corti.

Keywords: inner ear, hair cells, degeneration, innervation, neurotrophins, conditional deletion

OPEN ACCESS

Edited by:
Marta Magarinos, Universidad Autonoma de Madrid, Spain

Reviewed by:
Fernando Giraldez, Universitat Pompeu Fabra, Spain
Ricardo Romero-Guevara, University of Florence, Italy

***Correspondence:**
Bernd Fritzsch, Department of Biology, College of Liberal Arts and Sciences, University of Iowa, 143 Biology Building, 129 E Jefferson Street, Iowa City, IA 52242-1324, USA
bernd-fritzsch@uiowa.edu

Received: *19 January 2015*
Accepted: *28 February 2015*
Published: *18 March 2015*

Citation:
Kersigo J and Fritzsch B (2015) Inner ear hair cells deteriorate in mice engineered to have no or diminished innervation. Front. Aging Neurosci. 7:33. doi: 10.3389/fnagi.2015.00033

Introduction

It is estimated that over 900 million people worldwide will have at least a 25 dB reduction in hearing sensitivity by 2025 [http://hearinghealthmatters.org/hearinginternational/2011/incidence-of-hearing-loss-around-the-world/]. Even mild hearing loss (26–40 dB HL) may deprive people from their accustomed way of communication (Yamasoba et al., 2013), promote cognitive decline (Lin et al., 2013), and possibly increase the risk for developing dementia, including Alzheimer's disease (Lin and Albert, 2014). Clinically, hearing loss is multifactorial in its etiology, having both genetic and environmental (noise exposure, ototoxic drugs, neurotoxic drugs, etc.) components (Kopecky and Fritzsch, 2011; Makary et al., 2011; Huisman and Rivolta, 2012; Rivolta, 2013).

Sensorineural hearing loss is a common type of age-related hearing loss (AHL) and mainly results from loss of cochlear hair cells (HCs) and/or spiral ganglion neurons (SGNs). Potentially more devastating is a decline in vestibular function which typically starts about a decade after the onset of hearing loss (Rauch, 2001). Vestibular dysfunction can increase the risk of falling, resulting in fractures and subsequent morbidity of the elderly. Recently the hallmarks of aging were reviewed and cell communication was found to be a major aspect that defines which cell will survive and which will die (López-Otín et al., 2013), possibly underlying the diversity of cellular reactions that has been stressed in recent papers studying hair cell loss after ototoxic treatments (Taylor et al., 2012). Here we evaluate the historically controversial influence of innervation on hair cell viability in the ear using newly developed models of targeted deletion of neurotrophins.

Human temporal bone studies of the cochlea suggest that neuronal and HC loss are unrelated as over 90% of neuronal loss can occur without loss of HCs (Otte et al., 1978; Makary et al., 2011). Animal studies also suggest that innervation and HC loss can happen independently of each other (Perez and Bao, 2011; Kidd and Bao, 2012) except for inconclusive data that report the loss of some HCs after afferent innervation to the inner ear was cut (Sugawara et al., 2005). In the vestibular system of humans, there appears to be a somewhat matching decline of both vestibular ganglion neurons (VGNs) and HCs over time (Rauch, 2001). Earlier claims in studies involving adult guinea pigs show complete loss of HCs in vestibular sensory epithelium 4 months after vestibular nerve transection (Favre and Sans, 1991) have not been confirmed in other investigations in humans (Suzukawa et al., 2005) leaving the loss of vestibular hair cells after loss of innervation open to interpretation. To date, a large portion of the studies addressing the dependency of inner ear hair cell survival on innervation utilize surgical techniques with potential flaws: either incomplete surgical denervation or inadvertent disruption of blood supplies may affect data (Sugawara et al., 2005). Despite over 50 years of work on this subject, it is fair to say that no unequivocal answer has been reached largely due to technical limitations in all but one study that shows complete loss of all vestibular hair cells after surgical denervation (Favre and Sans, 1991).

Of note, in contrast to these disputed effects related to surgical removal of innervation on adult hair cells, data on mutant mice that lack all innervation to the ear by various mutations have established that absence of innervation has no short-term effect on HC development (Fritzsch et al., 1997a; Ma et al., 2000; Yang et al., 2011). In fact, removing neurotrophin receptors eliminates innervation without affecting hair cell development (Fritzsch et al., 1997a). This absence of any apparent effect of denervation contrasts with all other sensory cells, which seemingly depend on innervation either for complete differentiation or viability (Fritzsch et al., 1998). For example, severing gustatory nerves results in rapid loss of taste bud sensory cells, which can reappear after nerve fibers grow back into the skin (Farbman, 2003; Fei et al., 2014). However, some embryonic differentiation of taste sensory cells can occur in the absence of innervation (Fritzsch et al., 1997b; Ito et al., 2010) and gustatory nerve fibers cannot induce taste buds if the molecular competence of the epidermis is changed by mutating *Sox2* (Okubo et al., 2006, 2009). These data suggest that initial formation of taste sensory cells occurs autonomously, much like hair cells in the ear (Ma et al., 2000) but innervation is needed to maintain sensory cells. Similar to taste buds, electroreceptive sensory cells and organs depend on innervation for maintenance. Hair cells die within hours after severing the nerve and organs disappear rapidly through cell death after nerve fibers are cut and reappear rapidly upon reinnervation (Fritzsch et al., 1990). Transplantation studies have shown that the initial development of electroreceptive organs may be autonomous (Northcutt et al., 1995), again suggesting that afferents maintain but do not induce electroreceptive sensory cells. Neither taste buds nor electroreceptors have an efferent innervation, clearly indicating the role of afferents for maintenance. Electroreceptive sensory cells are closely related to the mechanosensory HCs of the lateral line, neuromasts (Duncan and Fritzsch, 2012), which also seem to depend on innervation for long term viability. In bony fish and amphibians, the hair cells of neuromasts are lost after months of denervation (Jones and Singer, 1969). These data suggest that possibly all placode derived sensory cells can differentiate autonomously but require innervation for viability. Among placode derived sensory cells, inner ear hair cells appear to be unique: like other placode derived sensory cells they have autonomous development in the absence of innervation but may not depend on afferent innervation for long term viability.

A new approach using a transgenic mutation resulting in the targeted deletion of neurotrophins to test the potential influence of afferents and efferents on HC viability, without compromising blood supply, could clarify this issue. Previous work has shown that mice lacking neurotrophins or their receptors are born with little to no innervation (Ernfors et al., 1995; Silos-Santiago et al., 1997; Fritzsch et al., 2004) but these mice die soon after birth. Mice with ear-specific conditional deletions of the two relevant neurotrophins in the ear (*Pax2-cre; Ntf3*$^{f/f}$, *Bdnf*$^{f/f}$) are viable for several months but are deaf and show vestibular and cerebellar motor control defects. We raised these mice for up to 10 months and investigated the pattern of remaining HCs and innervation using Myo7a, tubulin, and neurofilament (NF) immunohistochemistry, myelinated nerve fiber staining, and SEM. These mice show an age-dependent, progressive loss of HCs that correlates with the reduction of innervation in the cochlea and vestibular organs and suggests a yet to be determined, variable threshold of innervation for different organs and different hair cells within a given organ.

Material and Methods

Mouse Breeding and Collection

Pax2-cre mice (Ohyama and Groves, 2004) were crossed with floxed *Ntf3* (Bates et al., 1999) (aka *NT3*) and floxed *Bdnf* mice (Gorski et al., 2003) to generate conditional, ear-specific and viable mutants that lack neurotrophin expression in the ear. Breeding pairs consist of mice carrying the *Pax2-cre* together with heterozygosity of the floxed neurotrophins (*Pax2-cre; Ntf3*$^{f/+}$; *Bdnf*$^{f/+}$). These mice were crossed with mice homozygotic for

floxed alleles of both neurotrophins (*Ntf3* $^{f/f}$; *Bdnf*$^{f/f}$). 1 in 8 mice were doubly homozygotic for both floxed genes and also expressed cre. Combinations of cre with heterozygotic floxed *Bdnf* and homozygosity of *Ntf3* (*Pax2-cre; Ntf3*$^{f/f}$; *Bdnf*$^{f/+}$) or homozygosity for floxed Bdnf and heterozygosity for Ntf3 (*Pax2-cre; Ntf3*$^{f/+}$; *Bdnf*$^{f/f}$) are also included here. These mice lose much of their innervation of the organ of Corti and in case of loss of all *Bdnf*, also all innervation to canal cristae (Fritzsch et al., 2004). Because of the further delay in innervation loss in the apical half of the cochlea, we concentrated on the basal turn for this presentation except where stated differently.

Mice were genotyped within 3 days after birth. Non-desired littermates were eliminated to increase the viability of vestibular defected mutant mice (due to loss of Bdnf). Mice were raised to the designated age of 1, 2, 4, 7–10 months and were sacrificed. Six mutant animals were collected per the three genotypes whenever possible together with age-matched control littermates at the designated age to minimize genetic background effects. Data were pooled across two or more litters to eliminate any genetic background bias. Given that we had to cross three distinct mutant lines carrying the Pax2-cre, the floxed Bdnf and the floxed Ntf3 into a mixed mouse line, we do not expect strain specific effects of time delay as previously reported (Taylor et al., 2012). We cannot exclude that some strain specific background effects are present in our mixed lines. Nevertheless, we consider the best comparison to be with littermates with a different genotype but housed under identical circumstances in the same box to avoid undo bias introduced by unknown genetic background effects.

For the present analysis we concentrated on three genotypes: *Pax2-cre; Ntf3*$^{f/f}$; *Bdnf*$^{f/f}$; *Pax2-cre; Ntf3*$^{f/f}$; *Bdnf*$^{f/+}$and *Pax2-cre; Ntf3*$^{f/+}$; *Bdnf*$^{f/f+}$. The latter two genotypes had each only one single allele of neurotrophin left whereas the first had no neurotrophin expression left in the ear. In every case we used age matched controls to compare the effect of mutations. Animals without a cre or without floxed neurotrophin alleles were designated as control animals.

Control and mutant mice were raised together to a defined age, euthanized by deep anesthesia with an intraperitoneal injection of Avertin (1.25% tribromoethanol solution; 0.025 ml/g of body weight). Absence of blink and paw withdrawal reflex was used as evidence for proper depth of anesthesia. Once all reflexes had seized the chest was opened and the mouse was transcardially perfused with 4% paraformaldehyde (PFA) in 0.1 M Phosphate buffer using appropriate-sized needles assuring immediate death. After perfusion, ears were dissected and fixed overnight in 4% PFA and decalcified in 10% EDTA for 2–3 weeks, depending on age. The method of anesthesia is consistent with *AVMA Guidelines on Euthanasia* and is approved by the University of Iowa Institutional Animal Care and Use Committee (IACUC; protocol #1403046).

Immunostaining

Cochleae were micro-dissected, split into near equal sized basal and apical turn sections and immunostained for Myo7a (HCs), tubulin and neurofilament (neuronal processes). Cell nuclei were stained with Hoechst stain according to existing protocols (Jahan et al., 2013).

Lipophilic Dye Tracing

Small pieces of dye-soaked filter paper (Fritzsch et al., 2005a; Tonniges et al., 2010) were implanted into the cochlear nuclei (NeuroVue™ Maroon) or the efferent fiber tract (NeuroVue™ Red) in animals fixed in 4% PFA. Fixed tissue was kept at 60°C for ∼48–96 h to allow for dye diffusion from the hindbrain to the ear. Ears were micro-dissected, split into a basal and apical turn and mounted on a slide in glycerol. To avoid diffusion of dye out of the lipid bilayer into the glycerol used as mounting medium, images were taken immediately with a Leica TCS SP5 confocal microscope.

Imaging

Immunostained cochlea halves were mounted flat on a slide using glycerol, coverslipped and imaged using a Leica SP5 confocal microscope. Data sets were generated by collecting stacks at 3–6 μm steps (depending on the magnification) in 100–200 μm long segments at three different positions: the basal hook region, near the apical tip and at approximately the middle of the cochlea.

SEM Imaging

Selected ears of animals at late stages of HC loss were imaged using SEM to detail the loss and aberration of hair bundles and the reorganization of supporting cells after induced HC loss as recently described (Jahan et al., 2010). Ears designated for SEM were postfixed in 2.5% glutaraldehyde followed by 1.0% OsO4 fixation. The cochlea apex was cut away from the cochlear base with fine scissors resulting in an apical turn and a basal ¾ turn. OsO4 stains all myelinated nerve fibers black and images were taken after OsO4 staining to verify completion of nerve fiber loss or partial loss, depending on the genotype. Images of osmicated ears were taken on a Leica dissection scope using identical settings for mutant and control animals. SEM preparations were critical point dried, sputter coated and viewed with a Hitachi S-4800 scanning electron microscope. HC and supporting cell reorganization were interpreted according to known effects of aminoglycoside toxicity (Taylor et al., 2012). Cochlea and vestibular organs of age matched control and mutant littermates were processed together but differed in being either left or right ear for easy identification.

In situ Hybridization

Both the floxed *Bdnf* and the floxed *Ntf3* have been used in the ear for targeted deletion but only the Bdnf has been used before with Pax2-cre (Zilberstein et al., 2012; Zuccotti et al., 2012). We therefore verified the absence of *Ntf3* in Pax2-cre mice at birth to show that indeed there was no detectable level of Ntf3 at this late stage, consistent with the innervation phenotype. *In situ* hybridization was performed as described previously (Duncan et al., 2011) using a probe specific for *Ntf3* (courtesy of L. Reichardt). Previous work has already demonstrated the effectiveness of Pax2-cre to excise the floxed alleles of *Bdnf* (Zuccotti et al., 2012) and the effects agreed with previously described losses of *Bdnf*.

Results

Complete Absence of the Neurotrophins *Ntf3* and *Bdnf* (*Pax2-cre; Ntf3$^{f/f}$; Bdnf $^{f/f}$*)

Mice without any neurotrophins were difficult to maintain past postnatal day 21 (P21). Morbidity past 2 months was very high causing loss of all but one animal collected at 4 month of age. Morbidity may relate to aberrations in the cerebellum previously demonstrated in mutants lacking both neurotrophin receptors (Silos-Santiago et al., 1997). Given the presence of the neurotrophin *Ntf3* in cochlear nuclei (Maricich et al., 2009) and the delayed expression of *Pax2-cre* in the cochlear nuclei (Ohyama and Groves, 2004), more afferent fibers should survive past birth compared to the neurotrophin double null mutant mice which lose all innervation at or around birth, depending on the background (Ernfors et al., 1995; Yang et al., 2011). Indeed, P10 mice had limited afferent and more profound efferent supply to the cochlea (**Figure 1**) labeled through selective application of lipophilic dyes to cochlear nuclei and efferent fibers bundles, respectively (Simmons et al., 2011). No afferent or efferent fibers were detected in these animals in the basal turn. Immunostaining for tubulin also showed limited innervation at P10. Development of HCs (shown by Myo7a immunostaining) appeared normal (**Figure 1**). Likewise, no alteration in supporting cells could be detected using the immunostaining for tubulin (**Figure 1**). Complete absence of any innervation in these conditional null mutants for both neurotrophins (*Pax2-cre; Bdnf$^{f/f}$; Ntf3$^{f/f}$*) seemed to occur around P21 as neither tracing nor immunstaining for tubulin or neurofilament showed any fiber to the ear in these (data not shown) and older mice (**Figure 2**). However, even at this stage there was no change in hair cells, suggesting that at least until P21 partial or complete afferent and efferent loss has no effect on early differentiation of hair cells in the organ of Corti or the vestibular organs.

The most profound effect of the complete loss of innervation was in a 4 month old double conditional null mouse, the oldest mouse of this genotype obtained thus far. Absence of innervation was verified with OsO4 as previously described (Retzius, 1884; Postigo et al., 2002). OsO4 labels all myelinated nerve fibers in control littermates including a high density of radial fiber bundles connecting the spiral ganglion neurons with the organ of Corti (**Figures 1A,B**). Neither the cochlea (**Figures 2A′,B′**) nor the vestibular region (**Figure 2C**) showed any myelinated nerve fibers in the mutant mice, confirming the complete absence of innervation of vestibular and auditory organs by myelinated nerve fibers. Neither neurofilament and tubulin nor Myo7a showed positive immunostaining (data not shown). However, such negative results could be due to numerous problems, including loss of hair cells and fibers or their ability to express such epitopes in detectable amounts. We next investigated the degree of differentiation of the organ of Corti HCs using SEM.

The organ of Corti of 4 month old mice with no innervation showed a nearly complete loss of almost all outer hair cell (OHCs) and over 60% of inner hair cells (IHCs) throughout the basal turn (**Figures 3**, **4**). This contrasted with control littermates that showed a normal complement of three rows of OHCs and 1 row of IHCs with rarely any loss of HCs (**Figure 3A**, insert). The

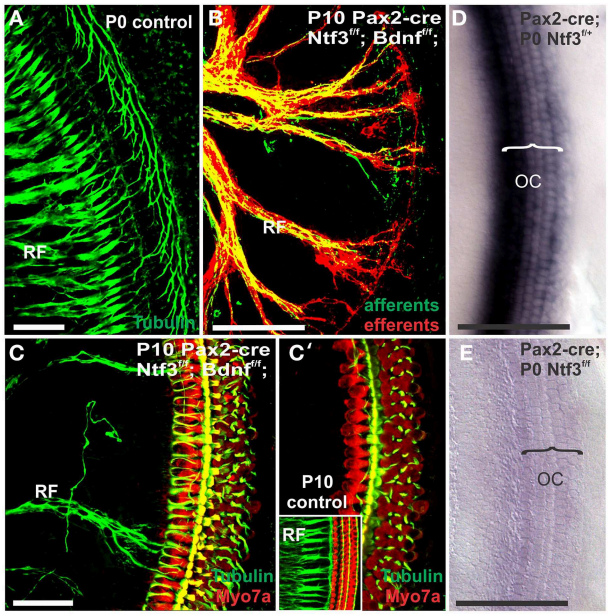

FIGURE 1 | Conditional deletion of floxed *Ntf3* and floxed *Bdnf* in the ear using *Pax2-cre* leads to near complete loss of afferents by P10 (B,C,C′) compared to innervation in a control at birth (A) or 10 days (insert in C′) indicating it is a true loss of afferents and not just delayed innervation. Lipophilic dye labeling reveals that efferent fibers (red) reach to the IHCs **(B)** but also form tunnel-crossing fibers to OHCs. Afferents (green in **B**) are nearly absent and reduced to few radial bundles in the middle turn. Immunostaining for tubulin (green in **B**) shows very few fibers (both afferents and efferents) left in the middle turn **(C)** but not in the base **(C′)**. Note that all hair cells, immunostained for Myo7a, are normally developed and surrounded by supporting cells (stained in green with anti-tubulin). *In situ* hybridization for *Ntf3* **(D,E)** shows a strong signal in control animals **(D)** but no signal above background after conditional deletion of Ntf3 using Pax2-cre **(E)**. Bar = 100 μm **(A,B,D,E)** and 50 μm in **(C,C′)**.

distribution of remaining HCs showed some aggregation near the very tip of the base but moving up only a few 100 μm toward the middle turn we found stretches of organ of Corti void of hair cells (**Figures 3**, **4**). In fact, throughout most of the basal turn the OHC/supporting cell area had nearly disappeared in this mutant (**Figures 3A–C**) as compared to conrol littermates (**Figure 3A**, insert). Remaining OHCs showed reduced numbers of stereocilia with variable height, the more central stereocilia usually being much shorter compared to those more lateral (**Figure 5C**). The few remaining scattered inner hair cells showed a partial fusion of stereocilia, mostly organized as a single row with more or less extensive gaps between them (**Figures 3**, **4**). Many remaining inner hair cells had only few stereocilia left on either side whereas other stereocilia showed various stages of shortening and fusion (**Figures 4**–**6**). Some IHCs showed a ballooning expansion protruding into the scala media, as previously described following otoxic treatment (Taylor et al., 2008), sometimes accompanied by barely recognizable stereocilia in the same cell (**Figure 5A**).

In some parts of the organ of Corti lacking any hair cells, the inner pillar cells also partially or completely dedifferentiated allowing continuity between the inner and outer spiral sulcus

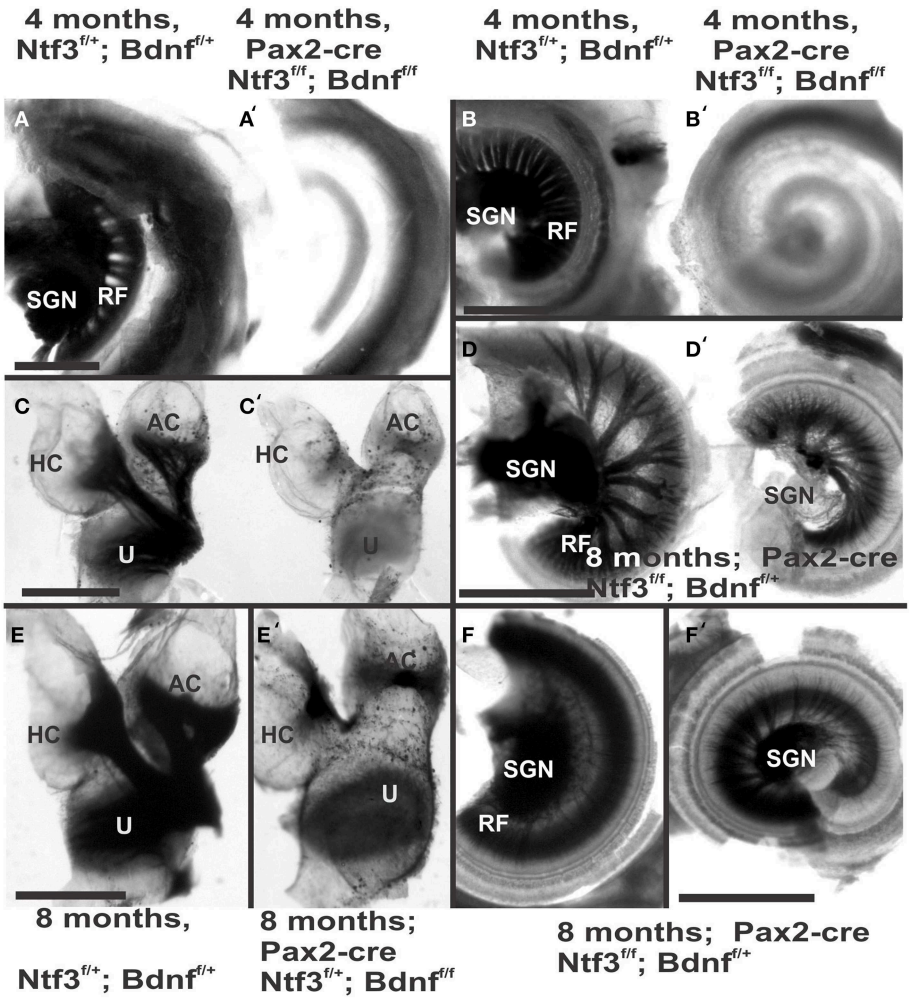

FIGURE 2 | Osmication labels all myelinated nerve fibers and is used here to assess completeness of nerve fiber loss. Inner ears of the 4 month old control **(A,B,C)** and *Pax2-cre; Ntf3*$^{f/f;}$ *Bdnf* $^{f/f}$ mutant mice **(A′,B′,C′,D,D′)** of 7 months old *Pax2-cre; Ntf3* $^{f/f;}$ *Bdnf* $^{f/+}$ mutant mice, and **(E,F)** are inner ears of 7 months old control and *Pax2-cre; Ntf3*$^{f/+;}$ *Bdnf* $^{f/f}$ mutant mice. Note the myelin in the spiral ganglion neurons (SGN) in the control littermate **(A,B)** and complete absence of any myelin staining in both the basal **(A′)** and apical turn **(B′)** of mice with a conditional deletion of both neurotrophins **(A′,B′)**. Likewise, there are no myelinated nerve fibers to the horizontal (HC) or anterior canal cristae (AC) of the conditional mutants **(C′)** in stark contrast to the control littermate **(C)**. *Pax2-cre; Ntf3*$^{f/f;}$ *Bdnf* $^{f/+}$ has some innervation remaining after 11 weeks to the middle turn **(D)** and apex **(D′)** while the basal hook region (top left in **D**) is devoid of any radial fibers. *Pax2-cre; Ntf3*$^{f/+;}$ *Bdnf* $^{f/f}$ mutants have no nerve fibers to the canal cristae **(E,E′)** and reduced innervation to the base and the apex **(F,F′)**. These data show that a single allele of *Bdnf* provides enough support to rescue many neurons for at least several weeks **(D,D′)** and that a single allele of Ntf3 is less effective for long term innervation (compare **D,F**). Bar indicates 500 μm.

(ISS/OSS **Figure 3B**). We could not find a consistent relationship between loss of IHCs, OHCs and changes in inner pillar cells (IPCs). In some areas where all HCs were lost IPCs were near normal but were disrupted in others near remaining HCs (**Figures 3B**, **4C**). The IPCs had the bundle of tubulin filaments protruding as little bumps due to the steep inclination of the IPC head toward the OSS. Where IHCs were lost, IPCs expanded laterally to fill the reticular lamina gap left by lost IHCs. These lateral expansions of IPCs either abutted the border cells (BC) of the ISS (**Figure 3**) or appeared to have a remaining layer of inner phalangeal cells with numerous short microvilli between the remaining IPCs and BCs (**Figure 4**). We presume these cells are remaining inner phalangeal cells (IPhC) as their numerous short microvilli resemble in detail those of IPhCs found between adjacent IHCs in areas that had IHCs. At places, the IPCs were partially dedifferentiated (**Figures 3**–**5**) leaving their heads standing freely over the remaining OPCs and the expanded OSS (**Figures 3**, **4**). In other places we could not identify IPCs and BCs of the ISS seemed to approximate Claudius cells (CC) of the OSS (**Figure 3B**; asterisk).

Overall, the organ of Corti showed dramatic regional variation of cellular changes with profound variability along the length of the basal turn, ranging from stretches of nearly flat epithelium (**Figure 3B**) to near normal. Nevertheless, these changes imply a putative temporal progression toward the more differentiated middle turn: OHCs were lost more rapidly and the outer

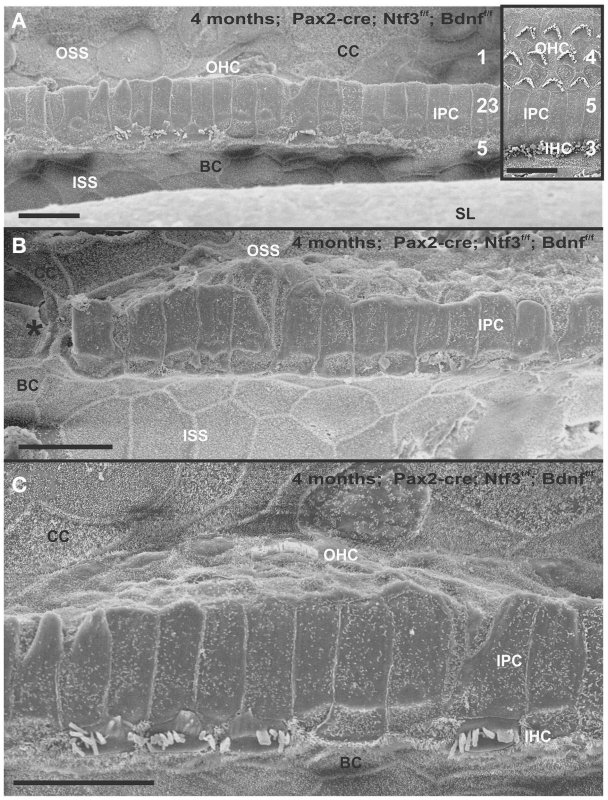

FIGURE 3 | Four month old *Pax2-cre; Ntf3*$^{f/f}$*; Bdnf* $^{f/f}$ mutant shows partial or complete loss of HCs along the organ of Corti (A–C) that contrasts sharply with control littermates that have no obvious defects in HCs (insert in A). Except for small regions (asterisk in **B**) where border cells (BC) of the inner spiral sulcus (ISS) seem to approximate Claudius cells (CC) of the outer spiral sulcus (OSS), inner pillar cells (IPCs) are present even in areas lacking all hair cells. Outer hair cells (OHC) are mostly lost at this stage in the basal turn whereas inner hair cells (IHC) show partial loss. Numbers in **(A)** indicate remaining HCs (5) and IPCs (23) that should normally form a ratio of IPC:OHC:IHC of 5:4:3 as in control animals (insert in **A**). In mutants this ratio is 7: 3:1. **(C)** shows a tilted and enlarge version of **(A)** to reveal the single OHC barely visible on the steep slope of the reticular lamina. Bar equals 10 μm.

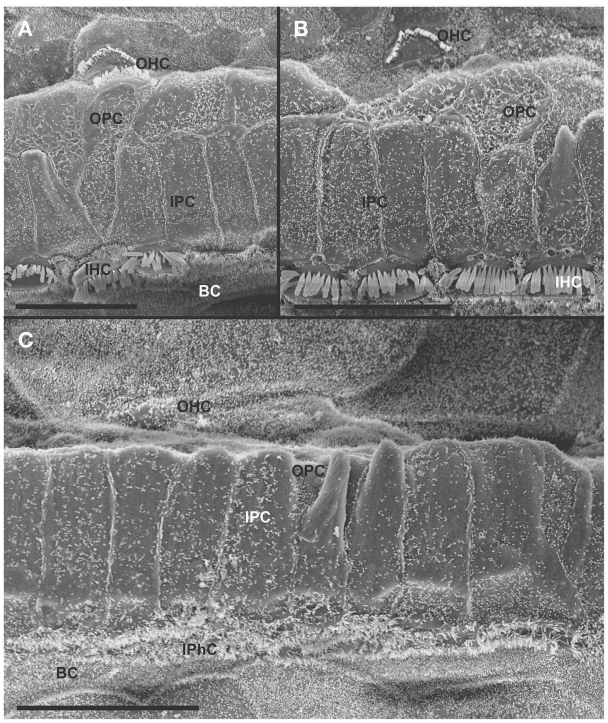

FIGURE 4 | Details of the organ of Corti reorganization after 4 months of denervation indicate an uncoupling of changes of IPCs from either IHC or OHC loss. IPC protrusions above the underlying outer pillar cells (OPC) can be seen in the presence **(A,B)** or absence **(C)** of either IHCs, OHCs, or both IHCs and OHCs **(C)**. Note that loss of the first row of OHCs leads to an expansion of OPCs that becomes continuous **(A,B)**. In certain areas, cells are present between IPCs and BCs **(C)** with dense, short microvilli resembling the inner phalangeal cells (IPhC) between IHCs **(B)**. In other areas, medial expansions of the reticular head of IPCs seem to be in direct contact with border cells (BC in **A**). Bar equals 10 μm.

compartment dedifferentiates and was overgrown or replaced by CCs of the OSS. Many IHCs survived much longer compared to OHCs. Lost IHCs were replaced by expansions of the IPCs with or without retention of the inner phalangeal cells. IPCs were the longest remaining cells in the organ of Corti. When IPCs dedifferentiated this allowed BCs of the ISS to approximate CCs of the OSS, constituting what has been termed a flat epithelium (Izumikawa et al., 2008).

In summary, mutants lacking two neurotrophins allow the study of HC maintenance in the complete absence of any innervation (both afferent and efferent fibers) from approximately postnatal day 12 (P12) onward. Within the limits of the delayed loss of a few middle turn afferents and efferents, this model is consistent with some previous claims of HC development being independent of innervation. Consistent with the most controlled surgical approach to sever ear innervation (Favre and Sans, 1991), our data suggests that the HCs of the organ of Corti in mice have a survival capacity of around 100 days in the complete absence of any innervation from around P12 forward. Some OHCs and more near normal IHCs remain scattered between profoundly altered cellular organization of the OC indicates a large degree of local variation to the effect of postnatal loss of innervation. To further investigate the effect of limited innervation on long term HC viability, we next investigated hair cell viability using littermates with varying genotypes and long term maintenance of some innervation mainly to the middle turn of the cochlea.

Complete Absence of *Ntf3* and Incomplete Absence of *Bdnf (Pax2-cre; Ntf3*$^{f/f}$*; Bdnf* $^{f/+}$*)*

Previous work has shown that loss of a given neurotrophin has both a longitudinal and a radial effect. Loss of Ntf3 caused absence of basal turn spiral ganglion neurons with residual innervation spiraling along the inner hair cells from the middle turn spiral ganglion neurons (**Figure 6**). In contrast, loss of Bdnf caused only a reduced density of innervation in the apex with a reduction of afferents to the OHCs (Fritzsch et al., 2004; Yang et al., 2011). Either tubulin immunocytochemistry in neonates (**Figure 6**) or osmication in adults (**Figure 2D**) showed conditional deletion of Ntf3 with conditional deletion of only one allele

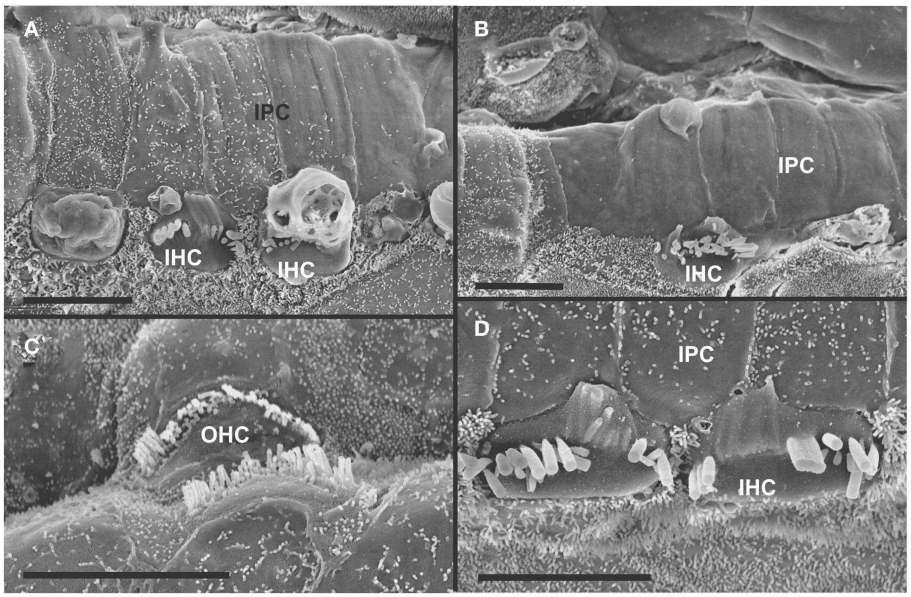

FIGURE 5 | Both IHCs (A,B,D) and OHCs (C) show variability in the length of stereocilia with partial or complete fusion and what appears to be resorption into the HCs. Some IHCs show globular protrusions expanding into the scala media, occasionally from IHCs that bear some stereocilia **(A,B)**. Note that IPCs typically have very short microvilli **(A,D)** but, at places, may entirely lack microvilli formation **(B)**. Bar equals 5 μm.

of Bdnf resulted in loss of all spiral ganglion neurons in the basal turn. Middle turn spiral ganglion neurons had processes spiraling along the inner spiral bundle to the base. Even 10 month old mutants (**Figure 7**) had some fibers innervating mostly IHCs and mostly in the upper middle turn.

In contrast to control littermates, 10 month old *Pax2-cre; Ntf3*$^{f/f}$; *Bdnf*$^{f/+}$ mutant mice showed no Myo7a positive staining throughout the basal turn (data not shown). We found Myo7a positive staining HCs in the middle turn and in the apex (**Figure 7C**). However, while control littermates (either no cre or no LoxP flanked neurotrophins) had near uniform Myo7a staining with occasional loss of one or two OHCs (**Figure 7B**), *Pax2-cre; Ntf3*$^{f/f}$; *Bdnf*$^{f/+}$ mutants showed a profound reduction of Myo7a with very few, mostly IHCs normally labeled (**Figure 7C**). Hoechst nuclear staining confirmed the presence of OHCs and IHCs (and the occasional loss of OHC) in control animals (**Figure 7B′**) while nuclear stain was difficult to use to identify HCs in the mutant due to large gaps and distribution of nuclei at different levels (**Figure 7C′**). Numerous fibers could be traced to IHCs and OHCs in control animals (**Figures 7B″,B‴**) whereas very few tunnel-crossing fibers were found in mutants (**Figure 7C″,C‴**). These data suggest a progressive loss of HCs in the mutant. However, it needs to be stressed that areas exist in the middle turn of mutants with fairly normal HC distribution that seemingly correlated with apparent higher level of innervation density, though the details require more quantification. Since 10 months seemed to be on the advanced end of HC loss in these mutants, we concentrated the SEM study on the 8 month old mutants to learn more about the cellular changes to expand beyond the data obtained in double null neurotrophin mutant mice.

At 8 month, the SEM data revealed a less severe deficit compared to 4 month old, denervated cochlea (**Figures 3**, **8**). Thus, a limited residual innervation maintains HCs under otherwise equal conditions for several more months compared to complete loss of innervation (**Table 1**). Most notable were differences in OHC vs. IHC loss and among the three rows of OHCs (**Figure 8**). Whereas in many cases there was no loss of OHCs in the third and second row, the first row of OHCs and in particular IHCs showed a regionally specific, severe loss (**Figure 8A**). This was in stark contrast to littermates that showed the well-known patchy loss of single OHCs that were scattered across all rows with a tendency to be more profound in the third row (**Figure 8E**). At places, most IHCs (**Figures 8B,C**) and nearly all OHCs of the first row (**Figure 8D**) were lost in mutants. In fact, in many instances, multiple IHCs were lost instead of the typical single OHCs (**Figure 8**). Thus, overall hair cell loss in the middle turn of mutants differed from age-matched littermates in showing loss of multiple adjacent HCs. Notably, there was virtually no loss of IHCs in control animals even at this age (**Figure 8E**). Closer examination showed fusion of multiple stereocilia in OHCs (**Figure 9B**) and IHCs (**Figures 9C–F**). This fusion in some IHCs was so advanced that only one or two prominent protrusions reached from IHCs into the scala media (**Figures 9E,F**). Loss of IHCs resulted in medial expansion of IPCs to either touch BCs (**Figures 9C,D**) or to leave inner phalangeal cells (IPhC) between them (**Figure 9E**). At places OPCs expanded into the outer compartment between the first rows of OHCs (**Figure 9A**). Loss of HCs in the first row of OHCs was usually filled by expansion of the lateral process of the OPCs (**Figure 9A**) but occasionally by a medial expansion of the first row of Deiter's cells (**Figure 9B**) generating a continuity of

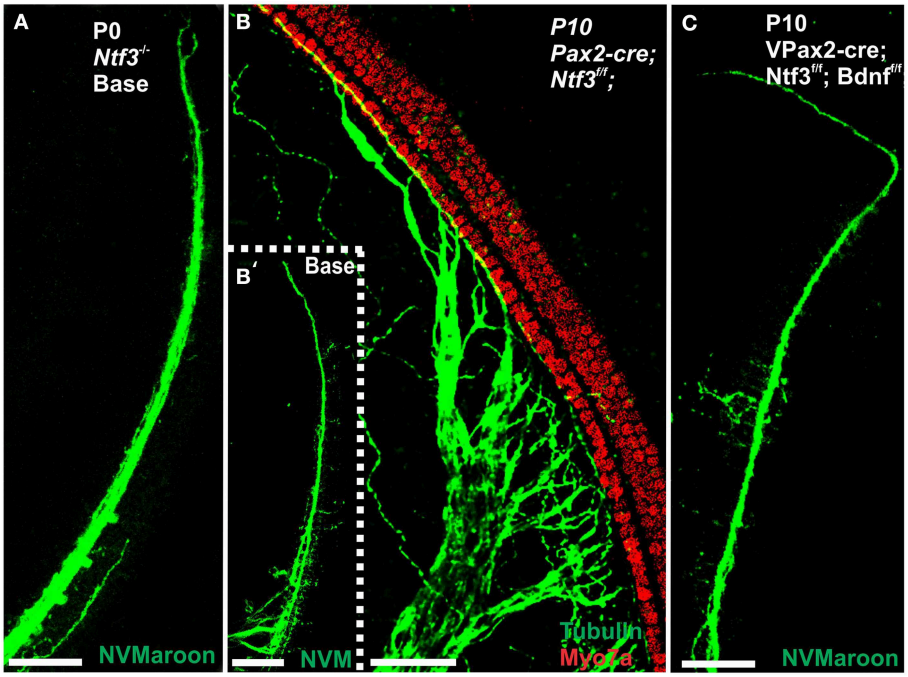

FIGURE 6 | Loss of innervation of the cochlear base is shown in mice with a complete deletion of *Ntf3* (A). A conditional deletion of *Ntf3* using *Pax2-cre* **(B)** or a conditional deletion of both *Bdnf* and *Ntf3* in the ear. Note that there is, at the most, a few fibers spiraling along the IHCs from the middle turn in either mutant and no matter the technique used (lipophilic dye tracing with NVMaroon, **A,C**; immunocytochemistry with anti-tubulin, **B′**). Importantly, conditional deletion of *Ntf3* using *Pax2-cre* requires the additional elimination of one or two alleles of *Bdnf* before the phenotype approaches that of the unconditional null for *Ntf3* **(A,C)**. Note that the reduction of innervation has no apparent effect on early development of hair cells visualized with anti-Myo7a staining **(B)**. Bar equals 50 μm.

different types of supporting cells without any HC between them. This interpretation is consistent with a recent report showing that Deiter's cells function as scavengers that engulf dying hair cells (Anttonen et al., 2014).

Complete Absence of *Bdnf* and Incomplete Absence of *Ntf3 (Pax2-cre; Ntf3$^{f/+}$; Bdnf $^{f/f}$)*

Previous work had demonstrated a limited effect of loss of Bdnf on cochlear innervation but complete loss of canal cristae (Fritzsch et al., 2004; Yang et al., 2011). Consistent with these embryonic data, we find no innervation left to the canal cristae of *Pax2-cre;* Ntf3$^{f/+}$;*Bdnf*$^{f/f}$ (**Figures 2E,E′**). In contrast to the loss of vestibular innervation and a severe reduction of the vestibular ganglion (data not shown) the innervation of the organ of Corti was reduced (**Figures 2F,F′**). Interestingly enough, fewer fibers were present to the basal turn but without the profound loss of all basal turn afferents characteristic for mice null for *Ntf3* (**Figure 2D**). *Bdnf* expression changes from embryonic apical to neonatal basal expression (Flores-Otero et al., 2007) and more profound effects in the basal turn have been noted before in *Pax2-cre; Bdnf*$^{f/f}$ mice (Zuccotti et al., 2012). It appears that heterozygosity of *Ntf3* profoundly compounds the effect of simple loss of *Bdnf*, resulting in reduced innervation of the cochlea (**Figures 2E,F**). This confirms that long term loss of one neurotrophin combined with haploinsufficiency of the second neurotrophin increases innervation defects suggestive of previously proposed simple quantitative compounding effects (Yang et al., 2011). Each of these different combinations of partial Bdnf loss (*Pax2-cre; Ntf3*$^{f/f}$; *Bdnf*$^{f/+}$) or partial *Ntf3* loss (*Pax2-cre;* Ntf3$^{f/+}$; *Bdnf*$^{f/f}$) have clear differences in the remaining innervation (**Figures 2D,F**) pattern, despite the fact that in each case only one of the four neurotrophin alleles remains. We next confirmed the reduction of innervation in the *Pax2-cre; Ntf3*$^{f/+}$; *Bdnf*$^{f/f}$ using immunocytochemistry (**Figure 7A**).

At 4 months the first effects of partial denervation in the basal turn appeared (**Figure 7A**). In fact, at this stage these mice already showed a loss of OHCs that was more obvious compared to a 10 month old control animal (**Figures 7A,B**). Specifically, multiple outer hair cells were missing, mostly in the base. As in other mutants, it appears that OHCs are preferentially missing in the first row compared to the second row (**Figure 7**). There was also some limited effect in IHCs which were less regular in their distribution, making them more difficult to assess by nuclear staining alone. Most of the remaining fibers that traced to OHCs showed features consistent with efferents (**Figure 7A″**). An occasional type II afferent fiber was identified (Simmons et al., 2011).

Our SEM data mostly confirmed previous changes in mutants at a cellular level but also showed surprising longitudinal and radial effects. Most interesting was that stretches of IHCs were missing in the basal turn (**Figure 10B**) of 7 month old mice whereas all IHCs were usually present in the apex (**Figure 10A**).

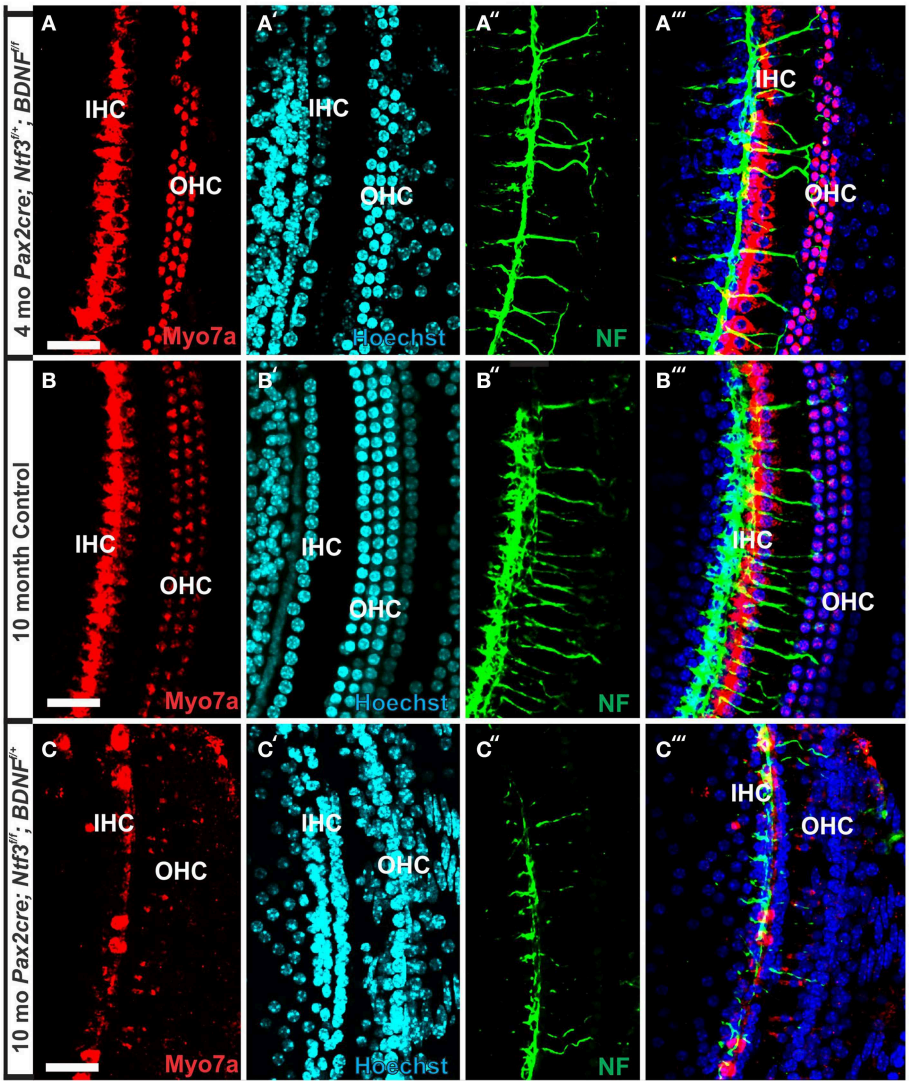

FIGURE 7 | Conditional deletion of *Bdnf* combined with heterozygosity of *Ntf3* using *Pax2-cre* leads to reduced innervation and sporadic OHC loss by 4 months (A″,A‴). In contrast, control littermates have a dense innervation and near continuous rows of IHC/OHCs, revealed with anti-neurofilament staining even at 10 months **(B″)** of the basal part of the middle turn. All remaining HCs stain positive for anti-Myo7a **(A–C)**. Note the regular appearance of HC nuclei with only an occasional OHC missing at this age **(B′)** compared to loss of nuclei in 4 months old partially denervated cochlea **(A′)**. The combined staining shows that nuclei (blue) and HCs (red) are the clear target of the many fibers **(B‴)**. In mutants lacking *Ntf3* and retaining only one allele of *Bdnf*, very few nerve fibers remain **(C″)**, many nuclei of OHC/IHCs are missing or are disorganized **(C′)**. Only few Myo7a positive IHCs or OHCs remain in mutants **(C)** and many have nearly undectable levels of Myo7a labeling **(C,C‴)**. Bar equals100 μm.

There were many losses of HCs in the second and third row of OHCs in the apex whereas the basal turn showed more losses in the first row. In particular, IHCs showed similar phenotypes in terms of fusion of stereocilia as previously encountered in the other mutations of this background (**Figures 10C,C′,C″**). Such fusion and reduced length of stereocilia was also found in OHCs were some cells showed short stereocilia on one side of the cell and only bumps of apparently fused stereocilia on the other side (**Figure 10B**). Overall, the changes in HCs and the pattern of loss with a large reduction in IHCs was similar to the other incompletely denervated mutant line analyzed here.

Mice without *Bdnf* have severe loss of all vestibular innervation at birth (Ernfors et al., 1995) but, in particular, the canal cristae loses all innervation (Fariñas et al., 2001; Fritzsch et al., 2004). Consistent with these known embryonic defects, there was no innervation of canal cristae at any postnatal stage (**Figures 2C′,E′**). Indeed, in 7 month old mutants we found only a limited innervation of the utricle but no innervation of the canal cristae (**Figures 11A′,B′**). There was also a noticeable reduction in size of the posterior canal cristae (**Figures 11C,D**) and the utricle (**Figures 11A,B**). Closer examination showed numerous calyces around type I vestibular hair cells in the control littermates but only a very rare

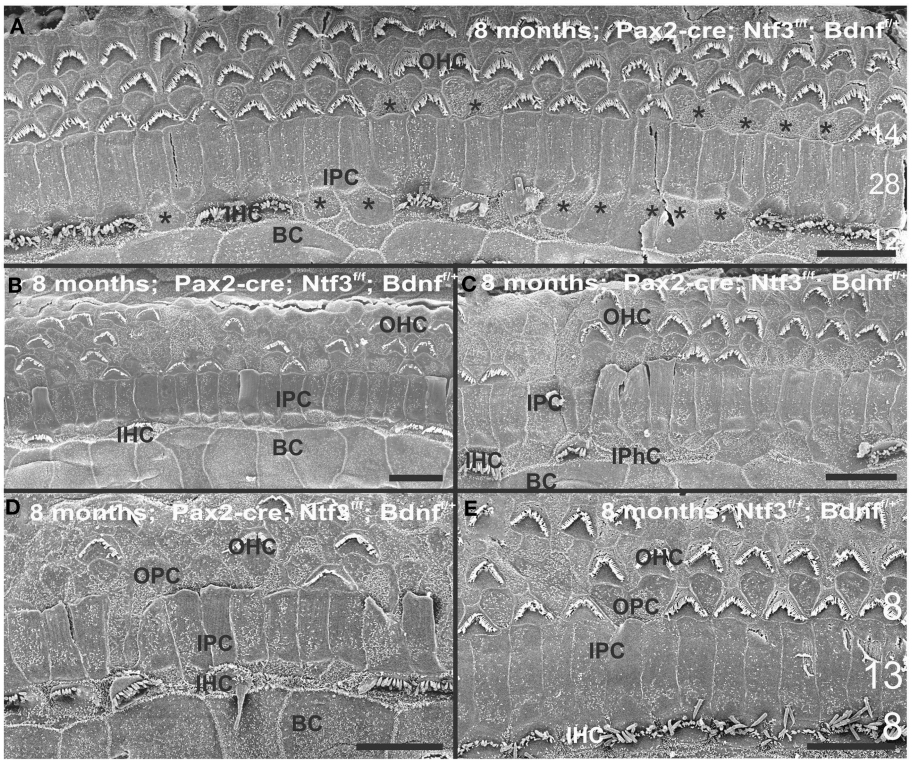

FIGURE 8 | The upper middle turn of an 8 month old *Pax2-cre; Ntf3$^{f/f}$; Bdnf$^{f/+}$* mutant mouse (A–D) is compared with a control littermate (E; no Pax2-cre). Mutant mice lack many OHCs and IHCs, sometimes as single cells and sometimes as partial rows (asterisks in **A**). In contrast, control animals show sporadic loss only of OHCs with a tendency to be more profound in the third row **(E)**. Spaces of lost IHCs are typically filled by medial expansions of IPCs that directly contact border cells (BC) of the inner spiral sulcus (ISS). Lost OHCs of the first row are mostly replaced by expansions of OPCs but sometimes by medial expansions of the first row of Dieter's cells. Due to the loss of OHCs and in particular IHCs, the ratio of IPC:OHC:IHC differs between control (13:8:8) and mutants (14:7:6). Bar indicates 10 μm.

calyx in the mutants (inserts in **Figures 11A″,B″**) consistent with a previous report that calyx formation requires normal Bdnf signaling through the TrkB receptor (Sciarretta et al., 2010).

SEM data also suggested a smaller utricular area compared to the control littermates. Only minor changes were found in HCs such as incomplete stereociliary bundles. However, such changes were difficult to document due to the density of stereocilia in the utricle. However, the posterior canal cristae appeared reduced in size compared to the anterior canal crista (**Figures 11C,D**) and had stretches of hair cells without long stereocilia (**Figure 12D**), consistent with gaps in HCs shown by immunostaining (**Figure 11D**). Some of the HCs in these areas had partially fused stereocilia (**Figures 12F,G**) that were lying flat on the surface of the epithelium (arrows in **Figures 12F,G**). Bundles were composed of stereocilia of uneven size and uneven length. Further quantification is needed to verify how much of the obvious shrinkage is due to loss of calyces and/or due to hair cell loss.

In summary, changes in HCs after partial denervation require at least twice as long to develop compared to complete denervation (**Figure 13**; **Table 1**). The overall changes at the hair cell level are somewhat similar and consist of fusion of stereocilia and shortening, both in IHCs and OHCs (**Figure 13**) and the vestibular epithelia **(Figure 12**). The reorganizations of the remaining supporting cells is more obvious in the organ of Corti and shows medial expansion of IPCs into the territory of lost IHCs and lateral expansion of OPCs into the territory of the lost first row of OHCs. The simple fact that in our mixed background we find profound loss of IHCs even with partial denervation, combined with the unusual phenotypes of reduced Myo7a immunopositivity, and fusion of stereocilia suggests that

TABLE 1 | Percent remaining hair cells quantified from three areas of 200 μm length near the base.

Genotype	% remaining HC 4 months (base)		% remaining HC 7–8 months (base)	
	IHC	OHC	IHC	OHC
Pax2-cre; Ntf3$^{f/f}$; Bdnf$^{f/f}$	44%	8%	na	
Pax2-cre; Ntf3$^{f/f}$; Bdnf$^{f/+}$	na		51%	62%
Pax2-cre; Ntf3$^{f/+}$; Bdnf$^{f/f}$	na		11%	72%
control; Ntf3$^{f/+}$; Bdnf$^{f/+}$	100%	98%	100%	82%

All data are means form 6 ears, except for the 4 months double null mutant that are from a single mutant.

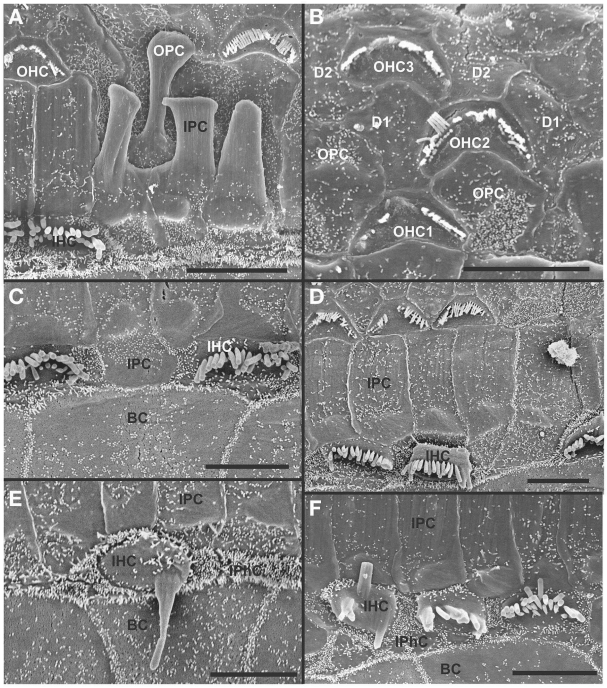

FIGURE 9 | Both OHCs (A,B,D) and IHCs (C–F) show various degrees of resorption and fusion of stereocilia in this 8 month old *Pax2-cre; Ntf3*$^{f/f}$*; Bdnf*$^{f/+}$ as well as patchy loss and locally different degrees of reorganization of supporting cells. IPCs always expand medially to close the reticular lamina over lost IHCs. However, IPCs may either directly contact **(C,D)** border cells (BC) or a layer of cells with numerous short microvilli, presumably inner phalangeal cells (IPhC), may be wedged between IPCs and BCs **(A,E,F)**. OPCs usually expand to complete the reticular lamina if the first row of OHCs is lost **(A)** but sometimes may expand to the second row of OHCs **(B)**. First row Deiter's cells (D1 in **B**) may occasionally expand to close the reticular lamina in places of lost first row of OHCs (OHC1 in **B**). Bar indicates 5 μm.

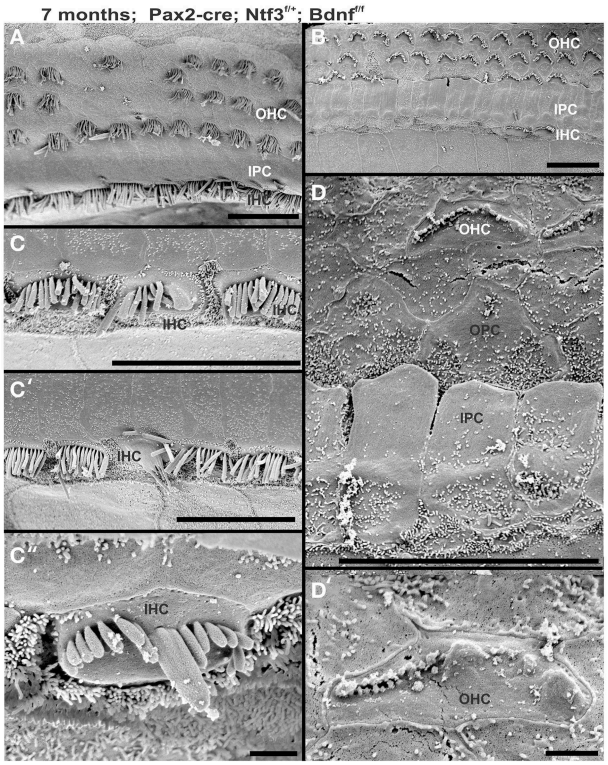

FIGURE 10 | Development of stereocilia and distribution of surviving hair cells is shown in a 7 month old *Pax2-cre; Ntf3*$^{f/+}$*; Bdnf*$^{f/f}$ null mutant mouse. Note that the apex shows a continuous row of IHCs **(A)** whereas the base has large stretches where there is only an occasional IHC left **(B)**. OHCs show loss in either region but the appears is more obvious in the innermost row of OHCs in the base whereas it is more obvious in the two outermost rows in the apex. IHCs show various unusual fusions of stereocilia **(C,C′,C″)** while others adjacent to these fused stereocilia appear normal. The few remaining OHCs in the upper middle turn show very short stereocilia **(D,D′)** if stereocilia are present at all. OHCs may show small bumps instead of stereocilia **(D′)**. Bar indicates 20 μm in **(A–C′)** and 5 μm in **(C″,D′)**.

these effects are mediated by yet to be determined compounds associated with innervation.

Discussion

Denervation Defects HCs

Overall, our data suggest a time line of innervation dependency of cochlear HCs of ∼4–8 months with loss of all OHCs and many IHCs of the basal turn in the absence of any innervation at 4 months (**Figures 3**, **4**, **13**). This is within the same range previously reported for the vestibular HCs after transection of the vestibular nerve without compromising the blood supply (Favre and Sans, 1991). In contrast, in mice, most vestibular HCs require at least 7 months of complete denervation before noticeable changes can be identified (**Figure 12**). The time line of several months of viability of denervated hair cells also agrees with published data on the lateral line mechanosensory cells in salamanders and frogs (Jones and Singer, 1969). Different to these obvious effects on long term maintenance, both *in vitro* and *in vivo* data clearly demonstrate that maturation and short-term survival of inner ear HCs is possible in the complete absence of any innervation (Fritzsch et al., 1998, 2005b). Our data confirm a normal complement of HCs at P12 even when little innervation remains (**Figures 1**, **7**). Contradictory data should be reconsidered in the light of partial and/or difficult to detect remaining innervation and the time lapse between denervation and analysis as well as the time at which denervation is initiated (Sugawara et al., 2005). Loss of hair cells in complete denervation cases should not be dismissed as likely due to blood supply problems (Sugawara et al., 2005; Suzukawa et al., 2005) as blood supply is not an issue in our mutant mice.

Recent data suggest that altered synaptic activity can induce inner ear HC loss over a long period of time (Kidd and Bao, 2012) but does not show a clear overall correlation between loss of HCs and loss of neurons (Perez and Bao, 2011). Most recently physiological defects were found in OHCs after long term efferent disruption (Liberman et al., 2014). The molecular basis of neurotrophic support from sensory epithelia to sensory neurons is well-known (Fritzsch et al., 2004; Bailey and Green,

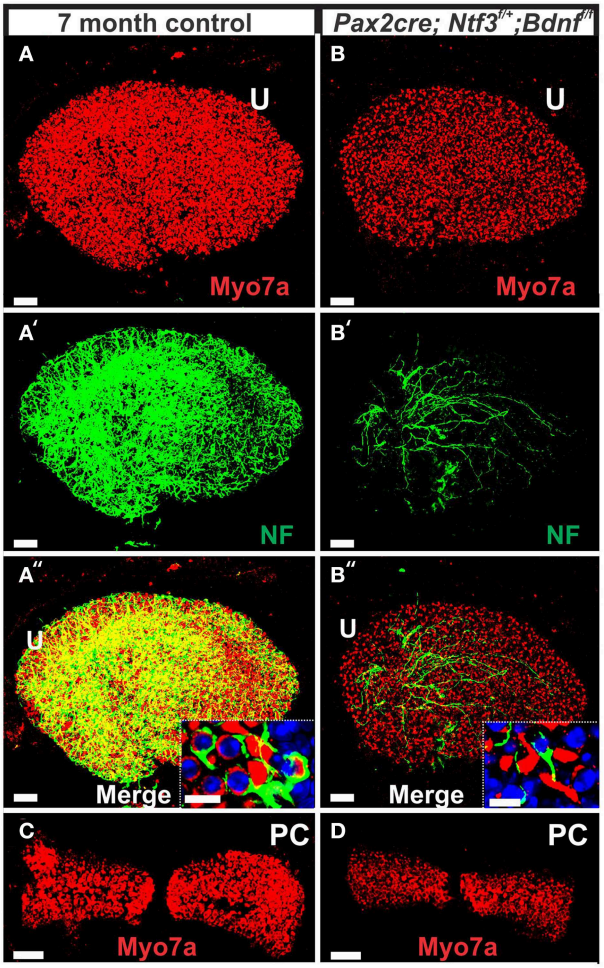

FIGURE 11 | This comparison of 7 months old control mouse vestibular organs (A,C) with a *Pax2-cre; Ntf3*$^{f/+}$*; Bdnf* $^{f/f}$ littermate shows changes in size and innervation density. Hair cells revealed with Myo7a **(A–D)** and their innervation **(A′,A″,B′,B″)** shows smaller sensory epithelia in mice lacking *Bdnf* and one allele of *Ntf3* (*Pax2-cre; Bdnf* $^{f/f}$*; Ntf3*$^{f/+}$) compared to the control littermate. Note that only the utricle (U) receives limited innervation in the mutant **(B′,B″)**. In contrast to the frequent calyces engulfing type I vestibular hair cells (insert in **A″**), mutants have only rare and partial calyces (insert in **B″**). The reduction in size of sensory epithelium is most profound in the posterior canal crista (PC in **C,D**) that is completely denervated and the only epithelium without any innervation throughout development. Bar indicates 50 μm **(A–D)** and 10 μm (inserts).

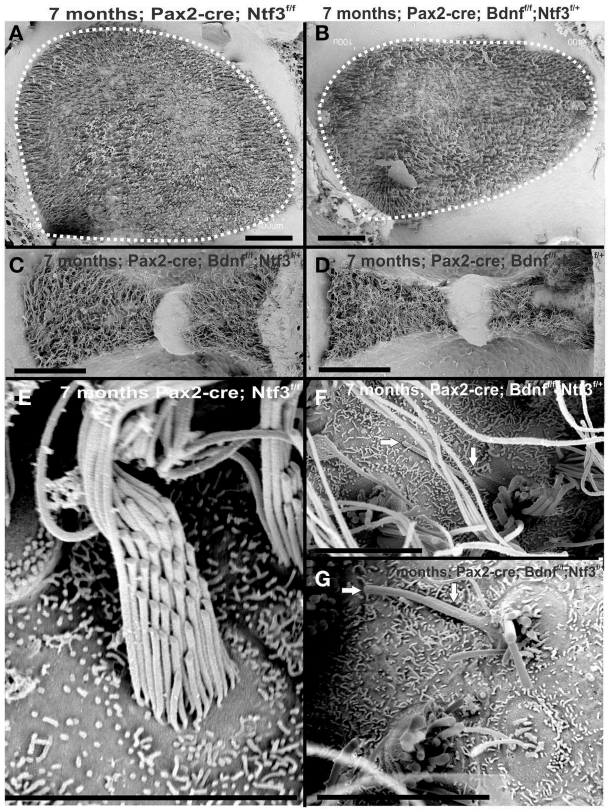

FIGURE 12 | The 7 month old mice lacking *Bdnf* and one allele of *Ntf3* (*Pax2-cre; Bdnf* $^{f/f}$*; Ntf3*$^{f/+}$) by *Pax2-cre* shows reduced size of sensory epithelia most obvious in a comparison of the utricle with that of a control littermate (dotted line in A,B). Interestingly, there is a size difference in the mutant between the anterior canal crista **(C)** and the posterior canal crista **(D)**. While the anterior canal crista is close to the remaining innervation of the utricle in this model and may transiently receive limited innervation, the posterior canal crista is removed from the limited innervation in the basal turn of the cochlea. Vestibular hair cells in the control animal show the normally bundled organization **(E)** whereas many aberrant bundles are found in the hair cells of the posterior canal crista around the "balding" region shown in the right hemicrista **(D,F,G)**. These hair cells show splayed bundles of stereocilia with fused stereocilia, and stereocilia of variable length that occasionally appear to be lying flat on the remaining epithelium (arrows in **F,G**). Bar indicates 50 μm **(A–D)** and 20 μm **(E–G)**.

2014). Neither the molecular basis of afferent support on developing auditory nucleus neurons (Levi-Montalcini, 1949; Rubel and Fritzsch, 2002) nor the molecular basis of innervation on the physiology of HCs (Liberman et al., 2014) or the long term viability of hair cells (**Figure 13**; **Table 1**) is known. The fact that neurons die after embryonic (Pan et al., 2011) or adult HC loss in rodents (Alam et al., 2007) but not in humans (Linthicum and Fayad, 2009) indicates some yet to be molecular defined species-specific differences. Adding to this emerging complexity of adult HC-SGN interactions are recent data on loss of afferent innervation and SGNs after frequent sound exposures that seemingly does not affect HCs (Kujawa and Liberman, 2009), at least not if the neuronal loss spares over 10% of the SGNs (Makary et al., 2011). Evaluating our model in other mammalian species could verify if the effects described here are unique to the genetic background of our conditional deletion mice or can be expanded to other mammals or even humans. Previous work on dependency of cochlear nucleus neurons on innervation shows a profound critical phase and delayed loss of innervation has progressively less effects on cochlear nucleus neuron viability (Rubel and Fritzsch, 2002). Our denervation experiment is certainly earlier and more complete compared to other attempts and our effects could indicate a critical phase of hair cell dependency on innervation. The longer viability of hair cells in partially denervated mice could indicate that targeted deletions of neurotrophins at different time points are needed to exclude other interpretations.

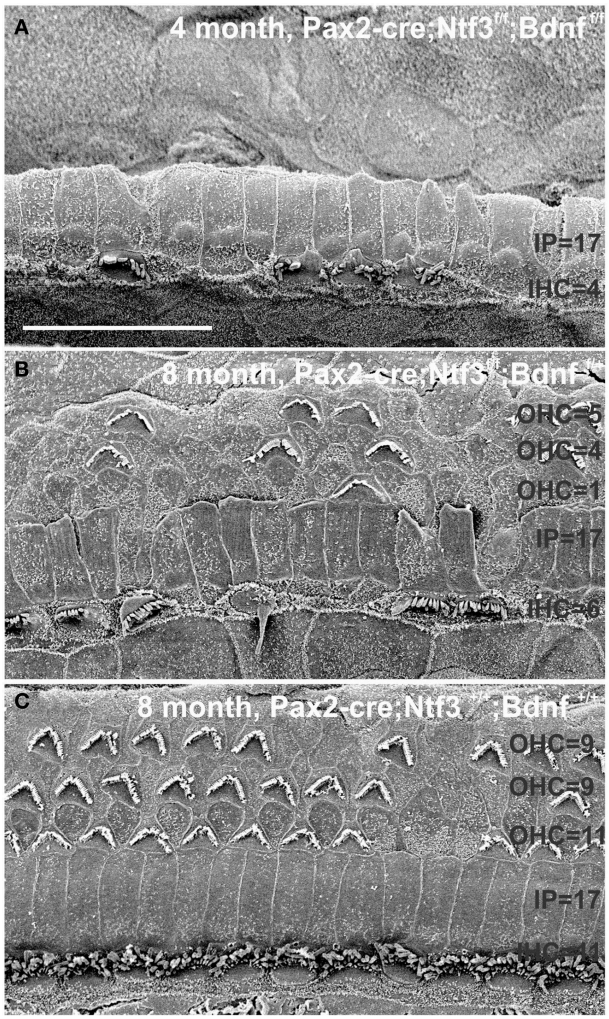

FIGURE 13 | This comparison shows the pertinent differences in complete loss of the entire outer compartment and nearly all OHCs in a 4 month old double neurotrophin conditional null mouse (A) as compared to a 8 month old mutant that retains one allele of *Bdnf* (B) and a 8 month old littermate control (C). Note that all mice have about 17 IPCs but a variable number of HCs. Control littermates retain all IHCs for at least 8 months, forming an approximate 4:3 ratio of IPCs and IHCs **(C)**. This changes to a 4:1 ratio in double null mutants **(A)** and a 3:1 ratio in partially denervated mice **(B)**. Note the variable loss of OHCs that is most profound in the first row in a mutant with incomplete loss of innervation **(B)** whereas it is more profound in the second and third row in control littermates. Bar equals 20 μm.

Available evidence suggests presence of neurotrophin receptors only on neurons (Ylikoski et al., 1993; Fariñas et al., 2001) but delayed expression of limited receptors needs to be verified using appropriate modern techniques to rule out any possible direct effect. Different cre lines such as a combination of Atoh1-cre (Matei et al., 2005) with induced delayed deletion in supporting cells using Fgfr3-creER (Anttonen et al., 2014) could result in more viable mice lacking all inner ear innervation. Another way to achieve denervation without affecting blood supply is by chemical treatment such as ouabain (Yuan et al., 2014). However, in this model type II neurons and efferents remain and HC are sensitive to ouabain (Fu et al., 2012).

Limited Innervation Can Provide Long Term HC Support

Our data and those gathered in other systems (Fritzsch et al., 1998) raise the possibility that compromised neuronal viability provides some feedback for long-term integrity of mechanosensory HCs in the inner ear but apparently with a large time delay, that is even longer with a limited innervation of less than 10%. We base this suggestion on quantification of spiral ganglion neuron loss in *Ntf3* null mice (∼85%) and *Bdnf* null mice (∼7%) that combines to ∼92% loss of SGNs (Bianchi et al., 1996; Fariñas et al., 2001). Assuming that there is a simple additive effect, this suggests that most papers claiming no effect of severe reduction of innervation on hair cell viability need to be revisited to determine exactly how much innervation was left when HCs appear to be normal and at which age all innervation was indeed lost. In addition, as innervation falls below 10% it appears that a very profound time delay exists before HCs are compromised that would be problematic for many studies dealing with mice that show premature age related HC loss. How this support of HCs is distributed between efferents and afferents remains to be elucidated but data on other sensory systems without efferents clearly point out the importance of afferents (Fritzsch et al., 1990). In fact, the unusual feature of our model is the effect on IHCs which receive only transient innervation during development and in certain circumstances in the adult system (Simmons et al., 2011; Lauer et al., 2012). Therefore, for IHCs, it appears likely that their high density of afferent innvervation plays a major role (Fritzsch et al., 2015). Such an interpretation is consistent with the preferential IHC loss in our models with diminished innervation. The apparent preferential loss of the first row of outer hair cells could relate to the difference in innervation density between IHCs and OHCs, assuming that afferents release a diffusible factor that can reach a short distance comparable to neurotrophins (Fritzsch et al., 2004).

Reconciling Literature Discrepancies

Cutting the cochlear nerve has led to contradictory, variable and inconclusive data (Sugawara et al., 2005) possibly due to a difficult mix of surgery related blood supply disturbance and incomplete elimination of all innervation, differences between experimental animals and the possible effect of a critical phase of HCs on innervation. We reason that all these data could be reconciled if it could be established that mechanosensory HCs of the ear depend on a yet to be defined critical threshold of afferent and efferent innervation during a critical phase, comparable to other sensory cells (Fritzsch et al., 1998) and cochlear nucleus neurons (Rubel and Fritzsch, 2002). However, neuronal dependency may take a longer time to manifest itself in the case of mechanosensory HCs of the ear compared to other sensory systems (Favre and Sans, 1991) but is comparable in its timeline to the mechanosensory lateral line system (Jones and Singer, 1969). Consistent with our anatomical data, long-term viability (Walsh et al., 1998) and function of outer hair cells (OHCs) might depend on efferent innervation (Liberman et al., 2014), whereas minor alterations

in synaptic transmission may affect viability of inner hair cells (IHCs) exposed to loud sound (Zuccotti et al., 2012). Ideally, one would like to eliminate a neurotrophic factor (Lindholm and Saarma, 2010; Bailey and Green, 2014) to show effects we describe here in the presence of innervation, comparable to the loss of spiral ganglion cells in neurotrophin mutants in the presence of hair cells (Fritzsch et al., 2004) to verify the nature of this molecule (or molecules). Whether such molecules could also be the basis for the unknown support of developing cochlear nucleus neurons (Levi-Montalcini, 1949; Rubel and Fritzsch, 2002) remains to be seen.

Partial Denervation May Aid in the Study of Age-related HC Loss

This mouse model, with no or with greatly diminished innervation, allows us to test the hypothesis that cochlear HCs depend on innervation but have a different time constant compared to other sensory systems and that vestibular HCs are even more resilient. Unfortunately, our partially denervated model is more difficult to interpret. There is a well-known dependency of cochlear innervation on support provided by the normally developed organ of Corti (Bailey and Green, 2014). This support will obviously decline as the organ of Corti dedifferentiates upon loss of HCs (Alam et al., 2007; Pan et al., 2011, 2012). It is possible that additional loss of innervation due to loss of HCs may accelerate regionally specific HC loss (a possible negative feedback loop). However, this is of no concern for the general problem investigated here, namely that mechanosensory HCs depend on a limited level of innervation for long-term viability. Such feedback loops have not been apparent in previous work simply because the loss of neurons in most cases studied over long periods is far less (Makary et al., 2011) compared to our presumed 93–100% loss of neurons. Only sparing HC loss has been reported after efferent deletion (Walsh et al., 1998), in contrast to our massive loss of HCs within 4 months after all afferents and efferents have been deleted (**Figure 13**). More recent work has suggested the existence of such a feedback loop regulating functionality of OHCs after complete elimination of efferents (Liberman et al., 2014). Unfortunately efferents depend on afferents for homing (Simmons et al., 2011) and thus early afferent loss will result in efferent loss as well. Our model thus cannot easily distinguish between afferent and efferent long term support.

Comparison to Models of Induced HC Loss

Overall, the loss of hair cells and reorganizations of the organ of Corti to eventually turn into a flat epithelium presented here follows, to a large extent, changes observed after aminoglycoside treatment (Taylor et al., 2012, 2008). However, while hair cells are lost rapidly after aminoglycoside treatment (Taylor et al., 2008) or carboplatin treatment (Ding et al., 2012) it takes weeks to months (depending on the mouse line) for the organ of Corti to reorganize (Taylor et al., 2012). In the case of complete denervation, we see progression of HC loss and reorganization over several months with profound local variation. Our data suggest that there is a correlation with changes in Myo7a expression (**Figure 7**) and fusion or resorption of stereocilia (**Figure 9**) that resembles the degeneration of HCs in Myo7a mutant mice (Self et al., 1998). This similarity is even more profound in Myo6 mutants that show fusion of stereocilia of IHCs and OHCs (Self et al., 1999; Hertzano et al., 2008) remarkably similar to our data (**Figures 5**, **9**, **10**, **12**). Conditional deletion of Cdc42 leads preferentially to IHC loss through stereocilia fusion (Ueyama et al., 2014) that is nearly identical to mice with incomplete denervation. However, while Cdc42 mice lose IHCs after 8 weeks, IHCs take over 4 months to degenerate even in completely denervated mice. It remains unclear if this correlation indicates some causality. If so, it could indicate that altered expression of Myo6, Cdc42 and other proteins associated with stereocilia homeostasis (Kitajiri et al., 2010; Sekerková et al., 2011) could underlie not only innervation dependent hair cell maintenance but may play a role in age dependent, variable loss of HCs through interference with the stereocilia homeostasis (Lenz et al., 2010). Like age dependent HC loss (Otte et al., 1978; Keithley and Feldman, 1982; Wright et al., 1986), loss of HCs in our model is highly variable with rather different time lines for individual HCs that is even more different with residual presence of some innervation. Combined, our data strongly support the conclusion of local variability of effects after aminoglycoside treatment (Taylor et al., 2012) and support the argument raised by Taylor et al. (2012) that attempts to regenerate an organ of Corti requires a close look at this variability of local effects. Given the variable residual presence of IPCs, IPhCs or nothing, strategies must be designed to take the local variations in supporting cell viability into account when attempting to restore a functional organ of Corti. Our data support the notion of molecular uniqueness and independence of IPCs (Fritzsch et al., 2015) that have been shown to survive long term in other molecular models of HC loss (Pauley et al., 2008) as well as in our model (**Figure 13**).

Translational Aspects

Previous work has shown that subcritical sound levels can result in long-term loss of some innervation (Kujawa and Liberman, 2009). It is possible that such retraction of nerve fibers is accelerated through compromised neurotrophin signaling (Wang and Green, 2011), accelerating additional loss of innervation caused by sound. Such a possible loop can eventually result in loss of HCs as consequences of mutation related to reduced signaling of neurotrophins or other molecules such as Igf-1 (Varela-Nieto et al., 2013) combined with reduced density of innervation. Given our data and those after aminoglycoside treatment that indicate profound local variations (Taylor et al., 2012), any treatment of the aging human cochlea to retain HCs or restore the organ of Corti needs to take local variation into account. This model could be used to develop expression profiles of remaining HCs to eventually identify genes (Liu et al., 2014) responsible for their viability focusing on interactions between Cdc42 and Myo6, the two mutants (Self et al., 1999; Ueyama et al., 2014) that have the greatest similarities with our denervation hair cell phenotype. Ultimately, we would need to identify the molecular basis of the neuronal signal to generate small molecular analogs to rescue HCs in the absence of innervation. Several candidate trophic factors exist (Bailey and

Green, 2014), some with unknown function or expression in the ear such as MANF (Lindholm and Saarma, 2010). Such molecules could possibly enhance viability of innervated HCs, rescuing them for longer periods to provide the growing aging population of the world with functional HCs for hearing and balance.

Acknowledgments

This work was supported by a base grant from NASA, a P30 from NIH and the office of the Provost of the University of Iowa. The authors wish to thank Dr. Andrew Forge for valuable comments and suggestions that helped improve an earlier version.

References

Alam, S. A., Robinson, B. K., Huang, J., and Green, S. H. (2007). Prosurvival and proapoptotic intracellular signaling in rat spiral ganglion neurons *in vivo* after the loss of hair cells. *J. Comp. Neurol.* 503, 832–852. doi: 10.1002/cne.21430

Anttonen, T., Belevich, I., Kirjavainen, A., Laos, M., Brakebusch, C., Jokitalo, E., et al. (2014). How to bury the dead: elimination of apoptotic hair cells from the hearing organ of the mouse. *J. Assoc. Res. Otolaryngol.* 15, 975–992. doi: 10.1007/s10162-014-0480-x

Bailey, E. M., and Green, S. H. (2014). Postnatal expression of neurotrophic factors accessible to spiral ganglion neurons in the auditory system of adult hearing and deafened rats. *J. Neurosci.* 34, 13110–13126. doi: 10.1523/JNEUROSCI.1014-14.2014

Bates, B., Rios, M., Trumpp, A., Chen, C., Fan, G., Bishop, J. M., et al. (1999). Neurotrophin-3 is required for proper cerebellar development. *Nat. Neurosci.* 2, 115–117. doi: 10.1038/5669

Bianchi, L. M., Conover, J. C., Fritzsch, B., DeChiara, T., Lindsay, R. M., and Yancopoulos, G. D. (1996). Degeneration of vestibular neurons in late embryogenesis of both heterozygous and homozygous BDNF null mutant mice. *Development* 122, 1965–1973.

Ding, D., Allman, B. L., and Salvi, R. (2012). Review: ototoxic characteristics of platinum antitumor drugs. *Anat. Rec.* 295, 1851–1867. doi: 10.1002/ar.22577

Duncan, J., Kersigo, J., Gray, B., and Fritzsch, B. (2011). Combining lipophilic dye, *in situ* hybridization, immunohistochemistry, and histology. *J. Vis. Exp.* 49:2451. doi: 10.3791/2451

Duncan, J. S., and Fritzsch, B. (2012). Evolution of sound and balance perception: innovations that aggregate single hair cells into the ear and transform a gravistatic sensor into the organ of corti. *Anat. Rec.* 295, 1760–1774. doi: 10.1002/ar.22573

Ernfors, P., Van De Water, T., Loring, J., and Jaenisch, R. (1995). Complementary roles of BDNF and NT-3 in vestibular and auditory development. *Neuron* 14, 1153–1164. doi: 10.1016/0896-6273(95)90263-5

Farbman, A. I. (2003). Neurotrophins and taste buds. *J. Comp. Neurol.* 459, 9–14. doi: 10.1002/cne.10588

Fariñas, I., Jones, K. R., Tessarollo, L., Vigers, A. J., Huang, E., Kirstein, M., et al. (2001). Spatial shaping of cochlear innervation by temporally regulated neurotrophin expression. *J. Neurosci.* 21, 6170–6180.

Favre, D., and Sans, A. (1991). Dedifferentiation phenomena after denervation of mammalian adult vestibular receptors. *Neuroreport* 2, 501–504. doi: 10.1097/00001756-199109000-00001

Fei, D., Huang, T., and Krimm, R. F. (2014). The neurotrophin receptor p75 regulates gustatory axon branching and promotes innervation of the tongue during development. *Neural Dev.* 9:15. doi: 10.1186/1749-8104-9-15

Flores-Otero, J., Xue, H. Z., and Davis, R. L. (2007). Reciprocal regulation of presynaptic and postsynaptic proteins in bipolar spiral ganglion neurons by neurotrophins. *J. Neurosci.* 27, 14023–14034. doi: 10.1523/JNEUROSCI.3219-07.2007

Fritzsch, B., Barbacid, M., and Silos-Santiago, I. (1998). Nerve dependency of developing and mature sensory receptor cells. *Ann. N.Y. Acad. Sci.* 855, 14–27. doi: 10.1111/j.1749-6632.1998.tb10543.x

Fritzsch, B., Matei, V. A., Nichols, D. H., Bermingham, N., Jones, K., Beisel, K. W., et al. (2005b). Atoh1 null mice show directed afferent fiber growth to undifferentiated ear sensory epithelia followed by incomplete fiber retention. *Dev. Dyn.* 233, 570–583. doi: 10.1002/dvdy.20370

Fritzsch, B., Muirhead, K. A., Feng, F., Gray, B. D., and Ohlsson-Wilhelm, B. M. (2005a). Diffusion and imaging properties of three new lipophilic tracers, NeuroVue(TM) Maroon, NeuroVue(TM) Red and NeuroVue(TM) Green and their use for double and triple labeling of neuronal profile. *Brain Res. Bull.* 66, 249–258. doi: 10.1016/j.brainresbull.2005.05.016

Fritzsch, B., Pan, N., Jahan, I., and Elliott, K. L. (2015). Inner ear development: building a spiral ganglion and an organ of Corti out of unspecified ectoderm. *Cell Tissue Res.* 384, 1–18. doi: 10.1007/s00441-014-2031-5

Fritzsch, B., Sarai, P. A., Barbacid, M., and Silos-Santiago, I. (1997b). Mice with a targeted disruption of the neurotrophin receptor trkB lose their gustatory ganglion cells early but do develop taste buds. *Int. J. Dev. Neurosci.* 15, 563–576. doi: 10.1016/S0736-5748(96)00111-6

Fritzsch, B., Silos-Santiago, I., Bianchi, L. M., and Farinas, I. (1997a). Effects of neurotrophin and neurotrophin receptor disruption on the afferent inner ear innervation. *Semin. Cell Dev. Biol.* 8, 277–284. doi: 10.1006/scdb.1997.0144

Fritzsch, B., Tessarollo, L., Coppola, E., and Reichardt, L. F. (2004). Neurotrophins in the ear: their roles in sensory neuron survival and fiber guidance. *Prog. Brain Res.* 146, 265–278. doi: 10.1016/S0079-6123(03)46017-2

Fritzsch, B., Zakon, H. H., and Sanchez, D. Y. (1990). Time course of structural changes in regenerating electroreceptors of a weakly electric fish. *J. Comp. Neurol.* 300, 386–404. doi: 10.1002/cne.903000309

Fu, Y., Ding, D., Jiang, H., and Salvi, R. (2012). Ouabain-induced cochlear degeneration in rat. *Neurotox. Res.* 22, 158–169. doi: 10.1007/s12640-012-9320-0

Gorski, J. A., Zeiler, S. R., Tamowski, S., and Jones, K. R. (2003). Brain-derived neurotrophic factor is required for the maintenance of cortical dendrites. *J. Neurosci.* 23, 6856–6865.

Hertzano, R., Shalit, E., Rzadzinska, A. K., Dror, A. A., Song, L., Ron, U., et al. (2008). A Myo6 mutation destroys coordination between the myosin heads, revealing new functions of myosin VI in the stereocilia of mammalian inner ear hair cells. *PLoS Genet.* 4:e1000207. doi: 10.1371/journal.pgen.1000207

Huisman, M. A., and Rivolta, M. N. (2012). Neural crest stem cells and their potential application in a therapy for deafness. *Front. Biosci.* 4, 121–132. doi: 10.2741/S255

Ito, A., Nosrat, I. V., and Nosrat, C. A. (2010). Taste cell formation does not require gustatory and somatosensory innervation. *Neurosci. Lett.* 471, 189–194. doi: 10.1016/j.neulet.2010.01.039

Izumikawa, M., Batts, S. A., Miyazawa, T., Swiderski, D. L., and Raphael, Y. (2008). Response of the flat cochlear epithelium to forced expression of *Atoh1*. *Hear. Res.* 240, 52–56. doi: 10.1016/j.heares.2008.02.007

Jahan, I., Pan, N., Kersigo, J., and Fritzsch, B. (2010). Neurod1 suppresses hair cell differentiation in ear ganglia and regulates hair cell subtype development in the cochlea. *PLoS ONE* 5:e11661. doi: 10.1371/journal.pone.0011661

Jahan, I., Pan, N., Kersigo, J., and Fritzsch, B. (2013). Beyond generalized hair cells: molecular cues for hair cell types. *Hear. Res.* 297, 30–41. doi: 10.1016/j.heares.2012.11.008

Jones, D. P., and Singer, M. (1969). Neurotrophic dependence of the lateral-line sensory organs of the newt, Triturus viridescens. *J. Exp. Zool.* 171, 433–442. doi: 10.1002/jez.1401710408

Keithley, E. M., and Feldman, M. L. (1982). Hair cell counts in an age-graded series of rat cochleas. *Hear. Res.* 8, 249–262. doi: 10.1016/0378-5955(82)90017-X

Kidd, A. R. III, and Bao, J. (2012). Recent advances in the study of age-related hearing loss: a mini-review. *Gerontology* 58, 490–496. doi: 10.1159/000338588

Kitajiri, S.-I., Sakamoto, T., Belyantseva, I. A., Goodyear, R. J., Stepanyan, R., Fujiwara, I., et al. (2010). Actin-bundling protein TRIOBP forms resilient rootlets of hair cell stereocilia essential for hearing. *Cell* 141, 786–798. doi: 10.1016/j.cell.2010.03.049

Kopecky, B., and Fritzsch, B. (2011). Regeneration of hair cells: making sense of all the noise. *Pharmaceuticals* 4, 848–879. doi: 10.3390/ph4060848

Kujawa, S. G., and Liberman, M. C. (2009). Adding insult to injury: cochlear nerve degeneration after "temporary" noise-induced hearing loss. *J. Neurosci.* 29, 14077–14085. doi: 10.1523/JNEUROSCI.2845-09.2009

Lauer, A. M., Fuchs, P. A., Ryugo, D. K., and Francis, H. W. (2012). Efferent synapses return to inner hair cells in the aging cochlea. *Neurobiol. Aging* 33, 2892–2902. doi: 10.1016/j.neurobiolaging.2012.02.007

Lenz, M., Prost, J., and Joanny, J. F. (2010). Actin cross-linkers and the shape of stereocilia. *Biophys. J.* 99, 2423–2433. doi: 10.1016/j.bpj.2010.07.065

Levi-Montalcini, R. (1949). The development of the acoustico—vestibular centres in the chick embryo in the absence of the afferent root fibers and of descending fiber tracts. *J. Comp. Neurol.* 91, 209–241. doi: 10.1002/cne.900910204

Liberman, M. C., Liberman, L. D., and Maison, S. F. (2014). Efferent feedback slows cochlear aging. *J. Neurosci.* 34, 4599–4607. doi: 10.1523/JNEUROSCI.4923-13.2014

Lin, F. R., and Albert, M. (2014). Hearing loss and dementia–who is listening? *Aging Ment. Health* 18, 671–673. doi: 10.1080/13607863.2014.915924

Lin, F. R., Yaffe, K., Xia, J., Xue, Q. L., Harris, T. B., Purchase-Helzner, E., et al. (2013). Hearing loss and cognitive decline in older adults. *JAMA Intern. Med.* 173, 293–299. doi: 10.1001/jamainternmed.2013.1868

Lindholm, P., and Saarma, M. (2010). Novel CDNF/MANF family of neurotrophic factors. *Dev. Neurobiol.* 70, 360–371. doi: 10.1002/dneu.20760

Linthicum, F. H. Jr., and Fayad, J. N. (2009). Spiral ganglion cell loss is unrelated to segmental cochlear sensory system degeneration in humans. *Otol. Neurotol.* 30, 418–422. doi: 10.1097/MAO.0b013e31819a8827

Liu, H., Pecka, J. L., Zhang, Q., Soukup, G. A., Beisel, K. W., and He, D. Z. (2014). Characterization of transcriptomes of cochlear inner and outer hair cells. *J. Neurosci.* 34, 11085–11095. doi: 10.1523/JNEUROSCI.1690-14.2014

López-Otín, C., Blasco, M. A., Partridge, L., Serrano, M., and Kroemer, G. (2013). The hallmarks of aging. *Cell* 153, 1194–1217. doi: 10.1016/j.cell.2013.05.039

Ma, Q., Anderson, D. J., and Fritzsch, B. (2000). Neurogenin 1 null mutant ears develop fewer, morphologically normal hair cells in smaller sensory epithelia devoid of innervation. *J. Assoc. Res. Otolaryngol.* 1, 129–143. doi: 10.1007/s101620010017

Makary, C. A., Shin, J., Kujawa, S. G., Liberman, M. C., and Merchant, S. N. (2011). Age-related primary cochlear neuronal degeneration in human temporal bones. *J. Assoc. Res. Otolaryngol.* 12, 711–717. doi: 10.1007/s10162-011-0283-2

Maricich, S. M., Xia, A., Mathes, E. L., Wang, V. Y., Oghalai, J. S., Fritzsch, B., et al. (2009). Atoh1-lineal neurons are required for hearing and for the survival of neurons in the spiral ganglion and brainstem accessory auditory nuclei. *J. Neurosci.* 29, 11123–11133. doi: 10.1523/JNEUROSCI.2232-09.2009

Matei, V., Pauley, S., Kaing, S., Rowitch, D., Beisel, K., Morris, K., et al. (2005). Smaller inner ear sensory epithelia in Neurog1 null mice are related to earlier hair cell cycle exit. *Dev. Dyn.* 234, 633–650. doi: 10.1002/dvdy.20551

Northcutt, R. G., Brandle, K., and Fritzsch, B. (1995). Electroreceptors and mechanosensory lateral line organs arise from single placodes in axolotls. *Dev. Biol.* 168, 358–373. doi: 10.1006/dbio.1995.1086

Ohyama, T., and Groves, A. K. (2004). Generation of Pax2-Cre mice by modification of a Pax2 bacterial artificial chromosome. *Genesis* 38, 195–199. doi: 10.1002/gene.20017

Okubo, T., Clark, C., and Hogan, B. L. (2009). Cell lineage mapping of taste bud cells and keratinocytes in the mouse tongue and soft palate. *Stem Cells* 27, 442–450. doi: 10.1634/stemcells.2008-0611

Okubo, T., Pevny, L. H., and Hogan, B. L. (2006). Sox2 is required for development of taste bud sensory cells. *Genes Dev.* 20, 2654–2659. doi: 10.1101/gad.1457106

Otte, J., Schuknecht, H. F., and Kerr, A. G. (1978). Ganglion cell populations in normal and pathological human cochleae. Implications for cochlear implantation. *Laryngoscope* 88, 1231–1246. doi: 10.1288/00005537-197808000-00002

Pan, N., Jahan, I., Kersigo, J., Duncan, J. S., Kopecky, B., and Fritzsch, B. (2012). A novel Atoh1 "self-terminating" mouse model reveals the necessity of proper Atoh1 level and duration for hair cell differentiation and viability. *PLoS ONE* 7:e30358. doi: 10.1371/journal.pone.0030358

Pan, N., Jahan, I., Kersigo, J., Kopecky, B., Santi, P., Johnson, S., et al. (2011). Conditional deletion of Atoh1 using Pax2-Cre results in viable mice without differentiated cochlear hair cells that have lost most of the organ of Corti. *Hear. Res.* 275, 66–80. doi: 10.1016/j.heares.2010.12.002

Pauley, S., Kopecky, B., Beisel, K., Soukup, G., and Fritzsch, B. (2008). Stem cells and molecular strategies to restore hearing. *Panminerva Med.* 50, 41–53.

Perez, P., and Bao, J. (2011). Why do hair cells and spiral ganglion neurons in the cochlea die during aging? *Aging Dis.* 2, 231–241.

Postigo, A., Calella, A. M., Fritzsch, B., Knipper, M., Katz, D., Eilers, A., et al. (2002). Distinct requirements for TrkB and TrkC signaling in target innervation by sensory neurons. *Genes Dev.* 16, 633–645. doi: 10.1101/gad.217902

Rauch, S. D. (2001). Vestibular histopathology of the human temporal bone. What can we learn? *Ann. N.Y. Acad. Sci.* 942, 25–33. doi: 10.1111/j.1749-6632.2001.tb03732.x

Retzius, G. (1884). *Das Gehörorgan der Wirbeltiere, Band 2: Das Gehörorgan der Reptilien, der Vögel und der Säugetiere*. Stockholm: Samson & Wallin.

Rivolta, M. N. (2013). New strategies for the restoration of hearing loss: challenges and opportunities. *Br. Med. Bull.* 105, 69–84. doi: 10.1093/bmb/lds035

Rubel, E. W., and Fritzsch, B. (2002). Auditory system development: primary auditory neurons and their targets. *Annu. Rev. Neurosci.* 25, 51–101. doi: 10.1146/annurev.neuro.25.112701.142849

Sciarretta, C., Fritzsch, B., Beisel, K., Rocha-Sanchez, S. M., Buniello, A., Horn, J. M., et al. (2010). PLCγ-activated signalling is essential for TrkB mediated sensory neuron structural plasticity. *BMC Dev. Biol.* 10:103. doi: 10.1186/1471-213X-10-103

Sekerková, G., Richter, C.-P., and Bartles, J. R. (2011). Roles of the espin actin-bundling proteins in the morphogenesis and stabilization of hair cell stereocilia revealed in CBA/CaJ congenic jerker mice. *PLoS Genet.* 7:e1002032. doi: 10.1371/journal.pgen.1002032

Self, T., Mahony, M., Fleming, J., Walsh, J., Brown, S., and Steel, K. P. (1998). Shaker-1 mutations reveal roles for myosin VIIA in both development and function of cochlear hair cells. *Development* 125, 557–566.

Self, T., Sobe, T., Copeland, N. G., Jenkins, N. A., Avraham, K. B., and Steel, K. P. (1999). Role of myosin VI in the differentiation of cochlear hair cells. *Dev. Biol.* 214, 331–341. doi: 10.1006/dbio.1999.9424

Silos-Santiago, I., Fagan, A. M., Garber, M., Fritzsch, B., and Barbacid, M. (1997). Severe sensory deficits but normal CNS development in newborn mice lacking TrkB and TrkC tyrosine protein kinase receptors. *Eur. J. Neurosci.* 9, 2045–2056. doi: 10.1111/j.1460-9568.1997.tb01372.x

Simmons, D., Duncan, J., de Caprona, D. C., and Fritzsch, B. (2011). "Development of the inner ear efferent system," in *Auditory and Vestibular Efferents*, eds D. K. Ryugo, R. R. Fay, and A. N. Popper (New York, NY: Springer), 187–216. doi: 10.1007/978-1-4419-7070-1

Sugawara, M., Corfas, G., and Liberman, M. C. (2005). Influence of supporting cells on neuronal degeneration after hair cell loss. *J. Assoc. Res. Otolaryngol.* 6, 136–147. doi: 10.1007/s10162-004-5050-1

Suzukawa, K., Yamasoba, T., Tsuzuku, T., and Kaga, K. (2005). Are vestibular sensory cells preserved after destruction of Scarpa's ganglion? A study based on metastatic tumors of temporal bone. *Otol. Neurotol.* 26, 1191–1195. doi: 10.1097/01.mao.0000194889.44023.30

Taylor, R. R., Jagger, D. J., and Forge, A. (2012). Defining the cellular environment in the organ of Corti following extensive hair cell loss: a basis for future sensory cell replacement in the Cochlea. *PLoS ONE* 7:e30577. doi: 10.1371/journal.pone.0030577

Taylor, R. R., Nevill, G., and Forge, A. (2008). Rapid hair cell loss: a mouse model for cochlear lesions. *J. Assoc. Res. Otolaryngol.* 9, 44–64. doi: 10.1007/s10162-007-0105-8

Tonniges, J., Hansen, M., Duncan, J., Bassett, M. J., Fritzsch, B., Gray, B. D., et al. (2010). Photo- and bio-physical characterization of novel violet and near-infrared lipophilic fluorophores for neuronal tracing. *J. Microsc.* 239, 117–134. doi: 10.1111/j.1365-2818.2009.03363.x

Ueyama, T., Sakaguchi, H., Nakamura, T., Goto, A., Morioka, S., Shimizu, A., et al. (2014). Maintenance of stereocilia and apical junctional complexes by Cdc42 in cochlear hair cells. *J. Cell Sci.* 127, 2040–2052. doi: 10.1242/jcs.143602

Varela-Nieto, I., Murillo-Cuesta, S., Rodriguez-de la Rosa, L., Lassatetta, L., and Contreras, J. (2013). IGF-I deficiency and hearing loss: molecular clues and clinical implications. *Pediatr. Endocrinol. Rev.* 10, 460–472.

Walsh, E. J., McGee, J., McFadden, S. L., and Liberman, M. C. (1998). Long-term effects of sectioning the olivocochlear bundle in neonatal cats. *J. Neurosci.* 18, 3859–3869.

Wang, Q., and Green, S. H. (2011). Functional role of neurotrophin-3 in synapse regeneration by spiral ganglion neurons on inner hair cells after excitotoxic trauma *in vitro*. *J. Neurosci.* 31, 7938–7949. doi: 10.1523/JNEUROSCI.1434-10.2011

Wright, A., Davis, A., Bredberg, G., Ulehlova, L., and Spencer, H. (1986). Hair cell distributions in the normal human cochlea. Acta oto-laryngologica. *Supplementum* 444, 1–48.

Yamasoba, T., Lin, F. R., Someya, S., Kashio, A., Sakamoto, T., and Kondo, K. (2013). Current concepts in age-related hearing loss: epidemiology and mechanistic pathways. *Hear. Res.* 303, 30–38. doi: 10.1016/j.heares.2013.01.021

Yang, T., Kersigo, J., Jahan, I., Pan, N., and Fritzsch, B. (2011). The molecular basis of making spiral ganglion neurons and connecting them to hair cells of the organ of Corti. *Hear. Res.* 278, 21–33. doi: 10.1016/j.heares.2011.03.002

Ylikoski, J., Pirvola, U., Moshnyakov, M., Palgi, J., Arumäe, U., and Saarma, M. (1993). Expression patterns of neurotrophin and their receptor mRNAs in the rat inner ear. *Hear. Res.* 65, 69–78. doi: 10.1016/0378-5955(93)90202-C

Yuan, Y., Shi, F., Yin, Y., Tong, M., Lang, H., Polley, D. B., et al. (2014). Ouabain-induced cochlear nerve degeneration: synaptic loss and plasticity in a mouse model of auditory neuropathy. *J. Assoc. Res. Otolaryngol.* 15, 31–43. doi: 10.1007/s10162-013-0419-7

Zilberstein, Y., Liberman, M. C., and Corfas, G. (2012). Inner hair cells are not required for survival of spiral ganglion neurons in the adult cochlea. *J. Neurosci.* 32, 405–410. doi: 10.1523/JNEUROSCI.4678-11.2012

Zuccotti, A., Kuhn, S., Johnson, S. L., Franz, C., Singer, W., Hecker, D., et al. (2012). Lack of brain-derived neurotrophic factor hampers inner hair cell synapse physiology, but protects against noise-induced hearing loss. *J. Neurosci.* 32, 8545–8553. doi: 10.1523/JNEUROSCI.1247-12.2012

Conflict of Interest Statement: The authors declare that the research was conducted in the absence of any commercial or financial relationships that could be construed as a potential conflict of interest.

frontiers in
AGING NEUROSCIENCE

MINI REVIEW ARTICLE
published: 05 February 2015
doi: 10.3389/fnagi.2015.00008

Cochlear injury and adaptive plasticity of the auditory cortex

Anna Rita Fetoni[1], Diana Troiani[2]*, Laura Petrosini[3] and Gaetano Paludetti[1]

[1] *Department of Head and Neck Surgery, Medical School, Catholic University of the Sacred Heart, Rome, Italy*
[2] *Institute of Human Physiology, Medical School, Catholic University of the Sacred Heart, Rome, Italy*
[3] *Department of Psychology, Sapienza University of Rome and IRCCS Santa Lucia Foundation, Rome, Italy*

Edited by:
Isabel Varela-Nieto, Consejo Superior de Investigaciones Científicas, Spain

Reviewed by:
Veronica Fuentes, University of Castilla-La Mancha, Spain
Maria E. Rubio, University of Pittsburgh, USA
Jiri Popelar, Academy of Sciences of the Czech Republic, Czech Republic

***Correspondence:**
Diana Troiani, Institute of Human Physiology, Medical School, Università Cattolica, Largo Francesco Vito 1, Rome 00168, Italy
e-mail: d.troiani@rm.unicatt.it

Growing evidence suggests that cochlear stressors as noise exposure and aging can induce homeostatic/maladaptive changes in the central auditory system from the brainstem to the cortex. Studies centered on such changes have revealed several mechanisms that operate in the context of sensory disruption after insult (noise trauma, drug-, or age-related injury). The oxidative stress is central to current theories of induced sensory-neural hearing loss and aging, and interventions to attenuate the hearing loss are based on antioxidant agent. The present review addresses the recent literature on the alterations in hair cells and spiral ganglion neurons due to noise-induced oxidative stress in the cochlea, as well on the impact of cochlear damage on the auditory cortex neurons. The emerging image emphasizes that noise-induced deafferentation and upward spread of cochlear damage is associated with the altered dendritic architecture of auditory pyramidal neurons. The cortical modifications may be reversed by treatment with antioxidants counteracting the cochlear redox imbalance. These findings open new therapeutic approaches to treat the functional consequences of the cortical reorganization following cochlear damage.

Keywords: presbycusis, noise-induced hearing loss, auditory cortex, pyramidal neurons, oxidative stress

INTRODUCTION: CHALLENGES FOR THE INVESTIGATION OF THE RELATION BETWEEN INNER EAR INJURY AND AUDITORY CORTEX PLASTICITY

Sensory-neural hearing loss is a disorder surprisingly frequent in the general population (Nelson et al., 2005) affecting severely the quality of life as reported by several assessments (Seidman and Standring, 2010). Hearing loss research provided evidence on two major causal insults, aging and noise trauma, and on a common predominant mechanism of damage affecting the organ of corti: the redox status imbalance. Mitochondrial production of reactive oxygen species (ROS) is indeed central to the free radical theory of aging (Lenaz, 2012; Orr et al., 2013). This theory has been implicated in the pathogenesis of virtually all age-associated diseases as well as in noise-induced hearing loss (NIHL), the second most common sensory-neural hearing deficit after age-related hearing loss (presbycusis) (Van Eyken et al., 2007; Someya et al., 2009; Fetoni et al., 2011). In both hearing pathologies, the increase of hearing threshold of about 40–50 dB affects predominantly the high-frequency region and is frequently associated to distressful and debilitating phantom sounds (Heffner and Harrington, 2002; Eggermont and Roberts, 2004; Weisz et al., 2006; Eggermont, 2008; Roberts et al., 2010). The current state of presbycusis and NIHL research suggests that sensory disruption due to damage of the organ of corti may trigger central mechanisms of homeostatic/maladaptive plasticity (Rauschecker, 1999; Syka, 2002; Caspary et al., 2008; Wang et al., 2011; Yang et al., 2011). Consistent with theories of homeostatic plasticity many studies have reported changes in excitatory, inhibitory, and neuromodulatory networks along the central auditory pathway (Liberman and Kiang, 1978; Abbott et al., 1999; Milbrandt et al., 2000; Salvi et al., 2000; Richardson et al., 2012; Engineer et al., 2013). Indeed, research focused selectively either on the analysis of cochlear damage within the organ of corti and its mechanisms or the functional adaptive changes of central and cortical networks. Despite the plethora of data achieved in recent years, a cohesive physiological framework underlying presbycusis and NIHL generation remains elusive inasmuch the relation between cochlear injury and cortical plasticity has been addressed only marginally. To this end, the current review will examine the convergence of factors related to auditory insults from a bottom-up perspective, coupling the acoustically- or aging-induced functional changes at peripheral level [e.g., hearing receptor and spiral ganglion neuron (SGN) function] with the central changes at the level of the pyramidal neurons in the auditory cortices. To gain insights into the relationship between cochlear damage and cortical rearrangement, this review will first address damage-induced ROS imbalance in the cochlea and the effect of antioxidant supplementation, and then the adaptive/maladaptive cortical rearrangement (diagram in **Figure 1A**).

OXIDATIVE STRESS AND REDOX BALANCE IN THE HAIR CELLS: THE ANTIOXIDANT PROTECTION

The loss of hair cells (HCs) induced by acoustic overexposure manifests as extensive outer hair cell (OHC) death, mainly the basally located OHCs, and frequency-delimited loss of inner hair cells (IHCs) scaling with the trauma severity (Spongr et al., 1992). This susceptibility to trauma appears to be conserved in certain models of ototoxicity, such as the exposure to aminoglycoside antibiotics

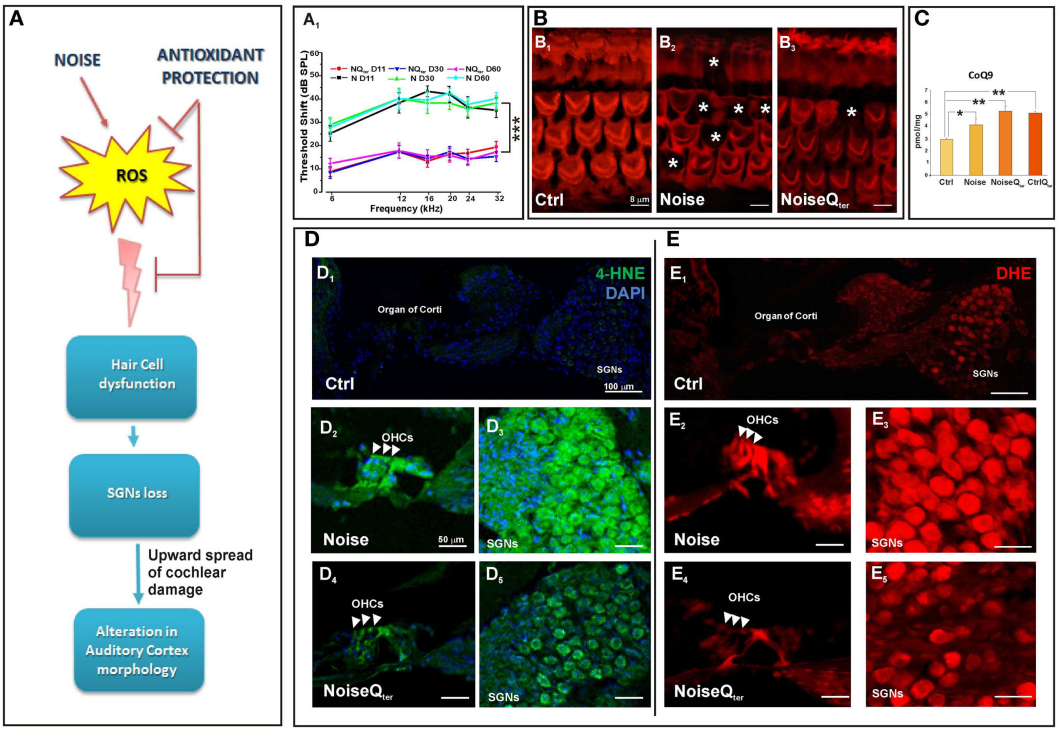

FIGURE 1 | In the rat, repeated noise exposure causes hearing loss and cochlear oxidative imbalance that is reduced by antioxidant treatment. The diagram in **(A)** is a schematic representation of the effect of antioxidant supplementation on the upward spread of noise-induced cochlear damage; reactive oxygen species (ROS) over production in cochlear structures induces hair cell dysfunction, spiral ganglion neurons (SGNs) loss and alterations in cortical pyramidal neurons. (A_1) The hearing loss has been evaluated by ABR threshold shift values (±SEM). Repeated noise exposure (100 dB, 10 kHz, 60 min/day for 10 consecutive days) induces threshold shift of ~40–45 dB for all frequencies tested with a peak between 16 and 24 kHz. NIHL is ameliorated by antioxidant treatment (Q_{ter}, 100 mg/kg × 10 days): the threshold shifts is ~10–15 dB at the end of noise sessions. ***$p < 0.0001$. **(B)** The quantitative assessment of HC survival has been determined by Rhodamine–Phalloidin (Rh–Ph) staining of HC apical pole 60 days after noise exposure. In control, typical distribution in three rows of OHCs and one row of inner hair cells (IHCs) is shown [indicated by asterisks in (B_1)], in noise exposed animals HC loss is observed mainly in the middle and basal turn [indicated by asterisks in (B_2)]. The amount of HC disappearance is significantly decreased by antioxidant treatment (B_3). **(C)** In order to demonstrate that the CoQ analog is protective against oxidative stress in the cochlea, the quantification of quinone levels (CoQ_9) has been performed by HPLC analysis at the end of Q_{ter} treatment. Interestingly, rats treated with Q_{ter} show higher quinone levels than in Ctrl and noise groups. The cochlear oxidative damage after noise exposure at day 11 has been detected using superoxide **(D)** and lipid peroxidation **(E)** markers. **(D)** Noise-induced superoxide production in the OHCs [indicated by arrow-heads in (D_2,D_4)] and SGNs (D_3,D_5) is reduced by Q_{ter} treatment. Similarly, Q_{ter} treatment significantly decreases the expression of 4-HNE mainly in OHCs [indicated by arrow-heads in (E_2,E_4)] and SGNs (E_3,E_5). Data are taken from Fetoni et al. (2013).

(Forge, 1985), or to platinum-derived cancer treatment drugs (Yorgason et al., 2006). Interestingly, there is an equivalency between loss developed following noise trauma and the loss acquired during aging, as in sensory presbycusis (Schuknecht, 1964; Schuknecht and Gacek, 1993; Ohlemiller, 2004). Ultimately, in models of sensory presbycusis and NIHL, the cochlear injury seems to converge upon auditory neuropathy (Stamataki et al., 2006; Sergeyenko et al., 2013; Gold and Bajo, 2014) and a ROS-dependent mechanism of damage (Henderson et al., 2006; Yamasoba et al., 2013).

Reactive oxygen species are formed as byproducts of mitochondrial respiration and examples of oxidizing reactive species are the superoxide anion radical (O_2), the hydroxyl radical (OH), and hydrogen peroxide (H_2O_2) (Bast and Haenen, 2013). Most research on the role of ROS in aging and NIHL has focused on two areas: defining the sites and mechanisms of ROS production and the resulting damage, and developing broad-acting antioxidants to decrease the damage caused by ROS (Someya et al., 2009; Orr et al., 2013). Considerable progress has been made in defining sites of production within the mitochondria and it is generally accepted that complex I and complex III have high capacities for production of superoxide/H_2O_2 and they are the sites most relevant to disease (Brand et al., 2013). Under basic metabolic conditions the intrinsic mitochondrial and cytosolic antioxidant machinery maintains redox homeostasis, the steady state between oxidative and reductive forces. However, if ROS are being produced in excess they create oxidative stress that affects various organelles and pathways in the cell, leading to apoptosis, or other forms of cell death, damaging mitochondria themselves and energy metabolism (Finkel, 2012; Böttger and Schacht, 2013). Our data on NIHL and ototoxicity models provide evidence on oxidative stress in the cochlea. Namely, enhanced superoxide production and lipid peroxidation in HCs and SGNs demonstrate the oxidative status after noise exposure and cisplatin-induced ototoxicity (Fetoni

et al., 2013, 2014). Among the biomarkers of lipid peroxidation, 4-hydroxy-2-nonenal (4-HNE) is one of the more sensitive and widely used *in vitro* and *in vivo* experimental models (Fetoni et al., 2010, 2013). A strong immunoreactivity for 4-HNE is detected in almost all OHCs in the damaged area in the first 24 h after the acoustic trauma in guinea pigs (Maulucci et al., 2014) and after cisplatin administration in rodents (Fetoni et al., 2014). Interestingly, an increasing level of free radical-induced lipid peroxidation is revealed in OHCs and SGNs in the first 3 days after exogenous insults; peroxidation then decreases in the following 7 days indicating that an early "window" for a successful therapeutic approach against exogenous factors occurs (Fetoni et al., 2010, 2013, 2014). During this period, several endogenous antioxidant pathways, which can be potentiated by exogenous supplementation, are activated to prevent the onset of HC damage. Vascular endothelial growth factor (VEGF), once regarded as an angiogenic factor implicated in antioxidant defense, is up-regulated at 1 and 7 days following intense noise exposure in the organ of corti. VEGF up-regulation can be temporally and spatially correlated to spontaneous recovery of auditory function that occurs in the first 7 post-damage days (Picciotti et al., 2006; Fetoni et al., 2009a). VEGF expression is also significantly reduced in aged mice (Picciotti et al., 2004). These findings suggest a possible interdependent relationship between aging and acoustic trauma on one hand, and oxidative stress mechanisms on the other hand, with potentially important therapeutic implications. Among the many intracellular pathways involved in the adaptive stress response, a relevant role is played by the inducible isoform of heme oxygenase (HO-1), the microsomal enzyme deputed to heme catabolism having antioxidant properties capable of scavenging peroxyl radicals and inhibiting lipid peroxidation (Barone et al., 2009). Several strategies to ameliorate redox status balance have been focused on antioxidant supplementation and there has been extensive research into the discovery of natural and newly designed antioxidants (Le Prell et al., 2007, 2011; Fetoni et al., 2010, 2014). Remarkably in the guinea-pig cochleae, the neuroprotective effect of the antioxidant Ferulic acid, when given 1 day before and for 3 days after noise exposure, is functionally related not only to its scavenging ability but also to the up-regulation of HO-1. These results fit the idea that antioxidants achieve their best cytoprotective capacity if given before and soon after the stressor. Also, in the model of cisplatin-induced oxidative stress HO-1 level is enhanced as an early endogenous, although insufficient, antioxidant response and this pathway is potentiated by the administration of the dietary antioxidant curcumin (Fetoni et al., 2014). Although the issue on the different mechanisms of cochlear oxidative stress/ROS generation in NIHL, ototoxicity and sensory presbycusis is not resolved, common to these hearing pathologies is mitochondrial dysfunction (Böttger and Schacht, 2013). The antioxidant ability to donate electrons of coenzyme Q_{10} (CoQ_{10}) in targeting mitochondrial dysfunction can be considered a promising approach inasmuch CoQ_{10} functions as an electron carrier from the protein complex I and II to complex III (Crane, 2001; Lenaz et al., 2007). As energy carrier, the CoQ_{10} factor continuously goes through oxidation–reduction cycle. In its reduced form, the CoQ_{10} holds electrons rather loosely, so CoQ_{10} will quite easily give up one or both electrons and, thus, act as antioxidant. CoQ_{10} inhibits lipid peroxidation by preventing the production of lipid peroxyl radicals, reduces the initial perferryl radical, which prevents propagation of lipid peroxidation, protects not only lipids but also proteins from oxidation. In addition, the reduced form of CoQ_{10} effectively regenerates vitamin E from the α-tocopheroxyl radical (Sohal and Forster, 2007). Considering that the efficacy of antioxidants is best tested in terms of their ability to maintain homeostasis CoQ_{10} analogs have been tested in NIHL. The synthetic analog of CoQ_{10}, idebenone, significantly prevents NIHL when administered in the peritraumatic period decreasing the apoptotic cascade activation and then avoiding HC loss (Sergi et al., 2006; Fetoni et al., 2008). Its efficacy seems to depend on the ability to intercept free radicals in both aqueous phases and lipid–water interfaces. On this basis, the protective role of CoQ_{10} against NIHL has been analyzed by comparing the efficacy of the native lipophilic CoQ_{10} molecule with that of a multi-composite formulation of CoQ_{10} with high water solubility and oral bioavailability, CoQ_{10} Terclatrate (Q_{ter}). The water soluble molecule is more effective as compared to the native CoQ_{10} in decreasing apoptosis as shown by the reduced expression of active caspase 3 and thus in improving hearing. The obtained results confirm that solubility of Q_{ter} improves the ability of CoQ_{10} in preventing oxidative injuries that result from mitochondrial dysfunction (Fetoni et al., 2009b, 2012, 2013). In fact, the systemic administration of Q_{ter} decreases superoxide production and 4-HNE expression in HCs and SGNs (**Figure 1**). Interestingly, reduced oxidative stress is consistent with the increased levels of the endogenous quinones (i.e., CoQ_9, the major form expressed in rats) after the administration of Q_{ter} indicating that the exogenous quinone can exert a protective effect on animal tissues. In fact, in the NoiseQ_{ter} group, CoQ_9 levels decrease at the end of treatment compared with the control Q_{ter} group, demonstrating that the exogenous quinone is used as scavenger during noise exposure to reduce the oxidative imbalance. This scavenging would thus prevent the functional and morphological cochlear damage (**Figures 1** and **2A,B**), the upward spread of the cochlear damage and the deafferentation consequences in the auditory cortex (**Figure 1A**).

INSULT-MEDIATED ADAPTIVE/MALADAPTIVE PLASTICITY IN THE AUDITORY CORTEX

Noise-induced hearing loss, ototoxicity, or age-induced damage to the peripheral hearing organ causes primarily alteration of the firing rates in the auditory nerve (Kraus et al., 2011), and compensatory changes at various levels of the central auditory pathway (Jin et al., 2005; Jin and Godfrey, 2006; Meidinger et al., 2006; Wang et al., 2006; Kraus et al., 2009; Kujawa and Liberman, 2009). The consequences of acoustic trauma have been investigated mainly through electrophysiological and neurochemical analyses, whereas morphological data in the central acoustic system are still scant (Bose et al., 2010; Gröschel et al., 2010). Nevertheless, following noise-induced acoustic trauma, decreased spine density paralleled by an increased dendritic length has been observed in the pyramidal neurons of auditory cortical areas (**Figure 2**) (Fetoni et al., 2013). Namely, pyramidal neurons belonging to layer II–III (L 2/3) and V–VI (L 5/6) of auditory cortices have been analyzed by using the Golgi–Cox technique from tissue collected two months after noise injury (**Figure 2C**). In both cortical layers

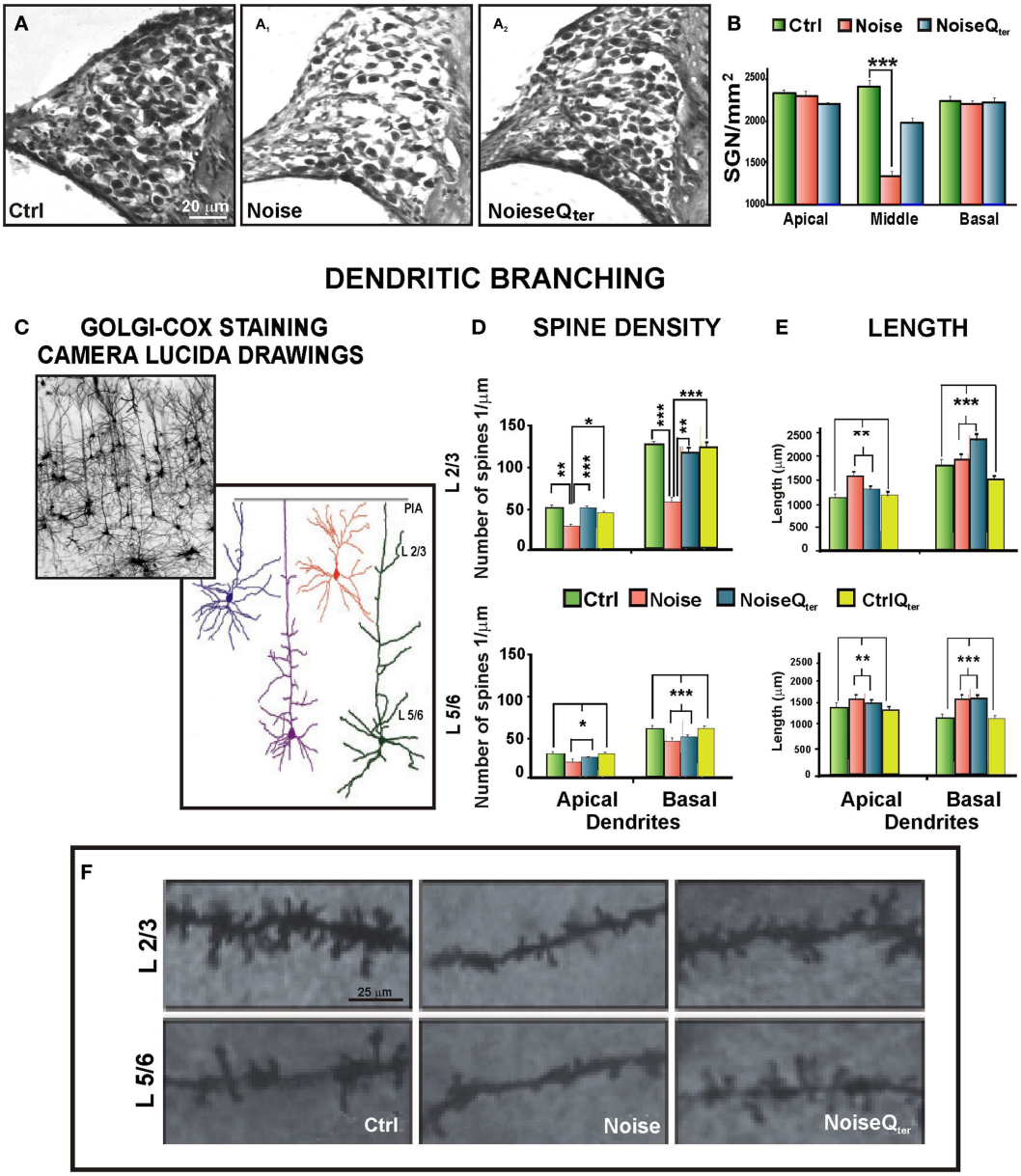

FIGURE 2 | Cortical morphological modifications induced by noise-induced cochlear damage and peripheral deafferentation are ameliorated by antioxidant treatment. **(A)** Repeated noise exposure induces SGN degeneration, soma appear smaller, their density is reduced, and fibers are thinner (A_1) compared with controls **(A)**. Q_{ter} administration preserves SGNs and fibers (A_2). **(B)** The graph shows SGN viability presented as number of cells per square millimeters, $***p < 0.0001$. **(C–F)** Auditory cortex pyramidal neurons belonging to L 2/3 and L 5/6 have been analyzed using Golgi–Cox technique from tissue collected at day 60 after noise exposure. **(C)** Golgi–Cox staining and Camera Lucida drawings of representative pyramidal neurons belonging to L 2/3 and L 5/6 of auditory cortices. **(D–E)** Histograms show the effects of noise exposure and antioxidant treatment (Q_{ter}) on dendritic spine density and length of L 2/3 (above) and L 5/6 (below) pyramidal neurons. Vertical bars indicate SEM, $*p < 0.05$, $**p < 0.001$, $***p < 0.0001$. **(D)** The acoustic trauma significantly decreases spine density in the apical and basal dendrites of both cortical layers. Q_{ter} treatment rescues control values of spine density for both apical and basal dendrites in L 2/3 but not in L 5/6. **(E)** In both layers, the acoustic trauma significantly increases neuronal length both in apical and basal dendrites. Q_{ter} treatment does not modify the dendritic length enhanced by the acoustic trauma in the apical and basal arborizations of L 2/3 and L 5/6 pyramidal neurons. **(F)** Photomicrographs visualize the spines of apical dendritic segments of pyramidal neurons belonging to L 2/3 and L 5/6 of the auditory cortex. Data are adapted from Fetoni et al. (2013).

and both apical and basal dendrites, the acoustic trauma significantly decreased spine density (**Figure 2D**) and increased dendritic length (**Figure 2E**). The distance from the soma of maximal spine concentration remained unaltered in the arborizations of L 2/3 while it was distally shifted in the apical and basal dendrites of L 5/6 reducing the efficacy of synapses on neuronal output (Fetoni

et al., 2013). In the absence of dendrite shrinkage, spine loss may be explained by excessive synaptic pruning attributable to enhanced synaptic competition. Hence, the spine loss that follows deafferentation may be caused by activity-dependent remodeling of neuronal connectivity and it could be a "trophic" response, whereby a diminished input cannot sustain a large number of excitatory connections. Alternatively, the deafferented cortical neuron could compensate for the reduced afferent drive by sensing global levels of activity and operating a homeostatic synaptic scaling (Turrigiano, 2008, 2012; Whitt et al., 2014). If so, the decrease in spine number could result in an up-regulated excitatory signaling and preserve relative synaptic efficacy. Literature on homeostatic plasticity (Caspary et al., 2008; Richardson et al., 2012; Gold and Bajo, 2014) describes how in response to changes in chronic neuronal activity, i.e., deafferentation, neural systems undergo compensatory changes in synaptic activity to stay within a relatively narrow operating range of the original neuronal activity (Turrigiano, 1999, 2007; Rich and Wenner, 2007). A number of plasticity studies have focused on the potential significance of the balance between excitation and inhibition to explain the adaptive and maladaptive homeostatic plasticity of cortical tonotopic map reorganization and tinnitus, respectively (Eggermont and Roberts, 2004; Roberts et al., 2010; Pienkowski and Eggermont, 2011; Wang et al., 2011). The cellular compensatory mechanisms involve the regulation of inhibitory and excitatory neurotransmission, since changes in one system produce reactive changes in the other one (Turrigiano, 2012). In response to increased neuronal activity, inhibitory and excitatory synaptic strengths are multiplicatively scaled up and down, respectively (Peng et al., 2010; Rannals and Kapur, 2011), to restore neuronal firing rate to normal levels. Indeed, dendrites and their spines are the main neuronal targets of plasticity (Feldman, 2012; Fortin et al., 2012; De Bartolo et al., 2014; Sala and Segal, 2014). Dendritic arbors and spines are then highly dynamic structures branching and retracting in response to the information they receive, so that dendritic length and spine number are related to the degree of connectivity and the complexity of information processing (McAllister, 2000). They provide the morphological substrate for lesion-induced and context-dependent plastic events (Kulkarni and Firestein, 2012).

Interestingly, systemic treatment with the antioxidant CoQ_{10} analog Q_{ter} in the rat NIHL model not only reduced the oxidative stress and cochlear damage but also prevented the alteration of the pyramidal dendritic pattern of the auditory cortex in a layer-selective mode (**Figures 2D–F**). Namely, the spine densities for both apical and basal dendrites were rescued to control values (**Figure 2D**) without modifying its distance from soma in L 2/3, but not in L 5/6 (Fetoni et al., 2013). However, the antioxidant treatment did not modify the dendritic length enhanced by the acoustic trauma in the apical and basal arborizations of L 2/3 and 5/6 pyramidal neurons (**Figure 2E**). As the other sensory cortices, the auditory cortex shows dense and well-developed L2/3, mainly involved in cortico-cortical circuits, and relatively sparse and reduced L5/6 (Linden and Schreiner, 2003; Paxinos and Watson, 2007). Thus, the neuronal rearrangement of the auditory cortex appears to engage mainly the cortico-cortical circuits and L2/3 homeostatic plastic changes are the substrate for cortical plasticity, as reported in other sensory cortices (Kotak et al., 2005; De Bartolo et al., 2009; Gelfo et al., 2009; Whitt et al., 2014). Overall, various forms of plasticity, including synaptic scaling, plasticity of intrinsic excitability, and changes in sensory-evoked inhibition and excitation–inhibition ratio, cooperate to modify the function of cortical circuits (Li et al., 2014; Whitt et al., 2014). This rich repertoire of synapse regulation and plasticity enables cortical circuits to respond with the greatest flexibility to changes in sensory input. On one hand, the several forms of homeostatic plasticity operating on different temporal and spatial scales may guarantee the apt compensatory responses to a wide range of sensory perturbations. Interestingly, in both juvenile and adult mammals, hearing loss restricted to a part of the audible frequency range can lead to a reorganization of cortical tonotopic maps (Pienkowski and Eggermont, 2011). Thus, the cortical modifications after NIHL, as illustrated in **Figure 2**, could be the structural basis of such a functional phenomenon for which within a few weeks from the onset of severe but restricted hearing loss, the cortical region related to the dysfunctional cochlear part becomes tuned to the sound frequencies, which stimulate the adjacent non-damaged part(s) (Eggermont and Komiya, 2000; Noreña and Eggermont, 2005). On the other hand, maladaptive cortical plasticity or impaired synaptic plasticity might contribute to the excess of plasticity as reported in focal and generalized form of dystonia (Quartarone and Pisani, 2011). It can be speculated that a deficit of synaptic "down-scaling" along with a deficient inhibition may underlie the excess of plasticity in tinnitus and the increased plasticity in the auditory cortex and/or multiple levels of the central auditory neuraxis can become maladaptive, giving rise to abnormal sensory patterns.

CONCLUSION

Mitochondrial production of ROS is implicated in the pathogenesis of virtually all age-associated diseases as well as in NIHL. As shown in the acoustic trauma model, noise exposure induces oxidative stress damage in the sensory epithelium of the organ of corti and degeneration of SGNs. The upward spread of cochlear oxidative damage appears to cause plastic rearrangement in the pyramidal layers (L 2/3 and L 5/6) of the auditory cortex. Antioxidants, such as Q_{ter}, Ferulic acid, and Idebenone, reduce the morphological and functional cochlear damage. The decrease of the peripheral oxidative imbalance reverses the upward spread of the cochlear damage and the deafferentation consequences in the auditory cortex, specifically in the highly plastic L 2/3. The present data demonstrate the capability of the auditory cortex to remodel its features in consequence of antioxidant therapy.

ACKNOWLEDGMENTS

This work has been supported by Fondi d'Ateneo UCSC and PRIN Grants, Italy. The Authors express their gratitude to Sara L. M. Eramo, Fabiola Paciello, Rolando Rolesi, and Paola De Bartolo for their helpful contribution. Special thanks to Romana Fato and Christian Bergamini for the HPLC analyses.

REFERENCES

Abbott, S. D., Hughes, L. F., Bauer, C. A., Salvi, R., and Caspary, D. M. (1999). Detection of glutamate decarboxylase isoforms in rat inferior colliculus following acoustic exposure. *Neuroscience* 93, 1375–1381. doi:10.1016/S0306-4522(99)00300-0

Barone, E., Calabrese, V., and Mancuso, C. (2009). Ferulic acid and its therapeutic potential as a hormetin for age-related diseases. *Biogerontology* 10, 97–108. doi:10.1007/s10522-008-9160-8

Bast, A., and Haenen, G. R. (2013). Ten misconceptions about antioxidants. *Trends Pharmacol. Sci.* 34, 430–436. doi:10.1016/j.tips.2013.05.010

Bose, M., Muñoz-Llancao, P., Roychowdhury, S., Nichols, J. A., Jakkamsetti, V., Porter, B., et al. (2010). Effect of the environment on the dendritic morphology of the rat auditory cortex. *Synapse* 64, 97–110. doi:10.1002/syn.20710

Böttger, C. E., and Schacht, J. (2013). The mitochondrion: a perpetrator of acquired hearing loss. *Hear. Res.* 303, 12–19. doi:10.1016/j.heares.2013.01.006

Brand, M. D., Orr, A. L., Perevoshchikova, I. V., and Quinlan, C. L. (2013). The role of mitochondrial function and cellular bioenergetics in ageing and disease. *Br. J. Dermatol.* 169(Suppl. 2), 1–8. doi:10.1111/bjd.12208

Caspary, D. M., Ling, L., Turner, J. G., and Hughes, L. F. (2008). Inhibitory neurotransmission, plasticity and aging in the mammalian central auditory system. *J. Exp. Biol.* 211(Pt 11), 1781–1791. doi:10.1242/jeb.013581

Crane, F. L. (2001). Biochemical functions of coenzyme Q10. *J. Am. Coll. Nutr.* 20, 591–598. doi:10.1080/07315724.2001.10719063

De Bartolo, P., Florenzano, F., Burello, L., Gelfo, F., and Petrosini, L. (2014). Activity-dependent structural plasticity of Purkinje cell spines in cerebellar vermis and hemisphere. *Brain Struct. Funct.* doi:10.1007/s00429-014-0833-6

De Bartolo, P., Gelfo, F., Mandolesi, L., Foti, F., Cutuli, D., and Petrosini, L. (2009). Effects of chronic donepezil treatment and cholinergic deafferentation on parietal pyramidal neuron morphology. *J. Alzheimers Dis.* 17, 177–191. doi:10.3233/JAD-2009-1035

Eggermont, J. J. (2008). The role of sound in adult and developmental auditory cortical plasticity. *Ear Hear* 29, 819–829. doi:10.1097/AUD.0b013e3181853030

Eggermont, J. J., and Komiya, H. (2000). Moderate noise trauma in juvenile cats results in profound cortical topographic map changes in adulthood. *Hear. Res.* 142, 89–101. doi:10.1016/S0378-5955(00)00024-1

Eggermont, J. J., and Roberts, L. E. (2004). The neuroscience of tinnitus. *Trends Neurosci.* 27, 676–682. doi:10.1016/j.tins.2004.08.010

Engineer, N. D., Møller, A. R., and Kilgard, M. P. (2013). Directing neural plasticity to understand and treat tinnitus. *Hear. Res.* 295, 58–66. doi:10.1016/j.heares.2012.10.001

Feldman, D. E. (2012). The spike-timing dependence of plasticity. *Neuron* 75, 556–571. doi:10.1016/j.neuron.2012.08.001

Fetoni, A. R., De Bartolo, P., Eramo, S. L., Rolesi, R., Paciello, F., Bergamini, C., et al. (2013). Noise-induced hearing loss (NIHL) as a target of oxidative stress-mediated damage: cochlear and cortical responses after an increase in antioxidant defense. *J. Neurosci.* 33, 4011–4023. doi:10.1523/JNEUROSCI.2282-12.2013

Fetoni, A. R., Eramo, S. L., Paciello, F., Rolesi, R., Podda, M. V., Troiani, D., et al. (2014). Curcuma longa (curcumin) decreases in vivo cisplatin-induced ototoxicity through heme oxygenase-1 induction. *Otol. Neurotol.* 35, e169–e177. doi:10.1097/MAO.0000000000000302

Fetoni, A. R., Ferraresi, A., Greca, C. L., Rizzo, D., Sergi, B., Tringali, G., et al. (2008). Antioxidant protection against acoustic trauma by coadministration of idebenone and vitamin E. *Neuroreport* 19, 277–281. doi:10.1097/WNR.0b013e3282f50c66

Fetoni, A. R., Ferraresi, A., Picciotti, P., Gaetani, E., Paludetti, G., and Troiani, D. (2009a). Noise induced hearing loss and vestibular dysfunction in the guinea pig. *Int. J. Audiol.* 48, 804–810. doi:10.3109/14992020903023140

Fetoni, A. R., Piacentini, R., Fiorita, A., Paludetti, G., and Troiani, D. (2009b). Water-soluble coenzyme Q10 formulation (Q-ter) promotes outer hair cell survival in a guinea pig model of noise induced hearing loss (NIHL). *Brain Res.* 1257, 108–116. doi:10.1016/j.brainres.2008.12.027

Fetoni, A. R., Mancuso, C., Eramo, S. L., Ralli, M., Piacentini, R., Barone, E., et al. (2010). In vivo protective effect of ferulic acid against noise-induced hearing loss in the guinea-pig. *Neuroscience* 169, 1575–1588. doi:10.1016/j.neuroscience.2010.06.022

Fetoni, A. R., Picciotti, P. M., Paludetti, G., and Troiani, D. (2011). Pathogenesis of presbycusis in animal models: a review. *Exp. Gerontol.* 46, 413–425. doi:10.1016/j.neuroscience.2010.06.022

Fetoni, A. R., Troiani, D., Eramo, S. L., Rolesi, R., and Paludetti, G. (2012). Efficacy of different routes of administration for coenzyme Q10 formulation in noise-induced hearing loss: systemic versus transtympanic modality. *Acta Otolaryngol.* 132, 391–399. doi:10.3109/00016489.2011.652307

Finkel, T. (2012). Signal transduction by mitochondrial oxidants. *J. Biol. Chem.* 287, 4434–4440. doi:10.1074/jbc.R111.271999

Forge, A. (1985). Outer hair cell loss and supporting cell expansion following chronic gentamicin treatment. *Hear. Res.* 19, 171–182. doi:10.1016/0378-5955(85)90121-2

Fortin, D. A., Srivastava, T., and Soderling, T. R. (2012). Structural modulation of dendritic spines during synaptic plasticity. *Neuroscientist.* 18, 326–341. doi:10.1177/1073858411407206

Gelfo, F., De Bartolo, P., Giovine, A., Petrosini, L., and Leggio, M. G. (2009). Layer and regional effects of environmental enrichment on the pyramidal neuron morphology of the rat. *Neurobiol. Learn. Mem.* 91, 353–365. doi:10.1016/j.nlm.2009.01.010

Gold, J. R., and Bajo, V. M. (2014). Insult-induced adaptive plasticity of the auditory system. *Front. Neurosci.* 8:110. doi:10.3389/fnins.2014.00110

Gröschel, M., Götze, R., Ernst, A., and Basta, D. (2010). Differential impact of temporary and permanent noise-induced hearing loss on neuronal cell density in the mouse central auditory pathway. *J. Neurotrauma* 27, 1499–1507. doi:10.1089/neu.2009.1246

Heffner, H. E., and Harrington, I. A. (2002). Tinnitus in hamsters following exposure to intense sound. *Hear. Res.* 170, 83–95. doi:10.1016/S0378-5955(02)00343-X

Henderson, D., Bielefeld, E. C., Harris, K. C., and Hu, B. H. (2006). The role of oxidative stress in noise-induced hearing loss. *Ear Hear.* 27, 1–19. doi:10.1097/01.aud.0000191942.36672.f3

Jin, Y. M., and Godfrey, D. A. (2006). Effects of cochlear ablation on muscarinic acetylcholine receptor binding in the rat cochlear nucleus. *J. Neurosci. Res.* 83, 157–166. doi:10.1002/jnr.20706

Jin, Y. M., Godfrey, D. A., and Sun, Y. (2005). Effects of cochlear ablation on choline acetyltransferase activity in the rat cochlear nucleus and superior olive. *J. Neurosci. Res.* 81, 91–101. doi:10.1002/jnr.20536

Kotak, V. C., Fujisawa, S., Lee, F. A., Karthikeyan, O., Aoki, C., and Sanes, D. H. (2005). Hearing loss raises excitability in the auditory cortex. *J. Neurosci.* 25, 3908–3918. doi:10.1523/JNEUROSCI.5169-04.2005

Kraus, K. S., Ding, D., Jiang, H., Lobarinas, E., Sun, W., and Salvi, R. J. (2011). Relationship between noise-induced hearing-loss, persistent tinnitus and growth-associated protein-43 expression in the rat cochlear nucleus: does synaptic plasticity in ventral cochlear nucleus suppress tinnitus? *Neuroscience* 194, 309–325. doi:10.1016/j.neuroscience.2011.07.056

Kraus, K. S., Ding, D., Zhou, Y., and Salvi, R. J. (2009). Central auditory plasticity after carboplatin-induced unilateral inner ear damage in the chinchilla: up-regulation of GAP-43 in the ventral cochlear nucleus. *Hear. Res.* 255, 33–43. doi:10.1016/j.heares.2009.05.001

Kujawa, S. G., and Liberman, M. C. (2009). Adding insult to injury: cochlear nerve degeneration after "temporary" noise-induced hearing loss. *J. Neurosci.* 29, 14077–14085. doi:10.1523/JNEUROSCI.2845-09.2009

Kulkarni, V. A., and Firestein, B. L. (2012). The dendritic tree and brain disorders. *Mol. Cell. Neurosci.* 50, 10–20. doi:10.1016/j.mcn.2012.03.005

Le Prell, C. G., Gagnon, P. M., Bennett, D. C., and Ohlemiller, K. K. (2011). Nutrient-enhanced diet reduces noise-induced damage to the inner ear and hearing loss. *Transl. Res.* 158, 38–53. doi:10.1016/j.trsl.2011.02.006

Le Prell, C. G., Hughes, L. F., and Miller, J. M. (2007). Free radical scavengers vitamins A, C, and E plus magnesium reduce noise trauma. *Free Radic. Biol. Med.* 42, 1454–1463. doi:10.1016/j.freeradbiomed.2007.02.008

Lenaz, G. (2012). Mitochondria and reactive oxygen species. Which role in physiology and pathology? *Adv. Exp. Med. Biol.* 942, 93–136. doi:10.1007/978-94-007-2869-1_5

Lenaz, G., Fato, R., Formiggini, G., and Genova, M. L. (2007). The role of coenzyme Q in mitochondrial electron transport. *Mitochondrion* 7(Suppl.), S8–S33. doi:10.1016/j.mito.2007.03.009

Li, L. Y., Xiong, X. R., Ibrahim, L. A., Yuan, W., Tao, H. W., and Zhang, L. I. (2014). Differential receptive field properties of parvalbumin and somatostatin inhibitory neurons in mouse auditory cortex. *Cereb. Cortex* doi:10.1093/cercor/bht417

Liberman, M. C., and Kiang, N. Y.-S. (1978). Acoustic trauma in cats. Cochlear pathology and auditory-nerve activity. *Acta Otolaryngol. Suppl.* 358, 1–63.

Linden, J. F., and Schreiner, C. E. (2003). Columnar transformations in auditory cortex? A comparison to visual and somatosensory cortices. *Cereb. Cortex* 13, 83–89. doi:10.1093/cercor/13.1.83

Maulucci, G., Troiani, D., Eramo, S. L., Paciello, F., Podda, M. V., Paludetti, G., et al. (2014). Time evolution of noise induced oxidation in outer hair cells: role of NAD(P)H and plasma membrane fluidity. *Biochim. Biophys. Acta* 1840, 2192–2202. doi:10.1016/j.bbagen.2014.04.005

McAllister, A. K. (2000). Cellular and molecular mechanisms of dendrite growth. *Cereb. Cortex* 10, 963–973. doi:10.1093/cercor/10.10.963

Meidinger, M. A., Hildebrandt-Schoenfeld, H., and Illing, R. B. (2006). Cochlear damage induces GAP-43 expression in cholinergic synapses of the cochlear nucleus in the adult rat: a light and electron microscopic study. *Eur. J. Neurosci.* 23, 3187–3199. doi:10.1111/j.1460-9568.2006.04853.x

Milbrandt, J. C., Holder, T. M., Wilson, M. C., Salvi, R. J., and Caspary, D. M. (2000). GAD levels and muscimol binding in rat inferior colliculus following acoustic trauma. *Hear. Res.* 147, 251–260. doi:10.1016/S0378-5955(00)00135-0

Nelson, D. I., Nelson, R. Y., Concha-Barrientos, M., and Fingerhut, M. (2005). The global burden of occupational noise-induced hearing loss. *Am. J. Ind. Med.* 48, 446–458. doi:10.1002/ajim.20223

Noreña, A. J., and Eggermont, J. J. (2005). Enriched acoustic environment after noise trauma reduces hearing loss and prevents cortical map reorganization. *J. Neurosci.* 25, 699–705. doi:10.1523/JNEUROSCI.2226-04.2005

Ohlemiller, K. K. (2004). Age-related hearing loss: the status of Schuknecht's typology. *Curr. Opin. Otolaryngol. Head Neck Surg.* 12, 439–443. doi:10.1097/01.moo.0000134450.99615.22

Orr, A. L., Ashok, D., Sarantos, M. R., Shi, T., Hughes, R. E., and Brand, M. D. (2013). Inhibitors of ROS production by the ubiquinone-binding site of mitochondrial complex I identified by chemical screening. *Free Radic. Biol. Med.* 65, 1047–1059. doi:10.1016/j.freeradbiomed.2013.08.170

Paxinos, G., and Watson, C. (2007). *The Rat Brain in Stereotaxic Coordinates.* Amsterdam: Elsevier.

Peng, Y. R., Zeng, S. Y., Song, H. L., Li, M. Y., Yamada, M. K., and Yu, X. (2010). Postsynaptic spiking homeostatically induces cell-autonomous regulation of inhibitory inputs via retrograde signaling. *J. Neurosci.* 30, 16220–16231. doi:10.1523/JNEUROSCI.3085-10.2010

Picciotti, P., Torsello, A., Wolf, F. I., Paludetti, G., Gaetani, E., and Pola, R. (2004). Age-dependent modifications of expression level of VEGF and its receptors in the inner ear. *Exp. Gerontol.* 39, 1253–1258. doi:10.1016/j.exger.2004.06.003

Picciotti, P. M., Fetoni, A. R., Paludetti, G., Wolf, F. I., Torsello, A., Troiani, D., et al. (2006). Vascular endothelial growth factor (VEGF) expression in noise-induced hearing loss. *Hear. Res.* 214, 76–83. doi:10.1016/j.heares.2006.02.004

Pienkowski, M., and Eggermont, J. J. (2011). Sound frequency representation in primary auditory cortex is level tolerant for moderately loud, complex sounds. *J. Neurophysiol.* 106, 1016–1027. doi:10.1152/jn.00291.2011

Quartarone, A., and Pisani, A. (2011). Abnormal plasticity in dystonia: disruption of synaptic homeostasis. *Neurobiol. Dis.* 42, 162–170. doi:10.1016/j.nbd.2010.12.011

Rannals, M. D., and Kapur, J. (2011). Homeostatic strengthening of inhibitory synapses is mediated by the accumulation of GABAA receptors. *J. Neurosci.* 31, 17701–17712. doi:10.1523/JNEUROSCI.4476-11.2011

Rauschecker, J. P. (1999). Making brain circuits listen. *Science* 285, 1686–1687. doi:10.1126/science.285.5434.1686

Rich, M. M., and Wenner, P. (2007). Sensing and expressing homeostatic synaptic plasticity. *Trends Neurosci.* 30, 119–125. doi:10.1016/j.tins.2007.01.004

Richardson, B. D., Brozoski, T. J., Ling, L. L., and Caspary, D. M. (2012). Targeting inhibitory neurotransmission in tinnitus. *Brain Res.* 1485, 77–87. doi:10.1016/j.brainres.2012.02.014

Roberts, L. E., Eggermont, J. J., Caspary, D. M., Shore, S. E., Melcher, J. R., and Kaltenbach, J. A. (2010). Ringing ears: the neuroscience of tinnitus. *J. Neurosci.* 30, 14972–14979. doi:10.1523/JNEUROSCI.4028-10.2010

Sala, C., and Segal, M. (2014). Dendritic spines: the locus of structural and functional plasticity. *Physiol. Rev.* 94, 141–188. doi:10.1152/physrev.00012.2013

Salvi, R. J., Wang, J., and Ding, D. (2000). Auditory plasticity and hyperactivity following cochlear damage. *Hear. Res.* 147, 261–274. doi:10.1016/S0378-5955(00)00136-2

Schuknecht, H. F. (1964). Further observations on the pathology of presbycusis. *Arch. Otolaryngol.* 80, 369–382. doi:10.1001/archotol.1964.00750040381003

Schuknecht, H. F., and Gacek, M. R. (1993). Cochlear pathology in presbycusis. *Ann. Otol. Rhinol. Laryngol.* 102, 1–16.

Seidman, M. D., and Standring, R. T. (2010). Noise and quality of life. *Int. J. Environ. Res. Public Health* 7, 3730–3738. doi:10.3390/ijerph7103730

Sergeyenko, Y., Lall, K., Liberman, M. C., and Kujawa, S. G. (2013). Age-related cochlear synaptopathy: an early-onset contributor to auditory functional decline. *J. Neurosci.* 33, 13686–13694. doi:10.1523/JNEUROSCI.1783-13.2013

Sergi, B., Fetoni, A. R., Paludetti, G., Ferraresi, A., Navarra, P., Mordente, A., et al. (2006). Protective properties of idebenone in noise-induced hearing loss in the guinea pig. *Neuroreport* 17, 857–861. doi:10.1097/01.wnr.0000221834.18470.8c

Sohal, R. S., and Forster, M. J. (2007). Coenzyme Q, oxidative stress and aging. *Mitochondrion* 7(Suppl.), S103–S111. doi:10.1016/j.mito.2007.03.006

Someya, S., Xu, J., Kondo, K., Ding, D., Salvi, R. J., Yamasoba, T., et al. (2009). Age-related hearing loss in C57BL/6J mice is mediated by Bak-dependent mitochondrial apoptosis. *Proc. Natl. Acad. Sci. U.S.A.* 106, 19432–19437. doi:10.1073/pnas.0908786106

Spongr, V. P., Boettcher, F. A., Saunders, S. S., and Salvi, R. J. (1992). Effects of noise and salicylate on hair cell loss in the chinchilla cochlea. *Arch. Otolaryngol. Head Neck Surg.* 118, 157–164. doi:10.1001/archotol.1992.01880020051015

Stamataki, S., Francis, H. W., Lehar, M., May, B. J., and Ryugo, D. K. (2006). Synaptic alterations at inner hair cells precede spiral ganglion cell loss in aging C57BL/6J mice. *Hear. Res.* 221, 104–118. doi:10.1016/j.heares.2006.07.014

Syka, J. (2002). Plastic changes in the central auditory system after hearing loss, restoration of function, and during learning. *Physiol. Rev.* 82, 601–636. doi:10.1152/physrev.00002.2002

Turrigiano, G. G. (1999). Homeostatic plasticity in neuronal networks: the more things change, the more they stay the same. *Trends Neurosci.* 22, 221–227. doi:10.1016/S0166-2236(98)01341-1

Turrigiano, G. G. (2007). Homeostatic signaling: the positive side of negative feedback. *Curr. Opin. Neurobiol.* 17, 318–324. doi:10.1016/j.conb.2007.04.004

Turrigiano, G. G. (2008). The self-tuning neuron: synaptic scaling of excitatory synapses. *Cell* 135, 422–435. doi:10.1016/j.cell.2008.10.008

Turrigiano, G. G. (2012). Homeostatic synaptic plasticity: local and global mechanisms for stabilizing neuronal function. *Cold Spring Harb. Perspect. Biol.* 4, a005736. doi:10.1101/cshperspect.a005736

Van Eyken, E., Van Camp, G., and Van Laer, L. (2007). The complexity of age-related hearing impairment: contributing environmental and genetic factors. *Audiol. Neurootol.* 12, 345–358. doi:10.1159/000106478

Wang, H., Brozoski, T. J., and Caspary, D. M. (2011). Inhibitory neurotransmission in animal models of tinnitus: maladaptive plasticity. *Hear. Res.* 279, 111–117. doi:10.1016/j.heares.2011.04.004

Wang, H. T., Luo, B., Zhou, K. Q., Xu, T. L., and Chen, L. (2006). Sodium salicylate reduces inhibitory postsynaptic currents in neurons of rat auditory cortex. *Hear. Res.* 215, 77–83. doi:10.1016/j.heares.2006.03.004

Weisz, N., Hartmann, T., Dohrmann, K., Schlee, W., and Norena, A. (2006). High-frequency tinnitus without hearing loss does not mean absence of deafferentation. *Hear. Res.* 222, 108–114. doi:10.1016/j.heares.2006.09.003

Whitt, J. L., Petrus, E., and Lee, H. K. (2014). Experience-dependent homeostatic synaptic plasticity in neocortex. *Neuropharmacology* 78, 45–54. doi:10.1016/j.neuropharm.2013.02.016

Yamasoba, T., Lin, F. R., Someya, S., Kashio, A., Sakamoto, T., and Kondo, K. (2013). Current concepts in age-related hearing loss: epidemiology and mechanistic pathways. *Hear. Res.* 303, 30–38. doi:10.1016/j

Yang, S., Weiner, B. D., Zhang, L. S., Cho, S. J., and Bao, S. (2011). Homeostatic plasticity drives tinnitus perception in an animal model. *Proc. Natl. Acad. Sci. U.S.A.* 108, 14974–14979. doi:10.1073/pnas.1107998108

Yorgason, J. G., Fayad, J. N., and Kalinec, F. (2006). Understanding drug ototoxicity: molecular insights for prevention and clinical management. *Expert Opin. Drug Saf.* 5, 383–399. doi:10.1517/14740338.5.3.383

Conflict of Interest Statement: The authors declare that the research was conducted in the absence of any commercial or financial relationships that could be construed as a potential conflict of interest.

Received: 01 December 2014; paper pending published: 15 December 2014; accepted: 21 January 2015; published online: 05 February 2015.

*Citation: Fetoni AR, Troiani D, Petrosini L and Paludetti G (2015) Cochlear injury and adaptive plasticity of the auditory cortex. Front. Aging Neurosci. **7**:8. doi: 10.3389/fnagi.2015.00008*

This article was submitted to the journal Frontiers in Aging Neuroscience.

frontiers in Aging Neuroscience

ORIGINAL RESEARCH
published: 11 March 2015
doi: 10.3389/fnagi.2015.00027

The influence of aging on the number of neurons and levels of non-phosporylated neurofilament proteins in the central auditory system of rats

*Jana Burianová *, Ladislav Ouda and Josef Syka*

Department of Auditory Neuroscience, Institute of Experimental Medicine of the Czech Academy of Sciences, Prague, Czech Republic

In the present study, an unbiased stereological method was used to determine the number of all neurons in Nissl stained sections of the inferior colliculus (IC), medial geniculate body (MGB), and auditory cortex (AC) in rats (strains Long Evans and Fischer 344) and their changes with aging. In addition, using the optical fractionator and western blot technique, we also evaluated the number of SMI-32-immunoreactive (-ir) neurons and levels of non-phosphorylated neurofilament proteins in the IC, MGB, AC, and visual cortex of young and old rats of the two strains. The SMI-32 positive neuronal population comprises about 10% of all neurons in the rat IC, MGB, and AC and represents a prevalent population of large neurons with highly myelinated and projecting processes. In both Long Evans and Fischer 344 rats, the total number of neurons in the IC was roughly similar to that in the AC. With aging, we found a rather mild and statistically non-significant decline in the total number of neurons in all three analyzed auditory regions in both rat strains. In contrast to this, the absolute number of SMI-32-ir neurons in both Long Evans and Fischer 344 rats significantly decreased with aging in all the examined structures. The western blot technique also revealed a significant age-related decline in the levels of non-phosphorylated neurofilaments in the auditory brain structures, 30–35%. Our results demonstrate that presbycusis in rats is not likely to be primarily associated with changes in the total number of neurons. On the other hand, the pronounced age-related decline in the number of neurons containing non-phosphorylated neurofilaments as well as their protein levels in the central auditory system may contribute to age-related deterioration of hearing function.

Keywords: SMI-32, neurofilaments, number of neurons, aging, auditory system

OPEN ACCESS

Edited by:
Marta Milo,
University of Sheffield, UK

Reviewed by:
Miguel A. Merchán,
University of Salamanca, Spain
Khaleel A. Razak,
University of California, USA

****Correspondence:***
Jana Burianová,
Department of Auditory Neuroscience, Institute of Experimental Medicine of the Czech Academy of Sciences, Vídeňská 1083, Prague 14220, Czech Republic
burianova@biomed.cas.cz

Received: *23 January 2015*
Paper pending published: *03 February 2015*
Accepted: *23 February 2015*
Published: *11 March 2015*

Citation:
Burianová J, Ouda L and Syka J (2015) The influence of aging on the number of neurons and levels of non-phosporylated neurofilament proteins in the central auditory system of rats.
Front. Aging Neurosci. 7:27.
doi: 10.3389/fnagi.2015.00027

Introduction

One intriguing feature of the naturally aging mammalian brain is its relatively slow rate of neuronal loss. Initial studies that used biased microscopic techniques rather overestimated its extent (Brody, 1955; Devaney and Johnson, 1980) while modern quantitative methods have adjusted these estimates, rendering the loss less dramatic, and not exceeding approximately 10% in the

case of human cortex (Pakkenberg and Gundersen, 1997). More detailed research in rodents have revealed variability across brain structures, but generally the decline in the number of neurons has been found to be marginal, falling below statistical significance in several brain areas, including the hippocampus (Rapp and Gallagher, 1996) and entorhinal cortex (Merrill et al., 2001). Therefore, naturally deteriorating brain function represented by cognitive processes cannot be simply accounted for by a numerical decline in the neuronal population.

Aging of the central auditory system has been intensively studied in an attempt to reveal the mechanisms underlying gradual age-related hearing loss (ARHL), or presbycusis. While peripheral alterations are relatively well documented (Schuknecht and Gacek, 1993; Gates and Mills, 2005; Buckiova et al., 2007) the central part of presbycusis remains far from being elucidated (for review see Syka, 2002; Caspary et al., 2008; Canlon et al., 2010) including the question of whether it develops independently or as a consequence of the restricted peripheral input. Studies in rodents have suggested that central presbycusis may result from disturbances of the inhibitory function mediated by GABAergic neurons in higher parts of the auditory pathway (Caspary et al., 2008). These studies demonstrated an age-related reduction in levels of mRNA and proteins or reduced immunoreactivity for glutamate decarboxylase (Ling et al., 2005; Burianova et al., 2009), a key GABA-synthesizing enzyme. In addition, the reduction was also present in calcium binding proteins such as parvalbumin, calbindin, and calretinin (Ouda et al., 2008, 2012a) which are prevalently found in the GABAergic neurons (Kubota et al., 1994; Gonchar and Burkhalter, 1997; Jinno and Kosaka, 2006; Gonchar et al., 2007). This is particularly important given the fact that GABAergic neurons play a crucial role during the processing of temporal parameters of complex sounds (Kawaguchi and Kubota, 1998; Bartos et al., 2007). Indeed, elderly people experience an inability to comprehend speech in a noisy environment (Pronk et al., 2013) and old rats display deficits in the detection and discrimination of gaps in a continuous noise (Suta et al., 2011).

There are other markers of aging in the central auditory system that reflect disturbances of its function. Non-phosphorylated epitopes of heavy and medium neurofilament subunits which are recognized by SMI-32 antibodies (Sternberger and Sternberger, 1983) could be such a candidate molecule. Together with a light subunit, these subunits form a neurofilament triplet thought to be associated with the level of myelination and the fast conduction of axons. Although SMI-32-ir neurons usually constitute a minority of the neuronal population in a particular central auditory brain structure (Ouda et al., 2012b), their conductance properties may play an important role in carrying and processing fast auditory signals. In the cerebral cortex, SMI-32-ir neurons are more abundant in layer V, often as subcortically projecting pyramidal neurons characterized by long apical dendrites (Ouda et al., 2012b) and bursts of action potentials (Voelker et al., 2004). SMI-32-ir neurons in the neocortex have been shown to be particularly vulnerable during Alzheimer's (Hof and Morrison, 1990) and Huntington (Cudkowicz and Kowall, 1990) disease, raising concerns over whether they are also poorly resistant during natural aging. These neurons have not yet been evaluated in the central auditory system, but related studies have confirmed age-related alterations in SMI-32 recognized epitope, indicating a progressive hyperphosphorylation of the neurofilaments (Vickers et al., 1992; Veeranna et al., 2011).

The main aim of the present study was originally to evaluate changes in SMI-32 immunoreactivity during natural aging in upper parts of the central auditory system, i.e., the inferior colliculus (IC), medial geniculate body (MGB), and auditory cortex (AC). However, these changes cannot be fully understood and properly interpreted without knowing whether there are age-related changes in the total number of neurons in each of the studied structures. Reliable knowledge of the total number of neurons in the different regions of the auditory system and their respective changes with aging can aid us in understanding the principles of presbycusis. To date, only a few unbiased assessments have been published with the aim of determining the total number of neurons in the nuclei and regions of the central auditory system of rats (Kulesza et al., 2002; Ouda et al., 2012b). Thus, the second aim of this study is to provide an unbiased estimate of the neuron numbers.

We employed an approach used in our previous work, comparing age-related changes occurring in Fischer 344 strain, known for its accelerated aging, including early onset of hearing loss, with Long Evans rats, which has preserved hearing function until late senescence.

Materials and Methods

Animals

In total, 22 Long Evans rats (14 young animals, 3–6 months old, and 8 aged animals, 29–35 months old), and 16 Fischer 344 rats (8 young animals, 3–4 months old, and 8 aged animals, 20–25 months old) were used in the experiments. Ages of the aged animals were intentionally chosen to be the highest possible, derived from the expected life span of the correspondent rat strain. All Long Evans rats were obtained from our local facility at the age of 2 months and reared in-house under the same conditions. All Fischer 344 rats were purchased at 2 months of age from Charles River Deutschland (Charles River Wiga GmbH, Sulzfeld, Germany) and then reared in-house under standard rearing conditions. All animals were housed in age-matched groups of two or three per cage under standard laboratory conditions in a constant environment and a 12/12 h normal light/dark cycle; food and water remained available *ad libitum*. We did not observe signs of any middle ear infection in any animal during their stay in our animal facility. The care and use of animals and all experimental procedures followed the principles of laboratory animal care and were performed in compliance with the guidelines of the Ethical Committee, Institute of Experimental Medicine of the Czech Academy of Sciences, and the Declaration of Helsinki.

Nissl Staining

Animals

Fourteen male Long Evans rats (10 young animals, 3–6 months old, and 4 aged animals, 29–33 months old) and 8 Fischer 344 rats (4 young animals, 3 months old, and 4 aged animals, 20–24 months old) were used in the experiments. Results obtained from the study of the young Long Evans rats have already been published (Ouda et al., 2012b).

Tissue Processing

Under deep anesthesia (ketamine 50 mg/kg + xylazine 8 mg/kg, *i.m.*) the animals were transcardially perfused with saline followed by 4% paraformaldehyde fixative in 0.1 M phosphate buffer (pH 7.4). Following 15 min of perfusion, the brains were removed, postfixed overnight at 4°C (same fixative), and then cryoprotected with 10, 20, and 30% sucrose in phosphate buffer for 1 day each.

Nissl Staining

Coronal serial sections (40 μm thick) were cut with a freezing microtome. Sections were mounted in serial order onto glass slides, air-dried, stained for Nissl substance using standard laboratory protocol with 1% cresyl violet and coverslipped. An illustration of the Nissl stained sections is provided in **Figure 1**.

Immunohistochemistry – SMI-32

Ten male Long Evans rats (6 young animals, 3–6 months old, and 4 aged animals, 29–33 months old) and 8 Fischer 344 rats (4 young animals, 3 months old, and 4 aged animals, 20–24 months old) were used. The results obtained from the young Long Evans rats have already been published (Ouda et al., 2012b). The tissue was processed as in 2.2.2. coronal serial sections (40 μm thick) were cut with a freezing microtome. Free-floating sections were preincubated in a blocking solution (5% low fat milk in PBS, 1 h) and then immersed in PBS containing the mouse monoclonal antibody SMI-32 against non-phosphorylated heavy and medium neurofilament subunits (1:1000, Covance Research Products, USA) for 18 h (4°C). Sections were incubated with a goat anti-mouse biotinylated secondary antibody (1:200, Sigma-Aldrich) for 1 h, and then with avidin-biotin-peroxidase complex (1:100, Vector Laboratories) for 1 h at room temperature. The reaction was visualized with 0.02% diaminobenzidine (DAB) and 0.01% hydrogen peroxide (15 min). Finally, the sections were mounted on slides, dehydrated and coverslipped.

Microscopy, Imaging and Stereological Quantification

The number of Nissl stained neurons was evaluated in all sections containing the IC, MGB, and AC, and delineated according to anatomical atlases (Zilles, 1985; Paxinos and Watson, 1998). In addition, the number of SMI-32-ir stained neurons was also evaluated in the rat visual cortex (VC).

In the rat brain, sections for the IC were sampled from bregma −8.0 to −9.2 mm, for the MGB from bregma −5.0 to −6.2 mm, for the AC from bregma −4.2 mm to −5.8 mm, and for the VC from bregma – 4.5 mm to – 9.2 mm (Zilles, 1985).

Estimates of the total number of neurons were inferred from the sample counts of Nissl positive nuclei. For this purpose an unbiased stereological method, the optical fractionator, was used. Measurements were performed using bright-field microscopy (Leica DMRXA microscope) equipped with an X-Y-Z motor stage and Stereo Investigator software (MicroBrightField, Inc., Colchester, VT, USA) was used to perform the optical dissector and nucleator protocol (West et al., 1991; Mayhew and Gundersen, 1996; Andersen and Gundersen, 1999).

First, we randomly selected a section containing the analyzed auditory structure, outlined the selected area of interest (5 × or 40 × objective lens) and then uniformly sampled it. The stereological probes were used in conjunction with a 100 × objective lens, while the counting frames used to obtain the sampling remained the same size in all the examined regions (2500 μm^2 – 50 × 50 μm) and were formed by two inclusion lines and two exclusion lines. The frequency of the samples depended on the size of the structure (section fraction). While the original thickness of the sections was 40 μm, due to the tissue processing, the average thickness was reduced to approximately 20 μm. The height of the optical dissector was held constant at 10 μm and the first and last 5 μm thicknesses of the section were omitted from the analysis (guard zones). Each neuron in the counting frame was counted when its nucleus came into maximum focus. To exclude glia cells from the analysis we identified them on the basis of their limited or non-visible cytoplasm and small dark nuclei.

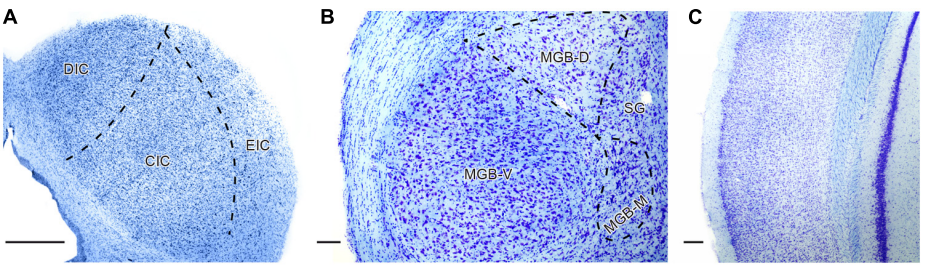

FIGURE 1 | Illustration of Nissl staining in the inferior colliculus (IC; A), medial geniculate body (MGB; B), and auditory cortex (AC; C) of young Long Evans rat with delineation of the principle subdivisions in the particular structure. DIC, dorsal cortex of the IC; CIC, central nucleus of the IC; EIC, external cortex of the IC; MGB-V, -D, -M – ventral, dorsal, medial divisions of the MGB; SG, suprageniculate nucleus of the MGB. Scale bar **(A,C)** = 200 μm, **(B)** = 100 μm.

The neuronal estimate for a given structure (Nest) was calculated as Nest = number of counted cells × area fraction × section fraction × dissector fraction.

The method of estimating the number of SMI-32-ir neurons was essentially the same as that used in the evaluation of the Nissl stained neurons. Specific differences are described elsewhere (Ouda et al., 2012b).

Western Blot Protein Analysis

Eight male Long Evans rats (4 young animals, 3–6 months old, and 4 aged animals, 30–35 months old) and 8 Fischer 344 rats (4 young animals, 4 months old, and 4 aged animals, 21–25 months old) were used in the experiments. Anesthetized rats (ketamine 35 mg/kg + xylazine 6 mg/kg, i.m.) were decapitated, their brains quickly extracted and rinsed in ice-cold physiological solution, and the ICs, ACs, and VCs were rapidly removed bilaterally. The samples included the whole IC, the Te1 + Te3 (Zilles, 1985) areas of the AC, and the V1 and V2 areas of the VC (Paxinos and Watson, 1998). All samples were immediately put into dry ice after extraction and stored frozen at −80°C until processed. For the analysis, ICs, ACs, and VCs were homogenized by a Potter–Elvehjem homogenizer in 0.05 M Tris–NaCl (pH 7.4) buffer with protease inhibitors (Sigma-Aldrich). The homogenate was centrifuged at 10,000*g* for 10 min at 4°C. To ensure similar protein loading, the total protein concentration of these extracts was determined using the Bradford method with BSA as the standard (Bradford, 1976). An absorbance of 595 nm was used. Samples (cytosolic fractions) were incubated in boiling water for 10 min at 80°C in sodium dodecyl sulfate–polyacrylamide gel electrophoresis buffer containing 10% glycerol, 2% SDS, 0.05% bromphenol blue and 4 M dithiotreitol. Samples were then subjected to Tris/Tricine/ SDS–PAGE on a 3% bis-acrylamide polyacrylamide gel at 30 mA/gel for 150 min on a Mini-Protean II apparatus (Bio-Rad; Ogita and Markert, 1979). After electrophoresis, the resolved proteins were transferred (Bio-Rad Mini Protean II transblot apparatus at 350 mA for 60 min at 4°C in 25 mM Tris, 192 mM glycine, 20% methanol, 0.1% SDS) to a nitrocellulose membrane (Amersham, Biosciences; Towbin et al., 1979). Equal loading and transfer of the western blot samples were further verified by reversible total protein staining of the nitrocellulose membrane with Ponceau-S reversible membrane staining. Loading control was made using the same amount of samples separated by SDS-PAGE in the same conditions and stained with sensitive Coomassie Blue. Membranes were incubated in 3% non-fat dry milk, in 10% Tris-buffered saline with 0.05% Tween 20 (TBST) for 65 min at room temperature to block non-specific protein binding. After being washed in TBST buffer (three times quickly, 3 × 5 min each), the membranes were probed overnight at 4°C with SMI-32-specific (mouse monoclonal, Covance Research Products, USA, 1:500 in TBST) or actin-specific (mouse monoclonal, Chemicon-Millipore, 1:3000 in TBST) primary antisera. The membranes were washed again and incubated with goat anti-mouse IgG antibody conjugated with horse radish peroxidase (Upstate, 1:7500 in TBST) for 2 h at room temperature. Before enhanced chemiluminescence (ECL), the membranes were washed as described above and stored in TBST for at least 2 h. For ECL, substrates A (Luminol solution) and B (H_2O_2 solution) were prepared, mixed 40:1 (Amersham Biosciences) just before use, and poured onto the membranes. The specific signals were detected on autoradiographic film (Kodak MXB). Films were developed at room temperature in a dark room, stopped, fixed, washed under running cold water, and air-dried. Scanning (Canon CanoScan 9000F) and ImageQuant software were used for quantifying the relative abundance of SMI-32 and actin in the individual samples. The amount of protein applied to the gel intentionally varied for each fraction in order to achieve linearity with the intensity × area (volume) of the band on the western blot. Samples from the compared experimental groups were run on the same gel and quantified on the same membrane. To ensure the specificity of SMI-32 and actin immunoreactive proteins, prestained molecular weight protein standards were used (Invitrogen). The levels of SMI-32 were calculated as the ratio of the optical density of the antibody of interest to the optical density of the antibody directed against actin.

Statistical Analysis

The statistical significance of the differences between the groups was assessed by Mann–Whitney *U* test with the use of GraphPad Prism software (version 4.0). *P*-values of 0.05 or less were considered statistically significant.

Results

Long Evans Rats

For Long Evans rats, the total numbers of neurons in the particular regions of the auditory pathway in young animals were previously evaluated by Ouda et al. (2012b) and the data obtained from the IC, MGB, and AC serve as the statistical comparison in the present paper. The observed age-related changes in the total number of neurons in all three structures were non-significant. In aged rats, the total number of neurons decreased by 7% in the IC, by 12% in the MGB and by 9% in the AC (**Figure 2**).

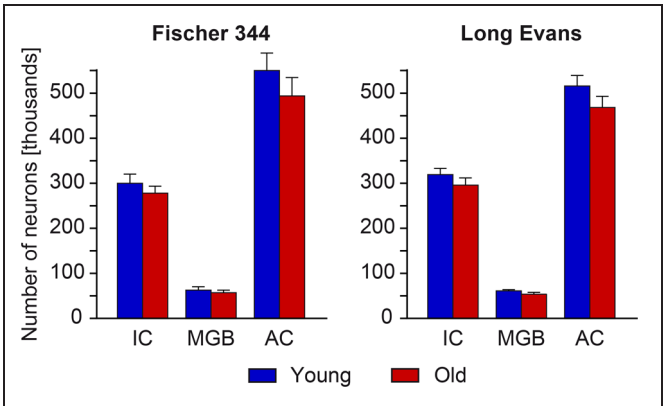

FIGURE 2 | Numerical estimates of the total number of neurons in the IC, MGB, and AC of young and old rats. With aging, we found only a mild and non-significant decline in the total number of neurons in all three analyzed auditory structures in both rat strains.

The distribution and number of SMI-32-ir neurons was also previously evaluated in Ouda et al. (2012b) and serves as the statistical comparison in the present paper. In both, young and old Long Evans rats, SMI-32-ir neurons were distributed relatively homogenously throughout the whole IC with higher density in the ventral and medial parts of the central nucleus of the IC, i.e., in the high-frequency region, which corresponds to a higher density of neurons apparent in the Nissl staining of this region. In the MGB, the SMI-32-ir neurons were much more prevalent in the ventral division and in the adjacent region of the dorsal division, while the dorsolateral parts of the dorsal division contained only a few positive cells. In the AC, SMI-32-ir neurons were scattered throughout cortical layers II–VI with a dominant position of intensely stained SMI-32-ir pyramidal neurons with thick immunopositive apical dendrites in layers III and V and a more heterogeneous population in layer VI (**Figure 3**).

In contrast with the mild changes in the total number of neurons, the age-related decline in the number of SMI-32-ir neurons was significant in all three examined structures. In the IC the number decreased by 17%, in the MGB by 18% and in the AC by 14% (all $P < 0.05$). In comparison with the AC, the age-related decrease was milder in the VC, 11%, and was not significant. (**Figure 4**). Western blot analysis revealed a significant age-related decline in the levels of non-phosphorylated neurofilaments (SMI-32 positive) in old Long Evans rats in comparison with young animals by 34% in the IC, 28% in the AC, and 21% in the VC (IC and AC $P < 0.001$; VC $P < 0.01$; **Figure 5**).

Fischer 344 Rats

In young Fischer 344 rats, the observed total numbers of neurons in the IC, MGB, and AC were similar to that found in young Long Evans rats. In addition to this, the observed age-related changes in the total number of neurons in all three structures were also relatively small and non-significant. In aged Fischer 344 rats, the total number of neurons decreased by 9% in the IC, by 11% in the MGB, and by 10% in the AC (**Figure 2**).

The distribution and quantity of SMI-32-ir neurons in the IC, MGB, and AC of young Fischer 344 rats corresponded with the situation present in young Long Evans rats. Also, as in old Long Evans rats, the number of SMI-32-ir neurons decreased significantly in Fischer 344 rats with aging. In the IC, their number decreased by 16%, in the MGB by 20%, and in the AC by 17% (all $P < 0.05$), while in the VC the decrease was lower, 13%, and was not significant (**Figure 4**). Western blot analysis revealed a significant age-related decline in the levels of non-phosphorylated neurofilaments (SMI-32 positive) in old Fischer 344 rats in comparison with young animals by 35% in the IC, 32% in the AC, and 25% in the VC (IC and VC $P < 0.001$; AC $P < 0.01$; **Figure 5**).

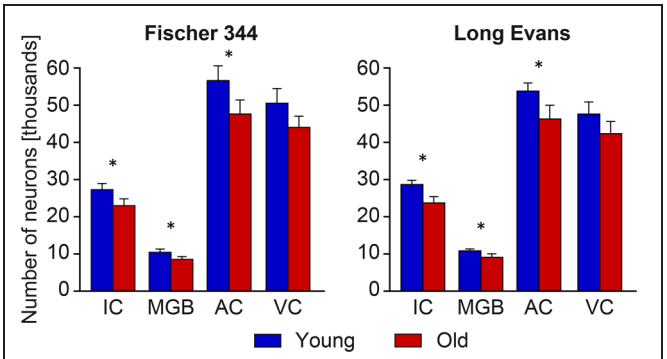

FIGURE 4 | Number of SMI-32-immunoreactive neurons in the IC, MGB, AC areas (AC – Te1 and Te3) and visual cortex (VC) in young and old rats of both the Long Evans and Fischer 344 rat strains. The error bars represent SEM (*$P < 0.05$).

Discussion

Age-Related Cell Loss in the Examined Auditory Structures

We demonstrated a non-significant age-related decline in both Long Evans and Fischer 344 rats in the IC, MGB, and AC. Our results fully support the view that natural age-related neuronal loss is much less prominent than previously thought. Biased non-stereological methods inferring neuron counts from neuron densities rendered estimates of the age-related neuronal loss in the human VC as high as nearly 50% (Devaney and Johnson, 1980). Later, stereological tools such as the optical dissector enabled the correction of these estimates so that the number of neurons in the whole human neocortex was believed not to reduce by more than 10% with aging (Pakkenberg and Gundersen, 1997). Due to fewer methodological constraints, more reports are available from rodent studies. Although the cerebellum (Rutten et al.,

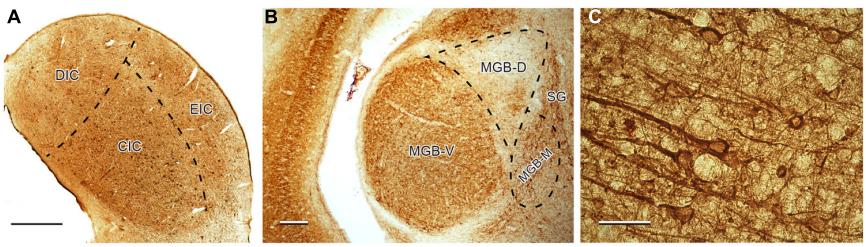

FIGURE 3 | Illustration of SMI-32 immunoreactivity in the IC (A), MGB (B), and in the Te1 auditory cortical area (C) in young Long Evans rats. DIC, dorsal cortex of the IC; CIC, central nucleus of the IC; EIC, external cortex of the IC; MGB-V, -D, -M, ventral, dorsal, medial divisions of the MGB; SG, suprageniculate nucleus of the MGB. Scale bar **(A,B)** = 200 μm, **(C)** = 50 μm.

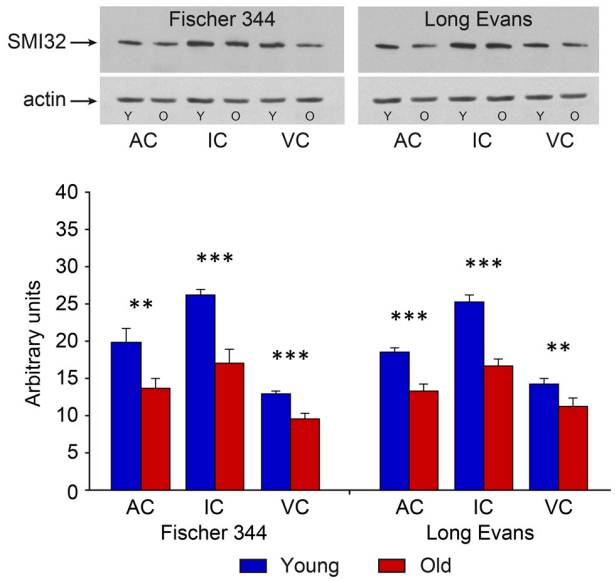

FIGURE 5 | Results of western blot SMI-32 analysis in young and old animals of both examined strains. Corresponding representative films of western blot analysis of SMI-32 (200 kDa) developed with the enhanced chemiluminescence (ECL) method. Actin, used as an internal control, was detected at the position corresponding to a molecular weight of 42 kDa. The abbreviations are: AC, auditory cortex; IC, inferior colliculus; VC, visual cortex, Y, young; O, old animals. Arbitrary units are calculated as the ratio of the optical densities of the examined protein and actin (in scanned films analyzed using ImageQuant software). The error bars represent SD (**$P < 0.01$, ***$P < 0.001$).

2007) as well as the prefrontal (Stranahan et al., 2012) and occipital cortices (Yates et al., 2008) have been reported to undergo mild neuronal loss, there are multiple brain regions that are resistant to significant age-related neuronal death. These include the hippocampus (Rapp and Gallagher, 1996; Rutten et al., 2007) and entorhinal cortices (Merrill et al., 2001) in which it has been convincingly demonstrated that a natural decline in function (cognitive capabilities) showed no correlation with the number of neurons of its neural substrate (Rapp and Gallagher, 1996; Merrill et al., 2001). Our data suggests that such a decline of function, not associated with neuronal loss, holds true also for the auditory system. Although we did not directly correlate cell numbers of the IC, MGB, and AC with any auditory functions in the present study, we can refer to previous work comparing corresponding cohorts of Long Evans rats. Aged animals of this strain were found impaired in auditory cortex-dependent temporal processing of auditory stimuli (Suta et al., 2011) as well as in responses to startle stimuli (Rybalko et al., 2012), a process thought to involve (among others) the IC.

The survival of neurons in the auditory pathway seems to follow the rule that regions proximal to the periphery are more vulnerable to cell death due to the negative impact of age-related degradation of the cochlea, while structures located more centrally are less affected. Accordingly, aged C57/BL/6J mice, which exhibit fast deterioration of cochlear function, display significant neuronal decline in the dorsal and posteroventral cochlear nuclei (Idrizbegovic et al., 2004). On the contrary, CBA/CaJ mice that have a more preserved cochlear function show only moderate loss of neurons in the dorsal cochlear nucleus (Idrizbegovic et al., 2001). Our current data apparently matches the above mentioned rule as we report relatively preserved neuronal populations in the upper parts of the auditory pathway. Importantly, this holds true also in Fischer 344 rats, i.e., the strain with cochlea degeneration in early senescence. Furthermore, results of our examination of the IC are in agreement with the previous (albeit not unbiased) neuronal estimates, reporting no significant loss in the whole IC of aged C57/BL/6J and CBA mice (Willott et al., 1994), and the central nucleus of the IC in F344 rats (Helfert et al., 1999). The finding that the rat AC does not display substantial neuronal decline is in line with recent data performed on the Long Evans strain by Ouellet and de Villers-Sidani (2014). These authors investigated the temporal trajectory of various neuron subpopulations and found that the total counts of neurons as revealed by Nissl staining showed a remarkable decline in number from P9 to P20, however, following this it slowed down and remained non-significant until the latest age studied (25 months). Thus, our data suggests an extension of this period up until 33 months. On the other hand, Martin del Campo et al. (2012) reported a subtle yet significant loss of neurons of C57/BL/6J mice in the deep (V–VI) cortical layers while the neuron number in the superficial layers remained preserved, suggesting that auditory cortex in the mice might be more vulnerable to neuronal loss than in the rats.

Age-Related Changes in the Central Auditory System: Involvement of Inhibitory Neurons

Our current data may also enhance the interpretation of previous studies comparing both strains of rats, focusing on the investigation of age-related changes in markers of the inhibitory system (Ouda et al., 2008, 2012a; Burianova et al., 2009). It should be noted here that statistical differences presented in Burianova et al. (2009) were further strengthened by adding more animals of both strains (Supplementary Figure S1). The significant age-related alterations in the markers of inhibitory system found in the cited studies are therefore not accompanied with substantial loss of neurons. We suggest that a diminished expression of proteins in the originally immuno-reactive neurons may be behind the age-related reduction in the detectable numbers of immuno-reactive neurons in the higher regions of the auditory pathway. Such a process could also explain the observed down-regulation of the number of GAD (Burianova et al., 2009) or calcium binding protein expressing neurons (Ouda et al., 2008, 2012a) reported in aged rats. Similarly, the up-regulation of expression or *de novo* expression of proteins in the previously non-expressing neurons, such as the increase in the number of PV-ir neurons in the primary AC of aged rats after intense auditory training (de Villers-Sidani et al., 2010) or the increase in the number of CR-ir neurons in the IC of old CBA mice (Zettel et al., 1997), also supports this hypothesis. The work of Ouellet and de Villers-Sidani (2014) clearly demonstrates how age-related changes in the number of inhibitory

cells labeled by a particular marker have their own pattern regardless of the total number of neurons. Further studies, aimed at identifying the rate of particular population cell loss and diminished (or increased) expression of the corresponding marker protein would provide valuable insight into the mechanisms of inhibition disturbance, a putative cause of central presbycusis.

Age-Related Loss of SMI-32-ir Neurons and Protein Levels

Immuno-reactivity for non-phosphorylated epitopes of heavy and medium neurofilament chains decreased in senescent rats of both strains to a similar degree in the IC, MGB, and AC. The decline was more robust when we evaluated the protein levels using western blot. The results are in accord with the study by Liu et al. (2013) that were conducted on C57BL/6 mice and found an almost three times lower level of protein labeled by SMI-32 in the neocortex of 12 months old mice compared to 5 months old mice. We further found a significant loss in the number of SMI-32-ir neurons (∼15–20%) in each examined structure. Since SMI-32-ir neurons only represent around 10–20% of the IC, MGB, or AC neurons (Ouda et al., 2012b), this statistically significant decline is not contradictory to the non-significant loss of the total number of neurons and may indicate a selective vulnerability of SMI-32-ir neurons to cell death. Indeed, such selective vulnerability has been documented in pathological states such as Alzheimer's (Hof and Morrison, 1990) and Huntington disease (Cudkowicz and Kowall, 1990). However, it is unlikely that the whole decline in SMI-32-ir neurons would be attributable to cell death. Instead, given the relatively large decline in the level of the protein compared to the decline in the number of immunoreactive neurons we believe that most of the decrease of SMI-32 immunoreactivity is due to the loss of the recognizable epitope caused by phosphorylation. The SMI-32 antibody recognizes a non-phosphorylated site on the carboxyl-terminal regions of the NF-M and NF-H subunits (Soifer et al., 1991). The C-terminal has been documented to undergo extensive phosphorylation during aging (Veeranna et al., 2011) likely as a result of the declining function of phosphatases. It is questionable whether this is a mechanism ensuring increased stability of neurofilaments or a sign of degrading function. Phosphorylation prevents neurofilaments from proteolysis (Goldstein et al., 1987; Pant and Veeranna, 1995) and regulates axonal transport (Shea and Lee, 2011). Moreover, it takes place particularly in axons, stabilizing, and maintaining their caliber, while non-phosphorylated neurofilaments, such as those labeled by SMI-32, remain in somata and dendrites (Sternberger and Sternberger, 1983). On the other hand, an altered neurofilament content is associated with many pathologies. While neurons in Alzheimer's disease are characterized by the accumulation of phosphorylated neurofilaments in the perikarya (Wang et al., 2001), multiple sclerosis reverses the natural pattern, i.e., dephosphorylation occurs in axons and hyperphosphorylation in perikarya and dendrites (Trapp et al., 1998). Collectively these data provide evidence that altering the phosphorylation status is not uncommon, both in health and disease, and thus suggests that our original SMI-32-ir cells may have been phosphorylated over time, becoming invisible to the labeling in senescence. However, how this specifically affects the processing of auditory signals remains largely unknown. Some insight could be gained by considering the distribution of SMI-32-ir neurons within brain networks and their morphological characteristics.

The Distribution of SMI-32-ir Neurons and Their Characteristics

Data about the distribution of SMI-32 immuno-reactivity comes mainly from anatomical examinations which utilize its site-specific staining pattern, enabling reliable parcellation of certain parts of the neocortex in cats (Mellott et al., 2010), macaques (Gabernet et al., 1999), rats (Van De Werd and Uylings, 2008), and other mammals, although subcortical examinations are much more sparse (Baizer, 2009; Ouda et al., 2012b). In the study of Ouda et al. (2012b), the authors found that in the rat central auditory system, SMI-32-ir neurons were present in virtually all studied structures although they formed only the minority of neurons (with the exception of medial nucleus of the trapezoid body) with an average content of 10–20%. Such a fraction was also reported in a study focused on the rat neocortex (Kirkcaldie et al., 2002). SMI-32-ir cells are usually larger than the average sized neurons (Campbell and Morrison, 1989; Tsang et al., 2000; Ouda et al., 2012b) with long projecting axons, e.g., motoneurons (Tsang et al., 2000). However, SMI-32 immunoreactivity is better correlated with the degree of myelination, rather than axon length (Kirkcaldie et al., 2002). Thus, SMI-32-ir cells are typically highly myelinated and are consequently fast conductors. In the cortex, they are predominantly type I pyramidal cortical neurons, characterized by burst activity (Molnár and Cheung, 2006). Collectively, these properties strongly suggest that SMI-32-ir neurons belong to the networks involved in processing complex sounds which require fast and time precise conduction of action potentials. These networks can also be seriously affected by the demyelination that accompanies natural aging (Peters, 2009; Tremblay et al., 2012), which would subsequently manifest in symptoms of central presbycusis. We can speculate that demyelination was associated with our decrease in SMI-32 immunoreactivity, but this would require further investigation. Although a direct link between presbycusis and age-related degradation of SMI-32 immunoreactivity is still yet to be revealed, there are physiological alterations indicating deteriorated function of fast conducting neurons that may potentially involve SMI-32-ir neurons. In rodents, these alteration include deteriorated processing of fast FM sweeps (Mendelson and Ricketts, 2001), slowing down of responses to the FM sweeps or increased variability to the same auditory stimuli (Trujillo and Razak, 2013).

In addition to the upper part of the auditory pathway, we evaluated SMI-32 immunoreactivity in the VC which also exhibited a significant age-related decline. Non-phosphorylated neurofilaments have been found in the monkey VC in association with myelin sheaths (Chaudhuri et al., 1996). In mice, myelination of the VC is altered during aging (Tremblay et al., 2012). Combined with our results, these studies suggest that in terms of SMI-32 immunoreactivity the age-related changes observed in the VC

parallel those in the AC although the decline is less pronounced. Its functional implications are, however, beyond the scope of this study.

Age-Related Changes and Comparisons Between the Two Rat Strains

It is a remarkable fact that the aforementioned age-related changes in neuron numbers or protein levels, GAD, calbindin, and calretinin share a mostly similar pattern in both Long Evans and Fischer 344 rats. This is also true for the presented results of SMI-32 immunoreactivity. The two strains differ substantially in age-related pathology of the peripheral auditory system. While Long Evans rats display a slow decline in auditory function, the Fischer 344 strain shows (Syka, 2010) (i) decreasing and eventually disappearing distortion product otoacoustic emissions (Popelar et al., 2006), (ii) as well as degenerative and collagen changes in the stria vascularis (Buckiova et al., 2006, 2007); these pathologies result in increased thresholds of auditory brain responses and qualitatively different responses to startle stimuli and their prepulse inhibition (Rybalko et al., 2012). The inter-strain comparison provides good evidence that age-related changes in the subcortical and cortical auditory structures develop independently (at least in part) of the peripheral condition. Our findings of no observable cell loss in both rat strains thus provide further support for periphery-independent aging of the auditory system.

Conclusion

In conclusion, we provided unbiased stereological estimates of neuronal numbers in the IC, MGB, and AC. Aging exerts small and non-significant effects on neuron numbers with a decline of about 10% in both examined rat strains. These data suggest that previously found significant declines of markers of inhibitory functions in the rat central auditory pathway, such as GAD (Burianova et al., 2009), parvalbumin (Ouda et al., 2008), and calbindin (Ouda et al., 2012a) cannot be accounted for by significant neuronal loss. Furthermore we report a decline of non-phosphorylated neurofilaments in rats which is presumably due to age related phosphorylation of the SMI-32 recognized epitope. This would interact with the process of myelination and consequently alter the conductance properties of neurons. In the central auditory system, this would seriously affect the processing of complex auditory stimuli. Importantly, age-related changes occur in both Long Evans and Fischer 344 in a similar pattern, suggesting that changes in the central auditory system develop independently of the functional state of the periphery.

Author Contributions

JB performed western blot evaluation, cell counting, and wrote the article. LO performed perfusions and cell counts analysis. JS coordinated and supervised the study as well as writing the article.

Acknowledgments

The authors wish to thank Mrs. J. Janouskova for the help with immunostaining and Mr. J. Setnicka for assistance with preparation of the figures. This study was supported by the Grant Agency of the Czech Republic P304/12/1342 and P304/12/G069.

Supplementary Material

The Supplementary Material for this article can be found online at: http://www.frontiersin.org/journal/10.3389/fnagi.2015.00027/abstract

References

Andersen, B. B., and Gundersen, H. J. (1999). Pronounced loss of cell nuclei and anisotropic deformation of thick sections. *J. Microsc.* 196, 69–73. doi: 10.1046/j.1365-2818.1999.00555.x

Baizer, J. S. (2009). Nonphosphorylated neurofilament protein is expressed by scattered neurons in the vestibular and precerebellar brainstem. *Brain Res.* 1298, 46–56. doi: 10.1016/j.brainres.2009.08.073

Bartos, M., Vida, I., and Jonas, P. (2007). Synaptic mechanisms of synchronized gamma oscillations in inhibitory interneuron networks. *Nat. Rev. Neurosci.* 8, 45–56. doi: 10.1038/nrn2044

Bradford, M. M. (1976). A rapid and sensitive method for the quantitation of microgram quantities of protein utilizing the principle of protein-dye binding. *Anal. Biochem.* 72, 248–254. doi: 10.1016/0003-2697(76)90527-3

Brody, H. (1955). Organization of the cerebral cortex. III. A study of aging in the human cerebral cortex. *J. Comp. Neurol.* 102, 511–516. doi: 10.1002/cne.901020206

Buckiova, D., Popelar, J., and Syka, J. (2006). Collagen changes in the cochlea of aged Fischer 344 rats. *Exp. Gerontol.* 41, 296–302. doi: 10.1016/j.exger.2005.11.010

Buckiova, D., Popelar, J., and Syka, J. (2007). Aging cochleas in the F344 rat: morphological and functional changes. *Exp. Gerontol.* 42, 629–638. doi: 10.1016/j.exger.2007.02.007

Burianova, J., Ouda, L., Profant, O., and Syka, J. (2009). Age-related changes in GAD levels in the central auditory system of the rat. *Exp. Gerontol.* 44, 161–169. doi: 10.1016/j.exger.2008.09.012

Campbell, M. J., and Morrison, J. H. (1989). Monoclonal antibody to neurofilament protein (SMI-32) labels a subpopulation of pyramidal neurons in the human and monkey neocortex. *J. Comp. Neurol.* 282, 191–205. doi: 10.1002/cne.902820204

Canlon, B., Illing, R., and Walton, J. (2010). "Cell Biology and physiology of the aging central auditory pathway," in *The Aging Auditory System*, eds S. Gordon-Salant, R. D. Frisina, A. N. Popper, and R. R. Fay (New York: Springer), 39–74.

Caspary, D. M., Ling, L., Turner, J. G., and Hughes, L. F. (2008). Inhibitory neurotransmission, plasticity and aging in the mammalian central auditory system. *J. Exp. Biol.* 211, 1781–1791. doi: 10.1242/jeb.013581

Chaudhuri, A., Zangenehpour, S., Matsubara, J. A., and Cynader, M. S. (1996). Differential expression of neurofilament protein in the visual system of the vervet monkey. *Brain Res.* 709, 17–26. doi: 10.1016/0006-8993(95)01217-6

Cudkowicz, M., and Kowall, N. W. (1990). Degeneration of pyramidal projection neurons in Huntington's disease cortex. *Ann. Neurol.* 27, 200–204. doi: 10.1002/ana.410270217

de Villers-Sidani, E., Alzghoul, L., Zhou, X., Simpson, K. L., Lin, R. C., and Merzenich, M. M. (2010). Recovery of functional and structural age-related

changes in the rat primary auditory cortex with operant training. *Proc. Natl. Acad. Sci. U.S.A.* 107, 13900–13905. doi: 10.1073/pnas.1007885107

Devaney, K. O., and Johnson, H. A. (1980). Neuron loss in the aging visual cortex of man. *J. Gerontol.* 35, 836–841. doi: 10.1093/geronj/35.6.836

Gabernet, L., Meskenaïte, V., and Hepp-Reymond, M. C. (1999). Parcellation of the lateral premotor cortex of the macaque monkey based on staining with the neurofilament antibody SMI-32. *Exp. Brain Res.* 128, 188–193. doi: 10.1007/s002210050834

Gates, G. A., and Mills, J. H. (2005). Presbycusis. *Lancet* 366, 1111–1120. doi: 10.1016/S0140-6736(05)67423-5

Goldstein, M. E., Sternberger, N. H., and Sternberger, L. A. (1987). Phosphorylation protects neurofilaments against proteolysis. *J. Neuroimmunol.* 14, 149–160. doi: 10.1016/0165-5728(87)90049-X

Gonchar, Y., and Burkhalter, A. (1997). Three distinct families of GABAergic neurons in rat visual cortex. *Cereb. Cortex* 7, 347–358. doi: 10.1093/cercor/7.4.347

Gonchar, Y., Wang, Q., and Burkhalter, A. (2007). Multiple distinct subtypes of GABAergic neurons in mouse visual cortex identified by triple immunostaining. *Front. Neuroanat.* 1:3. doi: 10.3389/neuro.05.003.2007

Helfert, R. H., Sommer, T. J., Meeks, J., Hofstetter, P., and Hughes, L. F. (1999). Age-related synaptic changes in the central nucleus of the inferior colliculus of Fischer-344 rats. *J. Comp. Neurol.* 406, 285–298. doi: 10.1002/(SICI)1096-9861(19990412)406:3<285::AID-CNE1>3.0.CO;2-P

Hof, P. R., and Morrison, J. H. (1990). Quantitative analysis of a vulnerable subset of pyramidal neurons in Alzheimers disease: II. Primary and secondary visual cortex. *J. Comp. Neurol.* 301, 55–64. doi: 10.1002/cne.903010106

Idrizbegovic, E., Bogdanovic, N., Willott, J. F., and Canlon, B. (2004). Age-related increases in calcium-binding protein immunoreactivity in the cochlear nucleus of hearing impaired C57BL/6J mice. *Neurobiol. Aging* 25, 1085–1093. doi: 10.1016/j.neurobiolaging.2003.11.004

Idrizbegovic, E., Canlon, B., Bross, L. S., Willott, J. F., and Bogdanovic, N. (2001). The total number of neurons and calcium binding protein positive neurons during aging in the cochlear nucleus of CBA/CaJ mice: a quantitative study. *Hear. Res.* 158, 102–115. doi: 10.1016/S0378-5955(01)00295-7

Jinno, S., and Kosaka, T. (2006). Cellular architecture of the mouse hippocampus: a quantitative aspect of chemically defined GABAergic neurons with stereology. *Neurosci. Res.* 56, 229–245. doi: 10.1016/j.neures.2006.07.007

Kawaguchi, Y., and Kubota, Y. (1998). Neurochemical features and synaptic connections of large physiologically-identified GABAergic cells in the rat frontal cortex. *Neuroscience* 85, 677–701. doi: 10.1016/S0306-4522(97)00685-4

Kirkcaldie, M. T., Dickson, T. C., King, C. E., Grasby, D., Riederer, B. M., and Vickers, J. C. (2002). Neurofilament triplet proteins are restricted to a subset of neurons in the rat neocortex. *J. Chem. Neuroanat.* 24, 163–171. doi: 10.1016/S0891-0618(02)00043-1

Kubota, Y., Hattori, R., and Yui, Y. (1994). Three distinct subpopulations of GABAergic neurons in rat frontal agranular cortex. *Brain Res.* 649, 159–173. doi: 10.1016/0006-8993(94)91060-X

Kulesza, R. J., Viñuela, A., Saldaña, E., and Berrebi, A. S. (2002). Unbiased stereological estimates of neuron number in subcortical auditory nuclei of the rat. *Hear. Res.* 168, 12–24. doi: 10.1016/S0378-5955(02)00374-X

Ling, L. L., Hughes, L. F., and Caspary, D. M. (2005). Age-related loss of the GABA synthetic enzyme glutamic acid decarboxylase in rat primary auditory cortex. *Neuroscience* 132, 1103–1113. doi: 10.1016/j.neuroscience.2004.12.043

Liu, Y., Staal, J. A., Canty, A. J., Kirkcaldie, M. T., King, A. E., Bibari, O., et al. (2013). Cytoskeletal changes during development and aging in the cortex of neurofilament light protein knockout mice. *J. Comp. Neurol.* 521, 1817–1827. doi: 10.1002/cne.23261

Martin del Campo, H. N., Measor, K. R., and Razak, K. A. (2012). Parvalbumin immunoreactivity in the auditory cortex of a mouse model of presbycusis. *Hear. Res.* 294, 31–39. doi: 10.1016/j.heares.2012.08.017

Mayhew, T. M., and Gundersen, H. J. (1996). If you assume, you can make an ass out of u and me: a decade of the disector for stereological counting of particles in 3D space. *J. Anat.* 188(Pt 1), 1–15.

Mellott, J. G., Van Der Gucht, E., Lee, C. C., Carrasco, A., Winer, J. A., and Lomber, S. G. (2010). Areas of cat auditory cortex as defined by neurofilament proteins expressing SMI-32. *Hear. Res.* 267, 119–136. doi: 10.1016/j.heares.2010.04.003

Mendelson, J. R., and Ricketts C. (2001). Age-related temporal processing speed deterioration in auditory cortex. *Hear. Res.* 158, 84–94. doi: 10.1016/S0378-5955(01)00294-5

Merrill, D. A., Chiba, A. A., and Tuszynski, M. H. (2001). Conservation of neuronal number and size in the entorhinal cortex of behaviorally characterized aged rats. *J. Comp. Neurol.* 438, 445–456. doi: 10.1002/cne.1327

Molnár, Z., and Cheung, A. F. (2006). Toward the classification of subpopulations of layer V pyramidal projection neurons. *Neurosci. Res.* 55, 105–115. doi: 10.1016/j.neures.2006.02.008

Ogita, Z. I., and Markert, C. L. (1979). A miniaturized system for electrophoresis on polyacrylamide gels. *Anal. Biochem.* 99, 233–241. doi: 10.1016/S0003-2697(79)80001-9

Ouda, L., Burianova, J., and Syka, J. (2012a). Age-related changes in calbindin and calretinin immunoreactivity in the central auditory system of the rat. *Exp. Gerontol.* 47, 497–506. doi: 10.1016/j.exger.2012.04.003

Ouda, L., Druga, R., and Syka, J. (2012b). Distribution of SMI-32-immunoreactive neurons in the central auditory system of the rat. *Brain Struct. Funct.* 217, 19–36. doi: 10.1007/s00429-011-0329-6

Ouda, L., Druga, R., and Syka, J. (2008). Changes in parvalbumin immunoreactivity with aging in the central auditory system of the rat. *Exp. Gerontol.* 43, 782–789. doi: 10.1016/j.exger.2008.04.001

Ouellet, L., and de Villers-Sidani, E. (2014). Trajectory of the main GABAergic interneuron populations from early development to old age in the rat primary auditory cortex. *Front. Neuroanat.* 8:40. doi: 10.3389/fnana.2014.00040

Pakkenberg, B., and Gundersen, H. J. (1997). Neocortical neuron number in humans: effect of sex and age. *J. Comp. Neurol.* 384, 312–320. doi: 10.1002/(SICI)1096-9861(19970728)384:2<312::AID-CNE10>3.0.CO;2-K

Pant, H. C., and Veeranna (1995). Neurofilament phosphorylation. *Biochem. Cell Biol.* 73, 575–592. doi: 10.1139/o95-063

Paxinos, G., and Watson, C. (1998). *The Rat Brain in Stereotaxic Coordinates*. San Diego: Academic Press Inc.

Peters, A. (2009). The effects of normal aging on myelinated nerve fibers in monkey central nervous system. *Front. Neuroanat.* 3:11. doi: 10.3389/neuro.05.011.2009

Popelar, J., Groh, D., Pelánová, J., Canlon, B., and Syka, J. (2006). Age-related changes in cochlear and brainstem auditory functions in Fischer 344 rats. *Neurobiol. Aging* 27, 490–500. doi: 10.1016/j.neurobiolaging.2005.03.001

Pronk, M., Deeg, D. J., Festen, J. M., Twisk, J. W., Smits, C., Comijs, H. C., et al. (2013). Decline in older persons ability to recognize speech in noise: the influence of demographic, health-related, environmental, and cognitive factors. *Ear Hear.* 34, 722–732. doi: 10.1097/AUD.0b013e3182994eee

Rapp, P. R., and Gallagher, M. (1996). Preserved neuron number in the hippocampus of aged rats with spatial learning deficits. *Proc. Natl. Acad. Sci. U.S.A.* 93, 9926–9930. doi: 10.1073/pnas.93.18.9926

Rutten, B. P., Schmitz, C., Gerlach, O. H., Oyen, H. M., De Mesquita, E. B., Steinbusch, H. W., et al. (2007). The aging brain: accumulation of DNA damage or neuron loss? *Neurobiol. Aging* 28, 91–98. doi: 10.1016/j.neurobiolaging.2005.10.019

Rybalko, N., Bureš, Z., Burianová, J., Popelář, J., Poon, P. W., and Syka, J. (2012). Age-related changes in the acoustic startle reflex in Fischer 344 and long evans rats. *Exp. Gerontol.* 47, 966–973. doi: 10.1016/j.exger.2012.09.001

Schuknecht, H. F., and Gacek, M. R. (1993). Cochlear pathology in presbycusis. *Ann. Otol. Rhinol. Laryngol.* 102, 1–16.

Shea, T. B., and Lee, S. (2011). Neurofilament phosphorylation regulates axonal transport by an indirect mechanism: a merging of opposing hypotheses. *Cytoskeleton (Hoboken)* 68, 589–595. doi: 10.1002/cm.20535

Soifer, D., Nicoletti, V., Cabane, K., Mack, K., and Poulos, B. (1991). Expression of the neurofilament protein NF-H in L cells. *J. Neurosci. Res.* 30, 63–71. doi: 10.1002/jnr.490300108

Sternberger, L. A., and Sternberger, N. H. (1983). Monoclonal antibodies distinguish phosphorylated and nonphosphorylated forms of neurofilaments in situ. *Proc. Natl. Acad. Sci. U.S.A.* 80, 6126–6130. doi: 10.1073/pnas.80.19.6126

Stranahan, A. M., Jiam, N. T., Spiegel, A. M., and Gallagher, M. (2012). Aging reduces total neuron number in the dorsal component of the rodent prefrontal cortex. *J. Comp. Neurol.* 520, 1318–1326. doi: 10.1002/cne.22790

Suta, D., Rybalko, N., Pelánová, J., Popelář, J., and Syka, J. (2011). Age-related changes in auditory temporal processing in the rat. *Exp. Gerontol.* 46, 739–746. doi: 10.1016/j.exger.2011.05.004

Syka, J. (2002). Plastic changes in the central auditory system after hearing loss, restoration of function, and during learning. *Physiol. Rev.* 82, 601–636.

Syka, J. (2010). The Fischer 344 rat as a model of presbycusis. *Hear. Res.* 264, 70–78. doi: 10.1016/j.heares.2009.11.003

Towbin, H., Staehelin, T., and Gordon, J. (1979). Electrophoretic transfer of proteins from polyacrylamide gels to nitrocellulose sheets: procedure and some applications. *Proc. Natl. Acad. Sci. U.S.A.* 76, 4350–4354. doi: 10.1073/pnas.76.9.4350

Trapp, B. D., Peterson, J., Ransohoff, R. M., Rudick, R., Mörk, S., and Bö, L. (1998). Axonal transection in the lesions of multiple sclerosis. *N. Engl. J. Med.* 338, 278–285. doi: 10.1056/NEJM199801293380502

Tremblay, M., Zettel, M. L., Ison, J. R., Allen, P. D., and Majewska, A. K. (2012). Effects of aging and sensory loss on glial cells in mouse visual and auditory cortices. *Glia* 60, 541–558. doi: 10.1002/glia.22287

Trujillo, M., and Razak, K. A. (2013). Altered cortical spectrotemporal processing with age-related hearing loss. *J. Neurophysiol.* 110, 2873–2886. doi: 10.1152/jn.00423.2013

Tsang, Y. M., Chiong, F., Kuznetsov, D., Kasarskis, E., and Geula, C. (2000). Motor neurons are rich in non-phosphorylated neurofilaments: cross-species comparison and alterations in ALS. *Brain Res.* 861, 45–58. doi: 10.1016/S0006-8993(00)01954-5

Van De Werd, H. J., and Uylings, H. B. (2008). The rat orbital and agranular insular prefrontal cortical areas: a cytoarchitectonic and chemoarchitectonic study. *Brain Struct. Funct.* 212, 387–401. doi: 10.1007/s00429-007-0164-y

Veeranna, Yang, D. S., Lee, J. H., Vinod, K. Y., Stavrides, P., Amin, N. D., et al. (2011). Declining phosphatases underlie aging-related hyperphosphorylation of neurofilaments. *Neurobiol. Aging* 32, 2016–2029. doi: 10.1016/j.neurobiolaging.2009.12.001

Vickers, J. C., Delacourte, A., and Morrison, J. H. (1992). Progressive transformation of the cytoskeleton associated with normal aging and Alzheimers disease. *Brain Res.* 594, 273–278. doi: 10.1016/0006-8993(92)91134-Z

Voelker, C. C., Garin, N., Taylor, J. S., Gähwiler, B. H., Hornung, J. P., and Molnár, Z. (2004). Selective neurofilament (SMI-32, FNP-7 and N200) expression in subpopulations of layer V pyramidal neurons in vivo and in vitro. *Cereb. Cortex* 14, 1276–1286. doi: 10.1093/cercor/bhh089

Wang, J., Tung, Y. C., Wang, Y., Li, X. T., Iqbal, K., and Grundke-Iqbal, I. (2001). Hyperphosphorylation and accumulation of neurofilament proteins in Alzheimer disease brain and in okadaic acid-treated SY5Y cells. *FEBS Lett.* 507, 81–87. doi: 10.1016/S0014-5793(01)02944-1

West, M. J., Slomianka, L., and Gundersen, H. J. (1991). Unbiased stereological estimation of the total number of neurons in thesubdivisions of the rat hippocampus using the optical fractionator. *Anat. Rec.* 231, 482–497. doi: 10.1002/ar.1092310411

Willott, J. F., Bross, L. S., and Mcfadden, S. L. (1994). Morphology of the inferior colliculus in C57BL/6J and CBA/J mice across the life span. *Neurobiol. Aging* 15, 175–183. doi: 10.1016/0197-4580(94)90109-0

Yates, M. A., Markham, J. A., Anderson, S. E., Morris, J. R., and Juraska, J. M. (2008). Regional variability in age-related loss of neurons from the primary visual cortex and medial prefrontal cortex of male and female rats. *Brain Res.* 1218, 1–12. doi: 10.1016/j.brainres.2008.04.055

Zettel, M. L., Frisina, R. D., Haider, S. E., and Oneill, W. E. (1997). Age-related changes in calbindin D-28k and calretinin immunoreactivity in the inferior colliculus of CBA/CaJ and C57Bl/6 mice. *J. Comp. Neurol.* 386, 92–110. doi: 10.1002/(SICI)1096-9861(19970915)386:1<92::AID-CNE9>3.0.CO;2-8

Zilles, K. (1985). *The Cortex of the Rat: A Stereotaxic Atlas*. Berlin, NY: Springer-Verlag.

Conflict of Interest Statement: The authors declare that the research was conducted in the absence of any commercial or financial relationships that could be construed as a potential conflict of interest.

frontiers in
AGING NEUROSCIENCE

ORIGINAL RESEARCH ARTICLE
published: 13 February 2015
doi: 10.3389/fnagi.2015.00004

Restricted loss of olivocochlear but not vestibular efferent neurons in the senescent gerbil (*Meriones unguiculatus*)

Susanne Radtke-Schuller[1,2]*, Sabine Seeler[1] and Benedikt Grothe[1,2]

[1] *Division of Neurobiology, Department Biology II, Ludwig-Maximilians-University, Munich, Germany*
[2] *IFB German Center for Vertigo and Balance Disorders, Munich, Germany*

Edited by:
Isabel Varela-Nieto, Consejo Superior Investigaciones Científicas, Spain

Reviewed by:
Veronica Fuentes, University of Castilla-La Mancha, Spain
Maria E. Rubio, University of Pittsburgh, USA

****Correspondence:***
Susanne Radtke-Schuller, Division of Neurobiology, Department Biology II, Ludwig-Maximilians-University, Großhaderner Strasse 2, 82152 Planegg-Martinsried, Munich, Germany
e-mail: radtke-schuller@bio.lmu.de

Degeneration of hearing and vertigo are symptoms of age-related auditory and vestibular disorders reflecting multifactorial changes in the peripheral and central nervous system whose interplay remains largely unknown. Originating bilaterally in the brain stem, vestibular and auditory efferent cholinergic projections exert feedback control on the peripheral sensory organs, and modulate sensory processing. We studied age-related changes in the auditory and vestibular efferent systems by evaluating number of cholinergic efferent neurons in young adult and aged gerbils, and in cholinergic trigeminal neurons serving as a control for efferents not related to the inner ear. We observed a significant loss of olivocochlear (OC) neurons in aged compared to young adult animals, whereas the overall number of lateral superior olive (LSO) cells was not reduced in aging. Although the loss of lateral and medial olivocochlear (MOC) neurons was uniform and equal on both sides of the brain, there were frequency-related differences within the lateral olivocochlear (LOC) neurons, where the decline was larger in the medial limb of the superior olivary nucleus (high frequency representation) than in the lateral limb (middle-to-low frequency representation). In contrast, neither the number of vestibular efferent neurons, nor the population of motor trigeminal neurons were significantly reduced in the aged animals. These observations suggest differential effects of aging on the respective cholinergic efferent brainstem systems.

Keywords: aging, cholinergic efferent systems, brainstem, olivocochlear neurons, superior olivary complex, vestibular, trigeminal, auditory

INTRODUCTION

Hearing deficits (presbycusis) and vertigo are symptoms of age-related auditory and vestibular disorders reflecting multifactorial changes in the peripheral and central nervous system. Presbycusis is also characterized by reduced speech recognition especially in noisy environments, slowed central processing of acoustic information, and impaired sound localization. The auditory and vestibular systems both evolved from the octavolateralis system (for review, see Köppl, 2011). Both sensory modalities use the same type of sensory receptor cells, i.e., hair cells, which receive direct efferent innervation by neurons of the same ontogenetic descent from rhombomere 4 (Bruce et al., 1997; Simmons, 2002). This cholinergic efferent synaptic transmission is a unique feature among sensory systems (for review, see Roberts and Meredith, 1992). Originating bilaterally in the brain stem, auditory efferent neurons and vestibular efferent neurons are the last links in elaborate descending neural pathways of the central auditory and vestibular systems (for reviews, see Holt et al., 2011; Schofield, 2011). These cholinergic descending projections exert central feedback control on the peripheral sensory organs, thereby modulating afferent information processing.

In mammals, the efferent olivocochlear (OC) system originates in the superior olivary complex (SOC) and consists of different components. Large medial olivocochlear (MOC) neurons are mainly located in the medial periolivary region (mainly in the ventral nucleus of the trapezoid body (VNTB). Additionally, some large OC neurons in the dorsal periolivary nucleus (DPO) are described as a sub-group of MOC neurons (rodents: Aschoff and Ostwald, 1987; Brown and Levine, 2008; cat: Warr et al., 2002). Small lateral olivocochlear (LOC) neurons are situated in and around the lateral superior olive (LSO) and display a discrete tonotopic projection to the cochlea (Guinan et al., 1984; Robertson et al., 1987). An additional group of larger LOC neurons, so-called shell neurons, is found at the margins of the LSO (Vetter and Mugnagnaini, 1992) and projects also tonotopically but to a broader frequency range (Warr et al., 1997). This sub-group is not as distinct in the gerbil as in other rodents and is therefore subsumed in the group of LOC neurons in this study. There can be considerable variation in the location, number and ratio of LOC and MOC neurons in gerbils (Aschoff et al., 1988; Kaiser et al., 2011). All OC neurons operate with acetylcholine as synaptic transmitter, and LOC neurons in addition use a variety of co-transmitters (Sewell, 2011).

Functionally, MOC neurons modulate the electromechanical amplification and gain in outer hair cells and thereby adjust the auditory nerve's dynamic range. They contribute to the protection of the auditory system from acoustic trauma and

contribute to extracting biologically important acoustic signals in noise (Guinan, 2011). Age-related decline of MOC functionality prior to outer hair cell degeneration has been demonstrated with distortion product otoacoustic emission (DPOAE) measurements in humans (Kim et al., 2002) and in CBA mice (Jacobson et al., 2003).

The function of the LOC system is less understood, but its neurons are known to modulate afferent activity of type I auditory nerve fibers through various neurotransmitter systems. The LOC efferents potentially protect the ear from acoustic overexposure and/or may balance the sensitivity of the two ears (Ruel et al., 2001; Darrow et al., 2006). Other reports have recently shown that the efferent auditory feedback neurons may have a protective function that slows down the progression of age-related cochlear hearing loss (Liberman et al., 2014). Age-related synaptic loss of MOC terminals and changes in LOC efferent innervation pattern has been shown to occur prior to hearing loss (Fu et al., 2010; Lauer et al., 2012), but it is still unknown whether age-related synaptic change is the cause or the consequence of neuronal cell loss (Jin et al., 2011). However, the age-related loss of OC neurons has not yet been evaluated directly.

The small group of efferent vestibular neurons is located in the medullary brainstem and similarly organized throughout mammals (gerbil: Perachio and Kevetter, 1989; Purcell and Perachio, 1997; Holt et al., 2011). About 90% of the efferent neurons belong to the larger group called "group *e*" (Goldberg and Fernandéz, 1980) and are located dorsolateral to the facial nerve genu between the abducens and superior vestibular nuclei. These neurons are anti-cholinetransferase (ChAT) immunopositive and in addition use a variety of co-transmitters (Perachio and Kevetter, 1989; Ryan et al., 1991), whereas neurons of the smaller group ventral to the genu do not stain for any of these markers (Perachio and Kevetter, 1989) and are not discussed further in this study. The responses of efferents and their effect on afferent discharge have been studied in detail (Holt et al., 2011), but the functions of the efferent vestibular system still remain elusive.

The objective of this study was to quantify and compare age-related loss of cholinergic efferent auditory and vestibular feedback neurons in senescent gerbils, a model species for human hearing (Ryan, 1976; Cheal, 1986). This decline was compared with age-related cell loss in the cholinergic motor trigeminal system. The observations suggest a differential impact of aging on these cholinergic brainstem systems.

MATERIALS AND METHODS

ANIMALS

Immunolabeling was conducted on the brain stem of 10 healthy Mongolian gerbils (*Meriones unguiculatus*) of both genders. The ages of the animals were either 3–5 month (young adults, $n = 5$) or 2.5–3.5 years (aged animals, $n = 5$). Animals were provided by the breeding facility of the Biocenter of the University of Munich (LMU). All experiments followed regulations on animal welfare approved by the Bavarian state government (AZ. Reg. v. Obb. 55.2-1-54.2531.8-211-10) and the European Communities Council Directive (86/609/EEC).

TISSUE PROCESSING

Gerbils were anesthetized by a lethal dose of i.p. administered Narcoren® (Merial GmbH, Halbergmoos, Germany) (200 mg/kg body weight). After the animals had reached a deep anesthetic state marked by a complete loss of the flexor reflex at all limbs, they were perfusion-fixed, first with Ringer solution supplemented with 0.1% heparin (Meditech Vertriebs GmbH, Parchim, Germany) and then with 4% paraformaldehyde (PFA). Brains were post-fixed in 4% PFA solution for at least 2.5 h up to overnight. Subsequently, the brains were oriented along standardized coordinates in an embedding chamber that was then filled with agarose. The standardized alignment before embedding guaranteed that the brains were cut in planes that corresponded as closely as possible to each other inter-individually and to a reference series (**Figure 1**). The resulting blocks were trimmed and the regions of interest were cut with a Leica VT 1200S vibratome (Leica Biosystems, Nussloch Germany) into 40 μm thick coronal sections of the brainstem. In order to achieve optimum comparability of results in young adult and aged animals, all procedures for tissue preparation and immunolabeling were applied to pairs or groups of young adult and aged healthy individuals together.

IMMUNOLABELING

We used ChAT antibody as marker for cholinergic neurons (Hedreen et al., 1983; Kaiser et al., 2011). Anti-chondroitinsulfate (CSPG) antibody was applied as a marker for perineuronal nets. Perineural nets are chondroitin sulfate proteoglycans which form an extracellular matrix that surrounds many neuronal somata, dendrites and synapses in net-like structures all over the brain. They ensheath most SOC principal neurons (gerbil: Lurie et al., 1997), and the neurons of the brainstem motor nuclei (including the motor trigeminal nucleus). CSPG antibody was therefore well-suited as an overview stain to delineate the SOC nuclei. Anti-microtubule-associated protein 2 (Map2) antibody was used to stain neuronal somata and dendrites.

The sections were washed and non-specific binding sites were saturated with a blocking solution containing 1% BSA, 1% Triton X-100 and 0.1% saponin for 1 h, then incubated in the primary antibody mix (diluted in blocking solution) at 4°C on a shaker. To ascertain the best incubation time, test sections were either incubated overnight, or incubated for two nights. The prolonged incubation time resulted in more intense staining but did not lead to an increased number of immunoreactive cells or a higher background. The specificity of all primary antibodies used has been previously published and the relevant publications are indicated for the respective antibodies. The primary antibodies used were: goat anti-ChAT (1:500 Millipore, AB144P; Kaiser et al., 2011), mouse anti-CSPG (1:500 Millipore, MAB5284; Andrews et al., 2012), chicken anti-Map2 (1:1000, Neuromics, CH22103; e.g., Rautenberg et al., 2009). Following extensive washing the sections were incubated with a combination of fluorescent secondary antibodies of different wavelength in blocking solution (1:400) for 4 h at room temperature or 18 h at 4°C on the shaker in the dark

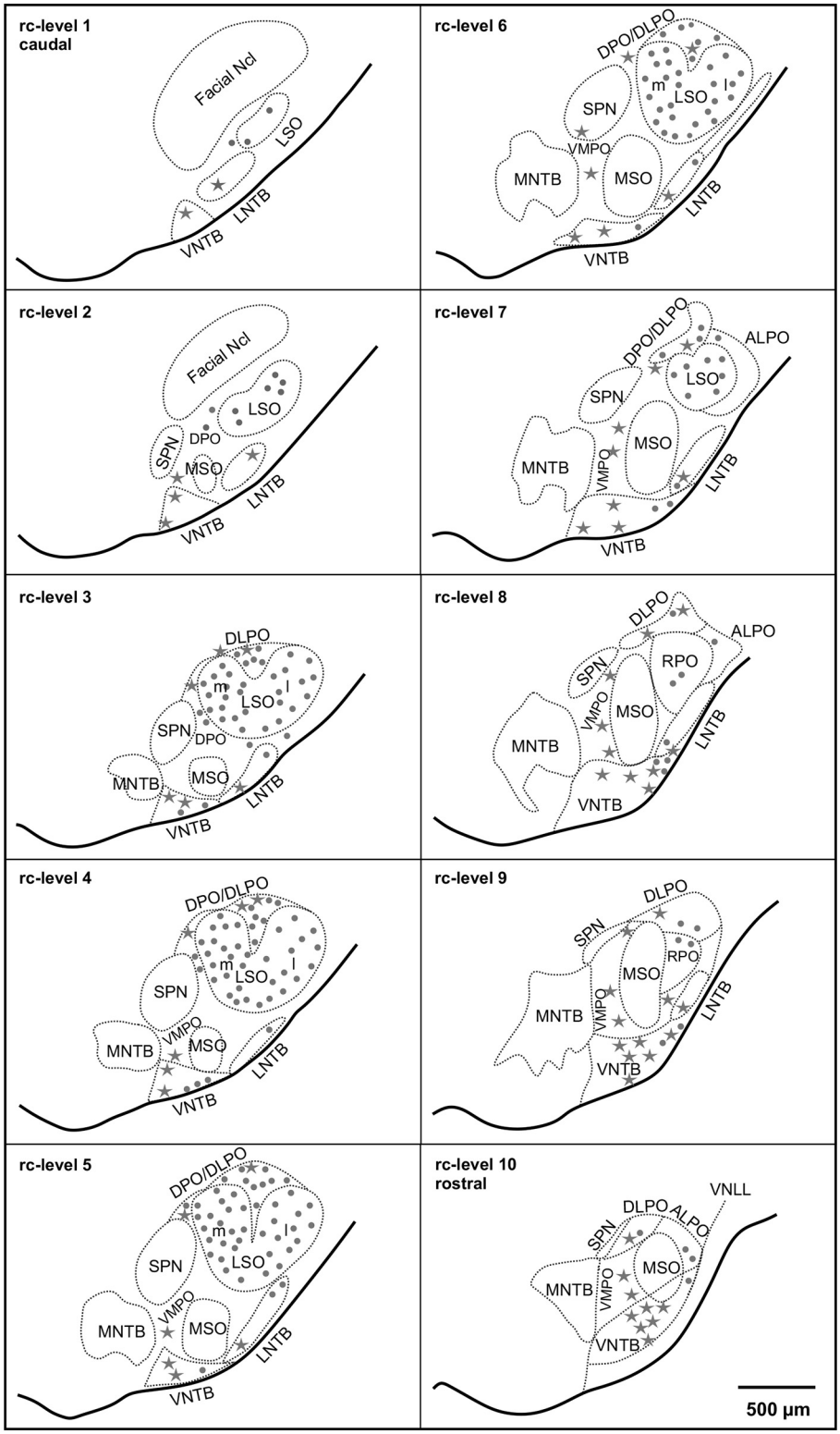

FIGURE 1 | Distribution of cholinergic neurons in the superior olivary complex (SOC) of the gerbil (*M. unguiculatus*). Reference series shows ventral outlines of the brainstem (solid lines) and the subdivisions of the SOC (dotted contours) at 10 rostrocaudal (rc) positions from facial nucleus (Facial Ncl) to the ventral nucleus of the lateral lemniscus (VNLL). Rc-level 1 indicates the most caudal and rc-level 10 the most rostral position. Dots: small cholinergic neurons comprising LOC neurons. Stars: large cholinergic neurons, including MOC neurons. The density of symbols represents roughly the relative frequency of occurrence of the respective cholinergic neurons within each subdivision.

(donkey anti goat (Alexa Fluor 488 Dianova 705-546-147), donkey anti mouse (Cy3, 570 nm; Dianova 715-166-151) and donkey anti chicken (Alexa Fluor 647 Dianova 703-606-155). After exhaustive washing, the sections were mounted with Vectashield® (Vector, Burlingame, CA, USA) and sealed with nail polish.

IMAGE ACQUISITION

For delineation of SOC nuclei and counting of cholinergic neurons, sections were imaged with a virtual slide microscope (VS120 S1, Olympus BX61VST, Olympus-Deutschland, Hamburg, Germany) at 10× magnification using the proprietary software dotSlide® (Olympus). All three colors of the secondary antibodies used for immunostaining were acquired sequentially and could be visualized separately or in overlay (**Figure 2**).

For counts of total neuron numbers in LSO, confocal optical sections were acquired with a Leica TCS SP5-2 confocal laser-scanning microscope (Leica Microsystems, Mannheim, Germany) with a Plan Fl20x/0.70 NA objective for the MAP2 stain. Stacks of eight-bit grayscale images were obtained with an axial distance of 3 μm between optical sections each averaged from four successive scans. Finer details (**Figure 3B**) were taken with a Plan 63x/NA1.32 oil immersion objective. For each optical

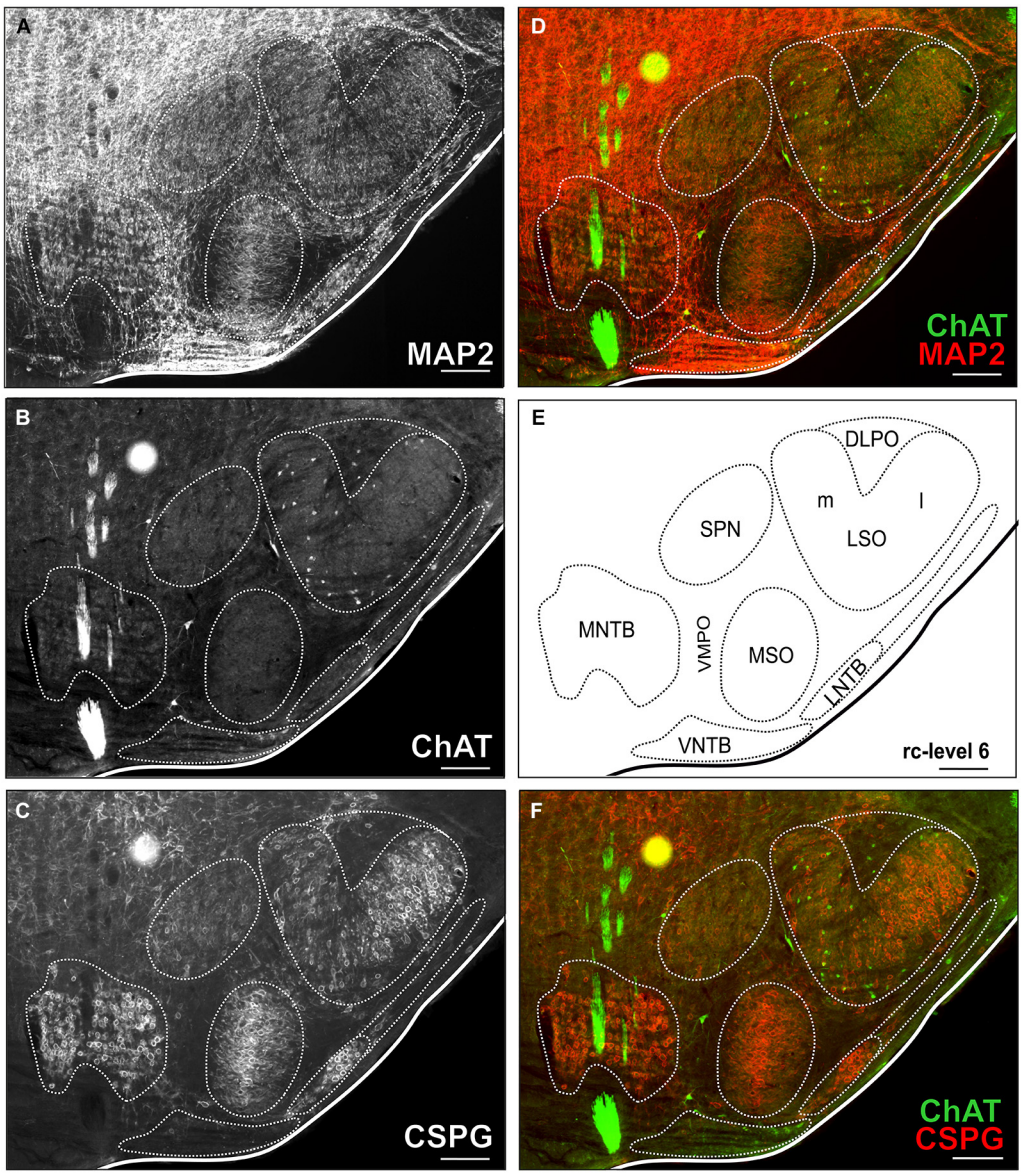

FIGURE 2 | Triple-stained example section of the SOC region of a young adult gerbil. The section corresponds to the reference series at rc-level 6 **(E)**. In **(A,B,C)** MAP2 stain, ChAT stain and CSPG stain are depicted alone with delineated SOC nuclei. Overlays of ChAT (Alexa Fluor 488, green) and MAP2 (Alexa Fluor 647, red) are shown in **(D)** and ChAT and CSPG (Cy 3, 570; red) in **(F)**. ChAT positive cells were easily detected in the ChAT stain alone as well as in overlay with both overview stains (MAP and CSPG). Scale bar in **(A–F)**: 500 μm.

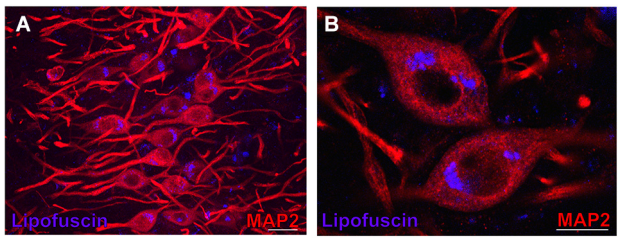

FIGURE 3 | Lipofuscin granules in medial superior olive (MSO) neurons of an aged gerbil. MSO neurons are MAP2 immunostained (Alexa Fluor 647, red). Lipofuscin granules have been excited with the DAPI excitation wavelengths and appear blue. Confocal images show a maximum projection of image stacks in **(A)** and a single optical image of 0.3 μm thickness in the enlargement in **(B)**. Scale bar in **(A)**: 50 μm and 20 μm in **(B)**.

section the images of one or two fluorochromes were collected sequentially. RGB stacks, montages of RGB optical sections, and maximum-intensity projections were assembled into tables by using ImageJ 1.37k plugins (NIH, USA) and Photoshop (CS6, Adobe Systems, San Jose, CA, USA). Figure images were arranged using CorelDRAW X6 (Corel Corporation, Ottawa, ON, Canada).

QUANTIFICATION AND ANALYSIS

Counting of cholinergic neurons

Cholinergic efferent neurons were counted using ChAT immunostaining in the ChAT, MAP2 and CSPG triple-labeled sections (refer to **Figure 2**). Outlines of the brainstem nuclei were determined in MAP2 and CSPG overview stains. The OC cell counts in the different SOC nuclei were related to a "standard series" of sections spaced 160 μm through the SOC, which was chosen from a young adult experimental animal (refer to **Figures 1**, **2**). The neuron group of vestibular efferents and the neurons of the motor trigeminal nucleus were easy to delineate as most of the neurons in these structures are cholinergic.

In aged animals the presence of autofluorescent lipofuscin granules affects the fluorescent image to some extent (see **Figures 4B,D,F,H**, **7B,D,F**). The lipofuscin granules are excitable by many wavelengths yielding different colors of emission, which makes them distinguishable from secondary fluorescent antibodies that are sensitive only to their specific excitation wavelength. Lipofuscin granules were excited by the excitation wavelength of Alexa Fluor 488 (secondary antibody used to label ChAT in green) as well as by the excitation wavelength of Cy3 (secondary antibody used to label the CSPG-positive perineuronal nets in red) as depicted in **Figures 4D,H**. Therefore lipofuscin granules appear bright yellow and are clearly distinguished from the green ChAT positive neurons (see **Figures 4B,D,F,H**, **7B,D,F**). Lipofuscin granules are also excitable with the DAPI excitation wavelength (350–360 nm) as shown in **Figures 3A,B**. Here neurons are stained with anti-MAP2 labeled with Cy3.

Based on the assumption that a soma that is not completely filled with lipofuscin granules is functional, we conservatively counted in aged animals all somata in which immunoreactivity for ChAT was still detectable.

The individual cholinergic somata were clearly identifiable within 40 μm slices. Double counting of somata was excluded as neurons were counted in every fourth slide in the series, i.e., at a distance of 160 μm between evaluated slices. The maximum diameter of cholinergic OC, vestibular and trigeminal somata are all below 50 μm and thus far below this distance (160 μm), so that double-counting of parts of a soma split due to slicing could not occur in the slices used for counting (120 μm apart). Cholinergic neurons in the images were marked on a separate layer in Photoshop (CS6 Extended, Adobe Systems, San Jose, CA, USA) and then counted with the aid of ImageJ plug-in "cell counter" (Kurt De Vos, Univ Sheffield, Academic Neurology[1]), separately on both sides of the brain. The cell numbers in the three interspersed slices between two evaluated slices were estimated by interpolation (Gleich et al., 2004; Kaiser et al., 2011). The underlying assumption was that the number of olivocochlear neurons does not change abruptly within the 160 μm of rostrocaudal extension and develops monotonically (Sanes et al., 1989). The counted and interpolated neuron numbers together represent the total number of cholinergic OC neurons within a virtual slice of 160 μm rostrocaudal width. Numbers of cholinergic neurons are always given for one side of the brain throughout the report.

Counting of LSO neurons

To assess the age-related loss of neurons in the SOC in general, MAP2 stained somata were counted in four pairs of young adult and aged animals. Somata were counted within restricted areas of interest (277 μm × 277 μm) of the lateral and medial limb of the LSO, respectively, in four sections spaced 160 μm corresponding to the rostrocaudal levels 3–6 of the standard reference series (**Figure 1**). Due to the much higher density of neurons (compared to cholinergic neurons) counting had to be performed on optical slices obtained from the 40 μm thick sections with the confocal microscope. Thirteen consecutive optical sections of 3 μm thickness each were used. The soma of each neuron was tracked individually through the stack and counted once in order to avoid double counting (West, 1993).

STATISTICAL ANALYSIS

Counting results of individuals and counts within or between groups were statistically treated with the program Prism6 (for Windows, GraphPad Software, San Diego, CA, USA[2]). Comparisons were performed with an unpaired *t*-test. Statistical significance is indicated with the *t* value, the degrees of freedom (df) and the *p* value. These indications are also included in the figure legends. Statistical significance was determined applying a criterion of $P < 0.01$.

RESULTS

OC NEURONS

The distribution of cholinergic neurons comprising LOC and MOC neurons in the SOC was evaluated in five pairs of healthy young adult gerbils (3–5 months old) and aged gerbils (between 2.5 and 3.5 years).

[1]http://rsb.info.nih.gov/ij/plugins/cell-counter.html
[2]www.graphpad.com

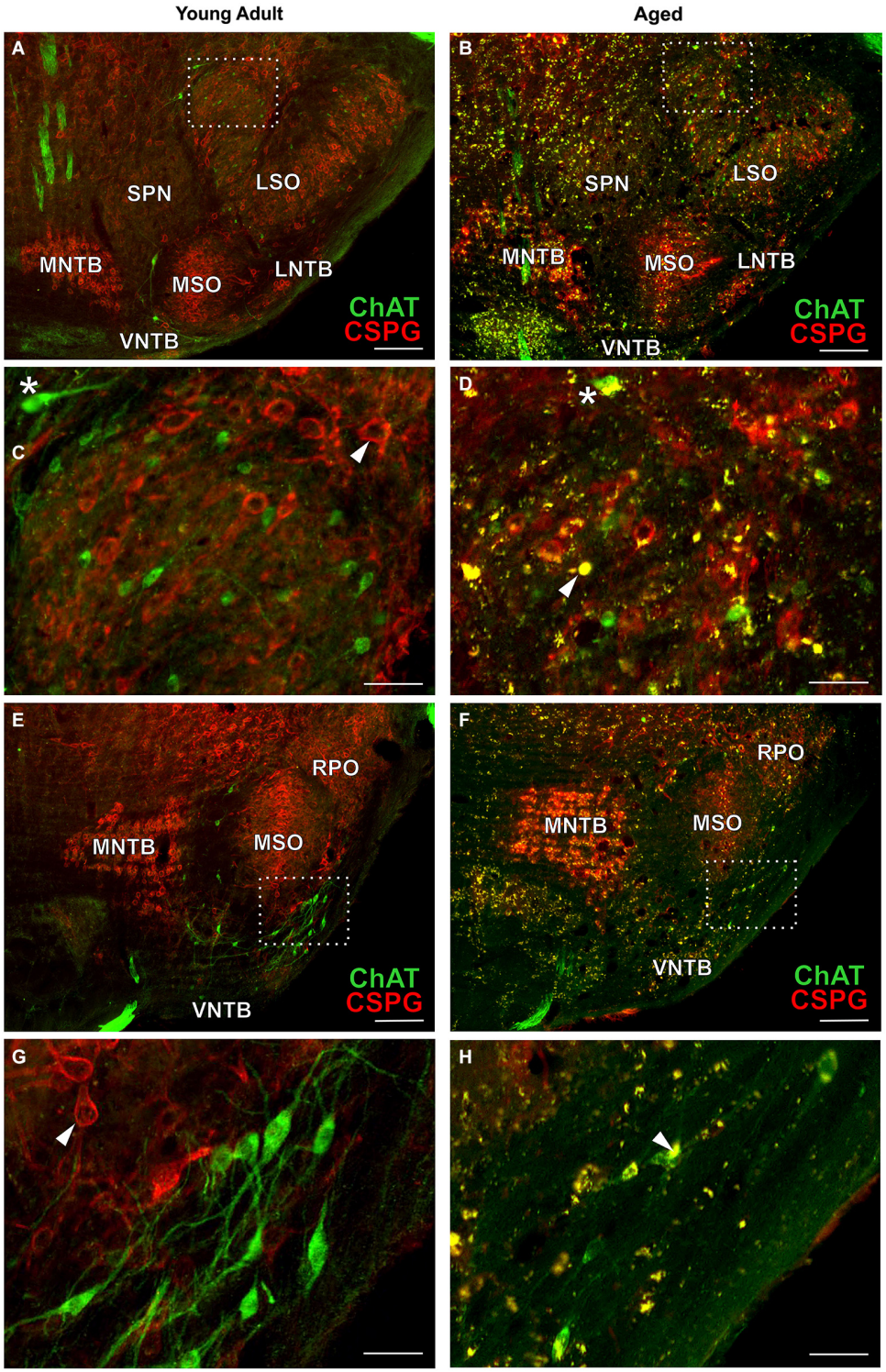

FIGURE 4 | OC neurons in SOC of young adult and aged gerbils. ChAT (Alexa Fluor 488, green) and CSPG (Cy 3, red) immunolabeling is shown. Arrowheads point towards a CSPG-positive perineuronal net in **(C,G)**. Note that OC neurons are not ensheathed in perineuronal nets. Autofluorescent lipofuscin granules appear yellow (arrowhead in **D**,**H**). LOC neurons: section at middle of SOC (rc-level 5) in young adult and aged gerbil **(A,B)** with enlargement of rectangular areas in medial LSO in **(C,D)**. MOC neurons: section at rostral SOC (rc-level 9) in young adult and aged gerbil **(E,F)**. VNTB/LNTB area within rectangle in **(E,F)** is enlarged in **(G,H)**. Stars in **(C,D)** mark presumed MOC neurons in DPO/DLPO. The presumed MOC soma in **(D)** is half-filled with lipofuscin granules (yellow). Scale bar in **(A,B,E,F)**: 200 μm; in **(C,D,G,H)**: 50 μm.

The distribution in young adult gerbils is in general similar to what has already been described in rodents (see Section Introduction), and is represented schematically in 10 standard slices through the SOC in **Figure 1**. The number of cholinergic neurons as a function of rostrocaudal location within the SOC is compiled in **Figure 5** for LOC and MOC neurons in parallel for young adult and aged animals, respectively. The small LOC neurons were numerous within the LSO but distributed sparsely in the border region to periolivary nuclei, notably in the dorsolateral periolivary nucleus (DLPO). A few small cholinergic neurons were found in untypical locations in the ventral and lateral nuclei of the trapezoid body (VNTB/LNTB **Figure 1**, rc-levels 3–10), in the dorsal/dorsolateral periolivary nuclei rostral to LSO and in the region of the anterolateral and rostral periolivary nuclei (DPO/DLPO, ALPO/RPO, **Figure 1**, rc-level 8–10). These neurons were analyzed separately. They displayed large individual variation but showed no significant difference between young adult and aged animals. MOC neurons occurred mostly in VNTB and in the ventromedial periolivary nucleus (VMPO). Some large cholinergic neurons were also found in the dorsal and dorsolateral periolivary nuclei (DPO/DLPO; **Figure 1**, rc-level 3–10; and **Figures 4A–D**). These neurons were presumed to be MOC neurons as they showed an age-related decline like the main group of MOC neurons (see below). No cholinergic neurons were detected in the medial superior olive (MSO), the medial nucleus of the trapezoid body (MNTB) and almost none in the superior periolivary nucleus (SPN).

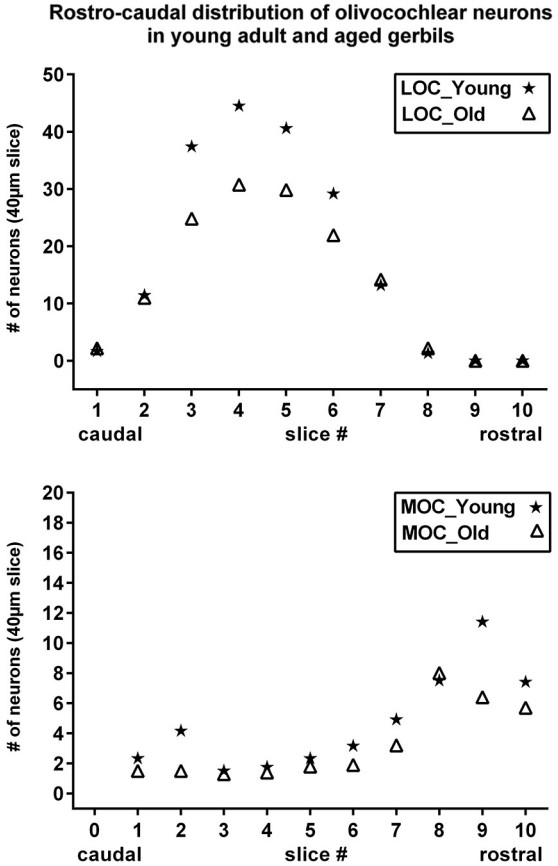

FIGURE 5 | Rostrocaudal distribution of olivocochlear neurons in young adult and aged gerbils. Number of LOC (upper) and MOC (lower) neurons are shown as a function of rostrocaudal location in the SOC. The slice numbers (abscissa) refer to the slices in **Figure 1**, and the values for young adult and aged animals are represented as stars and triangles, respectively. Values give the mean number of neurons in the respective slice of 40 µm thickness as counted in all five animals of each category.

COMPARISON OF OC NEURONS IN YOUNG ADULT AND AGED ANIMALS

Immunolabeling

Typical examples of OC neurons from a pair of young adult and aged gerbils are depicted in the upper panels of **Figure 4** for LOC (**Figures 4A–D**, rc-level 5) and in the lower panels for MOC (**Figures 4E–H**, rc-level 9). The principal nuclei of the SOC were prominently marked by the presence of perineuronal nets around their principal neurons as seen by the positive CSPG stain (red). In comparison, SPN, VMPO and VNTB staining of the nets was weak (**Figures 4A,B,E,F**; for detailed delineation of nuclei refer to **Figure 1**). LOC and MOC neurons were immunopositive for ChAT (green) but CSPG-negative, i.e., they did not possess perineuronal nets (**Figures 4C,D,G,H**, respectively). Overall we observed a key qualitative change of OC neurons in the aged brains: sections of aged animals were characterized by auto-fluorescent lipofuscin granules that accumulated in the neuronal somata during aging. As the fluorescence of lipofuscin granules is excited by a broad spectrum of wavelength, the granules stood out yellowish against the green cholinergic structures and the red perineuronal nets (see **Figure 4**, enlargements D and H). Perineuronal nets tended to fade, clump and dissolve with old age, which gave them a blurry appearance, but still helped to unequivocally delineate the SOC nuclei (**Figures 4B,F**). We also observed some of the spongiform lesions (**Figures 4F,H**) typical of aged gerbil brainstem tissue (Ostapoff and Morest, 1989).

Cell counts

Maximum cell counts of LOC neurons were found at rc-level 4 and 5, where LSO was at its largest cross section (**Figures 1**, **5**, upper panel, stars). Loss of LOC neurons in aged animals was prominent between rc-levels 3 and 6 (**Figure 5**, upper panel, triangles) which comprised the major volume of the LSO. MOC neurons extended over the entire rostrocaudal range of the SOC. Their number increased rostrally with a maximum between rc-levels 7 and 10 (**Figure 5**, lower panel, stars). In aged animals the loss of MOC cells spread throughout the rostrocaudal range with a maximum loss at rc-level 9 (**Figure 5**, lower panel, triangles). The counts of cholinergic OC neurons in young adult animals were fairly constant across individuals. Mean total number and standard deviation of mean (SEM) of LOC neurons per hemisphere and animal was 724 ± 43 ($N = 10$). MOC neurons amounted to 190 ± 10 neurons per hemisphere ($N = 10$). LOC neurons outnumbered MOC neurons almost by a factor of four (with LOC comprising 79% vs. MOC comprising 21%, of all cholinergic OC neurons).

The mean total numbers in aged animals were 551 ± 26 ($N = 10$) for LOC and 131 ± 9 ($N = 10$) for MOC neurons. The LOC to MOC ratio had virtually not changed in aged animals (80.9% vs. 19.1%, respectively). The average OC neuron counts

of left and right hemispheres yielded similar numbers, and there was no sign of lateralization.

In **Figure 6A** the means of total LOC and total MOC numbers for the young adult and aged cohort are contrasted and deviations are given as standard error of means (SEM). The loss of LOC neurons in the aged animals compared to young adult individuals of 24% was significant (t = 4.436; df = 18; $p < 0.001$). Aged animals also showed a significant loss of MOC neurons of 31% (t = 4.357; df = 18; $p < 0.001$). LOC neuron number in the LSO turned out to be not equal (**Figure 6B**), with significantly more LOC neurons in the medial limb than in the lateral limb of LSO in young adult animals (+23.4%; t = 2.608; df = 18; p = 0.018). The loss of LOC neurons in aged animals relative to young adult animals was significant in the medial part of LSO (−36%; t = 4.888; df = 18; $p < 0.001$). There was a trend of mean LOC decrease in the lateral LSO portion in aged animals which, however, was statistically not significant (23.4%; t = 1.96; df = 18; $p < 0.1$, n.s.). LOC neuron number in the medial and lateral limb of the LSO of aged animals was therefore less different (7.8%; t = 0.657; df = 18; p = 0.5195, n.s.).

To find out whether a general decrease in neuron numbers with age could also explain the differential loss of LOC neurons, the total number of LSO neurons was counted in a standard area of interest within medial and lateral part of LSO in young adult and aged animals. **Figure 6C** shows that the age-related loss of LSO neurons was virtually equal in the medial and lateral LSO limb and amounted to 10% and 13%, respectively (medial: 10%; t = 1.891; df = 6; n.s.; and lateral: −13%; t = 1.471; df = 6; n.s.). The average loss in LSO neurons of only about 12% cannot account for the loss in OC neurons, which was almost three times as high. The larger loss of LOC neurons in the medial compared to lateral subdivision of LSO did also not follow the pattern of general LSO neuron number decrease with age in the respective LSO limbs.

COMPARISON OF AGE-RELATED NEURONAL LOSS OF AUDITORY WITH VESTIBULAR AND MOTOR TRIGEMINAL EFFERENTS

Cholinergic vestibular efferent neurons from young adult and aged gerbils (same animals as in **Figure 4**) are depicted in the upper two panels of **Figure 7**. Like OC neurons, the medium sized round shaped cholinergic vestibular efferent neurons stained positive for ChAT, but were not ensheathed by CSPG-positive neuronal nets. Compared to OC neurons in the aged animal (**Figures 4D,H**) cholinergic vestibular efferents were only moderately loaded with lipofuscin granules (**Figure 7D**). Their number was not significantly reduced as shown in **Figure 8** (young adult: 119 ± 11, n = 10; aged: 120 ± 14, n = 10; t = 0.0449; df = 18; n.s.).

The large efferent motor trigeminal neurons (**Figures 7E,F**) stained positive for ChAT, and also for CSPG. The salient CSPG-positive perineuronal nets distinguished them from the auditory and cholinergic vestibular efferents. In aged animals these nets around the somata showed marked deterioration (**Figure 7F**). The neurons accumulated only moderate amounts of lipofuscin granules and their number was slightly reduced, but this loss was barely significant (see **Figure 8**, young adult: 1234 ± 51, n = 10; aged: 1092 ± 66, n = 10; t = 2.155; df = 18; n.s.).

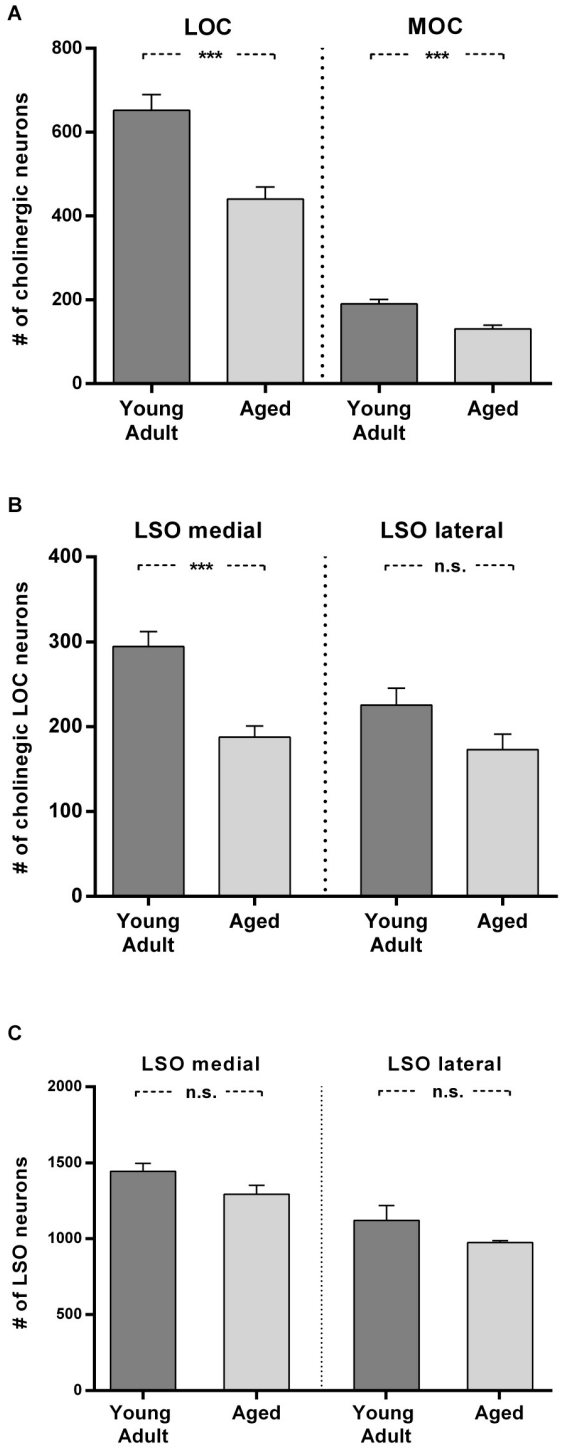

FIGURE 6 | Loss of olivocochlear (A,B) and LSO neurons in general (C) in aged compared to young adult animals. **(A)** The mean number of LOC and MOC neurons in one hemisphere is represented for young adult and aged animals. The decrease in OC numbers in aged animals relative to young adult animals is significant in LOC and MOC neurons (LOC: 24%: t = 4.436; df = 18; $p < 0.001$); MOC: 31%, t = 4.357; df = 18; $p < 0.001$). **(B)** LOC neuron numbers in medial and lateral part of LSO in young adult

(*Continued*

FIGURE 6 | Continued
and aged animals. The aged vs. young adult decrease of LOC neurons is −36% in the medial LSO portion (t = 4.888; df = 18; $p < 0.001$) and −23.4% in the lateral portion (t = 1.96; df = 18; n.s.). The difference of LOC numbers in the medial LSO vs. lateral LSO is not significant neither in young adult (t = 2,608; df = 18; p = 0.0178, n.s.) nor in aged (t = 0.657, df = 18; n.s.) animals. **(C)** Total number of LSO neurons within an area of interest of the medial and lateral portion of the LSO for young adult and aged animals. The left pair of columns gives the counts in the medial, the right one the counts in the lateral portion of LSO. LSO neurons exhibit only a moderate loss in both subdivisions with 10% in the medial LSO (t = 1.891; df = 6; n.s.) and 13% in the lateral LSO (t = 1.471; df = 6; n.s.). Neuron numbers are given as mean ± SEM. Dark gray columns: young adult animals, light gray columns: aged animals. ***$p < 0.001$.

DISCUSSION

The present study quantified the age-related loss of cholinergic efferent neurons in the auditory and vestibular systems and motor trigeminal nucleus. It revealed a loss of almost one third of the auditory efferents in aged gerbils in contrast to no or almost no neuronal loss of cholinergic vestibular efferents and neurons of the motor trigeminal nucleus. These observations suggest differential effects of aging on these three cholinergic brainstem systems.

The number and ratio of LOC and MOC neurons in young adult gerbils are in accord with the findings of Aschoff et al. (1988). The remarkable decline of auditory efferents with age was 31% for MOC and 24% for LOC neurons. Hence, the ratio of MOC to LOC neurons remained virtually constant in aged animals. The decline was equal in both hemispheres and showed little inter-individual variability. The decline of LOC neurons within LSO was significantly larger in the medial LSO than in its lateral part. This could not be explained by the comparably moderate and equally distributed general cell loss within LSO in aged animals of roughly 12%. Also, Gleich et al. (2004) observed that the number of neurons within the gerbil's LSO is only marginally affected by age (for review on age related changes in the SOC see Caspary et al., 2008). As auditory efferent neurons exert central feedback control on the cochlea and modulate information processing, their high loss should have serious functional consequences and could contribute to age-related hearing deficits.

MOC neurons protect hair cells from acoustic injury via a sound-evoked efferent reflex and are known to be involved in age-related decline of auditory processing (e.g., Kim et al., 2002; Jacobson et al., 2003; Fu et al., 2010). The functional role of the LOC neurons is less clear. LOCs could potentially prevent glutamate excitotoxicity at synaptic terminals of the auditory nerve (Pujol and Puel, 1999) by modulating the excitability of the nerve fibers (Ruel et al., 2001; Groff and Liberman, 2003). Recently, participation of olivo-cochlear neurons, especially MOCs in "hidden hearing loss" (Schaette and McAlpine, 2011) has been demonstrated (Furman et al., 2013): OC neurons have a protective effect against the selective loss of high-threshold auditory nerve fibers induced by moderate noise exposure (Maison et al., 2013). These fibers are most important for hearing-in-noise, which becomes increasingly more difficult with age, and is not necessarily correlated to a rise in auditory thresholds (Liberman et al., 2014). Thus age-related impairment of hearing-in-noise could result from the loss of efferent terminals.

Within the LSO a lateromedial tonotopic gradient from low to high frequencies is well established (e.g., gerbil: Sanes et al., 1989; rat: Kelly et al., 1998; cat: Tsuchitani and Bodreau, 1966; dog: Goldberg and Brown, 1968), and a lateral and medial limb of LSO can also be distinguished neuroanatomically. Consistent with previous observations of Kaiser et al. (2011), we found a higher density of LOC neurons in the medial, high-frequency processing LSO limb in young animals compared to the lateral low-frequency portion and significant age related loss of LOC neurons was only found in this portion of the LSO. Liberman et al. (2014) showed that MOC effects are most important to efferent-mediated protection in the apical half of the cochlea, whereas LOC contributions dominate in the basal half of the cochlear partition where high frequencies are processed. Thus the significant age-related loss of LOC neurons found in the medial portion of the LSO would predominantly affect the high frequency processing capabilities of the animals. This is also consistent with observations of age-related hearing loss in the high frequency range in gerbils and humans (e.g., Mills et al., 1990).

The cholinergic efferent vestibular feedback pathway, however, is not subject to such neuronal loss in old animals despite sharing a lot of features with the auditory efferent system. Efferent fiber stimulation results in complex effects on the activity of vestibular afferent neurons by increasing, inhibiting or having mixed biphasic effects on the electrical discharge of the afferent neurons (Soto and Vega, 2010). The functional significance of these effects is, however, still not fully understood.

Differences in functional shortcomings in the auditory and the vestibular system with age suggest a prevalence of loss of auditory efferents. In a longitudinal study Enrietto et al. (1999) investigated age-related decrease in auditory (pure tone and speech perception, detection threshold and speech discrimination score tested psychophysically) and vestibular responses (VOR measurements) in healthy older human subjects. The faster decrease in auditory responses was not correlated with age-related changes in the vestibular system. They concluded that the two systems may age at different rates in the same individual. Hence age-related dysfunction of the auditory system need not be correlated with any deterioration of the vestibular system, as has also been shown in C57BL/6 mice (Shiga et al., 2005). In contrast to the auditory system, age-associated degeneration of the peripheral vestibular system in C57BL/6 mice was not significantly correlated with any age-dependent changes in function and followed a different time course when compared to changes in auditory function.

The age-related loss of cholinergic efferent neurons of the motor trigeminal nucleus was found to be minimal in gerbils in accord with an earlier study of Sturrock (1987) that showed only sparse neuronal loss of trigeminal neurons in the aged mouse. However, other than auditory and cholinergic vestibular efferent neurons, motor trigeminal neurons do possess perineuronal nets and aging dramatically affects these nets. Among several other functions attributed to perineuronal nets, they have been

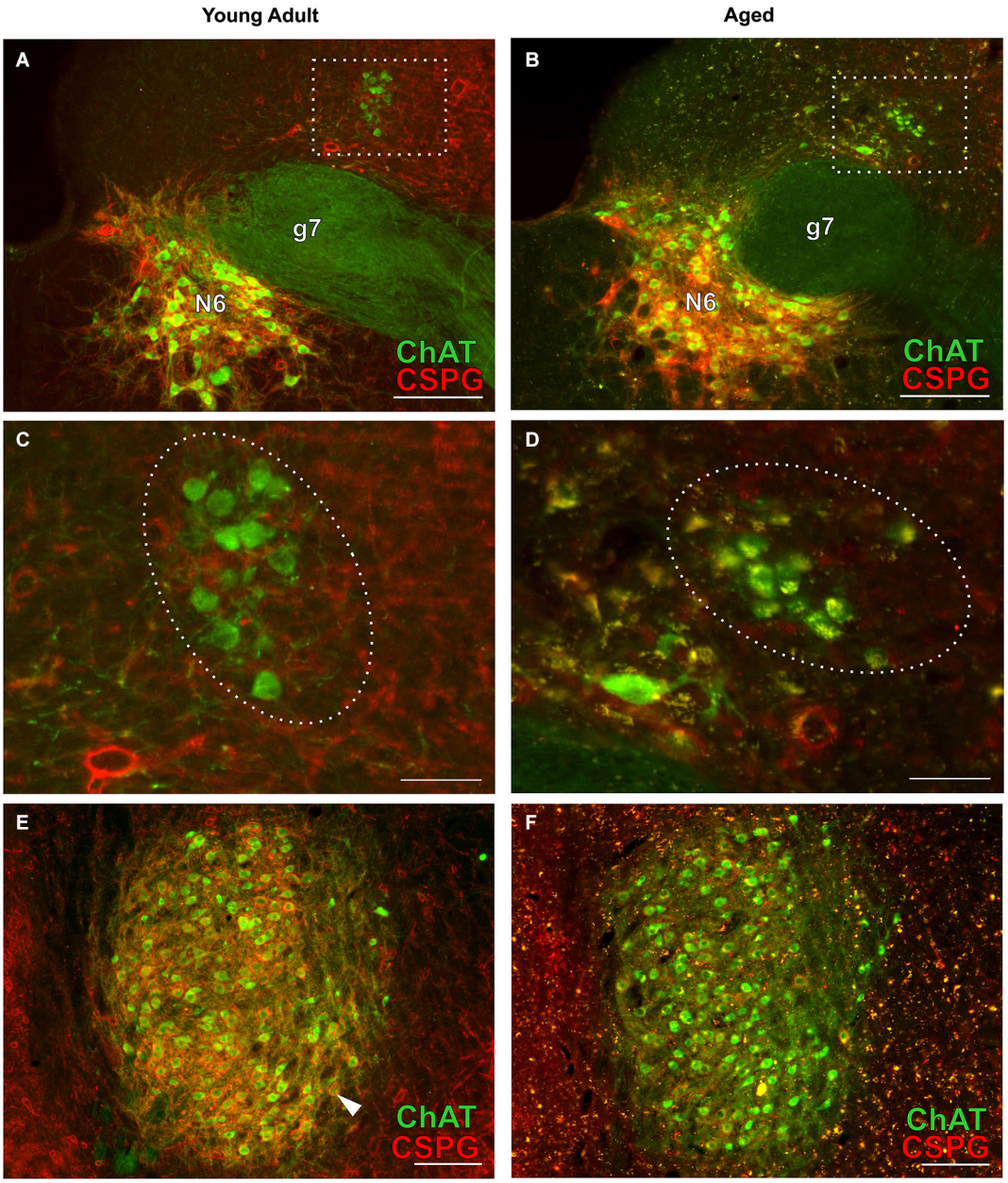

FIGURE 7 | Cholinergic neurons of the efferent vestibular system (A–D) and of the motor trigeminal nucleus (E,F) in young adult and aged gerbils. Micrographs were taken from the same series of a pair of young adult and aged gerbils as for the OC examples in **Figure 4**. ChAT (Alexa Fluor 488, green) and CSPG (Cy 3, red) immunolabeling is shown. The group of vestibular efferents in young adult and aged gerbil is accentuated by rectangles in **(A,B)**. **(C,D)** show enlargements of the rectangles in **(A,B)**, respectively. The groups of ChAT-positive and CSPG-negative efferent vestibular neurons are encircled. **(E,F)** give an overview of the motor trigeminal nucleus. ChAT-positive neurons of the young adult gerbil **(E)** are ensheathed in CSPG-positive perineuronal nets (arrowhead in **E**) whereas most cholinergic neurons of the aged gerbil **(F)** show degraded perineuronal nets and a comparably low amount of lipofuscin granules (yellow). N6: abducens nucleus; g7: genu of the facial nerve. Scale bar in **(A,B,E,F)**: 200 μm; in **(C,D)**: 50 μm.

shown to protect neurons from oxidative damage (Suttkus et al., 2012, 2014), but are themselves sensitive to excess oxidative stress (Cabungcal et al., 2013). Perineuronal nets might therefore be an effective protection from early functional impairment of trigeminal neurons with age. However, arguing against this, vestibular efferent neurons in the gerbil do not possess perineuronal nets and also showed no neuronal loss with aging.

Our results are in line with recent findings showing that during normal aging in humans and in animals, there is only a modest decline of neuronal number (probably no more than

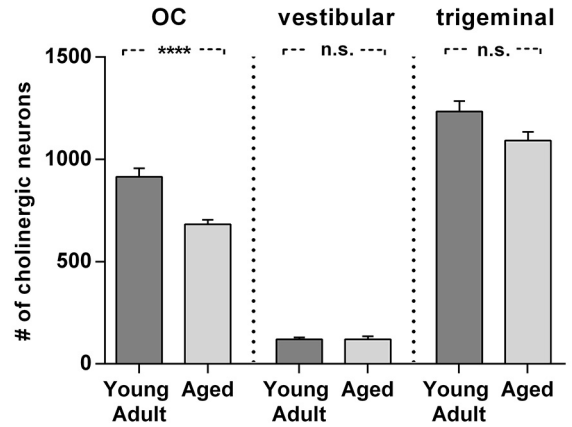

FIGURE 8 | Comparison of age related neuron loss in three cholinergic efferent systems. There is considerable loss in the olivocochlear efferent system (left) of 26% (t = 4,984; df = 18; $p < 0.0001$), whereas the vestibular efferent system (middle) is not affected by age and the trigeminal motor system (right) shows only a moderate neuronal loss of 12% (t = 2.155; df = 18; n.s.). Neuron numbers are given as mean ± SEM. Dark gray columns: young adult animals, light gray columns: aged animals. **** $p < 0.0001$.

10% (Morrison and Hof, 1997)). However, there is a specific age-related neuron loss in restricted neuronal populations of the nervous system (Pannese, 2011). In addition to a loss of cholinergic neurons, a functional decline with age might also be caused by dendritic, synaptic, and axonal degeneration as well as a decrease in trophic conditions of these neurons (Schliebs and Arendt, 2011).

Summarizing our findings, there is a significant loss in the auditory efferent system in senescent gerbils, with no counterpart in the vestibular efferent system or in the neuron population of the motor trigeminal nucleus. The observations support the concept of different mechanisms for age-associated changes in the different cholinergic systems of the brain stem.

AUTHOR CONTRIBUTIONS

Susanne Radtke-Schuller: conceived project, conducted experiments, analyzed and interpreted data, wrote manuscript. Sabine Seeler: conducted immunostaining, performed cell counts. Benedikt Grothe: conceived project jointly with Susanne Radtke-Schuller, interpreted data and jointly wrote manuscript.

ACKNOWLEDGMENTS

This research was funded by the BMBF (FKZ: EO 0901; IFB, German Center for Vertigo and Balance Disorders, TRF-7).

REFERENCES

Andrews, E. M., Richards, R. J., Yin, F. Q., Viapiano, M. S., and Jakeman, L. B. (2012). Alterations in chondroitin sulfate proteoglycan expression occur both at and far from the site of spinal contusion injury. *Exp. Neurol.* 235, 174–187. doi: 10.1016/j.expneurol.2011.09.008

Aschoff, A., Müller, M., and Ott, H. (1988). Origin of cochlea efferents in some gerbil species. A comparative anatomical study with fluorescent tracers. *Exp. Brain Res.* 71, 252–261. doi: 10.1007/bf00247485

Aschoff, A., and Ostwald, J. (1987). Different origins of cochlear efferents in some bat species, rats and guinea pigs. *J. Comp. Neurol.* 264, 56–72. doi: 10.1002/cne.902640106

Brown, M. C., and Levine, J. L. (2008). Dendrites of medial olivocochlear neurons in mouse. *Neuroscience* 154, 147–159. doi: 10.1016/j.neuroscience.2007.12.045

Bruce, L. L., Kingsley, J., Nichols, D. H., and Fritzsch, B. (1997). The development of vestibulocochlear efferents and cochlear afferents in mice. *Int. J. Dev. Neurosci.* 15, 671–692. doi: 10.1016/s0736-5748(96)00120-7

Cabungcal, J.-H., Steullet, P., Morishita, H., Kraftsik, R., Cuenod, M., Hensch, T. K., et al. (2013). Perineuronal nets protect fast-spiking interneurons against oxidative stress. *Proc. Natl. Acad. Sci. U S A* 110, 9130–9135. doi: 10.1073/pnas.1300454110

Caspary, D. M., Ling, L., Turner, J. G., and Hughes, L. F. (2008). Inhibitory neurotransmission, plasticity and aging in the mammalian central auditory system. *J. Exp. Biol.* 211, 1781–1791. doi: 10.1242/jeb.013581

Cheal, M. (1986). The gerbil: a unique model for research on aging. *Exp. Aging Res.* 12, 3–21. doi: 10.1080/03610738608259430

Darrow, K. N., Maison, S. F., and Liberman, M. C. (2006). Cochlear efferent feedback balances interaural sensitivity. *Nat. Neurosci.* 9, 1474–1476. doi: 10.1038/nn1807

Enrietto, J. A., Jacobson, K. M., and Baloh, R. W. (1999). Aging effects on auditory and vestibular responses: a longitudinal study. *Am. J. Otolaryngol.* 20, 371–378. doi: 10.1016/s0196-0709(99)90076-5

Fu, B., Le Prell, C., Simmons, D., Lei, D., Schrader, A., Chen, A. B., et al. (2010). Age-related synaptic loss of the medial olivocochlear efferent innervation. *Mol. Neurodegener.* 5:53. doi: 10.1186/1750-1326-5-53

Furman, A. C., Kujawa, S. G., and Liberman, M. C. (2013). Noise-induced cochlear neuropathy is selective for fibers with low spontaneous rates. *J. Neurophysiol.* 110, 577–586. doi: 10.1152/jn.00164.2013

Gleich, O., Weiss, M., and Strutz, J. (2004). Age-dependent changes in the lateral superior olive of the gerbil (*Meriones unguiculatus*). *Hear. Res.* 194, 47–59. doi: 10.1016/j.heares.2004.03.016

Goldberg, J. M., and Brown, P. B. (1968). Functional organization of the dog superior olivary complex: an anatomical and electrophysiological study. *J. Neurophysiol.* 31, 639–656.

Goldberg, J. M., and Fernandéz, C. (1980). Efferent vestibular system in the squirrel monkey: anatomical location and influence on afferent activity. *J. Neurophysiol.* 43, 986–1025.

Groff, J. A., and Liberman, M. C. (2003). Modulation of cochlear afferent response by the lateral olivocochlear system: activation via electrical stimulation of the inferior colliculus. *J. Neurophysiol.* 90, 3178–3200. doi: 10.1152/jn.00537.2003

Guinan, J. J. (2011). "Physiology of the medial and lateral olivocochlear systems," in *Auditory and Vestibular Efferents*, eds D. K. Ryugo, R. R. Fay and A. N. Popper (New York: Springer), 39–83.

Guinan, J. J., Warr, W. B., and Norris, B. E. (1984). Topographic organization of the olivocochlear projections from the lateral and medial zones of the superior olivary complex. *J. Comp. Neurol.* 226, 21–27. doi: 10.1002/cne.902260103

Hedreen, J. C., Bacon, S. J., Cork, L. C., Kitt, C. A., Crawford, G. D., Salvterra, P. M., et al. (1983). Immunocytochemical identification of cholinergic neurons in the monkey central nervous system using monoclonal antibodies against choline acetyltransferase. *Neurosci. Lett.* 43, 173–177. doi: 10.1016/0304-3940(83)90183-0

Holt, J. C., Lysakowski, A., and Goldberg, J. M. (2011). "The efferent vestibular system," in *Auditory and Vestibular Efferents*, eds D. K. Ryugo, R. R. Fay and A. N. Popper (New York: Springer), 135–187.

Jacobson, M., Kim, S., Romney, J., Zhu, X., and Frisina, R. D. (2003). Contralateral suppression of distortion-product otoacoustic emissions declines with age: a comparison of findings in CBA mice with human listeners. *Laryngoscope* 113, 1707–1713. doi: 10.1097/00005537-200310000-00009

Jin, D., Ohlemiller, K. K., Lei, D., Dong, E., Role, L., Ryugo, D. K., et al. (2011). Age-related neuronal loss in the cochlea is not delayed by synaptic modulation. *Neurobiol. Aging* 32, 2321.e13–2321.e23. doi: 10.1016/j.neurobiolaging.2010.05.011

Kaiser, A., Alexandrova, O., and Grothe, B. (2011). Urocortin-expressing olivocochlear neurons exhibit tonotopic and developmental changes in the auditory brainstem and in the innervation of the cochlea. *J. Comp. Neurol.* 519, 2758–2778. doi: 10.1002/cne.22650

Kelly, J. B., Liscum, A., van Adel, B., and Ito, M. (1998). Projections from the superior olive and lateral lemniscus to tonotopic regions of the rat's inferior colliculus. *Hear. Res.* 116, 43–54. doi: 10.1016/s0378-5955(97)00195-0

Kim, S., Frisina, D. R., and Frisina, R. D. (2002). Effects of age on contralateral suppression of distortion product otoacoustic emissions in human listeners with normal hearing. *Audiol. Neurootol.* 7, 348–357. doi: 10.1159/000066159

Köppl, C. (2011). "Evolution of the octavolateral efferent system," in *Auditory and Vestibular Efferents*, eds D. K. Ryugo, R. R. Fay and A. N. Popper (New York: Springer), 217–261.

Lauer, A. M., Fuchs, P., Ryugo, D. K., and Francis, H. W. (2012). Efferent synapses return to inner hair cells in the aging cochlea. *Neurobiol. Aging* 33, 2892–2902. doi: 10.1016/j.neurobiolaging.2012.02.007

Liberman, M. C., Liberman, L. D., and Maison, S. F. (2014). Efferent feedback slows cochlear aging. *J. Neurosci.* 34, 4599–4607. doi: 10.1523/JNEUROSCI.4923-13.2014

Lurie, D. I., Pasic, T. R., Hockfield, S. J., and Rubel, E. W. (1997). Development of Cat-301 immunoreactivity in auditory brainstem nucleiof the gerbil. *J. Comp. Neurol.* 380, 319–334. doi: 10.1002/(sici)1096-9861(19970414)380:3<319::aid-cne3>3.0.co;2-5

Maison, S. F., Usubuchi, H., and Liberman, M. C. (2013). Efferent feedback minimizes cochlear neuropathy from moderate noise exposure. *J. Neurosci.* 33, 5542–5552. doi: 10.1523/JNEUROSCI.5027-12.2013

Mills, J. H., Schmiedt, R. A., and Kulish, L. F. (1990). Age-related changes in auditory potentials of Mongolian gerbil. *Hear. Res.* 46, 201–210. doi: 10.1016/0378-5955(90)90002-7

Morrison, J. H., and Hof, P. R. (1997). Life and death of neurons in the aging brain. *Science* 278, 412–419. doi: 10.1126/science.278.5337.412

Ostapoff, E. M., and Morest, D. K. (1989). A degenerative disorder of the central auditory system of the gerbil. *Hear. Res.* 37, 141–162. doi: 10.1016/0378-5955(89)90036-1

Pannese, E. (2011). Morphological changes in nerve cells during normal aging. *Brain Struct. Funct.* 216, 85–89. doi: 10.1007/s00429-011-0308-y

Perachio, A. A., and Kevetter, G. A. (1989). Identification of vestibular efferent neurons in the gerbil: histochemical and retrograde labelling. *Exp. Brain Res.* 78, 315–326. doi: 10.1007/bf00228903

Pujol, R., and Puel, J.-L. (1999). Excitotoxicity, synaptic repair and functional recovery in the mammalian cochlea: a review of recent findings. *Ann. N Y Acad. Sci.* 884, 249–254. doi: 10.1111/j.1749-6632.1999.tb08646.x

Purcell, I. M., and Perachio, A. A. (1997). Three-dimensional analysis of vestibular efferent neurons innervating semicircular canals of the gerbil. *J. Neurophysiol.* 78, 3234–3248.

Rautenberg, P. L., Grothe, B., and Felmy, F. (2009). Quantification of the three-dimensional morphology of coincidence detector neurons in the medial superior olive of gerbils during late postnatal development. *J. Comp. Neurol.* 517, 385–396. doi: 10.1002/cne.22166

Roberts, B. L., and Meredith, G. E. (1992). "The efferent innervation of the ear: variations on an enigma," in *The Evolutionary Biology of Hearing*, eds D. B. Webster, R. R. Fay and A. N. Popper (New York: Springer), 185–210.

Robertson, D., Anderson, C. J., and Cole, K. S. (1987). Segregation of efferent projections to different turns of the guinea pig cochlea. *Hear. Res.* 25, 69–76. doi: 10.1016/0378-5955(87)90080-3

Ruel, J., Nouvian, R., Gervais d'Aldin, C., Pujol, R., Eybalin, M., and Puel, J.-L. (2001). Dopamine inhibition of auditory nerve activity in the adult mammalian cochlea. *Eur. J. Neurosci.* 14, 977–986. doi: 10.1046/j.0953-816x.2001.01721.x

Ryan, A. F. (1976). Hearing sensitivity of the mongolian gerbil, *Meriones unguiculatus*. *J. Acoust. Soc. Am.* 59, 1222–1226. doi: 10.1121/1.380961

Ryan, A. F., Simmons, D. M., Watts, A. G., and Swanson, L. W. (1991). Enkephalin mRNA production by cochlear and vestibular efferent neurons in the gerbil brainstem. *Exp. Brain Res.* 87, 259–267. doi: 10.1007/bf00231843

Sanes, D. H., Merickel, M., and Rubel, E. W. (1989). Evidence for an alteration of the tonotopic map in the gerbil cochlea during development. *J. Comp. Neurol.* 279, 436–444. doi: 10.1002/cne.902790308

Schaette, R., and McAlpine, D. (2011). Tinnitus with a normal audiogram: physiological evidence for hidden hearing loss and computational model. *J. Neurosci.* 31, 13452–13457. doi: 10.1523/JNEUROSCI.2156-11.2011

Schliebs, R., and Arendt, T. (2011). The cholinergic system in aging and neuronal degeneration. *Behav. Brain Res.* 221, 555–563. doi: 10.1016/j.bbr.2010.11.058

Schofield, B. R. (2011). "Central descending auditory pathways," in *Auditory and Vestibular Efferents*, eds D. K. Ryugo, R. R. Fay and A. N. Popper (New York: Springer), 261–291.

Sewell, W. F. (2011). "Pharmacology and neurochemistry of olivocochlear efferents," in *Auditory and Vestibular Efferents*, eds D. K. Ryugo, R. R. Fay and A. N. Popper (New York: Springer), 83–103.

Simmons, D. D. (2002). Development of the inner ear efferent system across vertebrate species. *J. Neurobiol.* 53, 228–250. doi: 10.1002/neu.10130

Shiga, A., Nakagawa, T., Nakayama, M., Endo, T., Iguchi, F., Kim, T.-S., et al. (2005). Aging effects on vestibulo-ocular responses in C57BL/6 mice: comparison with alteration in auditory function. *Audiol. Neurootol.* 10, 97–104. doi: 10.1159/000083365

Soto, E., and Vega, R. (2010). Neuropharmacology of vestibular system disorders. *Curr. Neuropharmacol.* 8, 26–40. doi: 10.2174/157015910790909511

Sturrock, R. R. (1987). Changes in the number of neurons in the mesencephalic and motor nuclei of the trigeminal nerve in the ageing mouse brain. *J. Anat.* 151, 15–25.

Suttkus, A., Rohn, S., Jäger, C., Arendt, T., and Morawski, M. (2012). Neuroprotection against iron-induced cell death by perineuronal nets—an in vivo analysis of oxidative stress. *Am. J. Neurodegen. Dis.* 1, 122–129.

Suttkus, A., Rohn, S., Weigel, S., Glöckner, P., Arendt, T., and Morawski, M. (2014). Aggrecan, link protein and tenascin-R are essential components of the perineuronal net to protect neurons against iron-induced oxidative stress. *Cell Death Dis.* 5:e1119. doi: 10.1038/cddis.2014.25

Tsuchitani, C., and Bodreau, J. C. (1966). Single unit analysis of cat superior olive S segment with tonal stimuli. *J. Neurophysiol.* 29, 684–697.

Vetter, D. E., and Mugnagnaini, E. (1992). Distribution and dendritic features of three groups of rat olivocochlear neurons. *Anat. Embryol. (Berl)* 185, 1–16. doi: 10.1007/bf00213596

Warr, W. B., Beck Boche, J., and Neely, S. T. (1997). Efferent innervation of the inner hair cell region: origins and terminations of two lateral olivocochlear systems. *Hear. Res.* 108, 89–111. doi: 10.1016/s0378-5955(97)00044-0

Warr, W., Beck Boche, J., Ye, Y., and Kim, D. O. (2002). Organization of olivocochlear neurons in the cat studied with the retrograde tracer cholera toxin-B. *J. Assoc. Res. Otolaryngol.* 3, 457–478. doi: 10.1007/s10162-002-2046-6

West, M. J. (1993). New stereological methods for counting neurons. *Neurobiol. Aging* 14, 275–285. doi: 10.1016/0197-4580(93)90112-o

Conflict of Interest Statement: The authors declare that the research was conducted in the absence of any commercial or financial relationships that could be construed as a potential conflict of interest.

Received: 07 November 2014; accepted: 11 January 2015; published online: 13 February 2015.

Citation: Radtke-Schuller S, Seeler S and Grothe B (2015) Restricted loss of olivocochlear but not vestibular efferent neurons in the senescent gerbil (Meriones unguiculatus). Front. Aging Neurosci. 7:4. doi: 10.3389/fnagi.2015.00004

This article was submitted to the journal Frontiers in Aging Neuroscience.

frontiers in Aging Neuroscience

ORIGINAL RESEARCH
published: 15 May 2015
doi: 10.3389/fnagi.2015.00063

Stochastic undersampling steepens auditory threshold/duration functions: implications for understanding auditory deafferentation and aging

Frédéric Marmel[1,2]*, *Medardo A. Rodríguez-Mendoza*[1] and *Enrique A. Lopez-Poveda*[1,2,3]

[1] Audición Computacional y Psicoacústica, Instituto de Neurociencias de Castilla y León, Universidad de Salamanca, Salamanca, Spain, [2] Grupo de Audiología, Instituto de Investigación Biomédica de Salamanca, Universidad de Salamanca, Salamanca, Spain, [3] Facultad de Medicina, Departamento de Cirugía, Universidad de Salamanca, Salamanca, Spain

It has long been known that some listeners experience hearing difficulties out of proportion with their audiometric losses. Notably, some older adults as well as auditory neuropathy patients have temporal-processing and speech-in-noise intelligibility deficits not accountable for by elevated audiometric thresholds. The study of these hearing deficits has been revitalized by recent studies that show that auditory deafferentation comes with aging and can occur even in the absence of an audiometric loss. The present study builds on the stochastic undersampling principle proposed by Lopez-Poveda and Barrios (2013) to account for the perceptual effects of auditory deafferentation. Auditory threshold/duration functions were measured for broadband noises that were stochastically undersampled to various different degrees. Stimuli with and without undersampling were equated for overall energy in order to focus on the changes that undersampling elicited on the stimulus waveforms, and not on its effects on the overall stimulus energy. Stochastic undersampling impaired the detection of short sounds (<20 ms). The detection of long sounds (>50 ms) did not change or improved, depending on the degree of undersampling. The results for short sounds show that stochastic undersampling, and hence presumably deafferentation, can account for the steeper threshold/duration functions observed in auditory neuropathy patients and older adults with (near) normal audiometry. This suggests that deafferentation might be diagnosed using pure-tone audiometry with short tones. It further suggests that the auditory system of audiometrically normal older listeners might not be "slower than normal", as is commonly thought, but simply less well afferented. Finally, the results for both short and long sounds support the probabilistic theories of detectability that challenge the idea that auditory threshold occurs by integration of sound energy over time.

Keywords: auditory deafferentation, auditory aging, auditory neuropathy, stochastic sampling, temporal processing, temporal integration

OPEN ACCESS

Edited by:
Isabel Varela-Nieto, Consejo Superior Investigaciones Científicas, Spain

Reviewed by:
Kathy Pichora-Fuller, University of Toronto Mississauga, Canada
Wendy Lecluyse, University Campus Suffolk, UK

***Correspondence:**
Frédéric Marmel, Audición Computacional y Psicoacústica, Instituto de Neurociencias de Castilla y León, Universidad de Salamanca, Calle Pintor Fernando Gallego 1, Salamanca 37007, Spain
frederic.marmel@gmail.com

Received: *18 December 2014*
Accepted: *11 April 2015*
Published: *15 May 2015*

Citation:
Marmel F, Rodríguez-Mendoza MA and Lopez-Poveda EA (2015) Stochastic undersampling steepens auditory threshold/duration functions: implications for understanding auditory deafferentation and aging. Front. Aging Neurosci. 7:63. doi: 10.3389/fnagi.2015.00063

Introduction

Hearing impairment is routinely diagnosed on the basis of elevated audiometric thresholds, i.e., on the basis of an increase in the lowest sound levels at which listeners can detect pure tones of different frequencies. It has long been known, however, that listeners can experience hearing difficulties not reflected in their audiometric thresholds (Kopetzky, 1948; King, 1954; for reviews see Lopez-Poveda, 2014; Plack et al., 2014). These hearing impairments are sometimes referred to as "hidden" hearing losses (Schaette and McAlpine, 2011). They include hyperacusis and tinnitus (Schaette and McAlpine, 2011) as well as deficits in temporal processing and related abilities, such as sound localization, temporal resolution, and/or speech-in-noise perception (Starr et al., 1991; Kraus et al., 2000; Zeng et al., 2005; Zeng and Liu, 2006; Zhao and Stephens, 2007). Behaviorally, studies of patients diagnosed with auditory neuropathy have well documented the association between impaired speech-in-noise perception and impaired temporal processing (Starr et al., 1991; Kraus et al., 2000; Zeng et al., 2005; Zeng and Liu, 2006). Impaired speech-in-noise perception and impaired temporal processing are also a frequent concern for older listeners with (near) normal hearing thresholds (CHABA, 1988; Pichora-Fuller and MacDonald, 2008; Fitzgibbons and Gordon-Salant, 2010; Humes and Dubno, 2010). Physiologically, recent studies have reported that noise exposure causes a permanent loss of auditory nerve fibers even though audiometric thresholds recover rapidly to the normal range (Kujawa and Liberman, 2009; Lin et al., 2011; Furman et al., 2013). Kujawa and Liberman (2009) argued that this deafferentation should "decrease the robustness of stimulus coding in low signal-to-noise conditions, for example speech in noise, where spatial summation via convergence of activity from groups of neurons must be important in signal processing" (p. 14083). Deafferentation also occurs with aging (Makary et al., 2011; Sergeyenko et al., 2013), which suggests that deafferentation could contribute to the speech-in-noise and temporal processing deficits observed in older listeners with (near) normal audiometry. The present study investigates how deafferentation could deteriorate temporal processing, in particular the detection of brief sounds. The present study also contributes to our understanding of the mechanisms underlying sound detection.

Lopez-Poveda and Barrios (2013) proposed a signal-processing analogy based on the stochastic nature of action potentials to explain how deafferentation could result in poorer temporal processing and speech-in-noise perception. They noted that the stochastic nature of action potentials imposes a limit to information encoding in the auditory nerve. Action potentials being stochastic means that individual auditory nerve fibers (ANFs) do not perfectly sample the waveform of the mechanical cochlear response in the cochlear region innervated by the fiber. Instead, an ANF can be seen as providing an undersampled, incomplete, representation of the mechanical response waveform in question. In a normal auditory nerve, a high-quality waveform representation would be granted by the pooling of the spike trains from all the ANFs in the nerve. Such a pooling mechanism is reminiscent of the "volley theory" (Wever, 1949) and has been shown to be effective for the encoding of speech sounds (Stevens and Wickesberg, 1999, 2002). In a deafferented nerve, however, the reduced number of ANFs would be less able to compensate for the limited information encoded by individual fibers.

In addition, Lopez-Poveda and Barrios (2013) argued that the stochastic nature of action potentials implies that a reduction of the number of ANFs would specifically degrade the coding of low-intensity and high-frequency sound features. They reasoned that the stochastic nature of action potentials means that the quantity of stimulus information conveyed by an individual ANF depends (1) on its instantaneous probability of firing as a function of stimulus intensity; and (2) on the stimulus duration. As the probability of an individual ANF firing increases with increasing sound pressure (Sachs and Abbas, 1974; Heil et al., 2011), a given ANF would be more likely to convey high-intensity than low-intensity sound features. Also, as action potentials occur stochastically in time, the probability of an individual ANF firing at least once in response to a stimulus increases with increasing the stimulus duration (Heil et al., 2008), which means that an individual ANF would be more likely to fire in response to a long sustained stimulus than to a short transient stimulus of equal intensity. As a result, acoustic features involving long intervals (low frequency features) would be more likely to be represented in the spike train of an individual ANF than acoustic features involving short intervals (high frequency features). In case of deafferentation, the comparatively fewer surviving ANFs might be insufficient to compensate for the limited information encoding of low-intensity and high-frequency features by individual ANFs.

Lopez-Poveda and Barrios (2013) tested their theory experimentally with a vocoder (see Section Stochastic Undersampling Vocoder, and **Figure 1**) designed to generate N stochastically undersampled versions of the stimulus per frequency channel, where the parameter N is the number of stochastic samplers and would roughly simulate N auditory nerve fibers. Lopez-Poveda and Barrios (2013) measured pure tone detection thresholds and speech recognition in quiet and in noise in young normal-hearing listeners, for stimuli processed with either a large or a small number of simulated fibers. Undersampled and non-processed stimuli were equalized for root-mean-square (rms) amplitude to make sure that performance was independent of differences in overall stimulus intensity. Instead, differences in performance would reflect changes in the distribution of stimulus energy along time, i.e., changes in the stimulus waveforms. Reducing the number of simulated fibers impaired speech recognition in noise but not in quiet, consistent with older listeners' impaired speech-in-noise perception (CHABA, 1988; Humes and Dubno, 2010). Pure-tone detection was slightly impaired both in noise and in quiet but detection thresholds were still within the normal range, which is consistent with the threshold recovery observed in noise-induced deafferentation studies (Kujawa and Liberman, 2009; Lin et al., 2011). These two results suggested that stochastic undersampling is a reasonable analogy to

explain how auditory deafferentation would cause speech-in-noise difficulties in listeners with (near) normal audiometric thresholds. The present study uses the stochastic undersampling analogy of Lopez-Poveda and Barrios (2013) to investigate how deafferentation could impair specific aspects of temporal processing.

We focus on threshold/duration functions, which are often referred to as "temporal integration" functions and describe the phenomenon of higher detection thresholds for shorter than for longer sound durations (Hughes, 1946; Garner and Miller, 1947). Auditory neuropathy patients have abnormally elevated detection thresholds for shorter durations (below approximately 30 ms) resulting in steeper threshold/duration functions than control listeners (Starr et al., 1991; Zeng et al., 2005). Even though "auditory neuropathy" is not always caused by alterations to the auditory nerve (Starr, 2009), deafferentation could be one possible cause of the steeper threshold/duration functions observed in these patients, given that the stochastic undersampling analogy of deafferentation predicts that short sounds are less likely to be represented in the response of ANFs than are long sounds. Poorer detection of short pure tones (15 ms) has also been reported to be a predictor of speech-in-noise perception in a group of listeners covering a wide range of ages (89 listeners, 21–82 years) whose thresholds were within the normal range for their age and for whom detection thresholds for longer (50 ms) tones did not correlate with age (Fostick and Babkoff, 2013; Fostick et al., 2013). The present study used the vocoder implementation of the stochastic undersampling principle (Lopez-Poveda and Barrios, 2013) to measure threshold/duration functions as a function of the degree of stochastic undersampling. As will be shown, reducing the number of stochastic samplers resulted in steeper threshold/duration functions. Therefore, stochastic undersampling, and so presumably deafferentation, could explain how deafferented listeners have trouble detecting short transient sounds.

We note that although threshold/duration functions are often referred to as "temporal integration" functions, the seminal explanation for absolute threshold that assumes that the auditory system integrates sound intensity over time (Green et al., 1957; Plomp and Bouman, 1959) has been challenged several times. Alternative mechanisms have been proposed: (1) the quantity integrated over time could be sound pressure rather than sound intensity (Heil and Neubauer, 2003); (2) there could be no long-term integration but instead a series of short "multiple looks", each providing independent information to be stored in memory and combined intelligently across looks (Viemeister and Wakefield, 1991); and (3) there could be no integration at all but instead a probability accumulation over time that would require no memory, with thresholds corresponding to the occurrence of a criterion number of stochastic detection events (Heil and Neubauer, 2003; Heil et al., 2013b) or even to one single detection event (Meddis and Lecluyse, 2011). In the present study, undersampled and non-processed stimuli were equated for rms amplitude (as in Lopez-Poveda and Barrios, 2013); hence stimuli of the same duration but processed with different degrees of stochastic undersampling will have the same energy and so any difference in their detectability will not be consistent with mechanisms based on long-term integration of intensity. Instead, the stochastic undersampling principle is reminiscent of the probabilistic approaches of sound detectability (Meddis and Lecluyse, 2011; Heil et al., 2013a,b) as they share the principle of enhanced stimulus representations for larger amplitudes and longer stimuli. A reduction in the number of stochastic samplers, which we use to simulate deafferentation, could be thought of as leading to a less efficient probability accumulation.

Materials and Methods

Participants

Nine participants (5 females) were tested. Their ages ranged from 24 to 33 years, with a mean of 27 years. All of them had audiometric thresholds less than 20 dB HL at octave frequencies spanning 250–8000 Hz (American National Standards Institute, 2004) and none reported any history of hearing impairment. All participants were tested in their right ear. Subjects were volunteers and were not paid for their service.

Stochastic Undersampling Vocoder

Figure 1 illustrates stochastic undersampling with $N = 10$ samplers, for a 20-ms broadband noise with an rms amplitude of 0.495 (which corresponds to a presentation level of 100 dB SPL with our apparatus). The noise was filtered through a bank of ten fourth-order Butterworth filters (only two are shown in **Figure 1**) with cut-off frequencies logarithmically spaced between 100 Hz and 10 kHz to roughly mimic frequency decomposition within the cochlea. For each filter output, multiple (N) "spike" trains were stochastically generated to roughly mimic N different possible encodings of the signal by N different "afferent fibers" innervating a given cochlear region. Each "spike" train was obtained by sample-wise comparisons of the absolute amplitude of the filtered signal (all "digital" amplitudes between 0 and 1) with an equal-length array of random numbers uniformly distributed between 0 and 1. A unity-amplitude "spike" was generated whenever the signal's absolute amplitude exceeded the corresponding random number. Thus, signals of higher intensities were more likely to generate "spikes" than signals of lower intensities. The resulting N "spike" trains per frequency band were aggregated into a single "spike" train using a sample-wise logical OR function; that is, unity amplitude "spikes" occurred in the aggregated response whenever a "spike" occurred in *any* of the N available "spike" trains. Thus, the larger the number of stochastic samplers (N), the more likely the aggregated response was to contain "spikes". An acoustic version of the aggregated "spike" train was then obtained by sample-wise multiplication of the train in question with the output of the filter in each band. The reconstructed signal from each frequency band was then filtered through its corresponding Butterworth filter to filter out distortion or energy splatter. Finally, the ten resulting signals (one per band) were sample-wise added to obtain a vocoded stimulus, whose rms amplitude was normalized to the rms amplitude of the original stimulus

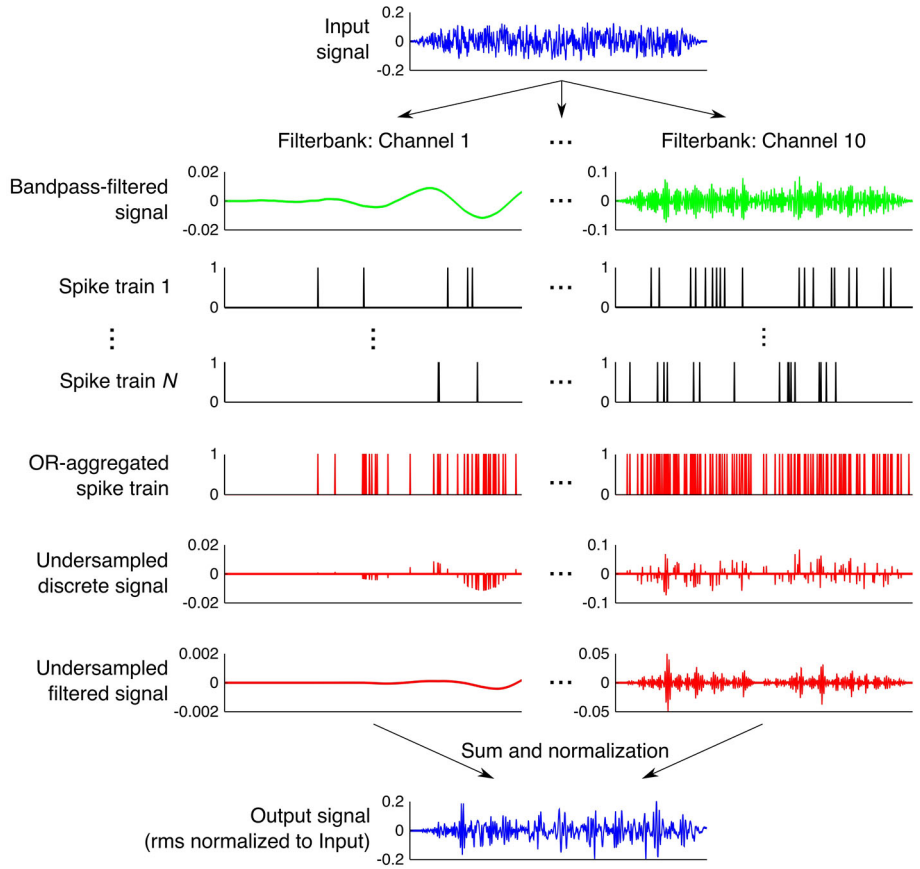

FIGURE 1 | Step-by-step illustration of the processing done by the stochastic undersampling vocoder. See Section Stochastic Undersampling Vocoder for a description.

so that stochastic undersampling would only affect the temporal distribution of energy and not the overall stimulus energy. For low-intensity signals and/or when using a small number N of stochastic samplers, it could happen that stochastic undersampling did not preserve any of the samples in the original stimulus (no "spikes" were generated). In those cases, rms normalization was not applied and the processed stimuli were left blank (a condition akin to having no stimulus).

Stimuli

All stimuli were broadband (20–10000 Hz) noises and had 2.5-ms cosine squared onset and offset ramps. Detection thresholds were measured as a function of stimulus duration, for stimulus duration (including the 2.5-ms ramps) of 5, 10, 20, 50, 100, 200, and 500 ms. Three different degrees of deafferentation were simulated by vocoding the stimuli with either 300 stochastic samplers per frequency channel, 1000 stochastic samplers per frequency channel, or by vocoding the stimuli without undersampling. As the undersampling of long stimuli was too computationally expensive to be made in real time, all stimuli were pre-generated so that the experimental software only had to load them from the computer hard drive. All stimuli were pre-generated for all sound levels between −10 and 80 dB SPL in 2-dB steps. For each level, three stimuli were pre-generated to avoid having exactly the same stimuli presented on different trials and—for each trial—the experimental software picked one of the three randomly. Some of the lower-intensity stimuli were left blank by the stochastic undersampling, mostly for short durations. As only three stimuli were generated per condition, the proportions of blank stimuli presented in the present study may have been different than what they would have been if the stimuli had been generated in real time. The implications of blank stimuli will be discussed in Section Implications for Mechanisms of Sound Detectability.

Apparatus

All stimuli were generated digitally using custom Matlab software (The Mathworks, Natick, Massachusetts, USA). Stimuli were digital-to-analog converted using an RME Fireface 400 sound card at a sampling rate of 44100 Hz and a resolution of 24 bits, and presented monaurally through circumaural Sennheiser HD580 headphones. Subjects sat in a double-wall sound booth during testing. Stimulus intensity (in dB SPL) was specified in reference to the acoustic sound level of a 1-kHz digital sinusoidal wave with maximal digital amplitude (i.e., peak amplitudes equal

to −1/+1). This calibration value was measured by placing the headphones on a KEMAR equipped with a Zwislocki coupler (Knowles DB-100) connected to a sound level meter (B&K 2238).

Procedure

The experimental procedure was controlled via custom Matlab software. Detection thresholds were estimated in a three-interval-three-alternative forced choice task (3I3AFC) using a two-down one-up adaptive procedure, which tracks the 70.7% point on the psychometric function (Levitt, 1971). One interval (randomly chosen) contained the stimulus while the two other intervals were silent. Lights flashing on a computer screen marked the three observation intervals. The lights had the same duration as the stimulus and were separated by 500 ms. Listeners were asked to identify which interval contained the stimulus by pressing the corresponding key on a computer keyboard. Visual feedback indicated whether their response was right or wrong. The stimulus level was initially set to 60 dB SPL and varied adaptively in 6-dB steps for the first three reversals and in 2-dB steps for the next nine reversals. The mean and the standard deviation of the stimulus levels on the last eight reversals were calculated. If the standard deviation was less than 6 dB, the mean was taken as an estimate of the detection threshold. Three such estimates were obtained for each experimental condition and their mean was taken as the final threshold.

Experimental procedures were approved by the Ethics Review Board of the University of Salamanca.

Statistical Analysis

Detection thresholds were compared with a repeated measures analysis of variance (ANOVA), using the degree of undersampling (without undersampling/300 samplers/1000 samplers) and the duration of the stimuli (5/10/20/50/100/200/500 ms) as within-subjects factors. Statistical results are reported with the Greenhouse-Geisser correction as the sphericity assumption was violated for duration.

Thresholds obtained for a given stimulus duration were compared across deafferentation conditions with *post hoc* two-tailed paired *t*-tests. The slopes of the threshold/duration functions were estimated for each participant and undersampling condition by fitting straight lines to the data (equations of the form: $threshold = a + b \times \ln[duration]$). For convenience, the estimated slopes will be reported as the decrease in threshold (in dB) per doubling duration (given by $b \times \ln[2]$). The mean slopes for each undersampling condition were compared using two-tailed paired *t*-tests.

Results

Individual and mean detection thresholds are plotted in **Figure 2**, which shows the data as analyzed statistically. To facilitate the comparison with figures from previous related studies (Florentine et al., 1988; Zeng et al., 1999, 2005), **Figure 3** re-plots mean detection thresholds relative to the mean thresholds obtained for the 500-ms stimuli. All listeners showed thresholds that decreased with increasing duration in all conditions. Undersampling, however, affected thresholds differently for durations shorter and longer than about 20–50 ms. For durations <20 ms, eight out of nine listeners (listener S2 being the exception) had lower thresholds without undersampling than when using 300 samplers, and thresholds obtained with 1000 samplers were intermediate. Results for durations longer than 20 ms were less consistent across listeners, but overall the differences between undersampling conditions decreased and sometimes reversed as most listeners had thresholds without undersampling that were comparable to or higher than at least one of the two undersampling conditions.

The ANOVA revealed a main effect of duration ($F_{(6,48)} = 366$; $p < 0.001$) but not of undersampling ($F_{(2,16)} = 2.27$; $p = 0.160$). Instead, duration and undersampling interacted. The effect of duration was larger with undersampling than in the control condition, and larger when using 300 samplers than with 1000 samplers ($F_{(12,96)} = 12.88$; $p < 0.001$). Thresholds for short sounds were higher with undersampling than without it, contrary to thresholds for long sounds that were lower with undersampling than without it. For short sounds of 5 and 10 ms, *post hoc* paired *t*-tests showed that thresholds were significantly lower without undersampling than with 1000 samplers (5 ms: $t_{(8)} = -5.63$; $p < 0.001$; 10 ms: $t_{(8)} = -7.11$; $p < 0.001$). They also revealed that thresholds were significantly lower with 1000 than with 300 samplers (5 ms: $t_{(8)} = -4.01$; $p < 0.005$; 10 ms: $t_{(8)} = -4.53$; $p < 0.005$). For long sounds of 200 and 500 ms, *post hoc* paired *t*-tests showed that thresholds were significantly higher without undersampling than with 300 samplers (200 ms: $t_{(8)} = 2.63$; $p < 0.05$; 500 ms: $t_{(8)} = 3.74$; $p < 0.01$). Thresholds were also higher with 1000 than with 300 samplers (200 ms: $t_{(8)} = 3.56$; $p < 0.01$; 500 ms: $t_{(8)} = 5.70$; $p < 0.001$). However, thresholds obtained with 1000 samplers were not different from thresholds obtained without undersampling (200 ms: $t_{(8)} = 0.75$; $p = 0.48$; 500 ms: $t_{(8)} = 0.55$; $p = 0.60$).

The slopes of the threshold/duration functions (**Figure 4**) indicated that thresholds in the absence of undersampling decreased by 1.81 dB for every doubling of duration whereas thresholds obtained with 300 and 1000 samplers decreased by respectively 3.12 and 2.35 dB for every doubling of duration. Hence, threshold/duration functions in the 1000 samplers and in the 300 samplers condition had slopes respectively 1.30 times and 1.73 times steeper than in the no undersampling condition. *Post hoc* paired *t*-tests confirmed shallower slopes in the absence of undersampling than when 1000 samplers were used ($t_{(8)} = 4.07$; $p < 0.01$), as well as shallower slopes when 1000 rather than 300 samplers were used ($t_{(8)} = 6.96$; $p < 0.001$).

Discussion

Stochastic Undersampling Impairs the Detection of Short Sounds, as Observed for Auditory Neuropathy Patients and Older Adults

We have shown that reducing the number of stochastic samplers leads to steeper threshold/duration functions with increased thresholds for the two shortest durations tested (5 and 10 ms). This result is consistent with the elevation of

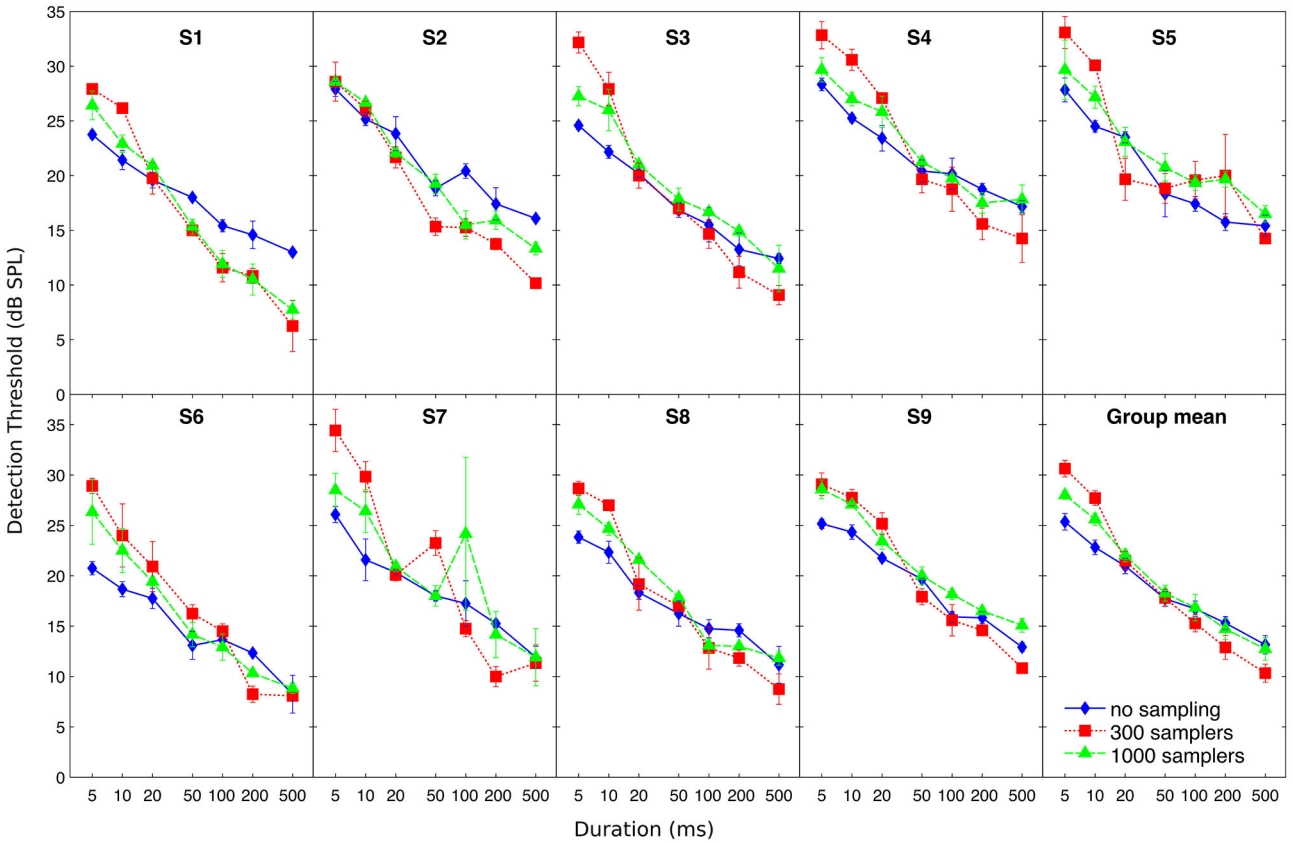

FIGURE 2 | Individual and mean detection thresholds as a function of stimulus duration. Different symbols illustrate detection thresholds for different undersampling conditions (no sampling, 300 samplers, and 1000 samplers), as indicated by the inset in the bottom-right panel. Error bars show ±1 standard error of the mean calculated over the three threshold estimates (for individual thresholds) or over the final individual threshold estimates (for the group mean).

detection thresholds for short sounds observed in patients diagnosed with auditory neuropathy (Starr et al., 1991; Zeng et al., 2005) and in older listeners with (near) normal audiometric thresholds (Fostick et al., 2013). Zeng et al. (2005) measured threshold/duration functions for broadband noise in a group of normal-hearing listeners and in a group of auditory neuropathy patients and found that the latter had elevated thresholds for stimuli with durations of 5 and 10 ms. The slopes of the threshold/duration functions were 1.3 times steeper for the patients than for the normal-hearing listeners (−3.9 vs. −3.0 dB per doubling duration); the same ratio observed here between slopes for the 1000-samplers and the no-undersampling conditions. The present results are also consistent with elevated detection thresholds observed for short 1-kHz tones in older listeners with audiometric thresholds in the normal range for their age (Fostick and Babkoff, 2013; Fostick et al., 2013). Listeners aged 61–82 years had thresholds for 15-ms tones that were 4.4 dB higher than listeners aged 21–40 years, even though the two groups had identical thresholds for 50-ms tones (Table 1 in Fostick and Babkoff, 2013).

Deafferentation, which comes with aging (Makary et al., 2011), could explain impaired short-tone detection in older listeners. One consequence of the stochastic nature of ANFs firing is that a loss of ANFs affects the representation of transient (short) waveforms more than sustained (long) waveforms. Thus, deafferentation may impair the detection of short sounds in a way perceptually similar to stochastic undersampling. Added to the finding of Lopez-Poveda and Barrios (2013) that stochastic undersampling leads to impaired intelligibility of speech in noise, the present results suggest that stochastic undersampling could be a common mechanism to explain how deafferentation results in impaired temporal processing and speech-in-noise intelligibility in older adults or in deafferented listeners with near normal audiometric thresholds. The present results also suggest that pure-tone audiometry for very short tones might be useful to assess the degree of deafferentation.

Implications for Mechanisms of Sound Detectability

The present results are of interest for understanding the mechanisms underlying the detectability of sounds with different durations. As explained in the Introduction, the classical theories of "temporal integration"—based on a long-term integration of intensity—would predict detection

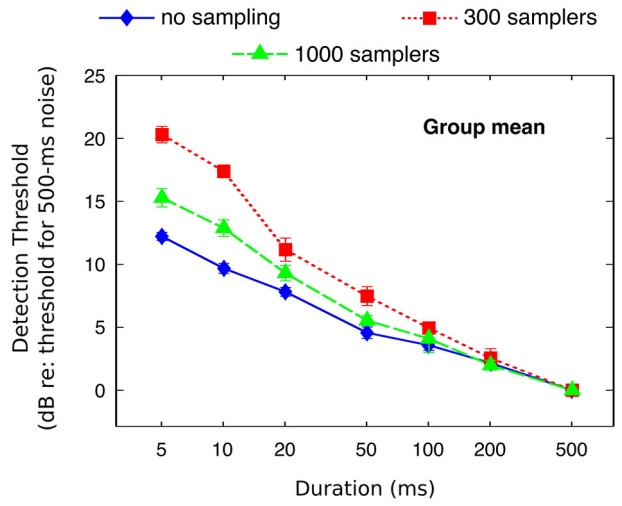

FIGURE 3 | Mean detection thresholds (from Figure 2) referenced to the thresholds for the 500-ms stimuli.

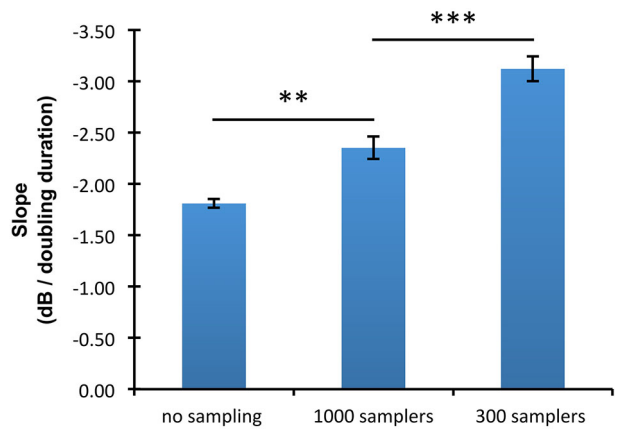

FIGURE 4 | Mean slopes of the threshold/duration functions in the three undersampling conditions (no sampling, 300 samplers, and 1000 samplers). Error bars show ±1 standard error of the mean calculated over the slopes estimated for each participant. Horizontal lines indicate the statistical comparisons made: two asterisks indicate a level of significance of $p < 0.01$, and three asterisks a level of significance of $p < 0.001$.

thresholds unaltered by stochastic undersampling because undersampled and non-processed stimuli were equated for rms amplitude. Instead, undersampling short stimuli (with 1000 or 300 stochastic samplers) increased detection thresholds, and undersampling long stimuli (with 300 samplers) decreased detection thresholds. Thus, the present results are not consistent with the classical theories of "temporal integration". The present results support instead the probabilistic theories of sound detectability (Meddis and Lecluyse, 2011; Heil et al., 2013a,b) that explain detection by a probability accumulation over time, with thresholds corresponding to a criterion number of detection events or to a single detection event.

Figure 5 illustrates how a probability accumulation of detection events could explain both the thresholds increase for short sounds and the thresholds decrease for long sounds. For short stimuli (5-ms stimuli on the top right panel), when plotting processed stimuli in the three sampling conditions and at the threshold level in the "no sampling" condition (25 dB SPL), it can be seen that processing with 1000 samplers kept very few samples, and that processing with 300 samplers removed all of the samples. If detectability depended on the occurrence of a criterion number of detection events, the limited number of samples in the two undersampled stimuli may not have been enough to trigger a criterion number of detection events. Thus, the limiting factor for detectability may have been the number of samples kept by the processing. Detectability in the two undersampled conditions was reached only at higher presentation levels, as higher intensities increase the probability of keeping any given sample, and hence increase the number of samples kept by the processing.

As explained in Sections Stochastic Undersampling Vocoder and Stimuli (and illustrated in **Figure 5**), stimuli of low intensities and short durations were sometimes left blank by the stochastic undersampling process. This phenomenon was expected and is a consequence of the decreasing probability for samplers to generate "spikes" in response to lower intensities and shorter stimuli. Indeed, blank stimuli (effectively silence tokens) may be thought of as conditions were the original stimulus was too weak to elicit a neural response. The use of blank stimuli during the adaptive procedure may have contributed to elevating thresholds. Using only three pre-generated stimuli per condition may have exaggerated this effect. To clarify the contribution of blank stimuli to the elevation of thresholds, **Figure 6** illustrates the actual levels ("output level") of the pre-generated stimuli as a function of their level before stochastic undersampling ("input level"), for the two shortest durations processed with 300 and 1000 stochastic samplers. Blank stimuli are also plotted as a function of "input level". The size of the symbols depicts the proportions of blank and non-blank stimuli, as indicated by the insets. Levels above 40 dB SPL were not plotted because none of the pre-generated stimuli was blank for those levels. It can be observed that blank stimuli were more frequent for lower intensities, for shorter durations, and when using 300 samplers. For the 300-samplers condition, blank stimuli were present within the range of individual threshold levels (shaded gray areas on **Figure 6**) and may have thus contributed to the observed elevation in threshold. On the other hand, for the 1000-samplers condition, blank stimuli were present only for levels about 10 dB or more below thresholds, hence their contribution to the thresholds elevation was probably negligible.

Contrary to short stimuli, detection of long (≥50 ms) stimuli was not limited by the number of samples since the easiest condition was the one with the fewest samples kept (i.e., thresholds were lowest in the 300-samplers condition). Instead, comparing on **Figure 5** (bottom right panel) the waveforms of long stimuli in the three sampling conditions suggests that their

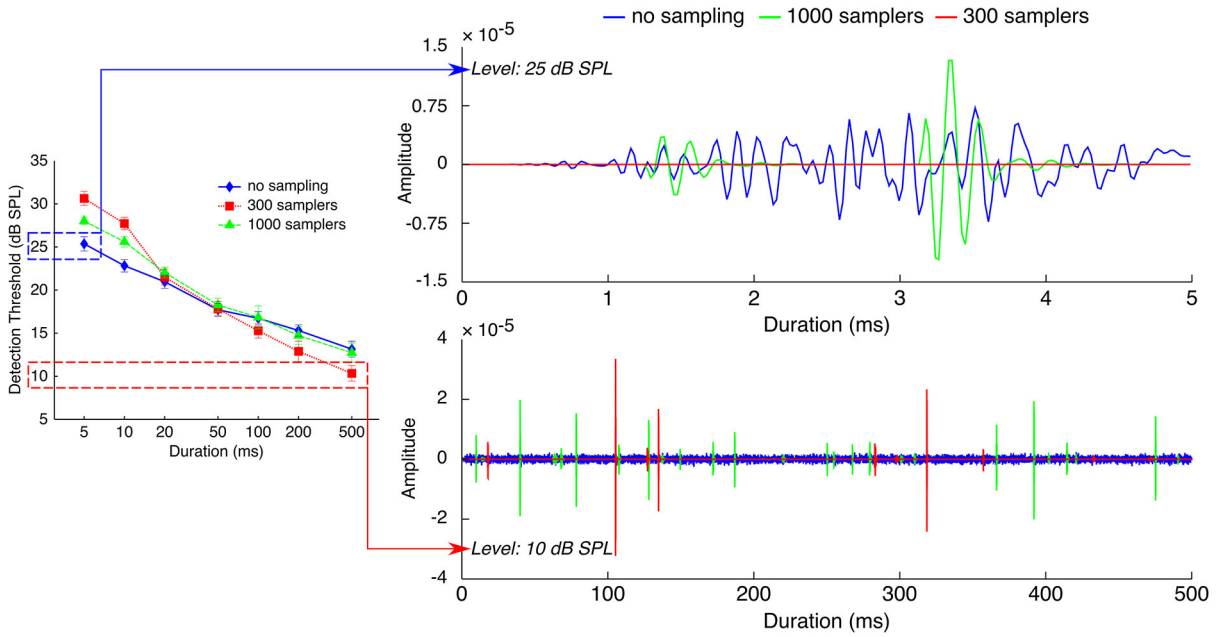

FIGURE 5 | Effects of stochastic undersampling on the waveforms of noise bursts with two different durations. **Top**. 5-ms noises at 25 dB SPL, the measured threshold level for the no-sampling condition. **Bottom**. 500-ms noises at 10 dB SPL, the measured threshold level for the 300-samplers condition. See Section Implications for Mechanisms of Sound Detectability for a description.

peak amplitudes may have been the limiting factor. The bottom right panel of **Figure 5** shows the waveforms of 500-ms stimuli in the three sampling conditions—all plotted at the threshold level of the 300-samplers condition (10 dB SPL). It can be seen that the 300-samplers condition was associated with larger peak amplitudes than the two other conditions. This is a result of the rms normalization: waveforms with fewer samples were scaled up to larger peak amplitudes to reach the rms amplitude of the control condition. Thus, a detection mechanism based on probability accumulation may have been more efficient in the 300-samplers condition because, at this low presentation level, only the larger peak amplitudes of the 300-samplers condition may have triggered detection events. In this view, the improvement of detection observed for long sounds would not be related to the stochastic undersampling *per se* but would be a side effect of the rms equalization.

Limitations of the Present Model

The present results appear inconsistent with the findings of physiological studies on the effects of noise-induced deafferentation in rodents (Kujawa and Liberman, 2009; Lin et al., 2011; Furman et al., 2013). The present stochastic undersampling model predicts that the neural representation of low intensities will be more degraded than the neural representation of high intensities. In the aforementioned studies, by contrast, ABR thresholds recovered quickly after noise exposure while supra-threshold neural amplitudes were permanently reduced. ABR thresholds are independent from stimulus duration and are similar in magnitude to behavioral thresholds for short sounds (Gorga et al., 1984). Hence, the recovery of ABR thresholds after deafferentation appears inconsistent with the threshold elevation for short sounds reported here. This inconsistency, however, may be more apparent than real. Lin et al. (2011), p. 614, discussed that deafferentation likely elicited a small threshold elevation (<5 dB) that could not be seen because of the 5-dB step size used to measure ABR thresholds, because of the number of ears tested, and because of the variance in ABR amplitudes. Indeed, ABRs thresholds in Figure 1A of Furman et al. (2013) were slightly elevated (5–10 dB) at frequencies corresponding to the octave-band noise (4–8 kHz) used to cause deafferentation. The mean threshold elevations observed here for 5-ms stimuli were +2.6 dB when using 1000 samplers and +5.3 dB when using 300 samplers, relative to thresholds in the no sampling condition (**Figure 2**). Hence, the increase of thresholds for short sounds elicited by stochastic undersampling in the present study is not inconsistent with the aforementioned physiological studies.

Both the recovery of ABR thresholds and the reduction of neural amplitudes at supra-threshold intensities in the aforementioned physiological studies have been accounted for by a loss of low- and medium-SR fibers, which only discharge at medium and high intensities. This points to a limitation of the present study, namely that the vocoder used here and in Lopez-Poveda and Barrios (2013) does not simulate different types of fibers. The vocoder as currently implemented may thus be unable to simulate the shallower growth of ABR wave I with increasing level reported in previous studies (Kujawa and Liberman, 2009; Lin et al., 2011; Furman et al., 2013). This, however, is not a limitation of the stochastic undersampling principle *per se*.

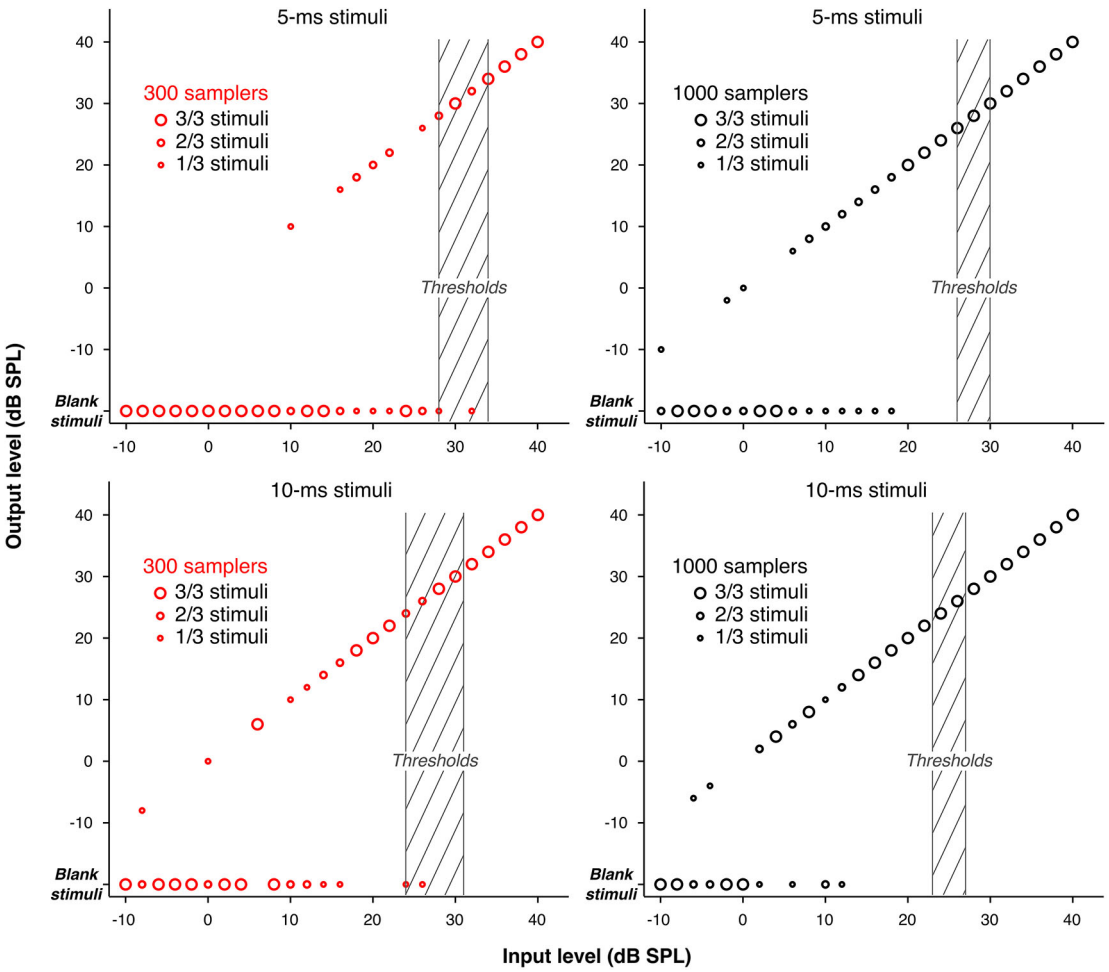

FIGURE 6 | Input/Output functions showing the actual levels of the pre-generated stimuli ("output level") as a function of their level before stochastic undersampling ("input level"), for the two shortest durations (5 and 10 ms), processed with 300 and 1000 stochastic samplers. Blank stimuli are also shown. The size of the circles marking the data points varies to indicate the proportions of blank and non-blank stimuli (either 1, 2, or 3 out of the 3 pre-generated stimuli) for each level. Levels above 40 dB SPL are not plotted because none of the stimuli pre-generated for those levels was blank. The shaded areas indicate the ranges of detection thresholds across participants.

Future work will investigate whether implementing the three ANFs types in the vocoder changes the results of the present study.

Slightly elevated detection thresholds would be compatible with the aforementioned physiological studies if a fraction of the fibers deafferented in those studies were high-SR fibers. Figures given in Furman et al. (2013) suggest that this may have been the case. Furman et al. (2013) estimated that low- and medium-SR fibers represented 47% of the ANFs in control ears and 29% of the "surviving" ANFs in noise-exposed ears (p. 580). The total neural loss after noise exposure was roughly 40% (p. 583, hence "surviving" rate = ∼60%). From these figures we can infer the following: (1) a control population of M fibers had $0.47 \times M$ low- and medium-SR fibers; (2) after noise exposure, the total number of fibers lost was $0.40 \times M$; and (3) after noise exposure, the remaining number of low- and medium-SR fibers was $0.29 \times (0.60 \times M)$. Thus, the proportion of ANFs lost that were low- or medium-SR ANFs can be estimated as $(0.47 \times M - 0.29 \times 0.60 \times M)/(0.40 \times M) = 0.74$. This suggests that deafferentation can be associated with a comparatively less but still substantial loss of high-SR fibers (26%), and thus that threshold elevation can be caused by deafferentation if the degree of deafferentation is sufficient.

In that respect, it may be noted that the (arbitrarily chosen) number of samplers used in the present study might have simulated a greater amount of deafferentation than observed in noise-exposure studies (Kujawa and Liberman, 2009; Lin et al., 2011; Furman et al., 2013) and age-related deafferentation studies (Makary et al., 2011; Sergeyenko et al., 2013). The 300- and 1000-samplers conditions corresponded to 3000 and 10000 simulated ANFs when summed across the ten vocoding channels, which spanned 100–10000 Hz. The 100–10000-Hz frequency range can be estimated to cover 77% of the length of the basilar membrane (BM) using the almost-exponential frequency-position function of Greenwood (1990) (with parameters set so that the full BM length span 20–20000 Hz). Given that the

density of inner hair cell (IHC) ribbon synapses is an inverted U-shaped function of the BM length peaking at 50% of the BM (Meyer et al., 2009), a BM section with a length of 77% the total BM length should encompass more than 77% of the total number of IHC ribbon synapses. Hence the 100–10000-Hz frequency range should correspond to at least 27000 ANFs in a non-deafferented ear (over a total of roughly 35000 ANFs; Miura et al., 2002), and the 300- and 1000-samplers conditions of the present study can be estimated to represent deafferentation rates of more than ∼90% and 60% respectively. In noise-exposure studies, the deafferentation was estimated to be ∼40% (Furman et al., 2013) and 50% (Kujawa and Liberman, 2009; Lin et al., 2011). Makary et al. (2011) reported a 30% loss of spiral ganglion cells in human temporal bones aged 91–100 years with no hair cells loss, and Sergeyenko et al. (2013) observed in mice that age-related cochlear synaptic degeneration (as indexed by presynaptic ribbons counts in IHC, their Figure 5C) was ∼10% larger than the loss of spiral ganglion cells. Hence age-related deafferentation would appear to be capped at ∼40%. Even considering that noise-related and age-related deafferentation would add up in real life, stochastic undersampling in the present study (and especially the 300-samplers condition) may have overestimated the amount of "ecological" age- and noise-related deafferentation.

Stochastic Undersampling as a Mechanism for Age-Related Degradation of Temporal Processing

The present results support stochastic undersampling as a valid signal-processing analogy to explain the deteriorating effect of deafferentation on temporal processing. As deafferentation is associated with aging (Makary et al., 2011; Sergeyenko et al., 2013), and as aging is associated with temporal processing difficulties even in the absence of audiometric loss (CHABA, 1988; Fitzgibbons and Gordon-Salant, 2010; Lopez-Poveda, 2014), the present results also argue that stochastic undersampling could explain age-related temporal processing deficits.

Evidence for auditory deficits related to age *per se* is difficult to obtain in humans as older listeners most often have some degree of cochlear hearing loss that acts as a confounding variable (Tremblay and Burkard, 2007; Fitzgibbons and Gordon-Salant, 2010). Interestingly, steeper threshold/duration functions as observed in the present study are the opposite result to what is usually observed in patients with cochlear (mechanical) hearing loss. Patients with cochlear hearing loss usually show elevated detection thresholds for all sound durations, with the elevation being larger for longer durations, resulting in shallower threshold/duration functions than normal-hearing listeners (Florentine et al., 1988; Gerken et al., 1990; Plack and Skeels, 2007). The larger threshold increase for longer durations has been explained by an increase of the "absolute" sensory threshold, i.e., the minimum sound level below which not a single stochastic detection event is generated (Neubauer and Heil, 2004; Meddis and Lecluyse, 2011). The present results, together with the previous finding of elevated detection thresholds for short but not long sounds in older adults with age-corrected normal audiometric thresholds (Fostick and Babkoff, 2013; Fostick et al., 2013), suggest that brief tone audiometry could potentially be useful when trying to disentangle the effects of age *per se* from the effects of age-related cochlear hearing loss. One known limitation to the use of brief tone audiometry is the large variability between listeners (Olsen, 1987). Conflicting effects of age *per se* and of age-related cochlear hearing loss on the threshold/duration functions of older listeners may explain a part of this variability. Combining brief tone audiometry with measures of cochlear hearing loss—such as standard audiometry, audiometry in threshold-equalizing noise (Moore et al., 2000), distortion product otoacoustic emission (Dorn et al., 2001; Lopez-Poveda et al., 2009), or temporal-masking curves (Nelson et al., 2001; Lopez-Poveda and Johannesen, 2012)—might help isolate the "deafferentation component" of hearing deficits in older listeners.

It should be stressed that the stochastic undersampling analogy was not conceived as a model of the physiological response of deafferented auditory nerves. Instead, it was meant to simulate a reduction of information in the nerve on the basis of the stochastic firing properties of neurons. However, stochastic undersampling in the nerve is not the only possible explanation for impaired temporal processing. Zeng et al. (2005) argued that the degraded temporal processing of auditory neuropathy patients could be explained by reduced synchronization between ANF responses or by deafferentation. Pichora-Fuller et al. (2007) found that simulating desynchronization by jittering the frequency components of speech stimuli could explain the poorer speech-in-noise intelligibility of older listeners with normal audiometric thresholds. Stochastic undersampling and deafferentation, however, offer a more parsimonious explanation than desynchronization because they do not postulate changes in the temporal properties of individual ANFs. In other words, according to the stochastic undersampling view, older adults may not have a "slower-than-normal" auditory processing but, more simply, they would have fewer functional ANFs.

A loss of functional ANFs appears early in the aging process as a consequence of cochlear synaptopathy (Sergeyenko et al., 2013). Age-related alterations in the auditory system cannot, however, be reduced to deafferentation. For example, age-related auditory deficits have been associated with alterations of the cochlear lateral wall that lead to a reduction of the endocochlear potential (Schmiedt, 2010) and hence to IHC and outer hair cell (OHC) dysfunction (Meddis et al., 2013; Saremi and Stenfelt, 2013). Stochastic undersampling may be used to simulate this and other pathologies. Indeed, stochastic undersampling can occur either by reducing the number of samplers (deafferentation) or by reducing the individual probability of firing of (sub)populations of samplers (ANFs) (Lopez-Poveda, 2014). Any alteration of the ear that would result in reduced probabilities of neural firing would also result in some samples of the stimulus waveform not being encoded in the auditory nerve, hence in a form of stochastic undersampling not related to deafferentation. Future work with vocoder implementations that include "abnormal" firing probabilities for the three types of ANFs may provide a way to study the effects

of various age-related auditory alterations independently. For example, OHC dysfunction would reduce auditory sensitivity to soft sounds and might be studied by reducing the probability of firing of high-spontaneous rate fibers, whereas deafferentation should be implemented as a reduction in the number of fibers, particularly of those with low- and medium-spontaneous rates. Age-related auditory deficits have also been associated with alterations central to the auditory nerve. For example, aging comes with a progressive weakening of GABAergic systems (i.e., reduced inhibitory neurotransmission) throughout the central auditory system (Canlon et al., 2010), which may at least partly result from a progressive deafferentation (Caspary et al., 1995). Deafferentation central to the auditory nerve has also been suggested by ABR data showing an age-related amplitude reduction of wave III apparent even after controlling for cochlear and auditory nerve changes reflected in wave I amplitude (Konrad-Martin et al., 2012). The stochastic undersampling analogy may thus be used also to study age-related neural alterations central to the auditory nerve, by using probability-intensity functions characteristic of central neurons instead of functions characteristic of ANFs.

Conclusions

1. Stochastic undersampling impairs the detection of short (<20 ms) sounds, consistently with the impairments observed in auditory neuropathy patients and in older listeners with (near) normal audiometric thresholds.
2. Insofar as deafferentation can produce stochastic undersampling and deafferentation comes with aging, the present results suggest that some of the temporal processing deficits of older adults could be due to deafferentation.
3. The present results suggest that deafferentation might be diagnosed using pure-tone audiometry with short tones.
4. Stochastic undersampling, as implemented here, impaired the detection of short sounds and, in certain conditions, improved the detection of long sounds. As rms amplitudes were equalized across undersampling conditions, the present results are not consistent with theories of detectability based on the integration of energy over the stimulus duration (the seminal temporal integration theory). Instead, the present results support probabilistic theories of detectability.

Acknowledgments

We thank Ray Meddis for insightful discussions, and Peter Heil and the two reviewers for helpful suggestions. This work was supported by the Spanish Ministry of Economy and Competitiveness (BFU2012-39544-C02).

References

American National Standards Institute. (2004). ANSI/ASA S3.21–2004: methods for manual pure tone threshold audiometry.

Canlon, B., Illing, R. B., and Walton, J. (2010). "Cell biology and physiology of the aging central auditory pathway," in *The Aging Auditory System*, eds S. Gordon-Salant, R. D. Frisina, A. N. Popper, and R. R. Fay (New York: Springer), 39–74.

Caspary, D. M., Milbrandt, J. C., and Helfert, R. H. (1995). Central auditory aging: GABA changes in the inferior colliculus. *Exp. Gerontol.* 30, 349–360. doi: 10.1016/0531-5565(94)00052-5

CHABA. (1988). Speech understanding and aging. *J. Acoust. Soc. Am.* 83, 859–895.

Dorn, P. A., Konrad-Martin, D., Neely, S. T., Keefe, D. H., Cyr, E., and Gorga, M. P. (2001). Distortion product otoacoustic emission input/output functions in normal hearing and hearing impaired human ears. *J. Acoust. Soc. Am.* 110, 3119–3131. doi: 10.1121/1.1417524

Fitzgibbons, P. J., and Gordon-Salant, S. (2010). "Behavioral studies with aging humans: hearing sensitivity and psychoacoustics," in *The Aging Auditory System*, eds S. Gordon-Salant, R. D. Frisina, A. N. Popper, and R. R. Fay (New York: Springer), 111–134.

Florentine, M., Fastl, H., and Buss, S. (1988). Temporal integration in normal hearing, cochlear impairment and impairment simulated by masking. *J. Acoust. Soc. Am.* 84, 195–203. doi: 10.1121/1.396964

Fostick, L., and Babkoff, H. (2013). Temporal and non-temporal processes in the elderly. *J. Basic Clin. Physiol. Pharmacol.* 24, 191–199. doi: 10.1515/jbcpp-2013-0049

Fostick, L., Ben-Artzi, E., and Babkoff, H. (2013). Aging and speech perception among the elderly: beyond hearing threshold and cognitive ability. *J. Basic Clin. Physiol. Pharmacol.* 24, 175–183. doi: 10.1515/jbcpp-2013-0048

Furman, A. C., Kujawa, S. G., and Liberman, M. C. (2013). Noise-induced cochlear neuropathy is selective for fibers with low spontaneous rates. *J. Neurophysiol.* 110, 577–586. doi: 10.1152/jn.00164.2013

Garner, W. R., and Miller, G. A. (1947). The masked threshold of pure tones as a function of duration. *J. Exp. Psychol.* 37, 293–303. doi: 10.1037/h0055734

Gerken, G. M., Bhat, V. K. H., and Hutchison-Clutter, M. (1990). Auditory temporal integration and the power function model. *J. Acoust. Soc. Am.* 88, 767–778. doi: 10.1121/1.399726

Gorga, M. P., Beauchaine, K. A., Reiland, J. K., Worthington, D. W., and Javel, E. (1984). Effects of stimulus duration on ABR thresholds and on behavioral thresholds. *J. Acoust. Soc. Am.* 76, 616–619. doi: 10.1121/1.391158

Green, D. M., Birdsall, T. G., and Tanner, W. P. (1957). Signal detection as a function of signal intensity and duration. *J. Acoust. Soc. Am.* 29, 523–531. doi: 10.1121/1.1908951

Greenwood, D. D. (1990). A cochlear frequency-position function for several species—29 years later. *J. Acoust. Soc. Am.* 87, 2592–2605. doi: 10.1121/1.399052

Heil, P., and Neubauer, H. (2003). A unifying basis of auditory thresholds based on temporal summation. *Proc. Natl. Acad. Sci. U S A* 100, 6151–6156. doi: 10.1073/pnas.1030017100

Heil, P., Neubauer, H., Brown, M., and Irvine, D. R. F. (2008). Towards a unifying basis of auditory thresholds: distributions of the first spikes latencies of auditory-nerve fibers. *Hear. Res.* 238, 25–38. doi: 10.1016/j.heares.2007.09.014

Heil, P., Neubauer, H., and Irvine, D. R. F. (2011). An improved model for the rate-level functions of auditory-nerve fibers. *J. Neurosci.* 31, 15424–15437. doi: 10.1523/JNEUROSCI.1638-11.2011

Heil, P., Neubauer, H., Tetschke, M., and Irvine, D. R. F. (2013a). A probabilistic model of absolute auditory thresholds and its possible physiological basis. *Adv. Exp. Med. Biol.* 787, 21–29. doi: 10.1007/978-1-4614-1590-9_3

Heil, P., Verhey, J. L., and Zoefel, B. (2013b). Modelling detection thresholds for sounds repeated at different delays. *Hear. Res.* 296, 83–95. doi: 10.1016/j.heares.2012.12.002

Hughes, J. W. (1946). The threshold of audition for short periods of stimulation. *Proc. R. Soc. Med.* 133, 486–490. doi: 10.1098/rspb.1946.0026

Humes, L. E., and Dubno, J. R. (2010). "Behavioral studies with aging humans: hearing sensitivity and psychoacoustics," in *The Aging Auditory System*, eds S. Gordon-Salant, R. D. Frisina, A. N. Popper, and R. R. Fay (New York: Springer), 111–134.

King, P. F. (1954). Psychogenic deafness. *J. Laryngol. Otol.* 68, 623–635. doi: 10.1017/S0022215100050052

Konrad-Martin, D., Dille, M. F., McMillan, G., Griest, S., McDermott, D., Fausti, S. A., et al. (2012). Age-related changes in the auditory brainstem response. *J. Am. Acad. Audiol.* 23, 18–35. doi: 10.3766/jaaa.23.1.3

Kopetzky, S. J. (1948). *Deafness, Tinnitus and Vertigo.* New York, NY: Nelson.

Kraus, N., Bradlow, A. R., Cheatham, M. A., Cunningham, J., King, C. D., Koch, D. B., et al. (2000). Consequences of neural synchrony: a case of auditory neuropathy. *J. Assoc. Res. Otolaryngol.* 1, 33–45. doi: 10.1007/s101620010004

Kujawa, S. G., and Liberman, M. C. (2009). Adding insult to injury: cochlear nerve degeneration after "temporary" noise-induced hearing loss. *J. Neurosci.* 29, 14077–14085. doi: 10.1523/JNEUROSCI.2845-09.2009

Levitt, H. (1971). Transformed up-down methods in psychoacoustics. *J. Acoust. Soc. Am.* 49, 467–477. doi: 10.1121/1.1912375

Lin, H. W., Furman, A. C., Kujawa, S. G., and Liberman, M. C. (2011). Primary neural degeneration in the Guinea pig cochlea after reversible noise-induced threshold shift. *J. Assoc. Res. Otolaryngol.* 12, 605–616. doi: 10.1007/s10162-011-0277-0

Lopez-Poveda, E. A. (2014). Why do I hear but not understand? Stochastic undersampling as a model of degraded neural encoding of speech. *Front. Neurosci.* 8:348. doi: 10.3389/fnins.2014.00348

Lopez-Poveda, E. A., and Barrios, P. (2013). Perception of stochastically undersampled sound waveforms: a model of auditory deafferentation. *Front. Neurosci.* 7:124. doi: 10.3389/fnins.2013.00124

Lopez-Poveda, E. A., and Johannesen, P. T. (2012). Behavioral estimates of the contribution of inner and outer hair cell dysfunction to individualized audiometric loss. *J. Assoc. Res. Otolaryngol.* 13, 485–504. doi: 10.1007/s10162-012-0327-2

Lopez-Poveda, E. A., Johannesen, P. T., and Merchán, M. A. (2009). Estimation of the degree of inner and outer hair cell dysfunction from distortion product otoacoustic emission input/output functions. *Audiolog. Med.* 7, 22–28. doi: 10.1080/16513860802622491

Makary, C. A., Shin, J., Kujawa, S. G., Liberman, M. C., and Merchant, S. N. (2011). Age-related primary cochlear neuronal degeneration in human temporal bones. *J. Assoc. Res. Otolaryngol.* 12, 711–717. doi: 10.1007/s10162-011-0283-2

Meddis, R., and Lecluyse, W. (2011). The psychophysics of absolute threshold and signal duration: a probabilistic approach. *J. Acoust. Soc. Am.* 129, 3153–3165. doi: 10.1121/1.3569712

Meddis, R., Lecluyse, W., Clark, N. R., Jürgens, T., Tan, C. M., Panda, M. R., et al. (2013). A computer model of the auditory periphery and its application to the study of hearing. *Adv. Exp. Med. Biol.* 787, 11–19; discussion 19–20. doi: 10.1007/978-1-4614-1590-9_2

Meyer, A. C., Frank, T., Khimich, D., Hoch, G., Riedel, D., Chapochnikov, N. M., et al. (2009). Tuning of synapse number, structure and function in the cochlea. *Nat. Neurosci.* 12, 444–453. doi: 10.1038/nn.2293

Miura, M., Sando, I., Hirsch, B. E., and Orita, Y. (2002). Analysis of spiral ganglion cell populations in children with normal and pathological ears. *Ann. Otol. Rhinol. Laryngol.* 111, 1059–1065. doi: 10.1177/000348940211101201

Moore, B. C. J., Huss, M., Vickers, D. A., Glasberg, B. R., and Alcántara, J. I. (2000). A test for the diagnosis of dead regions in the cochlea. *Br. J. Audiol.* 34, 205–224. doi: 10.3109/03005364000000131

Nelson, D. A., Schroder, A. C., and Wojtczak, M. (2001). A new procedure for measuring peripheral compression in normal-hearing and hearing-impaired listeners. *J. Acoust. Soc. Am.* 110, 2045–2064. doi: 10.1121/1.1404439

Neubauer, H., and Heil, P. (2004). Towards a unifying basis of auditory thresholds: the effects of hearing loss on temporal integration reconsidered. *J. Assoc. Res. Otolaryngol.* 5, 436–458. doi: 10.1007/s10162-004-5031-4

Olsen, W. O. (1987). Brief tone audiometry: a review. *Ear Hear.* 8, 13S–18S. doi: 10.1097/00003446-198708001-00005

Pichora-Fuller, M. K., and MacDonald, E. (2008). "Auditory temporal processing deficits in older listeners: a review and overview," in *Auditory signal processing in hearing-impaired listeners: Proceedings of the First International Symposium on Audiological and Auditory Research (ISAAR 2007)*, eds T. Dau, J. Buchholz, J. Harte, and T. Christiansen (Denmark: Centertryk A/S), 297–306.

Pichora-Fuller, M. K., Schneider, B. A., MacDonald, E., Pass, H. E., and Brown, S. (2007). Temporal jitter disrupts speech intelligibility: a simulation of auditory aging. *Hear. Res.* 223, 114–121. doi: 10.1016/j.heares.2006.10.009

Plack, C. J., Barker, D., and Prendergast, G. (2014). Perceptual consequences of "hidden" hearing loss. *Trends Hear.* 18:2331216514550621. doi: 10.1177/2331216514550621

Plack, C. J., and Skeels, V. (2007). Temporal integration and compression near absolute threshold in normal and impaired ears. *J. Acoust. Soc. Am.* 122, 2236–2244. doi: 10.1121/1.2769829

Plomp, R., and Bouman, M. A. (1959). Relation between hearing threshold and duration for tone pulses. *J. Acoust. Soc. Am.* 31, 749–758. doi: 10.1121/1.1907781

Sachs, M. B., and Abbas, P. J. (1974). Rate versus level functions for auditory nerve fibers in cats: tone-burst stimuli. *J. Acoust. Soc. Am.* 56, 1835–1847. doi: 10.1121/1.1903521

Saremi, A., and Stenfelt, S. (2013). Effect of metabolic presbyacusis on cochlear responses: a simulation approach using a physiologically-based model. *J. Acoust. Soc. Am.* 134, 2833–2851. doi: 10.1121/1.4820788

Schaette, R., and McAlpine, D. (2011). Tinnitus with a normal audiogram: physiological evidence for hidden hearing loss and computational model. *J. Neurosci.* 31, 13452–13457. doi: 10.1523/JNEUROSCI.2156-11.2011

Schmiedt, R. A. (2010). "The physiology of cochlear presbycusis," in *The Aging Auditory System*, eds S. Gordon-Salant, R. D. Frisina, A. N. Popper, and R. R. Fay (New York: Springer), 9–38.

Sergeyenko, Y., Lall, K., Liberman, M. C., and Kujawa, S. G. (2013). Age-related cochlear synaptopathy: an early-onset contributor to auditory functional decline. *J. Neurosci.* 33, 13686–13694. doi: 10.1523/JNEUROSCI.1783-13.2013

Starr, A. (2009). "Hearing and auditory neuropathy: lessons from patients, physiology and genetics," in *Neuropathies of the Auditory and Vestibular Eighth Cranial Nerves*, eds K. Kaga and A. Starr (Tokyo: Springer Japan), 3–9.

Starr, A., McPherson, D., Patterson, J., Don, M., Luxford, W., Shannon, R., et al. (1991). Absence of both auditory evoked potentials and auditory percepts dependent on timing cues. *Brain* 114, 1157–1180. doi: 10.1093/brain/114.3.1157

Stevens, H. E., and Wickesberg, R. E. (1999). Ensemble responses of the auditory nerve to normal and whispered stop consonants. *Hear. Res.* 131, 47–62. doi: 10.1016/s0378-5955(99)00014-3

Stevens, H. E., and Wickesberg, R. E. (2002). Representation of whispered word-final stop consonants in the auditory nerve. *Hear. Res.* 173, 119–133. doi: 10.1016/s0378-5955(02)00608-1

Tremblay, K. L., and Burkard, R. (2007). "Aging and auditory evoked potentials," in *Auditory Evoked Potentials: Scientific bases to Clinical Application*, eds R. Burkard, M. Don, and J. Eggermont (Baltimore: Lippincott Williams and Wilkins), 403–425.

Viemeister, N. F., and Wakefield, G. H. (1991). Temporal integration and multiple looks. *J. Acoust. Soc. Am.* 90, 858–865. doi: 10.1121/1.401953

Wever, E. G. (1949). *Theory of Hearing.* New York: Wiley.

Zeng, F. G., Kong, Y. Y., Michalewski, H. J., and Starr, A. (2005). Perceptual consequences of disrupted auditory nerve activity. *J. Neurophysiol.* 93, 3050–3063. doi: 10.1152/jn.00985.2004

Zeng, F. G., and Liu, S. (2006). Speech perception in individuals with auditory neuropathy. *J. Speech Lang. Hear. Res.* 49, 367–380. doi: 10.1044/1092-4388(2006/029)

Zeng, F. G., Oba, S., Garde, S., Sininger, Y., and Starr, A. (1999). Temporal and speech processing deficits in auditory neuropathy. *Neuroreport* 10, 3429–3435. doi: 10.1097/00001756-199911080-00031

Zhao, F., and Stephens, D. (2007). A critical review of King- Kopetzky syndrome: hearing difficulties, but normal hearing? *Audiolog. Med.* 5, 119–125. doi: 10.1080/16513860701296421

Conflict of Interest Statement: The authors declare that the research was conducted in the absence of any commercial or financial relationships that could be construed as a potential conflict of interest.

frontiers in
AGING NEUROSCIENCE

ORIGINAL RESEARCH ARTICLE
published: 16 February 2015
doi: 10.3389/fnagi.2015.00007

Swept-sine noise-induced damage as a hearing loss model for preclinical assays

Lorena Sanz[1,2,3†], Silvia Murillo-Cuesta[1,2,4*†], Pedro Cobo[5†], Rafael Cediel-Algovia[1,2,6], Julio Contreras[1,2,6], Teresa Rivera[1,2,3], Isabel Varela-Nieto[1,2,4†] and Carlos Avendaño[4,7†]

[1] Institute for Biomedical Research "Alberto Sols" (IIBM), Spanish National Research Council–Autonomous University of Madrid (CSIC-UAM), Madrid, Spain
[2] Centre for Biomedical Network Research (CIBER), Institute of Health Carlos III (ISCIII), Madrid, Spain
[3] Príncipe de Asturias University Hospital, University of Alcalá, Alcalá de Henares, Madrid, Spain
[4] Hospital La Paz Institute for Health Research (IdiPAZ), Madrid, Spain
[5] Institute for Physical and Information Technologies (ITEFI), Spanish National Research Council (CSIC), Madrid, Spain
[6] Veterinary Faculty, Complutense University of Madrid, Madrid, Spain
[7] Department of Anatomy, Histology and Neuroscience, Medical School, Autónoma University of Madrid, Madrid, Spain

Edited by:
Rodrigo Orlando Kuljiš, Zdrav Mozak Limitada, Chile
Gemma Casadesus, Case Western Reserve University, USA

Reviewed by:
Miguel A. Merchán, University of Salamanca, Spain
Jiri Popelar, Institute of Experimental Medicine AS CR, Czech Republic

***Correspondence:**
Silvia Murillo-Cuesta, Institute for Biomedical Research "Alberto Sols" (IIBM), Spanish National Research Council–Autonomous University of Madrid (CSIC-UAM), Arturo Duperier 4, 28029 Madrid, Spain
e-mail: smurillo@iib.uam.es

[†] *These authors have contributed equally to this work.*

Mouse models are key tools for studying cochlear alterations in noise-induced hearing loss (NIHL) and for evaluating new therapies. Stimuli used to induce deafness in mice are usually white and octave band noises that include very low frequencies, considering the large mouse auditory range. We designed different sound stimuli, enriched in frequencies up to 20 kHz ("violet" noises) to examine their impact on hearing thresholds and cochlear cytoarchitecture after short exposure. In addition, we developed a cytocochleogram to quantitatively assess the ensuing structural degeneration and its functional correlation. Finally, we used this mouse model and cochleogram procedure to evaluate the potential therapeutic effect of transforming growth factor β1 (TGF-β1) inhibitors P17 and P144 on NIHL. CBA mice were exposed to violet swept-sine noise (VS) with different frequency ranges (2–20 or 9–13 kHz) and levels (105 or 120 dB SPL) for 30 min. Mice were evaluated by auditory brainstem response (ABR) and otoacoustic emission tests prior to and 2, 14 and 28 days after noise exposure. Cochlear pathology was assessed with gross histology; hair cell number was estimated by a stereological counting method. Our results indicate that functional and morphological changes induced by VS depend on the sound level and frequency composition. Partial hearing recovery followed the exposure to 105 dB SPL, whereas permanent cochlear damage resulted from the exposure to 120 dB SPL. Exposure to 9–13 kHz noise caused an auditory threshold shift (TS) in those frequencies that correlated with hair cell loss in the corresponding areas of the cochlea that were spotted on the cytocochleogram. In summary, we present mouse models of NIHL, which depending on the sound properties of the noise, cause different degrees of cochlear damage, and could therefore be used to study molecules which are potential players in hearing loss protection and repair.

Keywords: cytocochleogram, hair cells, hearing loss, transtympanic, TGF-β inhibition, violet noise

INTRODUCTION

Noise-induced hearing loss (NIHL) is the most common form of acquired deafness in developed countries and therefore it is a public health priority (Sliwinska-Kowalska and Davis, 2012). Hearing impairment may be induced by a single impulsive noise or after repetitive exposure to moderate or high intensity noise (Kirchner et al., 2012). The cumulative damaging effects on the inner ear depend on the noise characteristics (frequency, level), chronicity and individual susceptibility to noise (Konings et al., 2009; Le Prell, 2012). Inner and particularly outer hair cells (IHC and OHC, respectively) especially those located in the basal turn of the cochlea in mammals, are very sensitive to noise damage. Thus, the disruption of stereocilia leads to a severe alteration in HC structural integrity that has been correlated to permanent threshold shifts (TS) in many species (Hamernik and Qiu, 2000; Chen and Fechter, 2003; Chen et al., 2003; Hu et al., 2006; Bohne et al., 2007; Harding and Bohne, 2009).

Mice models are essential tools for studying the pathophysiology of NIHL and for evaluating new potential therapies (Ohlemiller, 2006; Park et al., 2013). As reported in human cases, functional and structural alterations depend on noise level and duration of exposure, and also on strain susceptibility. Thus, C57BL/6 and BALB/c mice are particularly

Abbreviations: ABR, auditory brainstem responses; BM, basilar membrane; DPOAE, distortion product otoacoustic emissions; IHC, inner hair cell; NIHL, noise-induced hearing loss; OC, organ of Corti; OHC, outer hair cell; TS, threshold shift; V, violet noise; VS, violet swept-sine noise.

vulnerable to noise, whereas CBA/Ca mice appear to be more resistant (Ohlemiller et al., 2000, 2011; Ou et al., 2000a; Gratton et al., 2011). There are many reports on the functional and morphological characterization of different NIHL mouse models in which mice are usually exposed for a few (1–4) hours to high intensity (95–120 dB SPL) white or octave band noises, usually centered on low frequencies up to 10 kHz (Park et al., 2013). These frequencies are in the lowest frequency range of the mouse hearing spectrum (Greenwood, 1996). Exposures to noise over 10 kHz are much less frequent (i.e., 8–16 kHz in Kujawa and Liberman, 2009; 4–45 kHz in Ohlemiller et al., 2011). In this work we generated NIHL by short exposure to "violet" swept-sine noise (VS), a 10 s linear sweep in frequencies from 2 kHz to 20 kHz designed with high-pass filtering and linear with frequency gain (Cobo et al., 2009). Additionally VS noise with frequencies from just 9 to 13 kHz was used to injure a specific stretch of the basilar membrane (BM). To illustrate and quantify the distribution of HC along the length of the cochlea under the different conditions used, a cytocochleogram was performed, applying a stereological approach to previously published procedures (Ou et al., 2000b; Viberg and Canlon, 2004; Müller and Smolders, 2005; Müller et al., 2005; Boyce et al., 2010).

Here we describe the functional and morphological consequences, and their correlation, of exposure to VS noises of different sound levels and frequency ranges. We found that the characteristics of the VS noise determine the pattern of hair cell density along the cochlea and, accordingly, the ABR electrophysiological response. Therefore, the study of NIHL and of potential prevention and repair therapies could be further improved by refining the design of noise stimuli in experimental models. Furthermore, we tested the local actions of two peptides P17 or P144 inhibitors of transforming growth factor beta 1 (TGF-β1) to repair NIHL. TGF-β1 is a cytokine involved in the cochlear inflammatory response that is released early after cochlear injury caused by aminoglycoside (Wissel et al., 2006), antigens (Satoh et al., 2006), otitis media (Ghaheri et al., 2007) and noise exposure (Murillo-Cuesta et al., submitted). Our functional and cochleogram data indicated that a single local administration of either peptide did not exert a therapeutic effect on NIHL.

MATERIALS AND METHODS

MOUSE HOUSING AND HANDLING

The study was carried out on 2 month old male mice from CBA/CaOlaHsd (CBA) and C57BL/6JOlaHsd (C57) strains (Harlan Laboratories). Patterns of cochlear damage after noise exposure in these strains have been previously described; both strains show consistent lesions but different susceptibilities to noise injury (Ohlemiller et al., 2000, 2011; Ou et al., 2000a; Wang et al., 2002; Ohlemiller and Gagnon, 2007; Park et al., 2013). All procedures and animal handling were conducted in accordance with the European (2010/63/EU) and Spanish (RD 1201/2005) legislation on the experimental use of animals, and were approved by the Ethics Committee of the Spain National Research Council (CSIC).

HEARING EVALUATION

Auditory brainstem responses (ABR) and distortion product otoacoustic emissions (DPOAE) were obtained before and 2, 14 days and 28 days after noise exposure (**Figure 1**) with a System III Evoked Potential Workstation (Tucker-Davis Technologies, Alachua, FL, USA). Briefly, mice were anesthetized with ketamine (Imalgene, Merial, 100 mg/kg) and xilacyne (Rompun, Bayer, 10 mg/kg) and placed on a heating pad inside a soundproof acoustic chamber.

For the ABR test, click and tone burst stimuli (8, 16, 20, 28 and 40 kHz) were presented with an MF1 magnetic speaker (TDT) from 90 to 20 dB SPL in 5–10 dB SPL steps (Cediel et al., 2006; Riquelme et al., 2010; Murillo-Cuesta et al., 2012). Click stimuli were 0.1 ms and tone burst stimuli were 5 ms duration (2.5 ms each for rise and decay, without plateau). Threshold of click-evoked and tone-evoked ABR, peak latencies and amplitudes were determined. For DPOAE, an ER10B+ probe (Etymotic Research Inc., IL, USA) was inserted into the external auditory canal and mice were stimulated with two synchronic tones, whose frequencies (f1, f2; relation f1/f2 = 1.2) were calculated from a central frequency (F = 8, 10, 14, 18 and 22 kHz; f1 = F*0.909, f2 = F*1.09), and presented with decreasing intensity from 80 to 30 dB SPL (f1 level = f2 level). The distortion product 2f1–f2 was determined for each sound level from the FFT waveforms. DPOAE thresholds were defined as the minimum level of the primary tones that elicit a 2f1–f2 response higher than background noise.

NOISE EXPOSURE AND EXPERIMENTAL GROUPS

Mice were exposed for 30 min to noise in a reverberant chamber acoustically designed to reach maximum sound level with minimum deviation in the central exposure area (Cobo et al., 2009). Two sound stimuli, named violet (V) and violet swept-sine (VS), were designed with Wavelab Lite software (Steinberg Media Technologies GmbH, Hamburg, Germany). Both have a linear-with-frequency gain to compensate for the high frequency losses inside the chamber, and present a spectrum

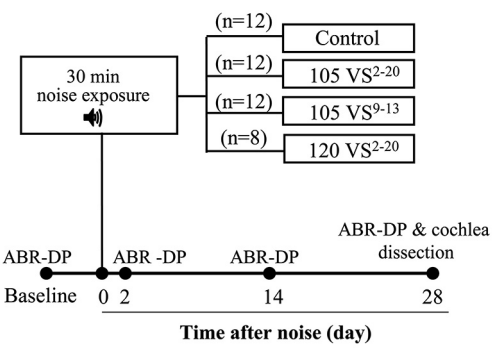

FIGURE 1 | Chronogram of the experiment. Mice were exposed to Violet Swept-sine (VS) noise with different intensities (105 or 120 dB SPL) and frequency ranges (2–20 or 9–13 kHz) for 30 min. Hearing was evaluated with Auditory Brainstem Responses (ABR) and Distortion Products of Otoacoustic Emissions (DP) before (baseline) and 2, 14 and 28 days after noise exposure. At the end of the study, cochleae were dissected and processed for histology and cell counting.

biased towards high frequencies, a kind of violet coloring. V noise was synthesized from white noise, whereas VS noise was a 10 s linear sweep in frequency from 2 kHz up to 20 kHz that was repeated during the 30 min of exposure. Specific characteristics of these stimuli are described in Cobo et al. (2009).

Preliminary experiments with V and VS noise were conducted in C57 and CBA mice in order to select the appropriate mouse strain and noise. For further studies, CBA mice were used and four experimental groups were established (**Figure 1**). Mice of the control group were not exposed (n = 12) whereas other mice were exposed to VS noise with the following level and frequency ranges: 105 dB SPL and 2–20 kHz (105 VS^{2-20}, n = 12), 120 dB SPL and 2–20 kHz (120 VS^{2-20}, n = 8), and 105 dB SPL and 9–13 kHz (105 VS^{9-13}, n = 12).

Finally, to evaluate the efficacy of P17 and P144 peptides, mice were exposed to 105 VS^{2-20} for 30 min and operated on 48 h after noise damage, once the increase in hearing thresholds was confirmed. The effect of noise exposure on hearing function was evaluated with the ABR test as described before, 2, 14 and 28 days after noise exposure.

DRUG ADMINISTRATION

Chemically synthesized peptide inhibitors with high affinity for TGF-β1 (Ezquerro et al., 2003) were gently defrosted, diluted and sonicated (only P144) to completely dissolve them. Local administration of inhibitors into the inner ear was performed 24 h after noise exposure, once the increase in hearing thresholds was confirmed. Briefly, the tympanic bulla was exposed via ventral surgical approach, and a bullostomy was performed at the posterolateral aspect using a small hook. Once the round window and stapedial artery were clearly visible, we applied directly 10 μl of a concentrated (40 mg/ml) P17 or P144 solution or saline (n = 6 each) to the round window using a gelatin sponge vehicle (Murillo-Cuesta et al., 2009).

COCHLEAR PROCESSING FOR HISTOLOGY AND HAIR CELL COUNTING

At the end of the experiment (**Figure 1**), mice were anesthetized with pentobarbital (Dolethal, Bayer, 150 mg/kg) and cochleae were extracted for light microscopy or HC counting. For histological evaluation, mice were perfused with 4% paraformaldehyde (in 0.1 M saline buffer, pH 7.4) and the cochleae were removed, fixed overnight, decalcified with 10% EDTA (0.3 M, pH 6.5) and embedded in paraffin as described (Riquelme et al., 2010; Murillo-Cuesta et al., 2012). Mid-modiolar 10 μm sections were Nissl-stained and evaluated with a Zeiss Diaplan microscope and a digital camera (Leitz DFC300 FXC). For HC counting, mice were sacrificed by cervical dislocation and the inner ear was carefully dissected. After removing the bony wall of the tympanic bulla and the stapes, the cochlea was exposed and two openings were performed, one between the round and oval windows and one in the apex, to circulate 300 μl paraformaldehyde. The cochleae were immersed in paraformaldehyde for 24 h and decalcified with EDTA for 4–6 days. Using an angled sharp micro scalpel, the bony and membranous labyrinths and the tectorial membrane were carefully removed to expose the organ of Corti (OC). Total removal of the BM along the entire cochlea is technically difficult; the basal-most region or "hook" is more delicate and it is easily injured during dissection. Therefore, the cochleogram shown in this work represents the 80% (range across cases: 70–85%) of the cochlea that can be dissected while maintaining cellular integrity. The 20% of the cochlea which is destroyed results in a loss of information regarding the 50–80 kHz frequencies, which, by definition, should not be greatly affected by noise containing frequencies in the range of 2–20 kHz (**Figure 2**).

OC was sectioned into two portions, one containing the apex and middle turns and the other containing the basal turn of the cochlea, placed on plates (Nunclon Microwell Plates, Sigma Aldrich) filled with PBS, and stored at 4°C. Samples were permeabilized with 0.5% Triton X-100 (Sigma-Aldrich) for 15 min, at room temperature on a shaker, and then incubated 1 h with 1:1000 phalloidin (R Alexa Fluor 488 phalloidin, Invitrogen) in PBS. After three washes in PBS, the samples were transferred to concave microscope slides (Menzel-Gläser) and mounted with Vectashield mounting medium with DAPI (Vector Laboratories). A total of 43 cochleae were obtained from the 22 animals (105 VS^{2-20}, n = 6), 120 VS^{2-20}, n = 6, 105 VS^{9-13}, n = 6, control non-exposed mice, n = 4).

STEREOLOGY AND COCHLEOGRAM PLOTTING

In order to plot a standardized cochleogram and to correlate cell damage with increased hearing thresholds at specific frequencies, a stereological approach was designed to determine the number and distribution of HCs along the length of the cochlea (Viberg and Canlon, 2004; Müller et al., 2005; Boyce et al., 2010; **Figure 2**). "Flattening" of the BM that resulted from cochlear extraction and mounting procedure helped to ensure an unbiased sampling of cells. High resolution photomicrographs of the OC samples were taken through a BX51 microscope with a DP70 camera (Olympus). These images were studied offline using CorelDRAW X3 software (Corel Corp., Ottawa, Ontario, Canada) to define an area of interest along the BM that included the rows of HCs, This area was further divided into sectors, each covering 5% of the total length, from apex to basal region. The OC samples were then evaluated with the same microscope under ultraviolet epi-illumination (Olympus U-RFL-T) with 4X and 40X magnification to detect phalloidin immunofluorescence, and previously defined sectors were located in the sample in order to perform cell counts. Interactive test grids and control of the motorized stage (Prior Scientific, Rockland, MA, USA) were provided by CAST stereological software package (v.2.3.2.0, Visiopharm, Hørsholm, Denmark). HC loss and stereocilia abnormalities are thought of as the principal correlate in NIHL. Since each HC is unequivocally represented by its hair bundle, phalloidin-stained stereocilia were used as counting units and HC were counted as present if the hair bundle was intact.

HC count was carried out by placing unbiased frames in a uniformly random sampling strategy on the focus planes of the

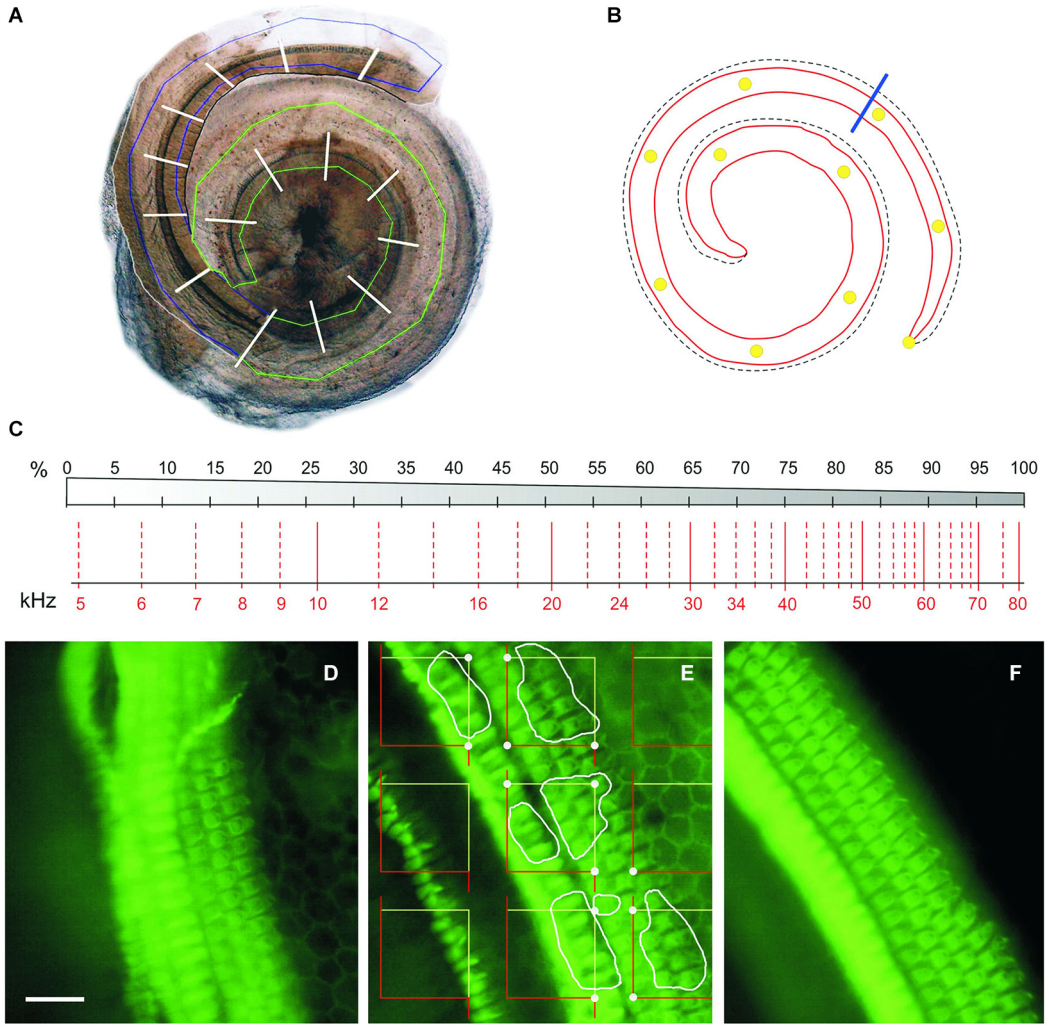

FIGURE 2 | Cochleogram and stereology. (A) Photomontage of digital images of the two blocks of a CBA mouse dissected cochlea. The region containing the BM is roughly delineated in green (apical-middle block) or blue (basal block); white traverses divide the whole length of the cochlea into 5% intervals. **(B)** Diagram of the BM of the same cochlea, with 10% intervals marked with yellow dots. The blue line separates the portion reconstructed in A (roughly 80% from the apex) from the basal quarter-turn, which was never included in the reconstruction. **(C)** Diagram showing a place-frequency map according to Viberg and Canlon (2004) and Müller et al. (2005), which combines a schematic drawing of the BM divided in 5% bins (top) and the corresponding frequency map (bottom). **(D–F)** Phalloidin-stained whole mounts of portions of the apical **(D)**, middle **(E)** and basal **(F)** cochlear turns in a control mouse. The stereological method used to estimate HC densities is summarized in **(E)**: A set of unbiased frames is randomly placed on the *stereociliary fringe*, the convex hull area bounding the hair tufts of the IHC and OHC; the HCs to be included in the count in this example are delineated by white profiles; dots highlight the frame corners that hit the stereociliary fringe, and serve to estimate the reference space sampled with the frames. Scale: 25 μm. IHC, inner hair cells; OHC, outer hair cells.

cilia. The reference space was considered the *stereociliary fringe*, that is, the convex hull area bounding the region containing the rows of hair tufts of the HCs.

The IHC and OHC cell densities were estimated for each sector as follows,

$$N_A(HC) = \frac{\sum Q(HC) \cdot 1000}{\sum a(SF)}$$

where N_A is the cell density expressed as number of cells/1000 μm^2, $\sum Q$ is the sum of HC counted within each sector, and $\sum a(SF)$ is the area of interest, in μm^2, sampled with the unbiased frames within the given sector. The precision of this method was approximated by computing the coefficient of error (CE) of the estimates (N_A) obtained on each sector, applying Cochran's equation for ratio estimators (eq. 10.32 in Howard and Reed, 2005). Our strategy yielded CE values of ∼17% (0.17 ± 0.015) in the control animals, and ∼21% (0.21 ± 0.020) in the noise-damaged groups.

Cytocochleograms were constructed by plotting the number of present OHCs or IHCs, or the OHC and IHC densities, as a function of percent distance from the apex of the cochlea.

STATISTICAL ANALYSIS

Data obtained from hearing test and hair cell counting were analyzed using v.19 IBM SPSS Statistics software. Results were expressed as mean ± SEM. Differences in ABR and DPOAE thresholds were analyzed using analysis of variance (ANOVA) with repeated measures. Bonferroni and T2 Tamhane *post hoc* tests (for equal or unequal variances, respectively) were used to make pairwise comparisons of the repeatedly measured data in different measurement times for each experimental group. ANOVA tests were also performed for comparison of HC numbers and densities among experimental groups. Results were considered significant at $p \leq 0.05$.

RESULTS

LONGITUDINAL STUDY OF HEARING-LOSS AFTER EXPOSURE TO DIFFERENT NOISE TYPES

Preliminary experiments were conducted in C57 and CBA mice in order to select the appropriate noise for subsequent cytocochleogram studies. Mice were exposed to noise for 30 min and threshold of click-evoked and tone-evoked ABR were determined before and at 1 h, and 3 and 7 days after exposure to noise. Results are summarized in **Table 1**. C57 mice exposed to noise at 120 dB SPL showed severe cochlear damage with irreversible TS, whereas following exposure at 100 dB SPL, baseline thresholds were practically recovered in the first week after insult, especially when V noise was used. CBA mice exposed to VS 105 dB SPL noise showed smaller TS than C57 mice, thus CBA was the strain chosen for further studies.

In these advanced studies, CBA mice from the four experimental groups (**Figure 1**) showed baseline thresholds of click-evoked and tone-evoked ABR below 20 dB SPL, without significant differences among them (**Figure 3A**). The control group maintained normal hearing thresholds throughout the experiment, with highly significant differences (Wald $\chi^2_{(3)} = 2282.9$, $p = 0.000$) when compared to all groups of noise-exposed mice. A click TS of around 50 dB occurred 2 days after noise exposure in all mice exposed to VS noise. No significant differences were found among damaged groups, although mice with the greatest TS were those exposed to 120 dB SPL noise. The evolution of click thresholds presented specific patterns for the three noise-exposed groups (**Figure 3A**). Thus, mice exposed to 120 VS^{2-20} noise showed a worsening of threshold 2 weeks after damage, with significant differences compared to exposure to 105 VS^{2-20} ($F_{(3)} = 202.64$, $p = 0.026$) and 105 VS^{9-13} ($p = 0.000$) noises. No differences were found between 105 VS^{2-20} and 105 VS^{9-13} noises at any time after insult, although the latter showed a non-significant but consistent small recovery of click thresholds. Similarly, baseline DPOAE thresholds were similar in all the experimental groups. Noise-exposed mice showed marked threshold increases in all the tested frequencies, with statistically significant differences compared to the control group, but without evident differences among them (**Figure 3B**).

In contrast, differences were found in the audiogram between exposure to 105 VS^{2-20} and 105 VS^{9-13} noises. Thus, mice exposed to VS^{9-13} noise showed higher TS 2-days after noise exposure, especially when high frequencies were tested (**Figure 4A**). Significant differences were found at stimuli frequencies of 16 ($F_{(3)} = 32.7$, $p = 0.002$), 20 ($F_{(3)} = 94.6$, $p = 0.000$), 28 ($F_{(3)} = 86.7$, $p = 0.000$) and 40 ($F_{(3)} = 177.1$, $p = 0.000$) kHz.

To study potentially selective damage on specific cochlear regions, the audiogram of mice exposed to VS^{9-13} noise was extended to include frequencies of 4 and 10 kHz. As expected, the TS at 10 kHz was larger than TS found at the nearby frequencies of 4, 8 and 16 kHz. This TS peak in the audiogram was maintained throughout the study (**Figure 4B**).

Statistical analysis of ABR latencies showed a significant decrease of the peak and interpeak latencies, especially I–II, in animals exposed to noise compared to baseline values. This reduction was similar in the three exposed groups, without significant differences, and persisted throughout the times examined (data not shown).

COCHLEAR MORPHOLOGY AND HAIR CELL DENSITY AFTER NOISE EXPOSURE

At the end of the experiment, CBA mice exposed for 30 min to VS stimulus showed some of the typical chronic cochlear alterations reported in this strain after noise damage (Wang et al., 2002); no gross differences were detected among 105 VS^{2-20}, 120 VS^{2-20} and 105 VS^{9-13} groups. The main cellular feature detected in Nissl-stained sections was fibrocyte loss in the spiral ligament and spiral limbus (**Figure 5**), whereas no evident changes in the gross anatomy of the OC were

Table 1 | Evolution of ABR threshold in response to click stimulus.

				ABR threshold (dB SPL)			
					Time after noise exposure		
Strain	**Stimulus**	**Level (dB SPL)**	**N**	**Baseline**	**1 h**	**3 days**	**7 days**
C57BL/6JOlaHsd	V^{2-20}	100	5	42 ± 3	55 ± 10	48 ± 12	41 ± 2
		120	3	43 ± 8	90 ± 10	90 ± 17	87 ± 12
	VS^{2-20}	100	4	42 ± 6	63 ± 5	60 ± 8	53 ± 5
		120	4	40 ± 8	88 ± 10	90 ± 8	83 ± 17
CBA/CaOlaHsd	VS^{2-20}	105	12	17 ± 5	n.d.	69 ± 4	70 ± 6

Exposure of mice to noxious noises at 100 dB SPL for 30 min induced moderate TS with almost complete recovery, especially when V^{2-20} noise was used. In contrast, 120 dB SPL noise exposure irreversibly damaged the cochlea. Exposure to VS^{2-20} noise in CBA mice was further selected to study functional effects and concomitant hair cell loss. V, violet noise; VS, violet swept-sine noise. Superscripts indicate the noise frequency range (in kHz).

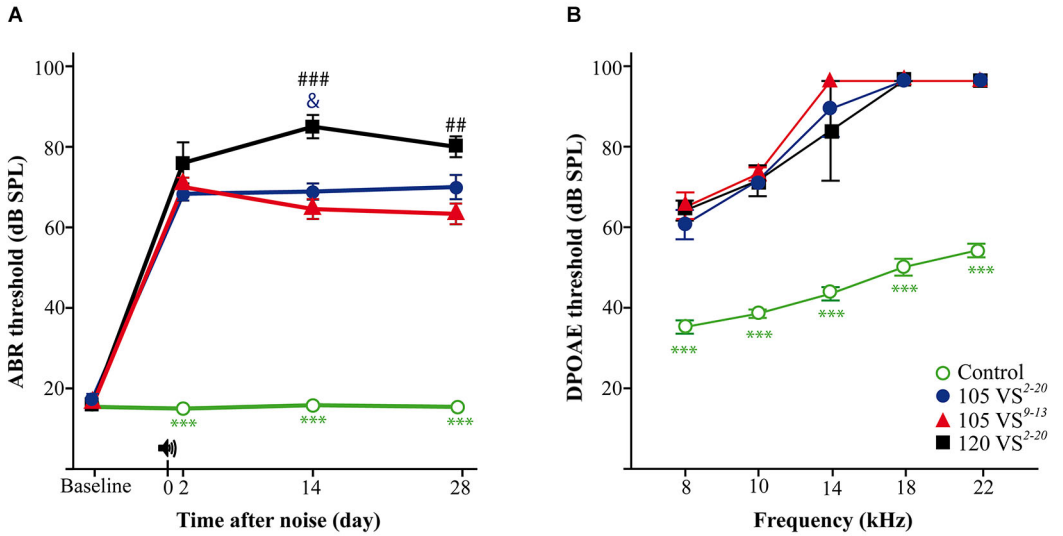

FIGURE 3 | Evaluation of hearing. (A) Evolution of threshold of click-evoked ABR. Control non-exposed mice ($n = 12$) maintained normal hearing thresholds along the study, with statistically significant differences ($p < 0.001$, ***) compared to noise damaged mice. Two days after noise insult, a notable TS occurred in exposed animals; at longer post-exposure periods, mice exposed to 120 VS^{2-20} ($n = 7$) showed significantly higher values compared to those exposed to 105 VS^{2-20} ($n = 11$, $p < 0.05$, &) and 105 VS^{9-13} ($n = 12$, $p < 0.01$, ##). **(B)** DPOAE thresholds at individual frequencies at the end of the experiment. 28 days after noise exposure (105 VS^{2-20}, $n = 5$; 105 VS^{9-13}, $n = 8$; 120 VS^{2-20}, $n = 4$) mice showed significant ($p < 0.001$, ***) higher DPOAE thresholds for all the frequencies as compared to control mice ($n = 6$). No significant differences were found among exposed animals. VS, violet swept-sine noise; superscripts indicate the noise frequency range (in kHz); the coefficient indicates the noise level in dB SPL.

observed. Stereocilia damage and HC loss were in fact evident in phalloidin-stained whole mount samples (**Figures 5C,F,G,J**). These preparations were further used for stereological hair cell counting. **Figure 2** shows that the whole length of the dissected BM was divided into 5% sectors from apical to basilar cochlear regions. Present IHC and OHC were counted and densities were estimated for each sector in control and noise exposed mice (**Figure 6**). Control non-exposed mice showed similar hair cell density values in all sectors, both for OHC (over 10 cell/1000 μm^2) and IHC (over 4 cell/1000 μm^2). Differences among noise-damaged mice were evident from sector 20 onwards, especially for OHC. Mice exposed to 120 VS^{2-20} noise showed a clear decrease in OHC density, mainly at the basal region, where no OHCs were detected. A similar but smaller density decrease was observed in 105 VS^{2-20} exposed mice when compared to those exposed to 120 VS^{2-20}. Whereas mice exposed to 105 VS^{9-13} noise showed an acute loss of OHCs in sectors 25 to 30%, and a progressive decrease of cellular density from sector 55% onwards (**Figures 6A,B**). Similar results were observed when IHC density was evaluated in all the experimental groups (**Figures 6C,D**).

Sectors were grouped into three cochlear regions (apical, 5–25%; middle, 30–55%; basal, 60–80%) for comparison (**Figure 6E**). As expected, the control group presented higher HC densities in the three regions compared to noise-exposed mice. A notable decrease in OHC density was observed in mice exposed to 120 VS noise, especially in the middle and basal regions. Mice exposed to 105 VS^{2-20} noise showed a gradual decrease of OHC density from apex to base, whereas in the group of mice exposed to 105 VS^{9-13} noise, OHC loss was evident in the basal region when compared to non-exposed mice ($p = 0.000$).

EVALUATION OF TGF-β1 INHIBITORS IN THE TREATMENT OF NIHL

NIHL mouse models and the cochleogram procedures were validated in a preclinical assay with TGF-β1 inhibitors (**Figure 7A**). Mice were exposed to 105 VS^{2-20} noise and after 2 days they were operated on for local delivery of a single dose of TGF-β1 inhibitor (P17, P144) or saline. Analysis of thresholds of click-evoked and tone-evoked ABR showed notable permanent TS 1 day after noise exposure and then a minimal recovery regardless of the treatment. No statistically significant differences were found in ABR thresholds in response to click or tone burst stimuli among mice treated with P17, P144 or saline at any of the times evaluated (1, 14 and 28 days after noise exposure) (**Figure 7B**).

At the end of the study, cochleae were collected to perform the cochleogram as described. As mentioned before, mice exposed to 105 VS^{2-20} noise showed a statistically significant decrease in HC number and density, both for IHCs and OHCs (data not shown). However, no significant differences were observed in cochleogram data between mice treated with TGF-β1 inhibitors and those with saline (**Figure 7C**).

DISCUSSION

NIHL is an important medical concern and reliable animal models are key to understanding its pathophysiology and developing new therapeutic strategies. In humans and mice,

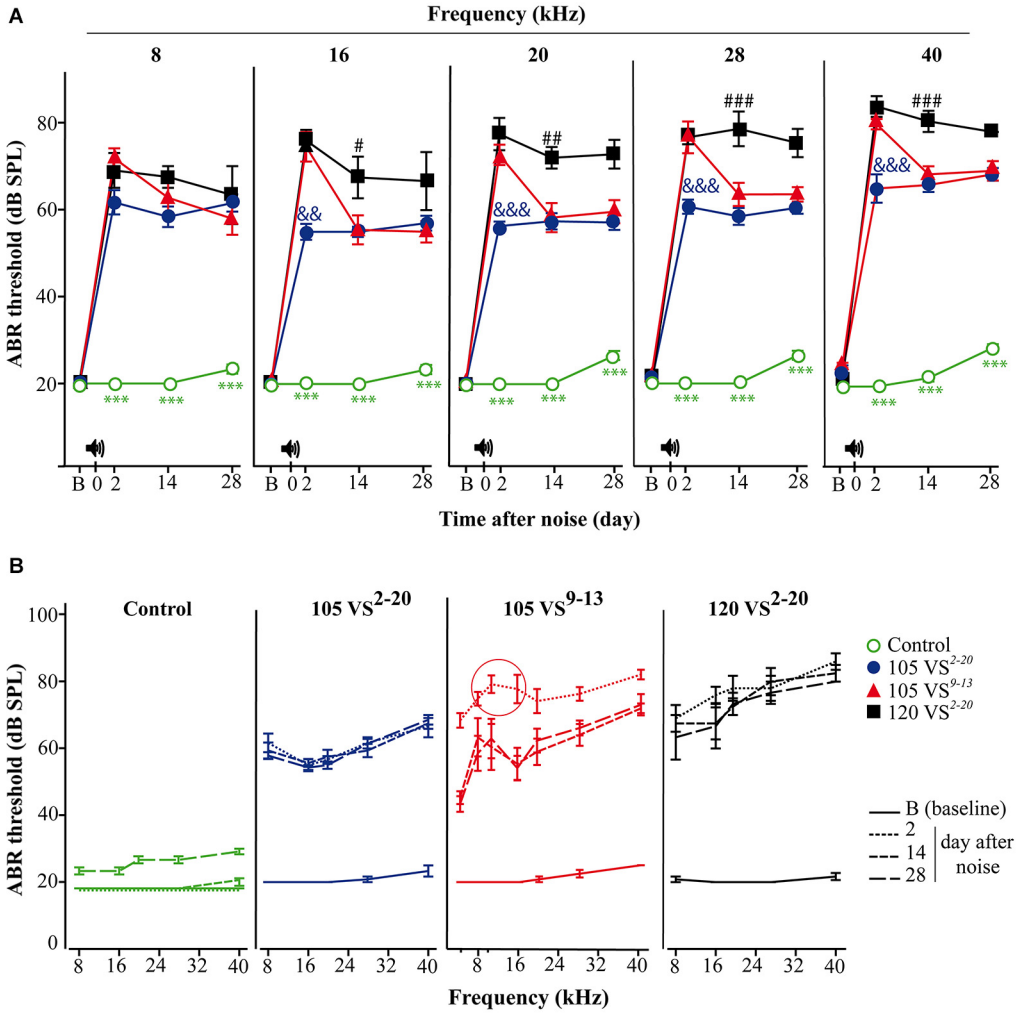

FIGURE 4 | Evolution of thresholds of tone-evoked ABR. (A) Control non-exposed mice (○, $n = 12$) maintained baseline **(B)** hearing thresholds and showed statistically significant differences ($p < 0.001$, ***) when compared to noise-damaged mice. Noise 120 VS^{2-20} (■, $n = 7$) induced the most severe damage (compared to 105 VS noises; # $p < 0.05$, ## $p < 0.01$, ### $p < 0.001$), whereas TSs in 105 VS^{2-20} (●, $n = 11$,) were significantly lower (compared to the other noises; && $p < 0.01$, &&& $p < 0.001$). Mice exposed to 105 VS^{9-13} (▲, $n = 12$,) showed significant early damage followed by a partial, but quick, recovery. **(B)** Mice exposed to VS noise showed an elevation in the audiogram, compared to control mice. A TS peak in the 105 VS^{9-13} was evident in response to 8 and 10 kHz. VS, violet swept-sine noise; superscripts indicate the noise frequency range (in kHz); the coefficient indicates the noise level in dB SPL.

noise exposure induces temporary or permanent hearing loss depending on the noise intensity and the individual susceptibility (reviewed in Davis et al., 2003). Other physical parameters of noise as frequency spectra, duration and intermittency also contribute to injury, but they are less frequently examined in NIHL studies (Mahendra Prashanth and Venugopalachar, 2011) or animal models.

In this work we demonstrate that by modulating noise characteristics, the hearing loss outcome in noise-exposed mice can vary largely. Thus, by modifying the physical properties of the sound, we have generated and characterized a range of experimental NIHL mouse models with the aim of obtaining experimental tools for studying human NIHL and for testing potential therapeutic strategies.

During the first 2 weeks after noise exposure, mice can show temporary and reversible increased threshold (temporal TS), but one month after injury, the auditory threshold elevation is considered permanent (permanent TS) (Hamernik and Qiu, 2000; Harding et al., 2002; Wang et al., 2002; Chen et al., 2003). Here we show that 30 min of exposure to VS noise of intensities of either 105 or 120 dB SPL could induce a notable increase in thresholds of click-evoked and tone-evoked ABR; the magnitudes of temporal and permanent TSs are proportional to the intensity as reported (Ohlemiller et al., 2000, 2011; Park et al., 2013). Interestingly, small changes in the noise frequency spectrum also induced different ABR profiles. Two days after exposure to 105 VS^{9-13} there was an acute TS greater than that observed after exposure to 105 VS^{2-20} noise, particularly at high frequencies.

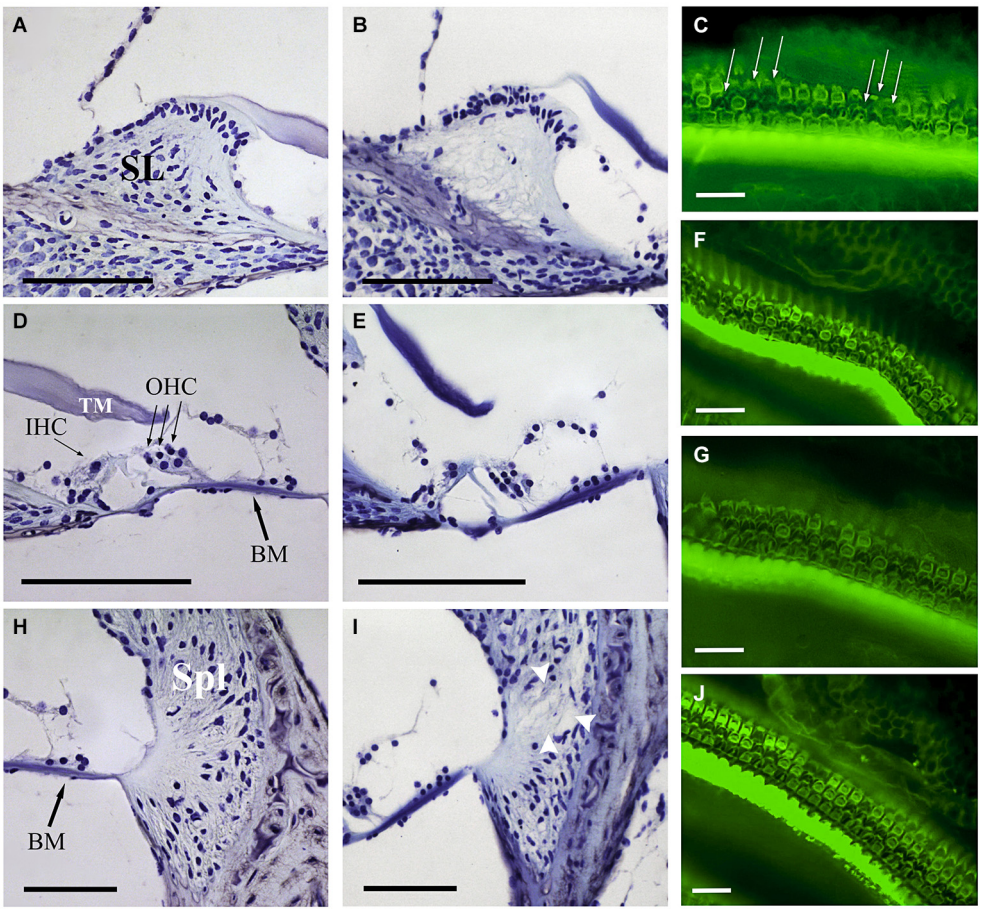

FIGURE 5 | Comparative study of cochlear morphology after noise insult. Comparison of the spiral limbus (SL) **(A,B)**, organ of Corti **(D,E)** and spiral ligament (Spl) **(H,I)** of control **(A,D,H)** and VS noise-exposed **(B,E,I)** mice at the cochlear middle level. Main features observed after short time noise exposure included fibrocyte loss at SL **(B)** and loss of type IV fibrocytes at Spl (white arrowheads at **I**). The organ of Corti reveals an essentially normal gross anatomy (no collapse of tunnel of Corti, Hensen cells or spaces of Nuel). The different noise exposure conditions show similar cytoarchitectural alterations with no evident differences among them. At the focal plane shown, phalloidin-stained whole mounts for actin exhibit the disrupted sequence (arrows in **C**) of otherwise well-defined outlines of OHC and a substantial OHC loss 28 days after VS noise insult **(C,F,G,J)**. Scale bars: 100 μm **(A,B,D,E,H,I)**, 25 μm **(C,F,G,J)**. BM, basilar membrane; IHC, inner hair cells; OHC, outer hair cells; TM, tectorial membrane; SL, spiral limbus; Spl, spiral ligament.

It is known that exposure to noise of a certain frequency does not induce a higher TS at that frequency, but rather at 0.5 to 2 octaves above that frequency, depending on the species (Ou et al., 2000a). Therefore, to assess functional impairment after noise exposure, it is necessary to measure thresholds of tone-evoked ABR over a range of frequencies by stimulation with multiple tone bursts. In this work we performed a large audiogram from 8 to 40 kHz. A notch was evident in the ABR audiogram from 105 VS^{9-13} noise-exposed mice with higher thresholds for pure tones at 8 and 10 kHz. Similar frequency-related variations in hearing thresholds have been reported in human studies. Exposures to broadband noise induce maximum TS at frequencies between 3 and 6 kHz but, if the noise is a pure tone, the higher the frequency, the greater the resulting TS (Mahendra Prashanth and Venugopalachar, 2011). In addition to level and frequency composition, other noise characteristics could influence the hearing outcome. Thus, swept-sine "intermittent" noises produce greater cochlear damage than "continuous" ones, including white, violet and broadband noises, possibly because they expose HCs to higher activity and stress.

Concomitantly with noise-induced TS, we observed a decrease in ABR peak latencies, which could be interpreted as acceleration in neural transmission along the auditory pathway. This observation is consistent with many studies both in human and animal models (Strelcyk et al., 2009; Scheidt et al., 2010; Henry et al., 2011), and diverse theories have been proposed, including recruitment phenomenon and hyperexcitability of central auditory fibers. Cochlear recruitment occurs when damaged HC call up those close to them to cover their activity, creating a paradoxical situation of hyperexcitability in the central auditory fibers, in which there is an abnormal increase in the response to sound (Moore, 2004; Sherlock and Formby, 2005). It is has been proposed that this is

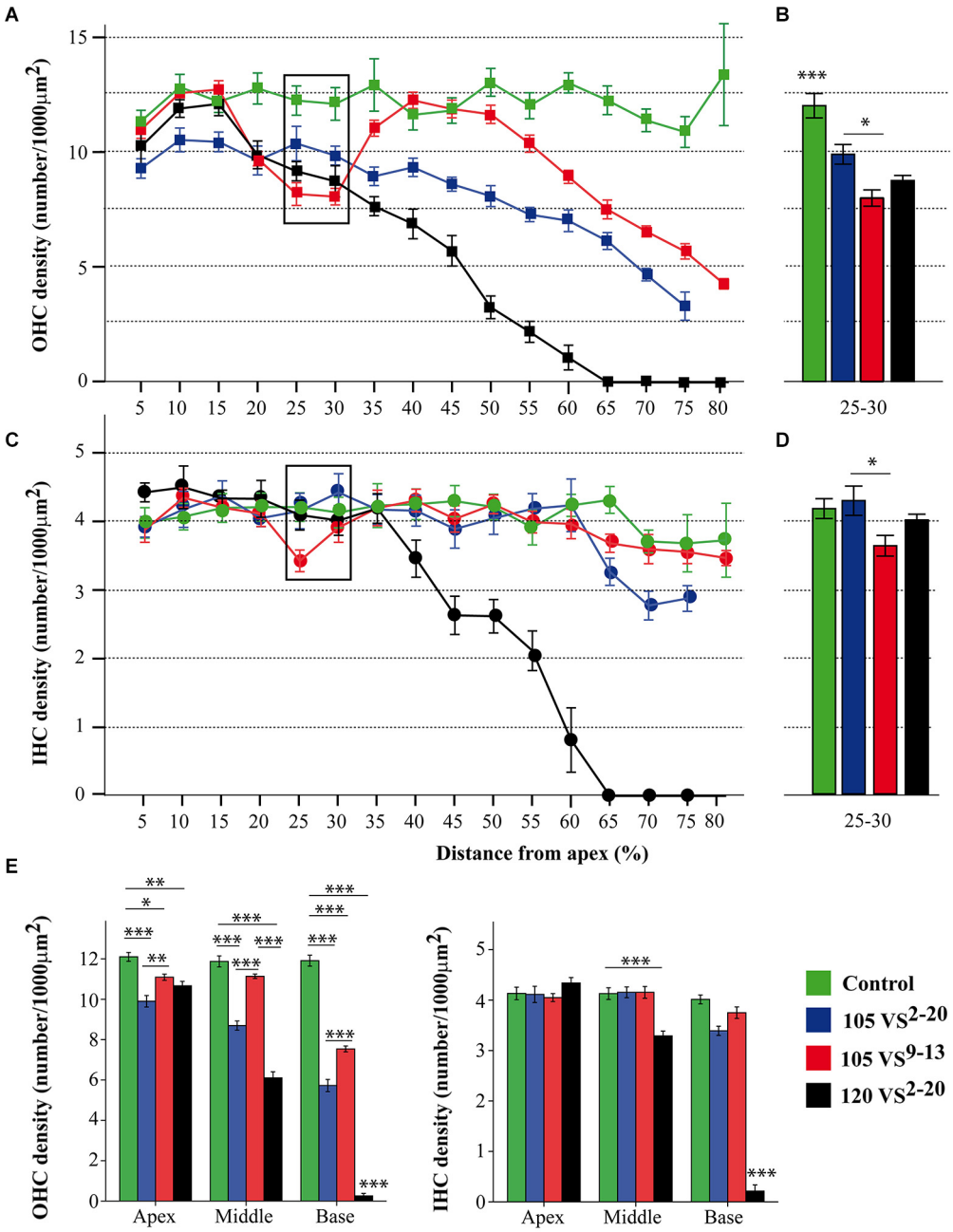

FIGURE 6 | Hair cell counting data. (A–D) Inner and outer hair cell density (mean ± SEM, expressed as number of cells/1000 μm^2) for each 5% sector across the total length of the BM **(A,C)** and focused on sectors 25–30 **(B,D)**. Exposure to 105 VS^{9-13} noise induced a significantly higher loss of hair cells in the cochlear region corresponding to sectors 25 and 30 (see **Figure 2C**) compared to exposure to 105 VS^{2-20} noise. **(E)** To better assess regional variations, sectors were grouped into three regions (apex, 5–25; middle, 30–55; base, 60–80) and the mean hair cell density was calculated. Statistically significant differences among groups were found, indicating that exposure to 120 VS^{2-20} noise induced the most severe damage, especially towards the basal region. * $p < 0.05$; ** $p < 0.01$; *** $p < 0.001$. VS, violet swept-sine noise; superscripts indicate the noise frequency range (in kHz); the coefficient indicates the noise level in dB SPL.

a mechanism for balancing neuronal activity after cochlear damage (Syka, 2002; Cai et al., 2009; Rybalko et al., 2011). However, the consequences of noise damage on ABR latencies are still unclear and other authors have observed increased values after exposure (Chen et al., 2002; Gourévitch et al., 2009). Wave amplitudes also decreased after noise-exposure, a pattern that was maintained throughout the study and which has been related to loss of afferent nerve terminals (Popelar et al., 2008; Kujawa and Liberman, 2009; Henry et al., 2011).

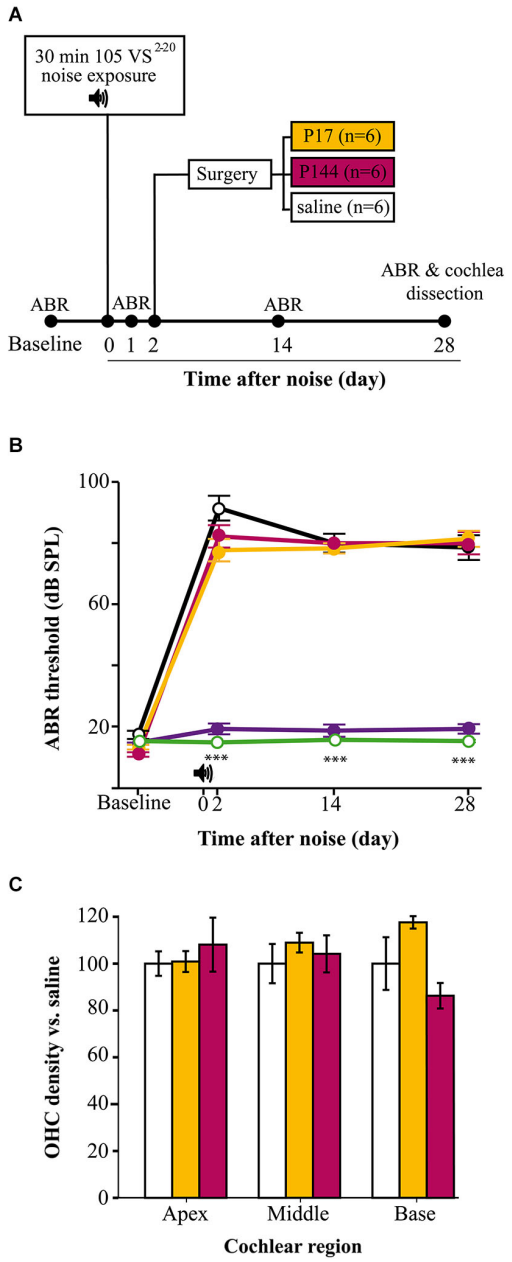

FIGURE 7 | TGF-β1 inhibitors in NIHL treatment. (A) Chronogram of the experiment. Mice were exposed for 30 min to VS noise at 105 dB SPL and after 2 days they were operated on to deliver P17, P144 or saline (n = 6 mice per group) to the inner ear through a bullostomy. ABR tests were performed before and 1, 14 and 28 days after noise exposure. **(B)** Evolution of threshold of click-evoked ABR in mice exposed to 105 VS^{2-20} noise for 30 min and treated locally with a single dose of TGF-β1 inhibitors P17 (orange line), P144 (pink) or saline (black), compared to non-exposed (green) and sham-operated (purple) mice . Noise induced notable TS in the first day after damage without noticeable recovery, compared to non-exposed controls (***$p \leq 0.001$). No significant differences were observed between mice treated with TGF-β1 inhibitors and those treated with saline. No statistically significant increase in click-evoked ABR threshold was observed in sham-operated mice. **(C)** Outer hair cell density (mean ± SEM, expressed as %) in mice treated with TGF-β1 inhibitors compared to saline

(*Continued*)

FIGURE 7 | Continued
expressed as %) in mice treated with TGF-β1 inhibitors compared to saline treated mice, in the three standard regions (apex, 5–25; middle, 30–55; base, 60–80) at the end of the experiment. No significant differences were observed between mice treated with P17 (orange bars) or P144 (pink) and those treated with saline (white) after exposure.

DPOAE is a method for early detection of NIHL in patients as their alteration may reflect subclinical cochlear changes that do not show up yet in the tone threshold audiometry (Attias et al., 2001; Martin et al., 2006; Fetoni et al., 2009). In parallel with changes in ABR parameters, we observed an increase in DPOAE thresholds in the three noise-exposed mice groups, without significant differences among them. DPOAE TS correlated with that observed in the ABR and also with the extent of OHC loss detected in the cochleogram, as described previously by other authors (Vázquez et al., 2004; Jamesdaniel et al., 2011; Park et al., 2013).

The CBA mouse strain has been reported to be more resistant to the harmful effects of noise than the C57 strain (Ohlemiller et al., 2011), a fact that was confirmed in our work by comparing two noise types, V and VS, at two intensities. C57 mice exposed to noise often showed an extreme response and became irreversibly profoundly deaf. Therefore CBA mice were used for further comparison of the lesions on different features caused by VS noises. CBA mice showed a characteristic noise-induced pattern of injury which includes changes in the spiral ligament, the limbus, the stria vascularis and the HC (Ou et al., 2000a; Wang et al., 2002; Ohlemiller et al., 2011; Park et al., 2013). In this study, in conjunction with the functional alterations observed, CBA mice exposed to VS noise showed cellular lesions in fibrocytes and HC. To fully characterize the effects of noise on HCs it is necessary to examine the entire OC from apex to base. However, surgical dissection of the organ of Corti is difficult, especially in the basal tip region or "hook", which is usually lost or artificially damaged. We estimated that this portion represents around 20% of the total length of the OC, therefore the cochleogram includes the 80% of the cochlea that maintained cellular integrity. Based on the frequency location map of the mouse cochlea by Ou et al. (2000b), this portion results in a loss of information on the 50–80 kHz frequencies. As mentioned before, noise exposure induces higher TS in a range of frequencies 0.5 to 2 octaves around the noise frequency. Therefore this hook region should not be much affected by our VS. To further study HC loss resulting from different VS noise exposures, stereological methods were applied to develop a cytocochleogram, a topographical map of the cochlea which associates frequencies to defined HC positions along the length of the BM, offering key information on the function to structure relationship, under both physiological and pathological conditions (Viberg and Canlon, 2004). Due to intraspecies BM length variation, it is preferable to construct percentage, rather than absolute length (in mm) cochleograms. When length values are expressed as percentages, this results in a linear topographic map that can be safely used to correlate the location of the HC (or a lesion thereof) to sound frequency by using appropriate frequency-place equations (Viberg and Canlon, 2004). For this

study with CBA mice, we chose to follow the Müller equation (Müller et al., 2005) and to plot the cytocochleogram dividing the length of the BM in 5% equidistant sectors from the apex to the base of the cochlea.

Cell counting procedures most often consist of direct counts of HC cell bodies or nuclei (or their absence from identified spots) at fixed length intervals from the apex, which may then be transformed into percentage distance from the cochlear apex (Nordmann et al., 2000; Minami et al., 2007; Harding and Bohne, 2009; Choudhury et al., 2011). We opted instead for estimating HC densities at regular 5% length intervals from the apex, an efficient and consistent novel procedure, which relied on applying a stereological method (Boyce et al., 2010) on phalloidin-stained stereocilia bundles as counting units. Single bundles are unambiguously identified on flat mounts of the cochlea, and their disappearance marks an irreversibly degenerating or already absent HC, since hair bundle loss is not recoverable in mammalian cochlear HC (Jia et al., 2009).

Using this cytocochleogram, we evidenced different patterns of HC loss depending on the level and frequency range of the VS noise, as well as a correlation with functional data. As reported for other sound stimuli in mice, VS noise induced a greater loss of OHC than IHC (Wang et al., 2002; Ohlemiller and Gagnon, 2007; Ohlemiller, 2008; Park et al., 2013). After exposure to noise with a particular range of frequencies, HC loss fundamentally occurs within the cochlear region that codifies this signal, but also outside this zone (Harding and Bohne, 2009). Consequently, we observed a notable HC loss, especially in OHC, in sectors 5–55% after exposure to 105 VS^{2-20} and a focal lesion in sectors 25–30% when 105 VS^{9-13} was used, but also we detected cell loss in the basal cochlear region. This is because the acoustic energy delivered by a noise is maximal in its frequency range and declines above and below it. As expected, after exposure to 120 VS^{2-20} noise the cochleogram showed generalized cochlear lesions with a marked decrease in HC density, with combined lesions in OHC and IHC and with large areas where no HC were detected.

The NIHL paradigm and cochleogram procedure shown here constitute valuable tools in preclinical assays of new molecules with potential therapeutic effects. Inhibitors are key regulators of the inflammatory and immune response in several tissues including the inner ear. Upregulation of TGF-β1 has been confirmed in some animal models with otic damage, including ototoxicity and antigen injection, chronic otitis media (Satoh et al., 2006; Wissel et al., 2006; Ghaheri et al., 2007) and NIHL (Murillo-Cuesta et al., submitted). In this context, the use of TGF-β1 inhibitors could be useful in ameliorating pathological changes in the cochlea after noise insult. Systemic treatment with P17 and P144 before noise exposure as well after damage has been shown to improve the TSs and the evolution of thresholds of click-evoked and tone-evoked ABR, compared to saline treated mice (Murillo-Cuesta et al., submitted). In order to deliver molecules to the inner ear with accuracy and to avoid adverse effects, new localized approaches to the cochlea are now being tested (Rivera et al., 2012). In this work we showed the functional and morphological results of a preclinical assay with TGF-β1 inhibitors applied to the middle ear using a gelatin sponge, after noise exposure. The potential therapeutic effect was evaluated with ABR and a cochleogram, as described. Mice exposed to noise showed a similar pattern of damage, both functional and morphological, with no significant differences compared to saline treated mice. Therefore, our results suggest that a single dose of these peptides is not enough to prevent noise damage.

In summary, we show that CBA mice exposed for 30 min to noise enriched in frequencies up to 20 kHz and presented in a swept-sine mode suffered a TS of around 50 dB. Depending on the intensity and frequency range, this noise induced specific functional and morphological changes, with a tonotopic correlation between the noise-frequency input and the injury output measured by means of functional data and cell density counting. The methodology described herein, combining standardized NIHL mouse models, friendly local delivery systems, and precise evaluation techniques such ABR and cochleogram, should be useful in further understanding NIHL and for evaluating novel therapeutic strategies.

AUTHORS AND CONTRIBUTORS

LS: acquisition, analysis, and interpretation of cytocochleogram data. SM-C: acquisition, analysis, and interpretation of functional data; drafting and revision of the manuscript. PC: substantial contribution to the conception and design of the noises and exposition chamber. RC: substantial contribution to the conception and design of the noises and exposition chamber. JC: acquisition, analysis, and interpretation of morphological data. TR: design of the work; revision of the manuscript. IVN: design of the work; analysis, and interpretation of data; drafting and revision of the manuscript. CA: design of the work, analysis and interpretation of data; critical revision of the manuscript.

ACKNOWLEDGMENTS

We warmly thank our colleagues from the Neurobiology of Hearing group for helpful discussions and for sharing unpublished data and procedures. We also thank the technical support of the Non-invasive Neurofunctional Evaluation facility (IIBm, CSIC-UAM and SEFALer, CIBERER). This work was supported by grants from MINECO (SAF2011-24391), Fundación de Investigación Médica Mutua Madrileña (FMM2012), European FP7-INNOVA2-AFHELO and FP7-PEOPLE-IAPP-TARGEAR to IVN and FIS PI 10/00394 for TR. S.M.-C. holds a CIBERER (ISCIII) postdoctoral contract.

REFERENCES

Attias, J., Horovitz, G., El-Hatib, N., and Nageris, B. (2001). Detection and clinical diagnosis of noise-induced hearing loss by otoacoustic emissions. *Noise Health* 3, 19–31.

Bohne, B. A., Harding, G. W., and Lee, S. C. (2007). Death pathways in noise-damaged outer hair cells. *Hear. Res.* 223, 61–70. doi: 10.1016/j.heares.2006.10.004

Boyce, R. W., Dorph-Petersen, K. A., Lyck, L., and Gundersen, H. J. (2010). Design-based stereology: introduction to basic concepts and practical approaches for estimation of cell number. *Toxicol. Pathol.* 38, 1011–1025. doi: 10.1177/0192623310385140

Cai, S., Ma, W. L., and Young, E. D. (2009). Encoding intensity in ventral cochlear nucleus following acoustic trauma: implications for loudness recruitment. *J. Assoc. Res. Otolaryngol.* 10, 5–22. doi: 10.1007/s10162-008-0142-y

Cediel, R., Riquelme, R., Contreras, J., Díaz, A., and Varela-Nieto, I. (2006). Sensorineural hearing loss in insulin-like growth factor I-null mice: a new model of human deafness. *Eur. J. Neurosci.* 23, 587–590. doi: 10.1111/j.1460-9568.2005.04584.x

Chen, T. J., Chen, S. S., Wang, D. C., and Hsieh, Y. L. (2002). Increased vulnerability of auditory system to noise exposure in mdx mice. *Laryngoscope* 112, 520–525. doi: 10.1097/00005537-200203000-00021

Chen, G. D., and Fechter, L. D. (2003). The relationship between noise-induced hearing loss and hair cell loss in rats. *Hear. Res.* 177, 81–90. doi: 10.1016/s0378-5955(02)00802-x

Chen, Y. S., Liu, T. C., Cheng, C. H., Yeh, T. H., Lee, S. Y., and Hsu, C. J. (2003). Changes of hair cell stereocilia and threshold shift after acoustic trauma in guinea pigs: comparison between inner and outer hair cells. *ORL J. Otorhinolaryngol. Relat. Spec.* 65, 266–274. doi: 10.1159/000075224

Choudhury, B., Adunka, O. F., Demason, C. E., Ahmad, F. I., Buchman, C. A., and Fitzpatrick, D. C. (2011). Detection of intracochlear damage with cochlear implantation in a gerbil model of hearing loss. *Otol. Neurotol.* 32, 1370–1378. doi: 10.1097/MAO.0b013e31822f09f2

Cobo, P., Murillo-Cuesta, S., Cediel, R., Moreno, A., Lorenzo-García, P., and Varela-Nieto, I. (2009). Design of a reverberant chamber for noise exposure experiments with small animals. *Appl. Acoust.* 70, 1034–1040. doi: 10.1016/j.apacoust.2009.03.005

Davis, R. R., Kozel, P., and Erway, L. C. (2003). Genetic influences in individual susceptibility to noise: a review. *Noise Health* 5, 19–28.

Ezquerro, I. J., Lasarte, J. J., Dotor, J., Castilla-Cortázar, I., Bustos, M., Peñuelas, I., et al. (2003). A synthetic peptide from transforming growth factor beta type III receptor inhibits liver fibrogenesis in rats with carbon tetrachloride liver injury. *Cytokine* 22, 12–20. doi: 10.1016/s1043-4666(03)00101-7

Fetoni, A. R., Garzaro, M., Ralli, M., Landolfo, V., Sensini, M., Pecorari, G., et al. (2009). The monitoring role of otoacoustic emissions and oxidative stress markers in the protective effects of antioxidant administration in noise-exposed subjects: a pilot study. *Med. Sci. Monit.* 15, PR1–PR8.

Ghaheri, B. A., Kempton, J. B., Pillers, D. A., and Trune, D. R. (2007). Cochlear cytokine gene expression in murine chronic otitis media. *Otolaryngol. Head Neck Surg.* 137, 332–337. doi: 10.1016/j.otohns.2007.03.020

Gourévitch, B., Doisy, T., Avillac, M., and Edeline, J. M. (2009). Follow-up of latency and threshold shifts of auditory brainstem responses after single and interrupted acoustic trauma in guinea pig. *Brain Res.* 1304, 66–79. doi: 10.1016/j.brainres.2009.09.041

Gratton, M. A., Eleftheriadou, A., Garcia, J., Verduzco, E., Martin, G. K., Lonsbury-Martin, B. L., et al. (2011). Noise-induced changes in gene expression in the cochleae of mice differing in their susceptibility to noise damage. *Hear. Res.* 277, 211–226. doi: 10.1016/j.heares.2010.12.014

Greenwood, D. D. (1996). Comparing octaves, frequency ranges and cochlear-map curvature across species. *Hear. Res.* 94, 157–162. doi: 10.1016/0378-5955(95)00229-4

Hamernik, R. P., and Qiu, W. (2000). Correlations among evoked potential thresholds, distortion product otoacoustic emissions and hair cell loss following various noise exposures in the chinchilla. *Hear. Res.* 150, 245–257. doi: 10.1016/s0378-5955(00)00204-5

Harding, G. W., and Bohne, B. A. (2009). Relation of focal hair-cell lesions to noise-exposure parameters from a 4- or a 0.5-kHz octave band of noise. *Hear. Res.* 254, 54–63. doi: 10.1016/j.heares.2009.04.011

Harding, G. W., Bohne, B. A., and Ahmad, M. (2002). DPOAE level shifts and ABR threshold shifts compared to detailed analysis of histopathological damage from noise. *Hear. Res.* 174, 158–171. doi: 10.1016/s0378-5955(02)00653-6

Henry, K. S., Kale, S., Scheidt, R. E., and Heinz, M. G. (2011). Auditory brainstem responses predict auditory nerve fiber thresholds and frequency selectivity in hearing impaired chinchillas. *Hear. Res.* 280, 236–244. doi: 10.1016/j.heares.2011.06.002

Howard, C. V., and Reed, M. G. (2005). *Unbiased Stereology. Three Dimensional Measurement in Microscopy.* 2nd Edn. New York: Garland Science/BIOS Scientific Publishers.

Hu, B. H., Henderson, D., and Nicotera, T. M. (2006). Extremely rapid induction of outer hair cell apoptosis in the chinchilla cochlea following exposure to impulse noise. *Hear. Res.* 211, 16–25. doi: 10.1016/j.heares.2005.08.006

Jamesdaniel, S., Hu, B., Kermany, M. H., Jiang, H., Ding, D., Coling, D., et al. (2011). Noise induced changes in the expression of p38/MAPK signaling proteins in the sensory epithelium of the inner ear. *J. Proteomics* 75, 410–424. doi: 10.1016/j.jprot.2011.08.007

Jia, S., Yang, S., Guo, W., and He, D. Z. (2009). Fate of mammalian cochlear hair cells and stereocilia after loss of the stereocilia. *J. Neurosci.* 29, 15277–15285. doi: 10.1523/JNEUROSCI.3231-09.2009

Kirchner, D. B., Evenson, E., Dobie, R. A., Rabinowitz, P., Crawford, J., Kopke, R., et al. (2012). Occupational noise-induced hearing loss: ACOEM task force on occupational hearing loss. *J. Occup. Environ. Med.* 54, 106–108. doi: 10.1097/JOM.0b013e318242677d

Konings, A., Van Laer, L., and Van Camp, G. (2009). Genetic studies on noise-induced hearing loss: a review. *Ear Hear.* 30, 151–159. doi: 10.1097/AUD.0b013e3181987080

Kujawa, S. G., and Liberman, M. C. (2009). Adding insult to injury: cochlear nerve degeneration after "temporary" noise-induced hearing loss. *J. Neurosci.* 29, 14077–14085. doi: 10.1523/JNEUROSCI.2845-09.2009

Le Prell, C. G. (2012). Noise-induced hearing loss: from animal models to human trials. *Adv. Exp. Med. Biol.* 730, 191–195. doi: 10.1007/978-1-4419-7311-5_43

Mahendra Prashanth, K. V., and Venugopalachar, S. (2011). The possible influence of noise frequency components on the health of exposed industrial workers–a review. *Noise Health* 13, 16–25. doi: 10.4103/1463-1741.73996

Martin, G. K., Stagner, B. B., and Lonsbury-Martin, B. L. (2006). Assessment of cochlear function in mice: distortion-product otoacoustic emissions. *Curr. Protoc. Neurosci.* Chapter 8:Unit8.21C. doi: 10.1002/0471142301.ns0821cs34

Minami, S. B., Yamashita, D., Ogawa, K., Schacht, J., and Miller, J. M. (2007). Creatine and tempol attenuate noise-induced hearing loss. *Brain Res.* 1148, 83–89. doi: 10.1016/j.brainres.2007.02.021

Moore, B. C. (2004). Testing the concept of softness imperception: loudness near threshold for hearing-impaired ears. *J. Acoust. Soc. Am.* 115, 3103–3111. doi: 10.1121/1.1738839

Müller, M., and Smolders, J. W. (2005). Shift in the cochlear place-frequency map after noise damage in the mouse. *Neuroreport* 16, 1183–1187. doi: 10.1097/00001756-200508010-00010

Müller, M., von Hünerbein, K., Hoidis, S., and Smolders, J. W. (2005). A physiological place-frequency map of the cochlea in the CBA/J mouse. *Hear. Res.* 202, 63–73. doi: 10.1016/j.heares.2004.08.011

Murillo-Cuesta, S., Camarero, G., González-Rodríguez, A., De La Rosa, L. R., Burks, D. J., Avendano, C., et al. (2012). Insulin receptor substrate 2 (IRS2)-deficient mice show sensorineural hearing loss that is delayed by concomitant protein tyrosine phosphatase 1B (PTP1B) loss of function. *Mol. Med.* 18, 260–269. doi: 10.1016/s1096-6374(12)60045-8

Murillo-Cuesta, S., García-Alcántara, F., Vacas, E., Sistiaga, J. A., Camarero, G., Varela-Nieto, I., et al. (2009). Direct drug application to the round window: a comparative study of ototoxicity in rats. *Otolaryngol. Head Neck Surg.* 141, 584–590. doi: 10.1016/j.otohns.2009.07.014

Nordmann, A. S., Bohne, B. A., and Harding, G. W. (2000). Histopathological differences between temporary and permanent threshold shift. *Hear. Res.* 139, 13–30. doi: 10.1016/s0378-5955(99)00163-x

Ohlemiller, K. K. (2006). Contributions of mouse models to understanding of age- and noise-related hearing loss. *Brain Res.* 1091, 89–102. doi: 10.1016/j.brainres.2006.03.017

Ohlemiller, K. K. (2008). Recent findings and emerging questions in cochlear noise injury. *Hear. Res.* 245, 5–17. doi: 10.1016/j.heares.2008.08.007

Ohlemiller, K. K., and Gagnon, P. M. (2007). Genetic dependence of cochlear cells and structures injured by noise. *Hear. Res.* 224, 34–50. doi: 10.1016/j.heares.2006.11.005

Ohlemiller, K. K., Rybak Rice, M. E., Rellinger, E. A., and Ortmann, A. J. (2011). Divergence of noise vulnerability in cochleae of young CBA/J and CBA/CaJ mice. *Hear. Res.* 272, 13–20. doi: 10.1016/j.heares.2010.11.006

Ohlemiller, K. K., Wright, J. S., and Heidbreder, A. F. (2000). Vulnerability to noise-induced hearing loss in 'middle-aged' and young adult mice: a dose-response approach in CBA, C57BL and BALB inbred strains. *Hear. Res.* 149, 239–247. doi: 10.1016/s0378-5955(00)00191-x

Ou, H. C., Bohne, B. A., and Harding, G. W. (2000a). Noise damage in the C57BL/CBA mouse cochlea. *Hear. Res.* 145, 111–122. doi: 10.1016/s0378-5955(00)00081-2

Ou, H. C., Harding, G. W., and Bohne, B. A. (2000b). An anatomically based frequency-place map for the mouse cochlea. *Hear. Res.* 145, 123–129. doi: 10.1016/s0378-5955(00)00082-4

Park, S. N., Back, S. A., Park, K. H., Seo, J. H., Noh, H. I., Akil, O., et al. (2013). Comparison of functional and morphologic characteristics of mice models of noise-induced hearing loss. *Auris Nasus Larynx* 40, 11–17. doi: 10.1016/j.anl.2011.11.008

Popelar, J., Grecova, J., Rybalko, N., and Syka, J. (2008). Comparison of noise-induced changes of auditory brainstem and middle latency response amplitudes in rats. *Hear. Res.* 245, 82–91. doi: 10.1016/j.heares.2008.09.002

Riquelme, R., Cediel, R., Contreras, J., la Rosa Lourdes, R. D., Murillo-Cuesta, S., Hernandez-Sanchez, C., et al. (2010). A comparative study of age-related hearing loss in wild type and insulin-like growth factor I deficient mice. *Front. Neuroanat.* 4:27. doi: 10.3389/fnana.2010.00027

Rivera, T., Sanz, L., Camarero, G., and Varela-Nieto, I. (2012). Drug delivery to the inner ear: strategies and their therapeutic implications for sensorineural hearing loss. *Curr. Drug Deliv.* 9, 231–242. doi: 10.2174/156720112800389098

Rybalko, N., Bureš, Z., Burianová, J., Popelář, J., Grécová, J., and Syka, J. (2011). Noise exposure during early development influences the acoustic startle reflex in adult rats. *Physiol. Behav.* 102, 453–458. doi: 10.1016/j.physbeh.2010.12.010

Satoh, H., Billings, P., Firestein, G. S., Harris, J. P., and Keithley, E. M. (2006). Transforming growth factor beta expression during an inner ear immune response. *Ann. Otol. Rhinol. Laryngol.* 115, 81–88. doi: 10.1177/000348940611500112

Scheidt, R. E., Kale, S., and Heinz, M. G. (2010). Noise-induced hearing loss alters the temporal dynamics of auditory-nerve responses. *Hear. Res.* 269, 23–33. doi: 10.1016/j.heares.2010.07.009

Sherlock, L. P., and Formby, C. (2005). Estimates of loudness, loudness discomfort and the auditory dynamic range: normative estimates, comparison of procedures and test-retest reliability. *J. Am. Acad. Audiol.* 16, 85–100. doi: 10.3766/jaaa.16.2.4

Sliwinska-Kowalska, M., and Davis, A. (2012). Noise-induced hearing loss. *Noise Health* 14, 274–280. doi: 10.4103/1463-1741.104893

Strelcyk, O., Christoforidis, D., and Dau, T. (2009). Relation between derived-band auditory brainstem response latencies and behavioral frequency selectivity. *J. Acoust. Soc. Am.* 126, 1878–1888. doi: 10.1121/1.3203310

Syka, J. (2002). Plastic changes in the central auditory system after hearing loss, restoration of function and during learning. *Physiol. Rev.* 82, 601–636. doi: 10.1152/physrev.00002.2002

Vázquez, A. E., Jimenez, A. M., Martin, G. K., Luebke, A. E., and Lonsbury-Martin, B. L. (2004). Evaluating cochlear function and the effects of noise exposure in the B6.CAST+Ahl mouse with distortion product otoacoustic emissions. *Hear. Res.* 194, 87–96. doi: 10.1016/s0378-5955(04)00130-3

Viberg, A., and Canlon, B. (2004). The guide to plotting a cochleogram. *Hear. Res.* 197, 1–10. doi: 10.1016/j.heares.2004.04.016

Wang, Y., Hirose, K., and Liberman, M. C. (2002). Dynamics of noise-induced cellular injury and repair in the mouse cochlea. *J. Assoc. Res. Otolaryngol.* 3, 248–268. doi: 10.1007/s101620020028

Wissel, K., Wefstaedt, P., Miller, J. M., Lenarz, T., and Stöver, T. (2006). Differential brain-derived neurotrophic factor and transforming growth factor-beta expression in the rat cochlea following deafness. *Neuroreport* 17, 1297–1301. doi: 10.1097/01.wnr.0000233088.92839.23

Conflict of Interest Statement: The authors declare that the research was conducted in the absence of any commercial or financial relationships that could be construed as a potential conflict of interest.

Received: 18 December 2014; accepted: 19 January 2015; published online: 16 February 2015.

Citation: Sanz L, Murillo-Cuesta S, Cobo P, Cediel-Algovia R, Contreras J, Rivera T, Varela-Nieto I and Avendaño C (2015) Swept-sine noise-induced damage as a hearing loss model for preclinical assays. Front. Aging Neurosci. 7:7. doi: 10.3389/fnagi.2015.00007

This article was submitted to the journal Frontiers in Aging Neuroscience.

frontiers in Aging Neuroscience

ORIGINAL RESEARCH
published: 19 May 2015
doi: 10.3389/fnagi.2015.00071

Nanoparticle mediated drug delivery of rolipram to tyrosine kinase B positive cells in the inner ear with targeting peptides and agonistic antibodies

Rudolf Glueckert[1,2], *Christian O. Pritz*[1,3], *Soumen Roy*[1†], *Jozsef Dudas*[1*] and *Anneliese Schrott-Fischer*[1]

[1] Department of Otolaryngology, Medical University of Innsbruck, Innsbruck, Austria, [2] University Clinics of Innsbruck, Tiroler Landeskrankenanstalten GmbH-TILAK, Innsbruck, Austria, [3] Department of Genetics, Institute of Life Sciences, Hebrew University of Jerusalem, Jerusalem, Israel

OPEN ACCESS

Edited by:
Isabel Varela-Nieto, Consejo Superior Investigaciones Científicas, Spain

Reviewed by:
Miguel A. Merchán, University of Salamanca, Spain
Michaël R. Paillasse, Affichem SA, France

***Correspondence:**
Jozsef Dudas, Department of Otolaryngology, Medical University of Innsbruck, Anichstr. 35, A-6020 Innsbruck, Austria
jozsef.dudas@i-med.ac.at

†Present Address:
Soumen Roy, Trinchieri Lab, Laboratory of Experimental Immunology, Cancer and Inflammation Program, National Cancer Institute, National Institutes of Health, Bethesda, MD, USA

Received: 09 February 2015
Accepted: 20 April 2015
Published: 19 May 2015

Citation:
Glueckert R, Pritz CO, Roy S, Dudas J and Schrott-Fischer A (2015) Nanoparticle mediated drug delivery of rolipram to tyrosine kinase B positive cells in the inner ear with targeting peptides and agonistic antibodies. Front. Aging Neurosci. 7:71. doi: 10.3389/fnagi.2015.00071

Aim: Systemic pharmacotherapies have limitation due to blood-labyrinth barrier, so local delivery via the round window membrane opens a path for effective treatment. Multifunctional nanoparticle (NP)-mediated cell specific drug delivery may enhance efficacy and reduce side effects. Different NPs with ligands to target TrkB receptor were tested. Distribution, uptake mechanisms, trafficking, and bioefficacy of drug release of rolipram loaded NPs were evaluated.

Methods: We tested lipid based nanocapsules (LNCs), Quantum Dot, silica NPs with surface modification by peptides mimicking TrkB or TrkB activating antibodies. Bioefficacy of drug release was tested with rolipram loaded LNCs to prevent cisplatin-induced apoptosis. We established different cell culture models with SH-SY-5Y and inner ear derived cell lines and used neonatal and adult mouse explants. Uptake and trafficking was evaluated with FACS and confocal as well as transmission electron microscopy.

Results: Plain NPs show some selectivity in uptake related to the *in vitro* system properties, carrier material, and NP size. Some peptide ligands provide enhanced targeted uptake to neuronal cells but failed to show this in cell cultures. Agonistic antibodies linked to silica NPs showed TrkB activation and enhanced binding to inner ear derived cells. Rolipram loaded LNCs proved as effective carriers to prevent cisplatin-induced apoptosis.

Discussion: Most NPs with targeting ligands showed limited effects to enhance uptake. NP aggregation and unspecific binding may change uptake mechanisms and impair endocytosis by an overload of NPs. This may affect survival signaling. NPs with antibodies activate survival signaling and show effective binding to TrkB positive cells but needs further optimization for specific internalization. Bioefficiacy of rolipram release confirms

LNCs as encouraging vectors for drug delivery of lipophilic agents to the inner ear with ideal release characteristics independent of endocytosis.

Keywords: inner ear, drug delivery, BDNF-TrkB signaling, rolipram, lipid core nanocapsules, polymerosom nanoparticles, quantum dot nano-suspensions, silica nanoparticle, explant culture

Introduction

Background

The problem of hearing impairment is growing. British MRC Institute of Hearing Research (www.hear-it.org, 2011) estimates that the total number of people suffering from hearing loss of more than 25 dB will exceed 700 million by 2015. Systemic pharmacological intervention to treat sensorineural hearing loss suffers to show significant effects. Due to the demographic development in all western countries age related hearing loss can be expected to increase continuously over the next decades. Effective pharmaceutical treatments are rare.

The isolated anatomical position, a blood-labyrinth barrier and low blood flow may be reasons that drugs do not reach therapeutic levels in the inner ear. Local inner ear treatment via the round window membrane (RWM) seems to be an effective natural pathway for drug application. Intratympanic administration of insulin like growth factor 1 (IGF-1) (Nakagawa et al., 2014) to treat sudden sensorineural hearing loss shows some promising results, studies of glucosteroids applied that way differ in their significance (Spear and Schwartz, 2011; Ng et al., 2014). New strategies for preserving low frequency hearing after cochlear implantation raise growing needs to protect sensorineural cells from trauma with effective treatments. There are candidate drugs that show efficacy to restore damage of the sensory receptor and spiral ganglion neurons (SGNs). Inhibition of caspases prevents or delays hair cell death and may preserve hearing/balance function (Wang et al., 2003; Cheng et al., 2005; Dinh and Van De Water, 2009) and neurotrophic factors have been shown to restore synaptic connection after noise trauma and promote neuron outgrowth after deafferenciation (Glueckert et al., 2008) as well as neural survival (Pettingill et al., 2011). Inhibition or scavenge of reactive oxygen species is another strategy to meliorate cell damage (Henderson et al., 2006; Yamasoba et al., 2013). Another putative therapeutic to provide anti-apoptotic signaling is rolipram, a posphodiesterase 4 inhibitor which affects neuronal survival via proteinkinase-A-mediated increase in cAMP responsive element binding protein activity and the expression of downstream targets as brain-derived neurotrophic factor (BDNF) and its high affinity receptor tropomyosin receptor kinase B (TrkB) (Asanuma et al., 1996; Nibuya et al., 1996).

Nanoparticle Mediated Drug Delivery (NPDD)

Nanoparticles (NPs) as vehicles to reach target cells in the inner ear may overcome limitations of pharmaceutical formulations and specifically target certain cell types. Some drugs show severe side effects (Suckfuell et al., 2007; Weissmiller and Wu, 2012), solubility, and stability may be poor (Gupta and Dixit, 2011), here NPs may act as a versatile tool to avoid off target effects on healthy tissue. Several NPs have been found to cross the RWM barrier (Moss and Wong, 2006; Roy et al., 2012; Liu et al., 2013), this is a prerequisite for atraumatic penetration of the inner ear. Fluid pathways in the cochlea (Rask-Andersen et al., 2006; Salt and Plontke, 2009) and *in vivo* experiments with NPs showed the feasibility to reach target structures via this route such as the sensory epithelium and SGNs (Tamura et al., 2005; Buckiova et al., 2012). Passive diffusion as well as magnetic force enhancement for paramagnetic NPs was reported to reach at least the basal portion of the cochlea (Tamura et al., 2005; Ge et al., 2007; Du et al., 2013). Cell-NP interactions largely depend on particles' physicochemical properties including surface charge, size, shape as well as surface chemistry that builds up the protein corona with body fluids under *in vivo* conditions (Shang et al., 2014) and adds new biological properties. Multivalent attachment of small molecules or antibodies adsorbed to the NP surface that interact with membrane associated proteins may activate cell's uptake machinery to internalize the particles. Cell specific internalization with drug bioefficacy and biosafety of the nanocarrier is the final aim. Within a European Union Consortium called "NanoEar" (contract nr. NMP-20043-.4.1.51-1) several NPs were developed to selectively target sensorineural structures within the cochlea as vehicles for future pharmacotherapies. Some results are presented here.

TrkB as Target for NPDD

In the inner ear SGNs are an indispensable element for the signal transduction from the hair cell to the brain (Bibel and Barde, 2000; Rubel and Fritzsch, 2002). In pathologic conditions, these cells are prone to cell death. For that reason, the preservation of those cells is paramount and renders these cells a target for NPDD. There is a neurotrophic relationship between hair cells and supporting cells, both providing neurotrophins, and SGNs, receiving the neutrophins (Zilberstein et al., 2012). Supplementation of BDNF and neurotrophin 3 (NT-3) after hair cell loss and subsequent damage to the supporting cells leads to a higher survival rate of SGNs (Deng et al., 2004; McGuinness and Shepherd, 2005; Wang and Green, 2011). Especially the TrkB is of particular interest because as alternative to BDNF, there is a number of agonistic molecules including antibodies (Cazorla et al., 2011) that circumvent the low stability of the BDNF protein. Since TrkB is expressed in adult human SGNs (Liu et al., 2011) and adult as well as developing mice inner ears (Bitsche et al., 2011), TrkB is an ideal target for NPDD targeting the SGNs. On the one hand, TrkB can act as label for SGNs to mediate specific binding and endocytosis of the NPDD. On the other hand, TrkB itself can be activated by an agonistic surface modification and thus contribute to mitogen-activated

protein kinase (MAPK), AKT and phospholipase C γ (PLCγ)-mediated neuronal survival signaling (Klein et al., 1989, 1993; Minichiello et al., 1998; Atwal et al., 2000; Watson et al., 2001; Mizoguchi and Nabekura, 2003; Gruart et al., 2007). In parallel the NPDD is still capable of delivering an anti-apoptotic drug such as rolipram (Meyer et al., 2012). Co-application of BDNF and rolipram strongly enhances the survival promoting effect of BDNF (Kranz et al., 2014). BDNF and rolipram may also stimulate the pro-apoptotic low affinity p75 receptor in parallel, so excessive stimulation needs to be prevented, as too much of pro survival signals may lead to tumorgenesis (Geiger and Peeper, 2007).

Targeting Ligands

Conjugated targeting ligands and other surface modifications on NPs serve various purposes like to mediate the permeation through epithelia, to activate signaling cascades, and to mediate the specific uptake in distinct cell populations. Ligands include small molecules, peptides, protein domains, antibodies, and nucleic acid aptamers, with all classes having unique attributes reviewed previously (Friedman et al., 2013). Conjugating targeting ligands such as in terms of surface modifications, antibodies have already demonstrated in several fields to function when surface-grafted (Beduneau et al., 2008; Ulbrich et al., 2009; Choi et al., 2011; Fiandra et al., 2013). For extracellular TrkB activation, the agonistic anti-TrkB antibody from clone 6B10 (NB110-94149) Novus Biologicals antiTrkB mouse monoclonal (at 1 $mg.ml^{-1}$ corresponds to 6.84 μM) was used to test TrkB activation in SH-SY5Y-G7 cells (passage 3). The agonistic anti-TrkB antibody 29D7 (Wyeth Research, Pfizer, Connecticut, USA) has already been shown to bind and activate TrkB when surface grafted to iron NPs (Steketee et al., 2011). Therefore, the use of 29D7 might be an appropriate means to establish an NPDD specifically targeting and activating SGN membrane resident TrkB. Here 29D7 monoclonal TrkB antibody-surface grafted 50 nm silica NPs (aTrkB NP) were used to assess the functionality of the antibody surface-modification to bind and activate TrkB in the HEI-OC1 and VOT-N33 cell culture model. The binding of TrkB by the immuno-NP in the cochlea and the localization after application was further tested in cochlea whole-organ-culture. Much smaller than antibodies short homing peptides offer several advantages such as high packing density, less immunogenicity and often higher purity, though design can be challenging. Typically these peptides are identified via the screening tool phage display (Kehoe and Kay, 2005; Deutscher, 2010), allowing selection of peptide sequences with increased affinities to a specific target of choice displayed on bacteriophage capsids that are collected and amplified with infected *E. coli*. Numerous sequences have been tested (Friedman et al., 2013), we designed peptides based on Ma et al. (2003) and summarized here (Ranjan et al., 2012).

Material and Methods

Nanocarriers and Ligands

Polymerosomes, lipid core nanocapsules (LNCs), silica as well as quantum dot NPs (QDotNPs) were used for the presented study. Peptide ligands are summarized in **Figure 5** and described previously (Ranjan et al., 2012). 29D7 monoclonal anti-TrkB-antibody was kindly provided by Wyeth Research, Pfizer®, Connecticut, USA and characterized previously (Steketee et al., 2011).

Polymerosomes: Amphiphilic block copolymers can self-assemble into polymersome NPs in an aqueous environment. Polymersomes are vesicular, nano-sized spheres that encapsulate an aqueous solution. The synthetic amphiphilic block copolymers consist of hydrophilic and hydrophobic units joined together. Poly lactic/glycolic acid is a charged biodegradable copolymer composed of lactic and glycolic acid monomers and forms here Polyethylene glycol-block-polycaprolactone (PEG-b-PCL) NPs. NP manufacturing and ligand ligation was described previously (Roy et al., 2010; Pritz et al., 2013b).

Lipid Core Nanocapsule (LNC) structure resembles that of lipoproteins with a lipidic core (triglycerides, mineral oils) surrounded by a amphiphilic shell formed by lecithin and stearate of Polyethlenglycol (PEG), where lecithin is located in the inner part of the shell. NPs synthesis and characterization is described here (Bastiat et al., 2013) in detail. Liposomes half-life can be extended by PEG-derivatized lipids (Uster et al., 1996).

Mesoporous **silica NPs** display high specific pore volume and surface area for high drug loadings. Particle size can be controlled more precisely and functionalization with different surface modification and tags make them ideal for imaging purposes. NPs were 50 nm in diameter and manufactured by MicroMod®, Rostock Germany and described previously (Pritz et al., 2013a), FITC fluorochrome served as visualization agent. 29D7 monoclonal anti-TrkB-antibody (Wyeth Research, Pfizer) surface-grafted silica NPs (42-36-501; S08412, MicroMod®) and bovine serum albumin (BSA) surface-grafted silica NPs (BSA-NP) (42-21-501; S08912, MicroMod®) were tested.

Quantum Dot NPs are made from emulsions, containing iron oxide, and quantum dots, they are composite NPs composed of two block copolymers, PLLA-mPEG: Poly(L-lactic acid)-block-poly(ethylene glycol). We investigated the internalization efficiency of these particles in neuronal-like cell cultures and cochlear explants. These NPs were manufactured by the Division of Functional Materials at the Royal Institute of Technology, Stockholm, Sweden, are biodegradable and resorbable with a hydrodynamic diameter of 423 (± 8) nm for orange QDotNPs and 200 (± 15) nm for green QDotNPs. CdO powder (Fluka) is added to a mixed solvent system containing 1-octadecene (Aldrich) and oleic acid (Sigma Aldrich), and heated at 160°C under nitrogen for 1 h, to obtain cadmium oleate. This is stored under nitrogen, and is usable for 2 weeks. Se powder is added to a mixed solvent system containing TOP (Trioctylphosphine, Fluka) and 1-octadecene and heated at 250°C under nitrogen for 1 h, to obtain trioctylphosphine selenide (TOPSe, Aldrich). This is stored under nitrogen and is usable for 2 weeks. In a typical synthesis, cadmium oleate is added to 1-octadecene and oleylamine (Fluka) in a 3-necked flask and the mixture is heated to 250°C under nitrogen. At this temperature, TOPSe is injected into this mixture. Depending on the desired size of the QDots, this reaction is stopped at variable times (typically ranging from 20 to 1800 s), by injecting

excessive amount of solvent at room temperature. QDots are a very stable fluorochrome and ideal for imaging purposes. Because of their extremely small size and optical resolution, they are also well suited for tracking the molecular dynamics of intracellular and/or intercellular molecular processes over long time scales (Pathak et al., 2006). Orange Quantum dots: CdSe/CdS quantum dots (with orange emission) were payloaded within the NPs, where PLGA: poly(lactic-co-glycolide) is used as a matrix material and carboxylic group as a surface. Green Quantum dots: CdSe/CdS quantum dots (with green emission) were payloaded within the NPs, where PLLA-mPEG: poly(L-lactic acid)-block-poly(ethylene glycol) is used as a matrix material and PEG as a surface. Characterization of CdSe quantum dots: A sample of NP suspension is characterized by ultraviolet and visible spectroscopy, and photoluminescence spectroscopy by depositing 1 ml of suspension in a polymethyl methacrylate cuvette at room temperature. Transmission electron microscope (TEM) analysis was performed after depositing one drop of NP suspension on a copper grid coated with formvar and carbon and letting to dry.

Cell Culture

HEI-OC1 cells were isolated by Dr. Federico Kalinec (Yorgason et al., 2010) and are used as a model for TrkB positive cells in the inner ear, when cultured under 33°C and 10% CO_2. Furthermore, after differentiation at 39°C and 5% CO_2 these cells represent a model for inner and outer hair cells of the mouse cochlea. Cells were grown as described previously (Pritz et al., 2013a). For size dependent uptake cells were plated on 21 × 26 mm cover slips. The cover slips were placed into 6-well plates; cells were plated at 10^4/ml. NP treatment occurred usually 24 h after plating. NPs were used in 500-, 1500- and 15,000- fold final dilution. For antibody coated silica NPs cells were plated 12 h before the start of the experiment. Cells were incubated with 9.5×10^9 NP.ml^{-1} 29D7 monoclonal TrkB-antibody (Wyeth Research, Pfizer) surface-grafted silica NPs (42-36-501 S08412, MicroMod®, Rostock Germany) and BSA surface-grafted silica NPs (42-21-501 S08912, MicroMod®). Each particle type was tested in two different conditions creating a competitive assay: binding and blocking conditions. Binding conditions: Cells were incubated with NPs at pH 7.4 in serum-free conditions in Dulbecco's Modified Eagle (DMEM) low-glucose Medium (E15-005 PAA Pasching, Austria) for 90 min. Blocking conditions: Cells were incubated with NPs at pH7.4 together with free 29D7 monoclonal TrkB-antibody (Pfizer®, USA) in 1 nM concentration (63-fold excess) for 90 min. The experiment was carried out at 4°C to prevent endocytosis and at 33°C the culturing temperature of the cells to permit endocytosis. According experiments were performed with BSA-grafted silica-NPs under same conditions. In each group 15–20 cells were analyzed.

The auditory neuroblast cell line **US/VOT-N33 (N33)**, which is conditionally immortal, was kindly provided by Matthew Holley and shall serve as an *in vitro* model for SGNs. Culture conditions were described previously (Nicholl et al., 2005). In brief, cells are grown in minimum essential medium (MEM) containing 10% fetal calf serum at 33°C, 10% CO_2 and after 3 h serum deprivation used for experiments. Antibody coated silica NPs were applied like with HEI-OC1 cells.

The **neuroblastoma cell line SH-SY5Y** was differentiated by all-trans-retinoic acid (ATRA) treatment that induces expression of TrkB, but not of TrkA receptor, and mediates biological responsiveness to receptors for the neurotrophins BDNF and NT-4/5 as described previously by our group (Ranjan et al., 2012). As an alternative to SH-SY5Y cells, **stable TrkB-transfected G7** cells were received from Garrett Brodeur, M.D. (Children's Hospital of Philadelphia, Philadelphia, Pennsylvania, USA) and maintained and cultured as referenced (Eggert et al., 2002). TrkB overexpressing SH-SY5Y cells were grown in the presence of the selection antibiotic as described elsewhere (Soumen et al., 2012). Cells were plated 12 h before the start of the experiment. Cells were serum starved for 3 h. Then cells were incubated with 5.5 nM BDNF, 1.9×10^{10} NP.ml^{-1} immuno-NP, 1.9×10^{10} NP.ml^{-1} immuno-NP and 9.5×10^9 NP.ml^{-1} BSA-NP for 90 min. Cells were rinsed three times in Tris-buffered saline (TBS) buffer and subsequently harvested with a cell scraper and lysed in lysis buffer (1% v/v NP-40, 50 mM Tris pH 8, 150 mM NaCl, 5 mM ethylenediaminetetraacetic acid (EDTA)). Protein quantification was subsequently performed by a Bradford assay (500-0001, BioRad, Vienna, Austria), at 595 nm using a BioPhotometer Plus (Eppendorf® Germany, Wien, Austria).

Western Blotting

Fifteen microgram of protein lysate was loaded in each slot. SDS-PAGE was carried out at 20 mA for 1 h in a 12% bisacrylamid gel using a Mighty Small II Deluxe Mini Vertical Electrophoresis Unit (SE260, Hoefer, Holliston, USA). Protein was subsequently transferred to a PVDF membrane (88518, Thermo Scientific®, Waltham USA) using a Maxi-BlotTank fully wet blotter (340.000, GP Kunststofftechnik, Germany) at 60 mA for 4 h at 4°C. Membranes were subsequently stained with anti-phospho-Erk1/2 antibody (#9101 Cell Signaling Technologies) in 1:1000 dilution and goat anti rabbit horseradish peroxidase (HRP) conjugated (31460, Thermo Scientific®) in 1:10 K dilution as described in detail in Wiedemann et al. (2006). Signal detection was performed by enhanced chemiluminescence using SuperSignal West Dura Chemilumenescent Substrate (37071,Thermo Scientific®) and CL-Xposure X-Ray films (34091, Thermo Scientific®). X-Ray films were subsequently scanned.

Organotypic Culture and Zero-gravity Whole Organ Culture of the Cochlea

Organotypic mouse culture was performed on neonatal P1–P3 mouse cochleae as described previously (Roy et al., 2010). Zero-gravity whole organ culture of adult cochlea was done with P18–P30 mice anesthetized by intraperitoneal injection of ketanmin hydrochlroid (84 μg.g^{-1} bodyweight, Ketasol® Graeub Veterinary Products, Bern Switzerland), 0.25 μg.g^{-1} bodyweight atropine sulfate (Atropium Sulfaticum, Nycomed® Austria GmbH, Linz, Austria), and 6.7 mg.g^{-1} bodyweight xylazin (Bayer® Healthcare, Berlin, Germany) in physiologic saline and subsequently killed by cervical dislocation. The cochleae were removed from the scull. All animal experiments

were approved by the Austrian Ministry of Science and Research and conformed to the Austrian guidelines on animal welfare and experimentation (BMWF-66011/0109-II/3b/2012). Stapes, RWM as well as the bone covering the apical portion of the cochlea and 270° along the basal turn covering the scala tympani was removed. The dissected cochleae were then transferred to culturing medium pre-warmed to 37°C. The culturing medium was composed of 100 $U.ml^{-1}$ penicillin (P7794-10MU, Sigma Aldrich, Vienna, Austria), B27 supplement (17504044, Invitrogen, Lofer, Austria), 5 mM L-glutamine (BE 17-505E, Lonza), Neurobasalmedium (21103-049, Invitrogen) at pH 7.4. The culturing was performed in a rotary cell culture system (RCCS-4SC, Synthecon® Incorporated, Housten, USA) in 10 ml disposable HARV-10 vessels (Synthecon® Incorporated) for 2 h. The culturing medium was then supplemented with 9.5×10^9 aTrkB NPs for immuno-conjugate NPs for 24 h or LNC particles loaded with rolipram as described by Meyer et al. (2012). LNCs were provided in a concentration of 4×10^{15} particles/ml with a hydrodynamic diameter of 52 ± 5 nm. 1:100 and 1:1000 dilution of LNC particles loaded with 2 μM rolipram with adding 50 μM cisplatin to the culture medium were tested in comparison with 50 μM cisplatin and culture medium alone for 24 and 48 h.

Processing of Cultured Cochleae

After culturing, cochleae were washed in phosphate buffered saline (PBS) and subsequently fixed in 2% paraformaldehyde in PBS overnight at 4°C. The specimens were decalcified using 20% EDTA in PBS for 4 h at 37°C. Specimens were then infiltrated by in an ascending series of 10 and 15% D-sucrose in PBS, and finally a mixture of 15% D-sucrose and 50% OCT-compound (4583, Tissue-Tek®, Finetek Sakura® Europe, Leiden, Netherlands). Final infiltration was performed in 100% OCT®-Compound overnight. Cochleae were rapidly frozen in OCT®-compound at −78°C as in a 1 + 1 EtOH:dry ice mixture. One half of the frozen cochleae were subsequently cryo-sectioned in 10 μm sections. The other half of the cochleae were thawed and post fixed in 2% glutaraldehyde in PBS at pH 7.4. Cochleae were than incubated in 1% OsO_4 for 1 h at 4°C in 0.05 M cacodylate buffer. Specimen were then dehydrated in an ascending EtOH series and embedded in Epon 812 (Electron Microscopy Science, Hatfield, UK, 14120) as described elsewhere (Thaler et al., 2011; Pritz et al., 2013a).

Immunostaining

Cell culture: early endosome antigen (EEA1) and lysosomal-associated membrane protein (LAMP-1) staining was performed as described previously (Pritz et al., 2013a). Rotary culture sections: After 3 × 5 min in PBS blocking and permeabilization (1 h 1% BSA and 5% normal goat serum in PBS + 0.05% Tween 20 at 4°C) primary antibodies rabbit-anti cleaved caspase-3 (CC3) 1:400, (Asp175, Cell signaling 9661L) Abcam® rabbit polyclonal anti-beta-III-Tubulin ab 1:200 or rabbit IgG isotype control was applied for 1 h at 4°C. After thorough wash in PBS, 2nd antibody Alexa® Fluor 647 F(ab')2 fragment goat anti rabbit (111-606-047, Jackson Immunoresearch®, PA, USA) 1:1500 in 0.5% (w/v) BSA was incubated overnight at 4°C in dark and subsequently 30 min 37°C and mounted with Vectashield® including DAPI (Vector Laboratories® Ltd, UK). Phalloidin FITC (Sigma® P5282; 1:80) was applied according to the manufacturer's protocol. Control samples were substituted with isotype matching rabbit immunoglobulins (rabbit polyclonal IgG Abcam®, ab27478, 1:200). These controls were consistently negative.

Confocal Microscopy

NP treated cells were illuminated by a 488 nm laser, at pinhole = 3 AU, resulting fluorescence was collected between 505 and 545 nm. Cochlea sections and NP treated cells were examined using Zeiss® LSM510 Meta (Zeiss®, Oberkochen Germany) using ZEN 2009. FITC was excited by 488 nm laser. For pairwise comparison of NP binding cells were imaged with a pinhole of 3 AU, illumination by a 488 nm laser, resulting fluorescence was collected from 505 to 545 nm. Due to the high autofluorescence in adult cochlea explant sections, the FITC in NPs was detected using lambda stacks from 490 to 700 nm. To distinguish FITC fluorescence from autofluorescence ratiometric detetection was performed. Fluorescence at 520 nm was divided by 565 nm. Alexa 647 was excited with a 633 nm Laser and detected with 650 bandpass filter, DAPI excited with 405 nm laser as described previously (Glueckert et al., 2008).

Transmission Electron Microscopy

For electron microscopy, epon blocks were sectioned to 80 nm sections. Electron microscopy was performed using a Zeiss® Libra 120 EFTEM (ZEISS, Oberkochen, Germany) as described in Pritz et al. (2013a) and Thaler et al. (2011).

Flow Cytometry

SHSY5Y cells were grown in DMEM/F12 1:1 medium (PAA, Linz, Austria) supplemented with 2 mM L-glutamine, penicillin (20 units/ml), streptomycin (20 mg/ml), and 15% (v/v) heat-inactivated fetal calf serum (PAA®) (Ranjan et al., 2012). Cells were maintained at 37°C in a saturated humidity atmosphere containing 95% air and 5% CO_2. Cells were seeded at an initial density of 10^4 cells/cm^2 in culture dishes (Unilab®, Innsbruck, Austria). All-trans-RA (Sigma®, Darmstadt, Germany) was added on the day of plating at a final concentration of 10 μM in DMEM/F12 with 15% fetal calf serum, and after that, daily. After 5 days in the presence of ATRA, cells were treated with LNC nanoparticles at 50 μg/ml final concentration for 5 or for 24 h, and analyzed by flow cytometry. The prepared LNCs contained Nile Red, which was used as a model of amphiphilic carried drug, and was also detectable by the excitation of the 488 nm laser source in flow cytometry. The particles were prepared without peptide conjugate and with A415, A747, scrambled Scr-A415, and scrambled Scr-A747 peptides, where A415 and A747 were intended as TrkB-targeting peptides, the other two were synthesized with scrambled sequences. The hydrodynamic diameter of the particles ranged 49–58 nm (**Figure 5**). LNCs labeled with Nile Red were intact particles in flow cytometer within the 24 h of experimentation. After the desired incubation period, cells were removed and collected from the culture dishes by trypsinization (PAA®) washed once with serum-containing culture medium and resuspended with Isoton II

sheath (Beckman Coulter®, Brea CA, USA) at 10^6 cells/ml sheath. Cell suspension was observed using a Coulter® XL-MCL flow cytometer (Beckman Coulter®) using the FL-2 channel with excitation of 488 nm and detection of the emission at 560–590 nm. These conditions are optimal for detecting Nile Red in lipid environment, as expected in LNCs (Greenspan and Fowler, 1985). Not stained cells were used as control and showed 0.9–2.1% Nile Red-like signal. These events were used for gating cells in the forward-side scatter scattergrams. The forward-side scatter scattergrams of LNC-incubated cells were comparable with the controls. The FL-2 signal of the LNC-treated cells has shown an increase. Percentage of cells showing increased signal (above the control level) was determined by the software Expo 32 (Coulter®), and was considered as Nile red positive cells.

Statistical Analysis

Experiments were planned as pair wise comparisons between binding and blocking conditions. When normal distribution was detected using Kolmogorov-Smirnov test, unpaired *t*-test was used at an alpha of 5%. When data was not normally distributed and transformation with monotonous functions failed to transform to normal distribution non-parametric tests were used.

Results

NP Uptake in Cochlear Tissue

The interface of LNCs, a highly packed monolayer of surfactants, has been modified by the post-insertion process carried out with pegylated amphiphilic phospholipids. This assay allowed us to introduce reactive amino groups on the surface, easily grafted with Rhodamine B molecules in the matrix material and was applied at a final concentration of 6.45×10^{14} particles/ml. **Figures 1A,B** shows the concentration gradient in different cell types in an organotypic culture of a mouse inner ear 3 days postnatal (P3). Penetration into the cytoplasm was observed all over the explant but enhanced staining was seen in the region of the SGNs, no signal was detected in any cell nuclei. Not the big bipolar neurons but smaller surrounding cells show highest uptake corresponding to satellite glia cells (SGC) that migrate from the neural crest to ensheath all neurons at a later stage of inner ear development. **Figure 1C** illustrates the anatomy of SGNs in a plastic embedded tissue with incomplete sheath of SGC. This depicts some selective nature of these LNC particles to show a preference for a certain cell type at a certain developmental stage.

Size-Dependent Internalization

NP size has a big influence on uptake kinetics and cell type selectivity. We tested different polymerosom NPs with zeta ξ potential = 1 mV and different mean hydrodynamic diameter (MHD) such as N115 (MHD = 70.2 nm), N116 (MHD = 91.2 nm) and N117 (MHD = 111.6 nm) in a concentration range in between 0.05 and 0.25 mg/ml with the different incubation time like as 2, 4, 6, 12 and 24 h in organotypic cultures of P1–P3 mice as described previously (Roy et al., 2010). Uptake of NPs was seen in an increasing time dependent manner from 2 to 24 h (**Figure 2**).

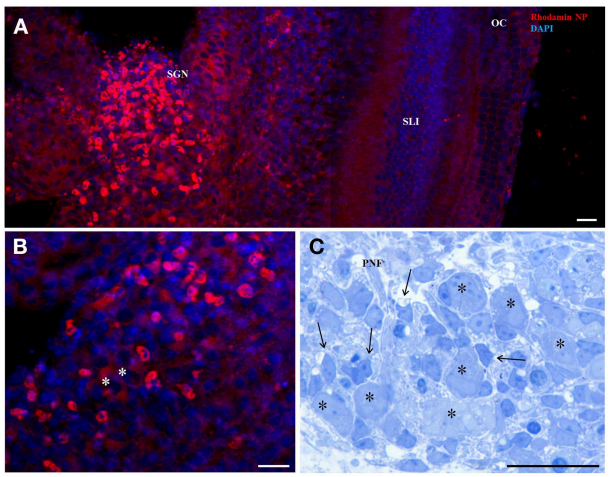

FIGURE 1 | 50 nm Rhodamin labeled LNC NPs without any surface functionalization after 24 h incubation in an organotypic cochlear culture (A,B confocal projection). Panel **(A)** shows higher uptake in in the region of the spiral ganglion neurons (SGN). Panel **(B)** is a magnified view of the SGN region and identifies small cells surrounding the neurons (asterisks) with intense staining. Panel **(C)** corresponds to this region in a semithin section with big type I neurons (asterisks) and satellite glia cells (arrows) that establish the glia sheath of neuron somata. SLI, spiral ligament; OC, organ of Corti; PNF, peripheral nerve fibers. Scale bars **(A)** 50 μm; **(B)** 20 μm; **(C)** 20 μm.

For a more detailed analysis we performed this experiment with LNCs in a size range of 25–100 nm in HEI-OC1 cell lines for 12 h in different dilutions of NPs (**Figure 3**). FITC was incorporated in the shell, neither payload nor ligand was added. After 12 h incubation in different dilutions of LNC25 (MHD = 25.2 nm), LNC50 (MHD = 53.39 nm), LNC100 (MHD = 102.9 nm), every NP tested showed most uptake in 1:200 dilution (see **Figure 3**). Further, the LNC25 was internalized most efficiently. The differences in uptake were even statistically highly significant at 200 fold dilution of NPs (LNC25 vs. LNC50 $p < 0.001$; LNC25 vs. LNC100 $p < 0.001$; LNC50 vs. LNC100 $p = 0.004$, Rank-Sum test, $n$small = 12). In 1500 and 15,000 fold dilution no statistical significant difference in uptake could be observed.

Big QDotNPs (**Figure 4**) were rather selectively found within cells in the spiral ganglion of organotypic cultures (P3). QDot orange as well as QDot green was located within the cytoplasm of cell somata of putative SGCs and SGNs (**Figure 4B**) and some cells in the sensory epithelium (arrowhead, **Figure 4A**), likely macrophage like cells. This result was surprising and suggests an interaction of QDotNPs with neuronal cells at that developmental stage. Since we tested only in an immature model we cannot predict SGNs behavior with mature-by SGC ensheathed-neurons in adult tissue.

Ligand Functionalized Nanocarriers

Small peptides with theoretical binding affinity for TrkB receptor (**Figure 5C**) were tested for specific binding and payload release (Nile red) with LNCs. After 5 days of ATRA treatment SHSY5Y cells were treated with LNC nanoparticles at 50 μg/ml final concentration for 5 or for 24 h, and analyzed by flow cytometry.

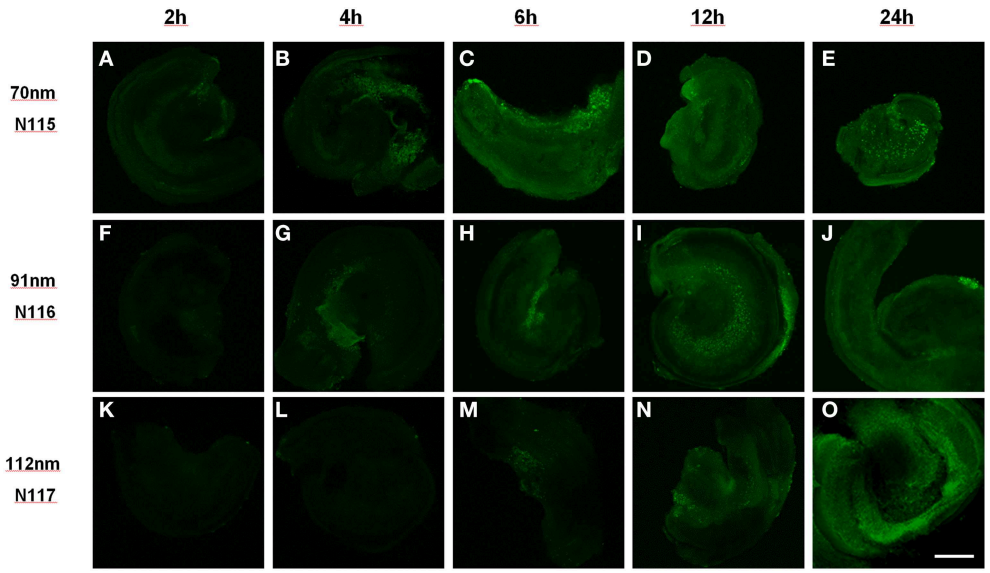

FIGURE 2 | Size dependent uptake of polymerosom NPs of different hydrodynamic diameter (N115 = 70 nm, N116 = 91 nm, N117 = 112 nm) in P3 mouse organotypic culture from 2 to 24 h of incubation: smallest particles show uptake within 2 h while biggest need 6 h. Scale bar 200 μm, **(A–E)** 70 nm , **(F–J)** 91 nm, **(K–O)** 112 nm particles exposed for 2 h **(A,F,K)**, 4 h **(B,G,L)**, 6 h **(C,H,M)**, 12 h **(D,I,N)** and 24 h **(E,J,O)**.

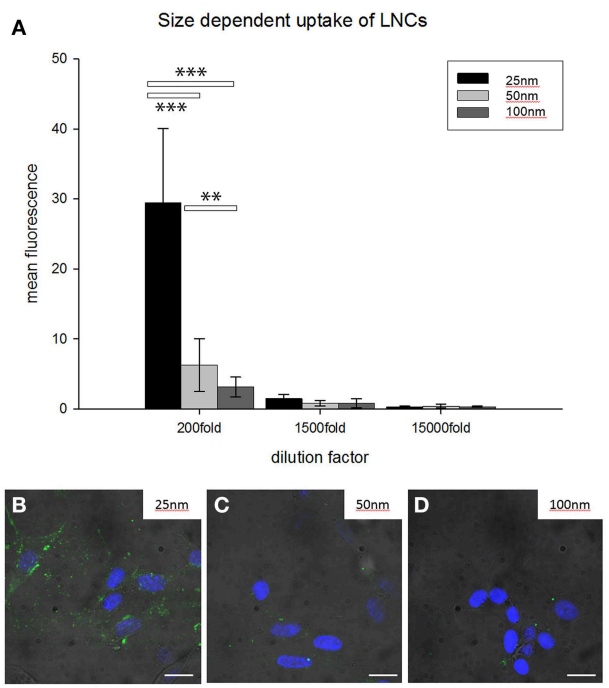

FIGURE 3 | Size-dependent internalization of unfunctionalized FITC-loaded LNCs in HEI-OC1 cells. (A) Bar chart classifies 25 nm-sized NPs to be internalized most efficiently while 100 nm LNCs were internalized with the least efficiency (**$p < 0.01$, ***$p < 0.001$, ANOVA, error bars denote standard deviation). 200–1500 times dilution of LNCs shows significant differences. **(B–D)** Representative examples of HEI-OC1 cells treated with FITC-loaded LNCs (200 times dilution); diameter of LNCs is denoted in the upper right of the micrograph. Green fluorescence is FITC from LNCs, blue fluorescence is DAPI, scale bars 10 μm.

The unconjugated LNC particles were detectable in almost all cells after 5 h (**Figures 5A,C**), which decreased to 77% of the cells after 24 h (**Figures 5B,C**). The peptide conjugated LNC particles were detected in 21–25% of the cells after 5 h and in 43–67% of the cells after 24 h (**Figures 5A–C**). The targeting or control sequence of the peptide did not have significant effect on the detection of Nile Red in the cells ($p > 0.05$, with One-Way ANOVA). Surface functionalization hampered NP/payload uptake in this cell line, peptide sequence did not show a significant effect. This suggests a peptide sequence independent uptake of LNC particles in SHSY5Y cells. Five hour treatment: Data were not normal distributed using the D'Agostino and Pearson omnibus normality test. Comparison of LNC with A415 with LNC with Scr-A415 using Mann-Whitney U-test: $p = 0.1242$.

Twenty four hour treatment: Data were not normal distributed using the D'Agostino and Pearson omnibus normality test. Comparison of LNC with A415 with LNC with Scr-A415 using Mann-Whitney *U*-test: $p = 0.100$.

A415 ligand conjugated polymerosom NP (FITC in the shell) incubated in cochlear explant cultures for 24 h showed some specifity for neuronal cells in the spiral ganglion (**Figures 6B,C**), while scrambled peptide showed same specifity but less uptake (**Figure 6D**, not quantified). Plain polymerosomes showed an even distribution of cellular uptake (**Figure 6A**). Also in this experiment small peptides change the uptake specifity, here a directional uptake into neurons is visible.

Extracellular-activated Kinase Activation with Agonistic TrkB Antibody

In order to assess, the capability to activate TrkB-downstream signaling with an agonistic anti-TrkB antibody, the ERK phosphorylation was assessed by western blotting of treated

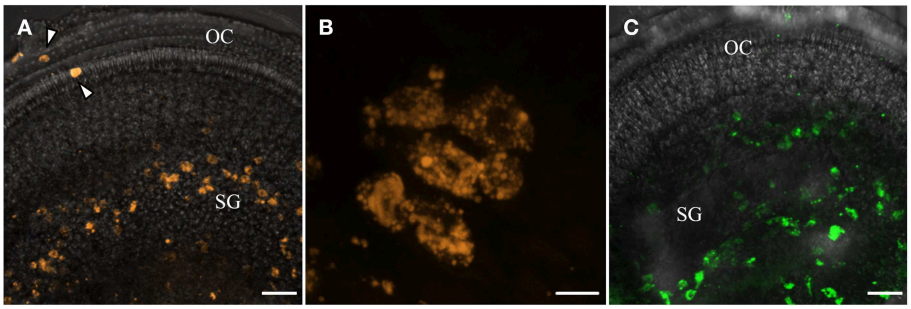

FIGURE 4 | Internalization of plain bigger QDot NPs shows selectivity for cells in the spiral ganglion (SG) in organotypic cultures with QDot orange (A,B) and QDot green NPs (C). Panel **(B)** is a higher magnified view of **(A)** that confirms NPs within the bigger spiral ganglion neuron cytoplasm.

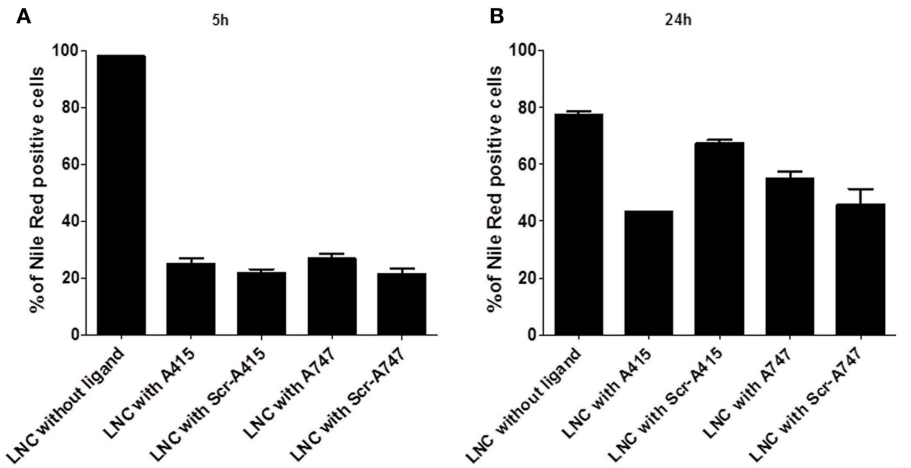

C

			% of Nile red positive cells	
Peptide conjugate	**Sequence**	**NP size, nm**	**in 5h**	**in 24h**
none		49.27	97.98 ± 0.6 %	77.5 ± 2.16 %
A415	CENLYFQSGSMAHPYFAR	57.68	25.13 ± 5.25 %	43.15 ± 0.44 %
Scr-A415	CENLYFQSGAYHMSAPFR	57.31	21.86 ± 3.41 %	67.6 ± 1.49 %
A747	GGGHHHQVYQVRSHWTGMHSGHD	57.34	27.1 ± 4.05 %	54.97 ± 7.34 %
Scr-A747	GGGVSDHQHHTMSHHYQWRHVGG	55.78	21.45 ± 4.96 %	45.77 ± 19.56 %

FIGURE 5 | Flow cytometry results of LNC NP uptake of functionalized TrkB targeting ligands (A415, A747) and scrambled control ligands (Scr-A415, Scr-A747) in comparison with unfunctionalized LNCs after 5 h (A) and 24 h (B) incubation. Nile Red payload is detected in percentage of positive cells, the table in **(C)** summarized peptide sequence, hydrodynamic NP diameter and quantitative flow cytometry data.

TrkB-overexpressing SH-SY5Y G7 cells. Phosphorylated ERK1/2 from SH-SYS5 G7 cells treated with 10 nM BDNF, 10 nM antiTrkB (6B10) and untreated were compared. After 30 min incubation with antiTrkB, slight ERK1/2 phosphorylation is visible (**Figure 7A**, **Table 1**). The phosphorylation is lower than observed with cells treated with 10 nM BDNF but clearly above the basal phosphorylation level.

Silica NP conjugated to 29D7 agonistic antibody (aTrkB NP) also showed effective neurotrophic signaling (**Figure 7B**). TrkB overexpressing SH-SY5Y G7 cells were treated with 5.5 nM BDNF, 1.9 × E10/ml aTrkB NPs, 1.9 × E9/ml aTrkB NPs and 1.9 × E10/mL BSA-linked NPs. 1.9 × E10/mL. aTrkB NPs were able to induce a phosphorylation response comparable to BDNF. When aTrkB NPs were diluted 10-fold the phosphorylation

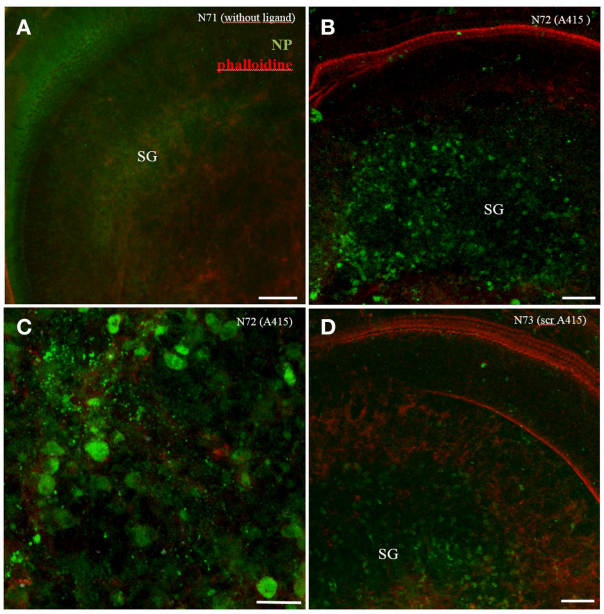

FIGURE 6 | Organotypic culture with A415 peptide functionalized polymerosom NPs after 24 h of incubation. While plain LNCs shows even distribution **(A)**, A415-LNC; **(B,C)** and scrambled A415(scr-A415-LNC); **(D)** reveal aggregation in the spiral ganglion (SG) region. Higher magnified view in **(C)** reveals signals mainly within bigger type I neurons. Phalloidine staining (red) indicates stereocilia positions within the sensory epithelium.

efficiency dropped to the level of the BSA grafted control particles.

When cells were treated with 5.5 nM BDNF (equals 100 ng.ml^{-1}) strong phosphorylation of ERK was induced (**Figure 7B**). A similarly strong phosphorylation was induced by 1.9×10^{10} NPs.ml^{-1} NPs, which carry agonistic TrkB antibodies on their surface immuno-conjugated NP. BSA coated control particle at a concentration of 1.9×10^{10} NP.ml^{-1} were not able to induce a similar magnitude of ERK phosphorylation. Also a 10-fold dilution of the aTrkB NPs resulted in a lower ERK phosphorylation (**Figure 7B**, **Table 2**).

Agonistic TrkB Antibody Binding Tests

Assessment of the binding capability of our immuno-conjugated NPs was performed in competitive assays (**Figures 8A–F**). Cells were exposed to aTrkB NPs alone, allowing specific and unspecific binding (**Figure 8A**) and in a competitive assay with inhibiting specific antibody-mediated binding of the aTrkB NP by an excess of free antibody (**Figure 8B**). When the experiment was performed at 4°C (**Figures 8C,D**), preventing endocytosis, under binding conditions, there were significantly more ($p = 0.001$, rank-sum test) NPs attached to the cells than under blocking conditions (**Figure 8C**). No statistical difference ($p = 0.450$, rank-sum test) was observed when the experiment was performed under identical conditions using BSA-NPs instead of aTrkB NPs (**Figure 8D**). This suggests an involvement of the antiTrkB-surface modification in the binding of the immuno-conjugated NP. When the experiments were performed at 33°C (**Figures 8E,F**), allowing endocytosis, there were more aTrkB NPs found to be associated with the cells than under blocking conditions (**Figure 8E**). However, difference was not significant ($p = 0.126$, rank-sum test). Using control BSA-NP, no significant difference ($p = 0.142$, rank-sum test) between binding and blocking conditions was observed (**Figure 8F**). These results suggest that under given conditions the surface modification is not playing a significant role for the endocytic uptake of immuno-conjugated NPs.

Trafficking of Antibody Conjugated Nanoparticles

aTrkB NPs were also tested for internalization and subcellular localizations in HEI-OC1 (**Figures 9A–H**) and VOT-N33 (**Figures 9I–P**) cells. In both cell lines NPs were found in early endosomes outlined by EEA1 (**Figures 9B,J**) as well as in LAMP1 (**Figures 9F,N**) positive late endosomes/lysosomes. After 1 h of incubation aTrKB-NPs localize in EEA1 positive endosomes in both cell lines and after 90 min in LAMP1 positive late endosomes/lysosomes (**Figures 9A–H**). Like reported previously with unfunctionalized silica NPs (Pritz et al., 2013a) NPs ended in large endosomes with non-overlapping intensity maxima of NP and endosomal marker (**Figures 9L,P**). We found unfunctionalized silica NPs surrounded by big LAMP-1 positive "rings" to resemble single-membrane compartments with multiple particles at TEM level. Since also in these experiments with aTrKB-NPs few NPs were observed in small vesicles, so clathrin or caveolin mediated endocytosis may be low. The big (>500 nm up to several μm) LAMP-1 positive vesicles resemble macropinosomes like we found with unfunctionalized particles at TEM level previously (Pritz et al., 2013a). This suggests that macropinocytosis may be a dominant uptake mechanism, further no evidence for endosomal escape of these nanocarriers was found.

Rotary Culture of NP-treated Inner Ears

When whole-organ-cultures were treated with aTrkB NPs for 2 and 8 h, NPs were found to be distributed throughout the cochlea. NPs were observed in the mesothelial/mesemchymal cells lining the perilymphatic fluid spaces. Dense agglomerations of immuno-conjugated NPs were found in the mesothelial layer of Reissner's membrane (**Figure 10A**) and tympanic covering layer cells underneath the basilar membrane. Infrequently, the aTrkB NPs were observed in the organ of Corti (**Figures 10A,B**) especially in inner hair cells (**Figure 10B**) and even less frequently the immuno-conjugated NPs were observed in the spiral ganglion (not shown). In order to overcome the limitations in spatial resolution of light microscopy electron microscopy was performed (**Figure 10C**). Ultrathin sections were screened for functionalized silica NPs. NPs were found to localize within tympanic covering layer cells of the basiliar membrane (**Figure 10C**). However, both outer and inner hair cells were not associated with NPs investigated at ultrastructural level. The basal pole of hair cells, where TrkB is exposed by the synaptic terminals, was not found to be associated with NPs. Also the endosomal compartment of hair cells was devoid of aTrkB NPs (not shown). Neither near nerve fibers in the lamina ossea spiralis nor within SGNs were particles detected at ultrastructural level. Based upon these observations, quantitative delivery to TrkB-positive cells such as SGNs and hair cells is very unlikely although

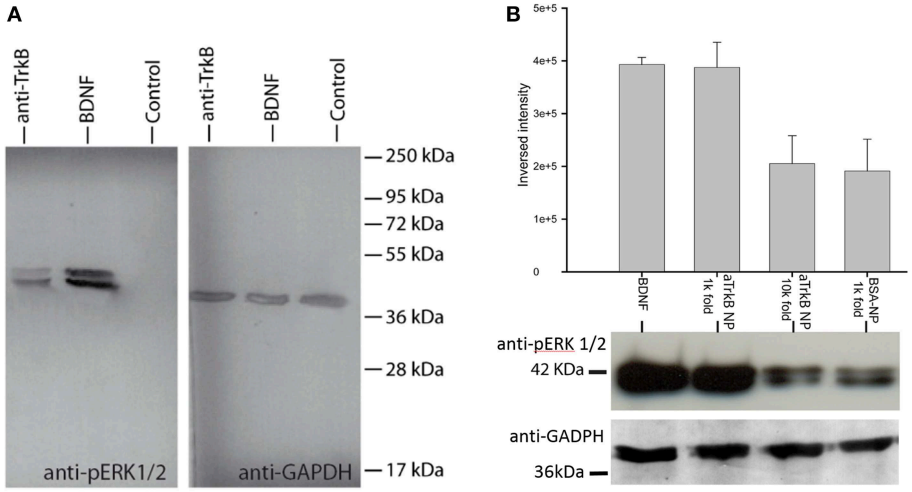

FIGURE 7 | ERK phosphorylation with anti-TrkB-antibody and anti-TrkB-antibody-functionalized silica NPs (aTrkB-NPs). (A) Agonistic anti-TrkB antibodies (6B10) without NPs applied to TrkB-overexpressing SH-SY5Y G7 cells induces ERK phosphorylation equivalent comparable to 5.5 nM BDNF application (10 nM BDNF shown). **(B)** Semi-quantitative comparison of ERK-activation by aTrkB-NPs (29D7) within TrkB-overexpressing SH-SY5Y cells compared to BSA-functionalized NPs: aTrkB-NPs in 1000-fold dilution elicited a similar activation of ERK as observed with 5.5 nM BDNF while BSA-functionalized NPs did not. At 10,000 fold dilution there is no significant difference to basal phosphorylation level. Western blot data are shown below.

TABLE 1 | Densitometric analysis SH-SY5Y G7 treated with anti-TrkB (6B10) antibody vs. BDNF presented as ratio over GAPDH expression.

Treatment	Mean density GAPDH	Mean density pERK	Ratio over GAPDH expression
Anti-TrkB (6B10)	35.002	24.5	0.699960002
BDNF 10 nM	30.477	83.345	2.734685172
Control	39.028	4.14	0.106077688

TABLE 2 | Densitometric analysis SH-SY5Y G7 treated with anti-TrkB (29D7) conjugated silica NP vs. BDNF presented as ratio over GAPDH expression ($N = 4$).

Treatment	Mean-pERK to GAPDH	SD pERK-related GAPDH
BDNF 5.5 nM	0.882019403	0.096842924
aTrkB NPs 1 k fold	0.972157927	0.130999313
aTrkB NPs 10 k fold	0.349104961	0.084694112
BSA-NP 1 k fold	0.698961261	0.00317995

some aggregation in inner hair cells is apparent at confocal level that conforms with TrkB expression in adult mice inner ears (Bitsche et al., 2011). Immunostaining of control adult inner ear cultures affirms the presence of an intact and innervated sensory epithelium (**Figure 10D**).

Rescuing SGNs with Rolipram-Loaded LNCs

Scheper and Colleagues demonstrated (Meyer et al., 2012) that rolipram-loaded LNCs can be used to prevent apoptosis of SGN culture. Here, we employed postnatal rotary culture of whole inner ears to test the potential of rolipram-loaded LNCs in a controllable environment. Rotary culture allows controlling both inducing apoptosis by chemical reagents and the treatment by NPs in controlled concentrations. In our model, we induced apoptosis by the application of 50 μM cisplatin (**Figure 11**). In cisplatin-treated cochleae, we observed a rise in CC3 immunoreactivity after 24 h of treatment (**Figure 11D**). However, when rolipram-loaded LNCs diluted 1000-fold applied together with cisplatin, the CC3 immunoreactivity was significantly reduced (**Figure 11A**). Analogous to the SGN similar effects were observed in the spiral ligament, which appears to be susceptible to apoptosis in the, cochlea culture. In this part of the cochlea, CC3 levels could also be rescued by the application of rolipram-loaded LNCs (**Figures 11G,J**). Controls are summarized in an **Supplementary Figure 1**. Together, this demonstrates that mouse rotary cultures of the cochlea is an efficient and sensitive test bed for the pharmacotherapy of the NPs. The rotary culture allows for exact control of concentration of reagents. It excludes the detrimental influence of animal behavior and is perfectly compatible with imaging-based analysis and biochemical interrogation.

Discussion

In the present study we demonstrated some principle application of nanocarriers for use of drug delivery to the inner ear. NP size influences uptake kinetics and may reflect different pathways into the cells. Mironava et al. reported that 45 nm Gold NPs penetrate dermal fibroblasts via clathrin-mediated endocytosis, while smaller 13 nm Gold NPs enter mostly via phagocytosis (Mironava et al., 2010). Mesoporus silica NP showed maximum uptake at a NP size of 50 nm; 30 and 110 nm showed significantly less uptake by HeLa cells (Lu et al., 2009). A NP core size of 30–50 nm seem to be an optimal size for active uptake (Shang et al., 2014) for most cells. Small spherical NPs have less interaction

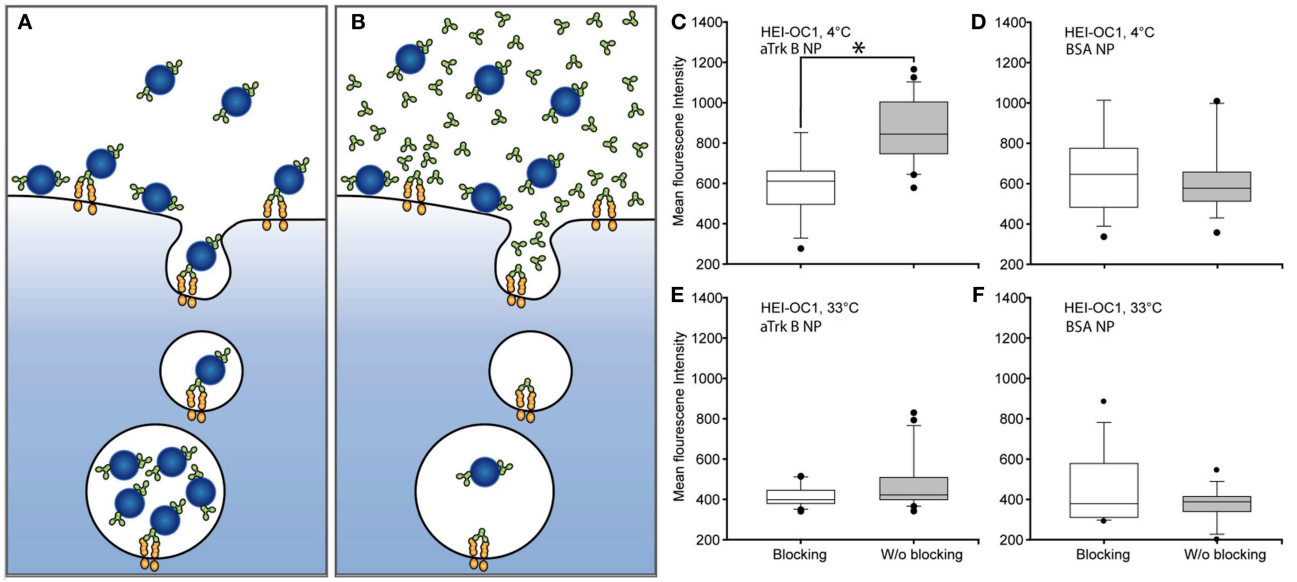

FIGURE 8 | Assessing the functionality of agonistic anti-TrkB (29D7)-surface grafted silica NPs (aTrkB-NP). Principle of competitive binding assays: **(A)** Under binding conditions, aTrkB-NPs are able to specifically und non-specifically bind to the cells. **(B)** Under blocking conditions the excess of free antibody should avoid the specific binding of the aTrkB-NPs leaving only non-specific interactions for binding. In theory a functional antiTrkB surface modification should lead to significantly higher binding and uptake of NPs under binding conditions. Panels **(C–F)** pairwise comparisons of blocking and binding conditions in HEI-OC1 cells. **(C)** HEI-OC1 cells incubated with aTrkB-NPs at 4°C, preventing endocytosis, showed significantly more binding under binding conditions ($p < 0.05$, rank-sum test). **(D)** The same experiment performed with BSA-NP did not show a significant difference ($p > 0.05$, rank sum test). **(E)** When the experiment was performed at 33°C, allowing endocytosis, no difference between binding and blocking conditions was observed ($p > 0.05$, rank sum test). **(F)** The application of BSA-NPs resulted in no difference ($p > 0.05$, rank sum test).

with the cell membrane, so small NP have to aggregate at the cell surface to trigger internalization (Jiang et al., 2010). Although we controlled NP composition and charge and used serum free media supplements, the NP corona will have been altered by some of these supplements and proteins secreted by cells and inner ear explants. Therefore, we can only speculate on uptake mechanisms varying with NP size. For unfunctionalized 50 nm silica particles we found macropinocytosis to be most relevant privileged by *in vitro* formation of NP agglomerates (Pritz et al., 2013a) and confocal imaging on the TrkB functionalized here show similar results. NP aggregation under *in vitro* conditions is poorly understood. Material properties such as particle size, morphology, and crystallinity are important parameters affecting nanoparticle colloidale stability (Gambinossi et al., 2014). The impact of aggregation cannot not easily predicted and needs to be evaluated NP by NP. Unfunctionalized LNCs highly penetrate cells and tissue of the inner ear and are able to release their cargo such as rolipram. LNCs are chemically stable and ideal to encapsulate hydrophobic cargos at high encapsulation rates. They displayed clear size dependency of internalization and did not show signs of toxicity compared to control experiments. In cochlear explants an enhanced uptake was identified for immature SGCs. Like in dorsal root ganglia there are cells to migrate from the neural crest and have the potential to generate glia and more than 20 different neuronal cell types, many of these cells undergo apoptosis (Raible and Ungos, 2006). The cells responsible for dead dorsal root ganglia neurons removal are satellite glial cell (SGC) precursors, rather than macrophages (Wu et al., 2009). These characteristics might be valid also for SGC in the immature cochlea and may explain enhanced uptake. Polymerosomes confirms that size is an important factor for kinetics of tissue penetration. On the big end of our NP portfolio QDot NPs demonstrated that also particles of several hundreds of nm show capability for uptake in SGCs and SGNs. Although we clearly found these particles also in the bipolar neurons uptake by immature SGCs and transcytosis to SGN may occur here, especially with those neurons that are already completely covered by their satellite sheath. Further, analysis might be valuable to study this possible pathway of NP transport.

As NPs are functionalized with small peptides internalization characteristics changes considerably. In our *in vitro* system using SHSY5Y cells the peptide functionalized LNCs showed worse uptake than the non-functionalized ones. In fact, this observation is in agreement with a previous report (Hirsjarvi et al., 2013). LNCs are subjected to surface modifications, including charged molecules (Perrier et al., 2010). Attaching for instance polysaccharides to the surface of LNCs offers the possibility of modifying the physicochemical and biological properties of the core particles. Surface modification of LNCs by post-insertion of the positively charged amphiphilic (Perrier et al., 2010) lipochitosan made the LNC surface more rigid, but

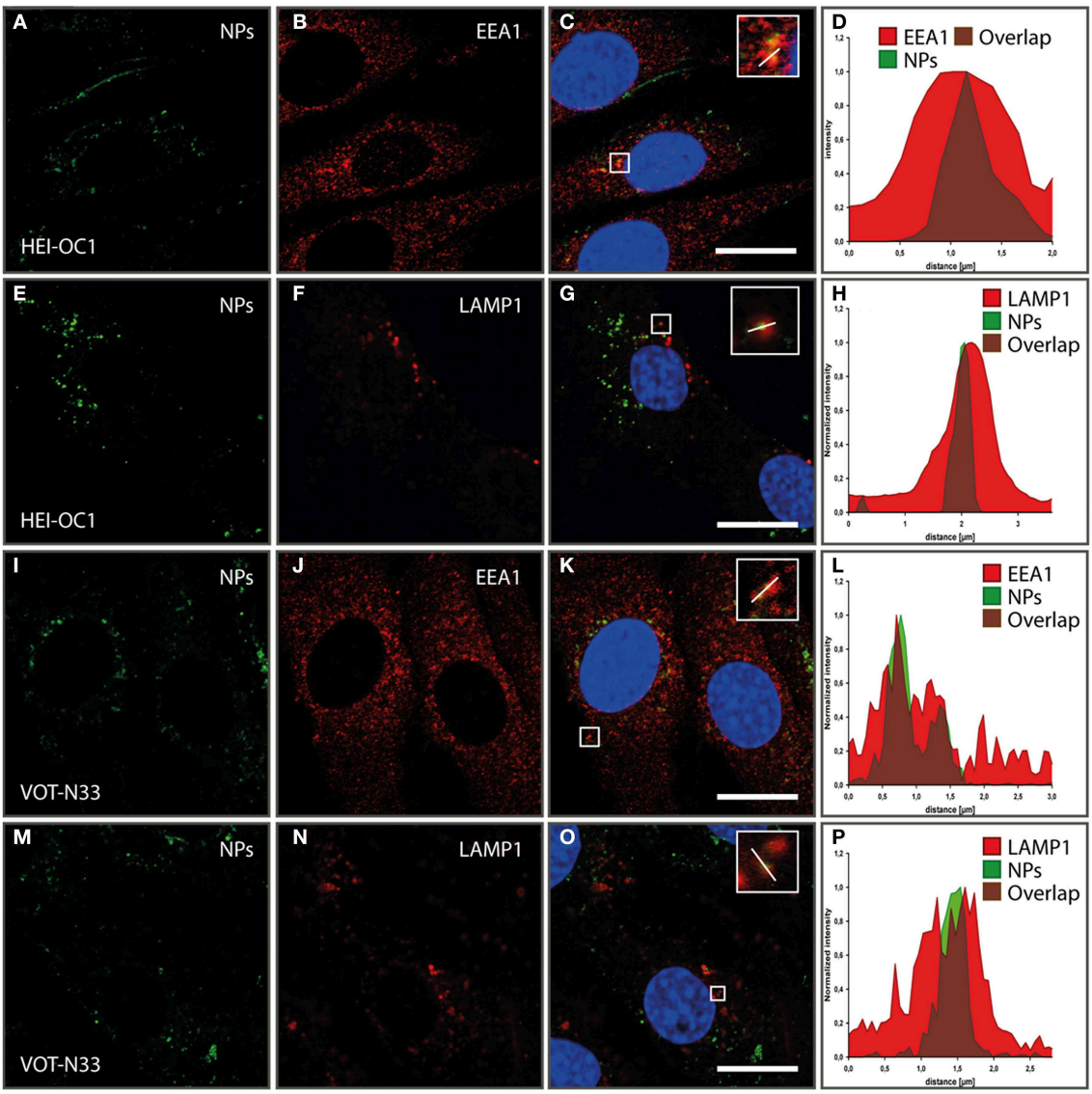

FIGURE 9 | Internalization and subcellular localization of aTrkB-silica NPs into HEI-OC1 (A–L) cells and VOT-N33 cells (I–P); (A–D). In HEI-OC1 cells after 1 h of incubation aTrkB-NPs localize in EEA1 positive endosomes. **(A)** EEA1 staining; **(B)** aTrKB-NPs, **(C)** Overlay; **(D)** luminance profile; scale bars 20 μm. **(E–H)** In HEI-OC1 cells 90 min after start of application aTrkB-NPs were found in LAMP1 positive late endosomes/lysosomes. **(E)** LAMP1 staining; **(F)** aTrkB-NPs, **(G)** Overlay; **(H)** luminance profile; scale bars 20 μm. Panels **(I–L)** in VOT-N33 cells after 1 h of incubation aTrKB-NPs localize in EEA1 positive endosomes. **(I)** EEA1 staining; **(J)** aTrkB-NPs, **(K)** Overlay; **(L)** luminance profile; scale bars 20 μm. Panels **(M–P)** in VOT-N33 cells 90 min after start of application aTrkB-NPs were found in LAMP1 positive late endosomes/lysosomes. **(M)** LAMP1 staining; **(N)** aTrkB-NPs, **(O)** Overlay; **(P)** luminance profile; scale bars 20 μm.

the neutral, higher molecular weighted lipodextran had no effect on the surface elasticity (Hirsjarvi et al., 2013). Although, these surface modified LNCs were better captured by the mononuclear phagocyte system, the neutral and charged molecules did not influence the *in vivo* biodistribution properties of LNCs in mice (Hirsjarvi et al., 2013). In addition, neuronal uptake mechanisms may not be identical with the mononuclear phagocyte system. With polymerosomes we found similar results in organotypic cultures. Here unfunctionalized particles showed an even uptake throughout the tissue while pattern differed with functionalized NPs. Here again a preference for the region of the spiral ganglion was found and appeared to be enriched with the targeting ligand. Further experiments investigating the kinetics of uptake in certain cell types would be necessary to prove specifity. However, adding moieties that can be used to target NPs into different cell types with high affinity is not an easy task. Surface modification of NPs often need to be introduced for providing functional groups that ca be conjugated with the ligand thereby changing the characteristics in and of themselves. To ensure ligand directed coupling with correct orientation and desired surface density

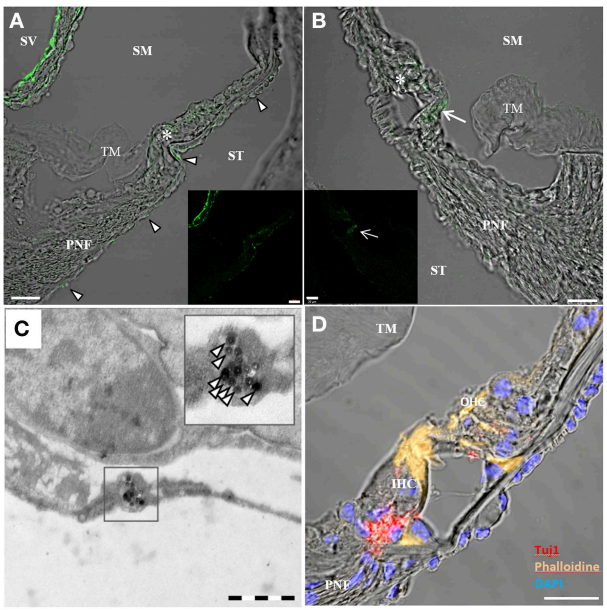

FIGURE 10 | Confocal imaging on rotary cultures of P25 mouse cochleae treated with aTrkB-silica-NPs. [**(A,B)** overlay, **(A)** inset green fluorescence, scale bars 20 μm] localized predominantly in the mesothelial covering layer of Reißner's membrane (RM) and tympanic covering layer cells underneath the basilar membrane (arrowheads in **A**). Some staining was observed within the sensory epithelium (asterisks). In **(B)** enhanced uptake was observed within the inner hair cell (arrow). **(C)** Transmission electron microscopy of aTrkB-NPs treated cochlea with NPs found in a tympanic covering layer cell (scale bar 1 μm). **(D)** Confocal projection of a control rotary culture showing the organ of Corti with Tuj1 positive nerve fibers underneath inner (IHC) and outer hair cells (OHC)-scale bar 20 μm. PNF, peripheral nerve fibers; TM, tectorial membrane; SM, scala media; ST, scala tympani; SM, scala media; SV, scala vestibuli.

may be a problem especially for very small particles (Friedman et al., 2013).

Antibody grafted NPs also face major challenges such as high specifity and affinity for target structures on cell surfaces. Further linker and nanocarrier material must not lower specific binding. Initial tests whether our antibody surface modification is functional and contributes both to enhanced binding and internalization in TrkB positive cells showed that the surface modification contributed to binding only. TrkB positive HEI-OC1 cells were exposed to functionalized NPs or to functionalized NPs and an excess of TrkB antibody inhibiting antibody-mediated binding of the immuno-NPs. When the experiment was performed at 4°C, inhibiting endocytosis, significantly more NPs were found on cells treated with only immuno-NPs than on cells treated with both free antibody and functionalized NPs. However when, the experiment was carried out at 33°C the significant difference was lost. This suggests that the binding of the functionalized NP is significantly determined by the specific antibody-TrkB interaction while the contribution of the antibody to the endocytosis of the membrane associated NP is negligible. This interpretation might be counterintuitive but it fits to the model of Decuzzi and Ferrari (2007). According to their model, for a NP the contribution of non-specific interactions such as electrostatic force to the early stages of endocytosis is as important as the specific interactions which are exerted by ligand surface modifications. The herein used 50 nm silica NP had an average of 3–5 antibodies grafted to the surface; the larger part of the NP surface was accessible to unspecific membrane-to-NP interactions. As a consequence, attractive unspecific interactions between NP and membrane might have been considerably larger than the specific interactions, thus governing the membrane wrapping process. Since the formation of the membrane invagination is the step determining the velocity in the endocytic process, the avidity of the immuno-conjugated NP-TrkB interaction might be insufficient to contribute with significant, specific interactions between NP and cell. It might appear that under given conditions the unspecific binding of NP to the cell is more significant for the endocytic uptake than the antibody-mediated binding. Taken together, this suggests for the herein used NPs the surface-grafting of TrkB antibodies was insufficient to significantly contribute to endocytosis of the NP.

A further explanation for the obtained results might be provided by macropinocytosis as source for "non-specific" internalization of the immuno-NPs. Since the aTrkB NPs were composed of the same matrix material as the NPs used previously (Pritz et al., 2013a), macropinocytosis might also have contributed substantially to the internalization of the aTrkB NPs as reported in the this study. In case of macropinocytosis, large amounts of extracellular liquid are internalized into the cell. Therefore, the internalization of NPs by macropinocytosis does not necessarily require membrane binding of the NPs. A high rate of non-specific ground-level internalization by macropinocytosis would explain the lacking difference between the binding and the blocking set-up. A factor which would lead to an increase in macropinocytosis-dependent internalization is NP clustering (Canton and Battaglia, 2012). As the binding and internalization experiments were conducted under serum-free conditions, only the "blocking" set-up with its 63-fold antibody excess provided enough soluble protein to cause protein-mediated NP-aggregation (Monopoli et al., 2011). An antibody-induced NP agglomeration could have led to an artificially higher internalization rate under "blocking" conditions. Moreover, also an excess of the aTrkB NPs itself might have been responsible for an increased non-specific binding of the immuno-NPs. The higher the concentration of the NPs, the higher the possibility for a non-specific pinocytic internalization by macropinocytosis. These considerations suggest that also a better control of the discussed experimental parameters as well as the colloidal stability is necessary to assess the true contribution of the antibody surface modification to the endocytosis of the immuno-NPs.

The insufficient contribution of NPs to internalization and tissue penetration suggest that an optimization of the nanocarrier system to selectively bind and activate TrkB with specific uptake in TrkB positive cells is necessary. Since a mismatch between specific and unspecific NP-to-membrane interactions is a likely source of error, an increase in specific interaction strength and a decrease in non-specific interaction would be beneficial. This can be achieved by increasing the number

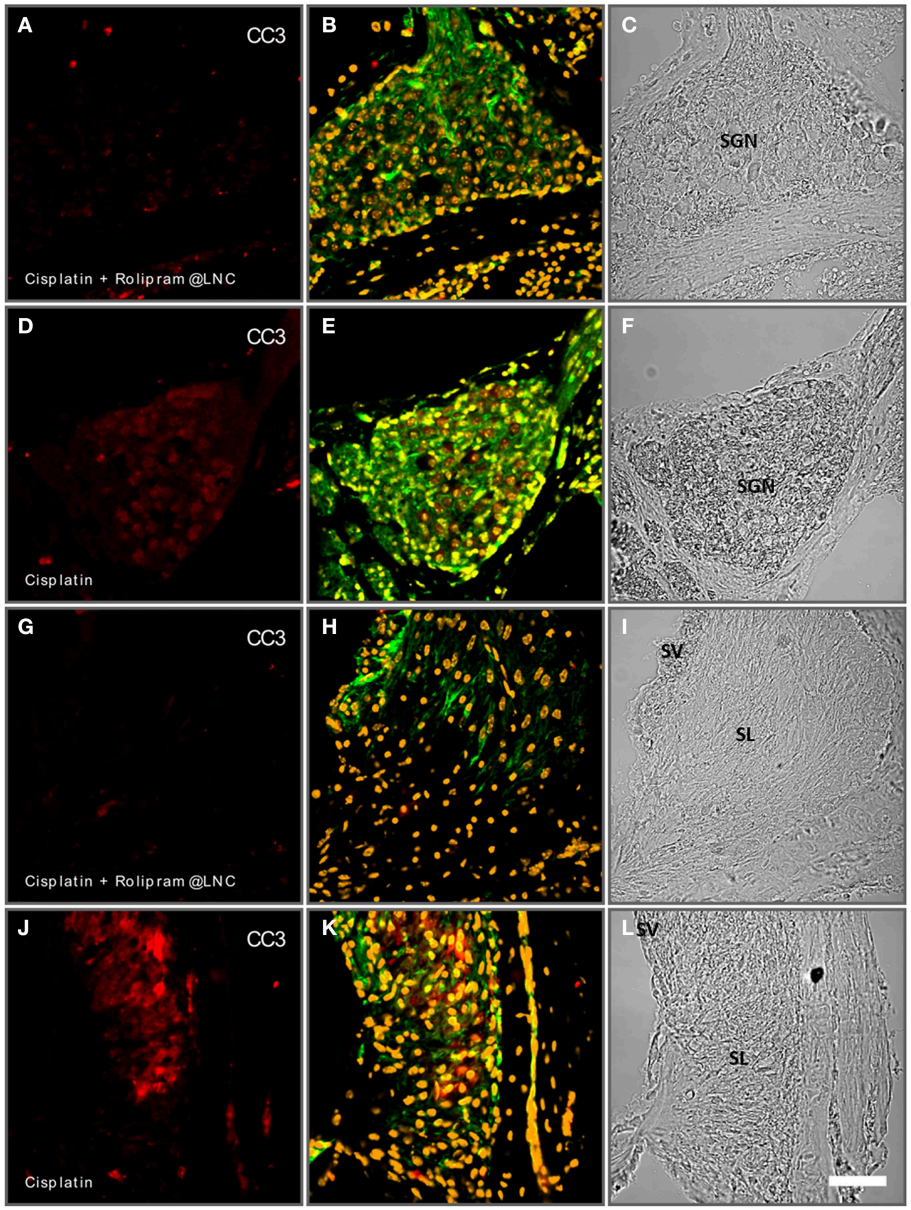

FIGURE 11 | Rolipram-loaded lipid nanocapsules (LNCs) partially rescue cisplatin-induced apoptosis in postnatal mouse cochlea cultures (P24). Spiral ganglion neurons (SGN) treated with cisplatin and rolipram-loaded LNCs exhibit less cleaved caspase 3 (CC3-red staining) immune reactivity **(A)** than controls exclusively treated with cisplatin **(D)**. In the spiral ligament (SL) cisplatin induces increased CC3 reactivity **(J)** while additional treatment with rolipram-loaded LNCs reduced the CC3-reacitivty **(G)**. **(A,D,G,J)** CC3 immunolabeling; **(B,E,H,K)** phalloidine labeling and DAPI staining; **(C,F,I,L)** bright field. Scale bar 50 μm.

of antibody molecules per NP. Silica NPs expose amino residues for surface functionalization. The remaining amino residues might be used for surface PEGylation. This would efficiently decrease non-specific interactions with the biological environment. For example, such a polymer brush is thought to minimize NP-protein-interactions (Vonarbourg et al., 2006a,b; Monopoli et al., 2011). The polymer coating could prevent non-specific interactions with the membrane/membrane proteins. In general a change of the particle type would also be an approach to solve these problems. LNCs would offer optimal membrane interaction properties. One the one hand, they minimize unwanted interactions by a PEG brush. On the other hand they exhibit a 10-fold higher avidity caused by a higher number of antibody molecules on the particle surface (Beduneau et al., 2007, 2008). However, we showed that there were enough aTrk-NPs or aggregates bound to TrkB positive cells present to activate neurotrophic signaling. This might partially compensate the slowing down and impairment of endocytosis as observed

with unfunctionalized silica NPs (Pritz et al., 2013a). Immuno-conjugated NPs showed similar trafficking pattern at confocal level that may pose a threat to important functions in the survival signaling in SGNs. Thus, (over-) load of silica NPs for cell types involved in sensorineural survival signaling needs to be minimized and a strategy for endosomal escape has to be applied for a use as drug carriers. In conclusion the surface chemistry of NPs aimed for TrkB-positive SGNs has still to be optimized and tested to guarantee a functional and specific antibody-based DD system customized for the SGNs.

Concerning the application of immuno-NPs to the whole-organ culture of cochleae, consistent results from TEM and confocal imaging show that the tissue permeation of the immuno-NPs was insufficient to reach TrkB positive cells in higher amounts. Antibody contribution to internalization of the immuno-NP-TrkB-complex is low as shown with our competitive blocking assay. TrkB is expressed in SGN in adult human (Liu et al., 2011) and in inner hair cells and neurons in young adult mice (Bitsche et al., 2011). Although some aggregation to inner hair cells was found our observations suggest that the permeation of the aTrkB NPs to those sites was not quantitative. The lack of tissue permeation might be caused by the specific physicochemical parameters of the silica NP. Since it was documented for *in vivo* experiments with other particles like LNCs (Zou et al., 2008), polymerosomes and liposomes (Buckiova et al., 2012) to locate within the cells of the organ of Corti, it might be necessary to switch to one of those carrier types. As a consequence, a fundamental change in the physicochemical properties of the carrier or a change to another type of nanocarrier is required to reach these TrkB-positive structures in the cochlea. Another problem for DD via the RWM into the ear presents the high phagocytic activity of the mesothelial covering layer cells lining the perilymphatic spaces. These cells form a loose layer. Like in other body cavities this cell type is able to phagocyte even bacteria and has function for antigen presentation (Visser et al., 1996). Strategies to selectively prevent this phagocytosis or better promote transcytosis toward endolymphatic compartments may be necessary. Analysis of fluid spaces in the human cochlea suggests rather easy accessibility for from scala tympani to SGNs (Rask-Andersen et al., 2006).

DD with targeting ligand NPs for the inner ear remain complex nevertheless the inner ear may be a good model organ for this approach with the possibility for local drug delivery to an organ isolated by a blood-labyrinth-barrier. Schuknecht was one of the first who experimented with intratympanic drug administration in the treatment of severe vertigo (Schuknecht, 1956). He reported success in Meniere symptomology with the intratympanic streptomycin injection but resulted also in profound hearing loss. However, the efficacy of his approach vs. systemic drug administration has been confirmed for various clinical indications. The major site of absorption of drugs is the RWM, the concentration of the drug in the inner ear depends greatly on the exposure time and drug concentration. To overcome rapid clearance by ciliated epithelia in the middle ear different hydrogels were used to immobilize a drug reservoir (Paulson et al., 2008). They tested chitosan-glycerophosphate hydrogels containing dexamethasone or gentamicin in the murine cochlea on the round window. We also previously reported permeation and distribution of paramagnetic particles loaded in an intelligent gel becoming solid at body temperature (Thaler et al., 2011). A cochlear implant is an artificial hearing device that can replace damaged hair cells in the cochlea. To minimize trauma during electrode insertion and reduce postsurgical inflammation reactions and fibrosis becomes more and more important especially in context with electro-acoustic stimulation of the cochlear nerve. Drug eluting electrodes are currently developed also using hydrogels (Hutten et al., 2014) or polymeric coatings (Ceschi et al., 2014). These carrier materials offer also great possibilities for nanocarriers and are already in use with human applications (Nakagawa et al., 2014).

Kikkawa et al. (2014) tested insulin like growth factor or heptatocyte growth factor in gelatine hydrogel coated electrodes. Their findings provide the first evidence that a hydrogel coated, growth factor-releasing electrode could attenuate insertion trauma and promote recovery from it. A combination that might be a DD strategy also for other inner ear damages.

Our experiments with rolipram loaded LNCs proved drug release by a nanocarrier. The drug delivery mechanism of LNCs is believed to be dependent on endocytosis and to involve endosomal escape (Paillard et al., 2010). For lipophilic cargo a slow and constant release from the LNC and a subsequent diffusion to the acceptor compartment has been demonstrated to accomplish subcellular DD with our HEI-OC1 cell line without the involvement of endocytosis (Bastiat et al., 2013). In contrast, amphiphilic cargo is confined to the LNC lumen. While amphiphilic cargo is confined in the surfactant shell of the LNC, lipophilic molecules are localizing in the lipophilic center of the LNCs, allowing diffusion of the cargo. Our rolipram loaded LNC NP in rotary cultures of adult inner ears demonstrate the bioefficacy of this drug release system to prevent apoptosis caused by cisplatin in the adult murine inner ear. Previous experiments could prove that incorporation of rolipram in LNCs increased the survival of SGNs significantly in *in vitro* cultures of immature neurons (Meyer et al., 2012). Without the use of any nanocarriers, concentration level of rolipram appeared to be very crucial as demonstrated in Kranz et al. (2014). Our rotary culture system proved as controllable system for adult inner ear tissue and could demonstrate this effect for the first time in adult inner ear tissue. LNCs may act as an appropriate system to deliver lipophilic drugs in low doses with a linear release characteristics suitable for inner ear application and do not feature initial burst release (Lamprecht et al., 2002). Thus, LNCs are one of the few carrier systems, which were able to demonstrate actual DD efficiency in the cochlea so far.

Acknowledgments

We gratefully thank Frederico Kalinec, Los Angeles USA for the HEI-OC1 cells and Matthew Holley, Sheffield, UK for the VOT-N33 cells. We also thank Pfizer® for 29D7 antiTrkB, a generous gift. This project was supported by a grant from the European Community 6th Framework program, NanoEar project, grant number: NMP4-CT-2006-026556, integrated project and Austrian Science Fund (FWF)-contract grant

number: P21848-N13. Many thanks to all scientist of NanoEar project especially our coordinator Ilmari Pyykko Department of Ear-, Nose-, and Throat Diseases at the University of Tampere in Finland, Andrea Foronara and Muhammed Mamoun from Royal Institute of Technology, Stockholm, Sweden for QDot particles, Alec Johnston and Tracy Newman from University Southampton, UK for polymerosome particles, Guillaume Bastiat and Patrick Saulnier INSERM U 1066, Angers, France for lipid core nanocapsules and Mario Bitsche for excellent technological work. This work is dedicated to Mario Bitsche (1970–2015). It was a privilege for us to work closely with him.

Supplementary Material

The Supplementary Material for this article can be found online at: http://journal.frontiersin.org/article/10.3389/fnagi.2015.00071/abstract

Supplementary Figure 1 | Control preparations for Rolipram-loaded lipid nanocapsules (P24, 48 hours incubation). Untreated spiral ganglion neurons (SGN) stained for cleaved caspase 3 (CC3-red staining) immune reactivity shows only few staining **(A)** as well as in the spiral ligament (SL) **(D)**. Treatment with rolipram (14 μM) shows no effect on CC3-reactivity **(G,J)**. **(A,D,G,J)** CC3 immunolabelling; **(B,E,H,K)** phalloidine labelling and DAPI staining; **(C,F,I,L)** bright field. Scale bar 50 μm.

References

Asanuma, M., Nishibayashi, S., Iwata, E., Kondo, Y., Nakanishi, T., Vargas, M. G., et al. (1996). Alterations of cAMP response element-binding activity in the aged rat brain in response to administration of rolipram, a cAMP-specific phosphodiesterase inhibitor. *Brain Res. Mol. Brain Res.* 41, 210–215. doi: 10.1016/0169-328X(96)00098-8

Atwal, J. K., Massie, B., Miller, F. D., and Kaplan, D. R. (2000). The TrkB-Shc site signals neuronal survival and local axon growth via MEK and P13-kinase. *Neuron* 27, 265–277. doi: 10.1016/S0896-6273(00)00035-0

Bastiat, G., Pritz, C. O., Roider, C., Fouchet, F., Lignieres, E., Jesacher, A., et al. (2013). A new tool to ensure the fluorescent dye labeling stability of nanocarriers: a real challenge for fluorescence imaging. *J. Control. Release* 170, 334–342. doi: 10.1016/j.jconrel.2013.06.014

Beduneau, A., Hindre, F., Clavreul, A., Leroux, J. C., Saulnier, P., and Benoit, J. P. (2008). Brain targeting using novel lipid nanovectors. *J. Control. Release* 126, 44–49. doi: 10.1016/j.jconrel.2007.11.001

Beduneau, A., Saulnier, P., Hindre, F., Clavreul, A., Leroux, J. C., and Benoit, J. P. (2007). Design of targeted lipid nanocapsules by conjugation of whole antibodies and antibody Fab' fragments. *Biomaterials* 28, 4978–4990. doi: 10.1016/j.biomaterials.2007.05.014

Bibel, M., and Barde, Y. A. (2000). Neurotrophins: key regulators of cell fate and cell shape in the vertebrate nervous system. *Genes Dev.* 14, 2919–2937. doi: 10.1101/gad.841400

Bitsche, M., Dudas, J., Roy, S., Potrusil, T., Schmutzhard, J., and Schrott-Fischer, A. (2011). Neurotrophic receptors as potential therapy targets in postnatal development, in adult, and in hearing loss-affected inner ear. *Otol. Neurotol.* 32, 761–773. doi: 10.1097/MAO.0b013e31821f7cc1

Buckiova, D., Ranjan, S., Newman, T. A., Johnston, A. H., Sood, R., Kinnunen, P. K., et al. (2012). Minimally invasive drug delivery to the cochlea through application of nanoparticles to the round window membrane. *Nanomedicine (Lond)* 7, 1339–1354. doi: 10.2217/nnm.12.5

Canton, I., and Battaglia, G. (2012). Endocytosis at the nanoscale. *Chem. Soc. Rev.* 41, 2718–2739. doi: 10.1039/c2cs15309b

Cazorla, M., Arrang, J. M., and Premont, J. (2011). Pharmacological characterization of six trkB antibodies reveals a novel class of functional agents for the study of the BDNF receptor. *Br. J. Pharmacol.* 162, 947–960. doi: 10.1111/j.1476-5381.2010.01094.x

Ceschi, P., Bohl, A., Sternberg, K., Neumeister, A., Senz, V., Schmitz, K. P., et al. (2014). Biodegradable polymeric coatings on cochlear implant surfaces and their influence on spiral ganglion cell survival. *J. Biomed. Mater. Res. Part B Appl. Biomater.* 102, 1255–1267. doi: 10.1002/jbm.b.33110

Cheng, A. G., Cunningham, L. L., and Rubel, E. W. (2005). Mechanisms of hair cell death and protection. *Curr. Opin. Otolaryngol. Head Neck Surg.* 13, 343–348. doi: 10.1097/01.moo.0000186799.45377.63

Choi, S., Lee, J., Kumar, P., Lee, K. Y., and Lee, S. K. (2011). Single chain variable fragment CD7 antibody conjugated PLGA/HDAC inhibitor immuno-nanoparticles: developing human T cell-specific nano-technology for delivery of therapeutic drugs targeting latent HIV. *J. Control. Release* 152(Suppl. 1), e9–e10. doi: 10.1016/j.jconrel.2011.08.089

Decuzzi, P., and Ferrari, M. (2007). The role of specific and non-specific interactions in receptor-mediated endocytosis of nanoparticles. *Biomaterials* 28, 2915–2922. doi: 10.1016/j.biomaterials.2007.02.013

Deng, Z., Wang, J., Qiu, J., Liu, S., Wang, C., and Yang, A. (2004). [Protection of NT3 gene transfection on the guinea pig cochlea treated with gentamicin]. *Lin Chuang Er Bi Yan Hou Ke Za Zhi* 18, 231–233.

Deutscher, S. L. (2010). Phage display in molecular imaging and diagnosis of cancer. *Chem. Rev.* 110, 3196–3211. doi: 10.1021/cr900317f

Dinh, C. T., and Van De Water, T. R. (2009). Blocking pro-cell-death signal pathways to conserve hearing. *Audiol. Neurootol.* 14, 383–392. doi: 10.1159/000241895

Du, X., Chen, K., Kuriyavar, S., Kopke, R. D., Grady, B. P., Bourne, D. H., et al. (2013). Magnetic targeted delivery of dexamethasone acetate across the round window membrane in guinea pigs. *Otol. Neurotol.* 34, 41–47. doi: 10.1097/MAO.0b013e318277a40e

Eggert, A., Grotzer, M. A., Ikegaki, N., Liu, X. G., Evans, A. E., and Brodeur, G. M. (2002). Expression of the neurotrophin receptor TrkA down-regulates expression and function of angiogenic stimulators in SH-SY5Y neuroblastoma cells. *Cancer Res.* 62, 1802–1808.

Fiandra, L., Mazzucchelli, S., De Palma, C., Colombo, M., Allevi, R., Sommaruga, S., et al. (2013). Assessing the *in vivo* targeting efficiency of multifunctional nanoconstructs bearing antibody-derived ligands. *ACS Nano* 7, 6092–6102. doi: 10.1021/nn4018922

Friedman, A. D., Claypool, S. E., and Liu, R. (2013). The smart targeting of nanoparticles. *Curr. Pharm. Des.* 19, 6315–6329. doi: 10.2174/13816128113199990375

Gambinossi, F., Mylon, S. E., and Ferri, J. K. (2014). Aggregation kinetics and colloidal stability of functionalized nanoparticles. *Adv. Colloid Interface Sci.* doi: 10.1016/j.cis.2014.07.015. [Epub ahead of print].

Ge, X., Jackson, R. L., Liu, J., Harper, E. A., Hoffer, M. E., Wassel, R. A., et al. (2007). Distribution of PLGA nanoparticles in chinchilla cochleae. *Otolaryngol. Head Neck Surg.* 137, 619–623. doi: 10.1016/j.otohns.2007.04.013

Geiger, T. R., and Peeper, D. S. (2007). Critical role for TrkB kinase function in anoikis suppression, tumorigenesis, and metastasis. *Cancer Res.* 67, 6221–6229. doi: 10.1158/0008-5472.CAN-07-0121

Glueckert, R., Bitsche, M., Miller, J. M., Zhu, Y., Prieskorn, D. M., Altschuler, R. A., et al. (2008). Deafferentation-associated changes in afferent and efferent processes in the guinea pig cochlea and afferent regeneration with chronic intrascalar brain-derived neurotrophic factor and acidic fibroblast growth factor. *J. Comp. Neurol.* 507, 1602–1621. doi: 10.1002/cne.21619

Greenspan, P., and Fowler, S. D. (1985). Spectrofluorometric studies of the lipid probe, nile red. *J. Lipid Res.* 26, 781–789.

Gruart, A., Sciarretta, C., Valenzuela-Harrington, M., Delgado-Garcia, J. M., and Minichiello, L. (2007). Mutation at the TrkB PLC{gamma}-docking site affects hippocampal LTP and associative learning in conscious mice. *Learn. Mem.* 14, 54–62. doi: 10.1101/lm.428307

Gupta, N. K., and Dixit, V. K. (2011). Bioavailability enhancement of curcumin by complexation with phosphatidyl choline. *J. Pharm. Sci.* 100, 1987–1995. doi: 10.1002/jps.22393

Henderson, D., Bielefeld, E. C., Harris, K. C., and Hu, B. H. (2006). The role of oxidative stress in noise-induced hearing loss. *Ear Hear.* 27, 1–19. doi: 10.1097/01.aud.0000191942.36672.f3

Hirsjarvi, S., Dufort, S., Bastiat, G., Saulnier, P., Passirani, C., Coll, J. L., et al. (2013). Surface modification of lipid nanocapsules with polysaccharides: from physicochemical characteristics to *in vivo* aspects. *Acta Biomater.* 9, 6686–6693. doi: 10.1016/j.actbio.2013.01.038

Hutten, M., Dhanasingh, A., Hessler, R., Stover, T., Esser, K. H., Moller, M., et al. (2014). *In vitro* and *in vivo* evaluation of a hydrogel reservoir as a continuous drug delivery system for inner ear treatment. *PLoS ONE* 9:e104564. doi: 10.1371/journal.pone.0104564

Jiang, X., Rocker, C., Hafner, M., Brandholt, S., Dorlich, R. M., and Nienhaus, G. U. (2010). Endo- and exocytosis of zwitterionic quantum dot nanoparticles by live HeLa cells. *ACS Nano* 4, 6787–6797. doi: 10.1021/nn101277w

Kehoe, J. W., and Kay, B. K. (2005). Filamentous phage display in the new millennium. *Chem. Rev.* 105, 4056–4072. doi: 10.1021/cr000261r

Kikkawa, Y. S., Nakagawa, T., Ying, L., Tabata, Y., Tsubouchi, H., Ido, A., et al. (2014). Growth factor-eluting cochlear implant electrode: impact on residual auditory function, insertional trauma, and fibrosis. *J. Transl. Med.* 12, 280. doi: 10.1186/s12967-014-0280-4

Klein, R., Parada, L. F., Coulier, F., and Barbacid, M. (1989). trkB, a novel tyrosine protein kinase receptor expressed during mouse neural development. *EMBO J.* 8, 3701–3709.

Klein, R., Smeyne, R. J., Wurst, W., Long, L. K., Auerbach, B. A., Joyner, A. L., et al. (1993). Targeted disruption of the trkB neurotrophin receptor gene results in nervous system lesions and neonatal death. *Cell* 75, 113–122. doi: 10.1016/0092-8674(93)90683-H

Kranz, K., Warnecke, A., Lenarz, T., Durisin, M., and Scheper, V. (2014). Phosphodiesterase type 4 inhibitor rolipram improves survival of spiral ganglion neurons *in vitro*. *PLoS ONE* 9:e92157. doi: 10.1371/journal.pone.0092157

Lamprecht, A., Bouligand, Y., and Benoit, J. P. (2002). New lipid nanocapsules exhibit sustained release properties for amiodarone. *J. Control. Release* 84, 59–68. doi: 10.1016/S0168-3659(02)00258-4

Liu, H., Chen, S., Zhou, Y., Che, X., Bao, Z., Li, S., et al. (2013). The effect of surface charge of glycerol monooleate-based nanoparticles on the round window membrane permeability and cochlear distribution. *J. Drug Target.* 21, 846–854. doi: 10.3109/1061186X.2013.829075

Liu, W., Kinnefors, A., Bostrom, M., and Rask-Andersen, H. (2011). Expression of TrkB and BDNF in human cochlea-an immunohistochemical study. *Cell Tissue Res.* 345, 213–221. doi: 10.1007/s00441-011-1209-3

Lu, F., Wu, S. H., Hung, Y., and Mou, C. Y. (2009). Size effect on cell uptake in well-suspended, uniform mesoporous silica nanoparticles. *Small* 5, 1408–1413. doi: 10.1002/smll.200900005

Ma, Z., Wu, X., Cao, M., Pan, W., Zhu, F., Chen, J., et al. (2003). Selection of trkB-binding peptides from a phage-displayed random peptide library. *Sci. China C Life Sci.* 46, 77–86. doi: 10.1007/BF03182687

McGuinness, S. L., and Shepherd, R. K. (2005). Exogenous BDNF rescues rat spiral ganglion neurons *in vivo*. *Otol. Neurotol.* 26, 1064–1072. doi: 10.1097/01.mao.0000185063.20081.50

Meyer, H., Stover, T., Fouchet, F., Bastiat, G., Saulnier, P., Baumer, W., et al. (2012). Lipidic nanocapsule drug delivery: neuronal protection for cochlear implant optimization. *Int. J. Nanomed.* 7, 2449–2464. doi: 10.2147/IJN.S29712

Minichiello, L., Casagranda, F., Tatche, R. S., Stucky, C. L., Postigo, A., Lewin, G. R., et al. (1998). Point mutation in trkB causes loss of NT4-dependent neurons without major effects on diverse BDNF responses. *Neuron* 21, 335–345. doi: 10.1016/S0896-6273(00)80543-7

Mironava, T., Hadjiargyrou, M., Simon, M., Jurukovski, V., and Rafailovich, M. H. (2010). Gold nanoparticles cellular toxicity and recovery: effect of size, concentration and exposure time. *Nanotoxicology* 4, 120–137. doi: 10.3109/17435390903471463

Mizoguchi, Y., and Nabekura, J. (2003). Sustained intracellular Ca2+ elevation induced by a brief BDNF application in rat visual cortex neurons. *Neuroreport* 14, 1481–1483. doi: 10.1097/00001756-200308060-00015

Monopoli, M. P., Walczyk, D., Campbell, A., Elia, G., Lynch, I., Bombelli, F. B., et al. (2011). Physical-chemical aspects of protein corona: relevance to *in vitro* and *in vivo* biological impacts of nanoparticles. *J. Am. Chem. Soc.* 133, 2525–2534. doi: 10.1021/ja107583h

Moss, O. R., and Wong, V. A. (2006). When nanoparticles get in the way: impact of projected area on *in vivo* and *in vitro* macrophage function. *Inhal.Toxicol.* 18, 711–716. doi: 10.1080/08958370600747770

Nakagawa, T., Kumakawa, K., Usami, S., Hato, N., Tabuchi, K., Takahashi, M., et al. (2014). A randomized controlled clinical trial of topical insulin-like growth factor-1 therapy for sudden deafness refractory to systemic corticosteroid treatment. *BMC Med.* 12:219. doi: 10.1186/s12916-014-0219-x

Ng, J. H., Ho, R. C., Cheong, C. S., Ng, A., Yuen, H. W., and Ngo, R. Y. (2014). Intratympanic steroids as a salvage treatment for sudden sensorineural hearing loss? A meta-analysis. *Eur. Arch. Otorhinolaryngol.* doi: 10.1007/s00405-014-3288-8. [Epub ahead of print].

Nibuya, M., Nestler, E. J., and Duman, R. S. (1996). Chronic antidepressant administration increases the expression of cAMP response element binding protein (CREB) in rat hippocampus. *J. Neurosci.* 16, 2365–2372.

Nicholl, A. J., Kneebone, A., Davies, D., Cacciabue-Rivolta, D. I., Rivolta, M. N., Coffey, P., et al. (2005). Differentiation of an auditory neuronal cell line suitable for cell transplantation. *Eur. J. Neurosci.* 22, 343–353. doi: 10.1111/j.1460-9568.2005.04213.x

Paillard, A., Hindre, F., Vignes-Colombeix, C., Benoit, J. P., and Garcion, E. (2010). The importance of endo-lysosomal escape with lipid nanocapsules for drug subcellular bioavailability. *Biomaterials* 31, 7542–7554. doi: 10.1016/j.biomaterials.2010.06.024

Pathak, S., Cao, E., Davidson, M. C., Jin, S., and Silva, G. A. (2006). Quantum dot applications to neuroscience: new tools for probing neurons and glia. *J. Neurosci.* 26, 1893–1895. doi: 10.1523/JNEUROSCI.3847-05.2006

Paulson, D. P., Abuzeid, W., Jiang, H., Oe, T., O'malley, B. W., and Li, D. (2008). A novel controlled local drug delivery system for inner ear disease. *Laryngoscope* 118, 706–711. doi: 10.1097/MLG.0b013e31815f8e41

Perrier, T., Saulnier, P., Fouchet, F., Lautram, N., and Benoit, J. P. (2010). Post-insertion into Lipid NanoCapsules (LNCs): from experimental aspects to mechanisms. *Int. J. Pharm.* 396, 204–209. doi: 10.1016/j.ijpharm.2010.06.019

Pettingill, L. N., Wise, A. K., Geaney, M. S., and Shepherd, R. K. (2011). Enhanced auditory neuron survival following cell-based BDNF treatment in the deaf guinea pig. *PLoS ONE* 6:e18733. doi: 10.1371/journal.pone.0018733

Pritz, C. O., Bitsche, M., Salvenmoser, W., Dudas, J., Schrott-Fischer, A., and Glueckert, R. (2013a). Endocytic trafficking of silica nanoparticles in a cell line derived from the organ of Corti. *Nanomedicine (Lond)* 8, 239–252. doi: 10.2217/nnm.12.91

Pritz, C. O., Dudas, J., Rask-Andersen, H., Schrott-Fischer, A., and Glueckert, R. (2013b). Nanomedicine strategies for drug delivery to the ear. *Nanomedicine (Lond)* 8, 1155–1172. doi: 10.2217/nnm.13.104

Raible, D. W., and Ungos, J. M. (2006). Specification of sensory neuron cell fate from the neural crest. *Adv. Exp. Med. Biol.* 589, 170–180. doi: 10.1007/978-0-387-46954-6_10

Ranjan, S., Sood, R., Dudas, J., Glueckert, R., Schrott-Fischer, A., Roy, S., et al. (2012). Peptide-mediated targeting of liposomes to TrkB receptor-expressing cells. *Int. J. Nanomedicine* 7, 3475–3485. doi: 10.2147/IJN.S32367

Rask-Andersen, H., Schrott-Fischer, A., Pfaller, K., and Glueckert, R. (2006). Perilymph/modiolar communication routes in the human cochlea. *Ear Hear.* 27, 457–465. doi: 10.1097/01.aud.0000233864.32183.81

Roy, S., Glueckert, R., Johnston, A. H., Perrier, T., Bitsche, M., Newman, T. A., et al. (2012). Strategies for drug delivery to the human inner ear by multifunctional nanoparticles. *Nanomedicine (Lond)* 7, 55–63. doi: 10.2217/nnm.11.84

Roy, S., Johnston, A. H., Newman, T. A., Glueckert, R., Dudas, J., Bitsche, M., et al. (2010). Cell-specific targeting in the mouse inner ear using nanoparticles conjugated with a neurotrophin-derived peptide ligand: potential tool for drug delivery. *Int. J. Pharm.* 390, 214–224. doi: 10.1016/j.ijpharm.2010.02.003

Rubel, E. W., and Fritzsch, B. (2002). Auditory system development: primary auditory neurons and their targets. *Annu. Rev. Neurosci.* 25, 51–101. doi: 10.1146/annurev.neuro.25.112701.142849

Salt, A. N., and Plontke, S. K. (2009). Principles of local drug delivery to the inner ear. *Audiol. Neurootol.* 14, 350–360. doi: 10.1159/000241892

Schuknecht, H. F. (1956). Ablation therapy for the relief of Meniere's disease. *Laryngoscope* 66, 859–870. doi: 10.1288/00005537-195607000-00005

Shang, L., Nienhaus, K., and Nienhaus, G. U. (2014). Engineered nanoparticles interacting with cells: size matters. *J. Nanobiotechnol.* 12:5. doi: 10.1186/1477-3155-12-5

Soumen, R., Johnston, A. H., Moin, S. T., Dudas, J., Newman, T. A., Hausott, B., et al. (2012). Activation of TrkB receptors by NGFbeta mimetic peptide conjugated polymersome nanoparticles. *Nanomedicine* 8, 271–274. doi: 10.1016/j.nano.2011.12.005

Spear, S. A., and Schwartz, S. R. (2011). Intratympanic steroids for sudden sensorineural hearing loss: a systematic review. *Otolaryngol. Head Neck Surg.* 145, 534–543. doi: 10.1177/0194599811419466

Steketee, M. B., Moysidis, S. N., Jin, X. L., Weinstein, J. E., Pita-Thomas, W., Raju, H. B., et al. (2011). Nanoparticle-mediated signaling endosome localization regulates growth cone motility and neurite growth. *Proc. Natl. Acad. Sci. U.S.A.* 108, 19042–19047. doi: 10.1073/pnas.1019624108

Suckfuell, M., Canis, M., Strieth, S., Scherer, H., and Haisch, A. (2007). Intratympanic treatment of acute acoustic trauma with a cell-permeable JNK ligand: a prospective randomized phase I/II study. *Acta Otolaryngol.* 127, 938–942. doi: 10.1080/00016480601110212

Tamura, T., Kita, T., Nakagawa, T., Endo, T., Kim, T. S., Ishihara, T., et al. (2005). Drug delivery to the cochlea using PLGA nanoparticles. *Laryngoscope* 115, 2000–2005. doi: 10.1097/01.mlg.0000180174.81036.5a

Thaler, M., Roy, S., Fornara, A., Bitsche, M., Qin, J., Muhammed, M., et al. (2011). Visualization and analysis of superparamagnetic iron oxide nanoparticles in the inner ear by light microscopy and energy filtered TEM. *Nanomedicine* 7, 360–369. doi: 10.1016/j.nano.2010.11.005

Ulbrich, K., Hekmatara, T., Herbert, E., and Kreuter, J. (2009). Transferrin- and transferrin-receptor-antibody-modified nanoparticles enable drug delivery across the blood-brain barrier (BBB). *Eur. J. Pharm. Biopharm.* 71, 251–256. doi: 10.1016/j.ejpb.2008.08.021

Uster, P. S., Allen, T. M., Daniel, B. E., Mendez, C. J., Newman, M. S., and Zhu, G. Z. (1996). Insertion of poly(ethylene glycol) derivatized phospholipid into pre-formed liposomes results in prolonged *in vivo* circulation time. *FEBS Lett.* 386, 243–246. doi: 10.1016/0014-5793(96)00452-8

Visser, C. E., Brouwer-Steenbergen, J. J., Schadee-Eestermans, I. L., Meijer, S., Krediet, R. T., and Beelen, R. H. (1996). Ingestion of Staphylococcus aureus, Staphylococcus epidermidis, and Escherichia coli by human peritoneal mesothelial cells. *Infect. Immun.* 64, 3425–3428.

Vonarbourg, A., Passirani, C., Saulnier, P., and Benoit, J. P. (2006a). Parameters influencing the stealthiness of colloidal drug delivery systems. *Biomaterials* 27, 4356–4373. doi: 10.1016/j.biomaterials.2006.03.039

Vonarbourg, A., Passirani, C., Saulnier, P., Simard, P., Leroux, J. C., and Benoit, J. P. (2006b). Evaluation of pegylated lipid nanocapsules versus complement system activation and macrophage uptake. *J. Biomed. Mater. Res. A* 78, 620–628. doi: 10.1002/jbm.a.30711

Wang, J., Van De Water, T. R., Bonny, C., De Ribaupierre, F., Puel, J. L., and Zine, A. (2003). A peptide inhibitor of c-Jun N-terminal kinase protects against both aminoglycoside and acoustic trauma-induced auditory hair cell death and hearing loss. *J. Neurosci.* 23, 8596–8607.

Wang, Q., and Green, S. H. (2011). Functional role of neurotrophin-3 in synapse regeneration by spiral ganglion neurons on inner hair cells after excitotoxic trauma *in vitro*. *J. Neurosci.* 31, 7938–7949. doi: 10.1523/JNEUROSCI.1434-10.2011

Watson, F. L., Heerssen, H. M., Bhattacharyya, A., Klesse, L., Lin, M. Z., and Segal, R. A. (2001). Neurotrophins use the Erk5 pathway to mediate a retrograde survival response. *Nat. Neurosci.* 4, 981–988. doi: 10.1038/nn720

Weissmiller, A. M., and Wu, C. (2012). Current advances in using neurotrophic factors to treat neurodegenerative disorders. *Transl. Neurodegener.* 1:14. doi: 10.1186/2047-9158-1-14

Wiedemann, F. R., Siemen, D., Mawrin, C., Horn, T. F., and Dietzmann, K. (2006). The neurotrophin receptor TrkB is colocalized to mitochondrial membranes. *Int. J. Biochem. Cell Biol.* 38, 610–620. doi: 10.1016/j.biocel.2005.10.024

Wu, H. H., Bellmunt, E., Scheib, J. L., Venegas, V., Burkert, C., Reichardt, L. F., et al. (2009). Glial precursors clear sensory neuron corpses during development via Jedi-1, an engulfment receptor. *Nat. Neurosci.* 12, 1534–1541. doi: 10.1038/nn.2446

Yamasoba, T., Lin, F. R., Someya, S., Kashio, A., Sakamoto, T., and Kondo, K. (2013). Current concepts in age-related hearing loss: epidemiology and mechanistic pathways. *Hear. Res.* 303, 30–38. doi: 10.1016/j.heares.2013.01.021

Yorgason, J. G., Kalinec, G. M., Luxford, W. M., Warren, F. M., and Kalinec, F. (2010). Acetaminophen ototoxicity after acetaminophen/hydrocodone abuse: evidence from two parallel *in vitro* mouse models. *Otolaryngol. Head Neck Surg.* 142, 814–819, 819 e811–819 e812. doi: 10.1016/j.otohns.2010.01.010

Zilberstein, Y., Liberman, M. C., and Corfas, G. (2012). Inner hair cells are not required for survival of spiral ganglion neurons in the adult cochlea. *J. Neurosci.* 32, 405–410. doi: 10.1523/JNEUROSCI.4678-11.2012

Zou, J., Saulnier, P., Perrier, T., Zhang, Y., Manninen, T., Toppila, E., et al. (2008). Distribution of lipid nanocapsules in different cochlear cell populations after round window membrane permeation. *J. Biomed. Mater. Res. B Appl. Biomater.* 87, 10–18. doi: 10.1002/jbm.b.31058

Conflict of Interest Statement: The authors declare that the research was conducted in the absence of any commercial or financial relationships that could be construed as a potential conflict of interest.

frontiers in Aging Neuroscience

MINI REVIEW
published: 15 May 2015
doi: 10.3389/fnagi.2015.00086

Synergistic effects of free radical scavengers and cochlear vasodilators: a new otoprotective strategy for age-related hearing loss

Juan Carlos Alvarado[1], Verónica Fuentes-Santamaría[1], Pedro Melgar-Rojas[1], María Llanos Valero[1], María Cruz Gabaldón-Ull[1], Josef M. Miller[2,3†] and José M. Juiz[1†]*

[1] Facultad de Medicina, Universidad de Castilla-La Mancha, Instituto de Investigación en Discapacidades Neurológicas (IDINE), Albacete, Spain, [2] Karolinska Institutet, Stockholm, Sweden, [3] Kresge Hearing Research Institute, University of Michigan, Ann Arbor, MI, USA

OPEN ACCESS

Edited by:
Marta Milo,
University of Sheffield, UK

Reviewed by:
Daniel Ortuño-Sahagún,
Centro Universitario de Ciencias de la Salud, Mexico
Matthew C. Holley,
University of Sheffield, UK
Marta Milo,
University of Sheffield, UK

***Correspondence:**
Juan Carlos Alvarado,
Facultad de Medicina, Universidad de Castilla-La Mancha, Instituto de Investigación en Discapacidades Neurológicas (IDINE), Campus de Albacete, Calle Almansa 14, 02006, Albacete, Spain
juancarlos.alvarado@uclm.es

† Senior contributor to this work.

Received: 15 January 2015
Paper pending published: 23 April 2015
Accepted: 30 April 2015
Published: 15 May 2015

Citation:
Alvarado JC, Fuentes-Santamaría V, Melgar-Rojas P, Valero ML, Gabaldón-Ull MC, Miller JM and Juiz JM (2015) Synergistic effects of free radical scavengers and cochlear vasodilators: a new otoprotective strategy for age-related hearing loss. Front. Aging Neurosci. 7:86. doi: 10.3389/fnagi.2015.00086

The growing increase in age-related hearing loss (ARHL), with its dramatic reduction in quality of life and significant increase in health care costs, is a catalyst to develop new therapeutic strategies to prevent or reduce this aging-associated condition. In this regard, there is extensive evidence that excessive free radical formation along with diminished cochlear blood flow are essential factors involved in mechanisms of other stress-related hearing loss, such as that associated with noise or ototoxic drug exposure. The emerging view is that both play key roles in ARHL pathogenesis. Therapeutic targeting of excessive free radical formation and cochlear blood flow regulation may be a useful strategy to prevent onset of ARHL. Supporting this idea, micronutrient-based therapies, in particular those combining antioxidants and vasodilators like magnesium (Mg^{2+}), have proven effective in reducing the impact of noise and ototoxic drugs in the inner ear, therefore improving auditory function. In this review, the synergistic effects of combinations of antioxidant free radicals scavengers and cochlear vasodilators will be discussed as a feasible therapeutic approach for the treatment of ARHL.

Keywords: antioxidants, vitamins, cochlear blood flow, magnesium, oxidative stress, presbyacusis, sensorineural hearing loss

Introduction

Despite the fact that age-related hearing loss (ARHL) affects more than one-third of the world population over 60 years-old, rising to more than two-third of those in their 70's (Ohlemiller and Frisina, 2008; Gopinath et al., 2009; Lin et al., 2011; Yamasoba et al., 2013), currently there is no available medical treatment for this age-related sensory dysfunction. This has led to an important humanitarian cost in terms of isolation, frustration, depression, cognitive decline and decrease in quality of life (World Health Organization, 2002, 2013; Huang and Tang, 2010; Kidd III and Bao, 2012; Ciorba et al., 2012), along with an enormous and growing economic burden in health care costs (World Health Organization, 2002, 2013; Huang and Tang, 2010). In an attempt to address this issue, recent research has focused on understanding the cellular mechanisms that participate in the development and progression of ARHL, in order to refine its diagnosis and facilitate the design of new therapeutic strategies to prevent or reduce this sensory impairment and it consequences. Animal models have been

valuable tools for the evaluation of this complex and multifactorial condition; and have provided significant information on the underlying genetic, molecular, histological and physiological factors associated with ARHL (Syka, 2002, 2010; Ohlemiller, 2006; Bielefeld et al., 2008, 2010; Fetoni et al., 2011; Alvarado et al., 2014). Previous studies have demonstrated that similar to that which occurs in other stress-related auditory pathologies, such as noise and drug-induced hearing loss (Ames et al., 1993; Ohlemiller, 2006; Chen et al., 2009; Bielefeld et al., 2010; Huang and Tang, 2010; Fetoni et al., 2011; Haider et al., 2014), an excess of free radical formation and blood flow reduction in the cochlea may be critical factors in triggering hearing loss associated with aging (Seidman et al., 2002; Bielefeld et al., 2010; Fetoni et al., 2011; Fujimoto and Yamasoba, 2014).

Free Radical Formation and Blood Flow Reduction in Cochlea

As part of normal cellular homeostasis, free radicals, notably reactive oxygen species (ROS), are continuously generated during aerobic respiration as by-products of redox reactions, mostly in mitochondria (Ames et al., 1993; Chen et al., 2009; Bielefeld et al., 2010; Huang and Tang, 2010; Fujimoto and Yamasoba, 2014). Free radicals are unstable molecular species that contain one or more unpaired electrons, which make them highly reactive (Halliwell, 2006; Halliwell and Gutteridge, 2007). It is noteworthy, that although all oxygen radicals are ROS, not all ROS are oxygen radicals, leading researchers to distinguish between oxygen non-radical species and reactive radical/non-radical species (e.g., reactive nitrogen species, reactive bromide species, and reactive chlorine species) (for a detailed summary of ROS, see Halliwell, 2006; Halliwell and Gutteridge, 2007). Under normal conditions, adequate intracellular ROS levels are essential to regulate many cell signaling pathways (Finkel, 2012; Ray et al., 2012; Sena and Chandel, 2012) and cellular homeostasis (Sena and Chandel, 2012), among other cellular functions. However, as a consequence of imbalances in production of free radicals and endogenous antioxidant systems, ROS concentrations may increase, become toxic, and cause oxidative stress-induced cell damage (Ames et al., 1993; Halliwell, 2006; Halliwell and Gutteridge, 2007; Chen et al., 2009; Sena and Chandel, 2012; Böttger and Schacht, 2013; Fujimoto and Yamasoba, 2014). As ROS-induced reactions proceed, other excessive free radicals, such as nitric monoxide, peroxide, superoxide, hydroxyl or peroxyl radicals (Ames et al., 1993; Seidman et al., 2002; Halliwell, 2006; Halliwell and Gutteridge, 2007; Uttara et al., 2009; Park and Yeo, 2013; Fujimoto and Yamasoba, 2014), interact causing oxidative damage of lipids and proteins in cell membranes and the cytosol, mitochondrial and nuclear genome mutations, and ultimately lead to cellular death (Ames et al., 1993; Uttara et al., 2009; Lee and Wei, 2012; Fujimoto and Yamasoba, 2014).

As postulated for several neurodegenerative diseases such as amyotrophic lateral sclerosis, Alzheimer's, Parkinson's and Huntington's diseases (Ames et al., 1993; Lin and Beal, 2006), the cascade of molecular events related to ROS overproduction may play a crucial role during the aging process (Ames et al., 1993; Ohlemiller, 2006; Chen et al., 2009; Bielefeld et al., 2010; Huang and Tang, 2010; Fetoni et al., 2011; Fujimoto and Yamasoba, 2014; Haider et al., 2014; Ortuño-Sahagún et al., 2014). Specifically, an excess of free radicals in the cochlear sensory epithelium, spiral ganglion neurons and cells of the stria vascularis may have a relevant role in the development of ARHL (**Figures 1A–D**; Ohlemiller, 2006; Chen et al., 2009; Bielefeld et al., 2010; Huang and Tang, 2010; Fetoni et al., 2011; Fujimoto and Yamasoba, 2014). Of importance, excessive ROS build up is clearly the key factor in the pathogenesis of other stress-induced otological conditions that also result in reduced auditory function, such as noise and drug induced hearing loss (**Figure 1E**; Ohinata et al., 2003; Le Prell et al., 2007a,b, 2014; Bielefeld et al., 2010; Fetoni et al., 2011). These findings provide the rationale to support the hypothesis that therapeutic strategies targeting ROS overproduction may be potentially useful not only for ameliorating noise and drug induced hearing loss but also to improve ARLH. Thus we propose that excessive free radical formation may provide a "common pathogenic pathway", shared by these pathologies (**Figure 1E**).

In addition to free radical generation in the cochlea, reduction in cochlear blood flow and vascular conductance during aging is another main contributor to cochlear damage. Consistent with this notion, during senescence there is a significant decrease in the circulating blood volume with reductions that may reach up to 20% in the cerebral flow (Park and Yeo, 2013). Despite the strong autoregulation of cochlear blood flow that occurs under normal conditions, the cochlea is no exception to this rule, as a significant decrease in blood flow regulation as well as in blood supply to the cochlea occurs during aging, particularly in the stria vascularis, in a number of animal models and man (Johnsson and Hawkins, 1972; Schuknecht and Gacek, 1993; Nakashima, 1999; Seidman et al., 1999; Seidman, 2000; Shi, 2011). Age-related alterations in the microvasculature of the stria vascularis, virtually the only vascularized epithelium in the body, have been found to correlate with the increase in auditory thresholds observed in presbyacusis, a condition known as strial or "metabolic" presbyacusis (Schuknecht and Gacek, 1993), as well as in noise and drug induced hearing loss, (Boettcher, 2002; Bielefeld et al., 2010; Fetoni et al., 2011; Shi, 2011; Lee, 2013; Ruan et al., 2014). The stria vascularis is pivotal in maintaining the endocochlear potential (EP; **Figure 1F**) as alterations in its structure and function induce a progressive decrease in the EP, finally affecting the cochlear amplification of acoustic signals (Gates and Mills, 2005; Schmiedt, 2010). Thus, diminished cochlear blood flow may contribute to damage to the stria vascularis and altered hair cell function (with or without cell death) and to aging-related increases in auditory thresholds (Shi, 2011; Lee, 2013). It is worth noting that recent evidence shows that there is a significant involvement of strial presbyacusis in the genesis of the ARHL, leading to the suggestion that alterations in the stria vascularis could be the major cause of hearing loss during aging (Schuknecht and Gacek, 1993; Gates and Mills, 2005; Schmiedt, 2010; Clinkard et al., 2013; Lee, 2013). In line with these observations, pharmacological up-regulation of cochlear blood flow could provide a vital treatment for ARHL.

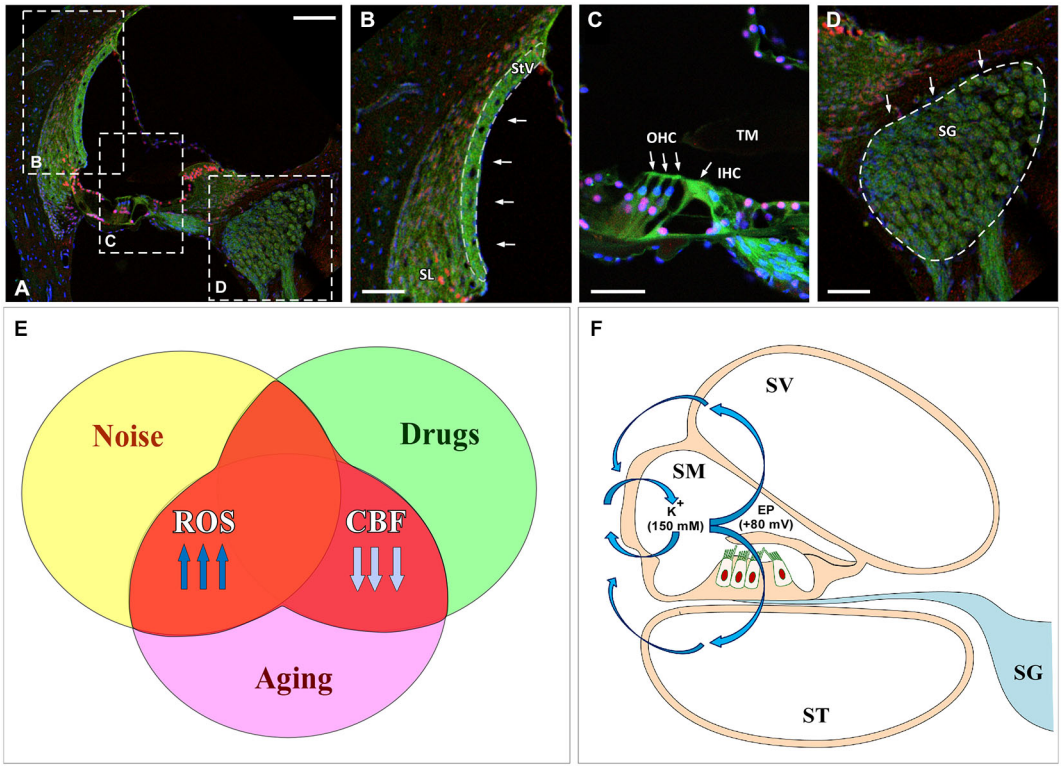

FIGURE 1 | Cochlear damage results in imbalances in free radical formation and cochlear blood supply in the inner ear following noise overstimulation, ototoxic drugs and aging. (A–D) Confocal images show target cochlear structures affected by oxidative stress and reduced CBF: the StV and SL **(B)**, outer and inner hair cells (arrows in **C**) and the SG **(D)**. Dashed line in **(B)** outlines the StV. Filamentous actin was stained with Phalloidin (green) and cell nuclei with caspase (red) and DAPI (blue). **(E)** Excessive ROS along with reduced CBF lead to oxidative stress-induced cell damage causing disruption of the inner ear structure and function. **(F)** Injury to the stria vascularis induces a dysregulation of the EP (blue arrows) that affects $K^{(+)}$ concentration, which in addition to diminished CBF, results in sensory epithelium disruption. Abbreviations: ROS, reactive oxygen species; CBF, cochlear blood flow; EP, endocochlear potential; SV, scala vestibuli; SM, scala media; ST, scala tympani; StV, stria vascularis; SL, spiral ligament; SG, spiral ganglion; TM, tectorial membrane; OHC, outer hair cells; IHC inner hair cell. Scale bars: 100 μm in **(A)**; 50 μm in **(B–D)**.

Free Radical Scavengers and Vasodilators

In the cell, there are different and overlapping antioxidant systems of defense against oxidative stress. The enzymatic systems involved include superoxide dismutase, glutathione peroxidase, glutathione reductase and catalases while the non-enzymatic scavengers are vitamins and micronutrients (**Figures 2A,B**; Halliwell, 2006; Halliwell and Gutteridge, 2007). As an excess of free radical formation is likely involved in the pathogenesis of many types of hearing loss, the administration of antioxidants has been used to minimize or avoid inner ear damage in conditions such as noise and drug induced hearing loss (Yamasoba et al., 1999; Seidman et al., 2002; Ohinata et al., 2003; Yamashita et al., 2005; Le Prell et al., 2007a, 2011; Fetoni et al., 2011). Although there is still controversy about the benefits of using free radical scavengers for the treatment of ROS induced cochlear damage (Uttara et al., 2009; Bielefeld et al., 2010; Park and Yeo, 2013), most studies seem to agree that antioxidants reduce structural and functional stress-induced pathology in the inner ear in experimental animals (Yamasoba et al., 1999; Ohinata et al., 2003; Yamashita et al., 2005; Le Prell et al., 2007b; Bielefeld et al., 2010; Fetoni et al., 2011). For instance, mannitol (Yamasoba et al., 1999), N-acetylcysteine (Kopke et al., 2005, 2007), acetyl-L-carnitine (Kopke et al., 2005), sallicylates combined with N-acetylcysteine (Kopke et al., 2000, 2005), trolox (Yamashita et al., 2005) or vitamins A, C, and E (Le Prell et al., 2007a, 2011) attenuate inner ear damage following noise-induce hearing loss. Similarly, D-methionine (Campbell et al., 2007), N-acetylcysteine (Tokgoz et al., 2011) or a combination of vitamins A, C, and E (Le Prell et al., 2014) also have been shown to protect the cochlea after drug ototoxicity.

This growing body of evidence supports the use of antioxidants to ameliorate pathological related to excess ROS. A clear example of this is the prevention and interruption of ROS-induced lipid peroxidation in cell membranes by vitamins A, C, and E (**Figures 2A,B**; Halliwell, 2006; Halliwell and Gutteridge, 2007). Given the key role of ROS in ARHL (Ohlemiller, 2006; Chen et al., 2009; Bielefeld et al., 2010; Huang and Tang, 2010; Fetoni et al., 2011; Fujimoto and Yamasoba, 2014), it is likely that free radical scavengers may provide a pharmacological approach to treat presbyacusis. Supporting this expectation the administration of resveratrol (Seidman et al., 2003) or L-carnitine

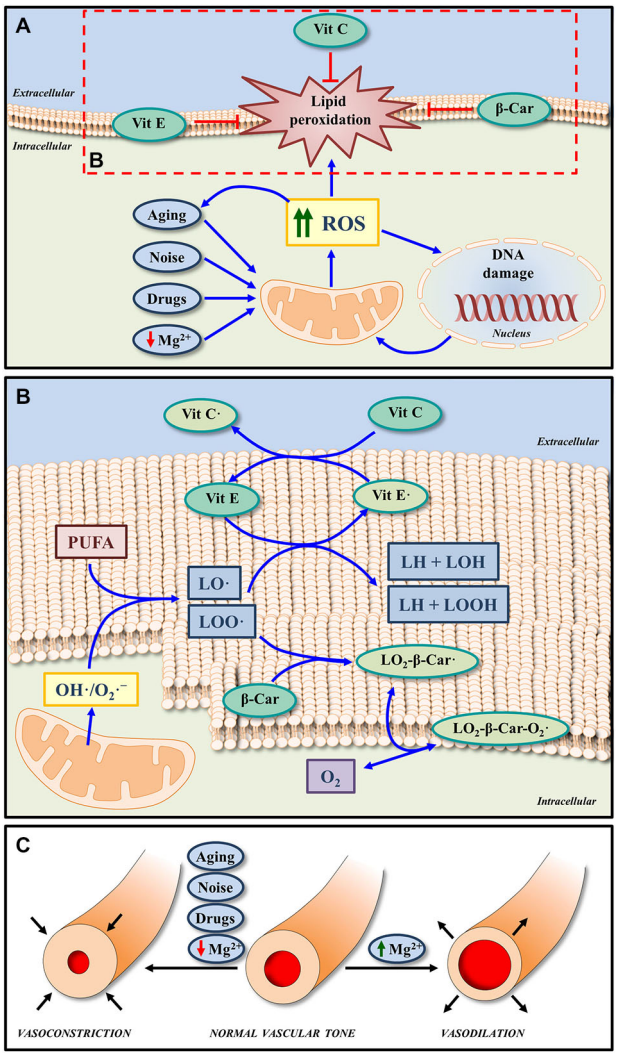

FIGURE 2 | Effects of micronutrients on oxidative stress and cochlea vasculature. (A) Increased ROS generation induced by noise, drugs, aging and even low extracellular Mg^{2+}, may lead to oxidative DNA damage and lipid peroxidation in the cell membrane. The non-enzymatic antioxidant system, which is composed by micronutrients such as Vit E, Vit C, and β-Car (metabolized to form Vit A) can block and/or revert lipid peroxidation, by reducing the impact of oxidative stress. **(B)** In response to ROS overproduction, peroxyl radicals of lipids (LOO·) and alkoxyl radicals of lipids (LO·) can be generated from polyunsaturated fatty acids (PUFA) of the cell membrane phospholipids. Both radicals can be scavenged by Vit E, one of the major antioxidants in the cell membrane. On the other hand, Vit C, considered one of the most important antioxidant molecules in the extracellular fluid, in addition to scavenging ROS, it can also protect cell membranes by regenerating Vit E from the oxidized form (Vit E·). Thus, the functions of both Vit E and Vit C in lipid peroxidation are coupled. Finally, the antioxidant activity of β-Car may also contribute to protect membranes from lipid peroxidation by scavenging LOO·. The reaction product (LO_2-β-Car·) can react in turn with an oxygen molecule to generate a new peroxyl radical (LO_2-β-Car-O_2·). **(C)** A byproduct of free radical formation in the inner ear (8-Iso-Prostaglandin $F_{2\alpha}$) is a powerful vasoconstrictor; and thus reduced blood flow is found with intense noise exposure, which may be blocked by an isoprostane blocker or a cochlear vasodilator, such as Mg^{2+}. Similarly Mg^{2+} will increase inner ear blood flow in the vascularly compromised aging ear.

(*Continued*)

FIGURE 2 | Continued

Abbreviations: ROS, reactive oxygen species; Vit A, vitamin A; Vit E, vitamin E; Vit C, vitamin C; β-Car, β-Carotene; Mg^{2+}, magnesium; O_2·-, superoxide radical; OH·, hydroxyl radicals.

(Derin et al., 2004) in Fischer 344 and Wistar rats respectively, or a combination of L-cysteine-glutathione mixed disulfide, ribose-cysteine, NW-nitro-L-arginine methyl ester, vitamin B12, folate, and ascorbic acid in C57BL/6 mice (Heman-Ackah et al., 2010) led to improved auditory function and delayed onset of ARHL. In possible contradiction, the administration of either vitamin C in senescent marker protein 30/gluconolactonase knockout mice, which cannot synthesize vitamin C (Kashio et al., 2009), N-acetyl-L-cysteine in the C57BL/6J mouse strain (Davis et al., 2007) or a combination of vitamins A, C, and E, L-carnitine and α-lipoic-enriched diet in CBA/J mice (Sha et al., 2012) did not improve auditory function or reduce ARHL. Negative results are of course more difficult to interpret. They may be due to inadequate dosing or to species differences or to the different experimental conditions used for the administration of antioxidants. Also, targeting a single factor responsible for the pathogenesis of the ARHL may not be sufficient to avoid or reduce the effects of aging on hearing.

Given the fact that strial presbyacusis could be at the origin of most forms of ARHL (Schuknecht and Gacek, 1993; Gates and Mills, 2005; Schmiedt, 2010; Clinkard et al., 2013; Lee, 2013), and that this pathology is caused at least in part by alterations in the microvasculature and decreased strial blood flow, the use of cochlear vasodilators to improve auditory thresholds during aging seems a reasonable option. Indirectly supporting this idea, the administration of hydrogen sulfide as a vasodilator following noise-induced hearing loss has been proven to have a protective effect on the inner ear as it reduces cochlear damage and improves auditory function (Li et al., 2011). A similar positive response on hearing was observed when using hydroxyethyl starch but not when pentoxifylline was administered in guinea pigs after noise trauma (Lamm and Arnold, 2000). As opposed to these latter findings, a recent study in guinea pigs concluded that the administration of pentoxifylline after noise overexposure produced a near-normal auditory brainstem response and reduced the damage to the organ of Corti (Kansu et al., 2011). Another potential cochlear vasodilator that has been used as otoprotector is Mg^{2+} (**Figure 2C**). Pharmacological properties of this cation include increased cochlear blood flow (Haupt and Scheibe, 2002), modulation of the NMDA glutamate receptor, regulation of influx of calcium into the sensory hair cells and also calcium channel permeability (Günther et al., 1989; Cevette et al., 2003; Le Prell et al., 2007b). The effectiveness of magnesium in protecting the cochlea from noise insult has been shown in guinea pigs (Ising et al., 1982; Scheibe et al., 2000; Miller et al., 2003; Le Prell et al., 2007a), CBA/J mice (Le Prell et al., 2011) and humans (Attias et al., 1994). Of relevance, magnesium has a greater otoprotective effect after noise trauma in CBA/J mice when coupled to free radical scavengers than that observed when either magnesium or antioxidants are used individually

as micronutrients (Le Prell et al., 2007a). Indeed together their protective effect is significantly greater than the sum of the individual agent protective effects. A similar combination of micronutrients has been demonstrated to reduce gentamicin-induced ototoxicity, reducing the threshold shift for frequencies at 12 kHz and below and protecting inner and outer hair cells in the upper half of the cochlea (Le Prell et al., 2014). As presbyacusis shares physiopathological alterations with noise and drug induced hearing loss, vasodilators like Mg^{2+} may protect the inner ear during aging (**Figure 2C**). Nonetheless, despite the benefits of using vasodilators for the treatment of hearing loss, as described in this review, there are no studies to date that have assessed its effects either individually or in combination on ARHL.

Conclusions

In the light of evidence presented in this review, focused on the key roles of free radicals and reduced blood flow in pathogenesis of stress-induced hearing loss, we propose that a combined therapy targeting these specific factors, which are well implicated in the genesis and/or progression of presbyacusis, may attenuate ear damage and therefore, improve auditory function during aging. While there is not yet an effective medication to prevent a multifactorial and complex pathological condition such as ARHL, a treatment based on the synergistic effects of natural micronutrients such as the antioxidants vitamins A, C and E and the vasodilator magnesium all with good safety profiles, seems to be an excellent and promising efficacious therapeutic alternative for the treatment of this sensory impairment associated with aging.

Author and Contributors

Drafting of the manuscript: JCA and VF-S. Design of figures: JCA, VF-S, PM-R, MCG-U. Critical revision of the manuscript for important intellectual content: JCA, VF-S, PM-R, MLV, JMM and JMJ.

Acknowledgments

This study was supported by the PROHEARING project of the 7th Framework Programme (FP7-HEALTH-2012-INNOVATON 304925).

References

Alvarado, J. C., Fuentes-Santamaría, V., Gabaldón-Ull, M. C., Blanco, J. L., and Juiz, J. M. (2014). Wistar rats: a forgotten model of age-related hearing loss. *Front. Aging Neurosci.* 6:29. doi: 10.3389/fnagi.2014.00029

Ames, B. N., Shigenaga, M. K., and Hagen, T. M. (1993). Oxidants, antioxidants and the degenerative disease of aging. *Proc. Natl. Acad. Sci. U S A* 90, 7915–7922. doi: 10.1073/pnas.90.17.7915

Attias, J., Weisz, G., Almog, S., Shahar, A., Wiener, M., Joachims, Z., et al. (1994). Oral magnesium intake reduces permanent hearing loss induced by noise exposure. *Am. J. Otolaryngol.* 15, 26–32. doi: 10.1016/0196-0709(94)90036-1

Bielefeld, E. C., Coling, D., Chen, G. D., Li, M., Tanaka, C., Hu, B. H., et al. (2008). Age-related hearing loss in the Fischer 344/NHsd rat substrain. *Hear. Res.* 241, 26–33. doi: 10.1016/j.heares.2008.04.006

Bielefeld, E. C., Tanaka, C., Chen, G. D., and Henderson, D. (2010). Age-related hearing loss: is it a preventable condition? *Hear. Res.* 264, 98–107. doi: 10.1016/j.heares.2009.09.001

Boettcher, F. A. (2002). Presbyacusis and the auditory brainstem response. *J. Speech Lang. Hear. Res.* 45, 1249–1261. doi: 10.1044/1092-4388(2002/100)

Böttger, E. C., and Schacht, J. (2013). The mitochondrion: a perpetrator of acquired hearing loss. *Hear. Res.* 303, 12–19. doi: 10.1016/j.heares.2013.01.006

Campbell, K. C., Meech, R. P., Klemens, J. J., Gerberi, M. T., Dyrstad, S. S., Larsen, D. L., et al. (2007). Prevention of noise- and drug-induced hearing loss with D-methionine. *Hear. Res.* 226, 92–103. doi: 10.1016/j.heares.2006.11.012

Cevette, M. J., Vormann, J., and Franz, K. (2003). Magnesium and hearing. *J. Am. Acad. Audiol.* 14, 202–212.

Chen, G. D., Li, M., Tanaka, C., Bielefeld, E. C., Hu, B. H., Kermany, M. H., et al. (2009). Aging outer hair cells (OHCs) in the Fischer 344 rat cochlea: function and morphology. *Hear. Res.* 248, 39–47. doi: 10.1016/j.heares.2008.11.010

Ciorba, A., Bianchini, C., Pelucchi, S., and Pastore, A. (2012). The impact of hearing loss on the quality of life of elderly adults. *Clin. Interv. Aging* 7, 159–163. doi: 10.2147/cia.s26059

Clinkard, D., Amoodi, H., Kandasamy, T., Grewal, A. S., Chen, S., Qian, W., et al. (2013). Changes in the cochlear vasculature and vascular endothelial growth factor and its receptors in the aging c57 mouse cochlea. *ISRN Otolaryngol.* 2013:430625. doi: 10.1155/2013/430625

Davis, R. R., Kuo, M. W., Stanton, S. G., Canlon, B., Krieg, E., and Alagramam, K. N. (2007). N-Acetyl L-cysteine does not protect against premature age-related hearing loss in C57BL/6J mice: a pilot study. *Hear. Res.* 226, 203–208. doi: 10.1016/j.heares.2006.07.003

Derin, A., Agirdir, B., Derin, N., Dinç, O., Güney, K., Ozcaglar, H., et al. (2004). The effects of L-carnitine on presbyacusis in the rat model. *Clin. Otolaryngol. Allied. Sci.* 29, 238–241. doi: 10.1111/j.1365-2273.2004.00790.x

Fetoni, A. R., Picciotti, P. M., Paludetti, G., and Troiani, D. (2011). Pathogenesis of presbycusis in animal models: a review. *Exp. Gerontol.* 46, 413–425. doi: 10.1016/j.exger.2010.12.003

Finkel, T. (2012). Signal transduction by mitochondrial oxidants. *J. Biol. Chem.* 287, 4434–4440. doi: 10.1074/jbc.r111.271999

Fujimoto, C., and Yamasoba, T. (2014). Oxidative stresses and mitochondrial dysfunction in age-related hearing loss. *Oxid. Med. Cell. Longev.* 2014:582849. doi: 10.1155/2014/582849

Gates, G. A., and Mills, J. H. (2005). Presbycusis. *Lancet* 366, 1111–1120. doi: 10.1016/s0140-6736(05)67423-5

Gopinath, B., Rochtchina, E., Wang, J. J., Schneider, J., Leeder, S. R., Mitchell, P., et al. (2009). Prevalence of age-related hearing loss in older adults: blue mountains study. *Arch. Intern. Med.* 169, 415–416. doi: 10.1001/archinternmed.2008.597

Günther, T., Ising, H., and Joachims, Z. (1989). Biochemical mechanisms affecting susceptibility to noise-induced hearing loss. *Am. J. Otol.* 10, 36–41.

Haider, S., Saleem, S., Perveen, T., Tabassum, S., Batool, Z., Sadir, S., et al. (2014). Age-related learning and memory deficits in rats: role of altered brain neurotransmitters, acetylcholinesterase activity and changes in antioxidant defense system. *Age* 36:9653. doi: 10.1007/s11357-014-9653-0

Halliwell, B. (2006). Reactive species and antioxidants. Redox biology is a fundamental theme of aerobic life. *Plant Physiol.* 141, 312–322. doi: 10.1104/pp.106.077073

Halliwell, B., and Gutteridge, J. M. C. (2007). *Free Radicals in Biology and Medicine.* 4th Edn. Oxford: Clarendon Press.

Haupt, H., and Scheibe, F. (2002). Preventive magnesium supplement protects the inner ear against noise-induced impairment of blood flow and oxygenation in the guinea pig. *Magnes. Res.* 15, 17–25. doi: 10.1007/pl00007505

Heman-Ackah, S. E., Juhn, S. K., Huang, T. C., and Wiedmann, T. S. (2010). A combination antioxidant therapy prevents age-related hearing loss in C57BL/6 mice. *Otolaryngol. Head Neck Surg.* 143, 429–434. doi: 10.1016/j.otohns.2010.04.266

Huang, Q., and Tang, J. (2010). Age-related hearing loss or presbyacusis. *Eur. Arch. Otorhinolaryngol.* 267, 1179–1191. doi: 10.1007/s00405-010-1270-7

Ising, H., Handrock, M., Günther, T., Fischer, R., and Dombrowski, M. (1982). Increased noise trauma in guinea pigs through magnesium deficiency. *Arch. Otorhinolaryngol.* 236, 139–146. doi: 10.1007/bf00454034

Johnsson, L. G., and Hawkins, J. E. Jr. (1972). Vascular changes in the human inner ear associated with aging. *Ann. Otol. Rhinol. Laryngol.* 81, 364–376. doi: 10.1177/000348947208100307

Kansu, L., Ozkarakas, H., Efendi, H., and Okar, I. (2011). Protective effects of pentoxifylline and nimodipine on acoustic trauma in Guinea pig cochlea. *Otol. Neurotol.* 32, 919–925. doi: 10.1097/mao.0b013e3182267e06

Kashio, A., Amano, A., Kondo, Y., Sakamoto, T., Iwamura, H., Suzuki, M., et al. (2009). Effect of vitamin C depletion on age-related hearing loss in SMP30/GNL knockout mice. *Biochem. Biophys. Res. Commun.* 390, 394–398. doi: 10.1016/j.bbrc.2009.09.003

Kidd III, A. R., and Bao, J. (2012). Recent advances in the study of age-related hearing loss: a mini-review. *Gerontology* 58, 490–496. doi: 10.1159/000338588

Kopke, R., Bielefeld, E., Liu, J., Zheng, J., Jackson, R., Henderson, D., et al. (2005). Prevention of impulse noise-induced hearing loss with antioxidants. *Acta Otolaryngol.* 125, 235–243. doi: 10.1080/00016480410023038

Kopke, R. D., Jackson, R. L., Coleman, J. K., Liu, J., Bielefeld, E. C., and Balough, B. J. (2007). NAC for noise: from the bench top to the clinic. *Hear. Res.* 226, 114–125. doi: 10.1016/j.heares.2006.10.008

Kopke, R. D., Weisskopf, P. A., Boone, J. L., Jackson, R. L., Wester, D. C., Hoffer, M. E., et al. (2000). Reduction of noise induced hearing loss using L-NAC and salicylate in the chinchilla. *Hear. Res.* 149, 138–146. doi: 10.1016/s0378-5955(00)00176-3

Lamm, K., and Arnold, W. (2000). The effect of blood flow promoting drugs on cochlear blood low, perilymphatic pO(2) and auditory function in the normal and noise-damaged hypoxic and ischemic guinea pig inner ear. *Hear. Res.* 141, 199–219. doi: 10.1016/s0378-5955(00)00005-8

Lee, K. Y. (2013). Pathophysiology of age-related hearing loss (peripheral and central). *Korean J. Audiol.* 17, 45–49. doi: 10.7874/kja.2013.17.2.45

Lee, H. C., and Wei, Y. H. (2012). Mitochondria and aging. *Adv. Exp. Med. Biol.* 942, 311–327. doi: 10.1007/978-94-007-2869-1_14

Le Prell, C. G., Gagnon, P. M., Bennett, D. C., and Ohlemiller, K. K. (2011). Nutrient-enhanced diet reduces noise-induced damage to the inner ear and hearing loss. *Transl. Res.* 158, 38–53. doi: 10.1016/j.trsl.2011.02.006

Le Prell, C. G., Hughes, L. F., and Miler, J. M. (2007a). Free radical scavengers vitamins A, C and E plus magnesium reduce noise trauma. *Free Radic. Biol. Med.* 42, 1454–1463. doi: 10.1016/j.freeradbiomed.2007.02.008

Le Prell, C. G., Ojano-Dirain, C., Rudnick, E. W., Nelson, M. A., DeRemer, S. J., Prieskorn, D. M., et al. (2014). Assessment of nutrient supplement to reduce gentamicin-induced ototoxicity. *J. Assoc. Res. Otolaryngol.* 15, 375–393. doi: 10.1007/s10162-014-0448-x

Le Prell, C. G., Yamashita, D., Minami, S. B., Yamasoba, T., and Miller, J. M. (2007b). Mechanisms of noise-induced hearing loss indicate multiple methods of prevention. *Hear. Res.* 226, 22–43. doi: 10.1016/j.heares.2006.10.006

Li, X., Mao, X. B., Hei, R. Y., Zhang, Z. B., Wen, L. T., Zhang, P. Z., et al. (2011). Protective role of hydrogen sulfide against noise-induced cochlear damage: a chronic intracochlear infusion model. *PLoS One* 6:e26728. doi: 10.1371/journal.pone.0026728

Lin, M. T., and Beal, M. F. (2006). Mitochondrial dysfunction and oxidative stress in neurodegenerative diseases. *Nature* 443, 787–795. doi: 10.1038/nature05292

Lin, F. R., Thorpe, R., Gordon-Salant, S., and Ferrucci, L. (2011). Hearing loss prevalence and risk factors among older adults in the United States. *J. Gerontol. A Biol. Sci. Med. Sci.* 66, 582–590. doi: 10.1093/gerona/glr002

Miller, J. M., Brown, J. N., and Schacht, J. (2003). 8-iso-prostaglandin F2α, a product of noise exposure, reduces inner ear flow. *Audiol. Neurootol.* 8, 207–221. doi: 10.1159/000071061

Nakashima, T. (1999). Autoregulation of cochlear blood flow. *Nagoya J. Med. Sci.* 62, 1–9.

Ohinata, Y., Miller, J. M., and Schacht, J. (2003). Protection from noise-induced lipid peroxidation and hair cell loss in the cochlea. *Brain Res.* 966, 265–273. doi: 10.1016/s0006-8993(02)04205-1

Ohlemiller, K. K. (2006). Contributions of mouse models to understanding of age- and noise-related hearing loss. *Brain Res.* 1091, 89–102. doi: 10.1016/j.brainres.2006.03.017

Ohlemiller, K. K., and Frisina, R. D. (2008). "Age-related hearing loss and its cellular and molecular bases," in *Auditory Trauma, Protection, and Repair*, eds J. Schacht, A. N. Popper, and R. R. Fay (New York: Springer), 145–194.

Ortuño-Sahagún, D., Pallàs, M., and Rojas-Mayorquín, A. E. (2014). Oxidative stress in aging: advances in proteomic approaches. *Oxid. Med. Cell. Longev.* 2014:573208. doi: 10.1155/2014/573208

Park, D. C., and Yeo, S. G. (2013). Aging. *Korean J. Audiol.* 17, 39–44. doi: 10.7874/kja.2013.17.2.39

Ray, P. D., Huang, B. W., and Tsuji, Y. (2012). Reactive oxygen species (ROS) homeostasis and redox regulation in cellular signaling. *Cell. Signal.* 24, 981–990. doi: 10.1016/j.cellsig.2012.01.008

Ruan, Q., Ma, C., Zhang, R., and Yu, Z. (2014). Current status of auditory aging and anti-aging research. *Geriatr. Gerontol. Int.* 14, 40–53. doi: 10.1111/ggi.12124

Scheibe, F., Haupt, H., and Ising, H. (2000). Preventive effect of magnesium supplement on noise-induced hearing loss in the guinea pig. *Eur. Arch. Otorhinolaryngol.* 257, 10–16. doi: 10.1007/pl00007505

Schmiedt, R. A. (2010). "The physiology of cochlear presbycusis," in *Aging Audit. Syst*, eds S. Gordon-Salant, R. D. Frisina, A. N. Popper, and R. R. Fay (New York: Springer), 9–38.

Schuknecht, H. F., and Gacek, M. R. (1993). Cochlear pathology in presbycusis. *Ann. Otol. Rhinol. Laryngol.* 102, 1–16.

Seidman, M. D. (2000). Effects of dietary restriction and antioxidants on presbyacusis. *Laryngoscope* 110, 727–738. doi: 10.1097/00005537-200005000-00003

Seidman, M. D., Ahmad, N., and Bai, U. (2002). Molecular mechanisms of age-related hearing loss. *Ageing Res. Rev.* 1, 331–343. doi: 10.1016/s1568-1637(02)00004-1

Seidman, M., Babu, S., Tang, W., Naem, E., and Quirk, W. S. (2003). Effects of resveratrol on acoustic trauma. *Otolaryngol. Head Neck Surg.* 129, 463–470. doi: 10.1016/s0194-5998(03)01586-9

Seidman, M. D., Quirk, W. S., and Shirwany, N. A. (1999). Mechanisms of alterations in the microcirculation of the cochlea. *Ann. N Y Acad. Sci.* 884, 226–232. doi: 10.1111/j.1749-6632.1999.tb08644.x

Sena, L. A., and Chandel, N. S. (2012). Physiological roles of mitochondrial reactive oxygen species. *Mol. Cell* 48, 158–167. doi: 10.1016/j.molcel.2012.09.025

Sha, S. H., Kanicki, A., Halsey, K., Wearne, K. A., and Schacht, J. (2012). Antioxidant-enriched diet does not delay the progression of age-related hearing loss. *Neurobiol. Aging* 33, 1010.e15–1010.e16. doi: 10.1016/j.neurobiolaging.2011.10.023

Shi, X. (2011). Physiopathology of the cochlear microcirculation. *Hear. Res.* 282, 10–24. doi: 10.1016/j.heares.2011.08.006

Syka, J. (2002). Plastic changes in the central auditory system after hearing loss, restoration of function and during learning. *Physiol. Rev.* 82, 601–636. doi: 10.1152/physrev.00002.2002

Syka, J. (2010). The Fischer 344 rat as a model of presbycusis. *Hear. Res.* 264, 70–78. doi: 10.1016/j.heares.2009.11.003

Tokgoz, B., Ucar, C., Kocyigit, I., Somdas, M., Unal, A., Vural, A., et al. (2011). Protective effect of N-acetylcysteine from drug-induced ototoxicity in uraemic patients with CAPD peritonitis. *Nephrol. Dial. Transplant.* 26, 4073–4078. doi: 10.1093/ndt/gfr211

Uttara, B., Singh, A. V., Zamboni, P., and Mahajan, R. T. (2009). Oxidative stress and neurodegenerative diseases: a review of upstream and downstream antioxidant therapeutic options. *Curr. Neuropharmacol.* 7, 65–74. doi: 10.2174/157015909787602823

World Health Organization. (2002). *Active Ageing, A Policy Framework.* Available online at: http://whqlibdoc.who.int/hq/2002/who_nmh_nph_02.8.pdf

World Health Organization. (2013). Deafness and hearing loss, Fact sheet N°300. Available online at: http://www.who.int/mediacentre/factsheets/fs300/en/index.html

Yamashita, D., Jiang, H. Y., Le Prell, C. G., Schacht, J., and Miller, J. M. (2005). Post-exposure treatment attenuates noise-induced hearing loss. *Neuroscience* 134, 633–642. doi: 10.1016/j.neuroscience.2005.04.015

Yamasoba, T., Lin, F. R., Someya, S., Kashio, A., Sakamoto, T., and Kondo, K. (2013). Current concepts in age-related hearing loss: epidemiology and mechanistic pathways. *Hear. Res.* 303, 30–38. doi: 10.1016/j.heares.2013.01.021

Yamasoba, T., Schacht, J., Shoji, F., and Miller, J. M. (1999). Attenuation of cochlear damage from noise trauma by an iron chelator, a free radical scavenger and glial cell line-derived neurotrophic factor *in vivo*. *Brain Res.* 815, 317–325. doi: 10.1016/s0006-8993(98)01100-7

Conflict of Interest Statement: The authors declare that the research was conducted in the absence of any commercial or financial relationships that could be construed as a potential conflict of interest.

frontiers in Aging Neuroscience

ORIGINAL RESEARCH
published: 20 March 2015
doi: 10.3389/fnagi.2015.00032

Transforming growth factor β1 inhibition protects from noise-induced hearing loss

Silvia Murillo-Cuesta[1,2,3], Lourdes Rodríguez-de la Rosa[1,2,3], Julio Contreras[1,2,4], Adelaida M. Celaya[1,2], Guadalupe Camarero[1,2,3], Teresa Rivera[1,2,5†] and Isabel Varela-Nieto[1,2,3†]*

[1] Institute for Biomedical Research "Alberto Sols" (IIBM), Spanish National Research Council–Autonomous University of Madrid (CSIC-UAM), Madrid, Spain, [2] Centre for Biomedical Network Research (CIBER), Institute of Health Carlos III (ISCIII), Madrid, Spain, [3] Hospital La Paz Institute for Health Research (IdiPAZ), Madrid, Spain, [4] Veterinary Faculty, Complutense University of Madrid, Madrid, Spain, [5] Príncipe de Asturias University Hospital, University of Alcalá, Alcalá de Henares, Madrid, Spain

Excessive exposure to noise damages the principal cochlear structures leading to hearing impairment. Inflammatory and immune responses are central mechanisms in cochlear defensive response to noise but, if unregulated, they contribute to inner ear damage and hearing loss. Transforming growth factor β (TGF-β) is a key regulator of both responses and high levels of this factor have been associated with cochlear injury in hearing loss animal models. To evaluate the potential of targeting TGF-β as a therapeutic strategy for preventing or ameliorating noise-induced hearing loss (NIHL), we studied the auditory function, cochlear morphology, gene expression and oxidative stress markers in mice exposed to noise and treated with TGF-β1 peptidic inhibitors P17 and P144, just before or immediately after noise insult. Our results indicate that systemic administration of both peptides significantly improved both the evolution of hearing thresholds and the degenerative changes induced by noise-exposure in lateral wall structures. Moreover, treatments ameliorated the inflammatory state and redox balance. These therapeutic effects were dose-dependent and more effective if the TGF-β1 inhibitors were administered prior to inducing the injury. In conclusion, inhibition of TGF-β1 actions with antagonistic peptides represents a new, promising therapeutic strategy for the prevention and repair of noise-induced cochlear damage.

Keywords: cochlear injury, inflammation, noise-induced hearing loss, protection, TGF-β

OPEN ACCESS

Edited by:
Paula I. Moreira, University of Coimbra, Portugal

Reviewed by:
Esperanza Bas Infante, University of Miami, USA
Diana Troiani, Human Physiology Medical School Catholic University, Italy

****Correspondence:***
Silvia Murillo-Cuesta, Institute for Biomedical Research "Alberto Sols" (IIBM), Spanish National Research Council–Autonomous University of Madrid (CSIC-UAM), Arturo Duperier 4, 28029 Madrid, Spain
smurillo@iib.uam.es

† These authors have contributed equally to this work.

Received: *18 December 2014*
Paper pending published: *30 December 2014*
Accepted: *28 February 2015*
Published: *20 March 2015*

Citation:
Murillo-Cuesta S, Rodríguez-de la Rosa L, Contreras J, Celaya AM, Camarero G, Rivera T and Varela-Nieto I (2015) Transforming growth factor β1 inhibition protects from noise-induced hearing loss. Front. Aging Neurosci. 7:32. doi: 10.3389/fnagi.2015.00032

Introduction

Noise-induced hearing loss (NIHL) is the second most common form of deafness and constitutes an important public health priority. Animal studies have shown that exposure to excessive noise produces loss of hair cells, damage to the nerve synapses and loss of fibrocytes (Wang et al., 2002; Hirose and Liberman, 2003), leading to sensorineural deafness. The severity of hearing loss depends on noise characteristics (level, frequency, duration and temporal pattern) and genetic susceptibility (Ohlemiller and Gagnon, 2007).

The main underlying molecular mechanisms in NIHL include free-radical formation and oxidative stress, which activate cell death pathways in the cochlea, reduced cochlear blood flow, disruption of the blood-labyrinth barrier, glutamate excitotoxicity, calcium imbalance

and cochlear inflammation (Henderson et al., 2006; Le Prell et al., 2007; Tan et al., 2013). Traditionally the cochlea was considered to be immunologically isolated because of the existence of the blood-labyrinth barrier. However, cochlear inflammation has been associated with many situations causing hearing loss, mainly otitis, autoimmune inner ear diseases and ototoxicity. In addition, in the last years inflammation has emerged as a key process in NIHL (Abi-Hachem et al., 2010; Tan et al., 2013).

Noise activates the local immune response, with early expression of proinflammatory cytokines in the cochlear resident macrophages (Okano et al., 2008), spiral ligament fibrocytes, strial cells and spiral ganglion neurons, including TNF-α, IL-1β and IL-6 (Ichimiya et al., 2000; Satoh et al., 2002; Fujioka et al., 2006; Tahera et al., 2006; Nakamoto et al., 2012; Tan et al., 2013; Zhang et al., 2013). These cytokines, along with other inflammatory mediators and cell adhesion molecules, induce the infiltration of blood monocytes and macrophages (Hirose et al., 2005; Tornabene et al., 2006) to phagocytize debris, and the secretion of more cytokines and growth factors (Yoshida et al., 1999). The inflammatory response is intended to limit the damage and promote further angiogenesis, fibroplasia and matrix synthesis, contributing to repair (Park and Barbul, 2004). However, it could also exacerbate pathological changes and produce bystander cell injury. Therefore, noise damaged cochlea represent a target for the application of otoprotective strategies based on controlling inflammation.

TGF-β is a member of a pluripotent cytokine superfamily with a key role in a variety of cellular processes such as proliferation, differentiation, extracellular matrix deposition and apoptosis during development, but also in postnatal stages (Massagué, 2012; Weiss and Attisano, 2013). In adult mammalians, TGF-β family members participate in the maintenance of tissue homeostasis, immune and inflammatory responses, angiogenesis and fibrogenesis (Dünker and Krieglstein, 2000; Prud'homme, 2007). The mammalian genome encodes for three isoforms (TGF-β 1, 2 and 3) with widespread tissue distribution and similar signaling cascades through TGF-β receptor types I, II and III (TGF-βR1, R2 and R3 or betaglycan) and SMAD2/3 proteins, which translocate to the nucleus and regulate gene transcription (Massagué, 2012). The three TGF-β isoforms are expressed in the embryonic cochlea in rodents with distinct patterns: TGF-β2 in the cochlear epithelium (Sanford et al., 1997; Paradies et al., 1998; Kim et al., 2006) and TGF-β1 and 3 in both epithelial and mesenchymal tissues (Pelton et al., 1991; Frenz et al., 1992; Paradies et al., 1998; Kim et al., 2006). Thus, TGF-β factors have been described to be involved in otic capsule formation (Liu et al., 2007), spiral ganglion formation and survival (Marzella et al., 1999; Okano et al., 2005), and indirectly in cochlear tonotopic organization (Son et al., 2012).

TGF-β1 is a master regulator of the immune response in several tissues, controlling the differentiation, proliferation, and activation of lymphocytes, macrophages and dendritic cells by autocrine and paracrine mechanisms (Letterio, 2000). Early after tissue damage, TGF-β1 modulates expression of adhesion molecules and induces chemoattraction and activation of leukocytes. These cells in turn secrete large amounts of interleukins, including TGF-β, which in a subsequent phase inhibit proliferation, differentiation and interleukin production (Letterio, 2000; Prud'homme, 2007; Mantel and Schmidt-Weber, 2011). Perturbations in the cytokine balance could modify dual TGF-β actions and contribute to immunopathology. In addition, several alterations of the immune system have been described in mice with targeted mutations in *Tgfb1*, including severe immune deregulation and lethal postnatal multi-organ inflammatory syndrome in *Tgfb1* knock-out mice (Shull et al., 1992; Kulkarni et al., 1993).

The role of TGF-β family factors in cochlear pathophysiology is not fully understood. Recent *in silico* analysis of genes relevant to hearing and deafness pointed to TGF-β1 as a nodal molecule in non-syndromic deafness and otic capsule development gene networks (Stamatiou and Stankovic, 2013). Although TGF-β1 is not among the classical proinflammatory cytokines, some studies in rodents have demonstrated an early increase in its expression during cochlear damage induced by aminoglycosides (Wissel et al., 2006), antigens (Satoh et al., 2006) and otitis media (Ghaheri et al., 2007), followed by a down-regulation as the response resolves, thus also supporting the immunomodulator role of TGF-β in the cochlea. Overexpression of TGF-β1 in the inner ear has also been related to fibrosis after cochlear damage (Kawamoto et al., 2003; Satoh et al., 2006), otosclerosis (Liu et al., 2007) and cochlear implantation trauma (Eshraghi et al., 2013). To our knowledge, there is no data concerning changes in TGF-β1 expression in NIHL, but a similar response to that observed in ototoxic or autoimmune labyrinthitis can be expected. Therefore, our hypothesis is that targeting TGF-β1 actions could help modulate the inflammatory response during noise-induced cochlear injury.

In this work we have studied the TGF-β signaling, gene expression and oxidative balance in the cochlea after noise exposure to clarify the role of TGF-β1 in NIHL. In addition, we have explored the potential of targeting this factor with two inhibitors of TGF-β1 as a therapeutic strategy to ameliorate the noise-induced functional, molecular and morphological changes.

Materials and Methods

Mouse Housing and Handling

Two month-old mice from three strains were used: C57BL/6JOlaHsd (C57), CBA/CaOlaHsd (CBA) and outbred HsdOla:MF1 (MF1) (Harlan Interfauna Ibérica, Spain). C57 mice are homozygous for a defective allele of the cadherin 23 gene (*Cdh23*^{ahl}), and are especially vulnerable to noise (Ohlemiller et al., 2000; Park et al., 2013). In contrast, CBA is a normal hearing, noise injury-resistant strain (Wang et al., 2002; Ohlemiller and Gagnon, 2007). In our hands, MF1 background shows normal hearing and it is moderately resistant to NIHL (Celaya et al., in preparation).

Mice were fed *ad libitum* with a standard diet and drinking water, and controlled following FELASA recommendations.

Animal experimentation was conducted in accordance with Spanish and European legislation and approved by the Spanish National Research Council (CSIC).

Hearing Evaluation and Noise Exposure

Hearing was evaluated by registering the auditory brainstem response (ABR) as described (Cediel et al., 2006). Click and 8–40 kHz tone burst stimuli (0.1 and 5 ms duration, respectively) were generated with SigGenRP™software (Tucker-Davis Technologies, Alachua, FL, USA) and presented monaurally at 30 or 50 pulses per second each, from 90 to 10 dBs relative to sound pressure level (dB SPL) in 5–10 dB SPL steps. The electrical response was amplified, recorded and averaged (1000 and 750 stimulus-evoked responses for click and tone burst, respectively). ABR thresholds were determined by visual detection and defined as the lowest intensity to elicit a reliable ABR wave with peaks I to IV clearly visible and medium peak amplitude over 200 nV. Peak and interpeak latencies were determined in the ABR trace in response to 20 dB SPL over the click evoked threshold.

The efficacy of TGF-β inhibitors was evaluated in a NIHL mice model. Briefly, conscious mice were confined in a wire mesh cage in the center of a reverberant chamber acoustically designed to reach maximum sound level with minimum deviation in the central exposure area (Cobo et al., 2009) and exposed to violet swept sine (VS) noise, at 100–120 dB SPL for short (30 min) or long (12 h) periods. VS noise was that was repeated during the 30 min of exposure.

VS noise was designed with Wavelab Lite software (Steinberg Media Technologies GmbH, Hamburg, Germany). It consists in a 10 s linear sweep in frequency, with a spectrum biased towards high frequencies (frequency range 2–20 kHz, VS^{2-20})and presented with a linear-with-frequency gain to compensate for the high frequency losses inside the chamber (Cobo et al., 2009; Sanz et al., 2015). The effect of noise exposure on hearing was evaluated with ABR tests as described above. The audiogram included tones from 8 to 40 kHz because exposure to noise of certain frequencies induces threshold shifts in octaves above those frequencies (Ou et al., 2000a,b; Sanz et al., 2015).

Drug Administration

Two chemically synthesized TGF-β inhibitors (P17 and P144) with 95% purity were used in the study (DIGNA Biotech, Pamplona, Spain). P17 (KRIWFIPRSSWYERA) is a soluble hydrophilic peptide derived from a phage library (Dotor et al., 2007), with 100% relative binding affinity for TGF-β1, 80% for TGF-β2 and 30% for TGF-β3 (Gil-Guerrero et al., 2008). P144 (TSLDASIIWAMMQN) is a poorly soluble hydrophobic peptide derived from the sequence of the extracellular region of TGF-β type III receptor and specifically designed to block the interaction with TGF-β1 (Ezquerro et al., 2003).

Peptides stored at −80°C were gently defrosted, diluted in saline and sonicated (P144) until a clear solution was obtained. Peptides were administered intraperitoneally at doses ranging from 2.5 to 10 mg/kg, once or twice daily. These doses were shown to be effective in animal models of inflammation and fibrosis as mentioned before. Control mice were injected IP with a similar volume of saline (0.1 ml/10 g).

Cochlear Morphology

At the end of every experiment, cochlear samples were taken for morphological evaluation. Cochlear samples were processed to obtain 5 μm thick paraffin sections following standard procedures. Cochlear morphology was studied in cresyl-violet (Fluka; Sigma Aldrich) stained sections with an Axiophot Zeiss microscope equipped with an Olympus DP70 digital camera as previously described (Riquelme et al., 2010).

Gene Expression and Protein Analysis

When indicated, protein and gene expression were measured by Western blotting and reverse transcription coupled to quantitative PCR Data shown are representative of those found in the different mouse strains studied whenever there were no observable differences due to mouse background. For protein analysis, cochlear extracts were prepared as reported (Sanchez-Calderon et al., 2010). Protein concentration was determined using a Micro BCA Protein Assay Kit (Pierce Biotechnology, Inc., Rockford, IL USA) with BSA as the standard. Cochlear proteins were subjected to gel electrophoresis and transferred to PVDF membranes in a Bio-Rad Trans Blot apparatus. After incubation with a blocking solution, the membranes were probed overnight at 4°C with the following primary antibodies: p-SMAD2 (Ser465/467) (Cell Signaling Technology, Danvers, MA, USA), p-p38 MAPK (Thr180/Tyr182), NOX-4 (Santa Cruz Biotechnology, Santa Cruz, CA, USA) each at a 1:1000 dilution and MnSOD (Merck Millipore, Billerica, MA, USA; 1 μg/ml). Blots were re-probed with SMAD2/3 (Santa Cruz Biotechnology, 1:1000), p38α (Santa Cruz Biotechnology, 1:1000), β-actin (Sigma-Aldrich Corp. St. Louis, MO, USA; 1:2500) or p44/42 MAPK (Cell Signaling Technology, 1:1000) as loading controls. Antibodies were prepared in TTBS containing 5% BSA for phosphorylation-specific antibodies or non-fat dried milk for others. The membranes were washed and incubated with the corresponding peroxidase-conjugated secondary antibodies for 1 h at room temperature. Immunoreactive bands were visualized by enhanced chemiluminescence (GE Healthcare Bio-Sciences, Pittsburgh, PA, USA) using X-ray films (Agfa, Mortsel, Belgium), and the bands were quantified by densitometry with NIH ImageJ software. Different exposure times were used to ensure that bands were not saturated.

For gene expression studies, cochlear samples were processed for RT-qPCR as reported (Rodríguez-de la Rosa et al., 2014). TaqMan MGB probes were obtained from Assay-by-Design^{SM} (Applied Biosystems) for amplification of *Tgfb1, Tgfb2, TgfbR1* and *TgfbR2* genes. The ribosomal phosphoprotein P0 (*Rplp0*) was used as endogenous control gene. The relative quantification values (RQ) between noise exposed and non-exposed mice were determined by the $2^{-\Delta\Delta}$Ct method as reported (Sanchez-Calderon et al., 2010), where $\Delta\Delta Ct = \Delta Ct_{exposed} - \Delta Ct_{non\text{-}exposed}$, and $\Delta Ct = Ct_{target} - Ct_{endogenous}$. Data were expressed as log10RQ mean.

Statistical Analysis

For ABR and Western blot results, statistical analysis was performed using IBM SPSS software (v.19.0). RT-qPCR data were analyzed using the Integromics Real Time StatMiner software package.[1] Data were expressed as mean ± standard error (SEM), and the results were considered significant at $p \leq 0.05$. Statistical significance was estimated by different tests for ABR, western blot and qRT-PCR data, which are specified in the figure legends.

Results

Noise Exposure Induces Changes in TGF-β Signaling, Gene Expression and Oxidative Balance in the Cochlea

Exposure to high level (100–120 dB SPL) VS^{2-20} noise induced a notably temporal threshold shift in the first 24 h after exposure and a gradual but limited recovery of ABR thresholds. The severity of hearing loss is related to noise intensity, with VS^{2-20} noise at 110 or 120 dB SPL inducing permanent changes that suggest irreversible cochlear damage (**Figure 1A**).

Next, the expression of *Tgfb* related genes (*Tgfb1*, *Tgfb2*, *TgfbR1* and *TgfbR2*) was studied in cochlear samples that were taken 4 and 24 h after challenge with VS^{2-20} noise at 110 dB SPL for 30 min. In general, RT-qPCR expression profiles of *Tgfb* related genes in noise exposed mice showed homogeneous distribution of Ct values and a higher correlation Pearson index compared to non-exposed controls. A statistical significant increase in the cochlear expression of *Tgfb1* was observed in mice exposed to noise 4 h after damage compared to non-exposed controls, (RQ value of 3.2 ± 0.5, $p = 0.03$). One day after exposure, a simultaneous increase in *Tgfb1* and *TgfbR1* and a decrease in *Tgfb2* and *TgfbR2* gene expression was observed in exposed mice compared to controls, although the change was statistically significant only for *TgfbR1* (RQ value of 1.2 ± 0.07, $p = 0.008$) (**Figure 1B**). In addition, p-SMAD2 protein levels, which propagate de TGF-β1 signal, as well as p-p38α, NOX-4 and MnSOD, which are related to cellular stress and oxidation, were determined prior to and 1, 3 and 14 days after noise exposure. Our results indicate a moderate and progressive increase in the phosphorylation of SMAD2 (ratio p-SMAD2/SMAD2/3) after noise exposure, compared to baseline values, although without statistically significant differences (**Figure 1C**). In addition, the levels of other stress-related molecules such as phospho-p38α, NOX-4 and MnSOD were also elevated in cochleae after noise damage, confirming the role of oxidative stress in the pathophysiology of NIHL. A statistically significant increase in the levels of the antioxidant enzyme MnSOD was observed in the first 24 h after exposure, whereas phosphorylation of p-38α MAPK rose significantly 2 weeks after injury. No differences were observed due to mouse strain (data not shown).

[1]http://www.integromics.com/genomics-data-analysis/pcr-analysis

These results confirm that inflammation and oxidative stress are key underlying mechanisms in NIHL and show that TGF-β1 plays a role in cochlear response to noise injury. In this context, the use of TGF-β1 inhibitors could represent a therapeutic strategy for ameliorating NIHL. To evaluate the safety profile and the efficacy of TGF-β1 inhibitor peptides P17 and P144 in the prevention and treatment of NIHL, different experiments were carried out and they are summarized in **Table 1**.

TGF-β1 Inhibitors Reduce Functional and Morphological Alterations After Noise-Exposure

Safety Assessment of P17 and P144

Initially, the safety of treatment with TGF-β1 inhibitors was evaluated. Systemic administration of either P17 or P144 peptides at doses ranging from 2.5 to 10 mg/kg/24 h for 15 days in MF1 and C57 mice was well-tolerated. None of the treated mice showed signs of systemic toxicity nor did they die, confirming previous reports in mice and rats (Ezquerro et al., 2003; Arribillaga et al., 2011; Baltanás et al., 2013). With regard to hearing, treatment with P17 and P144 did not increase ABR thresholds or peak latencies, and no significant differences were observed between drug-treated and saline control mice (**Table 2**). In addition, cochlear samples were taken after treatments to evaluate inner ear morphology. No gross alterations were found in the organ of Corti, spiral ganglion and stria vascularis, confirming the non-ototoxic and safe profile of both peptides (data not shown).

Pretreatment with P17 and P144 Reduces Threshold Shift After Noise Exposure

The potential of TGF-β1 inhibitors in preventing NIHL was evaluated by treating mice with P17 and P144 at 2.5 mg/kg/24 h or with saline at 0.1 ml/10 g/24 h for 15 days and then exposing them to VS^{2-20} noise at 100 dB SPL. ABR was performed before the treatment, and 1 day, 1, 2, 3 and 4 weeks after noise exposure. The experimental procedure was performed on mice from two genetic backgrounds, MF1 and C57, with different susceptibilities to noise damage. Under all the conditions studied, click thresholds did not change after treatment with P17 or P144, confirming the safety profile.

Mice treated with P17, P144 or saline showed a similar ABR temporal pattern in response to noise; a statistically significant increase in ABR thresholds was observed 1 day after noise exposure when compared to baseline values in the three groups (paired T test, $p \leq 0.001$), which was followed by a gradual decrease during the first 2 weeks and permanent threshold shifts from this moment on (**Figure 2A**). Compared to saline treatment, systemic injection of P144 and P17 attenuated the threshold shift that occurred in the first day after noise damage, and ameliorated hearing recovery in the following weeks. The preventive effect was more evident in MF1 than in C57 mice, the former showing statistically significant differences 1 and 7 days after noise with both peptides compared to saline (**Figure 2A**). Non-exposed mice of both strains did not show significant changes of their ABR thresholds over the time (data not shown).

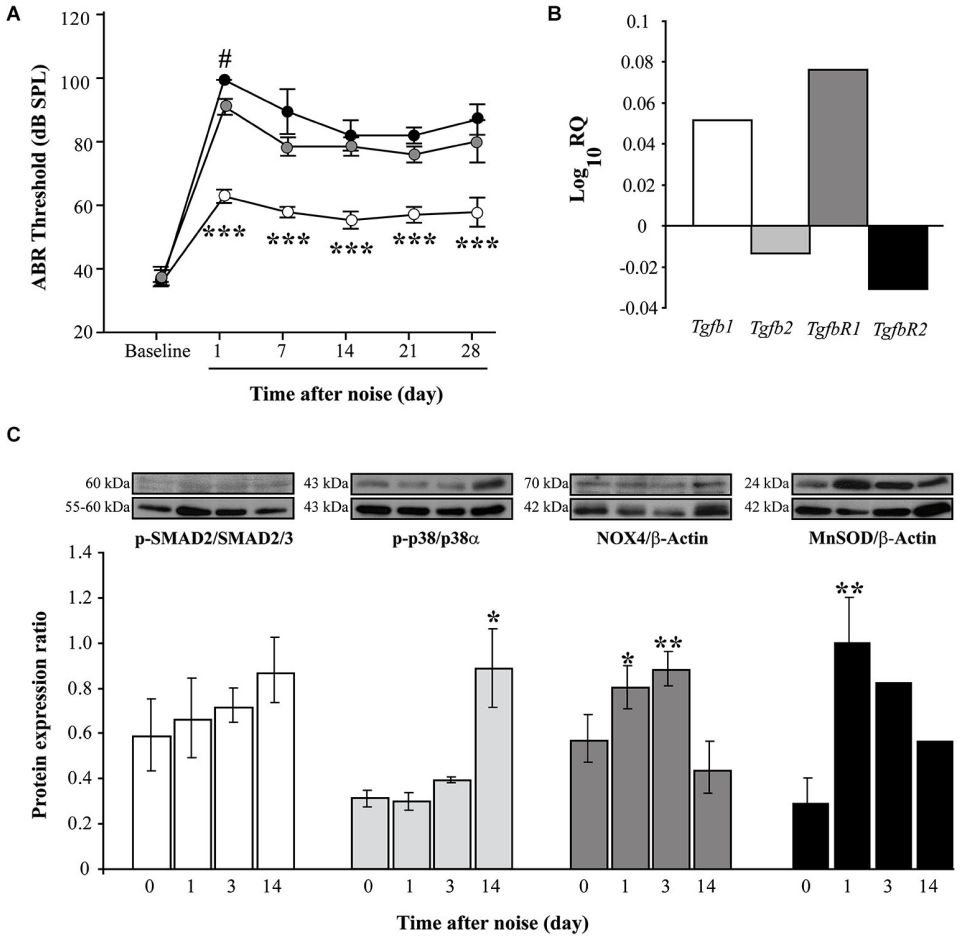

FIGURE 1 | Functional and molecular effects of noise exposure. **(A)** Evolution of ABR click thresholds (mean ± SEM, in dB SPL) in C57 mice exposed to VS^{2-20} noise at 100 (white circles), 110 (gray) or 120 (black) dB SPL (n = 6 per group) for 30 min. Statistically significant differences were found between mice exposed at 100 dB SPL and the other groups (paired T test, $^{***}p \leq 0.001$) and between 110 and 120 groups 1 day after exposure ($\#p \leq 0.05$). **(B)** Log_10RQ bar plot for *Tgb1*, T*gfb2*, *TgfbR1* and *TgfbR2* of cochlear samples, comparing noise exposed (VS^{2-20} at 110 dB SPL) with non-exposed CBA mice. Increase in the expression of *Tgfb1* and *TgfbR1* was observed in noise exposed mice compared to non-exposed, the latter with a statistical signifficant difference (p = 0.008, Limma test with Benjamini-Hochberg FDR method and 0.05 adjusted p-value threshold). **(C)** Time course of p-p38/p38α, p-SMAD2/SMAD2/3, NOX-4/β-actin and MnSOD/β-actin protein expression ratios in the cochlea of noise-exposed C57 mice (VS^{2-20} at 110 dB SPL), before and 1, 3 and 14 days after noise exposure (n = 3 mice for each determination). Representative blots are shown. Data shown as mean ± SEM. Statistically significant differences were found in p-p38, NOX4 and MnSOD levels after noise exposure compared to baseline values (paired T test, $^{*}p \leq 0.05$; $^{**}p \leq 0.01$).

TABLE 1 | Summary of the experiments performed with TGF-β1 inhibitors.

Study	Strain	Drug	Dosage	VS^{2-20} noise level/duration
Safety	MF1, C57	P17, P144	2.5 mg/kg/24 h/15 days	-
Pretreatment	MF1, C57	P17, P144	2.5 mg/kg/24 h /15 days	100 dB SPL/12 h
Treatment	C57	P17, P144	2.5 mg/kg/24 h /30 days	100 dB SPL /12 h
		P17, P144	2.5 mg/kg/12 h/15 days	100 dB SPL /30 min
		P17, P144	2.5 mg/kg/12 h/15 days	110 dB SPL /30 min
		P17, P144	2.5 mg/kg/12 h/15 days	120 dB SPL /30 min
	CBA	P144	10 mg/kg/24 h/ 15 days	110 dB SPL /30 min

Different mouse strains and doses were used to study cochlear toxicity and efficacy of TGF-β1 inhibitor peptides P17 and P144 in the treatment of NIHL. MF1, HsdOla:MF1; C57, C57BL/6JOlaHsd; CBA, CBA/CaOlaHsd; IP, intraperitoneal; VS^{2-20}, Violet Swept Sine noise, frequency range 2–20 kHz.

Mice exposed to noise also showed an early statistically significant increase in ABR latencies and a decrease in peak amplitudes, especially in those corresponding to cochlea and spiral ganglion (peak I), and then a recovery of baseline

TABLE 2 | Analysis of hearing parameters after treatment with TGF-β1 inhibitors.

Strain	Group	ABR Parameter	*n*	Baseline		After treatment	
				Mean	SEM	Mean	SEM
	SSF	Threshold		41	1.79	42	2.68
		IPL I-II		1.03	0.04	1.03	0.01
		IPL I-IV	5	2.63	0.03	2.57	0.03
		IPL II-IV		1.60	0.05	1.54	0.04
		AMP I		1260.22	178.17	1231.64	177.30
MF1	P17	Threshold		39	2.45	36	2.04
		IPL I-II		0.93	0.02	0.90	0.02
		IPL I-IV	6	2.66	0.03	2.50	0.01
		IPL II-IV		1.73	0.03	1.60	0.03
		AMP I		1184.65	206.14	1488.37	220.30
	P144	Threshold		36	0.82	34	0.82
		IPL I-II		0.92	0.01	0.90	0.01
		IPL I-IV	6	2.65	0.04	2.47	0.03
		IPL II-IV		1.73	0.03	1.57	0.02
		AMP I		1191.12	106.64	1411.01	115.87
	SSF	Threshold		43	1.22	39	1.63
		IPL I-II		1.01	0.02	0.98	0.02
		IPL I-IV	6	2.93	0.05	2.56	0.05
		IPL II-IV		1.92	0.04	1.58	0.05
		AMP I		1232.68	96.29	813.64	67.12
C57	P17	Threshold		43	1.22	42	1.63
		IPL I-II		0.91	0.04	0.91	0.01
		IPL I-IV	6	2.66	0.10	2.53	0.05
		IPL II-IV		1.75	0.07	1.62	0.05
		AMP I		974.21	127.11	730.55	98.24
	P144	Threshold		41	1.63	40	1.22
		IPL I-II		1.01	0.01	0.95	0.03
		IPL I-IV	6	2.82	0.05	2.61	0.04
		IPL II-IV		1.82	0.05	1.67	0.03
		AMP I		1075.09	155.36	778.55	59.05

ABR thresholds (in dB SPL), interpeak latencies (in ms) and peak I amplitude (in nV) in response to click stimulus before and after systemic (intraperitoneal) treatment with TGF-β1 inhibitor peptides P17 and P144 (at 2.5 mg/kg/24 h) or saline (at 0.1 ml/10 g/24 h) for 15 days in MF1 and C57 mice. No statistically significant differences were found between baseline and post-treatment values (paired T-tests). MF1, HsdOla:MF1; C57, C57BL/6JOlaHsd IPL, interpeak latency; AMP, peak amplitude.

values in the following weeks (**Figure 2B**). Our results showed that mice treated with TGF-β1 inhibitor peptides P17 and P144 exhibit a similar time-course of peak I latency and amplitude after noise, compared to saline treatment, suggesting that these molecules have a limited effect on nerve conduction.

Cochlear samples were taken at the end of the experiment (4 weeks after noise exposure) and processed for histological evaluation. Typical morphological alterations were observed in cochlear sections, including changes in stria vascularis, spiral limbus, spiral ligament and organ of Corti, although specific patterns of permanent damage were observed depending on the mouse strain and cochlear region, as described previously (Ohlemiller and Gagnon, 2007; Ohlemiller et al., 2011). In the MF1 strain, mice exposed to noise and treated with saline presented mainly a severe loss of spiral ligament fibrocytes from basal to medium cochlear areas but also a collapsed organ of Corti with lack of outer hair cells in the basal turn. Treatment with TGF-β1 inhibitor peptides P17 and P144 reduced cellular loss in the spiral ligament and favored maintenance of outer hair cells in the organ of Corti, even in basal regions (**Figure 3**).

Treatment with P17 and P144 Improves Functional and Morphological Alterations After Noise Exposure

Once the beneficial effect of TGF-β1 inhibitors in the prevention of NIHL was confirmed, we explored their therapeutic properties when administered after noise damage in C57 and CBA mouse strains. C57 mice were exposed to VS^{2-20} noise at 100, 110 or 120 dB SPL, and then treated with TGF-β1 inhibitors or saline. Cochlear samples were taken 1 and 3 days after noise for protein level evaluation, and also at the end the experiment (28 days after exposure) for morphological studies. In parallel, control non-exposed animals were also evaluated.

Initial experiments using the same dosage as in pre-treatment assays (2.5 mg/kg/24 h) for 15 or even 28 days after noise exposure, did not show statistically significant differences between drug-treated and saline-treated (0.1 ml/10 g/24 h) experimental groups (data not shown). This dose is in the lower range of the reported drug efficiency (Arribillaga et al., 2011) and both molecules have a short life span (Ezquerro et al., 2003), therefore the daily dose was doubled to 2.5 mg/kg/12 h and administered for 15 days. Even under these conditions, P17, P144 and saline treated mice showed similar ABR thresholds

after exposure to 120 dB SPL noise. This result indicates that TGF-β1 inhibitors were not able to restore hearing function after an acoustic trauma (data not shown). However, in non-traumatic exposures to noise intensities under 120 dB SPL, both inhibitors clearly improved the time course of hearing loss beginning the first week after noise-exposure. The favorable effect on the evolution of ABR thresholds was more evident in mice treated with P17 (**Figures 4A,B**), whereas P144 showed a subtle therapeutic effect, possibly because of its poorer pharmacokinetic profile. Statistically significant differences in ABR thresholds, compared to saline-treated mice, were observed when P144 doses were increased to the maximum recommended dose of 10 mg/kg/24 h for 15 days (**Figure 4C**). Thus, TGF-β1 inhibitors showed a dose-dependent therapeutic effect on NIHL.

As aforementioned, mice exposed to noise showed an early increase in p-p38α, p-SMAD2 and MnSOD protein levels in the cochlea regardless of treatment, in comparison to non-exposed control mice. In agreement with functional results, mice treated with TGF-β1 inhibitors showed significantly lower values of p-p38α and p-SMAD2 1 day after damage and a higher MnSOD level 3 days after insult when compared to saline-treated mice, suggesting that these peptides favored an anti-inflammatory and antioxidant state throughout TGF-β1 signalling inhibition (**Figure 5**).

Cochlear samples were taken for gross histology evaluation 4 weeks after noise exposure. Similarly to pre-treatment assays, treatment with TGF-β1 inhibitor peptides P17 and P144 attenuated the morphological alterations induced by VS^{2-20} noise compared to saline treated animals (data not shown). Differences were especially observed in the lateral wall structures and in the organ of Corti, depending on the mouse strain. In CBA mice, TGF-β1 inhibitors reduced the degenerative changes in the spiral ligament and the loss of fibrocytes, whereas in C57 mice, the protective effect was more evident in the organ of Corti, with maintenance of outer hair cells even in basal regions (data not shown).

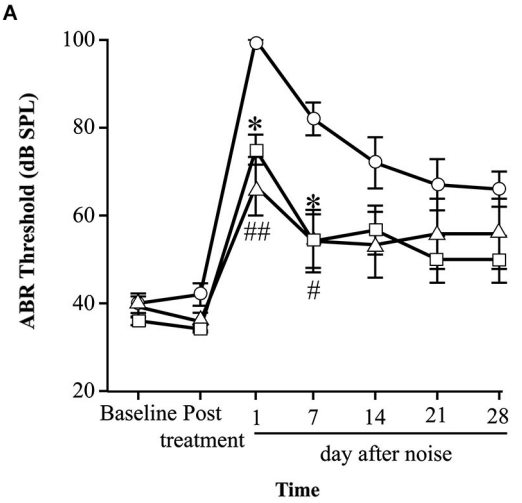

FIGURE 2 | Evolution of hearing after administration of TGF-β1 inhibitors before noise exposure. (A) Evolution of ABR thresholds (mean ± SEM, in dB SPL) in MF1 mice (n = 6 per group) treated with TGF-β1 inhibitors P17 or P144 at 2.5 mg/kg/24 h/15 days, or saline, and exposed to 100 dB VS noise overnight. Statistically significant differences (ANOVA with Bonferroni *post hoc* test, $p \leq 0.05$) were found between P17 (triangle, $^{*}p \leq 0.05$) or P144 (square, $\#p \leq 0.05$, $\#\#p \leq 0.01$,) and the saline group (circles), 1 and 7 days after exposure. **(B)** The evolution of peak I latency (mean ± SEM, in ms) in P17 (black bars), P144 (gray bars) and saline (white bars) treated mice showed a similar pattern. A statistically significant increase in peak I latency was observed 1 day after noise exposure in the three groups (paired T test compared to post-treatment values, $^{**}p \leq 0.01$).

Discussion

According to WHO, NIHL is an important medical concern in developed countries and currently efforts are being focused on preventing excessive noise exposure and on treating hearing loss (updated February 2014).[2]

Noise exposure induces a series of well-characterized morphological and functional changes in the cochlea, depending especially on the noise level, frequency, duration and temporal pattern (Wang et al., 2002; Hirose and Liberman, 2003; Ohlemiller, 2006; Park et al., 2013). The principal pathogenic mechanisms in NIHL include oxidative stress (Henderson et al., 2006) and inflammatory response, with an early local expression of cytokines and recruitment of immune cells (Tan et al., 2013), As occurred in ototoxicity, molecules with antioxidant and anti-inflammatory actions are being tested as potential otoprotective compounds (Bas et al., 2012; Fetoni et al., 2013).

The participation of the proinflammatory cytokines TNF-α, IL-1β and IL-6 in the cochlea after noise exposure has been reported (Ichimiya et al., 2000; Satoh et al., 2002; Fujioka et al., 2006; Tahera et al., 2006; Nakamoto et al., 2012; Tan et al., 2013), but the role of TGF-β is still undetermined. TGF-β family factors are key regulators of the immune and inflammatory response in several processes (reviewed in Mantel and Schmidt-Weber, 2011). In fact, an early increase in TGF-β expression in the inner ear has also been described in ototoxicity, immuno-mediated hearing loss and chronic otitis media (Satoh et al., 2006; Wissel et al., 2006; Ghaheri et al., 2007).

[2]http://www.who.int/mediacentre/factsheets/fs300/en/

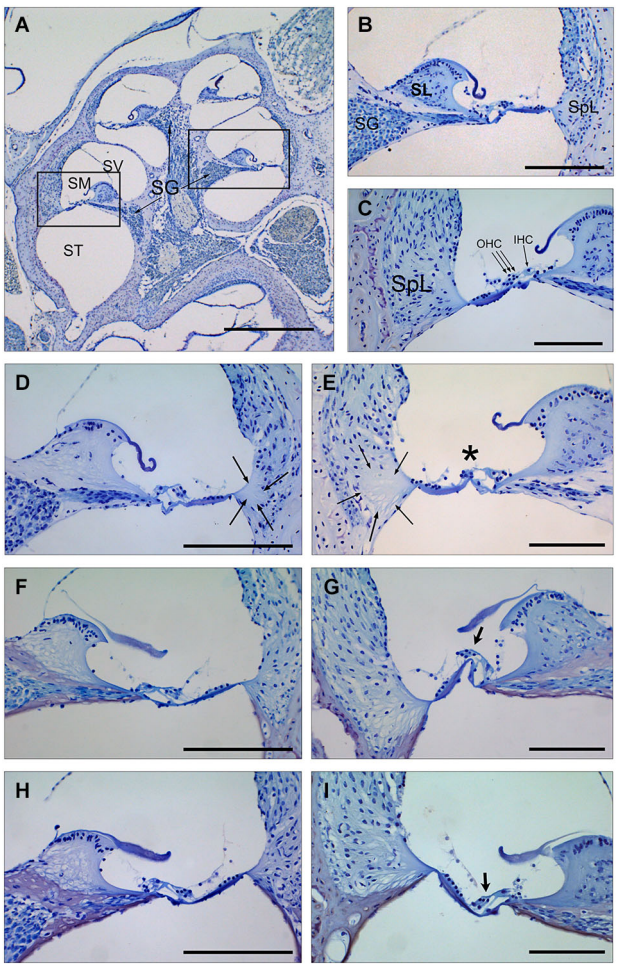

FIGURE 3 | Cochlear morphology in mice treated with TGF-β1 inhibitors before being exposed to noise. (A–C) Midmodiolar section **(A)** and detail of the scala media from middle **(B)** and basal **(C)** turns of the cochlea in a control non-exposed mouse, showing normal cytoarchitecture of spiral limbus (SL), spiral ligament (SpL) and organ of Corti with the outer and inner hair cells **(D–I)** Details of the spiral limbus, spiral ligament and organ of Corti from a representative MF1 mouse pre-treated with saline **(D,E)**, P17 **(F,G)** or P144 **(H,I)** before noise exposure. Mice treated with saline showed loss of fibrocyte cells in the spiral ligament (arrows) in the basal and middle turns of the cochlea and outer hair cells in the organ of Corti (asterisk) in the basal turn. In contrast, mice receiving TGF-β1 inhibitors presented preserved cochlear structures, with the presence of OHC even in the basal turn (arrows in **G**,**I**). Scale bars: A, K 0.5 mm; **(C–G)**, 100 μm. SG, spiral ganglion; SV, scala vestibule; SM, scala media; ST, scala tympani; SL, spiral limbus; SpL, spiral ligament; OHC, outer hair cells; IHC, inner hair cells.

In this work we show that in the first 24 h after noise exposure there is an increase in *Tgfb1* and *TgfbR1* cochlear gene expression, concomitantly with a decrease in *Tgfb2* and *TgfbR2*. These results point to the participation of TGF-β1 in the cochlear inflammatory response to noise injury, and suggest that TGF-β1 could play a role in the initial inflammatory phase. Thus, additional experiments from the group in a mice model of NIHL found a statistically significant 3-fold change in *Tgfb1* expression 4 h after noise challenge, compared to non-exposed animals (Celaya et al., in preparation). Similarly, up-regulation of the proinflammatory cytokines TNFα, IL-1β and IL-6 has been described to occur rapidly after noise exposure, reaching maximum level 3–6 h after noise exposure and maintaining high levels during the following 24–48 h (Fujioka et al., 2006; Tornabene et al., 2006). This quick inflammatory response presumably originates in resident cells, including bone marrow-derived macrophages, spiral ganglion cells and spiral ligament fibrocytes, but also from recruited immune cells. Thus, Satoh et al. found an increase in TGF-β1 immunostaining in the infiltrated inflammatory cells 3 h after the injection of keyhole limpet hemocyanin, which caused an exacerbated immune response in the mouse cochlea. These high levels of TGF-β1 persisted for 48 h and reverted to normal after 7 days as the response resolves (Satoh et al., 2006). TGF-β has been shown to possess dual actions in the inflammatory response to damage, with both pro and anti-inflammatory roles (Kawamoto et al., 2003; Sanjabi et al., 2009). Therefore, we can speculate that the observed initial release of the factor in the cochlea forms part of the early proinflammatory phase of cochlear response to noise damage. Indeed, our data show that its inhibition has an overall protective effect.

In our experiments, noise also induced an activation of the proinflammatory p38α MAPK in the cochlea. We studied the ratio of phosphorylated to total kinase levels as an index of activity in cochlear protein extracts, and we found an increase at 24 h and 2 weeks after VS^{2-20} noise exposure in the saline-treated mouse group. The activation of p38α after noise damage and its correlation with temporal and permanent threshold shifts have been previously reported in the cochlea of chinchilla (Jamesdaniel et al., 2011) and mouse (Meltser et al., 2010; Maeda et al., 2013).

We also confirmed elevated NOX-4 levels in the cochlea 1–3 days after noise exposure. NADPH oxidases (NOX) are enzymes that transport electrons across the plasma membrane and constitute an important source of superoxide radicals. Excessive production of superoxide increases levels of reactive oxygen and nitrogen species which could damage DNA and disrupt lipid and protein molecules leading to cell death by apoptosis (Henderson et al., 2006). Oxidative stress is a common pathogenic mechanism in cochlear damage secondary to noise, ototoxic drugs and aging. Thus, an increase in the expression of NOX-1 and NOX-4 isoforms and their regulatory subunits has been described in fibrocytes, epithelial cells and neurons from mice treated with cisplatin (Kim et al., 2010). In noise-exposed rats, it has been observed an up-regulation of NOX-1 and DUOX2 whereas NOX-3 was down-regulated (Vlajkovic et al., 2013).

In parallel to NOX-4, our data also confirmed an elevation of MnSOD protein level in the cochlea after noise damage exposure. Superoxide dismutases are key antioxidant enzymes directed toward the scavenging of free radicals to maintain the oxidative balance, and low levels are associated with an impaired response to cochlear damage in mice and rats (Keithley et al., 2005; Ying and Balaban, 2009). In addition, polymorphisms in the human *SOD2* gene that codifies for

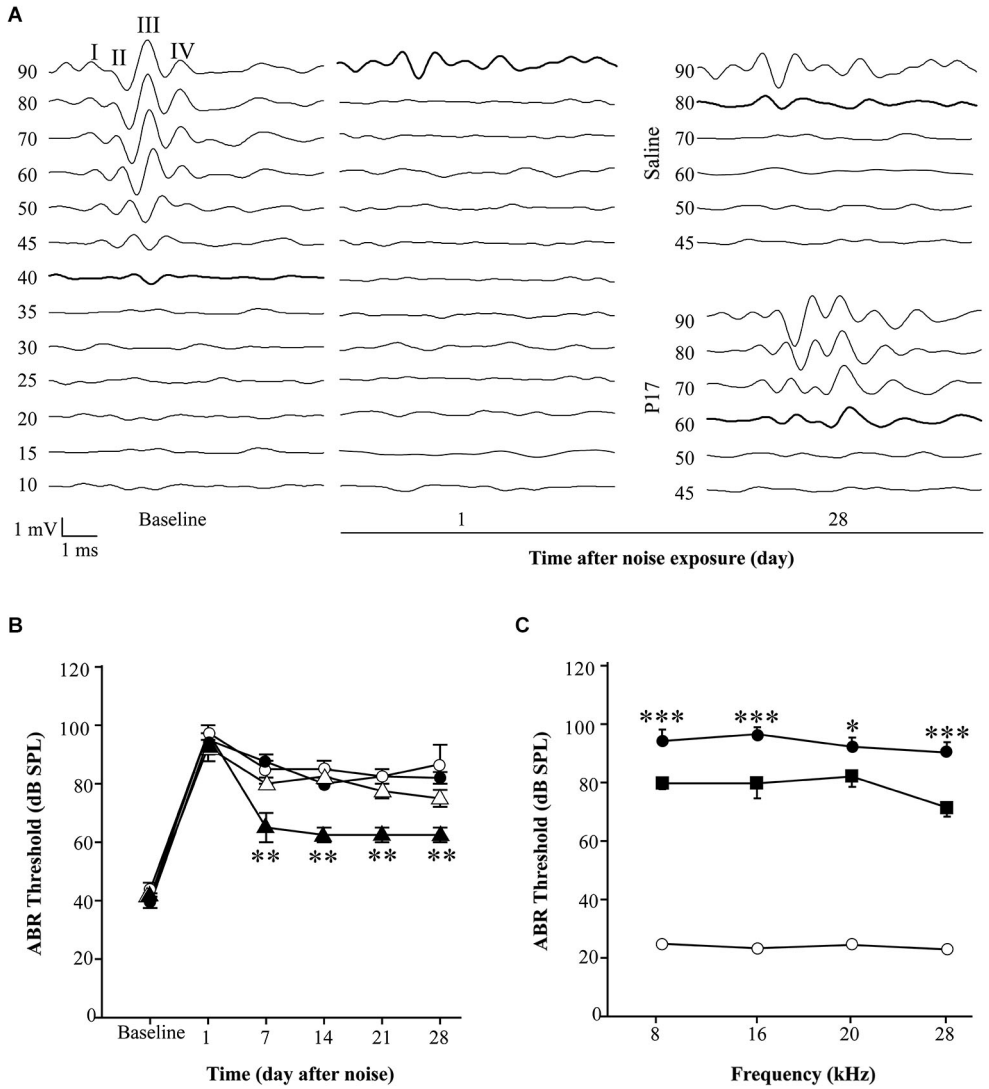

FIGURE 4 | Administration of TGF-β1 inhibitors after noise exposure. **(A)** Representative ABR waveforms in response to click stimulus in C57 exposed to VS^{2-20} noise at 110 dB SPL for 30 min and then treated with TGF-β1 inhibitor P17 at 2.5 mg/kg/12 h or saline for 15 days. Bold lines indicate the ABR threshold. **(B)** Evolution of click ABR thresholds (mean ± SEM, in dB SPL) in C57 mice exposed to VS^{2-20} noise at 110 dB SPL for 30 min and then treated with TGF-β1 inhibitor P17 (triangles) at 2.5 mg/kg or saline (circles) at 0.1 ml/10 g once (white symbols) or twice (black symbols) daily for 15 days (n = 6 per group). Statistically significant differences (paired T test, $^{**}p \leq 0.01$) were found between mice treated with P17 at 2.5 mg/kg/12 h and saline treated mice. Similar results were observed with P144 (data not shown). **(C)** Audiogram of CBA mice treated with P144 (black squares) at 10 mg/kg/day for 15 days after noise exposure (VS^{2-20} at 110 dB SPL, 30 min) showed statistically significant differences (paired T test, $^{*}p \leq 0.05$, $^{***}p \leq 0.001$) at the end of the treatment compared to saline treated mice (black circles). Non-exposed mice (white circles) maintained normal hearing thresholds throughout the study. Similar results were observed with P17 treatment (data not shown).

MnSOD enzyme, have been related to NIHL predisposition (Fortunato et al., 2004; Liu et al., 2010), suggesting that this enzyme is critical during the cochlear response to noise injury.

Taken together, our data confirm that inflammation and oxidative stress are central events in the physiopathology of NIHL and show that TGF-β1 participates in the early phases. Therefore, blocking of this proinflammatory cytokine could be useful in ameliorating pathological changes in the cochlea after noise insult. In this study we tested the therapeutic effect of TGF-β1 inhibitors P17 and P144 administered systemically both before and after noise exposure to explore their potential in prevention and repair situations, respectively. These peptides have demonstrated a strong TGF-β inhibitory effect in animal models of liver and pulmonary fibrosis and hypertension (Ezquerro et al., 2003; Arribillaga et al., 2011; Baltanás et al., 2013). In addition P144 has completed phase I and

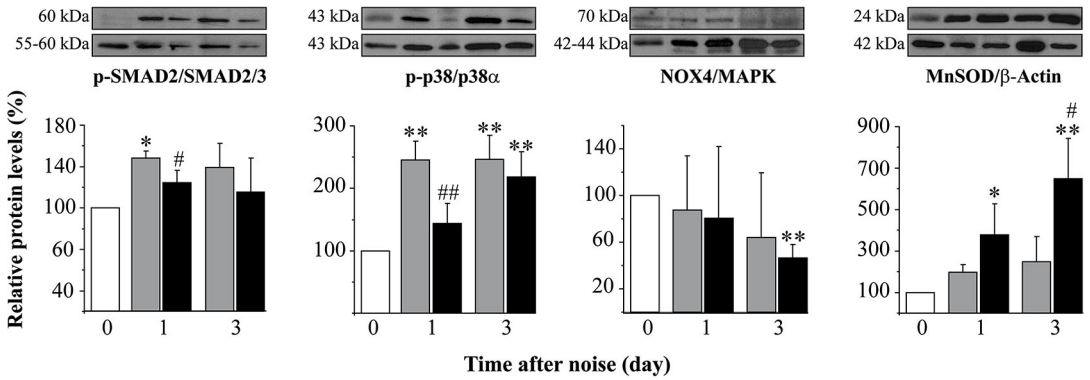

FIGURE 5 | Protein levels after noise exposure and treatment with TGF-β1 inhibitor. Time course of phospo-p38/p38α, phospho-SMAD2/SMAD2/3, NOX-4/MAPK and MnSOD/β-actin ratios relative (%) to non-exposed mice (white bars), in cochlear samples of noise-exposed (VS^{2-20} at 110 dB SPL) CBA mice (n = 3 mice for each determination) and treated with TGF-β1 inhibitor P144 at 10 mg/kg/24 h/15 days (black) or saline (gray). Representative blots are shown. Data are shown as mean ± SD. Statistically significant differences were found in p-p38, NOX4 and MnSOD levels after noise exposure compared to values in non-exposed mice (paired T test, $^{*}p \leq 0.05$; $^{**}p \leq 0.01$). Noise induced statistically significant increases in p-p38, p-SMAD2 and MnSOD ratios compared to non-exposed mice (paired T test, $^{*}p \leq 0.05$; $^{**}p \leq 0.01$). Treatment with P144 showed significantly lower levels of p-p38α and p-SMAD2 and higher levels of MnSOD compared to saline-treated mice (paired T test, $\#p \leq 0.05$; $\#\#p \leq 0.01$).

II clinical trial studies (NCT00656825, NCT00574613 from http://clinicaltrials.gov/ct2/home) and it has been designated as an orphan drug.

Systemic pre-treatment with P17 or P144 significantly reduced the temporal threshold shift observed 1 day after noise exposure. However, when the same dose of TGF-β1 inhibitors were administered after noise damage, the therapeutic effect was observed only after 1 week of treatment. Intraperitoneal administration of drugs could achieve rapidly high cochlear levels (Rivera et al., 2012). For example, steroids reach the highest concentration in the mouse cochlea only 25 min after injection (Kanzaki et al., 2012). On the other hand, up-regulation of proinflammatory cytokines, including TGF-β1, occurs in the first 3–6 h after noise exposure (Fujioka et al., 2006; Tornabene et al., 2006; Celaya et al., in preparation). Therefore, to reach effective local levels in the acute phase of noise-induced inflammation, drug delivery should be performed before or immediately after exposure. We hypothesize that this is the reason why a similar dose of TGF-β1 inhibitors (2.5 mg/kg/day/15 days) was more effective if administered prior to noise exposure rather than 1 day afterwards. The therapeutic effect of TGF-β1 inhibitors administered after noise exposure depended on the noise level and also on the peptide dosages. Thus, P17 and P144 were not able to improve the functional and structural damage that occurred after acoustic trauma with noise levels of 120 dB SPL. However, dose-dependent beneficial effects could be observed when these peptides were administered after exposure to non-traumatic 100 or 110 dB SPL noise. P17 induced a better recovery of ABR thresholds when administered at 5 mg/kg daily for 15 consecutive days, whereas P144 required 10 mg/kg daily dose to achieve similar effectiveness. This result might possibly reflect the pharmacological characteristics of these peptides, since P144 has a poorer solubility in saline than P17 (Ezquerro et al., 2003).

Concomitantly to functional improvement, mice treated with TGF-β1 inhibitors presented more favorable antioxidant and anti-inflammatory profiles than saline-treated mice. Thus, a significant decrease in the activation of the stress-related kinase p38α was observed in mice treated with TGF-β1 inhibitors 1 day after noise exposure compared to saline-treated mice, suggesting that these peptides contribute to decrease the activity of proinflammatory pathways after noise injury. Oxidative imbalance by excessive formation of free radical species is one of the main pathological mechanisms in NIHL (Henderson et al., 2006). Treatment of NIHL with TGF-β1 inhibitors also induces an increase in the levels of MnSOD compared to saline controls, therefore contributing to the scavenging of free radicals and recovery of the oxidative balance. Both the decrease in p38α and the increase in MnSOD activities should provide mice treated with TGF-β1 inhibitors a better resistance to NIHL.

The morphological substrate for this therapeutic effect seems to be the cochlear lateral wall, since noise-exposed mice treated with TGF-β1 inhibitors showed reduced pathological alterations in the spiral ligament when compared to those receiving saline. It has been well documented that noise exposure results in disruption of the lateral wall and causes strial edema and apoptosis of fibrocytes of the spiral ligament (Hirose and Liberman, 2003). The lateral wall is a central structure in the modulation of cochlear inflammatory and immune responses to insult, with resident macrophages and also fibrocytes secreting cytokines that modify the permeability of the blood-labyrinth barrier and attract immune cells from the vasculature. It is likely that TGF-β1 levels are increased in the spiral ligament after noise exposure, therefore acting as a proinflammatory cytokine. In addition, it has been reported that mononuclear phagocytes migrate into the murine cochlea after acoustic trauma (Hirose et al., 2005) and that

infiltrated inflammatory cells express TGF-β after antigen challenge (Satoh et al., 2006). Thus blocking this factor could be a good strategy for ameliorating noise-induced cochlear changes.

On the other hand, it is known that TGF-β1 stimulates the production of collagen fibers in fibrocytes and that excessive collagen synthesis could be deleterious. In this context, the inhibition of TGF-β1 has shown important effects on fibrotic diseases, including hepatic (Ezquerro et al., 2003), pulmonary (Arribillaga et al., 2011), myocardial (Hermida et al., 2009), skin (Santiago et al., 2005) and periprosthetic fibrosis (San-Martin et al., 2010). Therefore, reduction of excessive collagen formation in the spiral ligament after noise exposure could be a secondary beneficial action of TGF-β1 inhibitors in the cochlea.

In summary, in this study we show that TGF-β1 plays a central role in cochlear response to excessive noise exposure and that treatment with TGF-β1 inhibitors ameliorates NIHL.

Authors and Contributors

SM-C, acquisition of data, analysis and interpretation of data, drafting and revising the article, final approval of the version to be published. LR-dlR, acquisition of data, analysis and interpretation of data, drafting the article. JC, analysis and interpretation of data, drafting the article. GC, acquisition of data. TR, analysis and interpretation of data, revising the article, final approval of the version to be published. IV-N, design of the experiments, analysis and interpretation of data, revising the article, final approval of the version to be published.

Acknowledgments

We would like to thank our colleagues from the Neurobiology of Hearing group for their generous sharing of techniques and information. We also warmly thank Drs. Miguel Quintanilla (CSIC), Gemma Rodriguez-Tarduchy (CSIC), Javier Dotor (DIGNA Biotech) and Pablo Ortiz (OWL) for helpful discussions. This study was supported by grants from the Ministerio de Ciencia e Inovación (SAF2011-24391), DIGNA Biotech, the 7th Framework Programme projects AFHELO and TARGEAR for IVN and FIS PI 10/00394 for TR. SM-C, LRdR and GC hold contracts from CIBERER (SM, LRdR) and CSIC Junta para la Ampliación de Estudios programs (GC). The authors declare that they have no conflicts of interest.

Abbreviations

ABR, Auditory brainstem response; NIHL, Noise-induced hearing loss; OHC, Outer hair cells; TGF-β, Transforming growth factor beta; VS, Violet swept sine.

References

Abi-Hachem, R. N., Zine, A., and Van De Water, T. R. (2010). The injured cochlea as a target for inflammatory processes, initiation of cell death pathways and application of related otoprotectives strategies. *Recent Pat. CNS Drug Discov.* 5, 147–163. doi: 10.2174/157488910791213121

Arribillaga, L., Dotor, J., Basagoiti, M., Riezu-Boj, J. I., Borrás-Cuesta, F., Lasarte, J. J., et al. (2011). Therapeutic effect of a peptide inhibitor of TGF-beta on pulmonary fibrosis. *Cytokine* 53, 327–333. doi: 10.1016/j.cyto.2010.11.019

Baltanás, A., Miguel-Carrasco, J. L., San José, G., Cebrián, C., Moreno, M. U., Dotor, J., et al. (2013). A synthetic peptide from transforming growth factor-β_1 type III receptor inhibits NADPH oxidase and prevents oxidative stress in the kidney of spontaneously hypertensive rats. *Antioxid. Redox Signal.* 19, 1607–1618. doi: 10.1089/ars.2012.4653

Bas, E., Van De Water, T. R., Gupta, C., Dinh, J., Vu, L., Martinez-Soriano, F., et al. (2012). Efficacy of three drugs for protecting against gentamicin-induced hair cell and hearing losses. *Br. J. Pharmacol.* 166, 1888–1904. doi: 10.1111/j.1476-5381.2012.01890.x

Cediel, R., Riquelme, R., Contreras, J., Díaz, A., and Varela-Nieto, I. (2006). Sensorineural hearing loss in insulin-like growth factor I-null mice: a new model of human deafness. *Eur. J. Neurosci.* 23, 587–590. doi: 10.1111/j.1460-9568.2005.04584.x

Cobo, P., Murillo-Cuesta, S., Cediel, R., Moreno, A., Lorenzo-García, P., and Varela-Nieto, I. (2009). Design of a reverberant chamber for noise exposure experiments with small animals. *Appl. Acoust.* 70, 1034–1040. doi: 10.1016/j.apacoust.2009.03.005

Dotor, J., López-Vázquez, A. B., Lasarte, J. J., Sarobe, P., García-Granero, M., Riezu-Boj, J. I., et al. (2007). Identification of peptide inhibitors of transforming growth factor beta 1 using a phage-displayed peptide library. *Cytokine* 39, 106–115. doi: 10.1016/j.cyto.2007.06.004

Dünker, N., and Krieglstein, K. (2000). Targeted mutations of transforming growth factor-beta genes reveal important roles in mouse development and adult homeostasis. *Eur. J. Biochem.* 267, 6982–6988. doi: 10.1046/j.1432-1327.2000.01825.x

Eshraghi, A. A., Gupta, C., Van De Water, T. R., Bohorquez, J. E., Garnham, C., Bas, E., et al. (2013). Molecular mechanisms involved in cochlear implantation trauma and the protection of hearing and auditory sensory cells by inhibition of c-Jun-N-terminal kinase signaling. *Laryngoscope* 123(Suppl. 1), S1–S14. doi: 10.1002/lary.23902

Ezquerro, I. J., Lasarte, J. J., Dotor, J., Castilla-Cortázar, I., Bustos, M., Peñuelas, I., et al. (2003). A synthetic peptide from transforming growth factor beta type III receptor inhibits liver fibrogenesis in rats with carbon tetrachloride liver injury. *Cytokine* 22, 12–20. doi: 10.1016/s1043-4666(03)00101-7

Fetoni, A. R., De Bartolo, P., Eramo, S. L., Rolesi, R., Paciello, F., Bergamini, C., et al. (2013). Noise-induced hearing loss (NIHL) as a target of oxidative stress-mediated damage: cochlear and cortical responses after an increase in antioxidant defense. *J. Neurosci.* 33, 4011–4023. doi: 10.1523/JNEUROSCI.1009-13.2013

Fortunato, G., Marciano, E., Zarrilli, F., Mazzaccara, C., Intrieri, M., Calcagno, G., et al. (2004). Paraoxonase and superoxide dismutase gene polymorphisms and noise-induced hearing loss. *Clin. Chem.* 50, 2012–2018. doi: 10.1373/clinchem.2004.037788

Frenz, D. A., Galinovic-Schwartz, V., Liu, W., Flanders, K. C., and Van De Water, T. R. (1992). Transforming growth factor beta 1 is an epithelial-derived signal peptide that influences otic capsule formation. *Dev. Biol.* 153, 324–336. doi: 10.1016/0012-1606(92)90117-y

Fujioka, M., Kanzaki, S., Okano, H. J., Masuda, M., Ogawa, K., and Okano, H. (2006). Proinflammatory cytokines expression in noise-induced damaged cochlea. *J. Neurosci. Res.* 83, 575–583. doi: 10.1002/jnr.20764

Ghaheri, B. A., Kempton, J. B., Pillers, D. A., and Trune, D. R. (2007). Cochlear cytokine gene expression in murine chronic otitis media. *Otolaryngol. Head Neck Surg.* 137, 332–337. doi: 10.1016/j.otohns.2007.03.020

Gil-Guerrero, L., Dotor, J., Huibregtse, I. L., Casares, N., López-Vázquez, A. B., Rudilla, F., et al. (2008). *In vitro* and *in vivo* down-regulation of regulatory T cell activity with a peptide inhibitor of TGF-beta1. *J. Immunol.* 181, 126–135. doi: 10.4049/jimmunol.181.1.126

Henderson, D., Bielefeld, E. C., Harris, K. C., and Hu, B. H. (2006). The role of oxidative stress in noise-induced hearing loss. *Ear Hear.* 27, 1–19. doi: 10.1097/01.aud.0000191942.36672.f3

Hermida, N., López, B., González, A., Dotor, J., Lasarte, J. J., Sarobe, P., et al. (2009). A synthetic peptide from transforming growth factor-beta1 type III receptor prevents myocardial fibrosis in spontaneously hypertensive rats. *Cardiovasc. Res.* 81, 601–609. doi: 10.1093/cvr/cvn315

Hirose, K., Discolo, C. M., Keasler, J. R., and Ransohoff, R. (2005). Mononuclear phagocytes migrate into the murine cochlea after acoustic trauma. *J. Comp. Neurol.* 489, 180–194. doi: 10.1002/cne.20619

Hirose, K., and Liberman, M. C. (2003). Lateral wall histopathology and endocochlear potential in the noise-damaged mouse cochlea. *J. Assoc. Res. Otolaryngol.* 4, 339–352. doi: 10.1007/s10162-002-3036-4

Ichimiya, I., Yoshida, K., Hirano, T., Suzuki, M., and Mogi, G. (2000). Significance of spiral ligament fibrocytes with cochlear inflammation. *Int. J. Pediatr. Otorhinolaryngol.* 56, 45–51. doi: 10.1016/s0165-5876(00)00408-0

Jamesdaniel, S., Hu, B., Kermany, M. H., Jiang, H., Ding, D., Coling, D., et al. (2011). Noise induced changes in the expression of p38/MAPK signaling proteins in the sensory epithelium of the inner ear. *J. Proteomics* 75, 410–424. doi: 10.1016/j.jprot.2011.08.007

Kanzaki, S., Fujioka, M., Yasuda, A., Shibata, S., Nakamura, M., Okano, H. J., et al. (2012). Novel *in vivo* imaging analysis of an inner ear drug delivery system in mice: comparison of inner ear drug concentrations over time after transtympanic and systemic injections. *PLoS One* 7:e48480. doi: 10.1371/journal.pone.0048480

Kawamoto, K., Yagi, M., Stöver, T., Kanzaki, S., and Raphael, Y. (2003). Hearing and hair cells are protected by adenoviral gene therapy with TGF-α1 and GDNF. *Mol. Ther.* 7, 484–492. doi: 10.1016/s1525-0016(03)00058-3

Keithley, E. M., Canto, C., Zheng, Q. Y., Wang, X., Fischel-Ghodsian, N., and Johnson, K. R. (2005). Cu/Zn superoxide dismutase and age-related hearing loss. *Hear. Res.* 209, 76–85. doi: 10.1016/j.heares.2005.06.009

Kim, H. J., Kang, K. Y., Baek, J. G., Jo, H. C., and Kim, H. (2006). Expression of TGFbeta family in the developing internal ear of rat embryos. *J. Korean Med. Sci.* 21, 136–142. doi: 10.3346/jkms.2006.21.1.136

Kim, H. J., Lee, J. H., Kim, S. J., Oh, G. S., Moon, H. D., Kwon, K. B., et al. (2010). Roles of NADPH oxidases in cisplatin-induced reactive oxygen species generation and ototoxicity. *J. Neurosci.* 30, 3933–3946. doi: 10.1523/JNEUROSCI.6054-09.2010

Kulkarni, A. B., Huh, C. G., Becker, D., Geiser, A., Lyght, M., Flanders, K. C., et al. (1993). Transforming growth factor beta 1 null mutation in mice causes excessive inflammatory response and early death. *Proc. Natl. Acad. Sci. U S A* 90, 770–774. doi: 10.1073/pnas.90.2.770

Le Prell, C. G., Yamashita, D., Minami, S. B., Yamasoba, T., and Miller, J. M. (2007). Mechanisms of noise-induced hearing loss indicate multiple methods of prevention. *Hear. Res.* 226, 22–43. doi: 10.1016/j.heares.2006.10.006

Letterio, J. J. (2000). Murine models define the role of TGF-beta as a master regulator of immune cell function. *Cytokine Growth Factor Rev.* 11, 81–87. doi: 10.1016/s1359-6101(99)00031-3

Liu, W., Butts, S., Kim, H., and Frenz, D. A. (2007). Negative regulation of otic capsule chondrogenesis: it can make you Smad. *Ann. N Y Acad. Sci.* 1116, 141–148. doi: 10.1196/annals.1402.005

Liu, Y. M., Li, X. D., Guo, X., Liu, B., Lin, A. H., and Rao, S. Q. (2010). Association between polymorphisms in SOD1 and noise-induced hearing loss in Chinese workers. *Acta Otolaryngol.* 130, 477–486. doi: 10.3109/00016480903253587

Maeda, Y., Fukushima, K., Omichi, R., Kariya, S., and Nishizaki, K. (2013). Time courses of changes in phospho- and total- MAP kinases in the cochlea after intense noise exposure. *PLoS One* 8:e58775. doi: 10.1371/journal.pone.0058775

Mantel, P. Y., and Schmidt-Weber, C. B. (2011). Transforming growth factor-beta: recent advances on its role in immune tolerance. *Methods Mol. Biol.* 677, 303–338. doi: 10.1007/978-1-60761-869-0_21

Marzella, P. L., Gillespie, L. N., Clark, G. M., Bartlett, P. F., and Kilpatrick, T. J. (1999). The neurotrophins act synergistically with LIF and members of the TGF-beta superfamily to promote the survival of spiral ganglia neurons *in vitro*. *Hear. Res.* 138, 73–80. doi: 10.1016/s0378-5955(99)00152-5

Massagué, J. (2012). TGFβ signalling in context. *Nat. Rev. Mol. Cell Biol.* 13, 616–630. doi: 10.1038/nrm3434

Meltser, I., Tahera, Y., and Canlon, B. (2010). Differential activation of mitogen-activated protein kinases and brain-derived neurotrophic factor after temporary or permanent damage to a sensory system. *Neuroscience* 165, 1439–1446. doi: 10.1016/j.neuroscience.2009.11.025

Nakamoto, T., Mikuriya, T., Sugahara, K., Hirose, Y., Hashimoto, T., Shimogori, H., et al. (2012). Geranylgeranylacetone suppresses noise-induced expression of proinflammatory cytokines in the cochlea. *Auris Nasus Larynx* 39, 270–274. doi: 10.1016/j.anl.2011.06.001

Ohlemiller, K. K. (2006). Contributions of mouse models to understanding of age- and noise-related hearing loss. *Brain Res.* 1091, 89–102. doi: 10.1016/j.brainres.2006.03.017

Ohlemiller, K. K., and Gagnon, P. M. (2007). Genetic dependence of cochlear cells and structures injured by noise. *Hear. Res.* 224, 34–50. doi: 10.1016/j.heares.2006.11.005

Ohlemiller, K. K., Rosen, A. D., Rellinger, E. A., Montgomery, S. C., and Gagnon, P. M. (2011). Different cellular and genetic basis of noise-related endocochlear potential reduction in CBA/J and BALB/cJ mice. *J. Assoc. Res. Otolaryngol.* 12, 45–58. doi: 10.1007/s10162-010-0238-z

Ohlemiller, K. K., Wright, J. S., and Heidbreder, A. F. (2000). Vulnerability to noise-induced hearing loss in 'middle-aged' and young adult mice: a dose-response approach in CBA, C57BL and BALB inbred strains. *Hear. Res.* 149, 239–247. doi: 10.1016/s0378-5955(00)00191-x

Okano, T., Nakagawa, T., Kita, T., Kada, S., Yoshimoto, M., Nakahata, T., et al. (2008). Bone marrow-derived cells expressing Iba1 are constitutively present as resident tissue macrophages in the mouse cochlea. *J. Neurosci. Res.* 86, 1758–1767. doi: 10.1002/jnr.21625

Okano, J., Takigawa, T., Seki, K., Suzuki, S., Shiota, K., and Ishibashi, M. (2005). Transforming growth factor beta 2 promotes the formation of the mouse cochleovestibular ganglion in organ culture. *Int. J. Dev. Biol.* 49, 23–31. doi: 10.1387/ijdb.041905jo

Ou, H. C., Bohne, B. A., and Harding, G. W. (2000a). Noise damage in the C57BL/CBA mouse cochlea. *Hear. Res.* 145, 111–122. doi: 10.1016/s0378-5955(00)00081-2

Ou, H. C., Harding, G. W., and Bohne, B. A. (2000b). An anatomically based frequency-place map for the mouse cochlea. *Hear. Res.* 145, 123–129. doi: 10.1016/s0378-5955(00)00082-4

Paradies, N. E., Sanford, L. P., Doetschman, T., and Friedman, R. A. (1998). Developmental expression of the TGF beta s in the mouse cochlea. *Mech. Dev.* 79, 165–168. doi: 10.1016/S0925-4773(98)00184-1

Park, S.-N., Back, S.-A., Park, K.-H., Seo, J.-H., Noh, H.-I., Akil, O., et al. (2013). Comparison of functional and morphologic characteristics of mice models of noise-induced hearing loss. *Auris Nasus Larynx* 40, 11–17. doi: 10.1016/j.anl.2011.11.008

Park, J. E., and Barbul, A. (2004). Understanding the role of immune regulation in wound healing. *Am. J. Surg.* 187, 11S–16S. doi: 10.1016/s0002-9610(03)00296-4

Pelton, R. W., Saxena, B., Jones, M., Moses, H. L., and Gold, L. I. (1991). Immunohistochemical localization of TGF beta 1, TGF beta 2 and TGF beta 3 in the mouse embryo: expression patterns suggest multiple roles during embryonic development. *J. Cell Biol.* 115, 1091–1105. doi: 10.1083/jcb.115.4.1091

Prud'homme, G. J. (2007). Pathobiology of transforming growth factor beta in cancer, fibrosis and immunologic disease and therapeutic considerations. *Lab. Invest.* 87, 1077–1091. doi: 10.1038/labinvest.3700669

Riquelme, R., Cediel, R., Contreras, J., la Rosa Lourdes, R. D., Murillo-Cuesta, S., Hernandez-Sanchez, C., et al. (2010). A comparative study of age-related hearing loss in wild type and insulin-like growth factor I deficient mice. *Front. Neuroanat.* 4:27. doi: 10.3389/fnana.2010.00027

Rivera, T., Sanz, L., Camarero, G., and Varela-Nieto, I. (2012). Drug delivery to the inner ear: strategies and their therapeutic implications for sensorineural hearing loss. *Curr. Drug Deliv.* 9, 231–242. doi: 10.2174/156720112800389098

Rodríguez-de la Rosa, L., López-Herradón, A., Portal-Núñez, S., Murillo-Cuesta, S., Lozano, D., Cediel, R., et al. (2014). Treatment with N- and C-terminal peptides of parathyroid hormone-related protein partly compensate the skeletal abnormalities in igf-I deficient mice. *PLoS One* 9:e87536. doi: 10.1371/journal.pone.0087536

Sanchez-Calderon, H., Rodriguez-De La Rosa, L., Milo, M., Pichel, J. G., Holley, M., and Varela-Nieto, I. (2010). RNA microarray analysis in prenatal mouse cochlea reveals novel IGF-I target genes: implication of MEF2 and FOXM1 transcription factors. *PLoS One* 5:e8699. doi: 10.1371/journal.pone.0008699

Sanford, L. P., Ormsby, I., Gittenberger-De Groot, A. C., Sariola, H., Friedman, R., Boivin, G. P., et al. (1997). TGFbeta2 knockout mice have multiple

developmental defects that are non-overlapping with other TGFbeta knockout phenotypes. *Development* 124, 2659–2670.

Sanjabi, S., Zenewicz, L. A., Kamanaka, M., and Flavell, R. A. (2009). Anti-inflammatory and pro-inflammatory roles of TGF-beta, IL-10 and IL-22 in immunity and autoimmunity. *Curr. Opin. Pharmacol.* 9, 447–453. doi: 10.1016/j.coph.2009.04.008

San-Martin, A., Dotor, J., Martinez, F., and Hontanilla, B. (2010). Effect of the inhibitor peptide of the transforming growth factor beta (p144) in a new silicone pericapsular fibrotic model in pigs. *Aesthetic Plast. Surg.* 34, 430–437. doi: 10.1007/s00266-010-9475-0

Santiago, B., Gutierrez-Cañas, I., Dotor, J., Palao, G., Lasarte, J. J., Ruiz, J., et al. (2005). Topical application of a peptide inhibitor of transforming growth factor-beta1 ameliorates bleomycin-induced skin fibrosis. *J. Invest. Dermatol.* 125, 450–455. doi: 10.1111/j.0022-202x.2005.23859.x

Sanz, L., Murillo-Cuesta, S., Cobo, P., Cediel, R., Contreras, J., Rivera, T., et al. (2015). Swept-sine noise-induced damage as a hearing loss model for preclinical assays. *Front. Neurosci.* 7:7. doi: 10.3389/fnagi.2015.00007

Satoh, H., Billings, P., Firestein, G. S., Harris, J. P., and Keithley, E. M. (2006). Transforming growth factor beta expression during an inner ear immune response. *Ann. Otol. Rhinol. Laryngol.* 115, 81–88. doi: 10.1177/000348940611500112

Satoh, H., Firestein, G. S., Billings, P. B., Harris, J. P., and Keithley, E. M. (2002). Tumor necrosis factor-alpha, an initiator and etanercept, an inhibitor of cochlear inflammation. *Laryngoscope* 112, 1627–1634. doi: 10.1097/00005537-200209000-00019

Shull, M. M., Ormsby, I., Kier, A. B., Pawlowski, S., Diebold, R. J., Yin, M., et al. (1992). Targeted disruption of the mouse transforming growth factor-beta 1 gene results in multifocal inflammatory disease. *Nature* 359, 693–699. doi: 10.1038/359693a0

Son, E. J., Wu, L., Yoon, H., Kim, S., Choi, J. Y., and Bok, J. (2012). Developmental gene expression profiling along the tonotopic axis of the mouse cochlea. *PLoS One* 7:e40735. doi: 10.1371/journal.pone.0040735

Stamatiou, G. A., and Stankovic, K. M. (2013). A comprehensive network and pathway analysis of human deafness genes. *Otol. Neurotol.* 34, 961–970. doi: 10.1097/mao.0b013e3182898272

Tahera, Y., Meltser, I., Johansson, P., Bian, Z., Stierna, P., Hansson, A. C., et al. (2006). NF-kappaB mediated glucocorticoid response in the inner ear after acoustic trauma. *J. Neurosci. Res.* 83, 1066–1076. doi: 10.1002/jnr.20795

Tan, W. J. T., Thorne, P. R., and Vlajkovic, S. M. (2013). Noise-induced cochlear inflammation. *World J. Otorhinolaryngol.* 3, 89–99. doi: 10.5319/wjo.v3.i3.89

Tornabene, S. V., Sato, K., Pham, L., Billings, P., and Keithley, E. M. (2006). Immune cell recruitment following acoustic trauma. *Hear. Res.* 222, 115–124. doi: 10.1016/j.heares.2006.09.004

Vlajkovic, S. M., Lin, S. C., Wong, A. C., Wackrow, B., and Thorne, P. R. (2013). Noise-induced changes in expression levels of NADPH oxidases in the cochlea. *Hear. Res.* 304, 145–152. doi: 10.1016/j.heares.2013.07.012

Wang, Y., Hirose, K., and Liberman, M. C. (2002). Dynamics of noise-induced cellular injury and repair in the mouse cochlea. *J. Assoc. Res. Otolaryngol.* 3, 248–268. doi: 10.1007/s101620020028

Weiss, A., and Attisano, L. (2013). The TGFbeta superfamily signaling pathway. *Wiley Interdiscip. Rev. Dev. Biol.* 2, 47–63. doi: 10.1002/wdev.86

Wissel, K., Wefstaedt, P., Miller, J. M., Lenarz, T., and Stöver, T. (2006). Differential brain-derived neurotrophic factor and transforming growth factor-beta expression in the rat cochlea following deafness. *Neuroreport* 17, 1297–1301. doi: 10.1097/01.wnr.0000233088.92839.23

Ying, Y. L., and Balaban, C. D. (2009). Regional distribution of manganese superoxide dismutase 2 (Mn SOD2) expression in rodent and primate spiral ganglion cells. *Hear. Res.* 253, 116–124. doi: 10.1016/j.heares.2009.04.006

Yoshida, K., Ichimiya, I., Suzuki, M., and Mogi, G. (1999). Effect of proinflammatory cytokines on cultured spiral ligament fibrocytes. *Hear. Res.* 137, 155–159. doi: 10.1016/s0378-5955(99)00134-3

Zhang, F., Dai, M., Neng, L., Zhang, J. H., Zhi, Z., Fridberger, A., et al. (2013). Perivascular macrophage-like melanocyte responsiveness to acoustic trauma–a salient feature of strial barrier associated hearing loss. *FASEB J.* 27, 3730–3740. doi: 10.1096/fj.13-232892

Conflict of Interest Statement: The authors declare that the research was conducted in the absence of any commercial or financial relationships that could be construed as a potential conflict of interest.

frontiers in
AGING NEUROSCIENCE

MINI REVIEW ARTICLE
published: 29 January 2015
doi: 10.3389/fnagi.2015.00003

Targeting cholesterol homeostasis to fight hearing loss: a new perspective

Brigitte Malgrange[1], Isabel Varela-Nieto[2], Philippe de Medina[3]* and Michael R. Paillasse[3]*

[1] *GIGA-Neurosciences, Developmental Neurobiology Unit, University of Liege, Liege, Belgium*
[2] *Instituto de Investigaciones Biomédicas "Alberto Sols", CSIC-UAM. IdiPAZ, CIBERER Instituto de Salud Carlos III. Arturo Duperier 4, Madrid, Spain*
[3] *Affichem SA, Toulouse, France*

Edited by:
Rodrigo Orlando Kuljiš, Zdrav Mozak Limitada, Chile

Reviewed by:
Juan Carlos Alvarado, University of Castilla-La Mancha, Spain
Esperanza Bas Infante, University of Miami, USA

****Correspondence:***
Philippe de Medina and Michael R. Paillasse, Affichem SA, 9 rue Saint Joseph, Toulouse 31400, France
e-mail: p.demedina@affichem.com; m.paillasse@affichem.com

Sensorineural hearing loss (SNHL) is a major pathology of the inner ear that affects nearly 600 million people worldwide. Despite intensive researches, this major health problem remains without satisfactory solutions. The pathophysiological mechanisms involved in SNHL include oxidative stress, excitotoxicity, inflammation, and ischemia, resulting in synaptic loss, axonal degeneration, and apoptosis of spiral ganglion neurons. The mechanisms associated with SNHL are shared with other neurodegenerative disorders. Cholesterol homeostasis is central to numerous pathologies including neurodegenerative diseases and cholesterol regulates major processes involved in neurons survival and function. The role of cholesterol homeostasis in the physiopathology of inner ear is largely unexplored. In this review, we discuss the findings concerning cholesterol homeostasis in neurodegenerative diseases and whether it should be translated into potential therapeutic strategies for the treatment of SNHL.

Keywords: sensorineural hearing loss, cholesterol homeostasis, liver X receptor, excitotoxicity, oxysterol

INTRODUCTION

Hearing loss constitutes a major health problem affecting 16% of the adult population worldwide (Pleis and Lethbridge-Cejku, 2006). Aging is the main risk factor associated with hearing impairment. Age-related sensorineural hearing loss (SNHL) is the third most common disability of the elderly affecting about half of the population over 75 years old (Gates and Mills, 2005). SNHL prevalence dramatically increases and is expected to keep rising based on the rapidly increasing number of elderly people. SNHL is a pathology of the cochlea that is generally regarded as mechanical or chemical damage-induced hair cell death triggering spiral ganglion neuron (SGN) death and subsequent dysfunction of auditory nerve (Takeno et al., 1998). Recent researches in SNHL field have lead to a more complex vision of the relationship between inner ear damage and SNHL. Indeed, SGN loss without hair cell damage or death was observed (Ryals et al., 1999; White et al., 2000; Linthicum and Fayad, 2009). Because many cell types within the cochlea, including hair cells, SGN, and strial cells, decrease in number with age (Ohlemiller and Gagnon, 2004), the majority of age-related SNHL could be classified according to the type of cell degenerated: sensory (hair cell loss), neural (SGN loss), metabolic (strial dysfunction), and cochlear conductive (changes in the stiffness of the basilar membrane) (Schuknecht and Gacek, 1993). Consistent with this, auditory neuropathy and auditory synaptopathy were reported as a cause of SNHL. Auditory synaptopathy results from defects of the ribbon synapses between inner hair cells and SGN (Moser et al., 2013) leading to auditory neuropathy that is characterized by auditory nerve degeneration (Worthington and Peters, 1980; Starr et al., 1996). Auditory neuropathy is responsible for about 8% of SNHL cases and is notably associated with absent or abnormal ABR and poor speech understanding, particularly in noisy surroundings (Starr et al., 1996; Kraus et al., 2000; Madden et al., 2002).

Currently, no effective medication is available to prevent or treat SNHL. Cochlear implants bypass damaged hair cells by providing direct electrical stimulation of SGNs. This approach ameliorates speech production and perception in patients with a severe-profound SNHL (Harris et al., 1995; Bond et al., 2009). However, the beneficial effects of cochlear implants are strongly limited by both SGN degeneration and loss (Roehm and Hansen, 2005; Shibata et al., 2011). The neurotrophic and neuroprotective properties of neurotrophins were promising. However, first clinical trials led to variable results, showed bad distribution profiles and deleterious secondary effects such as abnormal proliferation of Schwann cells (Winkler et al., 1997), unwanted cell migration (Williams, 1991), or weight loss (Eriksdotter Jonhagen et al., 1998). Other trophic factors have shown effectiveness in modulating inner ear protection and repair, such as of insulin-like growth factor 1 (IGF-1). IGF-1 is effective in the protection from electrode trauma insertion in the guinea pig and in the recovery from sudden hearing loss in humans (Kikkawa et al., 2014; Nakagawa et al., 2014). This is promising, since, in men and mice, IGF-1 deficiency causes SNHL (Varela-Nieto et al., 2013) but more trials are needed. During the past few decades, other key mechanisms contributing to SNHL etiology were characterized. Indeed, noise-induced and age-related SNHL etiology was associated with ischemia, inflammation, excitotoxicity (excessive glutamate release), axonal degeneration, oxidative stress, and mitochondrial dysfunction (Menardo et al., 2012). Circulatory disturbance is considered as a plausible cause of idiopathic sudden SNHL (Kim, 1999; Merchant et al., 2008). Ischemia by itself causes excitotoxicity, failure of energy supply, and excess production of free radicals highlighting the

interconnection between these deleterious processes. Excitotoxicity is also considered as a major mediator of inner ear damage leading to deleterious effect on SGN function. New therapeutic approaches that target several of these deleterious processes should be effective for SNHL prevention and treatment.

Besides SNHL, these deleterious processes are also causative or characteristic factors of neurodegenerative diseases. Interestingly, cholesterol homeostasis and metabolism are central to numerous pathologies including neurodegenerative diseases (Liu et al., 2010; Vance, 2012) and regulate the above-mentioned processes involved in neuron survival and functionality (Laskowitz et al., 1997; Kang and Rivest, 2012). Consequently, interfering with cholesterol homeostasis should afford innovative therapeutic strategies to improve the care of SNHL. In this review, we discuss the underestimated potential of cholesterol homeostasis and metabolites as a new opportunity to better understand inner ear pathologies and afford innovative therapeutic strategies.

CHOLESTEROL HOMEOSTASIS IN BRAIN

Brain cholesterol is essential to ensure cell membrane structure, neurotransmitter release, signal transduction, and synaptogenesis (Pfrieger and Ungerer, 2011; Leoni and Caccia, 2013). Since the blood–brain barrier (BBB) prevents the uptake of lipoprotein from the circulation, all brain cholesterol is synthesized from acetyl-CoA through the rate-limiting enzyme HMGCoA reductase (HMGCR), tightly regulated by sterol-regulator element binding protein (**Figure 1**). In adult brain, neurons mostly rely on cholesterol from astrocytes, secreted by adenosine triphosphate-binding cassette (ABC) members A1 and G1, and bound to apolipoprotein E (ApoE) particles. Neurons then uptake these lipoproteins via receptors of the low density lipoprotein receptor family (i.e., LDL receptor, LDL receptor-related protein 1, and ApoE receptor 2). Cholesterol is notably required to form synapses (Goritz et al., 2002) in neuronal cells. Excess cholesterol is converted by Cyp46 into 24(S)-hydroxycholesterol [24(S)-OHC], then secreted directly or via ABCG4 to ApoE particles. Contrary to cholesterol, some oxysterols are able to cross the BBB, since 24(S)-OHC is excreted to circulation whereas 27-hydroxycholesterol (27-OHC) reaches the brain (**Figure 1**).

These oxysterols fluxes are important since most of those are endogenous ligands of liver X receptors (LXRs) (Janowski et al., 1996; Fu et al., 2001). LXRα and LXRβ are nuclear transcription

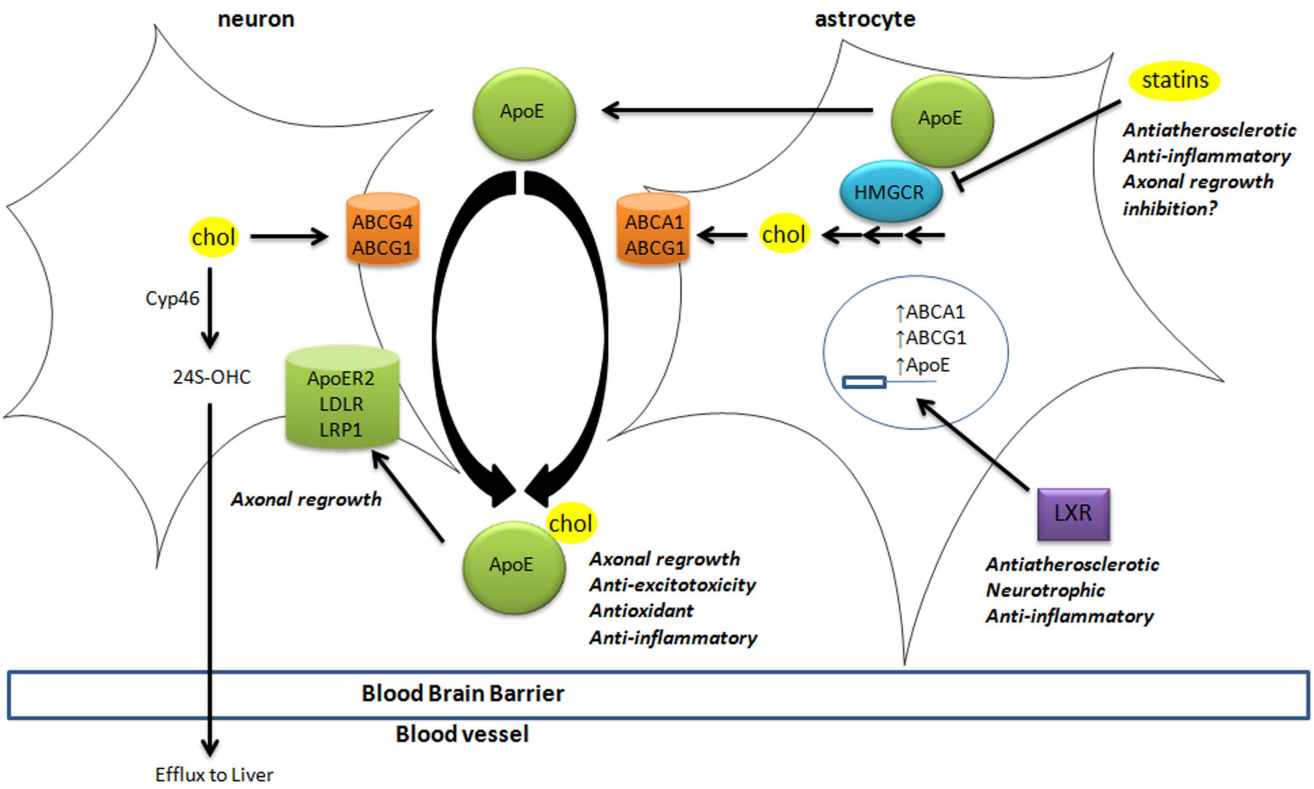

FIGURE 1 | Cholesterol homeostasis in brain. Cholesterol synthesis takes place in astrocytes, through activation of the rate-limiting enzyme HMGCR. Cholesterol is then loaded on ApoE particles by ABCA1 and ABCG1 transporters. LXR activation triggers the expression of ApoE, ABCA1, and ABCG1 at the transcriptional level. These lipoproteins are internalized by neurons via LDL-family receptors (LDLR, LRP1, and ApoER2). In neurons, cholesterol is metabolized into 24(S)-OHC by Cyp46 to be excreted through the blood–brain barrier to the liver. The impact of key players in cholesterol homeostasis (HMGCR, LXR, ApoE-lipoproteins, and LRP1) in processes associated with neurodegeneration is disclosed (italic). 24(S)-OHC, 24(S)-hydroxycholesterol; ABC, ATP-binding cassette; ApoER2, ApoE receptor 2; Cyp46, cytochrome P450 46A1 or cholesterol-24-hydroxylase; HMGCR, HMGCoA reductase; LDL, low density lipoprotein; LDLR, low density lipoprotein receptor; LRP1, LDL-related protein 1; LXR, liver X receptor.

factors that are master regulators of cholesterol homeostasis (Hong and Tontonoz, 2014), regulating the expression of the above-mentioned cholesterol transporters (**Figure 1**). For instance, the expression of ABCA1 and ABCG1 was reduced in astrocytes from LXR-invalidated mice, and LXR was shown to be essential for neurogenesis (Fan et al., 2008). Some oxysterols that are LXR ligands were detected in brain and display neurotrophic activity *in vitro* and *in vivo* (Schmidt et al., 1999; Sacchetti et al., 2009; Theofilopoulos et al., 2013).

Cholesterol homeostasis in the inner ear is largely unexplored. However, it is highly probable that similar mechanisms may rule cholesterol homeostasis in brain and cochlea. Indeed, neither brain nor cochlea can use cholesterol from the circulation and expression of cholesterogenic enzymes, cholesterol transporters, and LXR was reported in both.

CHOLESTEROL HOMEOSTASIS AND NEURODEGENERATIVE DISEASE

Deregulation of cholesterol balance is an increasingly recognized characteristic of chronic neurodegenerative diseases such as Parkinson's, Alzheimer's, and Huntington's diseases (Vance, 2012). Acute neuronal injury in stroke, brain trauma, or epileptic seizures also impact cholesterol homeostasis in the brain (Mahley, 1988; Adibhatla and Hatcher, 2008). Changes in brain cholesterol homeostasis were described during glutamate-mediated excitotoxicity, which is involved in the deleterious effect of numerous neurological stresses such as stroke, traumatic brain injury, and noise exposure. Nevertheless, roles of cholesterol and its metabolites are not clear (Ong et al., 2010; Sodero et al., 2012). Short-term glutamate mediated excitotoxicity induces a cholesterol loss from the synaptic membranes through the stimulation of 24(S)-OHC production potentially leading to excitotoxicity attenuation since cholesterol and oxysterols (notably 7-ketocholesterol and cholesterol epoxides, 7KC and 5,6-ECs, respectively) are promoters of exocytosis. Other study showed that longer exposure to a potent glutamate analog lead to increased level of cholesterol and oxysterols (notably 7KC and 5,6-ECs) in neurons of the damaged hippocampus that potentially propagate excitotoxicity and directly induce cytotoxicity. Consistently, inhibition of cholesterol synthesis by statins or depletion by methyl-β-cyclodextrin prevents excitotoxicity-induced neuronal death (Ponce et al., 2008).

On the other hand, cholesterol derived from astrocytes lipoprotein seems beneficial in neurons. Indeed, in glial cells, dramatic increase of ApoE produced was described after nerve injury in both central and peripheral nervous systems (Ignatius et al., 1986; Boyles et al., 1989), allowing axonal regrowth, and repair of injured neurons as shown in retinal ganglion neurons (Hayashi et al., 2004). An upregulation of ABCA1 was also observed *in vivo* during reinnervation of damaged hippocampus (Jasmin et al., 2014). In neurons, LDL receptor family supports ApoE beneficial action (Hayashi et al., 2004). For instance, LRP1 activation promotes axonal regeneration (Yoon et al., 2013) and induces neurotrophin receptor signaling (Shi et al., 2009). Altogether, these studies showed that ApoE-lipoproteins exert antioxidant, anti-inflammatory, and anti-excitotoxic activities and stimulate axonal regrowth by providing cholesterol to distal axons.

Numerous studies sustain the beneficial impact of LXR in neurodegeneration and as target for neuroprotective/regenerative treatments. LXR receptors disruption in mice is associated with severe neurodegeneration (Wang et al., 2002). The brain of LXR-invalidated mice displayed enlarged brain blood vessels, lipid deposits, proliferation of astrocytes, and loss of neurons. The impairment of cholesterol delivery from astrocytes to neurons should be a major cause of neurodegeneration observed in the LXR-invalidated mice. Consistently, LXR activation using synthetic ligands improves recovery in a rat model of acute brain ischemia (Namjoshi et al., 2013). In addition to homeostasis, role of LXR in inflammation is also major in diverse pathologies including neurodegenerative diseases (Steffensen et al., 2013). LXR activation prevents the transcription of inflammatory genes through the inhibition of NFκB pathway. In addition, synthetic LXR agonists reduce neuroinflammation in mice models of neurodegeneration and exert neuroprotective property *in vivo* (Sironi et al., 2008). Interestingly, some endogenous oxysterols do so *in vitro* and *in vivo* (Schmidt et al., 1999; Sacchetti et al., 2009; Theofilopoulos et al., 2013).

The studies related to brain cholesterol metabolites have essentially focused on 24(S)-OHC. It presents a Janus face, namely, the induction of cell death at high concentration (above 10 μM) and, at lower doses, an adaptive protective response against cytotoxic oxysterols. The former is due to increased exocytosis that may aggravate excitotoxic injury (Ma et al., 2010). The latter results from a stimulation of an LXR-dependant increase of ABCG1 that should promote the efflux of cytotoxic oxysterols formed during oxidative stress (Noguchi et al., 2014). Some observations describe other oxysterol players in the brain. 7alpha-hydroxycholesterol (7α-OHC), 7beta-hydroxycholesterol (7β-OHC), 5,6alpha-epoxycholesterol (5,6α-EC), 5,6beta-epoxycholesterol (5,6β-EC), and 7KC are self-oxidation products of cholesterol that were detected in rat hippocampus (**Figure 2**). The level of these oxysterols was strongly increased after excitotoxicity (Ong et al., 2010). They increase exocytosis, intracellular calcium concentrations, and cytotoxicity (in particular 7KC), and could so propagate excitotoxicity. Cholestane-3β,5α,6β-Triol (CT) was found in rat brain (Hu et al., 2014). This oxysterol is produced by the hydrolysis of 5,6α-EC and 5,6β-EC catalyzed by the cholesterol epoxide hydrolase (ChEH) enzymatic activity (De Medina et al., 2010). CT exhibits neuroprotective activity both *in vitro* and *in vivo* (**Figure 2**). Indeed, this oxysterol protects against glutamate-induced cytotoxicity and decreased neuronal injury in different animal models. These beneficial effects may stem from the ability of CT to bind and negatively modulate NMDA receptors. Moreover, CT level was increased with ischemic preconditioning and the subsequent neuroprotective effect were abolished by an inhibitor of ChEH. It is noteworthy that 5,6-ECs and 7KC that display neurotoxic effect are, respectively, substrates and inhibitor of ChEH suggesting a potential pathophysiological inter-relation between these oxysterols that have opposite effect on neurons.

Cholestenoic acids, intermediates in the metabolism of cholesterol to bile acids, are present in neural tissues. Among cholestenoic acids, 3β,7α-dihydroxycholest-5-en-26-oic acid and 3β-hydroxycholest-5-en-26-oic acid regulate motor neuron

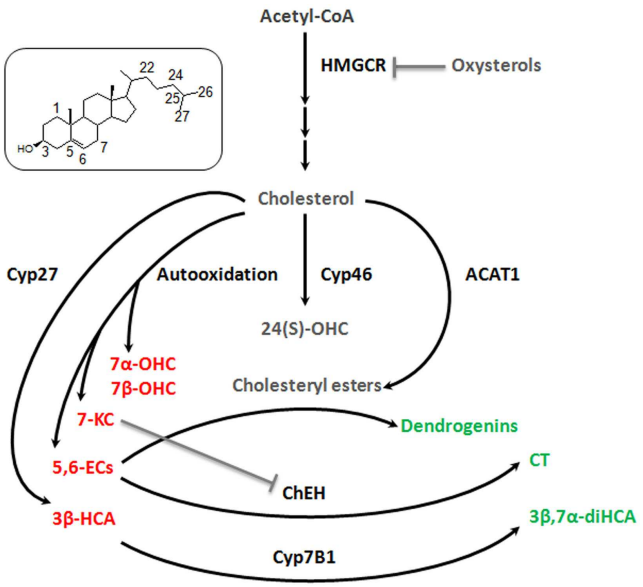

FIGURE 2 | Good and bad cholesterol metabolites in brain. As it was described decades ago for cardiovascular diseases and more recently for cancer, it appears that there is a balance between good and bad cholesterol in neurodegeneration process. Cholesterol is oxidized by different ways (enzymatic or auto-oxidation) to give rise to a large number of oxysterols. Some appear to be bad, as they stimulate exocytosis, excitotoxicity, apoptosis (7α-OHC, 7β-OHC, 5,6α-EC, 5,6β-EC, and 7KC, 3β-HCA – in red), some appear to be good as they exert neuroprotective, neurotrophic, or anti-inflammatory activities (CT, 3β,7α-diHCA, dendrogenins – in green) and finally some whose role is not clear, such as 24(S)-OHC and CE for which additional researches will be necessary to fully understand their involvement in neuroprotective or neurodegenerative processes (in gray). 7α-OHC, 7alpha-hydroxycholesterol; 7β-OHC, 7beta-hydroxycholesterol; 7KC, 7-ketocholesterol; 5,6α-EC, 5,6alpha-epoxycholesterol; 5,6β-EC, 5,6beta-epoxycholesterol; CT, cholestane-3β,5α,6β-triol; 3β,7α-diHCA, 3β,7α-dihydroxycholest-5-en-26-oic acid; 3β-HCA, 3β-hydroxycholest-5-en-26-oic acid; 24(S)-OHC, 24-hydroxycholesterol. Cyp27, cytochrome P450 27A1; Cyp46, cytochrome P450 46A1; Cyp7B1, cytochrome P450 7B1; ACAT-1, Acyl-CoA cholesterol acyltransferase; ChEH, cholesterol epoxide hydrolase; HMGCR, HMGCoA reductase.

function. 3β,7α-dihydroxycholest-5-en-26-oic acid promoted motor neuron survival in an LXR-dependant manner whereas 3β-hydroxycholest-5-en-26-oic acid triggers motor neuron loss (Theofilopoulos et al., 2014). These observations suggest a metabolic balance at the level of cholestenoic acids that may influence neurons fate (**Figure 2**). Cholesteryl esters (CEs) were detected in the brain (Martin and Bazan, 1992; Mulas et al., 2005). CEs are produced by the esterification of cholesterol with fatty acids catalyzed by Acyl-CoA: cholesterol acyltransferase (ACAT). CEs and ACAT-1 levels are increased in aging brain and in brain lesions. Moreover, increased expression of ACAT-1 and CEs level were reported in the hippocampus after excitotoxicity injury (Kim et al., 2011). Since excitotoxicity is associated with the production of cytotoxic oxysterols, esterification should sequester cholesterol to avoid this deleterious process. Conversely, cholesterol storage could also be deleterious by limiting the pool of cholesterol necessary to axonal regrowth, lipid raft functionality, and ApoE-lipoprotein delivery to neurons (Cutler et al., 2002). Whether CEs accumulation constitutes a neuroprotective response or participates in neuronal damage remains to be elucidated.

We previously reported that synthetic steroidal alkaloids resulting from the condensation of biogenic amines and 5,6α-epoxysterols display remarkable neurotrophic and neuroprotective activity *in vitro* (De Medina et al., 2009). Two of the most effective steroidal alkaloids identified to date are 5α-hydroxy-6β[2-(1H-imidazol-4-yl)ethylamino]cholestan-3β-ol, or dendrogenin A and 5α-hydroxy-6β-[3-(4-aminobutylamino)propylamino] cholest-7-en-3β-ol, or dendrogenin B. Dendrogenin B also promotes motor neuron survival (De Medina et al., 2009). In addition, these compounds induce proliferation and differentiation of neural stem cells (Khalifa et al., 2014). Dendrogenin A was recently characterized as a metabolite of 5,6α-EC in mammal tissues, including brain (De Medina et al., 2013). Thus, dendrogenins could be involved in the maintenance of nerve functional state including in inner ear.

As illustrated in **Figure 2**, cholesterol conversion in the brain is a double edged sword that can generate good or bad metabolites. A similar situation was reported for cancer (Silvente-Poirot and Poirot, 2014). This cholesterol balance should be involved in the normal and pathological physiology of the inner ear. To our knowledge, cholesterol metabolism has never been precisely studied in the inner ear.

CHOLESTEROL HOMEOSTASIS AND SNHL

Even if studies related to cholesterol homeostasis in inner ear are scarce, some reports support a relationship between cholesterol homeostasis deregulation and SNHL. Indeed, the genetic syndromes Niemann–Pick type C and Smith–Lemli–Opitz that affect, respectively, cholesterol intracellular transport and synthesis display devastating neurological phenotypes including SNHL (Di Berardino et al., 2007; King et al., 2014). Some epidemiology studies revealed that hypercholesterolemia predisposes to SNHL (Suzuki et al., 2000; Weng et al., 2013). Indeed, atherosclerosis, high plasma total cholesterol, and low HDL levels are positively correlated with SNHL. Medication used for prevention and treatment of atherosclerosis such as Simvastatin were described as otoprotective in mice (Cai et al., 2009). Consistently, ApoE knockout mice developed marked hyperlipidemia, atherosclerosis, and hearing impairment (Guo et al., 2005). The most plausible explanation is that hypercholesterolemia triggers the stenosis of spiral modiolar artery leading to cochlear ischemia and subsequent SNHL. Consequently, therapies that limit high plasma cholesterol level could be useful to prevent SNHL caused by cochlear ischemia.

THERAPEUTIC PERSPECTIVES

Cholesterol homeostasis and metabolism play an important role in neurodegenerative disease and interfere with major causative processes, which are also strongly associated with SNHL, suggesting that targeting cholesterol homeostasis should provide innovative strategies to prevent and attenuate SNHL (**Figure 1**). On this basis, we proposed some hypothesis to be explored for SNHL treatment.

Statins (HMGCR inhibitors) have been proposed as treatment for neurogenerative diseases including SNHL notably

through anti-atherosclerotic effect on cochlear artery and anti-inflammatory activity. Cholesterol-lowering agents should be useful to prevent ischemia and subsequent SNHL. However, this approach should be limited since damaged SGN need cholesterol from astrocyte-derived ApoE-lipoproteins for axonal regrowth. It might be preferable to use cholesterol-lowering agent not crossing the BBB at least in already damaged inner ear. An interesting approach might be a treatment with LXR agonists. These compounds also prevent atherosclerosis via the stimulation of cholesterol efflux rather than direct effect on cholesterogenesis. In the inner ear, LXR agonists might also promote axonal regrowth of SGN by inducing ApoE-lipoprotein formation in astrocytes. In addition, LXR agonists exhibit direct neurotrophic effect *in vitro* and anti-inflammatory activity. However, LXR ligands biological properties are closely related to their structure and to the cell types. For example, the 3β,7α-dihydroxycholest-5-en-26-oic acid and 3β-hydroxycholest-5-en-26-oic acid that both target LXR are, respectively, neuroprotective and neurotoxic (Theofilopoulos et al., 2014). This event is associated with differential recruitment of coactivators/corepressors and subsequent regulation of gene-expression patterns, which strongly depend on the structure of LXR/ligand complex (Huang et al., 2010). The discovery of the bona fide LXR ligand for SNHL treatment remains a difficult challenge. ApoE possesses antioxidant, anti-inflammatory, anti-excitotoxic, and neurotrophic properties and has been proved to be effective in treating brain injury in multiple mouse models. Consequently, it is plausible that ApoE or ApoE mimetics have beneficial effect for the prevention or the treatment of SNHL. Since LRP1 agonist exhibits axonal regrowth properties, this approach should also be considered.

This review highlights the good and the bad side of cholesterol metabolites in neurodegenerative diseases (**Figure 2**). First of all, the determination of the endogenous level of these cholesterol metabolites in healthy and damaged inner ear should be informative. The effect of the good cholesterol metabolites (i.e., CT, 3β,7α-dihydroxycholest-5-en-26-oic acid, dendrogenins) should be investigated in animal models of SNHL (aminoglycosides or noise exposure, presbycusis). Another approach that deserves to be studied is the blockage of bad cholesterol metabolites (i.e., 5,6-ECs, 7KC, 3β-hydroxycholest-5-en-26-oic acid). Since these oxysterols are mainly produced by auto-oxidation, the use of antioxidants seems sensible. Antioxidants have been extensively investigated and are suitable preventive agents for SNHL. At the level of cholesterol metabolism, it is probable that antioxidants block the production of both good and bad cholesterol metabolites potentially limiting their efficacy. It is noteworthy that 5,6-ECs and 3β-hydroxycholest-5-en-26-oic acid are converted, respectively, by ChEH and Cyp7B1 to produce CT and 3β,7α-dihydroxycholest-5-en-26-oic acid previously described as neuroprotective. Pharmacological interventions that stimulate ChEH and Cyp7B1 should be useful. However, concerning ChEH, the situation is more complex since CT will be formed at the expense of dendrogenins biogenesis that also arises from enzymatic transformation of 5,6α-EC (**Figure 2**). Gevokizumab, an antibody targeting pro-inflammatory cytokine IL1β is under clinical evaluation, for treatment of autoimmune inner ear disease. Development of antibodies against bad cholesterol metabolites is also a potential alternative for SNHL. Despite the impact of 24(S)-OHC and cholesterol esterification in neurodegenerative diseases remain unclear (**Figure 2**), their effect in the inner ear also deserve to be studied.

CONCLUDING REMARKS

This review proposes that the study of cholesterol homeostasis in the inner ear might afford new unexplored possibilities for the prevention and treatment of SNHL. Important tasks have to be done to achieve this aim. First: to characterize cholesterol homeostasis and metabolome in normal, aged, and damaged inner ear. Second: to determinate the impact of intervention of cholesterol homeostasis in SNHL. Third: to investigate whether cholesterol metabolites prevent, delay, or aggravate SNHL.

ACKNOWLEDGMENTS

This work was supported by the AFHELO project (FP7-309400, www.afhelo.eu) and TARGEAR project (FP7-612261, www.targear.eu), financed by the European Commission.

REFERENCES

Adibhatla, R. M., and Hatcher, J. F. (2008). Altered lipid metabolism in brain injury and disorders. *Subcell. Biochem.* 49, 241–268. doi:10.1007/978-1-4020-8831-5_9

Bond, M., Mealing, S., Anderson, R., Elston, J., Weiner, G., Taylor, R. S., et al. (2009). The effectiveness and cost-effectiveness of cochlear implants for severe to profound deafness in children and adults: a systematic review and economic model. *Health Technol. Assess.* 13, 1–330. doi:10.3310/hta13440

Boyles, J. K., Zoellner, C. D., Anderson, L. J., Kosik, L. M., Pitas, R. E., Weisgraber, K. H., et al. (1989). A role for apolipoprotein E, apolipoprotein A-I, and low density lipoprotein receptors in cholesterol transport during regeneration and remyelination of the rat sciatic nerve. *J. Clin. Invest.* 83, 1015–1031. doi:10.1172/JCI113943

Cai, Q., Du, X., Zhou, B., Cai, C., Kermany, M. H., Zhang, C., et al. (2009). Effects of simvastatin on plasma lipoproteins and hearing loss in apolipoprotein E gene-deficient mice. *ORL J. Otorhinolaryngol. Relat. Spec.* 71, 244–250. doi:10.1159/000236014

Cutler, R. G., Pedersen, W. A., Camandola, S., Rothstein, J. D., and Mattson, M. P. (2002). Evidence that accumulation of ceramides and cholesterol esters mediates oxidative stress-induced death of motor neurons in amyotrophic lateral sclerosis. *Ann. Neurol.* 52, 448–457. doi:10.1002/ana.10312

De Medina, P., Paillasse, M. R., Payre, B., Silvente-Poirot, S., and Poirot, M. (2009). Synthesis of new alkylaminooxysterols with potent cell differentiating activities: identification of leads for the treatment of cancer and neurodegenerative diseases. *J. Med. Chem.* 52, 7765–7777. doi:10.1021/jm901063e

De Medina, P., Paillasse, M. R., Segala, G., Poirot, M., and Silvente-Poirot, S. (2010). Identification and pharmacological characterization of cholesterol-5,6-epoxide hydrolase as a target for tamoxifen and AEBS ligands. *Proc. Natl. Acad. Sci. U. S. A.* 107, 13520–13525. doi:10.1073/pnas.1002922107

De Medina, P., Paillasse, M. R., Segala, G., Voisin, M., Mhamdi, L., Dalenc, F., et al. (2013). Dendrogenin A arises from cholesterol and histamine metabolism and shows cell differentiation and anti-tumour properties. *Nat. Commun.* 4, 1840. doi:10.1038/ncomms2835

Di Berardino, F., Alpini, D., Ambrosetti, U., Amadeo, C., and Cesarani, A. (2007). Sensorineural hearing-loss in the Smith-Lemli-Opitz syndrome. *Int. J. Pediatr. Otorhinolaryngol. Extra* 2, 169–172. doi:10.1016/j.pedex.2007.05.002

Eriksdotter Jonhagen, M., Nordberg, A., Amberla, K., Backman, L., Ebendal, T., Meyerson, B., et al. (1998). Intracerebroventricular infusion of nerve growth factor in three patients with Alzheimer's disease. *Dement. Geriatr. Cogn. Disord.* 9, 246–257. doi:10.1159/000017069

Fan, X., Kim, H. J., Bouton, D., Warner, M., and Gustafsson, J. A. (2008). Expression of liver X receptor beta is essential for formation of superficial cortical layers and migration of later-born neurons. *Proc. Natl. Acad. Sci. U. S. A.* 105, 13445–13450. doi:10.1073/pnas.0806974105

Fu, X., Menke, J. G., Chen, Y., Zhou, G., Macnaul, K. L., Wright, S. D., et al. (2001). 27-hydroxycholesterol is an endogenous ligand for liver X receptor in cholesterol-loaded cells. *J. Biol. Chem.* 276, 38378–38387. doi:10.1074/jbc.M105805200

Gates, G. A., and Mills, J. H. (2005). Presbycusis. *Lancet* 366, 1111–1120. doi:10.1016/S0140-6736(05)67423-5

Goritz, C., Mauch, D. H., Nagler, K., and Pfrieger, F. W. (2002). Role of glia-derived cholesterol in synaptogenesis: new revelations in the synapse-glia affair. *J. Physiol. Paris* 96, 257–263. doi:10.1016/S0928-4257(02)00014-1

Guo, Y., Zhang, C., Du, X., Nair, U., and Yoo, T. J. (2005). Morphological and functional alterations of the cochlea in apolipoprotein E gene deficient mice. *Hear. Res.* 208, 54–67. doi:10.1016/j.heares.2005.05.010

Harris, J. P., Anderson, J. P., and Novak, R. (1995). An outcomes study of cochlear implants in deaf patients. Audiologic, economic, and quality-of-life changes. *Arch. Otolaryngol. Head Neck Surg.* 121, 398–404. doi:10.1001/archotol.1995.01890040024004

Hayashi, H., Campenot, R. B., Vance, D. E., and Vance, J. E. (2004). Glial lipoproteins stimulate axon growth of central nervous system neurons in compartmented cultures. *J. Biol. Chem.* 279, 14009–14015. doi:10.1074/jbc.M313828200

Hong, C., and Tontonoz, P. (2014). Liver X receptors in lipid metabolism: opportunities for drug discovery. *Nat. Rev. Drug Discov.* 13, 433–444. doi:10.1038/nrd4280

Hu, H., Zhou, Y., Leng, T., Liu, A., Wang, Y., You, X., et al. (2014). The major cholesterol metabolite cholestane-3beta,5alpha,6beta-triol functions as an endogenous neuroprotectant. *J. Neurosci.* 34, 11426–11438. doi:10.1523/JNEUROSCI.0344-14.2014

Huang, P., Chandra, V., and Rastinejad, F. (2010). Structural overview of the nuclear receptor superfamily: insights into physiology and therapeutics. *Annu. Rev. Physiol.* 72, 247–272. doi:10.1146/annurev-physiol-021909-135917

Ignatius, M. J., Gebicke-Harter, P. J., Skene, J. H., Schilling, J. W., Weisgraber, K. H., Mahley, R. W., et al. (1986). Expression of apolipoprotein E during nerve degeneration and regeneration. *Proc. Natl. Acad. Sci. U. S. A.* 83, 1125–1129. doi:10.1073/pnas.83.4.1125

Janowski, B. A., Willy, P. J., Devi, T. R., Falck, J. R., and Mangelsdorf, D. J. (1996). An oxysterol signalling pathway mediated by the nuclear receptor LXR alpha. *Nature* 383, 728–731. doi:10.1038/383728a0

Jasmin, S. B., Pearson, V., Lalonde, D., Domenger, D., Theroux, L., and Poirier, J. (2014). Differential regulation of ABCA1 and ABCG1 gene expressions in the remodeling mouse hippocampus after entorhinal cortex lesion and liver-X receptor agonist treatment. *Brain Res.* 1562, 39–51. doi:10.1016/j.brainres.2014.03.016

Kang, J., and Rivest, S. (2012). Lipid metabolism and neuroinflammation in Alzheimer's disease: a role for liver X receptors. *Endocr. Rev.* 33, 715–746. doi:10.1210/er.2011-1049

Khalifa, S. A., De Medina, P., Erlandsson, A., El-Seedi, H. R., Silvente-Poirot, S., and Poirot, M. (2014). The novel steroidal alkaloids dendrogenin A and B promote proliferation of adult neural stem cells. *Biochem. Biophys. Res. Commun.* 446, 681–686. doi:10.1016/j.bbrc.2013.12.134

Kikkawa, Y. S., Nakagawa, T., Ying, L., Tabata, Y., Tsubouchi, H., Ido, A., et al. (2014). Growth factor-eluting cochlear implant electrode: impact on residual auditory function, insertional trauma, and fibrosis. *J. Transl. Med.* 12, 280. doi:10.1186/s12967-014-0280-4

Kim, J. H., Ee, S. M., Jittiwat, J., Ong, E. S., Farooqui, A. A., Jenner, A. M., et al. (2011). Increased expression of acyl-coenzyme A: cholesterol acyltransferase-1 and elevated cholesteryl esters in the hippocampus after excitotoxic injury. *Neuroscience* 185, 125–134. doi:10.1016/j.neuroscience.2011.04.018

Kim, J. S. (1999). Sensory symptoms restricted to proximal body parts in small cortical infarction. *Neurology* 53, 889–890. doi:10.1212/WNL.53.4.889

King, K. A., Gordon-Salant, S., Yanjanin, N., Zalewski, C., Houser, A., Porter, F. D., et al. (2014). Auditory phenotype of Niemann-Pick disease, type C1. *Ear Hear.* 35, 110–117. doi:10.1097/AUD.0b013e3182a362b8

Kraus, N., Bradlow, A. R., Cheatham, M. A., Cunningham, J., King, C. D., Koch, D. B., et al. (2000). Consequences of neural asynchrony: a case of auditory neuropathy. *J. Assoc. Res. Otolaryngol.* 1, 33–45. doi:10.1007/s101620010004

Laskowitz, D. T., Sheng, H., Bart, R. D., Joyner, K. A., Roses, A. D., and Warner, D. S. (1997). Apolipoprotein E-deficient mice have increased susceptibility to focal cerebral ischemia. *J. Cereb. Blood Flow Metab.* 17, 753–758. doi:10.1097/00004647-199707000-00005

Leoni, V., and Caccia, C. (2013). 24S-hydroxycholesterol in plasma: a marker of cholesterol turnover in neurodegenerative diseases. *Biochimie* 95, 595–612. doi:10.1016/j.biochi.2012.09.025

Linthicum, F. H. Jr., and Fayad, J. N. (2009). Spiral ganglion cell loss is unrelated to segmental cochlear sensory system degeneration in humans. *Otol. Neurotol.* 30, 418–422. doi:10.1097/MAO.0b013e31819a8827

Liu, J. P., Tang, Y., Zhou, S., Toh, B. H., McLean, C., and Li, H. (2010). Cholesterol involvement in the pathogenesis of neurodegenerative diseases. *Mol. Cell. Neurosci.* 43, 33–42. doi:10.1016/j.mcn.2009.07.013

Ma, M. T., Zhang, J., Farooqui, A. A., Chen, P., and Ong, W. Y. (2010). Effects of cholesterol oxidation products on exocytosis. *Neurosci. Lett.* 476, 36–41. doi:10.1016/j.neulet.2010.03.078

Madden, C., Hilbert, L., Rutter, M., Greinwald, J., and Choo, D. (2002). Pediatric cochlear implantation in auditory neuropathy. *Otol. Neurotol.* 23, 163–168. doi:10.1097/00129492-200203000-00011

Mahley, R. W. (1988). Apolipoprotein E: cholesterol transport protein with expanding role in cell biology. *Science* 240, 622–630. doi:10.1126/science.3283935

Martin, R. E., and Bazan, N. G. (1992). Changing fatty acid content of growth cone lipids prior to synaptogenesis. *J. Neurochem.* 59, 318–325. doi:10.1111/j.1471-4159.1992.tb08906.x

Menardo, J., Tang, Y., Ladrech, S., Lenoir, M., Casas, F., Michel, C., et al. (2012). Oxidative stress, inflammation, and autophagic stress as the key mechanisms of premature age-related hearing loss in SAMP8 mouse Cochlea. *Antioxid. Redox Signal.* 16, 263–274. doi:10.1089/ars.2011.4037

Merchant, S. N., Durand, M. L., and Adams, J. C. (2008). Sudden deafness: is it viral? *ORL J. Otorhinolaryngol. Relat. Spec.* 70, 52–60. doi:10.1159/000111048

Moser, T., Predoehl, F., and Starr, A. (2013). Review of hair cell synapse defects in sensorineural hearing impairment. *Otol. Neurotol.* 34, 995–1004. doi:10.1097/MAO.0b013e3182814d4a

Mulas, M. F., Demuro, G., Mulas, C., Putzolu, M., Cavallini, G., Donati, A., et al. (2005). Dietary restriction counteracts age-related changes in cholesterol metabolism in the rat. *Mech. Ageing Dev.* 126, 648–654. doi:10.1016/j.mad.2004.11.010

Nakagawa, T., Kumakawa, K., Usami, S., Hato, N., Tabuchi, K., Takahashi, M., et al. (2014). A randomized controlled clinical trial of topical insulin-like growth factor-1 therapy for sudden deafness refractory to systemic corticosteroid treatment. *BMC Med.* 12:219. doi:10.1186/s12916-014-0219-x

Namjoshi, D. R., Martin, G., Donkin, J., Wilkinson, A., Stukas, S., Fan, J., et al. (2013). The liver X receptor agonist GW3965 improves recovery from mild repetitive traumatic brain injury in mice partly through apolipoprotein E. *PLoS ONE* 8:e53529. doi:10.1371/journal.pone.0053529

Noguchi, N., Saito, Y., and Urano, Y. (2014). Diverse functions of 24(S)-hydroxycholesterol in the brain. *Biochem. Biophys. Res. Commun.* 446, 692–696. doi:10.1016/j.bbrc.2014.02.010

Ohlemiller, K. K., and Gagnon, P. M. (2004). Apical-to-basal gradients in age-related cochlear degeneration and their relationship to "primary" loss of cochlear neurons. *J. Comp. Neurol.* 479, 103–116. doi:10.1002/cne.20326

Ong, W. Y., Kim, J. H., He, X., Chen, P., Farooqui, A. A., and Jenner, A. M. (2010). Changes in brain cholesterol metabolome after excitotoxicity. *Mol. Neurobiol.* 41, 299–313. doi:10.1007/s12035-010-8099-3

Pfrieger, F. W., and Ungerer, N. (2011). Cholesterol metabolism in neurons and astrocytes. *Prog. Lipid Res.* 50, 357–371. doi:10.1016/j.plipres.2011.06.002

Pleis, J. R., and Lethbridge-Cejku, M. (2006). Summary health statistics for U.S. adults: National Health Interview Survey, 2005. *Vital Health Stat.* 232, 1–153.

Ponce, J., De La Ossa, N. P., Hurtado, O., Millan, M., Arenillas, J. F., Davalos, A., et al. (2008). Simvastatin reduces the association of NMDA receptors to lipid rafts: a cholesterol-mediated effect in neuroprotection. *Stroke* 39, 1269–1275. doi:10.1161/STROKEAHA.107.498923

Roehm, P. C., and Hansen, M. R. (2005). Strategies to preserve or regenerate spiral ganglion neurons. *Curr. Opin. Otolaryngol. Head Neck Surg.* 13, 294–300. doi:10.1097/01.moo.0000180919.68812.b9

Ryals, B. M., Dooling, R. J., Westbrook, E., Dent, M. L., Mackenzie, A., and Larsen, O. N. (1999). Avian species differences in susceptibility to noise exposure. *Hear. Res.* 131, 71–88. doi:10.1016/S0378-5955(99)00022-2

Sacchetti, P., Sousa, K. M., Hall, A. C., Liste, I., Steffensen, K. R., Theofilopoulos, S., et al. (2009). Liver X receptors and oxysterols promote ventral midbrain neurogenesis in vivo and in human embryonic stem cells. *Cell Stem Cell* 5, 409–419. doi:10.1016/j.stem.2009.08.019

Schmidt, A., Vogel, R., Holloway, M. K., Rutledge, S. J., Friedman, O., Yang, Z., et al. (1999). Transcription control and neuronal differentiation by agents that activate the LXR nuclear receptor family. *Mol. Cell. Endocrinol.* 155, 51–60. doi:10.1016/S0303-7207(99)00115-X

Schuknecht, H. F., and Gacek, M. R. (1993). Cochlear pathology in presbycusis. *Ann. Otol. Rhinol. Laryngol.* 102, 1–16.

Shi, Y., Mantuano, E., Inoue, G., Campana, W. M., and Gonias, S. L. (2009). Ligand binding to LRP1 transactivates Trk receptors by a Src family kinase-dependent pathway. *Sci. Signal.* 2, ra18. doi:10.1126/scisignal.2000188

Shibata, S. B., Budenz, C. L., Bowling, S. A., Pfingst, B. E., and Raphael, Y. (2011). Nerve maintenance and regeneration in the damaged cochlea. *Hear. Res.* 281, 56–64. doi:10.1016/j.heares.2011.04.019

Silvente-Poirot, S., and Poirot, M. (2014). Cancer. Cholesterol and cancer, in the balance. *Science* 343, 1445–1446. doi:10.1126/science.1252787

Sironi, L., Mitro, N., Cimino, M., Gelosa, P., Guerrini, U., Tremoli, E., et al. (2008). Treatment with LXR agonists after focal cerebral ischemia prevents brain damage. *FEBS Lett.* 582, 3396–3400. doi:10.1016/j.febslet.2008.08.035

Sodero, A. O., Vriens, J., Ghosh, D., Stegner, D., Brachet, A., Pallotto, M., et al. (2012). Cholesterol loss during glutamate-mediated excitotoxicity. *EMBO J.* 31, 1764–1773. doi:10.1038/emboj.2012.31

Starr, A., Picton, T. W., Sininger, Y., Hood, L. J., and Berlin, C. I. (1996). Auditory neuropathy. *Brain* 119(Pt 3), 741–753. doi:10.1093/brain/119.3.741

Steffensen, K. R., Jakobsson, T., and Gustafsson, J. A. (2013). Targeting liver X receptors in inflammation. *Expert Opin. Ther. Targets* 17, 977–990. doi:10.1517/14728222.2013.806490

Suzuki, K., Kaneko, M., and Murai, K. (2000). Influence of serum lipids on auditory function. *Laryngoscope* 110, 1736–1738. doi:10.1097/00005537-200010000-00033

Takeno, S., Wake, M., Mount, R. J., and Harrison, R. V. (1998). Degeneration of spiral ganglion cells in the chinchilla after inner hair cell loss induced by carboplatin. *Audiol. Neurootol.* 3, 281–290. doi:10.1159/000013800

Theofilopoulos, S., Griffiths, W. J., Crick, P. J., Yang, S., Meljon, A., Ogundare, M., et al. (2014). Cholestenoic acids regulate motor neuron survival via liver X receptors. *J. Clin. Invest.* 124, 4829–4842. doi:10.1172/JCI68506

Theofilopoulos, S., Wang, Y., Kitambi, S. S., Sacchetti, P., Sousa, K. M., Bodin, K., et al. (2013). Brain endogenous liver X receptor ligands selectively promote midbrain neurogenesis. *Nat. Chem. Biol.* 9, 126–133. doi:10.1038/nchembio.1156

Vance, J. E. (2012). Dysregulation of cholesterol balance in the brain: contribution to neurodegenerative diseases. *Dis. Model Mech.* 5, 746–755. doi:10.1242/dmm.010124

Varela-Nieto, I., Murillo-Cuesta, S., Rodriguez-De La Rosa, L., Lassatetta, L., and Contreras, J. (2013). IGF-I deficiency and hearing loss: molecular clues and clinical implications. *Pediatr. Endocrinol. Rev.* 4, 460–472.

Wang, L., Schuster, G. U., Hultenby, K., Zhang, Q., Andersson, S., and Gustafsson, J. A. (2002). Liver X receptors in the central nervous system: from lipid homeostasis to neuronal degeneration. *Proc. Natl. Acad. Sci. U. S. A.* 99, 13878–13883. doi:10.1073/pnas.172510899

Weng, T., Devine, E. E., Xu, H., Yan, Z., and Dong, P. (2013). A clinical study of serum lipid disturbance in Chinese patients with sudden deafness. *Lipids Health Dis.* 12, 95. doi:10.1186/1476-511X-12-95

White, J. A., Burgess, B. J., Hall, R. D., and Nadol, J. B. (2000). Pattern of degeneration of the spiral ganglion cell and its processes in the C57BL/6J mouse. *Hear. Res.* 141, 12–18. doi:10.1016/S0378-5955(99)00204-X

Williams, L. R. (1991). Hypophagia is induced by intracerebroventricular administration of nerve growth factor. *Exp. Neurol.* 113, 31–37. doi:10.1016/0014-4886(91)90143-Z

Winkler, J., Ramirez, G. A., Kuhn, H. G., Peterson, D. A., Day-Lollini, P. A., Stewart, G. R., et al. (1997). Reversible Schwann cell hyperplasia and sprouting of sensory and sympathetic neurites after intraventricular administration of nerve growth factor. *Ann. Neurol.* 41, 82–93. doi:10.1002/ana.410410114

Worthington, D. W., and Peters, J. F. (1980). Quantifiable hearing and no ABR: paradox or error? *Ear Hear.* 1, 281–285. doi:10.1097/00003446-198009000-00009

Yoon, C., Van Niekerk, E. A., Henry, K., Ishikawa, T., Orita, S., Tuszynski, M. H., et al. (2013). Low-density lipoprotein receptor-related protein 1 (LRP1)-dependent cell signaling promotes axonal regeneration. *J. Biol. Chem.* 288, 26557–26568. doi:10.1074/jbc.M113.478552

Conflict of Interest Statement: Philippe de Medina and Michael R. Paillasse are employees of Affichem Company. They are inventors of two patents in relation (among others) with neuroprotection/neuronal differentiation induced by aminooxysterols.

Received: 27 November 2014; accepted: 08 January 2015; published online: 29 January 2015.

*Citation: Malgrange B, Varela-Nieto I, de Medina P and Paillasse MR (2015) Targeting cholesterol homeostasis to fight hearing loss: a new perspective. Front. Aging Neurosci. **7**:3. doi: 10.3389/fnagi.2015.00003*

This article was submitted to the journal Frontiers in Aging Neuroscience.

frontiers in Aging Neuroscience

REVIEW
published: 23 April 2015
doi: 10.3389/fnagi.2015.00060

Sphingosine 1-phosphate signaling pathway in inner ear biology. New therapeutic strategies for hearing loss?

*Ricardo Romero-Guevara, Francesca Cencetti, Chiara Donati and Paola Bruni **

Department Scienze Biomediche Sperimentali e Cliniche "Mario Serio", University of Florence, Firenze, Italy

Hearing loss is one of the most prevalent conditions around the world, in particular among people over 60 years old. Thus, an increase of this affection is predicted as result of the aging process in our population. In this context, it is important to further explore the function of molecular targets involved in the biology of inner ear sensory cells to better individuate new candidates for therapeutic application. One of the main causes of deafness resides into the premature death of hair cells and auditory neurons. In this regard, neurotrophins and growth factors such as insulin like growth factor are known to be beneficial by favoring the survival of these cells. An elevated number of published data in the last 20 years have individuated sphingolipids not only as structural components of biological membranes but also as critical regulators of key biological processes, including cell survival. Ceramide, formed by catabolism of sphingomyelin (SM) and other complex sphingolipids, is a strong inducer of apoptotic pathway, whereas sphingosine 1-phosphate (S1P), generated by cleavage of ceramide to sphingosine and phosphorylation catalyzed by two distinct sphingosine kinase (SK) enzymes, stimulates cell survival. Interestingly S1P, by acting as intracellular mediator or as ligand of a family of five distinct S1P receptors ($S1P_1$–$S1P_5$), is a very powerful bioactive sphingolipid, capable of triggering also other diverse cellular responses such as cell migration, proliferation and differentiation, and is critically involved in the development and homeostasis of several organs and tissues. Although new interesting data have become available, the information on S1P pathway and other sphingolipids in the biology of the inner ear is limited. Nonetheless, there are several lines of evidence implicating these signaling molecules during neurogenesis in other cell populations. In this review, we discuss the role of S1P during inner ear development, also as guidance for future studies.

Keywords: sphingosine 1-phosphate, sensory hair-cells, inner ear neurogenesis, hearing loss, auditory neurons, neurotrophins, sphingolipids, growth factors

OPEN ACCESS

Edited by:
Marta Magarinos, Universidad Autonoma de Madrid, Spain

Reviewed by:
Norio Yamamoto, Kyoto University, Japan
Mercedes Garcia-Gil, University of Pisa, Italy

***Correspondence:**
Paola Bruni, Department Scienze Biomediche Sperimentali e Cliniche "Mario Serio", University of Florence, Viale GB Morgagni 50, 50134 Firenze, Italy
Tel: +39 055 2751204, Fax: +39 055 7830303
paola.bruni@unifi.it

Received: *23 January 2015*
Accepted: *08 April 2015*
Published: *23 April 2015*

Citation:
Romero-Guevara R, Cencetti F, Donati C and Bruni P (2015) Sphingosine 1-phosphate signaling pathway in inner ear biology. New therapeutic strategies for hearing loss? Front. Aging Neurosci. 7:60. doi: 10.3389/fnagi.2015.00060

Sphingosine 1-Phosphate as Sphingolipid Metabolite

Sphingolipids are a fascinating subclass of complex lipids known since a long time as key players in the correct structural organization of biological membranes. Subsequently to the understanding of their fundamental structural properties, it has been made clear that intermediates

in their biosynthesis and breakdown are indeed critical signaling molecules implicated in the regulation of essential biological events. In this regard, it is presently well accepted that the vast majority of the extracellular cues involved in the regulation of cell functioning exploits at least in part sphingolipid metabolism for the accomplishment of a variety of specific biological responses.

Among the various types of sphingolipids, sphingomyelin (SM) is of paramount relevance as potential source of bioactive sphingoid molecules. Numerous reviews focus on the intricate regulation of the sphingolipid pathway (Huwiler et al., 2000; Hannun and Obeid, 2008; **Figure 1**). Its breakdown, catalyzed by a small family of SMases, gives rise to the formation of ceramide, an intracellular mediator *per se*, as well as a central hub for the production of other critical bioactive compounds. Ceramide is composed by a sphingoid base, named sphingosine, linked to a fatty acid via an amide bond, thus, depending on the length of the fatty acid acyl chain, various types of ceramide do exist. Another metabolic pathway that can produce ceramide is represented by its *de novo* synthesis that begins with the condensation of palmitoyl-CoA and serine catalyzed by serine palmitoyl transferase to give 3-keto-dihydrosphingosine, then reduced to dihydrosphingosine, followed by acylation reaction performed by a family of six distinct ceramide synthases, several of which are co-expressed in many different cell systems (Stiban et al., 2010; Mullen et al., 2012). The last step involves the oxidation of dihydroceramide to ceramide which is dependent on the action of a specific desaturase. Accumulation of ceramide within the cell is associated with a number of biological responses including cell growth arrest, apoptotic cell death, cell senescence, stress response making the regulation of its intracellular content critical for the fate of a given cell type (Hannun and Obeid, 2011). Once produced, ceramide can be utilized in various distinct biosynthetic pathways. The most abundant sphingolipid in plasma membrane, named SM, is generated by SM synthases in a reaction that, via transfer of phosphocholine from phosphatidylcholine onto ceramide, yields also diacylglycerol (Taniguchi and Okazaki, 2014). Alternatively, ceramide can serve as backbone in the building of glycosphingolipids, the first step being catalyzed by glucosylceramide synthase (GCS), which produces glucosylceramide, the simplest member of this family (Messner and Cabot, 2010). In turn, by addition of a galactose moiety glucosylceramide is transformed into lactosylceramide, which, by addition of one or more monosaccharides, gives raise to individual ganglioside species, recognized as vital components of membrane microdomains with a role in cell-cell recognition, adhesion, and signal transduction (D'Angelo et al., 2013). Moreover, selective phosphorylation of ceramide brought about by ceramide kinase (CK) generates ceramide 1-phosphate, a bioactive sphingolipid regarded as a powerful pro-inflammatory mediator (Gomez-Muñoz et al., 2013).

Finally, it is worth noticing that also the catabolic route by which ceramide is degraded is responsible for the production of other bioactive sphingoid compounds, among which sphingosine 1-phosphate (S1P) plays a prominent role. S1P is produced by ceramide via two specific enzymatic reactions: at first ceramidases (CDase) catalyze ceramide deacylation to sphingosine (Mao and Obeid, 2008; Ito et al., 2014), then the sphingoid base is phosphorylated to S1P by sphingosine kinase (SK). Two distinct isoforms of SK exist, designated SK1 and SK2 (Takabe et al., 2008). They are ubiquitously expressed, each contributing to intracellular S1P production. Although in some instances SK1 and SK2 can have overlapping functions, in certain cell types they have been found to differ for intracellular localization, as well as for their biological role (Maceyka et al., 2012; Neubauer and Pitson, 2013). Catabolism of S1P is also under the control of multiple enzymes. S1P lyase catalyzes the irreversible breakdown of S1P to hexadecenal and phosphoethanolamine (Kumar and Saba, 2009), while two distinct specific S1P phosphatases by removing the phosphate moiety generate sphingosine, that can be further phosphorylated to S1P or employed to feed into the so called sphingolipid salvage pathway, responsible for ceramide biosynthesis from sphingolipid breakdown (Le Stunff et al., 2002).

S1P was discovered as an intracellular mediator more than 20 years ago, even though some of its intracellular targets have been identified only recently (Maceyka et al., 2012). Meanwhile, a large body of experimental evidence has been accumulated in favor of the critical role played by S1P as ligand of a family of five specific, high affinity, G protein coupled receptors named $S1P_{1-5}$ (Ishii et al., 2004; Meyer zu Heringdorf and Jakobs, 2007). The majority of these receptors are able to activate multiple heterotrimeric G proteins, making thus possible the triggering of a wide variety of signaling pathways as well as various biological responses. Notably, $S1P_1$, $S1P_2$ and $S1P_3$ are almost ubiquitous, while $S1P_4$ and $S1P_5$ expression appears to be limited to specific cell types such as those belonging to lymphoid and nervous tissue (Im et al., 2000; Kluk and Hla, 2002). Thus, taking into consideration the selective signaling downstream of individual S1P receptor subtypes, the final biological response evoked by S1P in a given cellular setting is specific, being often strictly dependent on the specific pattern of S1P receptor expressed. Exogenous S1P, mainly via ligation to one or more S1P receptors, is capable of regulating key biological processes, including cell proliferation, survival, motility as well as cell differentiation (Mendelson et al., 2014). Since ceramide and S1P are readily interconvertible lipids exerting opposite biological actions, the balance of their intracellular content is regarded as a biostat determining cell fate (Maceyka et al., 2002). Circulating plasma contains high nanomolar levels of S1P, whereas S1P availability within tissues is much lower (Schwab et al., 2005). The occurrence of such a gradient between blood and tissues is of utmost importance for the correct driving of lymphocyte and hematopoietic cell trafficking (Cyster and Schwab, 2012). Specific cell types such as erythrocytes, platelets and endothelial cells are responsible for the maintaining of the relatively high concentration of S1P in plasma (Pappu et al., 2007), although in principle every cell system can release endogenous S1P in the extracellular environment via the functioning of the widely expressed selective S1P transporter spinster-2 (SPNS2; Kawahara et al., 2009), as well as other less specific transporters such as several members of the ATP binding cassette (ABC) family (Nishi et al., 2014). Indeed, release of S1P by a given

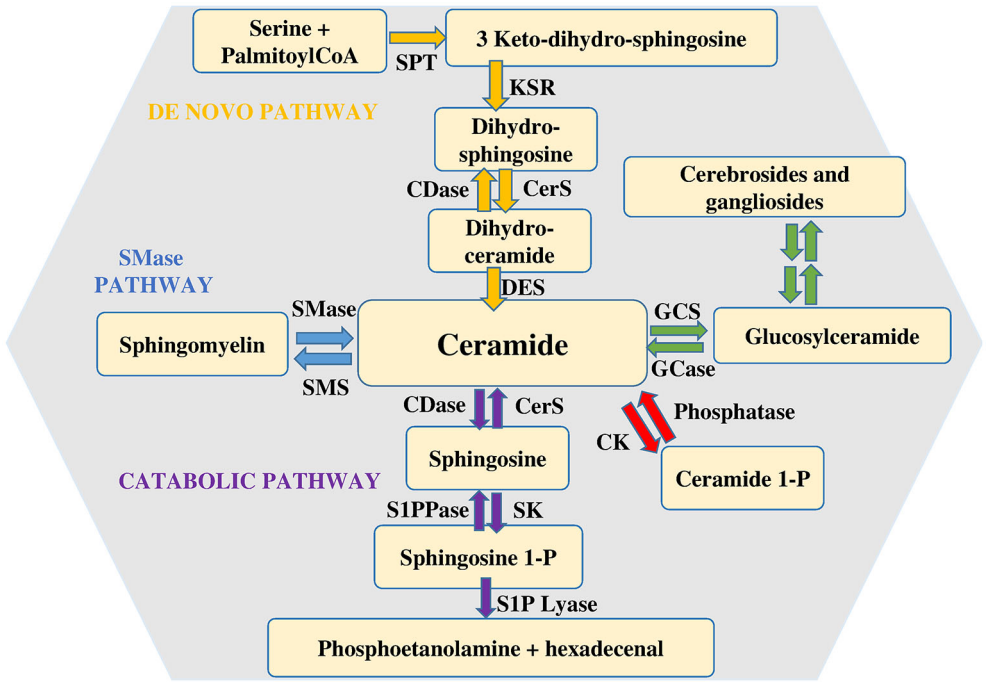

FIGURE 1 | Metabolism of sphingolipids. Ceramide is considered the hearth of sphingolipid metabolism. It can be formed by *de novo* synthesis and then converted to other bioactive lipids. Sphingosine 1-phosphate lyase (S1P lyase) catalyzes the irreversible exit from the pathway. Abbreviations: serine palmitoyl-CoA-acyltransferase (SPT), 3-ketosphinganine reductase (KSR), (dihydro)-ceramide synthase (CerS), ceramide desaturase (DES), ceramide kinase (CK), glucosylceramide synthase (GCS), glucosyl ceramidase (GCase), ceramidase (CDase), sphingosine-1-phosphate lyase (S1P lyase), sphingosine kinase (SK), sphingosine 1-phosphate phosphatase (S1PPase), sphingomyelin (SM) synthase (SMS), sphingomyelinase (SMase).

cell is regarded as a crucial step in the general mechanism by which this sphingolipid can act as paracrine or autocrine cue in the so called inside-out signaling (**Figure 2**). In this regard it has been clearly established that in a wide variety of cellular contexts intracellular S1P metabolism is tightly regulated by multiple extracellular agents including growth factors, hormones, cytokines and neurotransmitters and the subsequent functional interaction with S1P receptors is integral to their final biological actions (Takabe et al., 2008; Xia and Wadham, 2011; Maceyka et al., 2012). Interestingly, extensive experimental evidence has been provided for the occurrence of a complex cross-talk between S1P signaling axis and numerous different extracellular agents including: epithelial growth factor (EGF), platelet derived growth factor (PDGF), vascular endothelial growth factor (VEGF), IGF1, as well as tumor necrosis factor alpha (TNFα) and transforming growth factor beta (TGFβ), that comprises expression changes of S1P receptors and/or enzymes of S1P metabolism and/or S1P-dependent transactivation of enzyme-linked membrane receptors (Pyne et al., 2003; Takabe et al., 2008; Xia and Wadham, 2011; Maceyka et al., 2012; Donati et al., 2013a,b).

S1P Signaling Axis in Nervous Tissue

In keeping with the essential role of S1P metabolism and signaling for correct vertebrate development, S1P biosynthesis was found to be necessary for embryonal neurogenesis. Double knockout (KO) mice for SK1 and SK2 exhibited a severely disturbed neurogenesis, including neural tube closure, defects in angiogenesis and caused embryonic lethality (Mizugishi et al., 2005). The observed neural tube defect was ascribed to the absence of S1P and the consequent increased apoptosis of neuroepithelium. The biological action of S1P was mediated at least in part by $S1P_1$, given that *S1pr1* KO mice were found to display similar, even though milder, neural defects (Liu et al., 2000). A number of different studies have implicated S1P in the control of multiple biological events that occur in the various cell types present in central nervous tissue. Neural progenitor cells express S1P receptors and proliferate in response to S1P challenge (Harada et al., 2004); moreover, they are recruited by this bioactive sphingoid molecule toward a pathological area of the central nervous system (CNS) in a $S1P_1$-dependent manner (Kimura et al., 2007). In this regard, S1P-mediated migration of neural progenitor cells toward an area of brain injury was found to be enhanced by antagonizing $S1P_2$ (Kimura et al., 2008).

S1P is also efficacious in regulating proliferation of astrocytes (Sorensen et al., 2003; Bassi et al., 2006), specialized glial cells that by interacting with blood vessels and synapses regulate multiple aspects of brain homeostasis and functioning. Importantly, S1P was found to be secreted in response to fibroblast growth

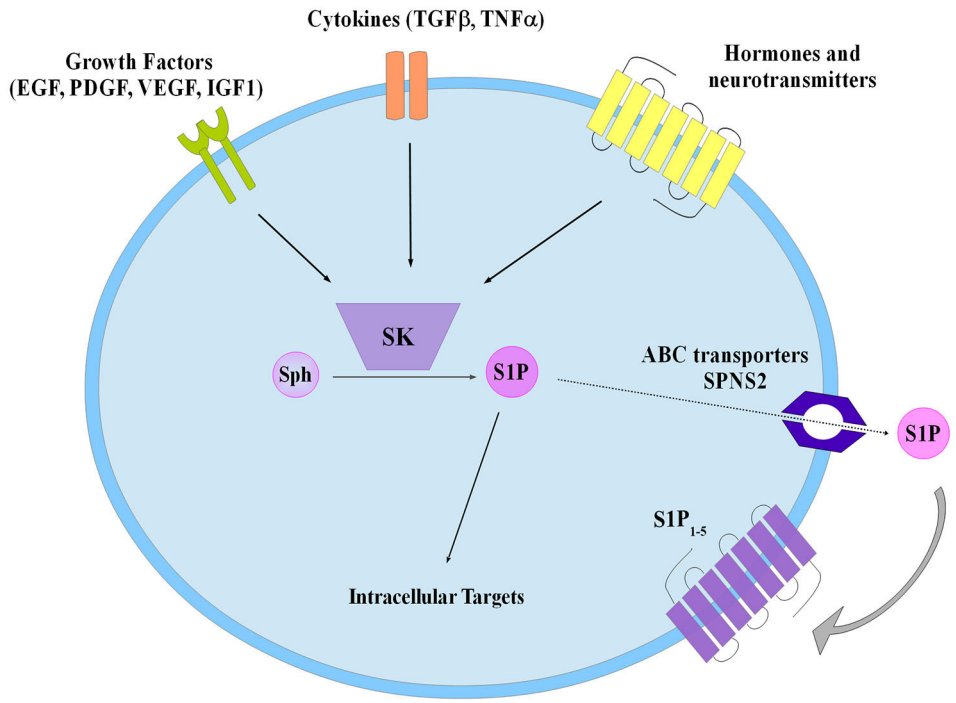

FIGURE 2 | Schematic diagram describing the inside-out signaling of S1P. Sphingosine kinase (SK) activation by different extracellular agents leads to S1P production that both can act via intracellular targets or is extracellularly released to bind specific S1P receptors ($S1P_{1–5}$). Transporters have been involved in S1P export such as the ATP binding cassette (ABC), and the specific spinster 2 (SPNS2).

factor 2 (FGF2) identifying an autocrine/paracrine mechanism of action of this sphingolipid in the proliferation of astrocytes, with a role in the FGF2-induced cell growth signaling (Bassi et al., 2006). Since a pilot study reported that S1P induces the expression of *Fgf2* mRNA in rat astrocytes (Sato et al., 2000), it is tempting to speculate that a positive feedback loop takes place between FGF2 and S1P signaling pathway in astrocytes.

The finding that $S1P_5$ is abundantly expressed in the white matter of brain (Im et al., 2001) led to the identification of this receptor subtype as predominantly present in oligodendrocytes, the myelinating cells of the CNS. In pre-oligodendrocytes S1P acting via $S1P_5$ elicited process retraction, whereas it promoted survival of mature cells (Jaillard et al., 2005). However, $S1P_5$ is not the unique transducer of S1P action in this cell type since $S1P_1$ was reported to be up regulated by PDGF in oligodendrocyte progenitors and implicated in the growth factor-induced mitogenesis (Jung et al., 2007).

A wealth of experimental data mainly performed in hippocampal neurons support an important role of S1P receptors in the modulation of neuronal excitability as well as synapse plasticity and transmission (Kajimoto et al., 2007; Sim-Selley et al., 2009; Kanno et al., 2010; Norman et al., 2010; Kempf et al., 2014). In agreement, aberrant S1P levels and S1P receptor signaling have been reported in a range of diseases of CNS. In multiple sclerosis patients S1P concentration in cerebrospinal fluid was augmented, in accordance with the chronic inflammation status associated with this degenerative disease (Kulakowska et al., 2010). S1P concentrations were selectively decreased in the cerebrospinal fluid of adult rats in an acute and an inflammatory pain model (Coste et al., 2008). Finally, region specific S1P content decline was recently observed during the course of Alzheimer's disease, primarily attributed to a loss of SK1 and SK2 in the hippocampus (Couttas et al., 2014).

It is important to underline that the recently developed fingolimod (FTY720) as oral therapy of multiple sclerosis directly targets S1P signaling pathway (Brinkmann et al., 2010). This compound is converted *in vivo* by SK2 into p-FTY720, that acts as high affinity agonist for all S1P receptors, except $S1P_2$, and results in sequestration of lymphocytes into secondary lymphoid tissues. Besides this key mechanism of action, nonimmunological CNS mechanisms for fingolimod efficacy in multiple sclerosis therapy were identified that implicate $S1P_1$ signaling in astrocytes as a key mediator, thus highlighting S1P signaling pathways within the CNS as targets for multiple sclerosis therapies (Choi et al., 2011). Intense recent studies aimed at exploring additional therapeutic applications of fingolimod, reviewed exhaustively in Brunkhorst et al. (2014), have produced very promising results that hopefully will enable the translation of some of these experimental findings into the clinics opening new avenues for the treatment of Alzheimer's disease, cerebral malaria, neuroblastoma and neuroprotection in cranial irradiation, among others.

An Overview of Inner Ear Morphogenesis

The mature inner ear of mammals is a remarkable structure composed by a myriad of exquisitely arranged cell types within a complex set of ducts and chambers: the vestibular system composed of the semicircular canals, the saccule and the utricle, and the auditory system formed by the cochlea, a convoluted structure where the organ of Corti (OC) resides. In this review we will emphasize the auditory system, in particular the spiral ganglion neurons (SGN), the innervation that transports the electrical stimulus from OC to the CNS. Although many questions are still open, the molecular events occurring from the initial formation of the otic placode, to the final complex tonotopic arrangement of mature SGN are starting to be understood. Several signaling pathways govern every stage in inner ear development, for example members of the FGF and WNT families are between the earliest signals triggering otic development. Later on, retinoic acid (RA) and IGF1 play an important role in the regionalization of the otic vesicle and the survival of auditory neuroblasts. Perhaps some of the most studied proteins involved in the development of SGN are neurotrophins, in particular brain-derived neurotrophic factor (BDNF) and neurotrophin 3 (NT3). The study of these neurotrophins and other signaling molecules involved in the formation and survival of SGN is also relevant from the point of view of therapeutic applications, since SGN are critical in the effectiveness of the cochlear implant.

In addition, in recent years several stem cell-based differentiation protocols have been proposed to create hair cells and sensory neurons that could be used in cell-replacement strategies (Oshima et al., 2010; Koehler and Hashino, 2014). Indeed it was recently shown that human embryonic stem cell-derived inner ear progenitors are able to restore hearing in deafened gerbils (Chen et al., 2012). It is worth mentioning that this and other protocols are developmentally-informed approaches, highlighting that a better understanding of inner ear development will be translated in more efficient differentiation protocols.

As previously mentioned, S1P signaling is functionally ubiquitous, and our group and others have shown that several cytokines, growth factors and morphogenetic cues modulate and are modulated by S1P receptors, S1P lyase and SKs.

We will briefly revisit the development of the inner and the main morphogenetic cues involved in the process and present the current knowledge on the interaction of such cues with S1P pathway in other systems. The evidence presented suggest that apart from the essential role of S1P signaling in hearing, it is worth looking at S1P pathway at earlier developmental stages.

The Pre-Placodal Region and the Formation of the Otic Placode

Preceding the formation of the otic placode, the border region between the neural plate and the lateral ectoderm acquires the competence to respond to otic inducing signals. This region surrounding the head ectoderm called the pre-placodal domain (PPD) is established by the cooperation of bone morphogenetic protein (BMP), WNT and FGF signals emanating from the mesenchyme and the neural plate.

In *X.laevis*, the PPD marker Six1 is expressed in animal caps when the BMP inhibitors noggin and cerberus are overexpressed (Brugmann et al., 2004). In line with this, BMP blocks the expression of Six1 in its endogenous domain while noggin expands it (Ahrens and Schlosser, 2005).

In the chick Wnt8a and BMPs are expressed posteriorly and laterally to the PPD and when these pathways are blocked, the expression of the PPD markers SIX4 and EYA2 expands beyond its endogenous territory (Litsiou et al., 2005). In both works it was also demonstrated that FGF signaling was necessary to fully induce the expression of the PPD markers ectopically (Ahrens and Schlosser, 2005; Litsiou et al., 2005).

The PPD is the common ground of all cranial placodes, characterized by the expression of members of DLX and FOX families of transcription factors in several species (Quint et al., 2000; McLarren et al., 2003; Hans et al., 2004). Experiments in the chick have shown that FGF2 is able to induce the early otic marker PAX2 in explants derived from any region within the PPD but not in lateral or trunk ectoderm (Martin and Groves, 2006). Similarly in the Zebrafish *fgf8* misexpression can enlarge the size of the otic vesicle only in the regions where PPD markers have been previously expressed (Hans et al., 2004).

FGF family are also important signals that initiate inner ear development across vertebrates. In particular, the role of FGF3 during otic induction is conserved in different species. However, other FGFs such as FGF8, FGF10, FGF19 are also involved depending on the species. For example, zebrafish embryos treated with the FGF receptor inhibitor SU5402, or *fgf3/fgf8* morpholino injected do not form otic vesicles neither express the placodal marker Pax8 (Phillips et al., 2001; Maroon et al., 2002). In the chick FGF19 and FGF3 have a synergistic effect during otic placode induction (Ladher et al., 2000), although FGF2 has also been shown to induce the expression of the otic markers PAX2 and DlX3 (Martin and Groves, 2006). In mice, FGF3 together with FGF10 play a redundant role during otocyst formation, double KO animals are completely devoid of otocyst (Alvarez et al., 2003; Wright and Mansour, 2003; Zelarayan et al., 2007). In line with this, FGF receptor 2 isoform IIIb (*Fgfr2IIIb*) KO mice, the receptor isoform for FGF3 and FGF10, present gross morphological defects in the inner ear (Xu et al., 1998; Pirvola et al., 2000).

In addition to the FGF signals, WNT plays also important role during the induction and formation of the otic placode. For example, it has been reported that WNT8A induces the expression of FGF3 before the appearance of otic placode markers in the chick (Ladher et al., 2000). In murine models, conditional expression and deletion of β-catenin (CTNNB1) within the PAX2 territory increases or diminishes respectively the size of the otic domain (Ohyama et al., 2006). In agreement, overexpression of *Dkk1* gene, a WNT signaling inhibitor, impairs the development of the otic placode (Freter et al., 2008).

In summary, FGFs together with a specific level of BMP and WNT signaling inhibition first establish the PPD. Then local

FGFs (e.g., FGF3 and FGF10) restrict the formation of the otic placode next to the hindbrain, which is then compartmentalized into otic and epidermis fates by the action of WNT signals.

To our knowledge, only one study has evaluated the direct involvement of S1P signaling during inner ear development (Hu et al., 2013), however there are reports indicating that S1P axis is involved in the signaling pathways that are required for the proper development of the inner ear. For example, in PC12 cells nerve growth factor (NGF) and FGF2, both important differentiation signals acting via tyrosine kinase receptors, increase the extracellular levels of S1P (Rius et al., 1997), suggesting that even different signaling molecules share in common the modulation of the S1P metabolism. Likewise, in astrocytes FGF2 can increase the activity of SK and the secretion of S1P, while S1P also induces the expression of FGF2 and phosphorylate ERK (Sato et al., 1999; Bassi et al., 2006), supporting the existence of a positive feedback regulatory loop between both signaling pathways in these cells. Analogous interaction of S1P and FGF signaling has been observed in human umbilical vein endothelial cells (HUVECs), where S1P induces the expression of VEGF, an important angiogenic factor. In these cells it was observed that the S1P-induced expression of FGF1 and its specific receptor FGFR1 preceded that of VEGF, since in cells treated with the FGFR inhibitor SU5402 or transfected with FGF1 and FGFR1 siRNA, S1P was unable to induce the VEGF expression (Chang et al., 2013). As observed in astrocytes, in HUVECs a mutual regulation between FGF and S1P signaling pathways occurs. For instance, it has been recently shown that FGF signaling is capable of regulating S1P metabolism by inducing the expression of SK1. In this system, the transcription factor KLF14, induced by FGF2, directly binds to the promoter region of SK1 gene (de Assuncao et al., 2014), establishing more clearly the mechanism of interaction between FGF and the S1P axis.

S1P plays also an important role in osteoblast differentiation. Osteoclast-conditioned medium induced the differentiation of human mesenchymal stem cells (hMSCs) towards osteoblasts. *SK1, BMP6, WNT10B* genes were highly expressed by osteoclasts and indeed when S1P signaling was blocked in hMSCs, differentiation and chemokinesis were reduced (Pederson et al., 2008). In addition, in osteoblasts it has been recently found that S1P axis increases BMP2-induced differentiation through the phosphorylation of ERK and Smad1/5/8 at a level higher than that observed following BMP2 treatment alone (Sato et al., 2012). Thus in this system S1P works as enhancer of the biological effect exerted by BMP signaling. Also in osteoblasts, S1P has been shown to interact with WNT signaling pathway by activating AKT, which inhibits GSK3β and lead to the nuclear traslocation of β-Catenin, downstream effector of WNT signaling. Indeed WNT3a-induced differentiation was impaired by the use AKT pharmacological inhibitors (Matsuzaki et al., 2013). These results and the known effects of BMP and WNT signaling in differentiation suggest that S1P could also behave as an enhancer of WNT signaling in bone formation similarly to its interaction with the BMP pathway.

Regionalization of the Otic Vesicle and the Development of Sensory Neurons

Although morphologically uniform, the otocyst is compartmentalized by the expression of otic markers allocated at different regions within the otocyst. Members of Notch, FGF, RA and SHH signaling pathways are involved in this process.

Although *Fgf3/Fgf10* double KO mice lack completely otic vesicle, the effect of single mutation affects only the expression patter of individual markers, such as DLX5 and PAX2, within the vesicle (Wright and Mansour, 2003). Indeed FGF3 and FGF10 are also expressed at different territories in the otocyst (Pirvola et al., 2000), suggesting that FGFs are important in otocyst regionalization.

RA is a morphogen with a known role in otic vesicle regionalization. In chick and mouse it was found that RA synthesis and degradation are allocated to the posterior and anterior ectoderm respectively, creating in this manner a RA gradient in the otic vesicle. Indeed exposure to RA posteriorise the entire otocyst, reducing the size of the prosensory domain, the area where sensory cells arise (Blentic et al., 2003; Bok et al., 2011). In the zebrafish RA expands anteriorly the expression of the transcription factor Tbx1 normally restricted to the posterior otic vesicle. This leads to increased Notch activation and reduction of the sensory domain (Radosevic et al., 2011).

RA also controls the expression pattern of FGF3 and FGF10, which may underlie the development of the sensory domain (Cadot et al., 2012; Economou et al., 2013). In this regard, it has been shown that FGF10 expression precedes the proneural genes *Neurog1* and *Neurod1* in the otocyst, and FGF10 overexpression increases the number of neuroblasts that delaminate (Alsina et al., 2004).

Sonic hedgehog (SHH) is another signaling molecule that participates in the formation of the otocyst ventromedial domain. *Shh* KO mice fail to maintain the expression of PAX2, OTX2, in the otocyst neurogenic region. As a consequence, ventral structures such as the cochlea and the cochlear ganglion never form (Riccomagno et al., 2002; Bok et al., 2007).

As early as E9 in the mouse, sensory neuroblast start to delaminate from the ventral neurogenic domain of the otocyst, the process continues until E14. Notch, neurotrophins and IGF1 are important in the differentiation and survival of neuroblast. Notch pathway has several functions, it restricts the non-neuronal domain of the otic vesicle posteriorly, and in the other hand, by mechanism of lateral inhibition limits the number of otic neuroblast that delaminate (NEUROD1+ cells) (Haddon et al., 1998; Abelló et al., 2007). In general, it has been observed that Notch signaling activation is necessary to the formation of sensory cells (Kiernan et al., 2006; Daudet et al., 2007). Indeed, the cell decision between neurogenic vs. sensory is regulated by Notch as NEUROG1+ cells restrict neighbor cells of adopting a neural fate but maintains them as sensory precursors (Raft et al., 2007). As neuroblasts (NEUROG1+) continue their way out of the otocyst, another transcription factor NEUROD1 is switched on. These genes are considered to be essential in the formation of the spiral ganglion. *Neurog1* and *Neurod1* KO mice lack completely innervation to the

cochlea which appears morphologically normal (Ma et al., 2000; Kim et al., 2001). However, *Neurod1* mutants form sensory neurons but these do not mature and undergo apoptosis. The expression of the neurotrophin receptors TRKB and TRKC failed in these animals, explaining the increased cell death.

Neurotrophins are important survival factors for many neuronal populations. The inner ear expresses two of them, BDNF and NT3 which are essential for the development of the SGNs. Double KO mice for either *Bdnf/Nt3* or their receptors *TrckB/TrckC* are devoid of cochlear innervation (Ernfors et al., 1995; Silos-Santiago et al., 1997). Their expression pattern forms a gradient for the topographic organization of the sensory neurons (Pirvola et al., 1992; Fariñas et al., 2001). For example BDNF expression starts at the apex of the cochlea at E12.5 and progresses towards the base as the hair cells mature while NT3 has an inverse base-to-apex expression pattern (Schimmang et al., 2003; Sugawara et al., 2007). In fact, exposure to one or the other changes the behavior of SGN towards apical or basal neurons regardless of their position (Adamson et al., 2002). It has been observed that BDNF and NT3 are able to differentially regulate important electrophysiological proteins such as AMPA receptors and synaptophisin (Flores-Otero et al., 2007).

There are other cues involved in the formation of the spiral ganglion. FGFs have been shown to influence the migration and neurite outgrowth of inner ear neuroblasts. In chick otocyst explants, the expression of the BDNF receptor, TRKB is induced by the treatment with FGF2, together with this change, neural progenitor migration and the axon outgrowth accelerates (Brumwell et al., 2000).

IGF1 also plays a role in the formation of mature spiral ganglion cells. *Igf1* KO mice are profoundly deaf by the third postnatal week. Although the cochlea seems normal at birth in these mice, the maturation of several structures of the inner ear such as the tectorial membrane and the spiral ganglion is impaired during the second and third postnatal week (Camarero et al., 2001). A marked apoptosis of SGNs, decreased soma size and an immature synapsis with the OC were observed in *Igf1* KO mouse. Thus IGF1 is prescindible for normal development but it is later required for the maturation and survival of spiral ganglion cells at postnatal stages. Nonetheless examination of the inner ear of *Igf1* KO at earlier developmental stages is still missing. In chick, IGF1 is necessary for the proliferation and further differentiation of auditory neuroblasts (Camarero et al., 2003). The biological effect of IGF1 in this model has been shown to be mediated by the activation of PI3K-AKT signaling pathway (Aburto et al., 2012).

Compelling evidence in several cellular settings models highlights the involvement of S1P axis in the signaling pathways discussed before. In human breast cancer cell lines for example, RA has shown an anti-proliferative effect mediated upon binding to the RA receptor RARα, leading to overproduction of ceramide and downregualtion of SK1. On the contrary, in cells transfected with a dominant-negative form of RARα, RA-induced growth inhibition is hampered, being accompanied by the increased expression and activity of SK1 (Somenzi et al., 2007). On the other hand S1P metabolism affects RA signaling: for example in colon cancer cells, S1P down-regulates the receptor RARβ, thus making cells refractory to RA-induced growth inhibition (Sun et al., 2012).

The cross-talk between neurotrophins and S1P metabolism is also well established. In PC12 and dorsal root ganglion cells, neuritogenesis induced by NGF depends in the membrane translocation of SK1 and the activation of $S1P_1$, while $S1P_2$ and $S1P_5$ have an inhibitory role in neurite formation (Toman et al., 2004). This underlines the importance of understanding the function of this pathway in a particular cell type, since different S1P receptors can trigger disparate biological functions.

In a mouse model of Rett syndrome, *Mecp2* KO, the S1P agonist p-FTY720 showed effectiveness in improving the symptoms of the disease, correlated with increased BDNF levels in several neuronal populations (Deogracias et al., 2012). In another study using cortical neurons p-FTY720 also induced the expression BDNF which protected cells against oligomeric amyloid-β toxicity in an *in vitro* model of Alzheimer disease (Doi et al., 2013). In oligodendrocytes, NT3-induced survival was found to be dependent upon SK expression and translocation (Saini et al., 2005).

Apart from differentiation and survival, it was demonstrated that NGF increased the number action potentials in sensory neurons through a SK1-dependent mechanism (Zhang et al., 2006), even S1P treatment alone was enough augment the number of action potentials in these cells. Thus, it seems that the modulation of S1P metabolism is common molecular mechanism to transmit several of the biological effects elicited by neurotrophins in diverse neuronal populations.

As regards the interaction of S1P with IGF1 signaling, it is important to recall that our laboratory recently found an involvement of S1P axis in IGF1 signaling. We proved that the myogenic effect of IGF1 in skeletal muscle cells is dependent on the activity of SK1 and SK2; if these kinases are blocked by pharmacological inhibitors or siRNA down-regulation, the expression of the myogenic markers myogenin and caveolin-3 is reduced (Bernacchioni et al., 2012). In the ear, IGF1 is currently being studied as a potential polypeptide to be used in the treatment of sensorineural hearing loss and the first results of a clinical trial involving 25 patients with sudden sensorineural hearing loss are very promising (Nakagawa et al., 2014; Yamamoto et al., 2014). Thus, from the point of view of medical application, it would be very interesting to investigate the potential involvement of S1P axis in IGF1 signaling in the context of the inner ear, and explore the possibility of using S1P or S1P receptor agonists/antagonists to prevent hearing loss.

In summary, the formation of the inner ear is a complex and dynamic process that involves the integration of signals such as WNTs, FGFs, RA, SHH and Notch ligands. The recognized interaction between these extracellular cues and S1P in other cell systems should prompt to study its possible involvement in the inner ear. This would shed light not only in the understanding of basic development of the inner ear, but also in the translation of more robust differentiation protocols to generate sensory cells *in vitro* from stem/progenitor cells.

The Role of Sphingolipid Signaling in the Inner Ear

It is still not clear the precise role of different sphingolipids in the biology of the inner ear, but there are several reports that highlight their importance and make them attractive targets that deserve further investigation.

For example it was recently found that the simplest ganglioside named GM3, generated by addition of a sialic acid to lactosylceramide in a reaction catalyzed by GM3 synthase, plays an important role in inner ear physiology. GM3 synthase (*St3gal5*) KO mice have been shown to be profoundly deaf due to specific deterioration of the OC (Yoshikawa et al., 2009). The hearing loss started as early as P14, progressing rapidly and by P17 KO mice were profoundly deaf with a substantial loss of hair cells. The molecular mechanism responsible for hearing loss was not determined. Although gangliosides GM3 and GT1b were expressed in the OC, SGN and stria vascularis (SV), no changes in K^+ and endocochlear potential (EP) were observed in the KO mice (Yoshikawa et al., 2009). Noteworthy, in rat organotipic cultures gangliosides GM1 and GM3 were shown to diminish gentamicin-induced hair cell death (Nishimura et al., 2010). In addition, in the *St3gal5* mutants there was an accumulation of other ganglioside species, whether these can induce apoptosis is unknown. In this regard, GM3 synthase deficient human fibroblasts showed increased apoptosis and accumulation of these ganglioside species (Liu et al., 2008). An alternative explanation could be that GM3-derived gangliosides could modulate growth factor response necessary for the maturation and survival. Indeed, in the work of Liu et al. fibroblasts of such patients have reduced EGF-induced proliferation and migration (Liu et al., 2008). It is important to mention that one of these patients was deaf (Fragaki et al., 2013).

Sphingomyelin, the most abundant sphingolipid in biological membranes, has also been demonstrated to be involved in hearing and maintenance of inner ear structures such as SV and hair cells and the EP. The SM synthase-1 (*Sms-1*) KO mouse presents hearing loss although this is milder than the one observed in *St3gal5* KO mouse and other mutant mouse strains discussed later, *Spns2* and *Sp1r2* KOs, and affects mainly the low and middle frequency hearing (Lu et al., 2012). These mice have a decreased EP compared with wild type (WT) of the same age, but the drop was not as robust as the ones observed in the *St3gal5*KO for example, perhaps accounting for the milder phenotype. Together with the SV defects and the decreased EP, there was an aberrant expression of the K^+ channel KCNQ1 in KO mice. However this was probably a secondary consequence, as its expression in the SV was only assessed at 3 months of age and the K^+ concentration was found to be equal at 1 month between KO and WT littermates.

Finally, only recently S1P signaling emerged as an important pathway in the development of the inner ear and there are only few reports describing its role. For instance, explants cultures of rat cochlea have shown that gentamicin-induced hair cell death can be reduced upon the addition of S1P or increased by the presence of ceramide in the culture media, suggesting that hair cells could respond to these sphingolipids (Nishimura et al., 2010). Moreover, a recent work provides some details on the molecular mechanism that is responsible for the protective effect of S1P on hair cells. Indeed, $S1P_{1-3}$ were found to be expressed in rat cochlea, both in spiral ganglion and OC, by non quantitative RT-PCR analysis and more interestingly an $S1P_2$ antagonist was capable to augment gentamicin-induced hair cell loss, pointing at a role of this receptor in inner ear cell survival (Nakayama et al., 2014). Therefore it is not clear if the effect of ceramide and S1P may also occur indirectly by a secreted signal released from supporting cells, where for example $S1P_2$ has been observed (Herr et al., 2007). Nonetheless, the insights could have an important implication for the use of these metabolites as otoprotective agents. In addition, it remains to be addressed if S1P and ceramide content change after ototoxic damage *in vivo* in the cochlea, this could shed new light into the role of these sphingolipids during hair cell degeneration.

Single *S1pr2* and double *S1pr2/S1pr3* KO have been shown to be profoundly deaf by the third postnatal week (MacLennan et al., 2006; Herr et al., 2007; Kono et al., 2007). Histological examination of the mutants at 6 weeks after birth shows a normal cochlear structure devoid of hair cells and auditory neurons. Kono et al. suggested that the loss of auditory function was caused by defects in the SV, a highly vascularized structure that maintains the EP. Indeed, well before the loss of hair cell and neurons, at postnatal week 2, a thickened SV with aberrant capillaries morphology and defects in the marginal cell boundaries could be observed (Kono et al., 2007). However, K^+ concentration and the EP were not measured in these mutant mice. Thus, the loss of hair cells could not be completely attributed to an altered EP. Recently, the S1P specific transporter SPNS2 was found to be involved in audition, as mutant mice showed a gradual and profound hearing loss starting from the second postnatal week (Chen et al., 2014). Similarly to the *S1pr2* KO mice, *Spns2* mutants showed defects in the SV characterized by thicker capillaries with increased branching, as well as abnormal marginal cell borders. These defects and a decrease in the EP were the earliest abnormalities observed in the *Spns2* KO (P14). Thus, it was concluded that SPNS2 is necessary to maintain the function of the SV and the EP, while the loss of hair cells and the downregulation of KCNQ1, KCNJ10, GJB2 and GJB6, known to maintain the EP, was secondary. This work is in agreement with the results obtained in the *S1pr2* KO mice (Kono et al., 2007), and suggests an involvement of the S1P-SPNS2-$S1P_2$ axis in the maintenance of the structure of the SV. However, how the S1P signaling maintains the EP is not clear, indeed, in the *Spns2* KO mice no permeability between perylimph and endolymph compartments, neither leakage from the capillaries of the SV was observed in the mutants (Chen et al., 2014). In this regard, S1P has shown to increase the excitability of cardiac fibroblast by activating the K^+ channel KIR6.1 in a $S1P_3$-dependent manner (Benamer et al., 2011) or increase the firing rate of rat hippocampal neurons (Norman et al., 2010), suggesting that this pathway

TABLE 1 | Knockout models for genes involved in sphingolipid metabolism and signaling have been found to present inner ear defects.

Gene	Model	Phenotype and function	References
Sphingosine 1-phosphate receptor 2 *(S1pr2)* Alternative names: *Edg5, H218, LPb2, S1P2, Gpcr13*	Mouse	At 1 month of age there was a profound hearing loss together with a decreased number of hair cells, at 4 months spiral ganglion neurons were completely absent as well. At P14 a thickened stria vascularis with disorganized marginal and basal cells was observed as well as thick vessels with excessive branches.	Kono et al. (2007)
		Approximately 40% of 2 months old KO mice displayed a vestibular phenotype, while invariably all mice were deaf from P22, the onset of degeneration of the Organ of Corti, characterized by an abnormally thin stria vascularis, loss of hair cells and a striated tectorial membrane.	MacLennan et al. (2006)
Sphingosine 1-phosphate receptor 3 *(S1pr3)* Alternative names: *Edg3, Lpb3, S1p3, AI132464*	Mouse	In combination with *S1pr2* knockout (KO), there was a progressive loss of hair cells and spiral ganglion neurons starting at 1 month of age.	Herr et al. (2007)
		The double KO *S1pr2* and *S1pr3* showed in addition to hearing loss, a vestibular phenotype not present in the single KO *S1pr2*.	Kono et al. (2007)
Sphingosine 1-phosphate receptor 2 *(s1pr2)* Alternative names: *mil, edg5, s1p2*	Zebrafish	Downregulation or overexpression of *s1pr2* gene reduced the size of the posterior otolith, altered its morphology at 48 h postfertilization and later, at 72 h disturbed the formation of the semi-circular canals. In addition, there was a decrease in the number of lateral line neuromast or these were shrunken with less hair cells and a higher proportion of apoptotic cells at 6 days postfertilization. Conversely *s1pr2* mRNA injection increased the number of posterior neuromast and the number of hair cell within the neuromast.	Hu et al. (2013)
Spinster homolog 2 *(Spns2)*	Mouse	Progressive hearing loss started at P14 and was almost complete by the third postnatal week, robust drop in the endocochlear potential was observed during this window followed by hair cell loss at 1 month of age. Other defects included an excessive branching of capillary net and reduced number of marginal cells in the stria vascularis, no vestibular problems were observed.	Chen et al. (2014)
Sphingomyelin synthase 1 *(Sgms1)* Alternative names: *Mob, Sms1, Sor1, C80702, Tmem23, AI841905, 9530058O11Rik*	Mouse	Auditory brain response analysis from 1 month of age onwards showed that the low and middle frequency hearing regions were the most affected. In line with the phenotype, there was a drop of approximately 20 mV in the endocochlear potential together with a thin and shortened stria vascularis in the mutants. Within the stria vascularis, the marginal cells look disorganized.	Lu et al. (2012)
ST3 beta-galactoside alpha-2, 3-sialyltransferase 5 *(St3gal5)* Alternative names: *3S-T, Siat9, GM3 synthase*	Mouse	Hearing loss evident at P14, selective degeneration of the organ of Corti while the rest of the cochlear structures were morphologically normal as well as the endocochlear potential.	Yoshikawa et al. (2009)

can regulate electrophysiological properties in diverse cell types. Another open question that deserves further investigation is the possible involvement of other S1P transporters in the inner ear. For instance in the *S1pr2* KO mice, a vestibular phenotype was observed while in the *Spns2* mutant only hearing function was disrupted. In this regard, it is unknown if in the vestibular system other S1P transporters may substitute the function of SPNS2. Only the MRP1 transporter has been found in the auditory and vestibular system and although it is known to transport S1P in other systems (Mitra et al., 2006), no vestibular phenotypes has been reported in the KO mice (Zhang et al., 2000). Other non-specific S1P transporters have been found in the mice sensory epithelia such as ABCG2 (Savary et al., 2007), but it is not known if it has role in regulating the extracellular levels of S1P. In fact, it is also unknown if the local release of S1P is necessary to maintain the EP as S1P has not been measured in the cochlea of WT or in *Spns2* KO mice.

In addition, a direct involvement of the S1P signaling in the maintenance of hair cells separate from the EP cannot be ruled out until cell type specific mutants become available. In this regard there are some indications that S1P signaling may have a direct role in sensory cells, evidenced for example by the localized expression of SPNS2 in outer hair cells (Chen et al., 2014), $S1P_2$ expression in supporting cells and $S1P_3$ in that area of SGN (Herr et al., 2007). Even more, the zebrafish ortholog of mammal *S1pr2*, miles-apart (*mil*) has been expressed during developmental stages at positions where the neuromast develop. In addition *mil* morphants have a reduced number of neuromasts in the lateral line while the mRNA transfected embryos have an excess of neuromasts. Equally, morphants and mRNA transfected animals presented patterning defects

in the otic vesicles (Hu et al., 2013). In summary, at least in the zebrafish $S1P_2$ is involved in the formation of the otic vesicle and hair cells. If it has a similar role in the mouse has not been studied yet although the gross morphology of the cochlea and the hair cells is normal at birth in the *S1pr2* KO mice.

Altogether these works indicate that sphingolipids are essential for normal hearing function, but their molecular targets are still to be discovered either in the sensory epithelium itself, the spiral ganglion and importantly, in the SV, that shows some of the earliest defects in the KO models. The results described before are summarized and presented in **Table 1**. Another important aspect to be explored in the future will be the relationship between different categories of sphingolipids, using cell lines derived from these animal models. Those studies will help us to pinpoint if there is a common mechanism involving hearing loss in the models described before. Such a task will be accomplished further with the help of cell lines with selective deletion of enzymes and receptors involved in S1P signaling axis, and possibly by using iPS-derived cells to uncover the role of S1P signaling during the differentiation of inner ear sensory cells.

Conclusions and Remaining Questions

Overall, the here reported experimental findings highlight the crucial role of S1P signaling axis in inner ear biology. However there are several remaining questions that deserve further investigation. The different animal models discussed here support that S1P signaling is necessary during inner ear maturation and hearing at postnatal age in mice. Nonetheless, to our knowledge only one study in the zebrafish has assessed the involvement of this pathway during development (Hu et al., 2013). Thus, it remains to be seen if deletion of S1P receptors or S1P-metabolizing enzymes in mice affect gene expression in the inner ear at early developmental stages.

Importantly, it is still necessary to investigate in more detail the molecular mechanism by which S1P axis is regulating inner ear function in postnatal age, such as the modulation of growth factor receptors, the expression of K^+ channels, critical for the EP, as well as the activation of prosurvival pathway in hair cells and sensory neurons. This is important and consistent with the variety of biological effects elicited by S1P in diverse cell types.

Future studies will confidently clarify the molecular mechanisms that regulate S1P metabolism and S1P receptor expression in the various aspects of inner ear sensory cell biology and hopefully they will disclose the therapeutic potential of S1P signaling pathway in hearing loss.

Acknowledgments

This work was supported by funds from FP7-PEOPLE-2013-IAPP-TARGEAR to PB.

References

Abelló, G., Khatri, S., Giráldez, F., and Alsina, B. (2007). Early regionalization of the otic placode and its regulation by the Notch signaling pathway. *Mech. Dev.* 124, 631–645. doi: 10.1016/j.mod.2007.04.002

Aburto, M. R., Magariños, M., Leon, Y., Varela-Nieto, I., and Sanchez-Calderon, H. (2012). AKT signaling mediates IGF-I survival actions on otic neural progenitors. *PLoS One* 7:e30790. doi: 10.1371/journal.pone.0030790

Adamson, C. L., Reid, M. A., and Davis, R. L. (2002). Opposite actions of brain-derived neurotrophic factor and neurotrophin-3 on firing features and ion channel composition of murine spiral ganglion neurons. *J. Neurosci.* 22, 1385–1396.

Ahrens, K., and Schlosser, G. (2005). Tissues and signals involved in the induction of placodal Six1 expression in Xenopus laevis. *Dev. Biol.* 288, 40–59. doi: 10.1016/j.ydbio.2005.07.022

Alsina, B., Abelló, G., Ulloa, E., Henrique, D., Pujades, C., and Giraldez, F. (2004). FGF signaling is required for determination of otic neuroblasts in the chick embryo. *Dev. Biol.* 267, 119–134. doi: 10.1016/j.ydbio.2003.11.012

Alvarez, Y., Alonso, M. T., Vendrell, V., Zelarayan, L. C., Chamero, P., Theil, T., et al. (2003). Requirements for FGF3 and FGF10 during inner ear formation. *Development* 130, 6329–6338. doi: 10.1242/dev.00881

Bassi, R., Anelli, V., Giussani, P., Tettamanti, G., Viani, P., and Riboni, L. (2006). Sphingosine-1-phosphate is released by cerebellar astrocytes in response to bFGF and induces astrocyte proliferation through Gi-protein-coupled receptors. *Glia* 53, 621–630. doi: 10.1002/glia.20324

Benamer, N., Fares, N., Bois, P., and Faivre, J. F. (2011). Electrophysiological and functional effects of sphingosine-1-phosphate in mouse ventricular fibroblasts. *Biochem. Biophys. Res. Commun.* 408, 6–11. doi: 10.1016/j.bbrc.2011.03.072

Bernacchioni, C., Cencetti, F., Blescia, S., Donati, C., and Bruni, P. (2012). Sphingosine kinase/sphingosine 1-phosphate axis: a new player for insulin-like growth factor-1-induced myoblast differentiation. *Skelet Muscle* 2:15. doi: 10.1186/2044-5040-2-15

Blentic, A., Gale, E., and Maden, M. (2003). Retinoic acid signalling centres in the avian embryo identified by sites of expression of synthesising and catabolising enzymes. *Dev. Dyn.* 227, 114–127. doi: 10.1002/dvdy.10292

Bok, J., Dolson, D. K., Hill, P., Rüther, U., Epstein, D. J., and Wu, D. K. (2007). Opposing gradients of Gli repressor and activators mediate Shh signaling along the dorsoventral axis of the inner ear. *Development* 134, 1713–1722. doi: 10.1242/dev.000760

Bok, J., Raft, S., Kong, K. A., Koo, S. K., Dräger, U. C., and Wu, D. K. (2011). Transient retinoic acid signaling confers anterior-posterior polarity to the inner ear. *Proc. Natl. Acad. Sci. U S A* 108, 161–166. doi: 10.1073/pnas.1010547108

Brinkmann, V., Billich, A., Baumruker, T., Heining, P., Schmouder, R., Francis, G., et al. (2010). Fingolimod (FTY720): discovery and development of an oral drug to treat multiple sclerosis. *Nat. Rev. Drug Discov.* 9, 883–897. doi: 10.1038/nrd3248

Brugmann, S. A., Pandur, P. D., Kenyon, K. L., Pignoni, F., and Moody, S. A. (2004). Six1 promotes a placodal fate within the lateral neurogenic ectoderm by functioning as both a transcriptional activator and repressor. *Development* 131, 5871–5881. doi: 10.1242/dev.01516

Brumwell, C. L., Hossain, W. A., Morest, D. K., and Bernd, P. (2000). Role for basic fibroblast growth factor (FGF-2) in tyrosine kinase (TrkB) expression in the early development and innervation of the auditory receptor: *in vitro* and *in situ* studies. *Exp. Neurol.* 162, 121–145. doi: 10.1006/exnr.2000.7317

Brunkhorst, R., Vutukuri, R., and Pfeilschifter, W. (2014). Fingolimod for the treatment of neurological diseases-state of play and future perspectives. *Front. Cell. Neurosci.* 8:283. doi: 10.3389/fncel.2014.00283

Cadot, S., Frenz, D., and Maconochie, M. (2012). A novel method for retinoic acid administration reveals differential and dose-dependent downregulation of Fgf3 in the developing inner ear and anterior CNS. *Dev. Dyn.* 241, 741–758. doi: 10.1002/dvdy.23748

Camarero, G., Avendano, C., Fernandez-Moreno, C., Villar, A., Contreras, J., de Pablo, F., et al. (2001). Delayed inner ear maturation and neuronal loss in postnatal Igf-1-deficient mice. *J. Neurosci.* 21, 7630–7641.

Camarero, G., Leon, Y., Gorospe, I., De Pablo, F., Alsina, B., Giraldez, F., et al. (2003). Insulin-like growth factor 1 is required for survival of transit-amplifying neuroblasts and differentiation of otic neurons. *Dev. Biol.* 262, 242–253. doi: 10.1016/s0012-1606(03)00387-7

Chang, C. H., Huang, Y. L., Shyu, M. K., Chen, S. U., Lin, C. H., Ju, T. K., et al. (2013). Sphingosine-1-phosphate induces VEGF-C expression through a MMP-2/FGF-1/FGFR-1-dependent pathway in endothelial cells *in vitro*. *Acta Pharmacol. Sin.* 34, 360–366. doi: 10.1038/aps.2012.186

Chen, J., Ingham, N., Kelly, J., Jadeja, S., Goulding, D., Pass, J., et al. (2014). Spinster homolog 2 (spns2) deficiency causes early onset progressive hearing loss. *PLoS Genet.* 10:e1004688. doi: 10.1371/journal.pgen.1004688

Chen, W., Jongkamonwiwat, N., Abbas, L., Eshtan, S. J., Johnson, S. L., Kuhn, S., et al. (2012). Restoration of auditory evoked responses by human ES-cell-derived otic progenitors. *Nature* 490, 278–282. doi: 10.1038/nature11415

Choi, J. W., Gardell, S. E., Herr, D. R., Rivera, R., Lee, C. W., Noguchi, K., et al. (2011). FTY720 (fingolimod) efficacy in an animal model of multiple sclerosis requires astrocyte sphingosine 1-phosphate receptor 1 (S1P1) modulation. *Proc. Natl. Acad. Sci. U S A* 108, 751–756. doi: 10.1073/pnas.1014154108

Coste, O., Brenneis, C., Linke, B., Pierre, S., Maeurer, C., Becker, W., et al. (2008). Sphingosine 1-phosphate modulates spinal nociceptive processing. *J. Biol. Chem.* 283, 32442–32451. doi: 10.1074/jbc.m806410200

Couttas, T. A., Kain, N., Daniels, B., Lim, X. Y., Shepherd, C., Kril, J., et al. (2014). Loss of the neuroprotective factor Sphingosine 1-phosphate early in Alzheimer's disease pathogenesis. *Acta Neuropathol. Commun.* 2:9. doi: 10.1186/2051-5960-2-9

Cyster, J. G., and Schwab, S. R. (2012). Sphingosine-1-phosphate and lymphocyte egress from lymphoid organs. *Annu. Rev. Immunol.* 30, 69–94. doi: 10.1146/annurev-immunol-020711-075011

D'Angelo, G., Capasso, S., Sticco, L., and Russo, D. (2013). Glycosphingolipids: synthesis and functions. *Febs J.* 280, 6338–6353. doi: 10.1111/febs.12559

Daudet, N., Ariza-Mcnaughton, L., and Lewis, J. (2007). Notch signalling is needed to maintain, but not to initiate, the formation of prosensory patches in the chick inner ear. *Development* 134, 2369–2378. doi: 10.1242/dev.001842

de Assuncao, T. M., Lomberk, G., Cao, S., Yaqoob, U., Mathison, A., Simonetto, D. A., et al. (2014). New role for Kruppel-like factor 14 as a transcriptional activator involved in the generation of signaling lipids. *J. Biol. Chem.* 289, 15798–15809. doi: 10.1074/jbc.m113.544346

Deogracias, R., Yazdani, M., Dekkers, M. P., Guy, J., Ionescu, M. C., Vogt, K. E., et al. (2012). Fingolimod, a sphingosine-1 phosphate receptor modulator, increases BDNF levels and improves symptoms of a mouse model of Rett syndrome. *Proc. Natl. Acad. Sci. U S A* 109, 14230–14235. doi: 10.1073/pnas.1206093109

Doi, Y., Takeuchi, H., Horiuchi, H., Hanyu, T., Kawanokuchi, J., Jin, S., et al. (2013). Fingolimod phosphate attenuates oligomeric amyloid beta-induced neurotoxicity via increased brain-derived neurotrophic factor expression in neurons. *PLoS One* 8:e61988. doi: 10.1371/journal.pone.0061988

Donati, C., Cencetti, F., and Bruni, P. (2013a). New insights into the role of sphingosine 1-phosphate and lysophosphatidic acid in the regulation of skeletal muscle cell biology. *Biochim. Biophys. Acta* 1831, 176–184. doi: 10.1016/j.bbalip.2012.06.013

Donati, C., Cencetti, F., and Bruni, P. (2013b). Sphingosine 1-phosphate axis: a new leader actor in skeletal muscle biology. *Front. Physiol.* 4:338. doi: 10.3389/fphys.2013.00338

Economou, A., Datta, P., Georgiadis, V., Cadot, S., Frenz, D., and Maconochie, M. (2013). Gata3 directly regulates early inner ear expression of Fgf10. *Dev. Biol.* 374, 210–222. doi: 10.1016/j.ydbio.2012.11.028

Ernfors, P., Van De Water, T., Loring, J., and Jaenisch, R. (1995). Complementary roles of BDNF and NT-3 in vestibular and auditory development. *Neuron* 14, 1153–1164. doi: 10.1016/0896-6273(95)90263-5

Fariñas, I., Jones, K. R., Tessarollo, L., Vigers, A. J., Huang, E., Kirstein, M., et al. (2001). Spatial shaping of cochlear innervation by temporally regulated neurotrophin expression. *J. Neurosci.* 21, 6170–6180.

Flores-Otero, J., Xue, H. Z., and Davis, R. L. (2007). Reciprocal regulation of presynaptic and postsynaptic proteins in bipolar spiral ganglion neurons by neurotrophins. *J. Neurosci.* 27, 14023–14034. doi: 10.1523/jneurosci.3219-07.2007

Fragaki, K., Ait-El-Mkadem, S., Chaussenot, A., Gire, C., Mengual, R., Bonesso, L., et al. (2013). Refractory epilepsy and mitochondrial dysfunction due to GM3 synthase deficiency. *Eur. J. Hum. Genet.* 21, 528–534. doi: 10.1038/ejhg.2012.202

Freter, S., Muta, Y., Mak, S. S., Rinkwitz, S., and Ladher, R. K. (2008). Progressive restriction of otic fate: the role of FGF and Wnt in resolving inner ear potential. *Development* 135, 3415–3424. doi: 10.1242/dev.026674

Gomez-Muñoz, A., Gangoiti, P., Arana, L., Ouro, A., Rivera, I. G., Ordonez, M., et al. (2013). New insights on the role of ceramide 1-phosphate in inflammation. *Biochim. Biophys. Acta* 1831, 1060–1066. doi: 10.1016/j.bbalip.2013.02.001

Haddon, C., Jiang, Y. J., Smithers, L., and Lewis, J. (1998). Delta-Notch signalling and the patterning of sensory cell differentiation in the zebrafish ear: evidence from the mind bomb mutant. *Development* 125, 4637–4644.

Hannun, Y. A., and Obeid, L. M. (2008). Principles of bioactive lipid signalling: lessons from sphingolipids. *Nat. Rev. Mol. Cell Biol.* 9, 139–150. doi: 10.1038/nrm2329

Hannun, Y. A., and Obeid, L. M. (2011). Many ceramides. *J. Biol. Chem.* 286, 27855–27862. doi: 10.1074/jbc.r111.254359

Hans, S., Liu, D., and Westerfield, M. (2004). Pax8 and Pax2a function synergistically in otic specification, downstream of the Foxi1 and Dlx3b transcription factors. *Development* 131, 5091–5102. doi: 10.1242/dev.01346

Harada, J., Foley, M., Moskowitz, M. A., and Waeber, C. (2004). Sphingosine-1-phosphate induces proliferation and morphological changes of neural progenitor cells. *J. Neurochem.* 88, 1026–1039. doi: 10.1046/j.1471-4159.2003.02219.x

Herr, D. R., Grillet, N., Schwander, M., Rivera, R., Müller, U., and Chun, J. (2007). Sphingosine 1-phosphate (S1P) signaling is required for maintenance of hair cells mainly via activation of S1P2. *J. Neurosci.* 27, 1474–1478. doi: 10.1523/jneurosci.4245-06.2007

Hu, Z. Y., Zhang, Q. Y., Qin, W., Tong, J. W., Zhao, Q., Han, Y., et al. (2013). Gene miles-apart is required for formation of otic vesicle and hair cells in zebrafish. *Cell Death Dis.* 4:e900. doi: 10.1038/cddis.2013.432

Huwiler, A., Kolter, T., Pfeilschifter, J., and Sandhoff, K. (2000). Physiology and pathophysiology of sphingolipid metabolism and signaling. *Biochim. Biophys. Acta* 1485, 63–99. doi: 10.1016/s1388-1981(00)00042-1

Im, D. S., Clemens, J., Macdonald, T. L., and Lynch, K. R. (2001). Characterization of the human and mouse sphingosine 1-phosphate receptor, S1P5 (Edg-8): structure-activity relationship of sphingosine1-phosphate receptors. *Biochemistry* 40, 14053–14060. doi: 10.1021/bi011606i

Im, D. S., Heise, C. E., Ancellin, N., O'Dowd, B. F., Shei, G. J., Heavens, R. P., et al. (2000). Characterization of a novel sphingosine 1-phosphate receptor, Edg-8. *J. Biol. Chem.* 275, 14281–14286. doi: 10.1074/jbc.275.19.14281

Ishii, I., Fukushima, N., Ye, X., and Chun, J. (2004). Lysophospholipid receptors: signaling and biology. *Annu. Rev. Biochem.* 73, 321–354. doi: 10.1146/annurev.biochem.73.011303.073731

Ito, M., Okino, N., and Tani, M. (2014). New insight into the structure, reaction mechanism and biological functions of neutral ceramidase. *Biochim. Biophys. Acta* 1841, 682–691. doi: 10.1016/j.bbalip.2013.09.008

Jaillard, C., Harrison, S., Stankoff, B., Aigrot, M. S., Calver, A. R., Duddy, G., et al. (2005). Edg8/S1P5: an oligodendroglial receptor with dual function on process retraction and cell survival. *J. Neurosci.* 25, 1459–1469. doi: 10.1523/jneurosci.4645-04.2005

Jung, C. G., Kim, H. J., Miron, V. E., Cook, S., Kennedy, T. E., Foster, C. A., et al. (2007). Functional consequences of S1P receptor modulation in rat oligodendroglial lineage cells. *Glia* 55, 1656–1667. doi: 10.1002/glia.20576

Kajimoto, T., Okada, T., Yu, H., Goparaju, S. K., Jahangeer, S., and Nakamura, S. (2007). Involvement of sphingosine-1-phosphate in glutamate secretion in hippocampal neurons. *Mol. Cell. Biol.* 27, 3429–3440. doi: 10.1128/mcb.01465-06

Kanno, T., Nishizaki, T., Proia, R. L., Kajimoto, T., Jahangeer, S., Okada, T., et al. (2010). Regulation of synaptic strength by sphingosine 1-phosphate in the hippocampus. *Neuroscience* 171, 973–980. doi: 10.1016/j.neuroscience.2010.10.021

Kawahara, A., Nishi, T., Hisano, Y., Fukui, H., Yamaguchi, A., and Mochizuki, N. (2009). The sphingolipid transporter spns2 functions in migration of zebrafish myocardial precursors. *Science* 323, 524–527. doi: 10.1126/science.1167449

Kempf, A., Tews, B., Arzt, M. E., Weinmann, O., Obermair, F. J., Pernet, V., et al. (2014). The sphingolipid receptor S1PR2 is a receptor for Nogo-a repressing

synaptic plasticity. *PLoS Biol.* 12:e1001763. doi: 10.1371/journal.pbio.1001763

Kiernan, A. E., Xu, J., and Gridley, T. (2006). The Notch ligand JAG1 is required for sensory progenitor development in the mammalian inner ear. *PLoS Genet.* 2:e4. doi: 10.1371/journal.pgen.0020004

Kim, W. Y., Fritzsch, B., Serls, A., Bakel, L. A., Huang, E. J., Reichardt, L. F., et al. (2001). NeuroD-null mice are deaf due to a severe loss of the inner ear sensory neurons during development. *Development* 128, 417–426.

Kimura, A., Ohmori, T., Kashiwakura, Y., Ohkawa, R., Madoiwa, S., Mimuro, J., et al. (2008). Antagonism of sphingosine 1-phosphate receptor-2 enhances migration of neural progenitor cells toward an area of brain. *Stroke* 39, 3411–3417. doi: 10.1161/STROKEAHA.108.514612

Kimura, A., Ohmori, T., Ohkawa, R., Madoiwa, S., Mimuro, J., Murakami, T., et al. (2007). Essential roles of sphingosine 1-phosphate/S1P1 receptor axis in the migration of neural stem cells toward a site of spinal cord injury. *Stem Cells* 25, 115–124. doi: 10.1634/stemcells.2006-0223

Kluk, M. J., and Hla, T. (2002). Signaling of sphingosine-1-phosphate via the S1P/EDG-family of G-protein-coupled receptors. *Biochim. Biophys. Acta* 1582, 72–80. doi: 10.1016/s1388-1981(02)00139-7

Koehler, K. R., and Hashino, E. (2014). 3D mouse embryonic stem cell culture for generating inner ear organoids. *Nat. Protoc.* 9, 1229–1244. doi: 10.1038/nprot.2014.100

Kono, M., Belyantseva, I. A., Skoura, A., Frolenkov, G. I., Starost, M. F., Dreier, J. L., et al. (2007). Deafness and stria vascularis defects in S1P2 receptor-null mice. *J. Biol. Chem.* 282, 10690–10696. doi: 10.1074/jbc.m700370200

Kulakowska, A., Zendzian-Piotrowska, M., Baranowski, M., Konończuk, T., Drozdowski, W., Górski, J., et al. (2010). Intrathecal increase of sphingosine 1-phosphate at early stage multiple sclerosis. *Neurosci. Lett.* 477, 149–152. doi: 10.1016/j.neulet.2010.04.052

Kumar, A., and Saba, J. D. (2009). Lyase to live by: sphingosine phosphate lyase as a therapeutic target. *Expert Opin. Ther. Targets* 13, 1013–1025. doi: 10.1517/14728220903039722

Ladher, R. K., Anakwe, K. U., Gurney, A. L., Schoenwolf, G. C., and Francis-West, P. H. (2000). Identification of synergistic signals initiating inner ear development. *Science* 290, 1965–1967. doi: 10.1126/science.290.5498.1965

Le Stunff, H., Galve-Roperh, I., Peterson, C., Milstien, S., and Spiegel, S. (2002). Sphingosine-1-phosphate phosphohydrolase in regulation of sphingolipid metabolism and apoptosis. *J. Cell Biol.* 158, 1039–1049. doi: 10.1083/jcb.200203123

Litsiou, A., Hanson, S., and Streit, A. (2005). A balance of FGF, BMP and WNT signalling positions the future placode territory in the head. *Development* 132, 4051–4062. doi: 10.1242/dev.01964

Liu, Y., Su, Y., Wiznitzer, M., Epifano, O., and Ladisch, S. (2008). Ganglioside depletion and EGF responses of human GM3 synthase-deficient fibroblasts. *Glycobiology* 18, 593–601. doi: 10.1093/glycob/cwn039

Liu, Y., Wada, R., Yamashita, T., Mi, Y., Deng, C. X., Hobson, J. P., et al. (2000). Edg-1, the G protein-coupled receptor for sphingosine-1-phosphate, is essential for vascular maturation. *J. Clin. Invest.* 106, 951–961. doi: 10.1172/jci10905

Lu, M. H., Takemoto, M., Watanabe, K., Luo, H., Nishimura, M., Yano, M., et al. (2012). Deficiency of sphingomyelin synthase-1 but not sphingomyelin synthase-2 causes hearing impairments in mice. *J. Physiol.* 590, 4029–4044. doi: 10.1113/jphysiol.2012.235846

Ma, Q., Anderson, D. J., and Fritzsch, B. (2000). Neurogenin 1 null mutant ears develop fewer, morphologically normal hair cells in smaller sensory epithelia devoid of innervation. *J. Assoc. Res. Otolaryngol.* 1, 129–143. doi: 10.1007/s101620010017

Maceyka, M., Harikumar, K. B., Milstien, S., and Spiegel, S. (2012). Sphingosine-1-phosphate signaling and its role in disease. *Trends Cell Biol.* 22, 50–60. doi: 10.1016/j.tcb.2011.09.003

Maceyka, M., Payne, S. G., Milstien, S., and Spiegel, S. (2002). Sphingosine kinase, sphingosine-1-phosphate and apoptosis. *Biochim. Biophys. Acta* 1585, 193–201. doi: 10.1016/S1388-1981(02)00341-4

MacLennan, A. J., Benner, S. J., Andringa, A., Chaves, A. H., Rosing, J. L., Vesey, R., et al. (2006). The S1P2 sphingosine 1-phosphate receptor is essential for auditory and vestibular function. *Hear. Res.* 220, 38–48. doi: 10.1016/j.heares.2006.06.016

Mao, C., and Obeid, L. M. (2008). Ceramidases: regulators of cellular responses mediated by ceramide, sphingosine and sphingosine-1-phosphate. *Biochim. Biophys. Acta* 1781, 424–434. doi: 10.1016/j.bbalip.2008.06.002

Maroon, H., Walshe, J., Mahmood, R., Kiefer, P., Dickson, C., and Mason, I. (2002). Fgf3 and Fgf8 are required together for formation of the otic placode and vesicle. *Development* 129, 2099–2108.

Martin, K., and Groves, A. K. (2006). Competence of cranial ectoderm to respond to Fgf signaling suggests a two-step model of otic placode induction. *Development* 133, 877–887. doi: 10.1242/dev.02267

Matsuzaki, E., Hiratsuka, S., Hamachi, T., Takahashi-Yanaga, F., Hashimoto, Y., Higashi, K., et al. (2013). Sphingosine-1-phosphate promotes the nuclear translocation of beta-catenin and thereby induces osteoprotegerin gene expression in osteoblast-like cell lines. *Bone* 55, 315–324. doi: 10.1016/j.bone.2013.04.008

McLarren, K. W., Litsiou, A., and Streit, A. (2003). DLX5 positions the neural crest and preplacode region at the border of the neural plate. *Dev. Biol.* 259, 34–47. doi: 10.1016/s0012-1606(03)00177-5

Mendelson, K., Evans, T., and Hla, T. (2014). Sphingosine 1-phosphate signalling. *Development* 141, 5–9. doi: 10.1242/dev.094805

Messner, M. C., and Cabot, M. C. (2010). Glucosylceramide in humans. *Adv. Exp. Med. Biol.* 688, 156–164. doi: 10.1007/978-1-4419-6741-1_11

Meyer zu Heringdorf, D., and Jakobs, K. H. (2007). Lysophospholipid receptors: signalling, pharmacology and regulation by lysophospholipid metabolism. *Biochim. Biophys. Acta* 1768, 923–940. doi: 10.1016/j.bbamem.2006.09.026

Mitra, P., Oskeritzian, C. A., Payne, S. G., Beaven, M. A., Milstien, S., and Spiegel, S. (2006). Role of ABCC1 in export of sphingosine-1-phosphate from mast cells. *Proc. Natl. Acad. Sci. U S A* 103, 16394–16399. doi: 10.1073/pnas.0603734103

Mizugishi, K., Yamashita, T., Olivera, A., Miller, G. F., Spiegel, S., and Proia, R. L. (2005). Essential role for sphingosine kinases in neural and vascular development. *Mol. Cell. Biol.* 25, 11113–11121. doi: 10.1128/mcb.25.24.11113-11121.2005

Mullen, T. D., Hannun, Y. A., and Obeid, L. M. (2012). Ceramide synthases at the centre of sphingolipid metabolism and biology. *Biochem. J.* 441, 789–802. doi: 10.1042/bj20111626

Nakagawa, T., Kumakawa, K., Usami, S., Hato, N., Tabuchi, K., Takahashi, M., et al. (2014). A randomized controlled clinical trial of topical insulin-like growth factor-1 therapy for sudden deafness refractory to systemic corticosteroid treatment. *BMC Med.* 12:219. doi: 10.1186/s12916-014-0219-x

Nakayama, M., Tabuchi, K., Hoshino, T., Nakamagoe, M., Nishimura, B., and Hara, A. (2014). The influence of sphingosine-1-phosphate receptor antagonists on gentamicin-induced hair cell loss of the rat cochlea. *Neurosci. Lett.* 561, 91–95. doi: 10.1016/j.neulet.2013.12.063

Neubauer, H. A., and Pitson, S. M. (2013). Roles, regulation and inhibitors of sphingosine kinase 2. *FEBS J.* 280, 5317–5336. doi: 10.1111/febs.12314

Nishi, T., Kobayashi, N., Hisano, Y., Kawahara, A., and Yamaguchi, A. (2014). Molecular and physiological functions of sphingosine 1-phosphate transporters. *Biochim. Biophys. Acta* 1841, 759–765. doi: 10.1016/j.bbalip.2013.07.012

Nishimura, B., Tabuchi, K., Nakamagoe, M., and Hara, A. (2010). The influences of sphingolipid metabolites on gentamicin-induced hair cell loss of the rat cochlea. *Neurosci. Lett.* 485, 1–5. doi: 10.1016/j.neulet.2010.08.014

Norman, E., Cutler, R. G., Flannery, R., Wang, Y., and Mattson, M. P. (2010). Plasma membrane sphingomyelin hydrolysis increases hippocampal neuron excitability by sphingosine-1-phosphate mediated mechanisms. *J. Neurochem.* 114, 430–439. doi: 10.1111/j.1471-4159.2010.06779.x

Ohyama, T., Mohamed, O. A., Taketo, M. M., Dufort, D., and Groves, A. K. (2006). Wnt signals mediate a fate decision between otic placode and epidermis. *Development* 133, 865–875. doi: 10.1242/dev.02271

Oshima, K., Shin, K., Diensthuber, M., Peng, A. W., Ricci, A. J., and Heller, S. (2010). Mechanosensitive hair cell-like cells from embryonic and induced pluripotent stem cells. *Cell* 141, 704–716. doi: 10.1016/j.cell.2010.03.035

Pappu, R., Schwab, S. R., Cornelissen, I., Pereira, J. P., Regard, J. B., Xu, Y., et al. (2007). Promotion of lymphocyte egress into blood and lymph by distinct sources of sphingosine-1-phosphate. *Science* 316, 295–298. doi: 10.1126/science.1139221

Pederson, L., Ruan, M., Westendorf, J. J., Khosla, S., and Oursler, M. J. (2008). Regulation of bone formation by osteoclasts involves Wnt/BMP signaling and the chemokine sphingosine-1-phosphate. *Proc. Natl. Acad. Sci. U S A* 105, 20764–20769. doi: 10.1073/pnas.0805133106

Phillips, B. T., Bolding, K., and Riley, B. B. (2001). Zebrafish fgf3 and fgf8 encode redundant functions required for otic placode induction. *Dev. Biol.* 235, 351–365. doi: 10.1006/dbio.2001.0297

Pirvola, U., Spencer-Dene, B., Xing-Qun, L., Kettunen, P., Thesleff, I., Fritzsch, B., et al. (2000). FGF/FGFR-2(IIIb) signaling is essential for inner ear morphogenesis. *J. Neurosci.* 20, 6125–6134.

Pirvola, U., Ylikoski, J., Palgi, J., Lehtonen, E., Arumäe, U., and Saarma, M. (1992). Brain-derived neurotrophic factor and neurotrophin 3 mRNAs in the peripheral target fields of developing inner ear ganglia. *Proc. Natl. Acad. Sci. U S A* 89, 9915–9919. doi: 10.1073/pnas.89.20.9915

Pyne, N. J., Waters, C., Moughal, N. A., Sambi, B. S., and Pyne, S. (2003). Receptor tyrosine kinase-GPCR signal complexes. *Biochem. Soc. Trans.* 31, 1220–1225. doi: 10.1042/bst0311220

Quint, E., Zerucha, T., and Ekker, M. (2000). Differential expression of orthologous Dlx genes in zebrafish and mice: implications for the evolution of the Dlx homeobox gene family. *J. Exp. Zool.* 288, 235–241. doi: 10.1002/1097-010x(20001015)288:3<235::aid-jez4>3.0.co;2-j

Radosevic, M., Robert-Moreno, A., Coolen, M., Bally-Cuif, L., and Alsina, B. (2011). Her9 represses neurogenic fate downstream of Tbx1 and retinoic acid signaling in the inner ear. *Development* 138, 397–408. doi: 10.1242/dev.056093

Raft, S., Koundakjian, E. J., Quinones, H., Jayasena, C. S., Goodrich, L. V., Johnson, J. E., et al. (2007). Cross-regulation of Ngn1 and Math1 coordinates the production of neurons and sensory hair cells during inner ear development. *Development* 134, 4405–4415. doi: 10.1242/dev.009118

Riccomagno, M. M., Martinu, L., Mulheisen, M., Wu, D. K., and Epstein, D. J. (2002). Specification of the mammalian cochlea is dependent on Sonic hedgehog. *Genes Dev.* 16, 2365–2378. doi: 10.1101/gad.1013302

Rius, R. A., Edsall, L. C., and Spiegel, S. (1997). Activation of sphingosine kinase in pheochromocytoma PC12 neuronal cells in response to trophic factors. *FEBS Lett.* 417, 173–176. doi: 10.1016/s0014-5793(97)01277-5

Saini, H. S., Coelho, R. P., Goparaju, S. K., Jolly, P. S., Maceyka, M., Spiegel, S., et al. (2005). Novel role of sphingosine kinase 1 as a mediator of neurotrophin-3 action in oligodendrocyte progenitors. *J. Neurochem.* 95, 1298–1310. doi: 10.1111/j.1471-4159.2005.03451.x

Sato, K., Ishikawa, K., Ui, M., and Okajima, F. (1999). Sphingosine 1-phosphate induces expression of early growth response-1 and fibroblast growth factor-2 through mechanism involving extracellular signal-regulated kinase in astroglial cells. *Brain Res. Mol. Brain Res.* 74, 182–189. doi: 10.1016/s0169-328x(99)00279-x

Sato, C., Iwasaki, T., Kitano, S., Tsunemi, S., and Sano, H. (2012). Sphingosine 1-phosphate receptor activation enhances BMP-2-induced osteoblast differentiation. *Biochem. Biophys. Res. Commun.* 423, 200–205. doi: 10.1016/j.bbrc.2012.05.130

Sato, K., Ui, M., and Okajima, F. (2000). Differential roles of Edg-1 and Edg-5, sphingosine 1-phosphate receptors, in the signaling pathways in C6 glioma cells. *Brain Res. Mol. Brain Res.* 85, 151–160. doi: 10.1016/s0169-328x(00)00262-x

Savary, E., Hugnot, J. P., Chassigneux, Y., Travo, C., Duperray, C., Van De Water, T., et al. (2007). Distinct population of hair cell progenitors can be isolated from the postnatal mouse cochlea using side population analysis. *Stem Cells* 25, 332–339. doi: 10.1634/stemcells.2006-0303

Schimmang, T., Tan, J., Müller, M., Zimmermann, U., Rohbock, K., Köpschall, I., et al. (2003). Lack of Bdnf and TrkB signalling in the postnatal cochlea leads to a spatial reshaping of innervation along the tonotopic axis and hearing loss. *Development* 130, 4741–4750. doi: 10.1242/dev.00676

Schwab, S. R., Pereira, J. P., Matloubian, M., Xu, Y., Huang, Y., and Cyster, J. G. (2005). Lymphocyte sequestration through S1P lyase inhibition and disruption of S1P gradients. *Science* 309, 1735–1739. doi: 10.1126/science.1113640

Silos-Santiago, I., Fagan, A. M., Garber, M., Fritzsch, B., and Barbacid, M. (1997). Severe sensory deficits but normal CNS development in newborn mice lacking TrkB and TrkC tyrosine protein kinase receptors. *Eur. J. Neurosci.* 9, 2045–2056. doi: 10.1111/j.1460-9568.1997.tb01372.x

Sim-Selley, L. J., Goforth, P. B., Mba, M. U., Macdonald, T. L., Lynch, K. R., Milstien, S., et al. (2009). Sphingosine-1-phosphate receptors mediate neuromodulatory functions in the CNS. *J. Neurochem.* 110, 1191–1202. doi: 10.1111/j.1471-4159.2009.06202.x

Somenzi, G., Sala, G., Rossetti, S., Ren, M., Ghidoni, R., and Sacchi, N. (2007). Disruption of retinoic acid receptor alpha reveals the growth promoter face of retinoic acid. *PLoS One* 2:e836. doi: 10.1371/journal.pone.0000836

Sorensen, S. D., Nicole, O., Peavy, R. D., Montoya, L. M., Lee, C. J., Murphy, T. J., et al. (2003). Common signaling pathways link activation of murine PAR-1, LPA and S1P receptors to proliferation of astrocytes. *Mol. Pharmacol.* 64, 1199–1209. doi: 10.1124/mol.64.5.1199

Stiban, J., Tidhar, R., and Futerman, A. H. (2010). Ceramide synthases: roles in cell physiology and signaling. *Adv. Exp. Med. Biol.* 688, 60–71. doi: 10.1007/978-1-4419-6741-1_4

Sugawara, M., Murtie, J. C., Stankovic, K. M., Liberman, M. C., and Corfas, G. (2007). Dynamic patterns of neurotrophin 3 expression in the postnatal mouse inner ear. *J. Comp. Neurol.* 501, 30–37. doi: 10.1002/cne.21227

Sun, D. F., Gao, Z. H., Liu, H. P., Yuan, Y., and Qu, X. J. (2012). Sphingosine 1-phosphate antagonizes the effect of all-trans retinoic acid (ATRA) in a human colon cancer cell line by modulation of RARbeta expression. *Cancer Lett.* 319, 182–189. doi: 10.1016/j.canlet.2012.01.012

Takabe, K., Paugh, S. W., Milstien, S., and Spiegel, S. (2008). "Inside-out" signaling of sphingosine-1-phosphate: therapeutic targets. *Pharmacol. Rev.* 60, 181–195. doi: 10.1124/pr.107.07113

Taniguchi, M., and Okazaki, T. (2014). The role of sphingomyelin and sphingomyelin synthases in cell death, proliferation and migration-from cell and animal models to human disorders. *Biochim. Biophys. Acta* 1841, 692–703. doi: 10.1016/j.bbalip.2013.12.003

Toman, R. E., Payne, S. G., Watterson, K. R., Maceyka, M., Lee, N. H., Milstien, S., et al. (2004). Differential transactivation of sphingosine-1-phosphate receptors modulates NGF-induced neurite extension. *J. Cell Biol.* 166, 381–392. doi: 10.1083/jcb.200402016

Wright, T. J., and Mansour, S. L. (2003). Fgf3 and Fgf10 are required for mouse otic placode induction. *Development* 130, 3379–3390. doi: 10.1242/dev.00555

Xia, P., and Wadham, C. (2011). Sphingosine 1-phosphate, a key mediator of the cytokine network: juxtacrine signaling. *Cytokine Growth Factor Rev.* 22, 45–53. doi: 10.1016/j.cytogfr.2010.09.004

Xu, X., Weinstein, M., Li, C., Naski, M., Cohen, R. I., Ornitz, D. M., et al. (1998). Fibroblast growth factor receptor 2 (FGFR2)-mediated reciprocal regulation loop between FGF8 and FGF10 is essential for limb induction. *Development* 125, 753–765.

Yamamoto, N., Nakagawa, T., and Ito, J. (2014). Application of insulin-like growth factor-1 in the treatment of inner ear disorders. *Front. Pharmacol.* 5:208. doi: 10.3389/fphar.2014.00208

Yoshikawa, M., Go, S., Takasaki, K., Kakazu, Y., Ohashi, M., Nagafuku, M., et al. (2009). Mice lacking ganglioside GM3 synthase exhibit complete hearing loss due to selective degeneration of the organ of Corti. *Proc. Natl. Acad. Sci. U S A* 106, 9483–9488. doi: 10.1073/pnas.0903279106

Zelarayan, L. C., Vendrell, V., Alvarez, Y., Domínguez-Frutos, E., Theil, T., Alonso, M. T., et al. (2007). Differential requirements for FGF3, FGF8 and FGF10 during inner ear development. *Dev. Biol.* 308, 379–391. doi: 10.1016/j.ydbio.2007.05.033

Zhang, Z. J., Saito, T., Kimura, Y., Sugimoto, C., Ohtsubo, T., and Saito, H. (2000). Disruption of mdr1a p-glycoprotein gene results in dysfunction of blood-inner ear barrier in mice. *Brain Res.* 852, 116–126. doi: 10.1016/s0006-8993(99)02223-4

Zhang, Y. H., Vasko, M. R., and Nicol, G. D. (2006). Intracellular sphingosine 1-phosphate mediates the increased excitability produced by nerve growth factor in rat sensory neurons. *J. Physiol.* 575, 101–113. doi: 10.1113/jphysiol.2006.111575

Conflict of Interest Statement: The authors declare that the research was conducted in the absence of any commercial or financial relationships that could be construed as a potential conflict of interest.